The genetic architecture of the human language connectome

Yasmina Nozha Mekki

université
PARIS-SACLAY

The genetic architecture of the human language connectome

L'architecture génétique du connectome du langage dans le cerveau humain

Thèse de doctorat de l'université Paris-Saclay

École doctorale n° 575, Electrical, Optical, Bio-Physics and Engineering (EOBE)
Spécialité de doctorat : Sciences de l'information et de la communication
Graduate School : Sciences de l'ingénierie et des systèmes, Référent : Faculté des sciences d'Orsay

Thèse préparée dans l'unité de recherche ***BAOBAB (Université Paris-Saclay, CEA, CNRS)***, sous la direction de **Vincent Frouin**, directeur de recherche, le co-encadrement de **Cathy Philippe**, docteure et de **Vincent Guillemot**, docteur.

Thèse soutenue à Paris-Saclay, le 15 février 2022, par

Yasmina Nozha Mekki

Composition du jury

Christophe Pallier Directeur de recherche, CEA NeuroSpin, Université Paris Saclay	Président
Hugues Aschard Directeur de recherche, Institut Pasteur	Rapporteur & Examinateur
Marie-Hélène Grosbras Directrice de recherche, Université Aix Marseille	Raporteure & Examinatrice
Vincent Frouin Directeur de recherche, CEA NeuroSpin, Université Paris Saclay	Directeur de thèse

THESE DE DOCTORAT
NNT : 2022UPAST019

Abstract

Language is an essential component of human life because of its central role in social interaction, cultural transmission, and for structuring our thoughts. Through developmental disorders of spoken and written language studies such as dyslexia, a growing number of genes have been identified and labelled as implicated in language etiology. Case-control studies suffering from a lack of statistical power, struggle to uncover significant variants. In parallel, neuroimaging studies have significantly contributed to the understanding of structural and functional aspects of language in the human brain. The recent availability of large-scale cohorts comprising both neuroimaging and genetics data such as the UK Biobank and the Human Connectome Project, have made it possible to study language in the general population via image-derived phenotypes (IDP). Indeed, these IDPs give access to biologically relevant measurements of individual variability and are consequently suitable for the search of genetic associations. In this thesis, we aim to first, highlight the inter-individual variation in brain structure and/or function of language; second, take advantage of this variability to study the genetic basis of the brain's infrastructure for language. For this, we used task-free functional connectivity (FC), extracted from perisylvian cortical regions as well as from anatomical connectivity (AC) measured using well-known language related white matter bundles determined from diffusion MRI. First, we present an in-depth study of language heritability using human language connectome as endophenotypes extracted from the two aforementioned large-scale cohorts. The results found are consistent with the heritability estimates reported in the literature and support that the language-related brain organization is partly underpinned by genetic. Secondly, using the significantly heritable FC endophenotypes, we performed a multivariate genome-wide association study on 32,186 participants from UK Biobank. Twenty genomic loci were found significantly associated with language FCs, out of which three were replicated in an independent sample (the UK Biobank non-British sample, N=4.754). The functional annotation highlighted noticeably the EPHA3 gene associated with FCs of the fronto-parieto-temporal semantic network, and the THBS1 gene with a potential role in the perceptual-motor interaction required for language processing. Finally, using the significantly heritable AC endophenotypes, we performed a multivariate genome-wide association study on 31.775 participants from UK Biobank. 278 genomic loci were found significantly associated with language ACs including those previously associated with FC endophenotypes. As a conclusion, this work contributed to uncovering the neurobiology

of human language using state-of-the-art genomic approaches and by developing novel language endophenotypes. The genes pinpointed in this work open new leads for investigations of neurobiology of language using animal and cellular models. Furthermore, as more and more cohorts are being built in the general population, this work strengthens our belief that multi-modal data collection in large-scale cohorts allow us to increase statistical power and to circumvent the small effect sizes in neuroimaging in order to investigate open neuroscience questions. Many other neuroscience fields could probably benefit from this type of methodology.

Résumé

Le langage est une composante essentielle de la vie humaine en raison de son rôle central dans les interactions sociales, la transmission culturelle, et la structuration de nos pensées. Grâce à l'étude des troubles du développement du langage parlé et écrit, tel que la dyslexie, un nombre croissant de gènes ont été identifiés et étiquetés comme étant impliqués dans leurs étiologies. Des études d'association cas-témoins sont mises en œuvre, mais souffrent d'un manque de puissance statistique et peinent à produire des résultats significatifs. Parallèlement à cela, des études de neuro-imagerie ont contribué de manière significative à la compréhension des aspects structurels et fonctionnels du langage dans le cerveau. La disponibilité récente des cohortes de grande taille comportant à la fois de la neuro-imagerie et de la génétique tels que "UK Biobank" et le "Human Connectome Project" a rendu possible l'étude du langage dans les populations générales via des phénotypes intermédiaires (endophénotypes). En effet, ceux-là donnent accès à des mesures biologiquement pertinentes de la variabilité individuelle des supports structurels et fonctionnels du langage et sont par conséquent adaptés à la recherche d'associations génétiques. Dans cette thèse, nous souhaitons d'une part, mettre en évidence la variation interindividuelle de la structure et/ou de la fonction cérébrale qui reflète des traits neurocognitifs spécifiques; d'autre part, tirer profit de cette variabilité pour mettre en évidence la base génétique de leur architecture cérébrale. Pour ce faire, nous avons étudié la neurobiologie du langage à l'aide de la connectivité fonctionnelle (CF) des régions corticales périsylviennes mesurée à l'état de repos, ainsi qu'à partir de la connectivité anatomique (CA) mesuré sur des faisceaux de matière blanche déterminé par l'IRM de diffusion et connus comme étant liés au langage. Tout d'abord, nous présentons une étude approfondie de l'héritabilité du langage en exploitant des endophénotypes du connectome du langage humain extraits des deux cohortes susmentionnées. Les résultats obtenus sont conformes aux estimations de l'héritabilité rapportées dans la littérature et confirment que l'organisation cérébrale liée au langage est en partie sous-tendue par la génétique. Deuxièmement, pour les endophénotypes de CF avec une héritabilité significative, nous avons réalisé une étude d'association multivariée pangénomique sur 32.186 participants de la cohorte UK Biobank. Vingt loci sont significativement associés aux CF du langage, dont trois sont répliqués dans un échantillon indépendant (ethnicité non britannique de UKB, N=4.754). L'annotation fonctionnelle approfondie pointe notamment vers le gène EPHA3 avec un rôle dans le réseau sémantique fronto-pariéto-temporal, et le gène THBS1 avec un rôle dans l'interaction perception-moteur,

requise dans le langage. Enfin, de la même manière, pour les endophénotypes de CA avec une héritabilité significative, nous avons effectué une étude d'association multivariée pangénomique sur 31.775 participants de la cohorte UK Biobank. 278 loci sont significativement associés aux CA du langage, dont ceux précédemment associés à des endophénotypes de CF. En conclusion, ce travail a permis d'étudier les bases génétiques du langage humain en utilisant des approches génomiques à l'état de l'art et ce, en développant des endophénotypes originaux associés au langage. Les gènes suggérés par l'analyse fournissent des pistes d'investigation dans des modèles animaux ou cellulaires du langage. Aussi, alors que de plus en plus de cohortes sont construites en population générale, ce travail renforce notre conviction que ce type de cohortes "multi-phénotypées" permet d'augmenter la puissance statistique et de pallier les faibles tailles d'effet en neuro-imagerie afin d'étudier des questions ouvertes en neuroscience. De nombreux autres domaines des neurosciences pourraient probablement bénéficier de ce type de méthodologie.

Contents

List of Figures xi

List of Tables xxi

Abbreviations and Acronyms xxv

1 State of the art 1

1.1 Genetic basis . . . 3
1.1.1 The genome and inter-individual variability . . . 4
1.1.2 From genotypes to phenotype . . . 6
1.2 Neuroanatomy basics . . . 6
1.2.1 Grey and white matter . . . 7
1.2.2 Gyri and Sulci . . . 7
1.2.3 Cells of the brain: From molecule to neurons and from neurons to brain . 8
1.3 How to determine the brain architecture? A neuroimaging approach . . . 9
1.3.1 Structural Neuroimaging . . . 10
1.3.2 Functional Neuroimaging . . . 13
1.4 A basic introduction to quantitative and molecular genetics methodology . . . 17
1.4.1 Heritability . . . 17
1.4.2 Endophenotypes . . . 18
1.4.3 Pleiotropy . . . 18
1.4.4 Candidate genes . . . 18
1.4.5 Genome-wide association study . . . 19
1.5 What are the bases of human language? A review of language approaches in human neurosciences . . . 21
1.5.1 Understanding language from aphasia . . . 21
1.5.2 Understanding language by brain imaging . . . 22
1.6 Complex and multifactorial aetiology: the pursuit of brain–language-genetics relationships . . . 29
1.6.1 Heritability of language . . . 30

1.6.2 Developmental language disorder related loci . . . 32
1.6.3 Genome-wide association studies of language abilities . . . 33
1.6.4 Moving Forward: Emergence of imaging-genetics approach . . . 35
1.7 Aim of this thesis . . . 39

2 Materials and methods 41
2.1 Cohorts . . . 42
2.1.1 UK Biobank . . . 42
2.1.2 Human Connectome Project . . . 45
2.2 Definition of brain regions and tracts of interest . . . 48
2.2.1 Functional connectomes . . . 48
2.2.2 Anatomical connectomes . . . 52
2.3 Rank-based inverse-normal transformation . . . 55
2.4 Heritability . . . 55
2.5 Genetic correlation . . . 56
2.6 Massive univariate and multivariate genome-wide association study . . . 56
2.7 Fine-mapping: identification of genomic risk loci and functional annotations . . . 59
2.7.1 FUMA: SNP2GENE . . . 59
2.7.2 FUMA: GENE2FUNC . . . 60
2.8 Protein networks . . . 60

3 Human language endophenotypes 63
3.1 Psychometric measures . . . 64
3.2 Language neural activation: a volume-based analysis . . . 67
3.3 Resting-state functional connectome . . . 69
3.4 Anatomical connectome . . . 70
3.5 Conclusion . . . 72

4 Heritability of human language 73
4.1 Pedigree-based heritability of behavioural and neuroimaging (endo)phenotypes: a twin study . . . 75
4.1.1 Cognitive behavioural assessment . . . 75
4.1.2 Brain neural activation . . . 76
4.1.3 Functional connectome . . . 76
4.2 SNP-based heritability of neuroimaging endophenotypes: a general population study . . . 77
4.2.1 Functional connectome . . . 77
4.2.2 Anatomical connectome . . . 80
4.3 Discussion . . . 80
4.4 Are heritability estimates inflated in twin studies? . . . 80
4.5 Conclusion . . . 84

5 Shared genetic variance between language-related performance, language-brain activations and language functional connectivity 85

5.1 Shared heritability between both resting-state functional connectivity and neural activations . . . 87

5.2 Shared heritability between both resting-state functional connectivity and language-related scores . . . 88

5.3 Shared heritability between both task activations and language-related scores . 88

5.4 Discussion . . . 89

6 The genetic architecture of human language functional connectome 91

6.1 Multivariate genome-wide association analysis . . . 93

6.2 Unraveling the genome: Evaluation of results from mvGWAS study of human language . . . 103

6.2.1 *Perceptual motor* interactions process driven by *THBS1* gene . . . 103

6.2.2 *Fronto-temporal semantic network* driven by *EPHA3* gene . . . 110

6.2.3 PrecR↔RolS and T1a↔T1a/HeschlR endophenotypes driven by *PLCE1*, *NOC3L* and *HELLS* genes . . . 115

6.3 Limitations . . . 117

6.4 Conclusions . . . 118

7 The genetic architecture of anatomical connectivity in human language 119

7.1 Multivariate genome-wide association studies . . . 120

7.2 Validation of lead SNPs associated with ACs. . . . 124

7.3 Functional annotations of genomic loci associated with language . . . 129

7.4 Discussion . . . 135

General Conclusions 137

Appendices **141**

A **143**

A.1 Population structure of Human connectome project data 143

B **145**

B.1 Pedigree-based heritability of behavioural and neuroimaging (endo)phenotypes: a twin study 145

B.2 SNP-based heritability of neuroimaging endophenotypes: a general population study 153

C **169**

C.1 (Endo)phenotypic correlation between both resting-state functional connectivity and neural activations 169

C.2 (Endo)phenotypic correlation between both resting-state functional connectivity and language-related scores 172

C.3 (Endo)phenotypic correlation between both task activations and language-related scores 177

D **180**

D.1 Genomic loci associated with heritable language anatomical connectivities using MOSTest 180

E Résumé en français (Abstract in French) **209**

Bibliography **215**

* * *
* *
*

List of Figures

1.1 **Description of the chromosome structure. (Source: https://www.genome.gov/).** 4

1.2 **Neuroanatomy of the brain ([Bui and Nguyen, 2019]).** A) Brain, Encephalon, Connections of the several parts of the brain, Cerebrum, Cerebellum, Pons, Cerebral; Superior; Middle; Inferior Peduncle, Medulla oblongata. B) Principal fissures and lobes of the cerebrum viewed laterally, Frontal Lobe, Parietal Lobe, Temporal Lobe, Occipital Lobe. 7

1.3 **Brain basics.** Example of a) the grey and white matter of the central nervous system (source : https://difference.guru/difference-between-white-and-gray-matter/), b) sulcus and gyrus. 8

1.4 **Schematic representation of the major cellular elements of the white matter (Source: [Johansen-Berg and Behrens, 2013]).** In this drawing, a neuronal cell body in the grey matter extends several short dendritic processes and a single, long axonal process. The axon, in the white matter, is surrounded by an insulating myelin sheath. This sheath is produced by oligodendrocytes. Generally, oligodendrocytes extend many processes, each of which wraps around a segment of an axon to form an internode. Internodes are separated from each other by small amyelinated regions called nodes of Ranvier. This specialized organisation of the myelin sheaths promotes saltatory conduction whereby electrical impulses "jump" from node to node as they pass along the axon from the neuronal cell body to the axon terminus. The white matter also contains astrocytes and microglia. Astrocytes are star-shaped glial cells that help maintain homeostasis by regulating local ion concentrations and extracellular fluid volume within the CNS. In the whiter matter, they extend processes to nodes of Ranvier and to blood vessels, where they contribute to blood–brain barrier function. Microglial cells, which are considered the immune cells of the CNS, help "mop up" debris and dying cells. 9

1.5 **Isotropic and anisotropic diffusion in the brain (Source:** [Pandit et al., 2013]**).** Fractional anisotropy image of a preterm born child reveals the nature of water diffusion within different brain tissue compartments (a). In the white matter of the corpus callosum (red), diffusion occurs preferentially along the axonal fibres, resulting in anisotropic diffusion (b). In the ventricular cerebro-spinal fluid (CSF; green), diffusion is unhindered and can be described as isotropic (c). Diffusion tensor ellipsoids representing anisotropic and isotropic diffusion are shown in b and c, respectively. Each tensor is expressed by three eigenvectors with values $\lambda 1$, $\lambda 2$ and $\lambda 3$. In isotropic diffusion $\lambda 1 = \lambda 2 = \lambda 3$, whereas in anisotropic diffusion the long axis of the ellipsoid aligns with the underlying white matter, and $\lambda 1$ is greater than $\lambda 2$ and $\lambda 3$. 11

1.6 **Principles of diffusion tensor imaging (DTI) tractography (Source:** [Catani and Forkel, 2019]**).** (A) Visualization of the diffusion tensor as an ellipsoid. The size and the shape of the tensor are defined by the three eigenvalues (1, 2, 3 in red), while the spatial orientation is described by the three eigenvectors (v1, v2, v3 in blue). In biological tissues, the tensor can vary between three possible configurations: (1) isotropy or weak anisotropy (equal or similar diffusivity along the three eigenvalues) is commonly observed, for example, inside the ventricles (isotropy) or in the gray matter (weak anisotropy); (2) planar anisotropy (unequal diffusivity between of one eigenvalue and the other two) is common in voxels containing, for example, two groups of crossing or diverging fibers; and (3) axial anisotropy is typical of voxels containing parallel fibers (unequal diffusivity between the axial eigenvalue and the two perpendicular eigenvalues). (B) Exemplified indices extracted from diffusion data, such as mean diffusivity (MD), fractional anisotropy (FA), principle eigenvector, and color-coded FA maps. (C) Streamline tractography is based on the assumption that in each white matter voxel the principal eigenvector (black arrows) is tangent to the main trajectory of the underlying fibers (black lines). Starting from a region of interest (red circle), the tractography algorithm propagates, voxel by voxel, a streamline (red) by piecing together neighboring principal eigenvectors. An example is shown in the neighboring panel where the streamlines are tracked on a principal eigenvector map and the tractography reconstruction of the arcuate fasciculus is visualized as 3D streamtubes. 12

1.7 Figure extracted from [Glover, 2011]. Block design fMRI experiment. A neural response to the state change from A to B in the stimulus is accompanied by a hemodynamic response that is detected by the rapid and continuous acquisition of MR images sensitised to BOLD signal changes. Using single- or multi-variate time series analysis methods, the average signal difference between the two states is computed for the scan and a contrast map generated. A statistical activation map is finally obtained using a suitable threshold for the difference; the map depicts the probability that a voxel is activated given the uncertainty due to noise and the small BOLD signal differences. 14

1.8 **Figure extracted from [Lee et al., 2013]. Surface plots of resting-state networks.** A: Default mode network, B: Somatomotor network, C: Visual network, D: Language network, E: Dorsal attention network, F: ventral attention network, G: Fronto-parietal control network. 15

1.9 **Principles of GWA illustrated with an example of a continuous endophenotype: a functional measure of the brain.** On the top figure, the y-axis is the endophenotype measure, and the x-axis represents the targeted genetic variant. This variant has two possible alleles: C and T. Each individual in the cohort will have a combination of CC, CT, TT alleles coded as 0, 1 or 2. The lower figure represent a Manhattan plot and is a figure-of-merit of GWASes. The y-axis is the -log10 of the p-value of the association, and the x-axis represents the SNP location along the genome. The most significant associations will have the smallest p-values and the -log10 of these p-values will have the highest height in the graph. The red dashed line corresponds to the $5e-8$ genomic threshold. The points above correspond to the genetic variants significantly associated with the studied phenotype. 20

1.10 **Neuroanatomy of language (Source: [Friederici, 2017]).** Anatomical and cytoarchitectonic details of the left hemisphere (LH). Top: The different lobes (frontal, temporal, parietal, occipital) are marked by colored borders. Major language-relevant gyri (inferior frontal gyrus (IFG), superior temporal gyrus (STG), middle temporal gyrus (MTG)) are color-coded, superior temporal sulcus (STS) located between STG and MTG is marked by an asterisk. Numbers indicate language-relevant Brodmann areas (BA) that Brodmann (1909) defined on the basis of cytoarchitectonic characteristics. The coordinate labels (see bottom left) superior (dorsal)/inferior (ventral) indicate the position of the gyrus within a lobe (e.g., superior temporal gyrus) or within a BA (e.g., superior BA 44). The horizontal coordinate labels anterior (rostral)/posterior (caudal) indicate the position within a gyrus (e.g., anterior superior temporal gyrus). Broca's area consists of the pars opercularis (BA 44) and the pars triangularis (BA 45). Located anterior to Broca's area is the pars orbitalis (BA 47). The frontal operculum (FOP) is located ventrally and medially to BA 44, BA 45. The premotor cortex (PMC) is located in BA 6. Wernicke's area is defined as BA 42 and BA 22. The primary auditory cortex (PAC) and Heschl's gyrus (HG) are located in a lateral to medial orientation in the temporal lobe. White matter fiber tracts, i.e., the dorsal and ventral pathways connecting the language-relevant brain regions are indicated by color-coded arrows (see bottom right). Reprinted from Friederici [2011]. The brain basis of language processing: From structure to function. Physiological Reviews, 91 (4): 1357–1392 . 23

1.11 **Overview of the meta-analysis (Source:** [Vigneau et al., 2006, 2011]**).** Each foci is color-coded according to its language components category: phonology (blue), semantic (red), and syntax (green). A) Distribution of the peaks in each hemisphere for each component. The 128 neuroimaging studies selected for our previous meta-analysis reported 728 activation peaks in the left hemisphere (left column). Among the 128, 59 studies reported 218 activation peaks in the right hemisphere (right column). Activation peaks detected during phonological tasks are indicated in blue (top row), lexico-semantic tasks in red (middle row) and sentence and text processing in green (bottom row). For this last component, peaks corresponding to contrast investigating comprehension are in green and those investigating syntax are in white. Peaks are projected onto a lateral view of the MNI single subject. B)Top: sagittal projection map of the 730 activation peaks. Bottom: clusters identified for phonological (blue), semantic (red), and syntactic (green) processing and obtained from the spatial clustering of the peaks. Clusters of different components that were not spatially distinct are circled (yellow). Error bars correspond to twice the standard error on the y and z stereotactic coordinates. The left hemisphere lateral surface rendering of the MNI single-subject brain template, together with the corresponding stereotactic grid, is displayed for anatomical reference. RolS, Rolandic sulcus; RolOp, Rolandic operculum; F3t, pars triangularis of the left inferior frontal gyrus; F3op, pars opercularis of the left inferior frontal gyrus; F3orb, pars orbitaris of the left inferior frontal gyrus; SMG, supramarginalis gyrus; PT, planum temporale; T1, superior temporal gyrus; T2, middle temporal gyrus; T3, inferior temporal gyrus; Prec, precentral gyrus; F2, middle frontal gyrus; PrF3op, precentral gyrus/F3op junction; STS, superior temporal sulcus; AG, angular gyrus; Fusa: anterior fusiform gyrus; a, anterior; p, posterior; l, lateral; m, middle; d, dorsal; v, ventral. 25

1.12 **Tractography-based reconstruction of the language networks from classical models to contemporary neurolinguistics (Source:** [Catani and Forkel, 2019]**).** (A) Classical language model with the arcuate fasciculus connecting Broca's region in the inferior frontal gyrus to Wernicke's region in the superior temporal gyrus. (B) Extension of the classical arcuate fasciculus sense strictu to include the anterior segment, connecting inferior frontal to inferior parietal lobe, and the posterior segment linking the inferior parietal to the temporal lobes. (C) Current model of an extended language network beyond the three segments of the arcuate fasciculus. The frontal aslant tract (FAT) connects the inferior frontal gyrus to the pre-supplementary motor cortex. The ventral network includes the uncinate fasciculus between the anterior temporal lobe and the orbital frontal and inferior frontal cortex, the temporal longitudinal fasciculus (TLF) between the posterior temporal lobe and the temporal pole, the inferior fronto-occipital fasciculus (IFOF) connecting the ventral frontal cortex to the occipital cortex, and the inferior longitudinal fasciculus (ILF) between the occipital and anterior temporal cortex. . 27

1.13 **Parent-offspring correlations for factor scores for specific cognitive abilities for adoptive, biological, and control parents and their children at 3, 4, 7, 9, 10, 12, 14, and 16 years (source: [Stromswold, 2001]).** Correlations are shown for verbal ability (a), spatial ability (b), speed of processing(c), and recognition memory (d). Parent-offspring correlations are weighted averages for mothers and fathers. The number of individuals range from 33 to 44 for biological fathers, 159 to 180 for biological mothers, 153 to 197 for adoptive parents, and 136 to 217 for control parents. 31

2.1 **Overview of the regions obtained from [Pallier et al., 2011].** Each language seed is color-coded according to its language category: phonology (blue), semantic (red), and syntax (green). ROIs of different components that were not spatially distinct are color-coded as pink (semantic/syntax), cyan (phonology/semantic) and white for the three language component. Different gyri and sulcus, known to be relevant for language: the inferior frontal gyrus (IFG), middle temporal gyrus (MTG), superior temporal gyrus (STG), and superior temporal sulcus (STS), are color-coded. Numbers in the left hemisphere (LH) represents language-relevant Brodmann areas (BA) which were defined on the basis of cytoarchitectonic characteristics. The pars opercularis (BA 44), the pars triangularis (BA 45) represents Broca's area. The pars orbitalis (BA 47) is located anterior to Broca's area. BA 42 and BA 22 represents Wernicke's area Friederici [2011]. Both supramarginal gyrus (BA40) and angular gyrus (BA39), also known as Geschwind's territory, are represented by green and yellow colors respectively. The primary motor cortex (BA4), the premotor cortex and the supplementary motor area (B6) are colored in orange. Within the left hemisphere, dorsal and ventral long-range fiber bundles connect language areas and are indicated by color-coded arrows. 49

2.2 **Overview of the regions obtained from the meta-analysis.** Each language seed is colour-coded according to its language category: phonology (blue), semantic (red), and syntax (green). ROIs of different components that were not spatially distinct are colour-coded as pink (semantic/syntax), cyan (phonology/semantic) and white for the three language component. For the sake of ROIs figure visibility, the coordinates were modified. The exact coordinates for each ROI are available in Table 2.2. Different gyri and sulcus, known to be relevant for language: the inferior frontal gyrus (IFG), middle temporal gyrus (MTG), superior temporal gyrus (STG), and superior temporal sulcus (STS), are color-coded. Numbers in the left hemisphere (LH) represents language-relevant Brodmann areas (BA) which were defined on the basis of cytoarchitectonic characteristics. Numbers in the right hemisphere (RH) represents the language-relevant BA counterpart. The pars opercularis (BA 44), the pars triangularis (BA 45) represents Broca's area. The pars orbitalis (BA 47) is located anterior to Broca's area. BA 42 and BA 22 represents Wernicke's area [Friederici, 2011]. Both supramarginal gyrus (BA40) and angular gyrus (BA39), also known as Geschwind's territory, are represented by green and yellow colours respectively. The primary motor cortex (BA4), the premotor cortex and the supplementary motor area (B6) are coloured in orange. Within the left hemisphere, dorsal and ventral long-range fibre bundles connect language areas and are indicated by colour-coded arrows. 50

2.3 **Spherical deconvolution tractography of frontal white matter connections. (Source:** [Rojkova et al., 2016]) For each tract a single participant map is supplied as a representative example of the individual anatomy. First (SLF I, light blue, no. 1), second (SLF II, dark blue, no. 2) and third (SLF III, pink, no. 3) branches of the superior longitudinal fasciculus; cingulum (yellow, no. 4); uncinate (pink, no. 5); long (LS, red, no. 6) and anterior (AS, green, no. 7) segments of the arcuate fasciculus; inferior fronto-occipital fasciculus (IFOF, no. 8); frontal corpus callosum (CC, no. 9); corticospinal tract (CST, no. 10); fronto-thalamic projections or anterior thalamic radiations (blue, no. 11); fronto-striatal projections (yellow, no. 12); fronto-pontine projections (no. 13); paracentral U tract (pink, no. 14); hand superior (green, no. 15), middle (yellow, no. 16) and inferior (red, no. 17) U tract; face U tract (blue, no. 18); frontal aslant tract (pink, no. 19); fronto-insular tract 1 (FIT 1, light blue, no. 20), 2 (FIT 2, dark blue, no. 21), 3 (FIT 3, red, no. 22), 4 (FIT 4, yellow, no. 23) and 5 (FIT 5, green, no. 24); frontal superior longitudinal (FSL, light blue, no. 25); frontal inferior longitudinal (FIL, pink, no. 26), frontal orbito-polar tract (FOP, yellow, no. 27) and fronto-marginal tract (FMT, red, no. 28). The overall visualization and screenshots were performed in Anatomist (http://brainvisa.info). 54

3.1 Distribution of the NIH measures collected by HCP team independently from the language fMRI task 65

3.2 Distribution of behavioral scores collected by HCP team during the language fMRI task, composed of MATH and STORY tasks 66

3.3 **First level model.** A) Design matrix used in the first level model. Predictors includes fMRI events and derivatives, twelve movement regressors and four drift features. B) Coefficients of the contrast, indexed by the names of the columns of the design matrix. 68

3.4 **Group analysis language task activation maps.** Group average activations for the HCP language task: story versus baseline is shown with a lower threshold of $z = \pm 10$. 68

3.5 **Functional connectome extraction pipeline** with two main steps: 1) Map of brain regions already defined on resting-state fMRI images. 2) Extraction of mean BOLD signal for each ROIs and quantifying functional interactions from these time series signal extracted. At the end of the second step, we obtain a functional connectome for each participants where each cell represents a resting-state functional connectivity. 70

3.6 **Functional connectome visualisation** Mean functional connectivity of the 300 and 15 endophenotypes, calculated using a shrinked estimate of partial correlation Marrelec et al. [2006] (estimated with a Ledoit-Wolf estimator Ledoit and Wolf [2004]) over 32,186 and 778 individuals using both UKB and HCP rsfMRI participants respectively. (a) Circos plot represents the mean FC estimated using SmPSS ROIs on UK Biobank. (b) Circos plot represents the mean FC estimated using SmPSS ROIs on HCP. (c) Circos plot represents the mean FC estimated using OcSS ROIs on UK Biobank. 70

3.7 **Anatomical connectome extraction pipeline** with one main steps consisting on mapping brain tracts of interest already defined on skeletonised images and extracting mean value for each tract of interest. At the end, we obtain an anatomical connectome for each participants where each cell represents an anatomical connectivity. 72

4.1 **Pedigree-based heritabilities of brain functional connectivities extracted using SmPSS ROIs.** Circle plot where all 25 regions are represented (19 ROIs on the left represent the left hemisphere and 6 ROIs on the right represent the right hemisphere) illustrating the FCs with significant pedigree-based heritability after false discovery rate correction at $p < 0.05$. Each link between two regions represents an endophenotype. The intensity of the color between two regions represents the pedigree-based heritability of an endophenotype as defined by the color bar. Please refer to Table B.1 for all pedigree-based heritability values. 77

4.2 **SNP-based heritabilities of brain functional connectivities extracted using OcSS ROIs.** Circle plot where all 6 regions are represented (6 ROIs on the left represent the left hemisphere. No region in the right hemisphere are included in OcSS ROIs.) illustrating the FCs with significant SNP-based heritability after false discovery rate correction at $p < 0.05$. Each link between two regions represents an endophenotype. The intensity of the color between two regions represents the SNP-based heritability of an endophenotype as defined by the color bar. Please refer to Table B.2 for all SNP-based heritability values. 78

4.3 **SNP-based heritabilities of brain functional connectivities extracted using SmPSS ROIs.** Circle plot where all 25 regions are represented (19 ROIs on the left represent the left hemisphere and 6 ROIs on the right represent the right hemisphere) illustrating the FCs with significant SNP-based heritability after false discovery rate correction at $p < 0.05$. Each link between two regions represents an endophenotype. The intensity of the color between two regions represents the SNP-based heritability of an endophenotype as defined by the color bar. Please refer to Table B.3 for all SNP-based heritability values. 79

4.4 **Comparison of heritabilities estimated according to different design parameters.** The endophenotypes extracted using SmPSS ROIs. Boxplots 1 and 2 display the heritability distributions estimated on UKB (using GCTA) and HCP (using SOLAR) respectively. Boxplot 3 : HCP-FCs using GCTA. Boxplot 4 : HCP-FCs using GCTA and considering the household effect. Boxplots 5 to 7 : HCP (using SOLAR) on rsfMRI sessions with the same duration as in UBK (6 min). 81

4.5 Comparison between heritabilities obtained with SOLAR on HCP (concatenation of the 4 runs) and the ones obtained with : (a) GCTA on HCP, (b) SOLAR on HCP taking into account the shared environment, (c) GCTA on UKB, (d) SOLAR on HCP (6 first minutes of the signal), (e) SOLAR on HCP (6 minutes in the middle of the signal), (f) SOLAR on HCP (6 last minutes of the signal) 82

4.6 Different cut of the resting-state time serie (6 minutes) obtained from HCP cohort. 83

6.1 **Multivariate GWAS analysis of the SmPSS resting state functional connectivity in 32,186 participants.** Manhattan plot for multivariate GWAS across 142 FCs. The red dashed line indicates the genome-wide significance threshold $p = 5e{-}8$. The Quantile-quantile plot is also shown. 93

6.2 Locus Zoom of the significant loci identified by the multiariate GWAS for functional connectivity. 96

6.3 **Genomic loci, eQTL associations and chromatin interactions identified via multivariate GWAS for functional connectivity.** Circos plot representing the genomic risk loci, and the genes associated with the loci by chromatin interactions and eQTLs. From outer layer to inner layer: Manhattan plot. Genomic risk loci are in blue. Genes mapped by chromatin interaction are in orange. Genes mapped by eQTL are in green. Genes mapped by both are in red. Chromatin interaction and eQTLs links follows the same color coding presented above. 97

6.4 Multivariate GWAS analysis of the OcSS resting state functional connectivity in 32,186 participants. Manhattan plot for multivariate GWAS accross 14 FCs. The red dashed line indicates the genome-wide significance threshold $p = 5e{-}8$. The Quantile-quantile plot is also shown. 98

6.5 **Regional effects.** Circle plot where all 25 regions are represented (19 ROIs on the left represent the left hemisphere and 6 ROIs on the right represent the right hemisphere) illustrating the lead SNPs identified from the multivariate GWAS for functional connectivity. Each link between two regions represents an endophenotype. The intensity of the color between two regions represents the Z-values from the univariate GWAS for each FCs as defined by the color bar. The absolute Z-values scaling is clipped at 8 ($p = 1.2e{-}15$). Positif effects of carrying the minor allele are shown in red, and negative in blue. 102

6.6 **Main results for the $15q14$ locus.** A) The two pairs of ROIs that forms the endpoints of the associated FCs reported as black bold lines. B) Effect sizes of the SNP rs1440802 for the two connections: (Prec↔F3opd) FC in green and (PrecR↔RolS) FC in yellow. C) Locus Zoom of the genomic region identified by the mvGWAS. Chromatin state of the genomic region. Brain tissue name abbreviations are the following; E054:Ganglion Eminence derived primary cultured neurospheres, E053: Cortex derived primary cultured neurospheres, E071: Brain Hippocampus Middle, E074: Brain Substantia Nigra, E068: Brain Anterior Caudate, E069: Brain Cingulate Gyrus, E072: Brain Inferior Temporal Lobe, E067:Brain Angular Gyrus, E073: Brain Dorsolateral Prefrontal Cortex, E070: Brain Germinal Matrix, E082: Fetal Brain Female, E081: Fetal Brain Male, E125: NH-A Astrocytes Primary Cells. The state abbreviations are the following; TssA: active transcription start site (TSS), TssFlnk: Flanking Active TSS, TxFlnk: Transcription at gene 5′ and 3′, Tx: Strong transcription, TxWk: Weak transcription, EnhG: Genic enhancers, Enh: Enhancers, ZNF/Rpts: ZNF genes & repeats, Het: Heterochromatin, TssBiv: Bivalent/Poised TSS, BivFlnk: Flanking Bivalent TSS/Enh, EnhBiv: Bivalent Enhancer, ReprPC: Repressed PolyComb, ReprPCWk: Weak Repressed PolyComb, Quies: Quiescent/Low. Expression quantitative trait loci (eQTL) associations (data source: eQTLGen [Võsa et al., 2018], PsychENCODE[Wang et al., 2018], DICE [Schmiedel et al., 2018], BIOS QTL browser [Zhernakova et al., 2017], GTEx/v8 [Consortium et al., 2017], eQTLcatalogue). D) Overlap of the genomic region risk region identified from FUMA for MOSTest results, (Prec↔F3opd) and (PrecR↔RolS). E) Gene expression from BrainSpan for the interesting genes prioritised by FUMA. . 110

6.7 **Main results for the** 3p11.1 **locus.** A) The pairs of ROIs that forms the endpoints of the associated FCs reported as black bold lines. B) Effect sizes of the SNP rs35124509 for the nine connections: (AG↔F3orb), (Pole↔STSp), (Pole↔T2ml), (T1a↔STSp), (STSp↔F3orb), (SMG↔T3p), (AG↔STSp), (F2p↔AG) and (T2ml↔SMG) FCs. C) Locus Zoom of the genomic region identified by the mvGWAS. Chromatin state of the genomic region. Brain tissue name abbreviations are the following; E054:Ganglion Eminence derived primary cultured neurospheres, E053: Cortex derived primary cultured neurospheres, E071: Brain Hippocampus Middle, E074: Brain Substantia Nigra, E068: Brain Anterior Caudate, E069: Brain Cingulate Gyrus, E072: Brain Inferior Temporal Lobe, E067:Brain Angular Gyrus, E073: Brain Dorsolateral Prefrontal Cortex, E070: Brain Germinal Matrix, E082: Fetal Brain Female, E081: Fetal Brain Male, E125: NH-A Astrocytes Primary Cells. The state abbreviations are the following; TssA: active transcription start site (TSS), TssFlnk: Flanking Active TSS, TxFlnk: Transcription at gene 5′ and 3′, Tx: Strong transcription, TxWk: Weak transcription, EnhG: Genic enhancers, Enh: Enhancers, ZNF/Rpts: ZNF genes & repeats, Het: Heterochromatin, TssBiv: Bivalent/Poised TSS, BivFlnk: Flanking Bivalent TSS/Enh, EnhBiv: Bivalent Enhancer, ReprPC: Repressed PolyComb, ReprPCWk: Weak Repressed PolyComb, Quies: Quiescent/Low. Expression quantitative trait loci (eQTL) associations (data source: eQTLGen [Võsa et al., 2018], PsychENCODE[Wang et al., 2018], DICE [Schmiedel et al., 2018], BIOS QTL browser [Zhernakova et al., 2017], GTEx/v8 [Consortium et al., 2017], eQTLcatalogue). D) Overlap of the genomic region risk region identified from FUMA for MOSTest results and the nine FCs mentioned above. E) Gene expression from BrainSpan for the interesting genes prioritised by FUMA. 115

7.1 **Multivariate GWAS analysis of the anatomical connectivity in 31,753 participants.** Manhattan plot for multivariate GWAS accross 313 FCs. The red dashed line indicates the genome-wide significance threshold $p = 5e{-}8$. The Quantile-quantile plot is also shown. 121

7.2 **Genomic loci, eQTL associations and chromatin interactions identified via multivariate GWAS for anatomical connectivity.** Circos plot representing the genomic risk loci, and the genes associated with the loci by chromatin interactions and eQTLs. From outer layer to inner layer: Manhattan plot. Genomic risk loci are in blue. Genes mapped by chromatin interaction are in orange. Genes mapped by eQTL are in green. Genes mapped by both are in red. Chromatin interaction and eQTLs links follows the same color coding presented above. Due to a high number of genes identified using eQTLs mapping (361) and chromatin interaction (874), the chromosome 17 circos plot represent only chromatin interaction.123

7.3 **Genome-wide gene-based association analysis of the anatomical connectivity in 31,753 participants.** genome-wide gene-based association analysis of 313 ACs using mvGWAS results as input. Input SNPs were mapped to 19,157 protein coding genes. The red dashed line indicates the Bonferroni-corrected significance threshold for gene-based analysis $p = 2.61e{-}6(0.05/19,157)$. The Quantile-quantile plot is also shown. 130

7.4 **Human language AC-associated genes integrated into a protein–protein interaction network.** Proteins are represented by nodes. Edges between nodes represent different types of protein–protein interactions according to the STRING [Szklarczyk et al., 2017] database (chapter 2.8), including known interactions (turquoise and dark purple represent interactions identified by curated databases and biological experiments, respectively) and interactions determined by co-expression. Coloured nodes represent the queried proteins. Only at least medium-confidence (> 0.4) links were retained, and disconnected proteins are not shown. 131

7.5 **MAGMA gene-property analysis.** A) Relation between gene-based association with human language AC and relatively higher mRNA expression in the human brain at particular ages, using BrainSpan data from 29 age groups. Asterisks indicate significant age groups meeting $p < 0.05$ with FDR correction. pcw: post-conceptional weeks. B) Relation between gene-based association with human language AC and relatively higher mRNA expression in the human brain at particular ages, using BrainSpan data from 11 developmental stages. Asterisks indicate significant groups meeting $p < 0.05$ with FDR correction. 134

A.1 **Overview of the first five principal components of the principal component analysis of the genotype data.** We can observe that the fifth principal component separate individual from the white ethnicity. 143

List of Tables

1.1 Summary of the linkage regions to reading disability (RD) and Specific language impairment (SLI) and the candidate genes within them (Source: Hagoort [2019]). . 32

1.2 Summary of the top genome-wide association signals from studies of reading and language traits (Source: Hagoort [2019]). 34

1.3 Summary of imaging genetics findings related to reading/language. (Source: Landi and Perdue [2019].) 36

1.4 Summary of the genome-wide association signals from studies of left-right asymmetry (source: Sha et al. [2021]). 38

2.1 Overview of the regions obtained from the meta-analysis. Each ROI is characterised by its abbreviated anatomical label defined by Vigneau et al. [2006, 2011] and is labelled according to the language component it belongs to: phonology, semantic, and syntax. 51

2.2 Centre of mass of the language processing regions of interests retained in both left and right hemispheres. Each ROI is characterised by its abbreviated anatomical label defined by [Vigneau et al., 2006, 2011] and its centre of mass MNI stereotactic coordinates (x, y, z, in mm). 52

4.1 **Heritabilities of language related behavioral scores.** Endophenotypes in bold represent language related behavioral scores with significant heritability after false discovery rate correction at $p < 0.05$. 75

4.2 **Heritabilities of language task activation.** Bold endophenotypes represents language task activation with significant heritability after false discovery rate correction at $p<0.05$. 76

5.1 **Shared heritabilities between both resting-state functional connectivity and neural activations.** Bold rows represents pairs of endophenotypes with significant shared heritability after false discovery rate correction at $p < 0.05$. For the sake of readability, only significant results are displayed. Pearson Correlation between pairs of endophenotypes are also shown. The asterisk represent significant endophenotypic correlation after false discovery rate correction at $p < 0.05$. Table C.1 summarises the endophenotypic correlation and their associated p-values. . . . 87

5.2 **Shared heritabilities between both task activations and language-related scores.** Bold rows represents pairs of endophenotypes with significant shared heritability after false discovery rate correction at $p < 0.05$. For the sake of readability, only significant results are displayed. Pearson Correlation between pairs of endophenotypes are also shown. The asterisk represent significant endophenotypic correlation after false discovery rate correction at $p < 0.05$. Table C.3 summarises the endophenotypic correlation and their associated p-values. 89

6.1 **Genomic loci associated with heritable language functional connectivities (SmPSS ROIs) using MOSTest.** Lead SNP: ID of the lead SNPs within each locus. Position: position of the SNP in the hg19 human reference genome. mvgwasP discovery -British-: MOSTest association P value obtained using the discovery sample. mvgwasP replication -non British-: MOSTest association P value obtained using the independent replication sample. Functionnal category: Functional consequence of the SNP on the gene obtained from ANNOVAR. 'Central' phenotypes: the phenotypes that contributed most to the multivariate association considering the genome-wide association threshold ($p = 5e - 8$). 99

6.2 **Genomic loci associated with heritable language functional connectivities (OcSS ROIs) using MOSTest.** Lead SNP: ID of the lead SNPs within each locus. Position: position of the SNP in the hg19 human reference genome. mvgwasP discovery -British-: MOSTest association P value obtained using the discovery sample. mvgwasP replication -non British-: MOSTest association P value obtained using the independent replication sample. Functionnal category: Functional consequence of the SNP on the gene obtained from ANNOVAR. 'Central' phenotypes: the phenotypes that contributed most to the multivariate association considering the genome-wide association threshold ($5e - 8$). 100

6.3 **The SNP-based genetic correlation analysis was estimated using GCTA software, for each pair of central FCs associated to** $15q14$**,** $3p11.1$ **or** $10q23.33$ **genetic loci.** Bold phenotypes represents pair of FCs with significant genetic correlation after false discovery rate correction at $p < 0.05$. 104

6.4 **Univariate associations of 2 lead SNPs with diffusion MRI indices.** Bold phenotypes represents tracts significantly associated with the lead SNP after Bonferroni correction ($p = 6.94e - 4(0.05/(3 * 9 + 5 * 9))$ 106

7.1 **Genomic loci associated with heritable language anatomical connectivities using MOSTest.** Lead SNP: ID of the lead SNPs within each locus. Position: position of the SNP in the hg19 human reference genome. mvgwasP discovery -British-: MOSTest association P value obtained using the discovery sample. mvgwasP replication -non British-: MOSTest association P value obtained using the independent replication sample. Functional category: Functional consequence of the SNP on the gene obtained from ANNOVAR. 'Central' endophenotypes: number of the endophenotypes that contributed most to the multivariate association considering the genome-wide association threshold ($5e-8$). 'Central' endophenotypes can be appreciated in the Table D.1. 125

7.2 **MAGMA gene-set analysis.** Gene-set attaining statistical significance following Bonferroni control for multiple test. 132

B.1 **Heritabilities of brain functional connectivities extracted using SmSSPAs ROIs.** Bold phenotypes represents FCs with significant heritability after false discovery rate correction at $p < 0.05$. 146

B.2 **Heritabilities of brain functional connectivities extracted using OcSS ROIs.** Bold phenotypes represents FCs with significant heritability after false discovery rate correction at p<0.05. 153

B.3 **Heritabilities of brain functional connectivities extracted using SmPSS ROIs.** Bold phenotypes represents FCs with significant heritability after false discovery rate correction at p<0.05. 154

B.4 **Heritabilities of brain anatomical connectivities.** Bold phenotypes represents ACs with significant heritability after false discovery rate correction at p<0.05. . . 161

C.1 **Pearson Correlation between both resting-state functional connectivity and neural activations.** Bold values represents pairs of endophenotypes with significant correlation after false discovery rate correction at $p < 0.05$. 169

C.2 **Pearson Correlation between both resting-state functional connectivity and language-related scores.** No significant correlation was observed after false discovery rate correction at $p < 0.05$. 172

C.3 **Pearson Correlation between both task activations and language-related scores.** Significant correlation was observed after false discovery rate correction at $p < 0.05$. 177

D.1 **Genomic loci associated with heritable language anatomical connectivities using MOSTest.** Lead SNP: ID of the lead SNPs within each locus. Position: position of the SNP in the hg19 human reference genome. mvgwasP discovery -British-: MOSTest association P value obtained using the discovery sample. mvgwasP replication -non British-: MOSTest association P value obtained using the independent replication sample. Functionnal category: Functional consequence of the SNP on the gene obtained from ANNOVAR. 'Central' phenotypes: the phenotypes that contributed most to the multivariate association considering the genome-wide association threshold ($5e-8$). 180

Abbreviations and Acronyms

Glossary of Acronyms and Abbreviations

AAL	Automated Anatomical Labeling
AC	Anatomical connectivity
AF	Arcuate fasciculus
AI	Assymetry index
AICHA	Atlas of Intrinsic Connectivity of Homotopic Areas
AMICO	Accelerated Microstructure Imaging via Convex Optimization
ANNOVAR	ANNOtate VARiation
BA	Brodmann areas
BGEN	Binary GEN
BOLD	Blood-oxygen level dependent
BrainSpan	Developmental stage
CADD	Combined Annotation Dependent Depletion
CAP	Colorado Adoption Project
CG	Candidate-gene
CNS	Central nervous system
CNV	Copy-number variants
CSF	Cerebro-spinal fluid
DEG	Differentially expressed gene
dbGaP	Database of Genotypes and Phenotypes
DLD	Developmental language disorders
dMRI	Diffusion magnetic resonance imaging
DNA	Deoxyribonucleic acid
DTI	Diffusion tensor imaging
DTIFIT	Diffusion Tensor Imaging Fitting
DW-MRI	Diffusion-weighted magnetic resonance imaging
DWI	Diffusion-weighted imaging
DZ	Dizygotic
EEG	Electroencephalography
EPI	Echo planar imaging

eQTL	Expression quantitative trait loci
FA	Fractional anisotropy
FAT	Frontal aslant tract
FC	Functional connectivity
FDR	False Discovery Rate
FIT	Fronto-insular tracts
fMRI	Functional Magnetic Resonance Imaging
FMRIB	Oxford Centre for Functional Magnetic Resonance Imaging of the Brain
FOP	Frontal operculum
FOV	Field-of-view
FSL	FMRIB Software Library
FWHM	Full width at half maximum
GCTA	Genome-wide complex trait analysis
GDC	Gradient distortion correction
GLM	General linear model
GO	Gene Ontology
GREML	Genome-based restricted maximum likelihood
GRM	Genetic relationship matrix
GTEx	Genotype-Tissue Expression
GWAS	Genome-wide association studies
h^2	Heritability
HCP	Human Connectome Project
HG	Heschl's gyrus
HRF	Hemodynamic response function
ICA	Independent Component Analysis
ICVF	Intra-cellular volume fraction - an index of white matter neurite density
IDP	Image derived phenotypes
IFG	Inferior frontal gyrus
IFOF	Inferior fronto-occipital fasciculus
ILF	Inferior longitudinal fasciculus
INT	Inverse normal transformation
iSECA	Independent SNP Effect Concordance Analysis
ISOVF	Isotropic or free water volume fraction
LD	Linkage disequilibrium
LDSC	Linkage disequilibrium score regression
LH	Left hemisphere
MAF	Minor allele frequency
MD	Mean diffusivity
MEG	Magnetoencephalography
MEGA	Multi-Ethnic Genotyping Array
MLM	Mixed effect linear model
MNI	Montreal Neurological Institute-Hospital

MO	Tensor mode
MOSTest	Multivariate Omnibus Statistical Test
MREC	Multi-Centre Research Ethics Committee
MRI	Magnetic Resonance Imaging
MTG	Middle temporal gyrus
mvGWAS	Multivariate genome-wide association study
MZ	Monozygotic
MetaPhat	Meta-Phenotype Association Tracer
MsigDB	Molecular Signatures Database
NIH	National Institute of Health
NODDI	Neurite Orientation Dispersion and Density Imaging
OD	Orientation dispersion index
OcSS	One-contrast sentences structure
PAC	Primary auditory cortex
PET	Positron emission tomography
PMAT	Penn Matrix Test
PMC	Premotor cortex
PNS	Peripheral nervous system
PPI	Protein-protein interaction
Polyphen	Polymorphism phenotyping
RD	Reading disability
REML	Restricted maximum likelihood
RL	Right hemisphere
RNA	RiboNucleic Acids
ROI	Region of interest
RdN	Reading network
rsfMRI	Resting-state functional magnetic resonance imaging
SE	Standard error
SENSAAS	SENtence Supramodal Areas AtlaS
SLF	Superior longitudinal fasciculus
SLI	Specific language impairment
SNP	Single Nucleotide Polymorphisms
SOLAR	Sequential Oligogenic Linkage Analysis Routines
SPECT	Single photon emission computed tomography
STG	Superior temporal gyrus
STS	Superior temporal sulcus
SmPSS	Supramodal phonology semantics and sentence processing
TBSS	Tract-Based Spatial Statistics
TE	Echo time
tfMRI	Task-based functional magnetic resonance imaging
TLF	Temporal longitudinal fasciculus
TR	Repetition time

UKB	UK Biobank
VBM	Voxel-based morphometry
WM	White matter
WMCA	Word-list Multimodal Cortical Atlas

Chapter 1

State of the art

Chapter Outline

1.1 Genetic basis . . . 6
1.1.1 The genome and inter-individual variability . . . 7
1.1.2 From genotypes to phenotype . . . 8
1.2 Neuroanatomy basics . . . 9
1.2.1 Grey and white matter . . . 10
1.2.2 Gyri and Sulci . . . 11
1.2.3 Cells of the brain: From molecule to neurons and from neurons to brain . . . 11
1.3 How to determine the brain architecture? A neuroimaging approach . . . 13
1.3.1 Structural Neuroimaging . . . 14
1.3.2 Functional Neuroimaging . . . 17
1.4 A basic introduction to quantitative and molecular genetics methodology . . . 21
1.4.1 Heritability . . . 21
1.4.2 Endophenotypes . . . 22
1.4.3 Pleiotropy . . . 22
1.4.4 Candidate genes . . . 22
1.4.5 Genome-wide association study . . . 23
1.5 What are the bases of human language? A review of language approaches in human neurosciences . . . 25
1.5.1 Understanding language from aphasia . . . 25
1.5.2 Understanding language by brain imaging . . . 26
1.6 Complex and multifactorial aetiology: the pursuit of brain–language-genetics relationships . . . 33
1.6.1 Heritability of language . . . 34
1.6.2 Developmental language disorder related loci . . . 36
1.6.3 Genome-wide association studies of language abilities . . . 37
1.6.4 Moving Forward: Emergence of imaging-genetics approach . . . 39
1.7 Aim of this thesis . . . 43

Language is a central component of human life. We live immersed in language as it underlies most human interactions; we use it to structure our thoughts, to communicate and interact with each other. Because it is so ubiquitous, it can seem simple, yet language is insufficiently understood as a phenomenon and process. Across different contexts and forms, researchers emphasize the special character of language compared to other human capacities. Accordingly, many difficult questions surround the topic of language. One of these concerns its origin: nature versus nurture. Language has an inherent dimension of learning, but also a natural instinctive tendency that is proven by the babbling of infants, for instance. Interestingly, this is not observed for other cultural practices and is specific to language. Language therefore exists in a unique space, at a junction between nature and culture, between individual and society.
As language is a phenomenon that is both biological and social, it can be approached with a wide variety of methods that includes methods and explanatory models of the formal and natural sciences, as well as the tools offered by the human and social sciences. The first approach focuses on the cognitive bases of language and the different aspects of the biological endowment that allow human species to learn and use languages. It weaves privileged relationships with cognitive neuroscience, human biology and also formal sciences which provides precise instruments for its modeling. The second approach on the other hand, will focus on the relationship between language and society, history, philologies, and literatures. The very nature of language, its complexity, its hybrid status justifies a plurality of approaches and methods [Luigi, 2021]. The present thesis is part of the first aforementioned approach and its main goal is to modestly contribute to the neurobiology of language question.
Interest in mapping genes for language skills has largely been driven by the need to understand the biological causes of language disability. Indeed, until recently, the biological foundations for language were mainly sought in lesion studies, where patients showed specific language impairments such as developmental language disorders and dyslexia. Imaging-genetics is an emerging scientific field that benefits from the maturity of non-invasive imaging techniques such as magnetic resonance imaging and high-throughput genotyping by DNA chips or sequencing. These techniques allow the systematic acquisition of anatomical and functional characteristics of an individual's brain along with its genotype. The ability to acquire these data in general population allows studies to be conducted on open questions of clinical or basic neuroscience. Data science tools - from big data hardware to analysis algorithms - open up the possibility of studying how genetics and environment modulate human brain function or anatomy and behaviour. With the recent availability of large-scale cohorts, it has made it possible to study language in the general population. The specific objective of this thesis is to highlight genes that underlie human language, contributing thus to our understanding of different processes required for language.

1.1 Genetic basis

In this section, we will present basic principles of genetics useful for understanding imaging-genetic studies. It has no intention to cover the genetic complexity but intend to provide brief definition of genetic terms necessary for the comprehension of the present work.

1.1.1 The genome and inter-individual variability

Genetic information is encoded in a macro-molecule called deoxyribonucleic acid (DNA). It is present in almost all living organisms, present in every cell (except for enucleated cells)) and identical throughout the body (except for gametes). A nucleotide is the basic building block of nucleic acids. DNA consists in two complementary strands of nucleotides. Its double helix structure was discovered in 1953 by Watson and Crick [Pray, 2008]. In human DNA, each strand comprises approximately 3,200,000,000 nucleotides. It is made up of four elementary bases called nucleosides: Adenine (A), Thymine (T), Guanine (G) and Cytosine (C) associated with a sugar (deoxyribose) and a triphosphate, the whole forming nucleotides. These bases work in pairs, one purine (Adenine or Guanine) paired with one pyrimidine (Thymine and Cytosine respectively) which allows physical stability of the molecule formed. The DNA macro-molecule is divided in humans into 22 pairs of autosomes (non-sexual chromosomes) and 1 pair of sexual chromosomes (XX or XY) (Fig. 1.1).

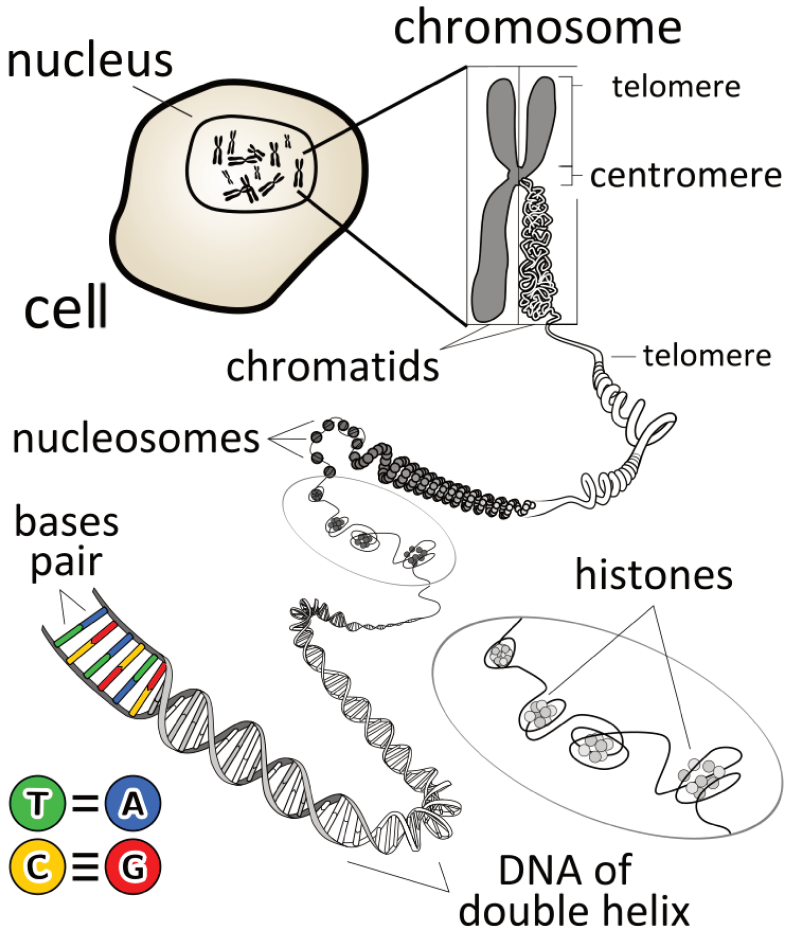

Figure 1.1 – **Description of the chromosome structure. (Source: https://www.genome.gov/).**

Along the DNA molecules, the genome has functional units called genes. These genes are DNA sequences made of exons and introns, transcribed into RiboNucleic Acids (RNA). Subsequently, only exons are translated into proteins. The human genome is estimated to contain approxim-

ately 23,000 genes. And these genes are separated by intergenic regions or non-coding DNA containing expression regulatory sequences such as promoters and enhancers and thus are involved in regulation of nearby genes expression. Nonetheless, the function of the major part of this non-coding DNA is still unknown. The sequence of nucleotide bases is important regarding the integrity of the genome. Its alteration can have consequences on the functional units produced. Genetic variations from a human reference sequence exist for each individual and are called genetic polymorphisms. Multiple mechanisms of polymorphisms are known. Relevant to our work, Single Nucleotide Polymorphisms (SNPs) are the smallest form of polymorphism and affects only one base pair. Except for rare cases, SNPs are bi-allelic polymorphisms. They represent markers of choice for researchers in order to establish a dense and precise mapping of the genome variations such as dbSNP [Sherry et al., 2001], HapMap [Gibbs et al., 2003], the 1000 genomes project [Consortium et al., 2015] . A SNP is categorised as common or rare variant and is characterised by its chromosomal position, its alleles and its minor allele frequency (See below for a definition).

More definitions to understand imaging-genetics

- Imputation is the process consisting in statistical inference of unobserved genotypes.
- Linkage disequilibrium (LD) is the non-random association of alleles from two or more polymorphic loci.
- Linkage analysis is a genetic approach aiming at establishing linkage between genetic markers and traits or diseases by examining patterns of inheritance among individuals within a family who exhibit the trait of interest and testing whether they co-segregate with the trait of interest, in a manner that is unlikely to have occurred by chance.
- Population stratification or genetic structure represents the presence of differences in allele frequencies between sub-populations in the studied population, due to their different genetic ancestries and can cause false positives in association studies.
- Hardy-Weinberg equilibrium models the behaviour of allelic and genotypic frequencies for a polymorphism. It states, under certain assumptions, that the allelic and genotypic frequencies of a polymorphism are stable within the population over generations.
- Minor allele frequency (MAF) is the frequency of the less frequent allele of a bi-allelic SNP, and it can vary depending on the considered population.
- epistasis is the phenomenon that describes an interaction between genes and/or genetic variations.
- pleiotropy is defined as the fact that one gene can have several different effects or functions, non necessarily independent from one another.

1.1.2 From genotypes to phenotype

Understanding the path from genotype to observable characteristics –phenotypes– is a major concern of molecular biology. A phenotype is almost always a multifactorial trait and results from the contribution of many proteins. The proteins are biological macro-molecules, made of a chain of amino acids and present in all living cells. A gene code for one protein, according to the genetic code: each amino acid in a protein is encoded by one or several triplets of nucleotides or codons. The process by which a gene is expressed into a protein is made of several steps: from each gene many messenger RNAs (ribonucleic acids) are produced (transcription), and are then edited (alternative splicing), translated into amino acid macro-molecules (translation) and finally matured in proteins (maturation). Interactions between proteins are important as they play a crucial role in cellular functions and biological processes, and produce phenotypes. Phenotype variability depends on the nature and/or the (relative) quantity of the potentially 23,000 concerned proteins.

Research on gene-phenotype association test for a non-random correlations between a phenotypic trait (qualitative or quantitative) and specific allelic variants. It can be carried out for just a single genetic marker (SNP), multiple sites within a gene, or across the entire genome. The research about mechanism underlying gene to phenotype manifestation is, on the other hand, beyond the scope of this study.

1.2 Neuroanatomy basics

The human brain is composed of three main parts: the cerebrum, cerebellum, and brainstem (Fig. 1.2a). The cerebrum is the largest part of the human brain and is made of two cerebral hemispheres separated by a deep *longitudinal fissure*, but remain connected via the corpus callosum. It has a folded appearance and is involved in higher functioning. It controls somatosensory, motor, language, cognitive thought, memory, emotions, hearing, and vision. Each hemisphere has a number of folds called **gyri** separated by grooves called **sulci**. They are divided into four main lobes separated by the *central sulcus*, *parieto-occipital sulcus*, and *lateral fissure (Sylvian fissure)*. The frontal lobe is situated anterior to the central sulcus while the parietal lobe is posterior to the central sulcus. The temporal lobe is separated from the frontal and parietal lobes by the lateral sulcus. Finally, the occipital lobe, located at the rear of the cerebrum, is separated from the parietal lobe by the parieto-occipital sulcus. These lobes, named after the bones of the skull that overlie them are distinguished by colors in Fig. 1.2b.

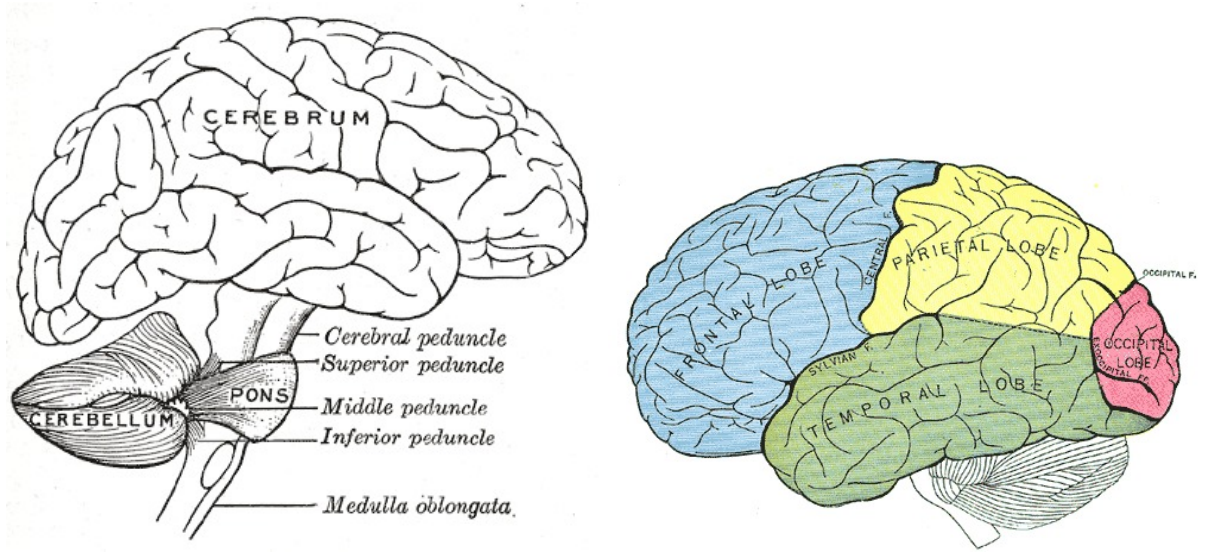

A) B)

Figure 1.2 – **Neuroanatomy of the brain ([Bui and Nguyen, 2019]).** A) Brain, Encephalon, Connections of the several parts of the brain, Cerebrum, Cerebellum, Pons, Cerebral; Superior; Middle; Inferior Peduncle, Medulla oblongata. B) Principal fissures and lobes of the cerebrum viewed laterally, Frontal Lobe, Parietal Lobe, Temporal Lobe, Occipital Lobe.

1.2.1 Grey and white matter

At a macroscopic scale, the human brain appears to be composed of grey matter and white matter (See Fig. 1.3a). The grey matter contains the neuronal cell bodies of the central nervous system and serves to process information. It is located on the surface of the gyri and nuclei (collection of neurons in the central nervous system). A distinction is made between cortical grey matter located in the cerebral cortex and subcortical ones. The latter are a group of diverse neural formations that lie beneath the cerebral cortex which includes the Hippocampus, Amygdala, and the basal ganglia. The white matter contains the fibre tracts of the neuronal axons wrapped in myelin and is found in the inner layer of the cortex. It is essential for impulse conduction as it supports the communication between various grey matter areas. It is composed of three types of fibres: commissural fibres, projection fibres, and association fibres. Commissural fibres connect the left-right cerebral hemispheres and are composed of anterior forceps that connect the lateral and medial surfaces of the two frontal lobes, and posterior forceps that connect the two occipital lobes. Projection fibres consist of efferent and afferent fibres that connect higher and lower brain centres. Association fibres interconnect lobes on the same side. Two subtypes of these association fibres exist: short association fibres – also called 'U'-fibres– lie beneath the grey substance of the cortex and connect adjacent gyri, while long association fibres connect distant areas of the same hemisphere.

1.2.2 Gyri and Sulci

The surface of the cerebrum is folded with a large number of gyri and sulci that give it its wrinkled appearance (Fig. 1.3b). These cortical foldings are variable from one individual to

another. The folding of the cerebral cortex creates gyri and grooves (sulci) that separate brain regions and increase the cortical surface area. This increasing of the surface area of the brain allows more neurons to be packed into the cortex so that it can process more information.

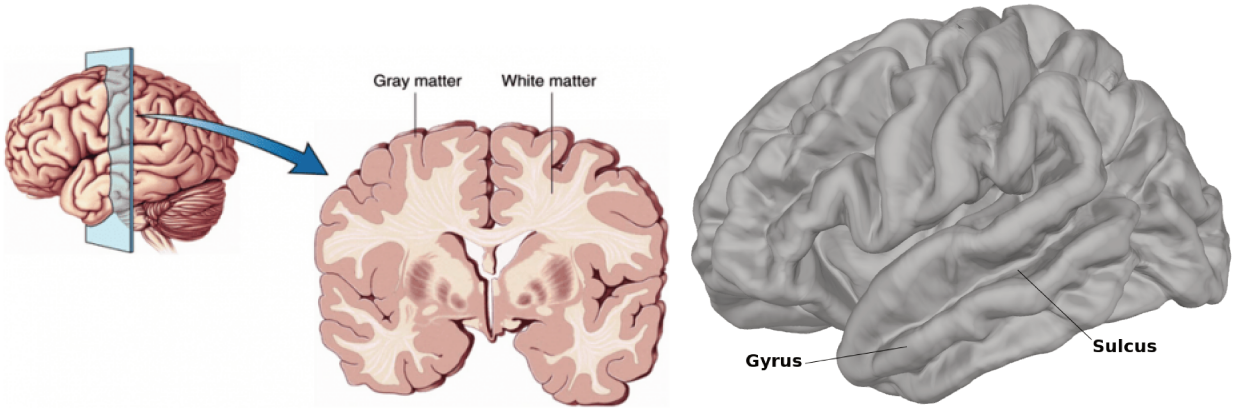

(a) (b)

Figure 1.3 – **Brain basics.** Example of a) the grey and white matter of the central nervous system (source : https://difference.guru/difference-between-white-and-gray-matter/), b) sulcus and gyrus.

1.2.3 Cells of the brain: From molecule to neurons and from neurons to brain

The central nervous system is made up of neurons and glial cells. Neurons are excitable cells, they vary in shape and size and can be classified according to their morphology and function. They have three basic parts: a cell body and two extensions called an axon and a dendrite. A nucleus is within the cell body, which controls the cell's activities and contains the cell's genetic material. Synapse is a structure that permit a transmission of signals (electric or chemical) from one neuron to another. The axon carries the information to another nerve cell (post synaptic neurons), while the dendrite receive information from other nerve cells (presynaptic neurons). Glial cells are nerve cells. Different types of glial cells are present in the central nervous system (CNS) and the peripheral nervous system (PNS). There are four types of glial cells in the CNS including oligodendrocytes, astrocytes, Ependymal and microglia. The microglia is found in all regions of the brain and spinal cord. It is implicated in the immunity process and plays an important role in neuron pruning during the neurodevelopment process. The oligodendrocytes and Schwann cells are found in the CNS and PNS respectively. They provide myelination to axons in the central and peripheral nervous system, respectively. The astrocytes are the most abundant type of macroglial cells in the central nervous system. The major nervous cell types are depicted schematically in the Fig. 1.4a.

The network of neurons is organised in a hierarchical way at different scales. Although this network is highly structured, it is important to note that the details of the structure can vary, both between individuals of the same species and over time in a given individual due to synaptic plasticity. Our understanding of the organisation and function of the different levels is strongly influenced by the available experimental techniques that will be described in the next section.

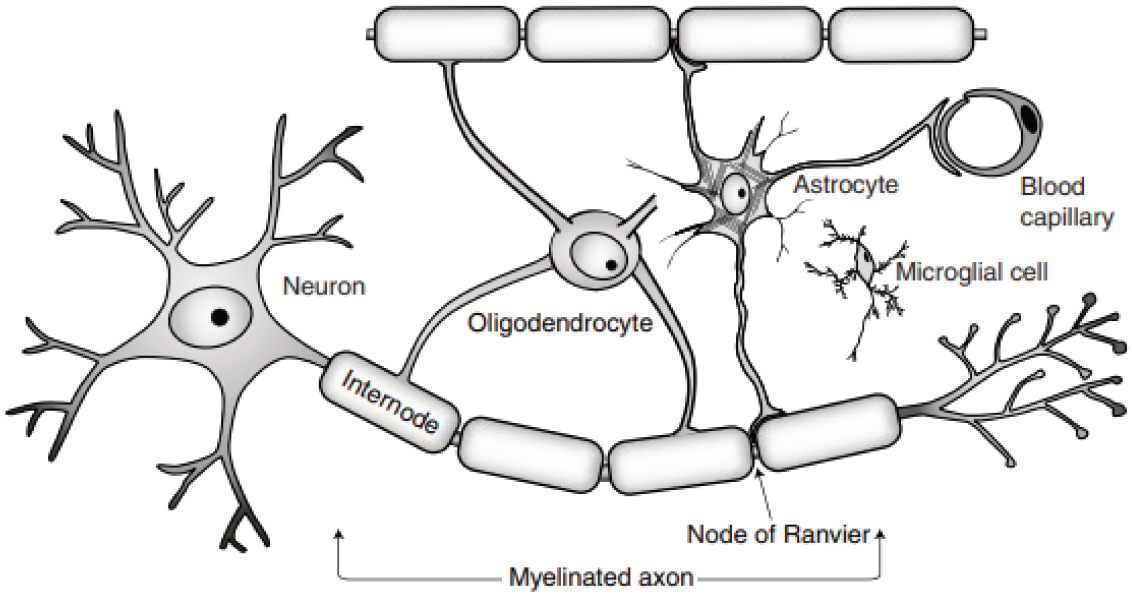

Figure 1.4 – **Schematic representation of the major cellular elements of the white matter (Source:** [Johansen-Berg and Behrens, 2013]**).** In this drawing, a neuronal cell body in the grey matter extends several short dendritic processes and a single, long axonal process. The axon, in the white matter, is surrounded by an insulating myelin sheath. This sheath is produced by oligodendrocytes. Generally, oligodendrocytes extend many processes, each of which wraps around a segment of an axon to form an internode. Internodes are separated from each other by small amyelinated regions called nodes of Ranvier. This specialized organisation of the myelin sheaths promotes saltatory conduction whereby electrical impulses "jump" from node to node as they pass along the axon from the neuronal cell body to the axon terminus. The white matter also contains astrocytes and microglia. Astrocytes are star-shaped glial cells that help maintain homeostasis by regulating local ion concentrations and extracellular fluid volume within the CNS. In the whiter matter, they extend processes to nodes of Ranvier and to blood vessels, where they contribute to blood–brain barrier function. Microglial cells, which are considered the immune cells of the CNS, help "mop up" debris and dying cells.

1.3 How to determine the brain architecture? A neuroimaging approach

The last century has witnessed the development of brain investigation techniques that include the use of various systems such as the positron emission tomography (PET), single photon emission computed tomography (SPECT), magnetic resonance imaging (MRI), functional MRI (fMRI), electroencephalography (EEG), or magnetoencephalography (MEG). These *in-vivo* predominant approaches are usually coupled with behavioural and cognitive ones to study how the brain functions [Friston, 2009]. They make it possible to discover different maps in the brain and can be used to determine the cognitive brain architecture by understanding the brain organisation such as brain connectivity, or spatiotemporal dynamics underlying cognitive functions [Friston, 1994, Liang and Lauterbur, 2000]. Relevant to this study, we will focus in this section on the presentation of the structural and functional MRI techniques.

Voxel-wise approach was for a long time the dominant approach to analyse brain images [Friston et al., 1994]. Such an approach requires massive computational and memory resources. In order to make inference with this approach it is usually necessary to correct drastically for a huge number of multiple comparisons which leads to low statistical power. **Image derived phenotypes (IDP)** approach has gained popularity and is increasingly used in the context of population imaging. Indeed, this approach that consists on summarising distinct measures of brain structure and function such as volume of grey matter in distinct brain regions, structural and functional connectivity metrics [Alfaro-Almagro et al., 2018, Elliott et al., 2018, Miller et al., 2016], can easily be shared by the neuroscience research community and alleviates the limitations of the voxel-wise approach: it mitigates the loss of statistical power compared to voxel-wise approach. For example assessing the functional connectome between region of interests significantly reduces the number of variables making it computationally and statistically more within our reach; For predictive modelling, it certainly has statistical benefits. The high dimensionality of the signal is a challenge in machine learning and IDPs approach is one way to circumvent it.

1.3.1 Structural Neuroimaging

Structural magnetic resonance imaging. Structural magnetic resonance imaging provides anatomical images with high contrast between grey and white matter.

Morphometric analysis of the structural neuroimaging is widely used for the study of the cortex; the fine layer of gray matter. Multiple IDPs might be derived using different softwares like Freesurfer (gray matter volume, surface local gyrification index) [Fischl and Dale, 2000] (https://surfer.nmr.mgh.harvard.edu/), Morphologist (sulcal size, pits, depth or number of *plis de passage*) (https://brainvisa.info/web/morphologist.html)to neuropathologies or behaviour [Lerch et al., 2017]. These features are obtained at the voxel-level and can be analyzed using either a voxel-wise [Ashburner and Friston, 2000] or pre-defined region of interest [Desikan et al., 2006] approaches. Multiple applications are possible, such as: cognitive ageing [Ritchie et al., 2015], brain evolution across species [Evans et al., 2006], general intelligence [Cox et al., 2019], and brain disease [Thompson et al., 2007].

Diffusion-weighted magnetic resonance imaging. Diffusion-weighted imaging is a noninvasive, *in vivo* MRI technique that quantifies water diffusion in biological tissues. It is used to measures and map the local structures by tracking the movement of the water molecules along the white matter bundles. It is used to identify the different fibber tracts in the human brain.

In general, the diffusion in brain tissue differentiate between tissues based on the diffusion of water molecules within them. The diffusion process is different depending on which type of tissue it is observed. Regarding the grey matter, the diffusion is unrestricted -isotropic diffusion-; the water molecules move in any possible direction. Concerning the white matter, the diffusion is restricted -anisotropic diffusion-; the displacement of water molecules is not random due to the presence of biological structures such as cell membranes, filaments, and nuclei (See Fig. 1.5).

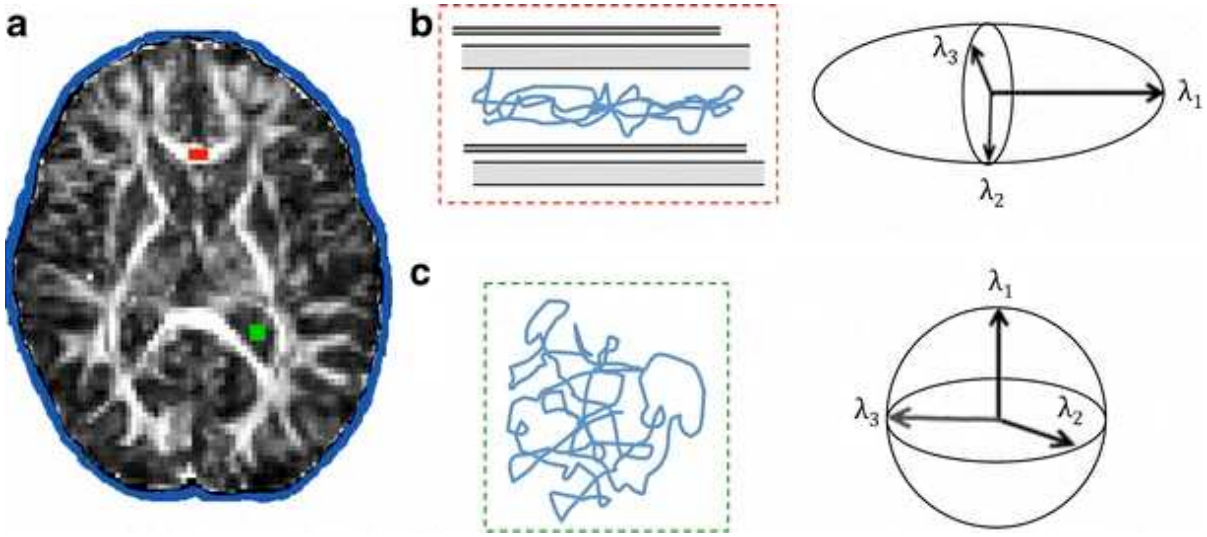

Figure 1.5 – **Isotropic and anisotropic diffusion in the brain (Source: [Pandit et al., 2013]).** Fractional anisotropy image of a preterm born child reveals the nature of water diffusion within different brain tissue compartments (a). In the white matter of the corpus callosum (red), diffusion occurs preferentially along the axonal fibres, resulting in anisotropic diffusion (b). In the ventricular cerebro-spinal fluid (CSF; green), diffusion is unhindered and can be described as isotropic (c). Diffusion tensor ellipsoids representing anisotropic and isotropic diffusion are shown in b and c, respectively. Each tensor is expressed by three eigenvectors with values $\lambda 1$, $\lambda 2$ and $\lambda 3$. In isotropic diffusion $\lambda 1 = \lambda 2 = \lambda 3$, whereas in anisotropic diffusion the long axis of the ellipsoid aligns with the underlying white matter, and $\lambda 1$ is greater than $\lambda 2$ and $\lambda 3$.

Within a single voxel, the shape of the diffusion profile can be described geometrically as an ellipsoid (the tensor) calculated from the diffusion coefficient values (eigenvalues, $\lambda 1 - \lambda 3$) and orientations (eigenvectors, $v1 - v3$) of its three principal axes (Fig. 1.6) [Catani and Forkel, 2019]. The mean diffusivity which represents the average water molecular displacement within a voxel, is obtained by taking the mean of the three eigenvalues ($\lambda 1, \lambda 2, and \lambda 3$). The degree to which diffusion is directionnally constrained can be determined based on the ratio of the eigenvalues to one another (e.g. fractional anisotropy). Overall, these indices provides complementary information about white matter micro-structures [O'Donnell and Westin, 2011, Thomason and Thompson, 2011].

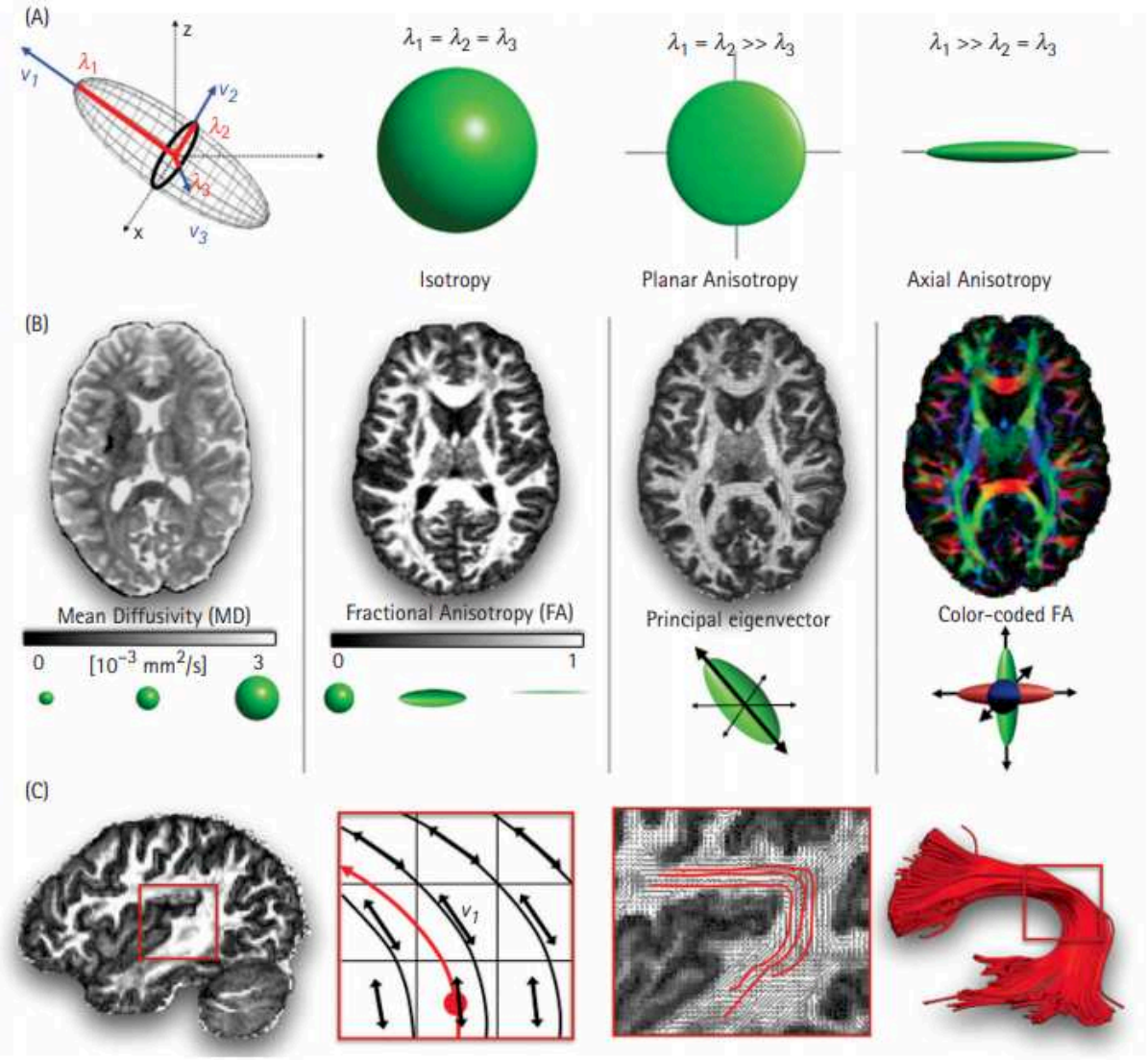

Figure 1.6 – **Principles of diffusion tensor imaging (DTI) tractography (Source: [Catani and Forkel, 2019]).** (A) Visualization of the diffusion tensor as an ellipsoid. The size and the shape of the tensor are defined by the three eigenvalues (1, 2, 3 in red), while the spatial orientation is described by the three eigenvectors (v1, v2, v3 in blue). In biological tissues, the tensor can vary between three possible configurations: (1) isotropy or weak anisotropy (equal or similar diffusivity along the three eigenvalues) is commonly observed, for example, inside the ventricles (isotropy) or in the gray matter (weak anisotropy); (2) planar anisotropy (unequal diffusivity between of one eigenvalue and the other two) is common in voxels containing, for example, two groups of crossing or diverging fibers; and (3) axial anisotropy is typical of voxels containing parallel fibers (unequal diffusivity between the axial eigenvalue and the two perpendicular eigenvalues). (B) Exemplified indices extracted from diffusion data, such as mean diffusivity (MD), fractional anisotropy (FA), principle eigenvector, and color-coded FA maps. (C) Streamline tractography is based on the assumption that in each white matter voxel the principal eigenvector (black arrows) is tangent to the main trajectory of the underlying fibers (black lines). Starting from a region of interest (red circle), the tractography algorithm propagates, voxel by voxel, a streamline (red) by piecing together neighboring principal eigenvectors. An example is shown in the neighboring panel where the streamlines are tracked on a principal eigenvector map and the tractography reconstruction of the arcuate fasciculus is visualized as 3D streamtubes.

1.3.2 Functional Neuroimaging

Functional Magnetic Resonance Imaging (fMRI) is a non-invasive technique that measures brain activity over time by detecting changes in blood-oxygen level dependent (BOLD) signal. The local oxygen level in the brain is coupled to the metabolic needs of neurons while these metabolic changes can be consequent due to task-induced cognitive state changes such as language or visual task. BOLD signal variations can also be observed in the case of free processes in the brain of an individual at rest [Glover, 2011].

Task-oriented functional magnetic resonance imaging. The conventional task-evoked fMRI experiments use different stimuli such as visual or auditory to alternately induce two or more different cognitive states of the brain. For example in a two-condition design, one state is called the experimental condition, while the other is denoted the control condition. The goal is to test the hypothesis that the signals differ between the two states [Glover, 2011]. For example, the individual perform a task 'A' involving processes 'P1', 'P2', 'P3', a task 'B' involving processes 'P1', 'P2'. The subtraction of the brain activation images obtained in tasks 'A' and 'B' makes it possible to isolate the region carrying out the 'P3' process (See Fig.1.7). This typical fMRI experiments allowed great progress in the understanding of the brain organisation. Nevertheless, task-induced fMRI experiments has revealed limits. The association between a high level function and a brain region is much more complex than what the subtractive approach can reveal. A brain region can be characterised by its multi-functional profile. Meta-analysis of a large number of studies on cognitive traits such as language are crucial to determine the degree of involvement of brain regions and give us a more global view. Moreover, the manifestation of a cognitive trait is the result of interaction within a network rather than a single area.

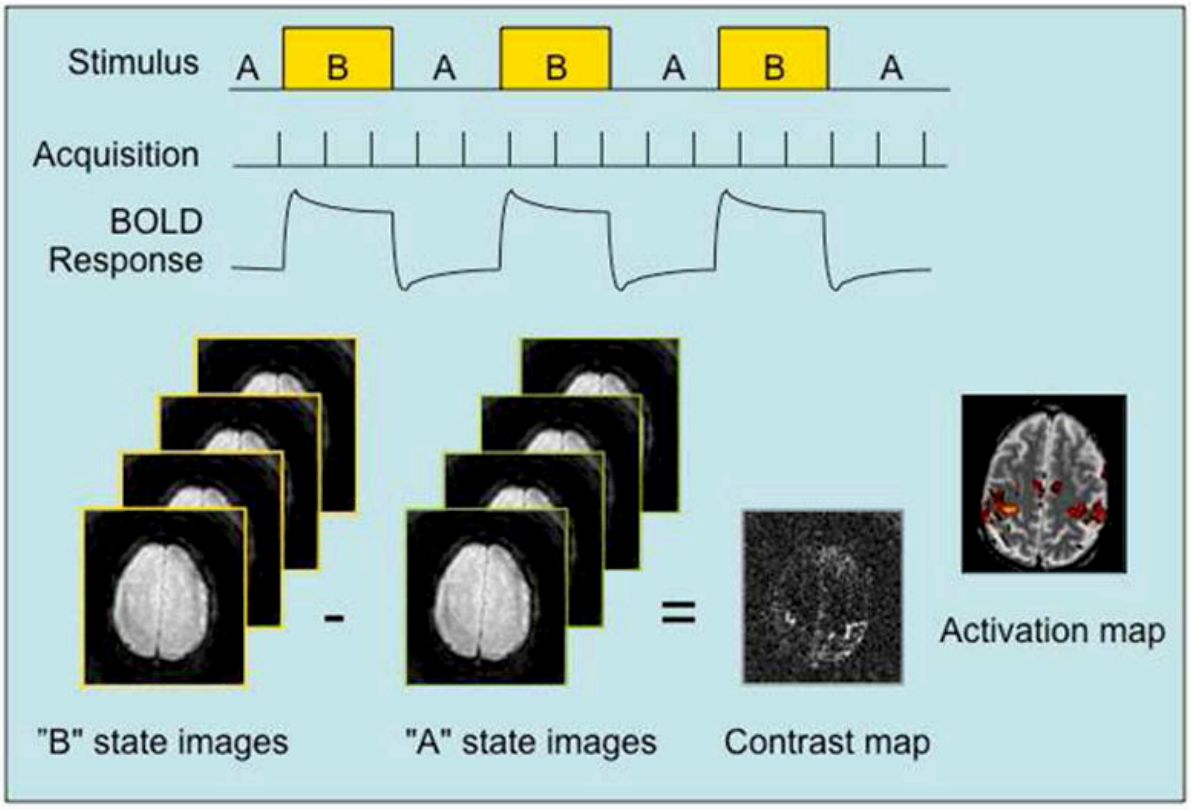

Figure 1.7 – Figure extracted from [Glover, 2011]. Block design fMRI experiment. A neural response to the state change from A to B in the stimulus is accompanied by a hemodynamic response that is detected by the rapid and continuous acquisition of MR images sensitised to BOLD signal changes. Using single- or multi-variate time series analysis methods, the average signal difference between the two states is computed for the scan and a contrast map generated. A statistical activation map is finally obtained using a suitable threshold for the difference; the map depicts the probability that a voxel is activated given the uncertainty due to noise and the small BOLD signal differences.

1.3.2.1 Resting-state functional magnetic resonance imaging

Resting-state functional MR images captures low-frequency fluctuation (< 0.1 Hz) in blood oxygenation and the significance of these fluctuation was initially presented by [Biswal et al., 1995]. It is paradigm free and as such it is easier to implement in very large cohorts like the UK Biobank. Indeed, during the resting-state scan, no explicit task is being performed and depending on the experience protocol, the participants are instructed to keep their eyes fixated on a crosshair, to relax, and to think of nothing in particular [Miller et al., 2016].

Functional images acquired during rest has recently emerged as a powerful tool and is a promising universal marker of brain function [Biswal et al., 2010]. Different network were identified using a paradigm free approach including the well known default mode network (See Fig. 1.8). This resting-state network was initially identified by [Raichle et al., 2001] using PET data and was further identified by fMRI by [Greicius et al., 2003]. In [Raichle et al., 2001] work, the researchers highlighted brain regions that were more active at rest than during task-oriented experience and observed that their activity decrease when cognitive tasks were performed. This

led to the hypothesis that a 'default mode' of the brain remained active in an organised fashion during the resting state.

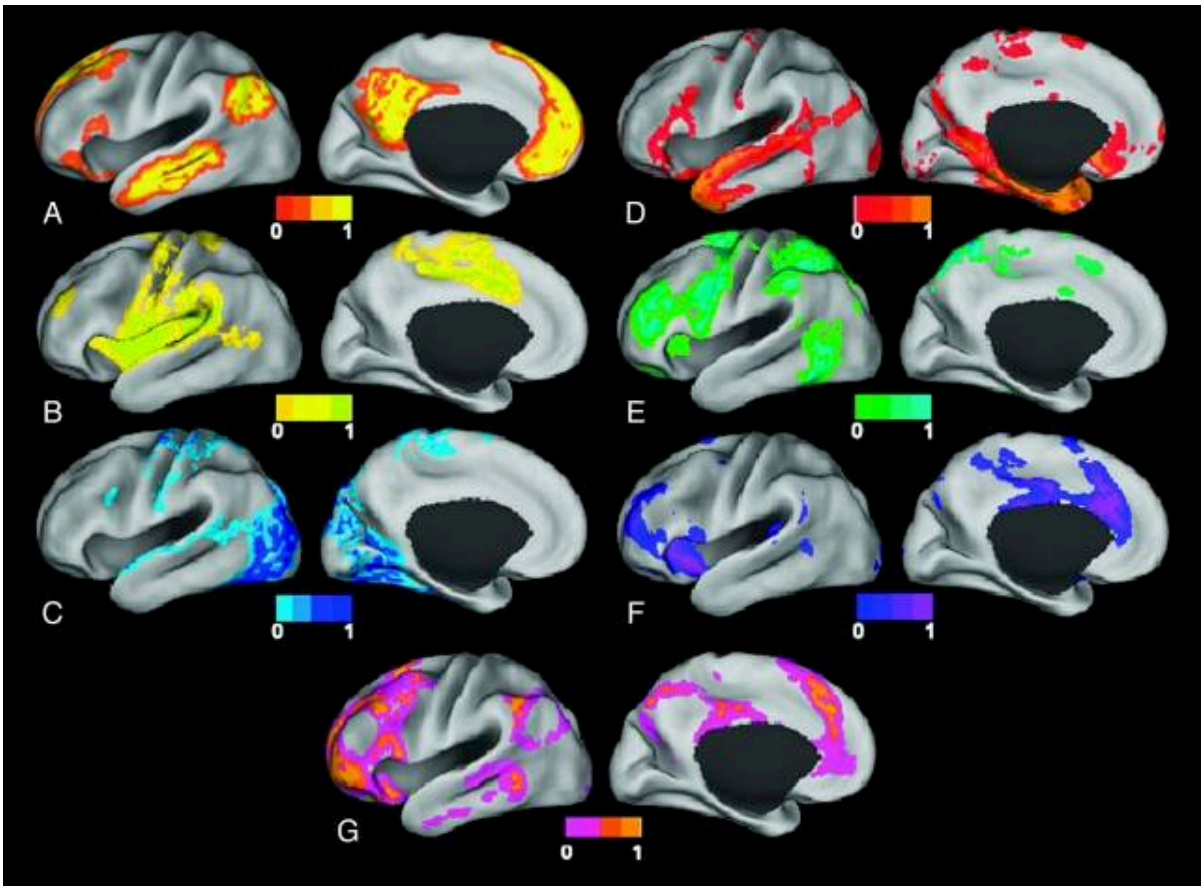

Figure 1.8 – **Figure extracted from [Lee et al., 2013]. Surface plots of resting-state networks.** A: Default mode network, B: Somatomotor network, C: Visual network, D: Language network, E: Dorsal attention network, F: ventral attention network, G: Fronto-parietal control network.

Despite low frequency blood-oxygen-level-dependent (BOLD) signals acquired in resting state condition and that rsfMRI does reflect large-scale circuit organisation [Biswal et al., 1995, Fox and Raichle, 2007], they are less used to study specific brain functions. However, a growing body of evidence suggests that there is a close correspondence between resting state networks and known cognitive task activation maps [Cole et al., 2014, Smith et al., 2009]. For example, [Tavor et al., 2016] showed that a prediction model relating FC estimated from rsfMRI to task-based activations can accurately predict individual differences in brain activity for unseen participants. In the [Smith et al., 2009] work, the authors analysed data from healthy volunteers comprising task maps from BrainMap database of functional imaging studies and resting-state fMRI maps. These maps were then associated with each other using (Pearson) spatial cross-correlation. They found close correspondence between the independent analyses of resting and activation brain dynamics. For example, the resting-state 'default mode network' were found to correspond to negative contrasts in cognitive paradigms. More specifically regarding language, several studies sought the brain dynamics and showed that resting-state FC map could map

language networks previously identified in task-based imaging studies [Hampson et al., 2006, Kelly et al., 2010, Koyama et al., 2010, Xiang et al., 2010]. Especially, [Xiang et al., 2010] used resting-state FC to infer the functional organisation of Broca's area and the perisylvian language networks by investigating their functional correlations and reported a clear topographical FC pattern in the left middle frontal, parietal, and temporal areas. On the other side, several studies have examined the relationship between resting-state FC and behavioural scores. Relevant to our work, these studies have shown that language-related performances like basic reading abilities are correlated to the strength of resting-state FC [Cheema et al., 2021, Cross et al., 2021, Koyama et al., 2011, Stevens et al., 2017]. [Koyama et al., 2011] reported a positive correlation between the reading scores and the resting-state FC between the fusiform gyrus and the inferior frontal gyrus (IFG) -pars opercularis-, belonging to the reading network (RdN). [Cheema et al., 2021] reported a positive correlation between reading fluency and the strength of FC between the left IFG and left supplementary motor area in a group without reading impairment. They also found that the stronger the FC between the supramarginal and the angular gyri, the higher is the word recognition accuracy score. Moreover, [Cross et al., 2021] showed that the FC between the pars triangularis and the right fusiform gyrus was positively correlated with rapid automatized naming performance. Finally, [Stevens et al., 2017] reported a positive correlation between accuracy on word classification and resting-state FC strength of the left occipitotemporal sulcus and Wernicke's area. Although the resting-state FC and behavioural (especially reading abilities) relationship are consistent through studies, the generalization of these findings should be taken with caution. First, the results might be sample dependant and not representative of the larger population of adult reader. Second, the reading tests represents relatively simple reading process and might not be generalized for more complex process (i.e. reading comprehension). Next, recent works suggest that mapping perisylvian language regions can be accomplished using either tbfMRI or rsfMRI [Branco et al., 2016, Jones et al., 2017, Lemée et al., 2019, Lu et al., 2017, Park et al., 2020, Tie et al., 2014]. Indeed, rsfMRI has been applied to mapping eloquent areas in surgical patients [Jones et al., 2017] and stroke patients [Klingbeil et al., 2019], where performing tbfMRI is not an option. Overall, these studies investigated the relevance of the rsfMRI approach in studying specific brain functions such as language, including its relationship with behavioral scores, task-based network at both individual and group levels. They also highlighted its advantages over task-based design, when certain population has difficulties to engage in specific tasks.

State-of-the-art analysis methods.

The preprocessing of resting-state functional MR images generally includes slice-timing correction, realignment, motion correction, high-pass temporal filtering, brain masking, spatial smoothing, co-registration to individual space using T1 template and registration to the MNI space to achieve spatial concordance between subjects.

Once these preprocessing steps are achieved, several methods can be used to analyse resting-state data. Each one has its own inherent advantages and disadvantages. In this section, we will provide a brief overview of some of the statistical and mathematical state-of-art approaches previously applied to rsfMRI data (For further discussion, see [Lee et al., 2013]).

- Data-driven approaches based on k-means or Ward clustering [Thirion et al., 2014], Independent Component Analysis (ICA) approaches [Beckmann and Smith, 2004, Calhoun et al., 2001], or dictionary learning [Mensch et al., 2016].
- Pre-defined reference anatomical atlases such as Automated Anatomical Labeling (AAL) [Tzourio-Mazoyer et al., 2002], or connectivity-based cortical landmarks such as SENtence Supramodal Areas AtlaS (SENSAAS) [Labache et al., 2019], Atlas of Intrinsic Connectivity of Homotopic Areas (AICHA) [Joliot et al., 2015], Word-list Multimodal Cortical Atlas (WMCA) [Hesling et al., 2019].
- Spheres of radius centred at coordinates identified using probabilistic activation maps identified during task-oriented fMRI experiments [Power et al., 2011].

1.4 A basic introduction to quantitative and molecular genetics methodology

In this section, we will briefly introduce basic genetic concepts useful for understanding imaging-genetic studies. Its unique aim is to provide the reader with sufficient knowledge to well understood the different studies presented further and is therefore not intended to be exhaustive.

1.4.1 Heritability

A pivotal question in biology is the heritability of a particular trait. In quantitative genetics, neuroimaging endophenotypes variance (among other traits) can be attributed to either genetic or environmental factors or their interactions. Heritability is defined as the proportion of variance for a particular phenotype, measured at a particular age, that is attributable to genetic variation [Visscher et al., 2008]. An observed phenotype is usually represented as the sum of the unobserved genotype (G) and unobserved environmental factors (E): Phenotype (P) = Genotype (G) + Environment (E). Likewise, the phenotypic variance of the observable phenotypes (σ^2_P) can be expressed as the sum of effects: $\sigma^2_P = \sigma^2_G + \sigma^2_E$. The broad sense heritability of a trait (H^2) is the proportion of phenotypic variance attributable to all sources of genetic variance: $H^2 = \sigma^2_G/\sigma^2_P$. The genetic variance can be partitioned into the variance of additive genetic effects (breeding values; σ^2_A), of dominance (interactions between alleles at the same locus) genetic effects (σ^2_D), and of epistatic (interactions between alleles at different loci) genetic effects (σ^2_I) [Visscher et al., 2008]: $\sigma^2_G = \sigma^2_A + \sigma^2_D + \sigma^2_I$. The narrow-sens heritability of a trait (h^2) is the proportion of phenotypic variance attributable to additive genetic: $h^2 = \sigma^2_A/\sigma^2_P$. It is the focus of most modern genetic investigation as a high proportion of genetic variance is additive [Hill et al., 2008]. Heritability estimates vary between 0 and 1 indicating either no genetic influence at all or complete genetic determination. In order to judge the value of endophenotypes and prioritise their study, it is common to rely on its heritability estimates. Indeed, a large and significant measure of heritability indicates that the trait of interest is significantly under genetic control and might be eligible for more extensive molecular genetic studies. Heritability is an important genetic concept however, its interpretation should be taken with caution.

First, heritability might be population-dependant in such, it summarises the strength of genetic influence on a specific trait measured in a specific population and may not be generalised to other cohorts where environmental influences and ancestry may differ [Thompson et al., 2013]. Second, heritability estimates is not much informative about which specific genes contribute to a trait, how many genes are involved, or the impact of any gene on it [Thompson et al., 2013]. For example, human height is a trait that is influenced by many genes with small effect [Yang et al., 2010].

1.4.2 Endophenotypes

Behaviour measures like language performance scores are not the direct expression of genetic effects. It is the manifestation of the combination of physiological characteristics as a result of molecular and cellular effects in the brain. Sometimes the physiological characteristic deficiencies may precede illness symptoms [Glahn et al., 2007, Gottesman and Gould, 2003] and they may be considered as biomarkers. The idea behind the concept of endophenotype is that these quantitative biomarkers considered as intermediate phenotype are more closely associated with gene effects than the complex phenotypic expression of a disease. The endophenotypes, like phenotypes, can be studied as regards heritability or genetic association. Such measures help our understanding of the individual neuroimaging variability and provide insight into genetic effects on the central nervous system. A certain number of putative endophenotypes have been proposed for functional and structural brain such as measures of structural and functional connectivity, and brain asymmetry.

1.4.3 Pleiotropy

Pleiotropy refers to the genetic effect of a single gene on two or more (endo)phenotypes. Neuroimaging allows us to generate numerous endophenotypes at a time regarding one individual. Pleiotropic effects have been observed in imgaging-genetic studies when considering phenome-wide association studies. Indeed, these ones allow us to identify association of a locus with interrelated endophenotypes.

1.4.4 Candidate genes

The candidate-gene (CG) design was the first and is still a widely used approach in neuroimaging-genetics field. It involves genotyped markers in genes chosen *a priori* and hypothetically related to the trait of interest. For example and relevant to our study, the well-known language related gene *FOXP2* was identified in the KE family, in which multiple close relatives suffered from similar disruptions of speech and language skills [Fisher et al., 1998]. Further candidate-gene studies focused on this particular gene because of *a priori* hypotheses about its etiological role in developmental language disorders (DLD). The candidate-gene design consists in comparing between groups classified according to their alleles on a specific gene (AA, AB, BB). The presence of a specific allele can be associated quantitatively and linearly with the trait of interest and several models can be adjusted to this end. The CG design is simple and offers relatively

straightforward interpretability of results; the gene of interest is generally well-known and its effect is often well-characterised. Despite these strengths, CG studies have been subject to important criticism. The significant findings of association regarding candidate genes approach have not been replicated when followed up in subsequent association studies. Additionally, in most cases, the biological mechanism of these candidate genes is poorly understood and only few have direct effect on the trait of interest. Indeed, most genes have indirect effects by modulating others mainly at the level of transcription, (post)translation in such proteins can have altered function in the presence of absence of others.

1.4.5 Genome-wide association study

Genome-wide association studies (GWAS) aim to identify associations of genotypes with (intermediate) phenotypes. GWAS can consider different type of genetic information; copy-number variants (CNV), sequence variations, or single nucleotide polymorphisms (SNP). The predominant strategy for identifying genomic loci associated with complex traits is through a massive *univariate-imaging univariate-genetic association study*. Univariate approaches involve the association between a single phenotype and each of millions isolated genetic variants. According to the nature of the endophenotype of interest -binary or continuous value-, various models can be adjusted. An example with endophenotypes extracted using fMRI data can be appreciated in the Fig. 1.9.

This state-of-the-art massive univariate approach results in a total of more than one million statistical tests. To assess significance, a consensus threshold $p = 5e - 8$ is considered by the genomic community. It is comparable to a Bonferroni correction of the traditional 0.05 type 1 error rate for one million statistical tests. Furthermore, a massive univariate approach ignores the biological information shared across multiple traits -the phenomenon called pleiotropy (See section 1.4.3)-. When several (endo)phenotypes are of interest, the number of tests significantly increase and it forces the users to adopt a stringent multiple comparison correction of the p-values to control the family-wise error rate. The colossal correction for multiple tests often leaves no significant associations. This limitation has led to the emergence of new multivariate statistical methods, designed to take into account the correlations among the biologically related (endo)pheontypes, classically encountered in imaging-genetic studies.

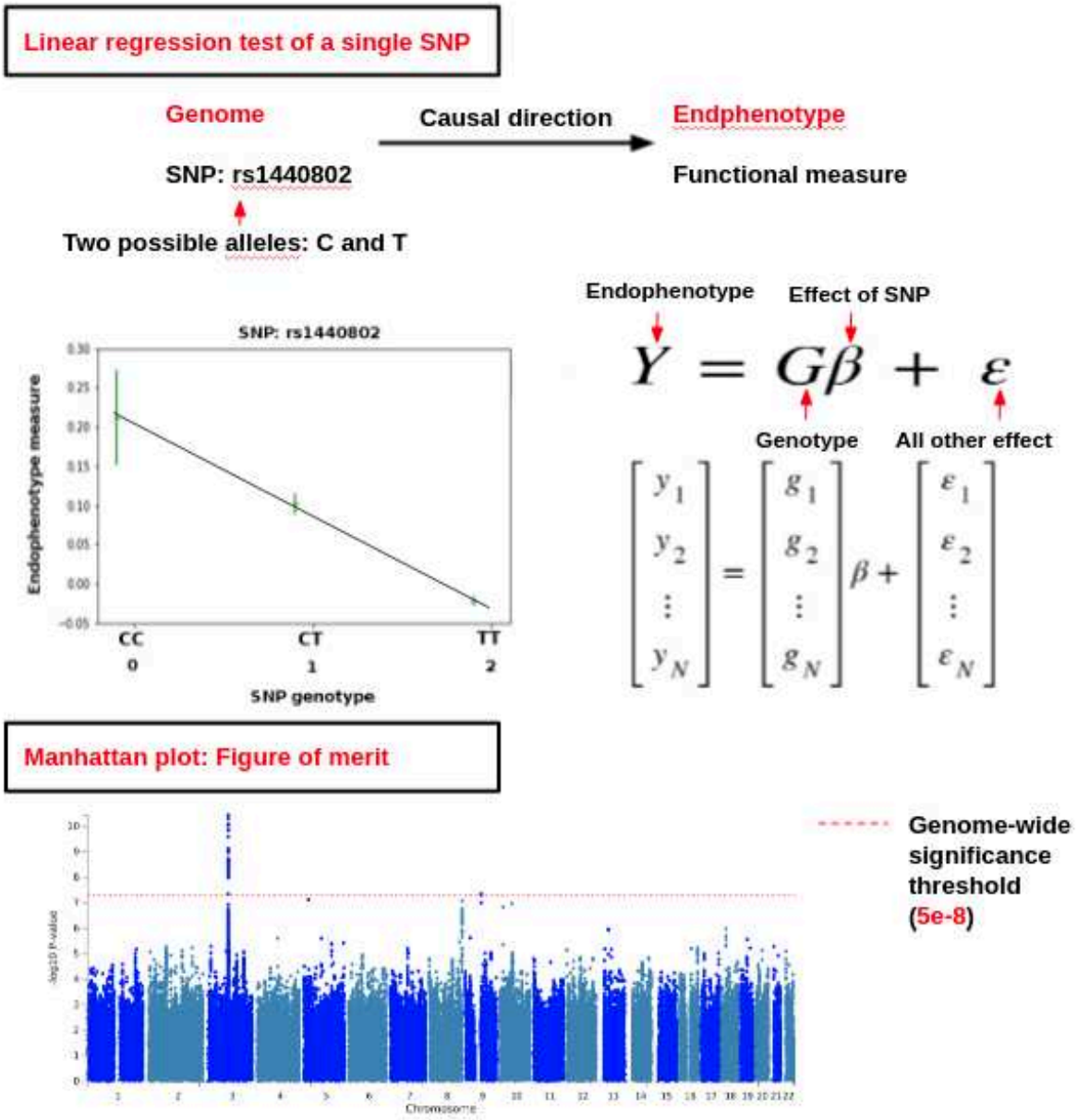

Figure 1.9 – **Principles of GWA illustrated with an example of a continuous endophenotype: a functional measure of the brain.** On the top figure, the y-axis is the endophenotype measure, and the x-axis represents the targeted genetic variant. This variant has two possible alleles: C and T. Each individual in the cohort will have a combination of CC, CT, TT alleles coded as 0, 1 or 2. The lower figure represent a Manhattan plot and is a figure-of-merit of GWASes. The y-axis is the -log10 of the p-value of the association, and the x-axis represents the SNP location along the genome. The most significant associations will have the smallest p-values and the -log10 of these p-values will have the highest height in the graph. The red dashed line corresponds to the $5e-8$ genomic threshold. The points above correspond to the genetic variants significantly associated with the studied phenotype.

Multivariate approaches quantify the simultaneous contributions of loci to multiple traits by taking advantage of their genotypic-phenotypic structures. Importantly, in the case of multivariate-imaging univariate-genetic association frameworks, several advantages are observable. First, by taking into account the cross-trait covariance, multivariate analyses increase the statistical power

in case of the presence of genetic correlation between the different traits [Allison et al., 1998, Zhu and Zhang, 2009]. Second, by performing a single test for association with a set of traits, multivariate procedures alleviate the multiple comparison correction [Klei et al., 2008, Zhu and Zhang, 2009]. Third, it improves the ability to detect susceptible genetic variants whose effects are too small to be detected in univariate analysis. Fourth, contrary to the massive univariate approach, multivariate GWASes have the advantage of leveraging the distributed nature of genetic effects and the presence of pleiotropy across modalities and is thus, more consistent with biology [Chavali et al., 2010]. More details about multivariate methods that exists in the litterature are presented in the chapter 2.6

1.5 What are the bases of human language? A review of language approaches in human neurosciences

Language is complex and multi-faceted. Its study is conducted within many different disciplines and from different theoretical angles such as descriptive linguistics, theoretical linguistics, sociolinguistics, computational linguistics, historical linguistics, and neurolinguistics. The present thesis, following on the neurolinguistics approach, addresses the historical and relevant aspects of the language-brain relationship. Historically, neurolinguistics is rooted in the development of aphasiology, the study of linguistic deficits occurring as the result of brain damage. With the emergence of new brain imaging technologies, our understanding of the anatomical organisation of linguistic functions has greatly matured. In the following sections, we will attempt to produce a basic summary of our current knowledge about the language-brain relationship. These ones do not claim to be exhaustive and are only intended to provide the reader with the necessary background to understand the aspects that we addressed and studied in the rest of the present manuscript.

1.5.1 Understanding language from aphasia

Most of the early knowledge about the language-brain relationship comes from the examination of individuals with language impairments following brain injury caused by accidents or diseases. Several types of aphasia exist suggesting that language processes undergo several stages and take place in different brain regions. Based on these aphasiology discoveries, Broca and Wernicke (and Lichtheim and many others) offered fundamental knowledge about language-brain relationship. Accordingly, a language neurobiology model have been proposed; the well-known "Broca-Wernicke-Lichtheim-Geschwind model". This classical model, yet obsolete, will be furthermore, briefly described.

1.5.1.1 The Broca-Wernicke-Lichtheim-Geschwind classical model

During the 19th century, language-brain researches were mainly *post mortem* driven. Based on aphasiology, neurologists like Broca and Wernicke offered fundamental knowledge about language-brain relationship. Historically, Broca first described the association between motor aphasia and a lesion in the middle part of 'tan' patient's left frontal lobe (Broca's aphasia)

shortly followed by Wernicke who reported a damage in the left posterior superior temporal gyrus, resulting in deficits in language comprehension (Wernicke's aphasia). He proposed that a disconnection between these both language brain areas lead to aphasia. Afterward, Ludwig Lichtheim and Norman Geschwind expanded his work and proposed the "Broca-Wernicke-Lichtheim-Geschwind" model, widely known as the "Wernicke-Geschwind" classical model. Two main functions are modelised through this model, comprehension and responding to the written words as well as comprehension and responding to spoken language. According to this model, the sounds of the words are transferred through the auditory pathways to the primary auditory cortex and then to Wernicke's area, where the meaning of the words is extracted. In order for a person to produce speech, from Wernicke's area to Broca's area via the arcuate fasciculus white matter tract, the meanings of words are sent. Next, morphemes are formed and then passed on to the motor cortex. Concerning the written word, information is transferred through the primary visual cortex to the angular gyrus and from there to the Wernicke's area. The Broca-Wernicke-Lichtheim-Geschwind model is now considered to be too simplified and to contain a certain number of errors. For example, this model is based on both Broca's and Wernicke's areas connected by the arcuate fasciculus. The localisation of these cortical region is still a matter of ambiguity. Furthermore, studies showed evidence that there is no single area in our brain dedicated to language processing such as speech comprehension but a set of cortical sites [Mesulam et al., 2015]. Due to its simplicity and usefulness for understanding the classical categorization of aphasic syndromes, this classical model remains widely studied. However, researchers believe that it should be re-evaluated [Dronkers, 2000, Nasios et al., 2019, Tremblay and Dick, 2016, Vigneau et al., 2006].

1.5.2 Understanding language by brain imaging

Until recently, language-related brain processes were mainly investigated using association between language deficits and *post-mortem* analysis of brain lesions. Today, advances in structural and functional imaging techniques have provided new insights into our understanding of brain-language relationship. In many aspects, the data obtained by these imaging methods confirmed what was known from studies about language impairments. However, these also demonstrate that language processing may be even more complex than previously thought.

Modular paradigm has shaped our understanding of brain-language function. However, accumulating evidence suggest that cognition in the brain is supported by an overlapping and interactive large-scale cognitive networks rather than modules [Fuster, 2002, Mesulam, 1990]. Contrary to single-study analysis, meta analysis approaches provide empirical support for this theoretical shift and has the advantage of identifying previously neglected regions involved in language processing. Here, we will start on reporting the state-of-the-art language brain areas and large-scale cognitive networks proposed by [Vigneau et al., 2006, 2011] in terms of cortical regions. Next, we will briefly introduce the Hickok and Poeppel's dual stream model as a modern network-based model as well as the language-relevant white matter tracts.

1.5.2.1 From Broca and Wernicke to the neuromodulation era: a brief neuroanatomy of language

In order to map the language network in the human brain, we need a coordinate system that subdivides the brain into relevant parts and applies labels to these parts. In this section and throughout the manuscript, to refer to the neuroanatomical location of a given function, we use the different gyri and sulci in the cortex. The anatomical details of both left and right hemisphere are represented in the Fig. 1.10. Furthermore, an old, yet still valid, widely used parcellation provided by Korbian Brodmann in 1909 is the cytoarchitectonic description of the cortical structure [Brodmann, 1909].

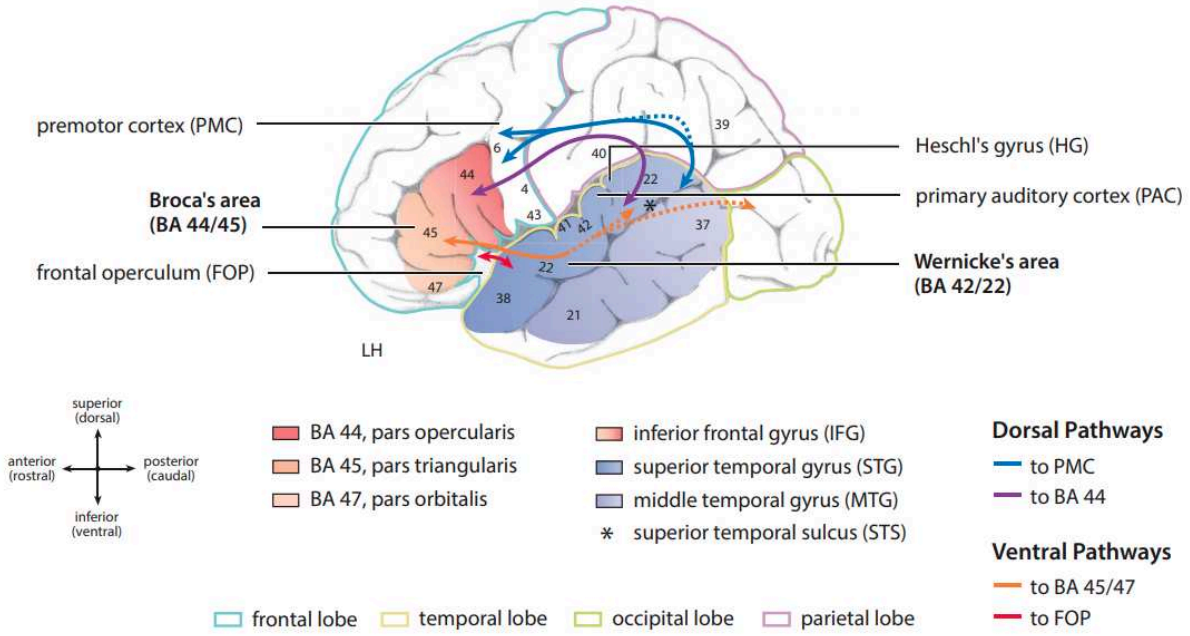

Figure 1.10 – **Neuroanatomy of language (Source: [Friederici, 2017]).** Anatomical and cytoarchitectonic details of the left hemisphere (LH). Top: The different lobes (frontal, temporal, parietal, occipital) are marked by colored borders. Major language-relevant gyri (inferior frontal gyrus (IFG), superior temporal gyrus (STG), middle temporal gyrus (MTG)) are color-coded, superior temporal sulcus (STS) located between STG and MTG is marked by an asterisk. Numbers indicate language-relevant Brodmann areas (BA) that Brodmann (1909) defined on the basis of cytoarchitectonic characteristics. The coordinate labels (see bottom left) superior (dorsal)/inferior (ventral) indicate the position of the gyrus within a lobe (e.g., superior temporal gyrus) or within a BA (e.g., superior BA 44). The horizontal coordinate labels anterior (rostral)/posterior (caudal) indicate the position within a gyrus (e.g., anterior superior temporal gyrus). Broca's area consists of the pars opercularis (BA 44) and the pars triangularis (BA 45). Located anterior to Broca's area is the pars orbitalis (BA 47). The frontal operculum (FOP) is located ventrally and medially to BA 44, BA 45. The premotor cortex (PMC) is located in BA 6. Wernicke's area is defined as BA 42 and BA 22. The primary auditory cortex (PAC) and Heschl's gyrus (HG) are located in a lateral to medial orientation in the temporal lobe. White matter fiber tracts, i.e., the dorsal and ventral pathways connecting the language-relevant brain regions are indicated by color-coded arrows (see bottom right). Reprinted from Friederici [2011]. The brain basis of language processing: From structure to function. Physiological Reviews, 91 (4): 1357–1392

Based on Brodmann's cytoarchitectonic parcellation, Broca's area for example, was subdivided into a posterior part (BA 44) and a anterior part (BA45) of the IFG. A subdivision that coincides with the neuroanatomical separation into pars opercularis and pars triangularis, respectively. A novel synthesis of old and new knowledge about the architecture of the language processing network is provided by the work of Vigneau et al. [2006, 2011]. In this study, the authors performed a large-scale meta-analysis of 946 brain language activation peaks collected from 129 task-based fMRI language studies from the literature (See Fig. 1.11a). This meta-analysis aimed at defining the composition of the phonological, semantic, and sentence processing networks in the fronto-parieto-temporal regions of the both cerebral hemispheres (See Fig. 1.11b). This work offers a global view of the language processing beyond the modular paradigm and accordingly, argues for large-scale architecture networks rather than modular organisation of language. The connections between different language regions distributed across the parieto-fronto-temporal cortex are ensured by the white matter bundles [Catani and Forkel, 2019, Catani et al., 2005]. These neuroanatomical white matter tracts can connect quite distant region and guarantee the information transfer between them. This short description show the complexity of the language brain relationship. More details about language-relevant fiber tracts will be given below.

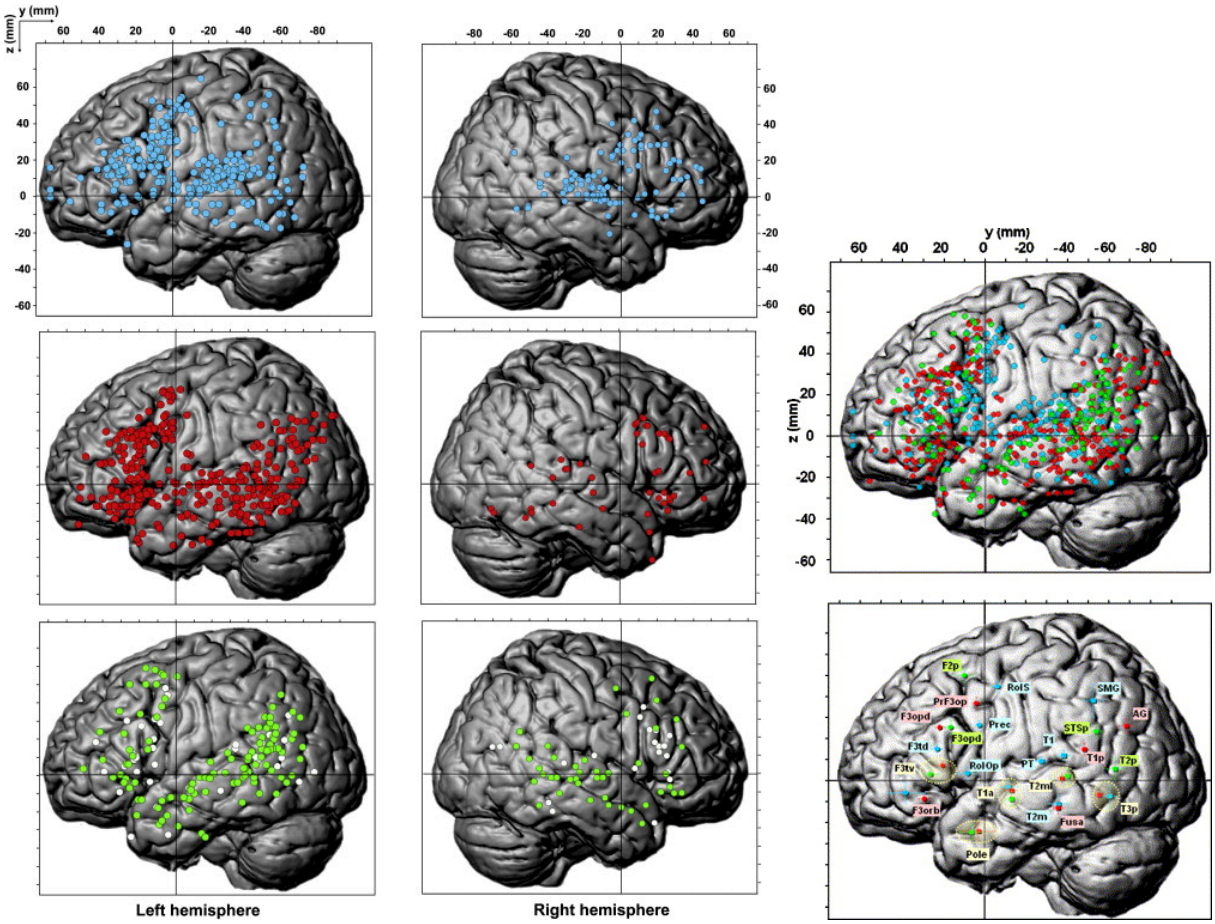

A) B)

Figure 1.11 – **Overview of the meta-analysis (Source:** [Vigneau et al., 2006, 2011]**).** Each foci is color-coded according to its language components category: phonology (blue), semantic (red), and syntax (green). A) Distribution of the peaks in each hemisphere for each component. The 128 neuroimaging studies selected for our previous meta-analysis reported 728 activation peaks in the left hemisphere (left column). Among the 128, 59 studies reported 218 activation peaks in the right hemisphere (right column). Activation peaks detected during phonological tasks are indicated in blue (top row), lexico-semantic tasks in red (middle row) and sentence and text processing in green (bottom row). For this last component, peaks corresponding to contrast investigating comprehension are in green and those investigating syntax are in white. Peaks are projected onto a lateral view of the MNI single subject. B)Top: sagittal projection map of the 730 activation peaks. Bottom: clusters identified for phonological (blue), semantic (red), and syntactic (green) processing and obtained from the spatial clustering of the peaks. Clusters of different components that were not spatially distinct are circled (yellow). Error bars correspond to twice the standard error on the y and z stereotactic coordinates. The left hemisphere lateral surface rendering of the MNI single-subject brain template, together with the corresponding stereotactic grid, is displayed for anatomical reference. RolS, Rolandic sulcus; RolOp, Rolandic operculum; F3t, pars triangularis of the left inferior frontal gyrus; F3op, pars opercularis of the left inferior frontal gyrus; F3orb, pars orbitaris of the left inferior frontal gyrus; SMG, supramarginalis gyrus; PT, planum temporale; T1, superior temporal gyrus; T2, middle temporal gyrus; T3, inferior temporal gyrus; Prec, precentral gyrus; F2, middle frontal gyrus; PrF3op, precentral gyrus/F3op junction; STS, superior temporal sulcus; AG, angular gyrus; Fusa: anterior fusiform gyrus; a, anterior; p, posterior; l, lateral; m, middle; d, dorsal; v, ventral.

1.5.2.2 The neuroanatomical pathways of language

Despite the huge amount of knowledge accumulated the last past decades regarding the language-brain relationship, no large-scale models of the functional anatomy of language has been proposed beyond the Broca-Wernicke-Lichtheim-Geschwind classical model. To remedy this situation, Hickok and Poeppel's [Hickok and Poeppel, 2004] proposed a model, free of fiber tracts connecting the language-related brain regions but by thinking of aspects of language processing in terms of sensory–conceptual mapping of speech and sensory–motor mapping. This model consists on a dual stream model – analogous to the visual system [Hickok and Poeppel, 2004], which emphasize speech processing during perception and production in "dorsal and "ventral" pathways (streams). Each of the pathways consists of more than one fiber bundle terminating in different cortical regions. In the recent years, with the advent of new imaging techniques, such as diffusion-weighted magnetic resonance imaging, researchers addressed this question by tracking *in vivo* in human brain the white matter fiber bundles and the results supported Hickok and Poeppel's dual stream model [Hickok and Poeppel, 2007], as detailed below.

The dorsal pathway involves a left hemispheric structure, the **arcuate fasciculus (AF)**, that connects Broca's region in the posterior frontal lobe to Wernicke's region in the posterior dorsal temporal lobe as stipulated in the Broca-Wernicke-Lichtheim-Geschwind model. However, [Catani et al., 2005] tracked the arcuate fasciculus using dMRI and suggested two dorsal, direct and indirect, pathways. The direct pathway known as the **arcuate fasciculus -long segment-** connects Wernicke's region with Broca's region, and the indirect pathway is mediated by the inferior parietal cortex. It consists of the **arcuate fasciculus -anterior segment-**, linking Broca's region to Geschwind's region (encompassing the angular (BA 39) and supramarginal (BA 40) gyrus), and the **arcuate fasciculus -posterior segment-** between Geschwind's region and Wernicke's region. The **superior longitudinal fasciculus (SLF)** is also a dorsal tract composed of three parallel longitudinal branches connecting the parietal and the frontal lobes. Historically, this fasciculus has been referred to as (AF/SLF) because both the AF and the SLF run partly in parallel. The superior branch (SLF I) runs from the superior parietal lobule and the precuneus to the superior frontal gyrus. The middle branch (SLF II) connects the angular gyrus (BA39) to the posterior regions of the middle frontal gyrus (BA6). The inferior branch (SLF III) connects the supramarginal gyrus and Broca's area (the pars opercularis, the pars triangularis and the pars orbitalis) [Rojkova et al., 2016].

The ventral pathway involves bilaterally distributed hemispheric structures. It was originally viewed as a unifunctional tract but was later revisited and several ventral fiber tracts were assigned as subserving sound-to-meaning mapping, specifically the **inferior fronto-occipital fasciculus**, a long-ranged tract connecting the inferior frontal regions (BA45 et BA47) with the temporal and occipital cortex, the **uncinate fasciculus** which connects the anterior temporal lobe (BA38) to the frontal operculum, and the **inferior longitudinal fasciculus** that connects the occipital and anterior temporal cortex.

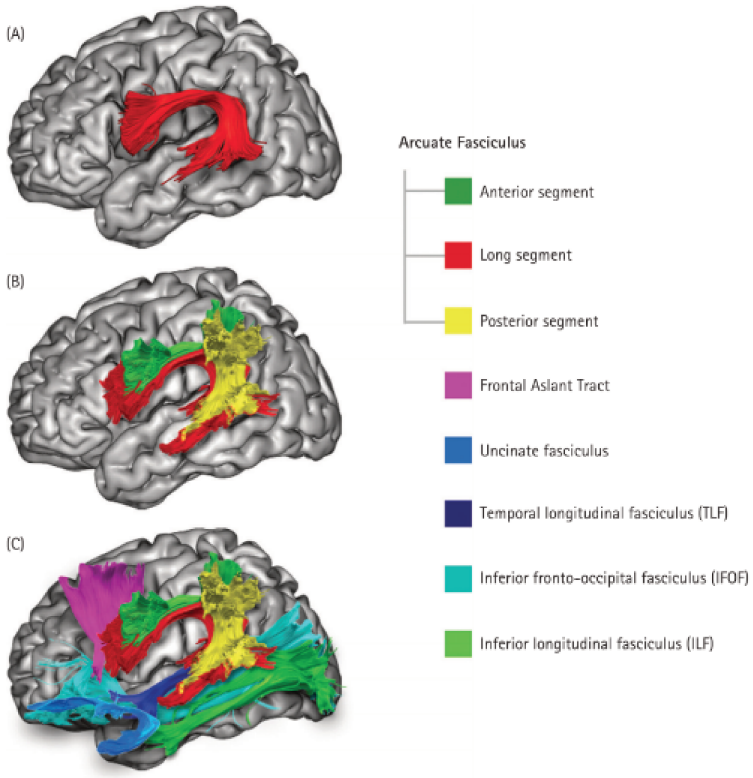

Figure 1.12 – **Tractography-based reconstruction of the language networks from classical models to contemporary neurolinguistics (Source:** [Catani and Forkel, 2019]**).** (A) Classical language model with the arcuate fasciculus connecting Broca's region in the inferior frontal gyrus to Wernicke's region in the superior temporal gyrus. (B) Extension of the classical arcuate fasciculus sense strictu to include the anterior segment, connecting inferior frontal to inferior parietal lobe, and the posterior segment linking the inferior parietal to the temporal lobes. (C) Current model of an extended language network beyond the three segments of the arcuate fasciculus. The frontal aslant tract (FAT) connects the inferior frontal gyrus to the pre-supplementary motor cortex. The ventral network includes the uncinate fasciculus between the anterior temporal lobe and the orbital frontal and inferior frontal cortex, the temporal longitudinal fasciculus (TLF) between the posterior temporal lobe and the temporal pole, the inferior fronto-occipital fasciculus (IFOF) connecting the ventral frontal cortex to the occipital cortex, and the inferior longitudinal fasciculus (ILF) between the occipital and anterior temporal cortex.

Additional structural networks relevant for communication are proposed [Catani and Bambini, 2014, Catani and Forkel, 2019, Rojkova et al., 2016]: *i)* the **frontal aslant tract (FAT)** is a recently described pathway that connects Broca's region to the supplementary and pre-supplementary motor area (BA6);*ii)* the **temporal longitudinal fasciculus (TLF)** is a recently described fasciculus connecting Wernicke's region to the anterior temporal pole; *iii)* The **fronto-insular tracts (FIT)** is a system composed of five U-shaped tracts that connects the frontal operculum to the insula. The four most anterior tracts link respectively the pars orbitalis -BA47- (FIT 1), the pars triangularis -BA45- (FIT 2), the pars opercularis -BA44- (FIT 3) and the precentral gyrus -BA6- (FIT 4) of the frontal lobe with the anterior insula. The most posterior tract (FIT 5) connects the subcentral gyrus -BA43- to the posterior insula. The Fig. 1.12 summarises these language-relevant white matter tracts.

What about the pathways in the right hemisphere and cross-hemispheric pathways?
The search of the implication of the right hemisphere in language have been, for a long time, neglected. Recent studies have demonstrate its involvement after aphasia resulting from left hemisphere but also its involvement alone or in interaction with the left hemisphere during auditory language comprehension in healthy individuals. These findings called for a structural description of the pathways within the right hemisphere and cross-hemispheric ones. Similar to the left hemisphere, the right hemisphere shows a dual-stream model with a lower density of fiber bundles compared to their left counterpart. The cross-hemispheric pathways is the corpus callosum. Its anterior and posterior parts have been discussed to be involved in language-related processes.

1.5.2.3 The neural bases of language processing networks

In [Vigneau et al., 2006], the authors identified and revisited different language processing networks. These are briefly described below.

Fronto-temporal auditory–motor network.
The motor theory of speech perception has been quite an old debate [Flinker et al., 2015, Galantucci et al., 2006, Liberman and Mattingly, 1985, Schwartz et al., 2008, Whalen, 2019]. [Vigneau et al., 2006] advocate for an audio–motor loop that includes an upper motor area for mouth motion control, a lower premotor area in the precentral gyrus that is dedicated to pharynx and tongue fine-movement coordination, and a sensory–motor integration region in the Rolandic operculum in the frontal lobe as well as the left planum temporale and Heschl's gyrus in the temporal lobe. These fronto-temporal areas, support of a perception–action cycle, are supposed to be connected through the arcuate fasciculus fibers [Vigneau et al., 2006].

Fronto-parietal working memory loops.
The phonological working-memory loop connects the dorsal part of the pars triangularis of the inferior frontal gyrus in the frontal lobe and the supramarginal gyrus in the parietal lobe connected by both the arcuate fasciculus [Catani et al., 2005] and U-fibers [Duffau et al., 2003]. These regions constitute the neural basis of a perception–action cycle defined above for phonological working memory.
The semantics working-memory loop includes a frontal area at the junction of the precentral gyrus and opercular part of the inferior frontal gyrus and the angular gyrus in the parietal lobe connected by the arcuate fasciculus. These regions constitute the perception–action cycle for semantic working memory.
The sentence and text comprehension working-memory loop includes the posterior part of the middle frontal gyrus and the posterior part of the superior temporal sulcus connected by the arcuate fasciculus.

Fronto-parieto-temporal semantic network
Research studies described the general semantic network to typically include left parieto-frontal-temporal areas [Binder et al., 2009]. [Vigneau et al., 2006] and [Lau et al., 2008] proposed neuroanatomical model for semantic processing that includes the angular gyrus in the posterior

inferior parietal lobe, the lateral temporal lobe, including the middle temporal gyrus, the anterior temporal cortex and the fusiform gyrus, the anterior and posterior inferior frontal gyrus.

1.6 Complex and multifactorial aetiology: the pursuit of brain–language-genetics relationships

Multiple factors influence language process. Both environment and genetics plays a crucial role. Environmental factors include home literacy environment, socio-economic status, and parental education [Peterson and Pennington, 2015]. Genetic factors also affect variation as language disabilities such as dyslexia are familial. Genetic factors are not restricted to language disabilities but also affect normal variation that support language performance. The molecular genetic framework underlying language genetic component is complex and heterogenic. Many genes are likely to contribute to it. Indeed, Today, there is broad agreement that language is a complex and multifactorial trait and is unlikely to be associated to only few genes but rather to many related genes and their interactions, contributing to neural pathways that are important to normal brain maturation and possibly language development (i.e. neuronal differentiation, migration, and connectivity), together with experience-dependent contributions from the environment [Fisher and Vernes, 2015]. Here, we will briefly summarise the results found to date regarding both heritability of multiple language subcomponent and genes supporting this trait.

1.6.1 Heritability of language

A pivotal question in biology is the heritability of a particular trait. It provide a quantitative estimation of its association with a set of genetic markers and thus, informs us about the richness of its contribution in the trait of interest. How much of language is genetic and how much learned? The heritability of language has been extensively reported in the literature and the work of [Stromswold, 2001] provides a meta-analysis of the available evidence concerning a possible genetic basis for human language. These previous studies have mainly focused on twins, adoption, and linkage studies of language.

Twin studies are based on the difference between monozygotic (MZ) and dizygotic (DZ) twins. The assumption underlying these studies is that MZ twins share 100% of their genetic material, whereas DZ twins share only 50% of their genetic material. In both cases, the twins share a substantially similar environment as they were raised by the same parents in the same household. If language has a genetic component, then language abilities of MZ twins should be more similar to each other than DZ are to each others. If no difference is observed, this suggests that the heritability of language is negligible. Different linguistic ability are reviewed for both individuals with or without developmental language disorders such as dyslexia and specific language impairments. These includes spoken and non spoken vocabulary, phenoeme, phonology, articulation, auditory and phonological short-term memory, articulation, morphology, syntax, reading and spelling (syntactic comprehension and production). These studies strongly suggest that genetic factors account for some of the individual differences in linguistic ability for both people with or without developmental language disorders [Stromswold, 2001].

The adoption studies compare adopted children's linguistic abilities with those of their adopted and biological relatives. If language has a genetic component, then linguistics ability of adopted children should resemble more to their biological relatives than to their adopted ones. Database such as the Colorado Adoption Project (CAP) [Rhea et al., 2013] offer a unique opportunity to disentangle nature and nurture regarding cognitive abilities including language trait. Taken as a whole, the adoption studies also suggest that genetic factors affect language abilities and more specifically, verbal performance (See Fig. 1.13).

Overall these results advocate for a genetic predetermination and heritability of human language. Depending on the language score test, age of the volunteers, or the methodology adopted, these genetic studies of language acquisition estimate the heritability of language to be between 1 and 82% [Dale et al., 2000, Ganger et al., 2002, Reznick et al., 1997, Stromswold, 2001]. Nevertheless, these results should be taken with caution. One limitation of these studies is regarding the generalizability of their results. Indeed, most of the twin studies included in this review involved relatively small numbers of twins. Regarding adopted studies, The results are mainly obtained using data from the same group of adopted children (CAP cohort), which can or cannot be representative of the general population. Furthermore, most of these studies did not take into account corrections regarding the multiple tests performed and thus, call for replications.

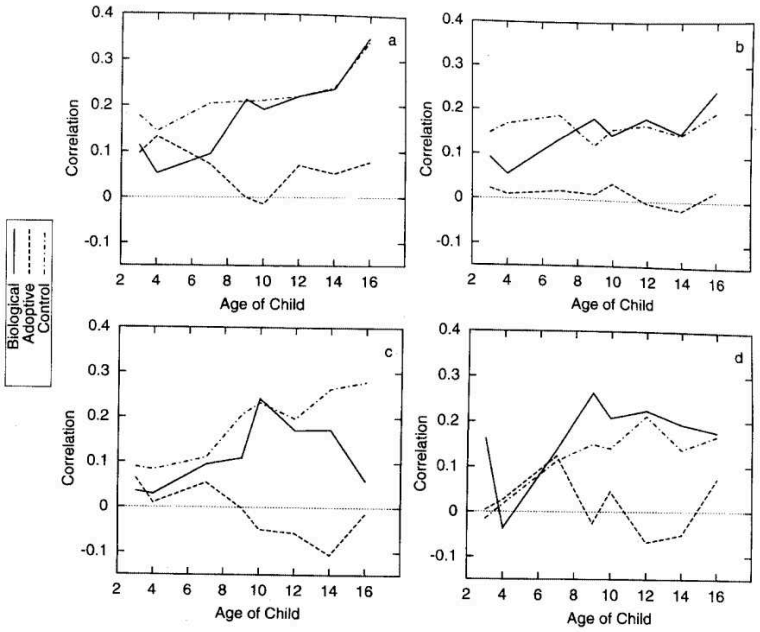

Figure 1.13 – **Parent-offspring correlations for factor scores for specific cognitive abilities for adoptive, biological, and control parents and their children at 3, 4, 7, 9, 10, 12, 14, and 16 years (source: [Stromswold, 2001]).** Correlations are shown for verbal ability (a), spatial ability (b), speed of processing(c), and recognition memory (d). Parent-offspring correlations are weighted averages for mothers and fathers. The number of individuals range from 33 to 44 for biological fathers, 159 to 180 for biological mothers, 153 to 197 for adoptive parents, and 136 to 217 for control parents.

To date, behavioural genetics investigations are the main type of studies that address this question. The recently available large-scale imaging-genetics cohorts provide an illuminating new tool to explore this question. Contrary to prior studies, recent studies propose to use image-derived phenotypes to explore this question by taking advantage of the UK Biobank cohort, a large-scale imaging-genetics resources constituted of unrelated volunteers introduced in the 2.1.1. The left–right hemispheric asymmetry is an important aspect of healthy brain organization for many functions including language. These studies focused on this aspect of the brain and reported the heritability of endophenotypes extracted from structural MRI [Carrion-Castillo et al., 2020, Le Guen et al., 2020, Sha et al., 2021]. Carrion-Castillo et al. [2020] evaluated the association between the planum temporale volume asymmetry with neurodevelopmental disorders including dyslexia, schizophrenia and autism and estimated its narrow-sens heritability to roughly 14%. Le Guen et al. [2020] evaluated the superior temporal assymetrical pit and estimated its narrow-sens heritability to 11%. The work of [Sha et al., 2021] offers a more general view of the left–right hemispheric asymmetry. They reported a significant narrow-sens heritability ranging from 2.2% for the assymetry index (AI) of entorhinal cortical thickness to 9.4% for the AI of superior temporal surface area. A discrepency between heritabilities reported by both [Carrion-Castillo et al., 2020, Le Guen et al., 2020] and [Sha et al., 2021] can be explained by the difference of phenotypes studies as well as the sample size used. Indeed, while [Carrion-Castillo et al., 2020, Le Guen et al., 2020] used a sample size of 18,057 and 16,515

participants respectively, [Sha et al., 2021] take advantages of a more recent release of 32,256 participants from the UK Biobank. Regarding functional brain aspect and to our knowledge, there is no study that extensively explored the heritability of human language. That being that, the heritability of functional MRI derived phenotypes in a brain-wide context has been evaluated by [Elliott et al., 2018] and although not specific to language cognitive trait, it allow us to frame the orders of magnitude of the heritability estimates. According to Elliott et al. [2018], the resting-state fMRI functional connectivity show the lowest levels of SNP heritability, compared to structural IDP.

1.6.2 Developmental language disorder related loci

Historically, before the emergence of the genotyping technology, genetic linkage was the only affordable method able to interrogate genetics regarding trait of interest. Consequently, the candidate genes that has been targeted for reading and language impairments has arisen from linkage analysis. These findings are briefly presented in the Table 1.1.

Table 1.1 – Summary of the linkage regions to reading disability (RD) and Specific language impairment (SLI) and the candidate genes within them (Source: Hagoort [2019]).

Classification	Locus name	cytogenetic position	Candidate gene	Associated phenotypes	Reference
Dyslexia	DYX1	15q21	DYX1C1	RD	[Taipale et al., 2003]
	DYX2	6p23–21.3	DCDC2, KIAA0319	RD	[Kaplan et al., 2002], [Deffenbacher et al., 2004]
	DYX3	2p15–16	MRPL19, C2ORF3	RD	[Anthoni et al., 2007]
		2p11		RD	[Kaminen et al., 2003]
	DYX4	6q11.2–q12		RD	[Petryshen et al., 2001]
	DYX5	3p12–q13	ROBO1	RD	[Hannula-Jouppi et al., 2005]
	DYX6	18p11.2		RD	[Fisher et al., 2002]
	DYX7	11p15.5		RD	[Hsiung et al., 2004]
	DYX8	1p36	KIAA0319L	RD	[Couto et al., 2008]
	DYX9	Xq27.2–q28		RD	[De Kovel et al., 2004]
Specific language impairment (SLI)	SLI1	16q23.1–q24	CMIP, ATP2C2	Phonological memory in an SLI cohort	[Newbury et al., 2009]
	SLI2	19q13.13–q13.41		SLI	[Consortium et al., 2004]
	SLI3	13q14.3–q31.1		SLI	[Consortium et al., 2004]
				Reading-IQ discrepancy in an SLI cohort	[Bartlett et al., 2002]
	SLI4	7q31–q36	CNTNAP2	Phonological memory in an SLI cohort including nonaffected family members	[Vernes et al., 2008]
	SLI5	2q36	TM4SF20	Language delay; exon 3 deletion co-segregated with language delay in Southeast Asian families	[Wiszniewski et al., 2013]
	Other	2p22		SLI	[Bartlett et al., 2004]
		17q23		Reading-IQ discrepancy in an SLI cohort	[Bartlett et al., 2004]
		7q31	FOXP2		[Fisher et al., 1998]

1.6.3 Genome-wide association studies of language abilities

Genome-wide association studies of reading and language abilities have used quantitative traits from both general population and case-control designs. The results are summarised in Table 1.2.

Table 1.2 – Summary of the top genome-wide association signals from studies of reading and language traits (Source: Hagoort [2019]).

Cytogenetic position	SNP	Closest known gene	Trait	SNP test, N	Total N	Reference
1p13.1	rs4839516		Single word reading	2,373,249 imputed	6,135 individuals (children and adolescents)	[Luciano et al., 2013]
2q31	rs12474600	CCDC141	Language factor	1,724,317 imputed	2,329 children	[Harlaar et al., 2014]
3p12.3	**rs7642482**	**ROBO2**	**Expressive vocabulary in 15 month olds**	**2,449,665 imputed/ genotyped**	**8,889 individuals (toddlers)**	[St Pourcain et al., 2014]
4p15.3	rs11945798		Single word reading	2,373,249 imputed	6,135 individuals (children and adolescents)	[Luciano et al., 2013]
4q26	rs482700		SLI	500,527 genotyped	163 SLI (based on test performance) and 4,117 controls (children)	[Eicher et al., 2013]
5p13	rs1353835 (maternal effect)		SLI	614,937 genotyped	278 families (297 SLI children)	[Nudel et al., 2014]
5q35.1	rs9313548	FGF18	RD	125,047 autosomal SNPs	718 families (400 with RD)	[Field et al., 2013]
6p24	rs479526		Reading and spelling factors	2,373,249 imputed	6,127 individuals (children and adolescents)	[Luciano et al., 2013]
7p21	rs6954796		Phonological memory	2,373,249 imputed	6,583 individuals (children and adolescents)	[Luciano et al., 2013]
7p21	rs13307587		Reading and spelling factors; single word reading	2,373,249 imputed	6,127 individuals (children and adolescents)	[Luciano et al., 2013]
7q32	rs59197085	CCDC136	Reading and language factor	5,518,496 imputed	1,862 SLI/RD children and their nonaffected siblings	[Gialluisi et al., 2014]
8q24.1	rs2590673		RD	500,527 genotyped	353 SLI (based on test performance) and 4,117 controls (children)	[Eicher et al., 2013]
10p15	rs17135159		Reading and spelling factors	2,373,249 imputed	6,127 individuals (children and adolescents)	[Luciano et al., 2013]
10q23.3	rs1326167		Language factor	1,724,317 imputed	2,329 children	[Harlaar et al., 2014]
10q25.3	rs180950		RD	500,527 genotyped	353 SLI (based on test performance) and 4,117 controls (children)	[Eicher et al., 2013]
10q21.2	rs3213056	CDK1	Reading and spelling factor	2,373,249 imputed	6,127 individuals (children and adolescents)	[Luciano et al., 2013]
11p15.2	rs10734234	INSC	Expressive vocabulary in 15 month olds	2,449,665 imputed/ genotyped	8,889 individuals (toddlers)	[St Pourcain et al., 2014]
12q15	rs11176749	CAND1	Expressive vocabulary in 15 month olds	2,449,665 imputed/ genotyped	8,889 individuals (toddlers)	[St Pourcain et al., 2014]
13q21.3	rs1928007		Single word reading	2,373,249 imputed	6,135 individuals (children and adolescents)	[Luciano et al., 2013]
14q12	**rs11158632 (paternal effect)**		**SLI**	**614,937 genotyped**	**278 families (297 SLI children)**	[Nudel et al., 2014]
14q23	rs11158345	PRKCH	Single word reading	2,373,249 imputed	6,135 individuals (children and adolescents)	[Luciano et al., 2013]
16q22	rs764255	C16orf47	Single word reading	2,373,249 imputed	6,135 individuals (children and adolescents)	[Luciano et al., 2013]

Cytogenetic position	SNP	Closest known gene	Trait	SNP test, N	Total N	Reference
16q23	rs7187223		Single word reading	2,373,249 imputed	6,135 individuals (children and adolescents)	[Luciano et al., 2013]
19p13.3	rs1654584	DAPK3	Expressive vocabulary in 15 month olds	2,449,665 imputed/ genotyped	8,889 individuals (toddlers)	[St Pourcain et al., 2014]
19p13.3	rs4807927	DAZAP1	Reading and spelling factors; single word reading	2,373,249 imputed	6,127 individuals (children and adolescents)	[Luciano et al., 2013]
21q11.2	rs2192161	ABCC13	Phonological memory	2,373,249 imputed	6,583 individuals (children and adolescents)	[Luciano et al., 2013]
22q12.3	rs5995177	RBFOX2	Reading and language factors	5,518,496 imputed	1,862 SLI/RD children and their non-affected siblings	[Gialluisi et al., 2014]

Bold entries achieved genome-wide significance. Note that a comprehensive summary of the effect allele effect size and P value is given in Carrion-Castillo et al. (2016) along with replication results for many of these SNPs.
Located within the gene.

1.6.4 Moving Forward: Emergence of imaging-genetics approach

The emerging field of neuroimgaing genetics seek to better understand the language-brain-genetic relationships by establishing intermediate phenotypes at the neural level. As for linkage mapping and candidate gene approaches, the predominant research were regarding language impairments such as reading disability and developmental language disorder. Going forward, and with the recent availability of large-scale cohorts such as UK Biobank 2.1.1, more and more research focus on normal population and novel candidate genes arised from large GWASes. Indeed, GWASes of normal variation have been successful in demonstrating the importance of common SNP variation (minor allele frequency > 0.01) [Davies et al., 2016]. Findings from these both approaches are detailed below.

1.6.4.1 Neuroimaging genetics studies in developmental disorders

A comprehensive summary of research employing a neuroimaging genetic approach to study neurodevelopmental disorders of spoken and written language is given in [Landi and Perdue, 2019]. In this work, the authors have limited their review to studies that includes population with specific reading disability (SRD) and developmental language disorder (DLD) and no additional neurological or psychiatric diagnosis. The table 1.3 reports these findings.

Table 1.3 – Summary of imaging genetics findings related to reading/language. (Source: Landi and Perdue [2019].)

Gene	Chr Location	Function	Design	Imaging	N	Age	Ethnic Background	Phenotype (language/reading)	References
BDNF	11p13	Neuronal survival; Neuronal proliferation; Synaptic growth	Continuous	fMRI	81	6–10	70 Caucasian 1 African-American 2 Hispanic 3 Asian 5 Mixed ethnicity	Reading	[Jasińska et al., 2016]
C2orf3/ GCFC2/ MRPL19	2p11-q11.2	Unknown	Continuous	MRI; DTI	332	3-20	European	Reading	[Eicher et al., 2016]
			Continuous		76	6–25	98%European		[Scerri et al., 2012]
CMIP	16q23.2-q23.3	T-cell signaling	Case/control	MRI	54	5–12	NR	Reading	[Skeide et al., 2016]
COL4A2	13q34	Type IV collagen subunit encoding	Case/control	MRI	54	5–12	NR	Reading	[Skeide et al., 2016]
COMT	22q11.21	Dopamine metabolism	Case/control	fMRI	86	6–10	83 Caucasian 3 African-American	Reading	[Landi et al., 2013]
NRSN1	6p22.3	Neurite growth	Case/control	MRI	54	5–12	NR	Reading	[Skeide et al., 2016]
ROBO1	3p12.3	Neuronal migration; Axon guidance	Case/control	MEG	10	19–51	Finnish	Reading	[Lamminmäki et al., 2012]
CCDC136/ FLNC	7q32.1	Unknown	Continuous	MRI	1275	18–35	NR	Reading/ Language	[Gialluisi et al., 2017]
DCDC2	6p22	Neuronal migration	Continuous	fMRI	82	7–12	EuropeanAmerican	Reading/ Language	[Cope et al., 2012]
			SRD	EEG	200	8–19	German		[Czamara et al., 2011]
			Continuous	MRI DTI	76	6–25	98% European		[Darki et al., 2012]
			Continuous	MRI DTI	76	6–25	98% European		[Darki et al., 2014]
			Continuous	MRI DTI	332	3–20	European		[Eicher et al., 2016]
			Case/control	DTI	47	16–21	NR		[Marino et al., 2014]
			Continuous	MRI	56	19–85	NR		[Meda et al., 2008]
DYX1C1	15q21.3	Neuronal migration	Continuous	MRI DTI	76	6–25	98% European	Reading/ Language	[Darki et al., 2012]
			Continuous	MRI DTI	76	6–25	98% European		[Darki et al., 2014]
FOXP2	7q31	Transcriptional regulation Neurogenesis	Case/control	MRI	34	9–27	European		[Belton et al., 2003]
			Case/control	fMRI	20	19–56	European		[Liégeois et al., 2003]
			Continuous	fMRI	94	M = 24.7	European	Reading/ Language	[Pinel et al., 2012]
			Continuous	MRI	54	5–12	NR		[Skeide et al., 2016]
			Case/control	PET MRI	34	NR	European		[Vargha-Khadem et al., 1998]
			Case/control	MRI	34	9–27	European		[Watkins et al., 2002]
			Case/control	fMRI	33	M = 11	German		[Wilcke et al., 2012]
			Continuous	MRI DTI	76	6–25	98% European		[Darki et al., 2012]
KIAA0319	6p22	Neuronal migration	Continuous	MRI DTI	76	6–25	98% European	Reading/ Language	[Darki et al., 2014]
			Continuous	MRI DTI	332	3–20	European		[Eicher et al., 2016]
			Continuous	fMRI	94	M = 24.7	Primarily Caucasian		[Pinel et al., 2012]
RBFOX2	22q12.3	Alternative exon splicing regulation	Continuous	MRI	1275	18–35	NR	Reading/ Language	[Gialluisi et al., 2017]
SETBP1	18q12.3	DNA replication, apoptosis, transcription, nucleosome assembly	Continuous	fMRI	73	5–12	116 Caucasian 2 African American 3 Hispanic 4 Asian 8 mixed 2 unreported	Reading/ Language	[Perdue et al., 2019]
SLC2A3	4q32.1	Neural glucose transport regulation	SRD	EEG	200	8–19	German	Reading/ Language	[Roeske et al., 2011]
			Continuous	rsfMRI DTI	34	9–12	NR		[Skeide et al., 2015]
ACOT13/THEM2	6p22.3	Cell proliferation	Continuous	MRI; DTI	332	3–20	European	Reading/ Language	[Eicher et al., 2016]
			Continuous	fMRI	94	M = 24.7	Primarily Caucasian		[Pinel et al., 2012]
CNTNAP2	7q35	Cell adhesion Voltage-gated	Continuous	DTI	328	M = 23.4	Caucasian	Language	[Dennis et al., 2011]
			Continuous	fMRI	108	M = 26.3	Japanese		[Koeda et al., 2015]
			Continuous	MRI	54	5–12	NR		[Skeide et al., 2016]
			Continuous	MRI DTI	114	NR	NR		[Tan et al., 2010]
			Continuous	MRI	1717	M = 24.3	Primarily European Caucasian		[Uddén et al., 2017]
			Continuous	fMRI	66	M = 20.5	Caucasian		[Whalley et al., 2011]

1.6.4.2 Neuroimaging genetics studies in general population

Recent works investigate the language-brain-genetics relationships in general population and novel potential genes arising from GWASes have been proposed. These studies with a main focus on the brain asymmetry. [Carrion-Castillo et al., 2020] reported two loci (2q37 and 10p14) significantly associated with the planum temporale volumetric asymmetry including a coding polymorphism within the gene *ITIH5* that is predicted to affect the protein's function and to be deleterious and a locus that affects the expression of the genes *BOK* and *DTYMK*. Additionally, [Le Guen et al., 2020] reported a locus near *DACT1* to be associate with the superior temporal

sulcus depth. Both finding based on structural IDPs were emphasised by [Sha et al., 2021] who through a multivariate analysis, identified twenty-one loci involved in the left-right asymmetry, an important aspect of healthy brain organisation for many functions including language. These authors yield broader insights into biological pathways by proposing a role of the cytoskeleton[1] in the left–right axis determination. Although these results are particularly interesting, the relationship between brain asymmetry and language is still poorly understood. The table 1.4 summarise these findings.

[1]Cytoskeleton have an essential role in many cellular processes, such as cellular division, migration, and intracellular transport.

Table 1.4 – Summary of the genome-wide association signals from studies of left-right asymmetry (source: Sha et al. [2021]).

Cytogenetic position	SNP	Functional category	Effect allele	Effect allele frequency	mvGWAS P value	Nearest gene	Trait	N SNP	Total N	Samples	Design	Reference
2p23.3	rs62130503	NcRNA intronic	T	0.05	1.2210e10	MAPRE3	Thalamus (SUB), parahippocampal (SA)	9,803,522	32,256	UKB -british sample-	Multivariate GWAS	[Sha et al., 2021]
2p23.3	rs12617392	Intronic	A	0.44	4.0210e11	CGREF1	Inferior temporal (SA), caudal anterior cingulate (SA), isthmus of cingulate (SA)	9,803,522	32,256	UKB -british sample-	Multivariate GWAS	[Sha et al., 2021]
2q37	rs7420166	intronic	A	0.26	7.5410e10	BOK	Planum temporale asymmetry	8,011,919	16,515		Univariate GWAS	[Carrion-Castillo et al., 2020]
3q24	rs2279829	3ÚTR	T	0.22	1.2610e9	ZIC4	Isthmus of cingulate (CT) , precuneus (SA) , posterior cingulate (CT) , fusiform (SA)	9,803,522	32,256	UKB -british sample-	Multivariate GWAS	[Sha et al., 2021]
5q15	rs869219775	Intergenic	T	0.14	3.0610e9	NR2F1	Inferior parietal (SA), transverse temporal (SA)	9,803,522	32,256	UKB -british sample-	Multivariate GWAS	[Sha et al., 2021]
6p21.33	rs7781	Downstream	G	0.24	1.6210e10	TUBB	Isthmus of cingulate (CT), rostral anterior cingulate (CT), pars triangularis (SA)	9,803,522	32,256	UKB -british sample-	Multivariate GWAS	[Sha et al., 2021]
7p14.3	rs6947352	Intronic	A	0.31	4.3810e8	BBS9	Banks of the superior temporal sulcus (SA)	9,803,522	32,256	UKB -british sample-	Multivariate GWAS	[Sha et al., 2021]
9q22.33	rs911934	Intergenic	G	0.70	2.3910e15	GALNT12	Inferior parietal (SA), isthmus of cingulate (SA) , precuneus (SA), paracentral (SA), supramarginal (SA), entorhinal (CT)	9,803,522	32,256	UKB -british sample-	Multivariate GWAS	[Sha et al., 2021]
10p14	rs41298373	Exonic	A	0.10	4.7510e38	ITIH5	Superior temporal (SA) , parahippocampal (SA), fusiform (SA) , inferior temporal (CT) , transverse temporal (SA)	9,803,522	32,256	UKB -british sample-	Multivariate GWAS	[Sha et al., 2021]
					2.0110e15		Planum temporale asymmetry	15,120,452	18,057		Univariate GWAS	[Carrion-Castillo et al., 2020]
12q13.12	rs10783306	Intergenic	C	0.33	9.9910e12	TUBA1B	Superior frontal (SA), entorhinal (SA), medial orbitofrontal (SA), pars triangularis (SA)	9,803,522	32,256	UKB -british sample-	Multivariate GWAS	[Sha et al., 2021]
14q23.1	rs160459	Intergenic	C	0.46	4.9810e12	DACT1	Banks of the superior temporal sulcus (SA), transverse temporal (SA), pericalcarine (SA)	9,803,522	32,256	UKB -british sample-	Multivariate GWAS	[Sha et al., 2021]
					4.2x10e12		superior temporal asymmetrical pit	8,011,919	16,515		Univariate GWAS	[Le Guen et al., 2020]
16q24.3	rs72813426	Intronic	G	0.24	2.4510e14	SPIRE2	Paracentral (SA), isthmus of cingulate (SA), middle temporal (SA)	9,803,522	32,256	UKB -british sample-	Multivariate GWAS	[Sha et al., 2021]
16q24.3	rs111398992	Intronic	T	0.13	5.9910e15	TUBB3	Isthmus of cingulate (CT), fusiform (SA), rostral anterior cingulate (CT), pericalcarine (SA)	9,803,522	32,256	UKB -british sample-	Multivariate GWAS	[Sha et al., 2021]
17q21.31	rs55938136	NcRNA intronic	G	0.22	4.9110e15	CRHR1	Parahippocampal (SA), middle temporal (SA), pallidum (SUB), hippocampus (SUB), pars triangularis (SA)	9,803,522	32,256	UKB -british sample-	Multivariate GWAS	[Sha et al., 2021]
17q21.31	rs35908989	Intronic	C	0.23	1.3410e8	MAPT	Supramarginal (SA), caudate (SUB)	9,803,522	32,256	UKB -british sample-	Multivariate GWAS	[Sha et al., 2021]
17q21.31	rs80103986	Intronic	T	0.20	5.1610e16	KANSL1	Parahippocampal (SA), middle temporal (SA), pallidum (SUB), hippocampus (SUB), pars triangularis (SA)	9,803,522	32,256	UKB -british sample-	Multivariate GWAS	[Sha et al., 2021]
19p13.3	rs11672092	Intronic	T	0.22	5.6910e10	TUBB4A	Isthmus of cingulate (CT), lateral orbitofrontal (SA), middle temporal (SA)	9,803,522	32,256	UKB -british sample-	Multivariate GWAS	[Sha et al., 2021]
20p12.1	rs6135555	Intronic	A	0.39	7.0010e9	MACROD2	Pericalcarine (SA), caudate (SUB)	9,803,522	32,256	UKB -british sample-	Multivariate GWAS	[Sha et al., 2021]
21q22.3	rs7283026	Intronic	C	0.27	8.4210e10	COL18A1	Supramarginal (SA), transverse temporal (SA)	9,803,522	32,256	UKB -british sample-	Multivariate GWAS	[Sha et al., 2021]
22q13.31	rs9615351	Exonic	G	0.25	3.0210e8	CELSR1	Isthmus of cingulate (CT), transverse temporal (SA)	9,803,522	32,256	UKB -british sample-	Multivariate GWAS	[Sha et al., 2021]
Xp22.33	rs12400461	Intergenic	C	0.58	1.2410e8	ASS1P4	Inferior temporal (SA), pars opercularis (SA)	9,803,522	32,256	UKB -british sample-	Multivariate GWAS	[Sha et al., 2021]

Bold entries were replicated in an external sample

1.6.4.3 Discussion

Several approaches combined with a variety of (endo)phenotypes have been considered for the language-brain-genetic study. Through linkage analysis and after with genome-wide association studies, numerous findings were highlighted regarding language trait. These illustrate the complex neurobiological underpinnings of human language. Whether regarding targeted genetic association or exploratory genome-wide association study, replication of genetic associations with language (endo)phenotypes has emerged as an important limitation in the literature. Additional concerns regarding sample size and power, correction for multiple testing, unreported effect size have been arised regarding neuroimaging field. Accordingly, language-brain studies should be interpreted with caution.

Notwithstanding the literature regarding genetic of human language is quite rich, we are still

quite far from understanding which part of the genome codes for language, or how genetic differences lead to different language abilities.

1.7 Aim of this thesis

The main aim of this thesis was to improve our understanding of the genetic underpinnings of human language. To this end, we investigated common genetic variants that might affect human language related quantitative trait. We determined the inter-individual variations in brain function and structure that reflect specific language as neurocognitive traits and studied the potential associations between the observed inter-individual variability of language trait and the genotype profile.This study took advantage of two well known large-scale cohorts suitable for imaging-genetic studies; the UK Biobank and the Human Connectome Project. These two large-scale cohorts comprise detailed genotyping and a wide variety of endophenotypes ranging from health/activity questionnaires, extended demographics to neuroimaging and clinical health records.

First, in chapter 3, we present an experimental design set up to highlight interesting endophenotypes representative of human language. Different imaging modalities were considered. Using resting-state fMRI, we built endophenotypes estimating rsfMRI functional connectivities between perisylvian cortical ROIs drawn from an exhaustive meta-analysis of task-based fMRI language studies. Using diffusion MRI, we determined endophenotypes from well-known language related white matter bundles. Using task-based fMRI, we extracted language-brain activation using the perisylvian cortical ROI aforementioned.

Second, in chapter 4, we provided a contribution to the study of human language heritability by presenting in-depth results on it using both psychometric and imaging derived endophenotypes as presented in the chapter 3 using the two aforementioned large-scale resources currently available.

Third, in chapter 5, we performed bivariate genetic analyses to quantify the shared genetic influence between human language performance, and brain functional manifestations of language represented by both neural activation measured in language task fMRI experiments and functional connectivity estimated in resting-state fMRI. To this end, we took advantage of the Human Connectome Project cohort which comprises language-related scores, language task-based fMRI data as well as resting-state fMRI data.

Fourth, in chapter 6, we contributed to enlighten the genetic architecture of language functional connectivity by exhibiting potential key genes related to language processing. We performed a multivariate genome-wide association study on 32,186 participants from UK Biobank using significantly heritable resting-state FC endophenotypes as highlighted in the chapter 4. The results obtained were then subjected to a replication study in an independent sample (N=4,754). Next we performed an extensive functional annotations of each genomic risk locus which allowed us to suggest new genes with a role in different aspects of the language processing system.

Fifth, in Chapter 7, we adopted a similar experimental design than the one presented in the chapter 6 to study the genetic architecture of anatomical connectivity. We performed a mvGWAS between genetic variants and diffusion features measured in well-known language-related

white matter bundles, on 31,775 participants from UK Biobank. The findings suggested new candidate genes involved in different brain organisation.
Finally, in the general conclusion, we have summarised and reviewed the main findings of the experimental chapters (i.e. chapter 4 to 7), and discussed future perspectives of the genetics of human language, in relation to the complementary approaches that were considered within these studies.

* * *
* *
*

Chapter 2

Materials and methods

Chapter Outline

2.1 Cohorts 46
2.1.1 UK Biobank 46
2.1.2 Human Connectome Project 49
2.2 Definition of brain regions and tracts of interest 52
2.2.1 Functional connectomes 52
2.2.2 Anatomical connectomes 56
2.3 Rank-based inverse-normal transformation 59
2.4 Heritability 59
2.5 Genetic correlation 60
2.6 Massive univariate and multivariate genome-wide association study 60
2.7 Fine-mapping: identification of genomic risk loci and functional annotations . . . 63
2.7.1 FUMA: SNP2GENE 63
2.7.2 FUMA: GENE2FUNC 64
2.8 Protein networks 64

In this chapter, we present the two cohorts and the statistical methods that we used to answer the questions regarding the genes that underlie human language processing in order to see how genetic variation influences this system variation. In the first part of this chapter, we introduce the two imaging-genetics cohorts used in the manuscript. We provide as well, details on the demographics, the neuroimaging and the genetic data available in both UK Biobank (UKB) and the Human Connectome Project (HCP). The second part of this chapter concerns the definition of the regions of interest that underlie language in human brain. This step is crucial and difficult to determine as the adequate choice of ROIs may vary depending on different conditions such as the experimental design or pathologies. This choice constitutes the entry point of our study and will lay the foundations for the neuroimaging genetic studies performed. Image-derived phenotypes will be extracted using these ROIs. Details on the standard methods used in the literature to estimate these endophenotypes will be discussed further. The next sections of this chapter describe the state-of-the-art genetic methods that are today largely adopted by the imaging-genetics community. More precisely, the heritability and genetic correlation estimation, as well as genome-wide association studies (GWAS) using massive univariate methods will be described. Also, innovative multivariate approaches for GWAS will be presented. Finally, the last part is dedicated to presenting how to relate the candidate variants identified from GWAS to biological functions or processes. This step is performed through a statistical fine-mapping and proteomics interactions. It is essential in order to select and prioritise genetic variants linked to language.

2.1 Cohorts

To investigate the neurobiology of language in human brain, we took advantage of two well known large-scale cohorts; the UK Biobank and the Human Connectome Project. These open-acces cohorts comprises detailed genotyping, neuroimaging data and cognitive-behavioural assessments which make them suitable for imaging-genetics studies.

2.1.1 UK Biobank

The UK Biobank is an open-access longitudinal population-wide cohort that includes 500k participants from all over the United Kingdom [Sudlow et al., 2015]. Data collection comprises detailed genotyping and a wide variety of endophenotypes ranging from health/activity questionnaires, extended demographics to neuroimaging and clinical health records. All participants provided informed consent and the study was approved by the North West Multi-Centre Research Ethics Committee (MREC).

This study used the February 2020 release (UK BioBank application number #64984). This release consisted of 41,670 participants, age range between 40 to 70 years (21,135 females, mean age=54.9 $\pm$7.47 years), with genotyping and brain imaging data including resting-state functional MRI and/or diffusion MRI. Furthermore, to avoid any possible confounding effects related to ancestry, we restricted our analysis to individuals with British ancestry using the sample quality control information provided by UK Biobank [Bycroft et al., 2018]. A final

cohort of 35,366 volunteers (18,298 females, mean age = 55.1 ±7.43 years) were included. The potential remaining cryptic population structure can be a severe confound to genetic association studies [Marchini et al., 2004]. It was accounted for by considering the first ten principal components (Data field 22009) of the principal component analysis of the genetic data and were included as covariates. We used the 5,286 non-British individuals drawn from the UK Biobank as an independent replication dataset. The age range of these participants was 40 to 70 (2,837 females, mean age = 53 ±7.59 years). It is noteworthy that UK Biobank uses its 22 centres across the UK to collect brain imaging. Three scanning centres were represented in our sample (Cheadle, Reading, and Newcastle). This difference in scanning hardware may lead to a site-specific variability in the imaging. To overcome this limitation, we identified the imaging centre information (Data field 54) and considered the scanning site as a confound-regressor variable. Details about data acquisition parameters, data processing of multi-modalities of MRI images used in our studies as well as details about genetic data and the quality control applied will be summarised and presented below. For additional technical details, refer to the UK Biobank Brain Imaging Documentation (v.1.7, January 2020) as well as to [Alfaro-Almagro et al., 2018, Miller et al., 2016].

2.1.1.1 Data acquisition details on UKB samples

Two MRI modalities were considered throughout the manuscript as each of them potentially captures unique neurobiological details: resting state functional MRI (rsfMRI) and diffusion-weighted MRI (DW-MRI). The acquisition parameters used for each modality are described here.

Resting-state functional MRI data. Resting-state functional MRI (rsfMRI) captures low-frequency fluctuations in blood oxygenation from which functional connectivity is then estimated Biswal et al. [1995]. rsfMRI data were acquired on 3T Siemens Skyra scanner using the following parameters:

- Resolution: $2.4 \times 2.4 \times 2.4 mm^3$,
- Field-of-view matrix: $88 \times 88 \times 64$,
- Repetition time (TR) = 0.735 s,
- Echo time (TE) = 39 ms,
- Acquisition time = 6 min.

As a result, 3D volumes of the volunteers' brain are acquired every 0.735s during 6 minutes resulting in 490 brain volumes in time represented by a 4D image. All images were acquired in Anterior-Posterior phase encoding direction. During the resting-state scan, participants were instructed to keep their eyes fixated on a crosshair, to relax, and to think of nothing in particular [Miller et al., 2016].

Diffusion-weighted MRI data. Diffusion-weighted imaging is a noninvasive, *in vivo* MRI technique that quantifies water diffusion in biological tissues. It is used to map structures and

measures their local organisation by tracking the movements of water molecules contained in the brain tissues. The Diffusion-weighted MRI (DW-MRI) images were acquired using a 3T Siemens Skyra scanner with the following parameters;

- Resolution: $2 \times 2 \times 2mm^3$,
- Five non diffusion-weighted image b=0 s/mm^2,
- Diffusion-weighting of b=1000, and 2000 s/mm^2 with 50 directions each,
- Acquisition time: 7 min,

2.1.1.2 Data processing details on UKB samples

All the MRI data preprocessing steps were carried out by UK Biobank brain imaging team using FSL software (http://www.fmrib.ox.ac.uk/fsl). The preprocessing applied to each modality is described here.

Resting-state functional MRI data. We applied the following preprocessing pipeline on rsfMRI data before we extracted the IDPs. It includes motion correction using MCFLIRT [Jenkinson et al., 2002], grand-mean intensity normalisation, high-pass temporal filtering (Gaussian-weighted least-squares straight line fitting, with $\sigma = 50.0$ s) including the unwarping of EPI (echo planar imaging) and co-registration to T1 template and gradient non-linearity distortion correction (GDC), brain masking, and registration to the MNI (Montreal Neurological Institute-Hospital) space. The rsfMRI volumes were further cleaned using ICA-FIX (Independent Component Analysis followed by FMRIB's ICA-based X-noiseifier [Beckmann and Smith, 2004, Griffanti et al., 2014, Salimi-Khorshidi et al., 2014] for automatically identifying and removing artefacts.

Diffusion-weighted MRI data. We applied the following preprocessing pipeline on dMRI data before we extracted the IDPs. It includes: correction for eddy current distortions, head motion and has outlier-slices (individual slices in the 4D data) corrected, using Eddy (https://fsl.fmrib.ox.ac.uk/fsl/fslwiki/EDDY) [Andersson and Sotiropoulos, 2015]. A gradient distortion correction (GDC) is applied to these corrected images, resulting in the 4D output file. The preprocessed images were then further fed into the software DTIFIT (Diffusion Tensor Imaging Fitting procedure from FSL) to model the 50 diffusion directions to generate DTI outputs, e.g. FA (fractional anisotropy), MO (tensor mode), MD (mean diffusivity). In addition to the DTI fitting, the preprocessed images were fed into NODDI (Neurite Orientation Dispersion and Density Imaging) [Zhang et al., 2012] estimates using AMICO (Accelerated Microstructure Imaging via Convex Optimization) [Daducci et al., 2015]. This enabled modeling the biological properties of fiber tracts visible in the form of ICVF (intra-cellular volume fraction - an index of white matter neurite density), ISOVF (isotropic or free water volume fraction) and OD (orientation dispersion index, a measure of within-voxel tract disorganisation). Furthermore, in order to facilitate cross-subject comparisons on fiber tract based IDPs, all the outputs were aligned onto a common space with TBSS (Tract-Based Spatial Statistics) [Smith et al., 2006].

2.1.1.3 Genetic data: genotyping and imputation

The UK Biobank genetic data contain genotypes for 488,377 participants. Genotyping was performed using the UK BiLEVE Axiom array by Affymetrix [Wain et al., 2015] on a subset of 49,950 participants (807,411 markers) and the UK Biobank Axiom array on 438,427 participants (825,927 markers). Both arrays are extremely similar and share 95% of common SNP probes. Further details are available in [Bycroft et al., 2018]. Genotype imputation is the process of statistically infer unobserved genotypes using a reference panel haplotypes. It densifies the number of SNPs that can be tested, and facilitates combining GWAS summary statistics across studies. The process of imputation is twofold: pre-phasing, and imputation. First, in the pre-phasing step, a statistical method is applied to genotype data to infer the underlying haplotypes of each individual. Second, the inferred haplotypes are combined with a reference panel (*UK10K haplotype* reference merged with *1000 Genomes Phase 3* reference panel) and the unobserved genotypes are predicted (imputed). The imputation process is extensively described here https://biobank.ctsu.ox.ac.uk/crystal/ukb/docs/impute$_u kb_v$1.*pdf*. Imputation was carried out with the IMPUTE4 program (https://jmarchini.org/software/). The result of the imputation process is a dataset with 93,095,623 autosomal SNPs, short indels and large structural variants in 487,442 individuals. The imputed genotypes, obtained from the UK Biobank repository, were provided in BGEN file format (https://enkre.net/cgi-bin/code/bgen/dir?ci=trunk) and consisted of 93,095,623 autosomal SNPs, short indels, and large structural variants. See [Bycroft et al., 2018] for more details.

Quality control protocol. Before all analyses, the genetic data underwent a stringent quality control protocol, excluding participants with unusual heterozygosity, high missingness (Data field 22027), sex mismatches, such as discrepancy between genetically inferred sex (Data field 22001) and self-reported sex (Data field 31). Variants with minor allele frequency (MAF) < 0.01 were filtered out from the imputed genotyping data using PLINK 1.9 [Chang et al., 2015] to retain the common variants only.

2.1.2 Human Connectome Project

The Human Connectome Project (HCP) is an open-access population-wide cohort study that includes 1,206 participants with extensive MRI, behavioural measurements, and whole genome genotyping data, released in April 2018 [Van Essen et al., 2013]. All participant are healthy young adult twins and non-twin siblings ranged in age from 22 to 37 years old and free from current psychiatric or neurological illnesses. They provided informed consent and the study was approved by the Institutional Review Board of Washington University.

This study used the HCP S1200 release. This release consisted of 1,113 volunteers, age range between 22 to 37 years (606 females, mean age=28.8$\pm$3.7 years), who underwent an MRI experience. Furthermore, to avoid any possible confounding effects related to ancestry, we restricted our analysis to individuals identified as Caucasian using the sample quality control information provided by the Human Connectome Project [Van Essen et al., 2013]. The potential remaining cryptic population structure were accounted for by considering the first four principal compon-

ents of the principal component analysis of the genotype data covering 78.75% of the explained variance (See Fig. A.1). These were included as covariates. Details about data acquisition parameters, data processing of multi-modalities of MRI images used in our studies as well as details about genetic data and the quality control applied will be summarised and presented below. For additional technical details, refer to the the Human Connectome Project S1200 Subjects Data Release Reference Manual (10 April 2018) (https://www.humanconnectome.org/) and to [Van Essen et al., 2013].

2.1.2.1 Data acquisition details on HCP samples

Two MR imaging modalities were considered in the manuscript as each of them potentially captures unique neurobiological details: resting state functional MRI (rsfMRI) and task-based functional MRI (tfMRI). Briefly, the acquisition parameters used for each modality are described here.

Resting-state functional MRI data.
Resting-state functional MRI (rsfMRI) data were acquired on 3T Siemens "Connectom Skyra" scanner using the following parameters:

- Resolution: $2.0 \times 2.0 \times 2.0 mm^3$,
- Field-of-view matrix: $208 \times 180 mm$,
- Repetition time (TR) = $720 ms$,
- Echo time (TE) = $33.1 ms$,
- Acquisition time = 14 : 33 min.

As a result, 3D volumes of the volunteers' brain are acquired every 720 ms during 14:33 minutes resulting in 1200 brain volumes in time represented by a 4D image. All images were collected over two scanning sessions. Each session consists of two runs that were acquired in an alternate opposite phase encoding directions (right-to-left (RL) and left-to-right (LR)), for a total of approximately 1 h of resting-state data collected for each participant. During the resting-state scan, participants were instructed to keep their eyes open with relaxed fixation on a projected bright cross-hair on a dark background and presented in a darkened room [Van Essen et al., 2013].

Task-based functional MRI data.
Task-based functional MRI images captures changes in the activity of the neuronal populations and seek to induce different neural states in the brain [Logothetis, 2008]. The task-based functional MRI (tfMRI) images were acquired on 3T Siemens "Connectom Skyra" scanner with the same EPI pulse sequence parameters as for rsfMRI data:

- Resolution: $2.0 \times 2.0 \times 2.0 mm^3$,
- Field-of-view matrix: $208 \times 180 mm$,

- Repetition time (TR) = 720ms,
- Echo time (TE) = 33.1ms,
- Acquisition time = 14 : 33 min.

Seven tasks of two runs each were acquired in an alternate opposite phase encoding directions (L/R, R/L): Working Memory (Duration=5:01 min, Frames per run=405), Gambling (Duration=3:12 min, Frames per run=253), Motor (Duration=3:34 min, Frames per run=284), Language (Duration=3:57 min, Frames per run=316), Social Cognition (Duration=3:27 min, Frames per run=274), Relational Processing (Duration=2:56 min, Frames per run=232), Emotion Processing (Duration=2:16 min, Frames per run=176). These tasks are described in more detail in [Barch et al., 2013]. During the task-based experience, stimuli were projected onto a computer screen behind the volunteer's head and the screen was viewed by a mirror positioned approximately 8 cm above the volunteer's face. Relevant to our work, we will describe the language task experiment implemented in the HCP cohort.

The language task.

The language task implemented in the Human Connectome Project cohort was developed by Binder and colleagues [Binder et al., 2011]. It consists of two runs that each interleaves 4 blocks of a story task and 4 blocks of a mathematics task. The story task presents participants with brief auditory stories adapted from Aesop's fables, followed by a 2-alternative forced choice question about the topic of the story. The example provided in the original Binder paper (p. 1466) is "For example, after a story about an eagle that saves a man who had done him a favour, participants were asked, "Was that about revenge or reciprocity?". The math task aurally presents to participants a series of arithmetic operations (e.g., "fourteen plus twelve"), followed by "equals" and then two choices (e.g., "twenty-nine or twenty-six"). Participants requires to complete these arithmetic operations. The math task is adaptive in order to try to maintain a similar level of difficulty across participants. The length of each block varies (average of approximately 30 seconds), but the task was designed so that both task blocks length match. Refer to [Binder et al., 2011] and to HCP manual (https://www.humanconnectome.org/) for more details.

2.1.2.2 Data processing details on HCP samples

All the MR data preprocessing steps were carried out by the HCP brain imaging team using the minimal preprocessing pipeline described in [Glasser et al., 2013]. Briefly, the preprocessing of resting-state functional MR images includes correction for B0 distortion, registration to the participant's structural scan, normalisation to the 4D mean, brain masking, and non linear warping to MNI space. The volumes were denoised as well by using 24 confound time series derived from the motion estimation (3 rotations, 3 translations, their first derivatives and all 12 resulting regressors squared) followed by ICA-FIX denoising. The spatial preprocessing steps for task-based functional MRI are identical to those used for rsfMRI.

2.1.2.3 Genetic data: genotyping

The HCP genetic data contain genotypes for 1,142 of the 1206 total released participants, including 149 pairs of genetically-confirmed monozygotic twins (298 participants) and 94 pairs of genetically-confirmed dizygotic twins (188 participants). Overall, there are 457 different families in the study, as determined by genetic analysis. These data were released on the database of Genotypes and Phenotypes (dbGaP) on March 1st, 2018. Genotyping data were obtained under dbGaP application number #17771 (dbGaP Study Accession: phs001364.v1.p1). Genotyping completed on Infinium Multi-Ethnic Genotyping Array (MEGA) chip with PsychChip and ImmunoChip content (2,052,643 markers). Further details are available in [Elam et al., 2021, Van Essen et al., 2012] and https://www.ncbi.nlm.nih.gov/.

2.2 Definition of brain regions and tracts of interest

In the chapter 1.3, we introduced state-of-art methods that are generally used to analyse MRI data. In this work, we have chosen to address the genetics of the human language connectome using the region of interest approach. The first step of this approach consists on identifying a set of functional regions of interest that fits our needs. This step is an important, albeit difficult, choice. In this section, we provide details about the choice of the ROIs and the tools used to generate them regarding both human language functional and anatomical connectivity.

2.2.1 Functional connectomes

Different methods to estimate the functional connectomes exists in the literature (see chapter 1.3.2 for more details). During my thesis, we focused on the ROIs-based approach. This choice was motivated by two complementary reasons. First, as participants during resting-state are not engaged in any language task-experiments, the use of regions identified through task paradigm, ensures the validity of the resting-state signal masked regarding language processing. Second, this approach provides a greater interpretability regarding the different subprocesses implied by these regions. This is achieved by taking advantage of the richness of the knowledge acquired during task experiences and the derived contrasts. In this work, two sets of regions of interest were employed for defining the language network. At the beginning of this thesis, we had chosen a set of regions of interest that includes the perisylvian regions which cover both Broca and Wernicke's areas. Later, we decided to look at a more extended language network and identified a meta-analysis regrouping and analysing a significant number of scientific reports. This meta-analysis offered a more general view of the language regions, a rich interpretation of the regions' classification regarding language components (phonology, semantic and syntax) and more importantly, it offers potentially a more consensual set of ROIs within the neuroscientific community. These sets of regions will be successively defined below. To refer to the regions defined under each set of ROIs, we use the following terms: Supramodal phonology, semantics and sentence processing (SmPSS) for the latter one, and one-contrast sentences structure (OcSS) for the former one. The core steps of the used pipeline for the functional connectome estimation are common to both UK Biobank and HCP imaging data. It is estimated from each set of brain

ROIs that form brain parcellations (nodes) by measuring their pairwise interactions termed as functional connectivity (edges). It is worth noting that all regions with less than 100 voxels were excluded from the derived analyses.

One-contrast sentences structure (OcSS). OcSS was defined based on the probabilistic activation map of a single fMRI contrast [Pallier et al., 2011]. This atlas of 7 supramodal areas, estimated on a group of 20 healthy participants, is based on activation during language comprehension. These regions of interest are located in the frontal and temporal lobe and refer to the inferior frontal activations centred on the pars triangularis (BA45/44) and pars orbitalis (BA 45/47) and along the superior temporal sulcus from its anterior part to the temporal pole junction. These ROIs are summarised in Fig. 2.1.

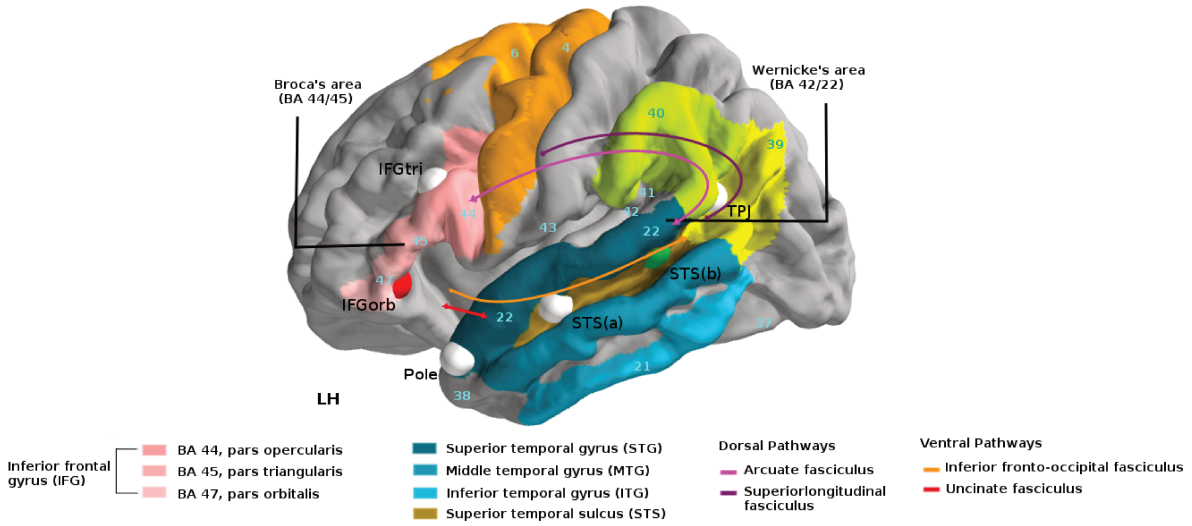

Figure 2.1 – **Overview of the regions obtained from** [Pallier et al., 2011]. Each language seed is color-coded according to its language category: phonology (blue), semantic (red), and syntax (green). ROIs of different components that were not spatially distinct are color-coded as pink (semantic/syntax), cyan (phonology/semantic) and white for the three language component. Different gyri and sulcus, known to be relevant for language: the inferior frontal gyrus (IFG), middle temporal gyrus (MTG), superior temporal gyrus (STG), and superior temporal sulcus (STS), are color-coded. Numbers in the left hemisphere (LH) represents language-relevant Brodmann areas (BA) which were defined on the basis of cytoarchitectonic characteristics. The pars opercularis (BA 44), the pars triangularis (BA 45) represents Broca's area. The pars orbitalis (BA 47) is located anterior to Broca's area. BA 42 and BA 22 represents Wernicke's area Friederici [2011]. Both supramarginal gyrus (BA40) and angular gyrus (BA39), also known as Geschwind's territory, are represented by green and yellow colors respectively. The primary motor cortex (BA4), the premotor cortex and the supplementary motor area (B6) are colored in orange. Within the left hemisphere, dorsal and ventral long-range fiber bundles connect language areas and are indicated by color-coded arrows.

Supramodal areas: phonology, semantics and sentence processing (SmPSS). We leverage a large-scale meta-analysis of 946 activation peaks (728 peaks in the left hemisphere, 218 peaks in the right hemisphere) obtained from a meta-analysis of 129 task-based fMRI language studies [Vigneau et al., 2006, 2011]. The identified fronto-parietal-temporal activation foci revealed via a hierarchical clustering analysis, 50 distinct, albeit partially overlapping, clusters of activation foci for phonology, semantics, and sentence processing: 30 clusters in the left hemisphere and 20 in the right hemisphere.

Because this overlap could unduly increase the co-activation between regions and to avoid a deconvolution bias in the estimation of the functional connectivity, we proceeded as follows. First,

because the clustering process was performed for each component independently, we checked whether pairs of clusters belonging to different language-component networks were spatially distinct considering the significance of their mean Euclidean distance with paired t-tests. We identified areas that are common to multiple language components; in the temporal lobe, the anterior part of the superior temporal gyrus (T1a) area appears to be common to all three language components, the anterior part of the superior temporal sulcus (Pole) and Lateral/middle part of the middle temporal gyrus (T2ml) are common to semantic and sentence's clusters and the posterior part of the left inferior temporal gyrus (T3p) to semantic and phonology clusters. In the frontal lobe, the L|R dorsal part of the pars opercularis (F3opd) and the ventral part of the pars triangularis (F3tv) are common to semantic and syntactic clusters. In these cases, we retained the larger cluster and assigned it multiple labels. Second, ROIs were obtained for each cluster by building a 3D convex-hull of the peaks in the MNI space and were then subjected to a morphological opening operation. Third, in case of overlap between the convex-hull ROIs, the common region between the two ROIs was attributed to the most representative in terms of the number of peaks. This preprocessing resulted in 25 multilabelled ROIs: 19 in the left hemisphere and 6 in the right hemisphere which are summarised in Fig. 2.2 and Table 2.1.

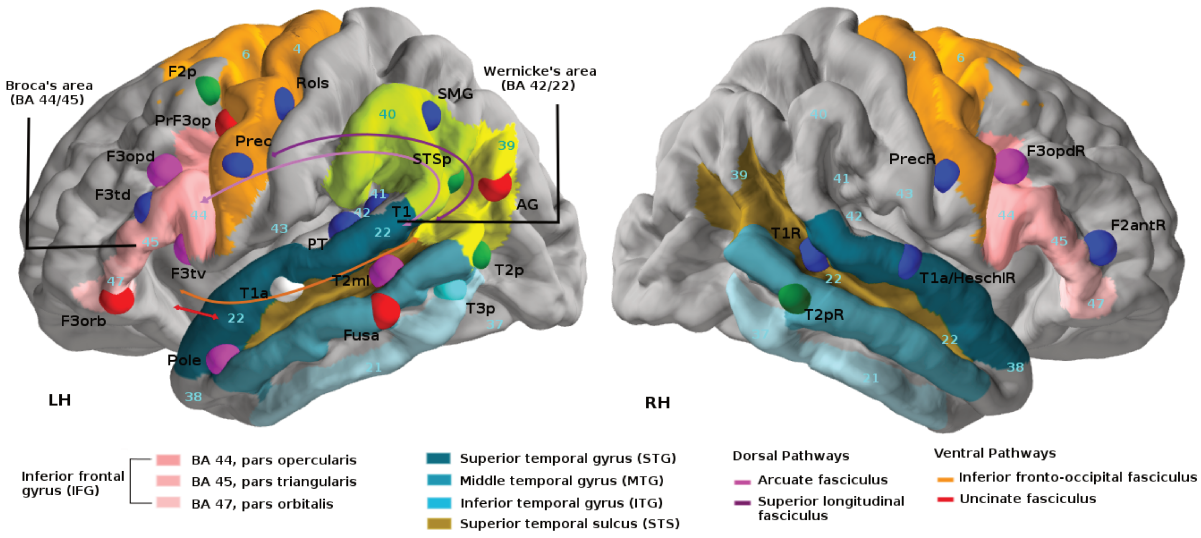

Figure 2.2 – **Overview of the regions obtained from the meta-analysis.** Each language seed is colour-coded according to its language category: phonology (blue), semantic (red), and syntax (green). ROIs of different components that were not spatially distinct are colour-coded as pink (semantic/syntax), cyan (phonology/semantic) and white for the three language component. For the sake of ROIs figure visibility, the coordinates were modified. The exact coordinates for each ROI are available in Table 2.2. Different gyri and sulcus, known to be relevant for language: the inferior frontal gyrus (IFG), middle temporal gyrus (MTG), superior temporal gyrus (STG), and superior temporal sulcus (STS), are color-coded. Numbers in the left hemisphere (LH) represents language-relevant Brodmann areas (BA) which were defined on the basis of cytoarchitectonic characteristics. Numbers in the right hemisphere (RH) represents the language-relevant BA counterpart. The pars opercularis (BA 44), the pars triangularis (BA 45) represents Broca's area. The pars orbitalis (BA 47) is located anterior to Broca's area. BA 42 and BA 22 represents Wernicke's area [Friederici, 2011]. Both supramarginal gyrus (BA40) and angular gyrus (BA39), also known as Geschwind's territory, are represented by green and yellow colours respectively. The primary motor cortex (BA4), the premotor cortex and the supplementary motor area (B6) are coloured in orange. Within the left hemisphere, dorsal and ventral long-range fibre bundles connect language areas and are indicated by colour-coded arrows.

Table 2.1 – Overview of the regions obtained from the meta-analysis. Each ROI is characterised by its abbreviated anatomical label defined by Vigneau et al. [2006, 2011] and is labelled according to the language component it belongs to: phonology, semantic, and syntax.

Hemisphere	Regions of interest	Phonology	Semantic	Sentence
Left hemisphere	Planum temporale (PT)	✓		
	Rolandic sulcus (RolS)			
	Superior temporal gyrus (T1)	✓		
	Supramarginalis gyrus (SMG)	✓		
	Precentral gyrus (Prec)			
	Dorsal part of the pars triangularis of the inferior frontal gyrus (F3td)	✓		
	Anterior fusiform gyrus (Fusa)		✓	
	Opercular part of the inferior frontal gyrus (PrF3op)		✓	
	Angular gyrus (AG)			
	Pars orbitaris of the left inferior frontal gyrus (F3orb)			
	Posterior part of the middle frontal gyrus (F2p)			✓
	Posterior ending of the superior temporal gyrus (STSp)			
	Posterior part of the middle temporal gyrus (T2p)			✓
	Temporal pole (Pole)			
	Lateral/middle part of T2 (T2ml)		✓	✓
	Posterior part of the left inferior temporal gyrus (T3p)	✓	✓	
	Dorsal part of the pars opercularis (F3opd)			
	Ventral part of the pars triangularis (F3tv)		✓	✓
	Anterior part of T1 (T1a)	✓	✓	✓
Right hemisphere	Anterior part of the middle frontal gyrus (F2antR)	✓		
	Precentral gyrus (PrecR)			
	Anterior part of tT1 overlapping the Heschl's gyrus (T1a/HeschlR)	✓		
	Superior temporal gyrus (T1R)	✓		
	Middle part of the STS (T2pR)			✓
	Upper part of the pars opercularis of F3 (F3opdR)		✓	✓

Table 2.2 – Centre of mass of the language processing regions of interests retained in both left and right hemispheres. Each ROI is characterised by its abbreviated anatomical label defined by [Vigneau et al., 2006, 2011] and its centre of mass MNI stereotactic coordinates (x, y, z, in mm).

Hemisphere	ROIs	x	y	z
Left hemisphere	Prec	-46.76	2.01	25.85
	RolS	-45.28	-9.40	44.17
	F3orb	-35.82	35.30	-10.77
	T3p	-45.90	-56.48	-7.35
	F3td	-42.15	25.10	14.54
	T2p	-39.30	-65.25	2.05
	SMG	-40.68	-50.25	40.86
	T1a	-54.07	-11.85	-5.85
	F3tv	-45.20	14.24	4.23
	STSp	-47.12	-56.92	24.07
	PrF3op	-39.61	2.90	39.34
	Fusa	-35.27	-37.17	-12.89
	T1	-50.46	-38.56	14.32
	T2ml	-54.99	-39.62	-2.84
	F2p	-34.72	10.94	48.80
	F3opd	-43.90	21.97	25.70
	PT	-59.89	-28.11	8.67
	Pole	-45.00	5.19	-26.79
	AG	-43.93	-70.85	22.20
Right hemisphere	T1R	51.84	-38.51	3.40
	F3opdR	49.67	14.93	27.48
	F2antR	46.64	39.80	5.06
	T2pR	54.76	-42.11	-7.73
	T1a/HeschlR	56.54	-13.38	0.81
	PrecR	52.68	-1.49	24.15

2.2.2 Anatomical connectomes

The core steps of a pipeline for the anatomical connectivity estimation are common to both UK Biobank and HCP imaging data. Although the UK Biobank team provides two types of meaningful diffusion IDPs, these do not include all key language white matter tracts making them not the most adapted to our study. Starting from this observation, we identified one set of tracts of interest that comprises well-known language white matter bundles and used it as a standard-space mask. Details about this atlas are provided below.

Atlas of Human-language Brain Connections Spherical deconvolution tractography of frontal white matter connections was performed by [Rojkova et al., 2016], resulting in a probabilistic atlas of the interlobar, commissural, projection and short U-shaped tracts in a population with a large age range. This atlas provides probabilistic maps of the well known white matter tracts that connects the different brain areas including language brain areas. The latter are represented by the three branches of the superior longitudinal fasciculus (SLF I, II, III), the uncinate fasciculus, the three segments of the arcuate fasciculus (anterior, long, posterior), the

inferior fronto-occipital fasciculus (IFOF), the frontal U-shaped tracts, the frontal aslant tract (FAT), five U-shaped fronto-insular tracts (FITs) and the frontal corpus callosum which connect both hemispheres. These tracts are summarised in Fig.2.3

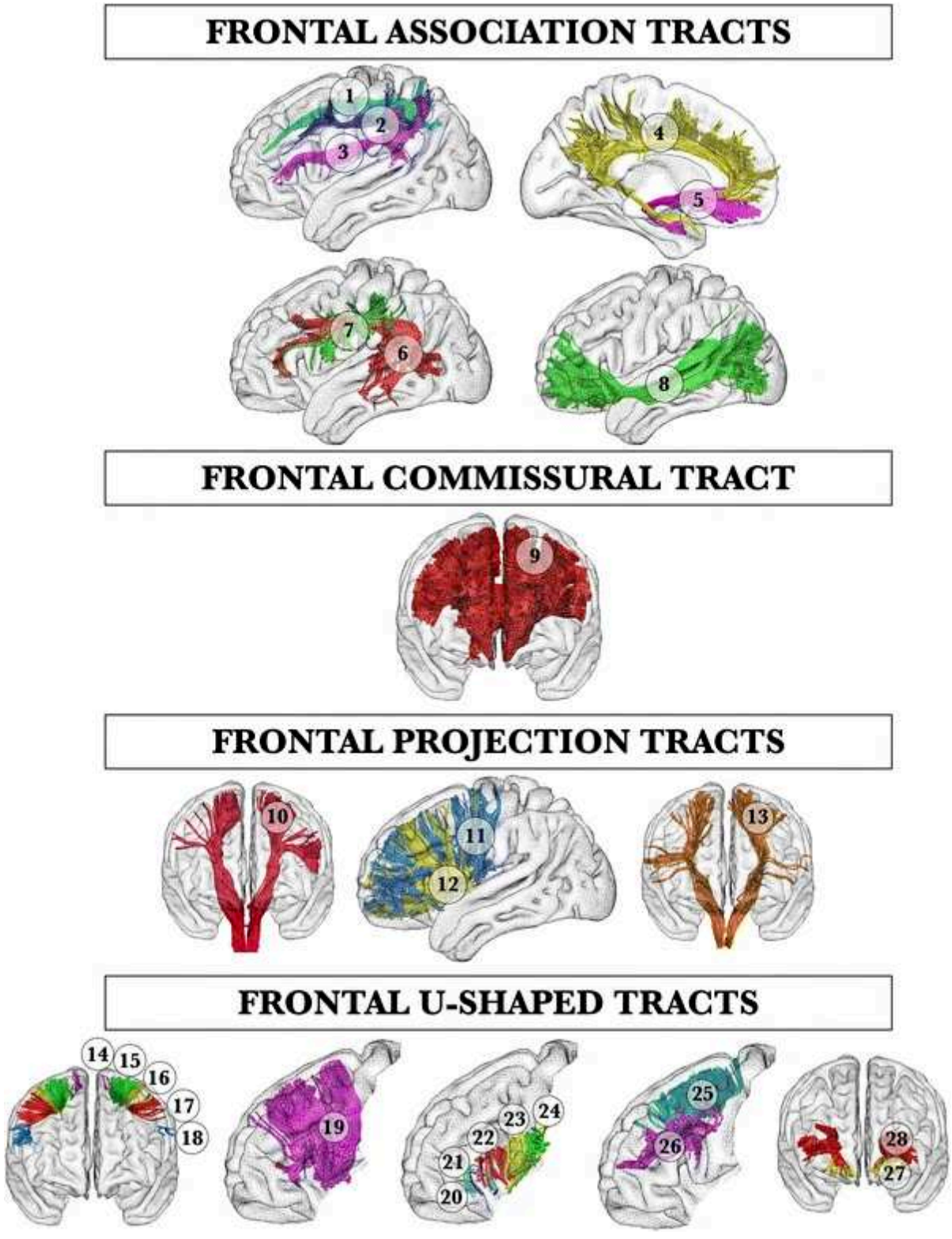

Figure 2.3 – **Spherical deconvolution tractography of frontal white matter connections. (Source:** [Rojkova et al., 2016]**)** For each tract a single participant map is supplied as a representative example of the individual anatomy. First (SLF I, light blue, no. 1), second (SLF II, dark blue, no. 2) and third (SLF III, pink, no. 3) branches of the superior longitudinal fasciculus; cingulum (yellow, no. 4); uncinate (pink, no. 5); long (LS, red, no. 6) and anterior (AS, green, no. 7) segments of the arcuate fasciculus; inferior fronto-occipital fasciculus (IFOF, no. 8); frontal corpus callosum (CC, no. 9); corticospinal tract (CST, no. 10); fronto-thalamic projections or anterior thalamic radiations (blue, no. 11); fronto-striatal projections (yellow, no. 12); fronto-pontine projections (no. 13); paracentral U tract (pink, no. 14); hand superior (green, no. 15), middle (yellow, no. 16) and inferior (red, no. 17) U tract; face U tract (blue, no. 18); frontal aslant tract (pink, no. 19); fronto-insular tract 1 (FIT 1, light blue, no. 20), 2 (FIT 2, dark blue, no. 21), 3 (FIT 3, red, no. 22), 4 (FIT 4, yellow, no. 23) and 5 (FIT 5, green, no. 24); frontal superior longitudinal (FSL, light blue, no. 25); frontal inferior longitudinal (FIL, pink, no. 26), frontal orbito-polar tract (FOP, yellow, no. 27) and fronto-marginal tract (FMT, red, no. 28). The overall visualization and screenshots were performed in Anatomist (http://brainvisa.info).

2.3 Rank-based inverse-normal transformation

The rank-based inverse normal transformation (INT) [Beasley et al., 2009] transforms the sample distribution of a continuous variable to make it appear more normally distributed. It is commonly used in genetic researches and applied during genome-wide association studies of non-normally distributed traits. It consists on creating a modified rank variable and then computing a new transformed value of the phenotype for the ith individual:

$$y_i^{'} = \Phi^{-1}(\frac{r_i - c}{N - 2c + 1}), c \in [0, \frac{1}{2}] \tag{2.1}$$

where r_i is the ordinary rank of the measure for ith individual, N represents the sample size, Φ^{-1} denotes the standard normal quantile, $y_i^{'}$ is the value after transformation, and $c = \frac{3}{8}$ as recommended by [Blom, 1958]. Other such INTs are minor variations, with c replaced by other values. In MOSTest [van der Meer et al., 2020], the authors used $c = \frac{1}{2}$.

2.4 Heritability

Heritability is defined as the proportion of a variance for a particular phenotype, measured at a particular age, that is attributable to genetic variation [Visscher et al., 2008]. Please refer to chapter 1.4.1 for more details on its definition. This section is dedicated to the approaches and bioinformatic tools that are usually used by the genetic community for the heritability estimation. The proportion of additive genetic variance in the neuroimaging phenotypic variance, also called narrow-sense heritability, can be estimated using either the pedigree information using SOLAR (Sequential Oligogenic Linkage Analysis Routines) or the genotyped SNPs information from common genetic variant using genome-based restricted maximum likelihood (GREML) [Yang et al., 2011]. Briefly, these are detailed below.

Pedigree analysis.

The heritability estimation for imaging-genetic cohorts that include groups of related individuals is performed using extended pedigrees. The pedigree based variance components linkage method, as implemented in the SOLAR software [Almasy and Blangero, 1998], estimates the narrow-sense heritability defined as the proportion of the phenotypic variance explained by the additive genetic variance: $h^2 = \frac{\sigma_g^2}{\sigma_p^2}$. The variance of a quantitative phenotype is given by $\sigma_p^2 = \sigma_g^2 + I\,\sigma_e^2$, where σ_g^2 is the genetic variance due to the additive genetic factors and σ_e^2 is the variance due to individual environment.

Assuming that all environmental effects are uncorrelated among family members, the covariance matrix Ω for a pedigree of individuals is given by $\Omega = 2\,\Phi\,\sigma_g^2 + I\,\sigma_e^2$, where Φ is the kinship matrix representing the pairwise kinship coefficient among all individuals. It is noteworthy that it is a strong assumption that in many situation will not hold. Significance of the estimated heritability is determined by testing the null hypothesis $\sigma_g^2 = 0$ (no linkage). In order to do that, a comparison is done between the likelihood of the model in which σ_g^2 is constrained to zero with that of the model where σ_g^2 is estimated. Prior to heritability estimation, phenotype values were adjusted with respect to both *sex* and *age* covariates. In this thesis, we used SOLAR software

package [Almasy and Blangero, 1998] to estimate the heritability from the pedigree information. Outputs from SOLAR comprise the heritability value, the significant p-value and the standard error (SE) for a given phenotype.

SNP-based heritability estimation.
Contrary to the pedigree analysis, this approach computes the narrow-sense heritability based only on the genotyping data which is used to estimate the degree of relationship between unrelated individuals: the so-called genetic relationship matrix (GRM). It is noteworthy that the independence between participant is critical for the validity of the SNP-based heritability. In order to do that, the following steps are followed: first, a quantitative control consisting in filtering the SNPs is done via PLINK [Purcell et al., 2007]. The following parameters were used: missing genotype $< 5\%$, minor allele frequency $< 1\%$, Hardy-Weinberg equilibrium $< 10^{-6}$. The SNPs in moderate linkage disequilibrium (with a $r^2 of 0.9$)) are kept. Next, the GRM is first estimated with the remaining SNPs and is then fitted by a mixed effect linear model (MLM) in order to identify the amount of variance attributed to the selected set of SNPs via the restricted maximum likelihood (REML) method. Prior to heritability estimation, phenotype values were adjusted for *sex*, *genotype array type*, *age*, *aqcuisition center* and the first 10 *genetic principal components* provided by UK Biobank to account for population structure. In this thesis, we used the Genome-wide complex trait analysis (GCTA) Yang et al. [2011] to estimate the heritability from the single nucleotide polymorphisms (SNPs) genotyped information. Similarly to SOLAR Almasy and Blangero [1998], outputs from GCTA comprise the heritability value, the significant p-value and the standard error (SE) for a given phenotype.

2.5 Genetic correlation

Genetic correlation is a key population parameter that describes the shared genetic architecture of complex traits and diseases [Ni et al., 2018]. It is the proportion of additive genetic covariance of pairs of endophenotypes. It can be estimated by current state-of-the-art methods, i.e., Bivariate genome-based restricted maximum likelihood (Bivariate GREML) [Lee et al., 2012] (https://cnsgenomics.com/software/gcta/Overview), linkage disequilibrium score regression (LDSC) [Bulik-Sullivan et al., 2015] (https://github.com/bulik/ldsc), or independent SNP Effect Concordance Analysis (iSECA) (https://neurogenetics.qimrberghofer.edu.au/iSECA/) [Nyholt, 2014]. The bivariate-GREML approach requires individual-level population-based SNPs genotype data while the two latter do not require individual-level genotype data but instead use GWAS summary statistics.

2.6 Massive univariate and multivariate genome-wide association study

As stated in chapter 1.4.5, the predominant strategy for identifying genomic loci associated with complex traits is through massive univariate genome-wide association studies (GWAS). Univariate approaches involve the association between a single phenotype and each of millions

isolated genetic variants. According to the nature of the endophenotype of interest -binary or continuous value-, various models can be adjusted. For example, for quantitative phenotypes, the following linear model is fitted:

$$y = G\beta_G + X\beta_X + e \tag{2.2}$$

where y is the phenotype vector, G is the genotype matrix for the current variant, X is the fixed-covariate matrix and contains an intercept column, and e is the error term subject to least-squares minimisation.

This state-of-the-art massive univariate approach results in a total of more than one million statistical tests. To assess significance, a consensus threshold $p = 5e - 8$ is considered by the genomic community. It is comparable to a Bonferroni correction of the traditional 0.05 type 1 error rate for one million statistical tests. However, this approach raise a certain number of limitations. A massive univariate approach ignores the biological information shared across multiple traits -the phenomenon called pleiotropy (See section 1.4.3)-. When several (endo)phenotypes are of interest, the number of tests significantly increase and it forces the users to adopt a stringent multiple comparison correction of the p-values to control the family-wise error rate. The colossal correction for multiple tests often leaves no significant associations. This limitation has led to the emergence of new multivariate statistical methods, designed to take into account the correlations among the biologically related (endo)pheontypes, classically encountered in imaging-genetic studies.

On the other hand, multivariate approaches quantify the simultaneous contributions of loci to multiple traits by taking advantage of their genotypic-phenotypic structures. Importantly, multivariate frameworks offer several advantages. These were listed in chapter 1.4.5 and we will take the liberty of listing them here as well for the sake of clarity. First, by taking into account the cross-trait covariance, multivariate analyses increase the statistical power in case of the presence of genetic correlation between the different traits [Allison et al., 1998, Zhu and Zhang, 2009]. Second, by performing a single test for association with a set of traits, multivariate procedures alleviate the multiple comparison correction [Klei et al., 2008, Zhu and Zhang, 2009]. Third, it improves the ability to detect susceptible genetic variants whose effects are too small to be detected in univariate analysis. Fourth, contrary to the massive univariate approach, multivariate GWASes have the advantage of leveraging the distributed nature of genetic effects and the presence of pleiotropy across modalities and is thus, more consistent with biology [Chavali et al., 2010].
To date, several multivariate approaches to genome-wide association study have been proposed; MQFAM implemented in the genetic association analysis software PLINK (MV-PLINK) [Ferreira and Purcell, 2009] is based on canonical correlation analysis, a Bayesian multiple phenotype test implemented in SNPTEST (MV-SNPTEST) [Marchini et al., 2007], the R package MultiPhen (MultiPhen) [O'Reilly et al., 2012] tests the linear combination of phenotypes for each SNP by performing ordinal regression, a Bayesian model comparison and model averaging for multivariate regression in BIMBAM (MV-BIMBAM) [Guan and Stephens, 2008, Stephens,

2013], the Principal Component of Heritability Association Test (PCHAT) [Klei et al., 2008], a Trait-based Association Test that uses Extended Simes procedure (TATES) [Van der Sluis et al., 2013], MultiABEL implements Pillai's trace MANOVA [Pillai, 1955] to calculate multivariate p-value from summary statistics, adaptive multi-trait association test (aMAT) [Wu, 2020], Multi-Trait Analysis of GWAS (MTAG) [Turley et al., 2018], METAL [Willer et al., 2010], genome-wide association meta-analysis (GWAMA) [Mägi and Morris, 2010], Joint Analysis of GWAS Summary Statistics (JASS) [Julienne et al., 2020] and Multivariate Omnibus Statistical Test (MOSTest) [van der Meer et al., 2020].

Comparative studies have shown the utility of multivariate methods listed as it substantially boost statistical power and gene discovery over univariate tests [Galesloot et al., 2014, Porter and O'Reilly, 2017]. However, imaging-genetic community struggles to adopt these methods due to the lack of interpretation. Indeed, an important challenge is to identify "central" phenotypes driving the multivariate association from ones with minor contributions to the genotype-phenotypes association statistic. To date and to our knowledge, there is one bioinformatic tool; Meta-Phenotype Association Tracer (MetaPhat) [Lin et al., 2020] that address this issue by performing decomposition and tracing the traits of highest and lowest statistical importance to identify subsets of central traits at each associated variant.

In our work, we used the Multivariate Omnibus Statistical Test (MOSTest) [van der Meer et al., 2020] to conduct our multivariate analysis. Briefly, MOSTest is a twofold method. First, a univariate GWAS on each of pre-residualised and normalised (rank-based inverse-normal transformation) endophenotypes is carried out using a standard additive model of linear association between genotypes and each phenotype. Statistical significance was assessed from Pearson's correlation coefficient. Second, the MOSTest statistic ${\chi_j}^2$, for the jth SNP is calculated as a Mahalanobis norm ${\chi_j}^2 = \boldsymbol{z_j^T \tilde{R}^{-1} z_j}$, where $\boldsymbol{z_j} = (z_1 j, \ldots, z_K j)$ is the vector of z-scores of jth SNP across K phenotypes and $\boldsymbol{\tilde{R}}$ is the K-by-K correlation matrix of $\boldsymbol{\tilde{Z}}$; matrix of z-scores, calculated from association tests on a randomly permuted genotype vector of each SNP.

In this thesis, we performed a multivariate genome-wide association study (mvGWAS) between the filtered imputed genotypes described in the genetic quality control section 2.1.1.3 and the significantly heritable endophenotypes (see chapter 4), using MOSTest [van der Meer et al., 2020] described above. All endophenotypes were pre-residualised controlling for covariates including sex, genotype array type, age, recruitment site, and first ten genetic principal components provided by UK Biobank. In addition, as mentioned above, MOSTest performs a rank-based inverse-normal transformation (see section 2.3) of the residualised endophenotypes to ensure that the inputs are normally distributed. The distributions across the participants of all endophenotypes were visually inspected before and after covariate adjustment. MOSTest generated summary statistics that capture the significance of the association across language endophenotypes. To account for multiple testing over the whole genome, statistically significant SNPs were considered as those reaching the genome-wide threshold $p = 5\text{e}{-8}$.

2.7 Fine-mapping: identification of genomic risk loci and functional annotations

To further process the output from the multivariate genome-wide association study, the FUMA online platform v1.3.6a [Watanabe et al., 2017] with default parameters was used. FUMA aims to use functional, biological information to prioritise genes based on GWAS outcomes. It is organised as two separate processes; SNP2GENE and GENE2FUNC. Details of these two processes are presented below.

2.7.1 FUMA: SNP2GENE

SNP2GENE consists in a multi-step process which characterises genomic loci, annotates candidate SNPs in genomic loci and performs a SNP-to-gene mapping using three different strategies. It also perform gene-based and gene-set genome-wide association analyses using MAGMA [de Leeuw et al., 2015]

Characterization of significant hits.

The SNP2GENE process allows us to identify distinct, significantly associated genomic loci, and independent lead SNPs within those loci.

The characterization of significant hits process allows us to identify distinct, significantly associated genomic loci, and independent lead SNPs within those loci. *UKB release2b 10k white British* is used as a reference panel to calculate LD across SNPs and genes. SNPs with genome-wide significant mvGWAS p-values $p < 5e{-}8$ and independent from each other at $r^2 < 0.6$ were identified. For each of these SNPs, all known SNPs, regardless of being available in the input, that had $r^2 \geq 0.6$ with them were included for further annotation (candidate SNPs). Based on the identified independent significant SNPs, independent lead SNPs were also defined among them as having low LD ($r^2 < 0.1$) with any others. Additionally, each genomic locus can contain multiple independent significant SNPs and lead SNPs. Indeed, if LD blocks of independent significant SNPs are closely located to each other ($< 250kb$, default parameter), they are merged into one genomic locus.

SNPs were annotated for functional consequences on gene functions using ANNOVAR [Wang et al., 2010], Combined Annotation Dependent Depletion (CADD) scores [Kircher et al., 2014], and 15-core chromatin state prediction by ChromHMM [Ernst and Kellis, 2012] by matching chromosome, position, reference, and alternative alleles.

Additionally, RegulomeDB v2.0 [Boyle et al., 2012] was queried externally to annotate SNP. Coding hit SNPs are also annotated with polymorphism phenotyping v2 (Polyphen-2) [Ramensky et al., 2002].

SNPs were mapped to genes at significant mvGWAS loci using three different strategies; positional mapping, expression quantitative trait loci (eQTL) mapping, and chromatin interaction mapping.

Gene-level analyses.

FUMA implements different methods that enable to summarise SNP associations at the gene level and to associate the set of genes to biological pathways.
Gene-based association analysis was performed using mvGWAS summary statistics as input into MAGMA [de Leeuw et al., 2015]. This process examines the joint association signals of all SNPs within a given gene (including 50 kb upstream to 50 kb downstream of the gene), while considering the LD between the SNPs. FUMA applies a Bonferroni correction for the number of tested genes to identify significant gene associations.
Gene-set enrichment analysis was performed using MAGMA [de Leeuw et al., 2015], to test for enrichment of association of predefined gene sets. This process is performed for curated gene sets and the Gene Ontology (GO) terms [gen, 2021, Ashburner et al., 2000] obtained from the Molecular Signatures Database (MsigDB) [Subramanian et al., 2005]. A Bonferroni correction is applied considering all tested gene sets.
Gene-property analysis was performed using MAGMA [de Leeuw et al., 2015] to test if genes are over-represented in developmental stages and considering gene expression from BrainSpan data source from 11 developmental stages (from early prenatal to middle adulthood) and 29 different age groups (from 8 post-conceptional weeks to 40 years old). An FDR correction was used to correct for multiple testing.

2.7.2 FUMA: GENE2FUNC

GENE2FUNC provides information on expression of prioritised genes and tests for enrichment of the set of genes in pre-defined pathways. It offers four main views regarding gene expression per tissue types (GTEx) or developmental stage (BrainSpan), enrichment of differentially expressed gene (DEG) sets in a certain tissue compared to all other tissue types, enrichment of input genes in gene sets using hypergeometric tests, and gene table with input genes mapped to OMIM ID, UniProt ID, Drug ID of DrugBank and linked to GeneCards.

2.8 Protein networks

Interactions between proteins are important as they play a crucial role in cellular functions and biological processes. Multiple databases track the protein-protein interaction network using both physical interaction and functional associations. For example, the STRING database [Szklarczyk et al., 2017] gathers interaction experiments where physical interactions are identified and take into account experimental evidence that includes:

- Conserved neighbourhood: genes that occur repeatedly in close neighbourhood in (prokaryotic) genomes
- Co-occurrence: the presence or absence of linked proteins across species.
- Fusion: individual gene fusion events per species.
- Co-expression: identify genes that show similar expression pattern across many different conditions.

- Experiments: significant protein interaction datasets, gathered from other protein-protein interaction databases.
- Databases: curated knowledge from manually annotated databases of protein complexes as well as molecular pathways.
- Automatic text mining: process the vast biomedical literature and extract from the abstracts of scientific literature.

In this work, we used curated experimental protein-protein interaction (PPI) observations from the STRING [Szklarczyk et al., 2017] database (https://string-db.org/, version 11.5), and sought for a functional enrichment through this analysis.

* * *
* *
*

Chapter 3

Human language endophenotypes

Chapter Outline

3.1 Psychometric measures 68
3.2 Language neural activation: a volume-based analysis 71
3.3 Resting-state functional connectome 73
3.4 Anatomical connectome 75
3.5 Conclusion 76

In chapters 1 and 2, we presented basic principles of imaging and genetics useful for understanding imaging-genetic studies as well as the data and statistical methods explored. Large-scale neuroimaging studies usually summarise the imaging data into image-derived phenotypes (IDPs), which reduces raw data into a compact set of biologically meaningful measures. Compared to the traditional voxel level approach, the IDPs approach is simple, and effectively reduces the high-dimensional data into interpretable, compact, convenient features. However, IDPs remain indirect measures of the biological process of interest and meaningful interpretation requires care. Here, we provide the standard pipelines used to extract novel endophenotypes covering both psychometric and image derived phenotypes that encompass the human language connectome. To this end, the two well-known large-scale UK Biobank and HCP cohorts were used. These endophenotypes will be subjects to heritability analysis and genetic association studies as described further in the chapters 4 to 7. Genetic association analysis with complex cognitive traits can be enriched through the use of different information on trait development.

3.1 Psychometric measures

Two types of behavioural scores are available in the HCP cohort. Cognitive performance scores measured during the MRI session and psychometric measures acquired using standardized tests from the National Institute of Health (NIH), independently from the task performed inside the MRI scanner. These latter ones includes fluid intelligence, working memory, and language assessments such as vocabulary comprehension and oral reading decoding. A brief description taken as it is from (https://nihtoolbox.force.com/s/article/nih-toolbox-scoring-and-interpretation-guide) is presented below. The NIH measure consists of:

- Oral reading recognition: measured by the oral reading recognition Test. The participants are asked to read and pronounce letters and words as accurately as possible. Higher scores indicate better reading ability.
- Vocabulary Comprehension: measured by the Picture Vocabulary Test. The participants are presented with an audio recording of a word and four photographic images on the computer screen and is asked to select the picture that most closely matches the meaning of the word. Higher scores indicate higher vocabulary ability.
- Fluid Intelligence: measured by the Penn Matrix Test (PMAT) which measures fluid intelligence via non-verbal reasoning. Participants are presented with patterns made up of 2x2, 3x3 or 1x5 arrangements of squares, with one of the squares missing. They must pick one of five response choices that best fits the missing square on the pattern. Two features are declined from this test: the number of correct answers and the median reaction time (RT) for correct answers.
- Working Memory: measured by the List Sorting Working Memory Test. The participants sequence different visually and orally presented stimuli. Pictures of different foods and animals are displayed with both a sound clip and written text that name the item. The task has two different conditions: 1-List and 2-List. In the 1-List condition, participants

are required to order a series of objects (either food or animals) in size order from smallest to largest. In the 2-List condition, participants are presented both food and animals and are asked to report the food in size order, followed by the animals in size order.

The distribution of these psychometric measures can be appreciated in Fig.3.1

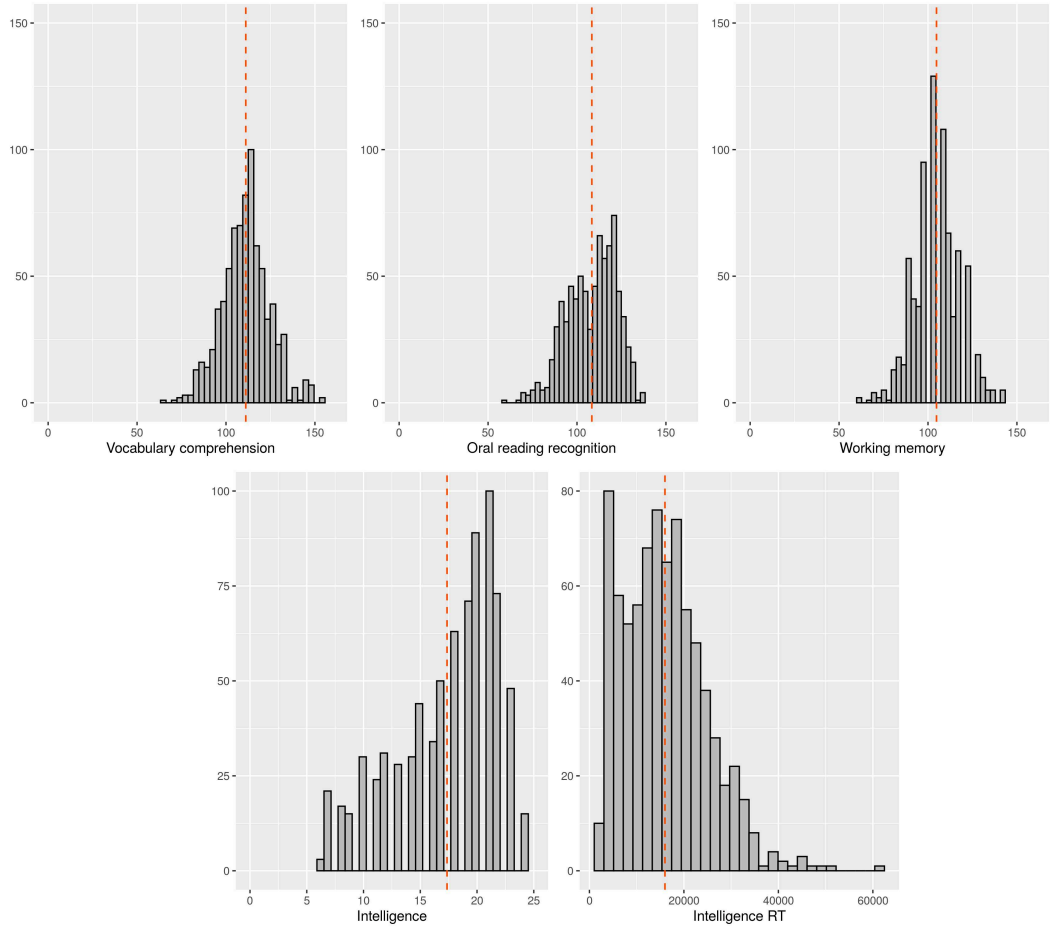

Figure 3.1 – Distribution of the NIH measures collected by HCP team independently from the language fMRI task

The cognitive performance scores measured during the MRI session consist of:

- Language task math: three features are measured, namely the accuracy percentage during math condition in language task, the median reaction time for correct trials and the average difficulty level of the presented stimuli.
- Language task overall: three features are measured, namely the average of accuracy from each condition in language task, the average of median reaction time from each condition in language task.
- Language task story: three features are measured, namely the accuracy percentage during story condition in language task, the median reaction time for correct trials and the average difficulty level of the presented stimuli.

The distribution of these psychometric measures can be appreciated in Fig.3.2

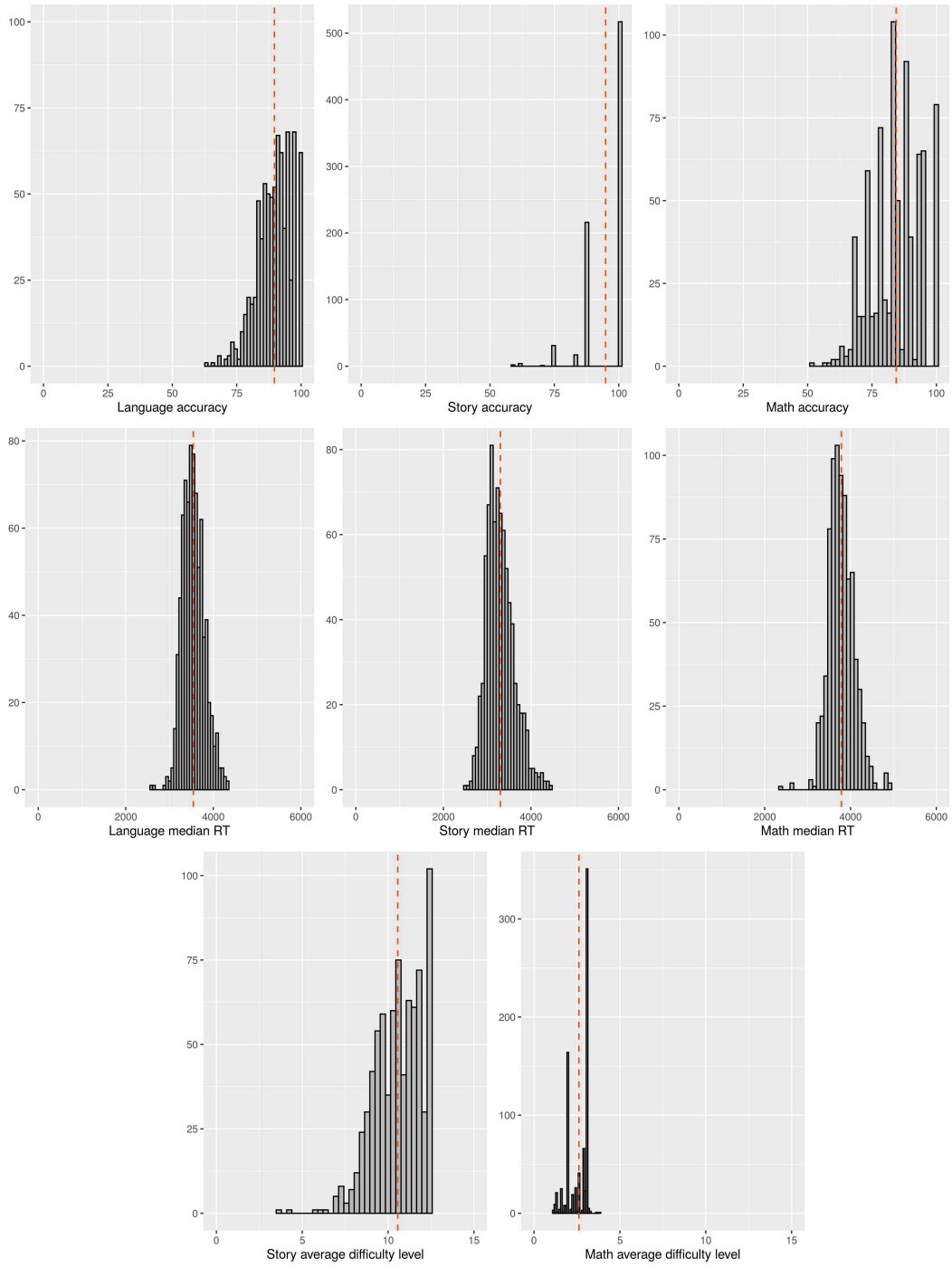

Figure 3.2 – Distribution of behavioral scores collected by HCP team during the language fMRI task, composed of MATH and STORY tasks

3.2 Language neural activation: a volume-based analysis

As described in the chapter 1.3.2, task-based fMRI (tfMRI) measures BOLD signal changes between task-stimulated states such as visual, auditory, or language and control states (resting state). These data are presented as a succession of 3D images that vary in time (4D image) and which reflect the state of the brain at a given moment regarding the cerebral stimulation of the experiment set up. The analysis of task-based fMRI data consist of participant-level and group-level analyses. The participant-level known as the first level consists of fitting a general linear model (GLM) using the task-based fMRI data and performing a t-test or an F-test according to the condition one wants to highlight; either a condition versus baseline or a combination of conditions (possibly two-, three- or higher-dimensional) that explains a significant proportion of the signal. The group-level, also known as the second level consists on averaging the activation across participants. Both first-level and second-level analysis are described in the chapter 1.3.2. In this section, we will describe the methodology applied to analyse the language task-based fMRI data in the HCP cohort and the pipeline used to extract the endophenotypes related to language.

Concerning the first level, activity estimates were computed for the preprocessed functional time series (4D image) using a GLM implemented in Nilearn. Two predictors of interest were included in the GLM model design: the story predictor covered the variable duration of a short story, question, and response period ($\sim 30s$), and the math predictor covered the duration of a set of math questions designed to roughly match the duration of the story blocks. These predictors were convolved with a double gamma "canonical" hemodynamic response function (HRF) to generate the main model regressors. To compensate for slice-timing differences and variability in the HRF delay across regions, temporal derivative terms derived from each predictor were added and were treated as confounds of no interest. A cosine drift model was used. To correct for autocorrelations in the fMRI data, an autoregressive AR1 noise model was used. Finally, we applied to the task-volume, a spatial smoothing using an unconstrained 3D Gaussian kernel of full width at half maximum $(FWHM) = 4mm$. The Fig.3.3 represents the design matrix used to fit the GLM model. At the end, we obtain a β-map for each participants. To access the estimated β coefficients of the GLM model, we used the contrast represented in the Fig.3.3 to perform a story versus baseline contrast. The role of the contrast is to select columns of the model –and potentially weight them– to study the associated statistics. In order to get statistical significance, we form a t-statistic, and convert it into z-scale. The values are scaled across voxels to match a standard Gaussian distribution (mean=0, variance=1). At the end, we obtain a z-map for each individuals.

Regarding the second level, activity estimates were computed for the individual β-maps using a GLM implemented in Nilearn followed by a t contrast. The Fig3.4 shows the activations for the story versus baseline (The intercept of the general linear model being considered as baseline). The intercept reflects the mean of the residual BOLD time series after removing variance explained by all other regressors.

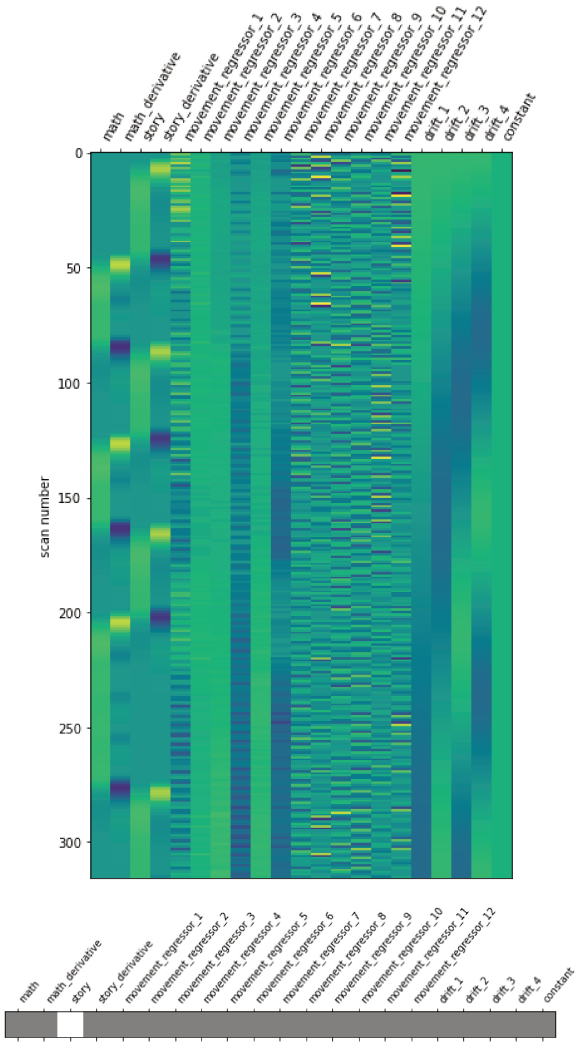

Figure 3.3 – **First level model.** A) Design matrix used in the first level model. Predictors includes fMRI events and derivatives, twelve movement regressors and four drift features. B) Coefficients of the contrast, indexed by the names of the columns of the design matrix.

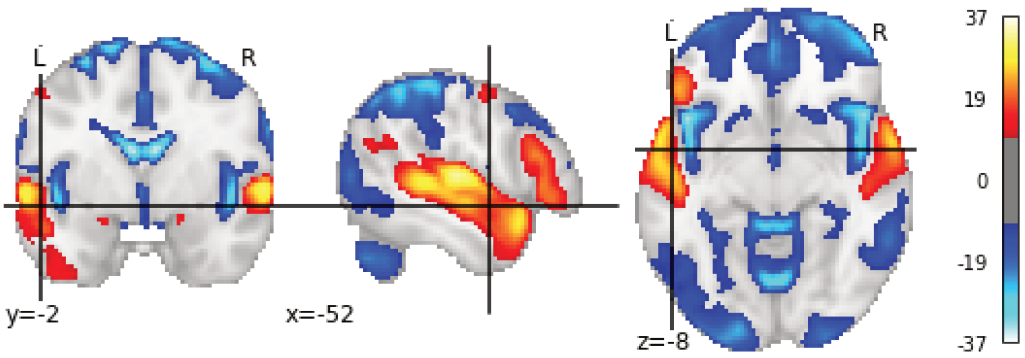

Figure 3.4 – **Group analysis language task activation maps.** Group average activations for the HCP language task: story versus baseline is shown with a lower threshold of $z = \pm 10$.

Estimating neural activation endophenotypes.
In this work, we estimated task-based neural activation in HCP, using perisylvian cortical areas as regions of interest (ROI) introduced in chapter 2.2.1. The obtained first-level z maps were masked using the ROIs and averaged for each individual. This resulted in 25 language neural activation regarding the SmPSS set of regions.

3.3 Resting-state functional connectome

As discussed in the chapter 1.3.2, intrinsic brain activity assessed while at rest can recover specific brain functional activations making it a good surrogate of functional neuronal processes. The identification of brain networks from fMRI data whether from resting-state or task-based, is often attempted by first, identifying a set of functional "nodes" such as ICAs maps or spatial ROIs. Next, conducting a connectivity analysis between the regions, based on the fMRI time-course signal averaged in each region. In the next section, we will summarise the pipeline undertaken in this work for the functional connectivity estimation.

Estimating functional connectome endophenotypes.
In this work, we estimated task-free FC in UK Biobank [Bycroft et al., 2018], using perisylvian cortical areas as regions of interest (ROI) introduced in chapter 2.2.1. Different measures can be considered regarding the estimation of the connectivity between nodes as highlighted in the chapter 1.3.2. General correlation-based approaches are known to be quite successful [Smith et al., 2011]. The simplest measure of pairwise similarity between two timeseries is covariance and in case of normalisation of the timeseries, we refer to it as *full correlation*. The correlation between two timeseries does not imply that the functional connection between two nodes is direct. Indeed, the correlation coefficient might give misleading results if there is a third node that is numerically related to both initial nodes. *Partial correlation* overcomes this limitation by ruling out indirect effects in the correlation structure. In this thesis, we chose to use the *Partial correlation* as it offers a more accurate interpretation of our results.
Overall, the functional connectivity estimation was performed by applying the following steps: the preprocessed resting-state BOLD signal was masked using the ROIs and averaged at each time volume. A connectome matrix was computed using Nilearn [Abraham et al., 2014] for each participant using a shrunk [Ledoit and Wolf, 2004] estimate of partial correlation [Marrelec et al., 2006] (See Fig. 3.5). This resulted in 300 ($= 25 \times 24/2$) and 15 ($= 6 \times 5/2$) edges connecting language ROIs for each individual for both the SmPSS and OcSS sets of regions, respectively. Each edge —also denoted functional connectivity (FC)— is further considered as a candidate endophenotype.

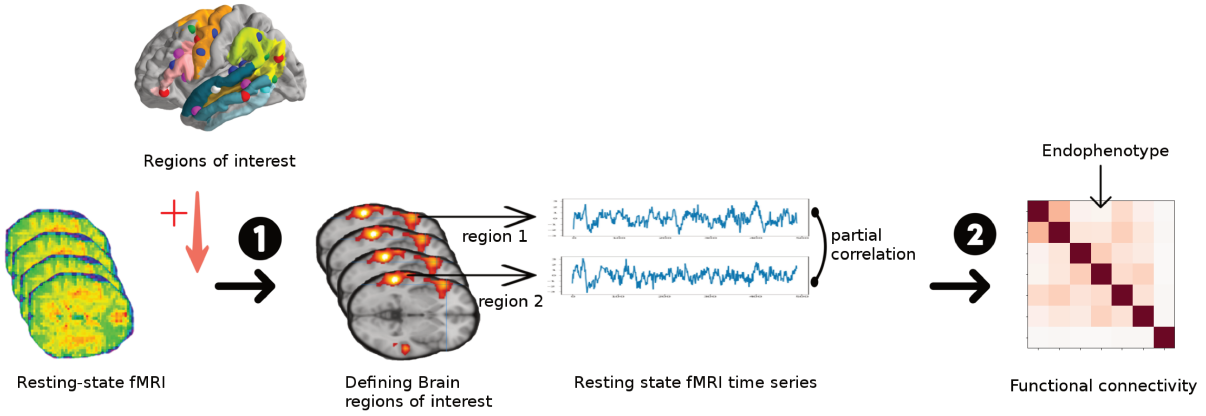

Figure 3.5 – **Functional connectome extraction pipeline** with two main steps: 1) Map of brain regions already defined on resting-state fMRI images. 2) Extraction of mean BOLD signal for each ROIs and quantifying functional interactions from these time series signal extracted. At the end of the second step, we obtain a functional connectome for each participants where each cell represents a resting-state functional connectivity.

This pipeline was applied to both UKB and HCP cohorts and the endophenotypes extracted can be appreciated in the Fig.3.6

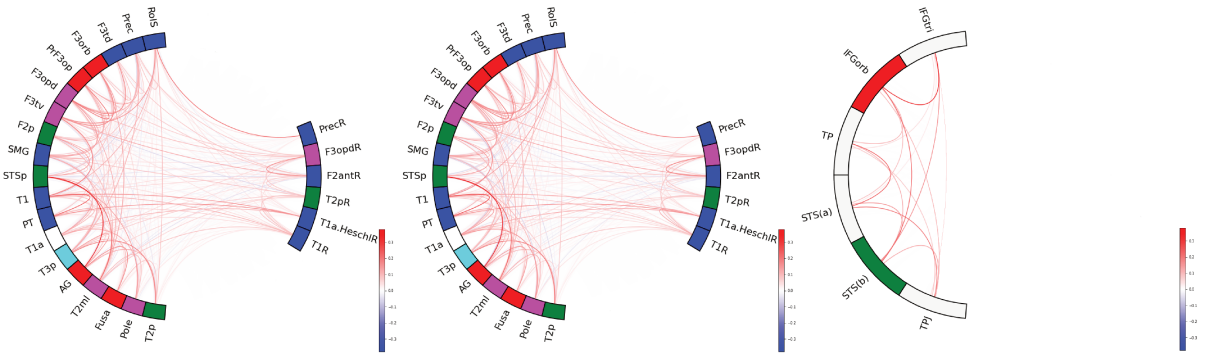

(a) (b) (c)

Figure 3.6 – **Functional connectome visualisation** Mean functional connectivity of the 300 and 15 endophenotypes, calculated using a shrinked estimate of partial correlation Marrelec et al. [2006] (estimated with a Ledoit-Wolf estimator Ledoit and Wolf [2004]) over 32,186 and 778 individuals using both UKB and HCP rsfMRI participants respectively. (a) Circos plot represents the mean FC estimated using SmPSS ROIs on UK Biobank. (b) Circos plot represents the mean FC estimated using SmPSS ROIs on HCP. (c) Circos plot represents the mean FC estimated using OcSS ROIs on UK Biobank.

3.4 Anatomical connectome

Diffusion-weighted imaging quantifies water diffusion in biological tissues and is used to identify the different fibber tracts in the human brain by tracking the directional diffusion of water in the brain. It provides a number of measures that can be used for statistical and genetic analyses. Regarding the heritability of structural connectivity, several genetic studies showed that DTI measures are heritable and therefore worthy targets for more in-depth genetic analysis.

More details are provided in the chapter 1.3.1. In the next section, we will summarize the methodological steps undertaken for the endophenotypes estimation.

Estimating anatomical connectome endophenotypes.
The anatomical connectivity endophenotypes are estimated using a set of 35 white matter tract masks defined from the probabilistic atlas [Rojkova et al., 2016] introduced in the chapter 1.5.2.2 and that are enumerated below: The arcuate fasciculus (long, anterior, and posterior segments), the superior longitudinal fasciculus (I, II, III), the inferior fronto-occipital fasciculus, the uncinate fasciculus, the frontal inferior longitudinal, the frontal superior longitudinal, the inferior longitudinal fasciculus, the frontal aslant tract, the fronto-insular tracts (1-5) and the corpus callosum.
In this thesis, we mainly conduct phenotypic multivariate analysis. Overlapping white matter tracts might be a serious limitation regarding the interpretation of the mvGWAS results. Indeed, the identification of the set of tracts that weight the most in the multivariate association becomes difficult. In light of this observation, we apply a stringent threshold at 90% of probabilities, defined after a visual inspection, in order to reduce significantly the overlap and allow us a fine interpretation of our results. Finally, the images derived phenotypes (IDPs) are estimated as follow: first, a binarisation of the set of 35 white matter tracts is performed to generate the tract-masks. Next, for each individuals, and for each DTI/NODDI output image type, an IDPs is generated by averaging the skeletonised images across the set of the tracts of interest. As these structural white matter tracts are assessed by 9 indices: fractional anisotropy (FA) maps, tensor mode (MO), mean diffusivity (MD), intracellular volume fraction (ICVF), isotropic volume fraction (ISOVF), mean eigenvectors (L1, L2, L3), and orientation dispersion index (OD), $315 = 35 \times 9$ dMRI endophenotypes are derived. Fig.3.7 summarize the methodological steps for the endophenotypes estimation.

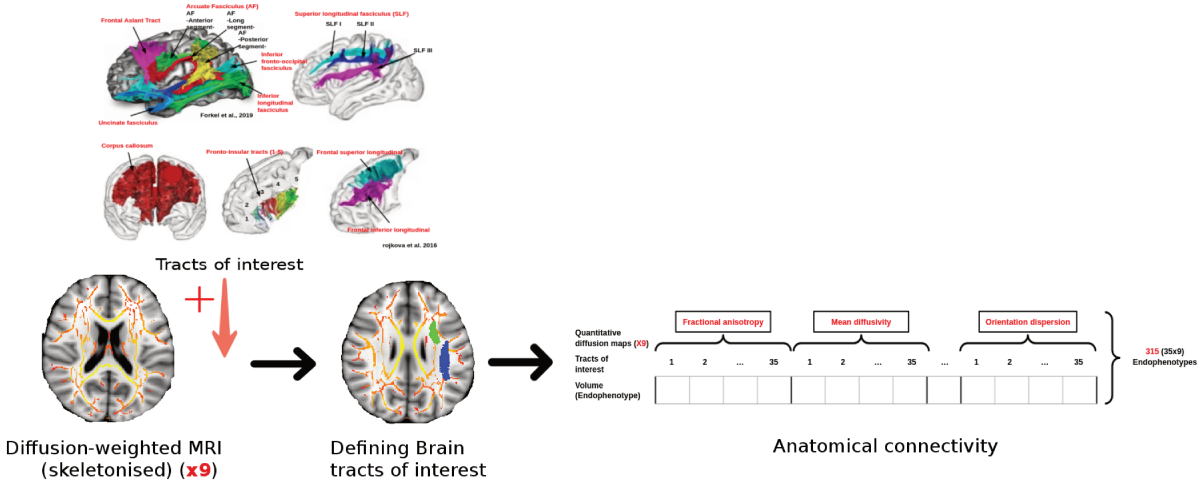

Figure 3.7 – **Anatomical connectome extraction pipeline** with one main steps consisting on mapping brain tracts of interest already defined on skeletonised images and extracting mean value for each tract of interest. At the end, we obtain an anatomical connectome for each participants where each cell represents an anatomical connectivity.

3.5 Conclusion

Multi-modal data collection in large-scale cohorts offers us a great opportunity to investigate open neuroscience questions from different perspectives. A valuable aspect of this work has been to exhibit different (endo)phenotypes regarding human language trait. These quantitative endophenotypes reflects human brain inter-individual variability. In order to ensure that these endophenotypes represents human language as cognitive process of interest, we adopted a region of interest approach. Whether for cortical regions or white matter tracts, the ROIs were carefully chosen. These ones were previously associated with language impairment, and/or identified in task based fMRI as supporting language and in case of WM tracts, reach language cortical regions. In the next chapter, we will investigate and show that many of these (endo)phenotypes are heritable and therefore worthy targets for more in-depth genetic analysis.

* * *
* *
*

Chapter 4

Heritability of human language

Chapter Outline

4.1 Pedigree-based heritability of behavioural and neuroimaging (endo)phenotypes: a twin study . . . 79
4.1.1 Cognitive behavioural assessment . . . 79
4.1.2 Brain neural activation . . . 80
4.1.3 Functional connectome . . . 80
4.2 SNP-based heritability of neuroimaging endophenotypes: a general population study . . . 81
4.2.1 Functional connectome . . . 81
4.2.2 Anatomical connectome . . . 83
4.3 Discussion . . . 83
4.4 Are heritability estimates inflated in twin studies? . . . 83
4.5 Conclusion . . . 87

How do we decide if a cognitive trait such as language is genetically influenced? In quantitative genetics, heritability reflect cognitive traits variance that can be attributed to genetics versus environmental factors or their interactions. The traits may be either language related behaviour or language brain image derive measures (IDP). In chapter 1.4.1, the heritability concept has been detailed. Relevant to our study, heritability of human language has been extensively reported in the literature as revealed by reviews of the field [Stromswold, 2001]. Previous studies have mainly focused on twins, adoption, and linkage studies of language. The predominant genetics investigations concerns behavioural traits. With the recent availability of large-scale imaging-genetics cohorts, researches have addressed the heritability of language hypothesis regarding the left–right hemispheric asymmetry measured from neuroimaging [Carrion-Castillo et al., 2020, Le Guen et al., 2020, Sha et al., 2021]. Details about all these studies are provided in the chapter 1.6.1. However, we could not help but notice a lack of researches of the heritability of language regarding other available modalities. Thus, the present contribution seeks to provide elements of answers regarding this scientific question by taking advantage of the different (endo)phenotypes exhibited during this thesis and presented in the previous chapter. In this chapter, we use pedigree and real whole genome genotyping data as well as psychometric measures (chapter 3.1) and MRI data including task-based fMRI (see chapter 3.2), resting-state fMRI (see chapter 3.3), and diffusion-weighted MRI (see chapter 3.4) from the two cohorts introduced in the chapter 2.1; the Human Connectome Project (HCP) and the UK Biobank (UKB).
The objective of the present work is two-fold: *i)* to contribute to the study of language heritability and compare the obtained results with the literature; *ii)* to filter the endophenotypes for the multivariate genome-wide association study presented in both chapter 6 and 7.
Furthermore, the estimation of heritability reported by pedigree studies have been subject of multiple concerns as the estimation might be inflated [Hofer et al., 2018, Stromswold, 2001, van der Lee et al., 2017]. The possible origins of these discrepancies will be further discussed.

4.1 Pedigree-based heritability of behavioural and neuroimaging (endo)phenotypes: a twin study

Using SOLAR, we estimated the pedigree-based heritabilities of each endophenotypes. As covariates, the sex, the age, the ethnicity (Hispanic or not), and the first four principal components of the principal component analysis of the genetic data were considered. To account for multiple tests, a 0.05 threshold on False Discovery Rate (FDR) adjusted p-values was applied.

4.1.1 Cognitive behavioural assessment

The pedigree-based heritability (h^2) was estimated for each of the language scores we described in the chapter 3.1. After a FDR correction for multiple testing, all language scores have a significant pedigree-based heritability (Table 4.1), ranging from 19.4% for the language task math median reaction time to 71.7% for the oral reading recognition.

Table 4.1 – **Heritabilities of language related behavioral scores.** Endophenotypes in bold represent language related behavioral scores with significant heritability after false discovery rate correction at $p < 0.05$.

Endophenotype	heritability	P value	SE	FDR P value
Oral reading recognition	71.7%	4.74E-30	0.038	6.16E-29
Vocabulary Comprehension	64.2%	1.78E-24	0.045	1.16E-23
Fluid Intelligence	60.0%	9.54E-19	0.055	4.13E-18
Working Memory	50.2%	5.50E-15	0.058	1.79E-14
Language task math accuracy	43.5%	8.39E-12	0.061	2.18E-11
Language task overall accuracy	41.5%	3.94E-10	0.065	8.54E-10
Language task story difficulty level	36.9%	1.00E-07	0.069	1.86E-07
Fluid Intelligence reaction time	34.0%	3.00E-07	0.069	4.87E-07
Language task math difficulty level	34.1%	1.30E-06	0.071	1.88E-06
Language task story accuracy	19.9%	1.38E-03	0.068	1.64E-03
Language task overall median reaction	20.6%	1.38E-03	0.072	1.64E-03
Language task story median reaction time	19.5%	1.68E-03	0.069	1.82E-03
Language task math median reaction time	19.4%	2.87E-03	0.072	2.87E-03

4.1.2 Brain neural activation

The pedigree-based heritability (h^2) was estimated for each of the neural activations measured in the 25 SmPSS regions. In order to take into account the multiple tests, FDR correction on the p values was applied. This revealed 16 regions out of the 25, whose language activation displays a significant pedigree-based heritability (Table 4.2), ranging from 14.4% for the T2pR to 34.9% for the T1.

Table 4.2 – **Heritabilities of language task activation.** Bold endophenotypes represents language task activation with significant heritability after false discovery rate correction at p<0.05.

Endophenotype	heritability	P value	SE	FDR P value
F2p	32.9%	2.00E-07	0.065	1.25E-06
T1R	32.3%	2.00E-07	0.064	1.25E-06
T1	34.9%	1.00E-07	0.065	1.25E-06
T2ml	33.0%	2.00E-07	0.064	1.25E-06
SMG	31.1%	5.00E-07	0.064	2.50E-06
T1a.HeschlR	30.5%	1.10E-06	0.066	4.58E-06
Pole	31.1%	4.90E-06	0.070	1.75E-05
AG	27.2%	7.90E-06	0.064	2.47E-05
T1a	27.9%	1.07E-05	0.066	2.97E-05
STSp	28.0%	7.34E-05	0.076	1.83E-04
PT	23.4%	1.47E-04	0.066	3.34E-04
PrF3op	21.2%	2.40E-04	0.062	5.00E-04
F3orb	19.8%	1.66E-03	0.070	3.19E-03
F3opdR	17.8%	3.22E-03	0.067	5.76E-03
F3opd	16.2%	5.39E-03	0.065	8.98E-03
T2pR	14.5%	8.50E-03	0.063	1.33E-02
F2antR	11.0%	4.59E-02	0.067	6.57E-02
Fusa	10.9%	4.73E-02	0.068	6.57E-02
PrecR	10.6%	6.05E-02	0.070	7.96E-02
F3td	8.7%	8.10E-02	0.064	1.01E-01
Prec	7.7%	1.05E-01	0.063	1.25E-01
T3p	7.5%	1.18E-01	0.065	1.34E-01
T2p	5.4%	1.99E-01	0.065	2.16E-01
F3tv	4.6%	2.40E-01	0.066	2.50E-01
RolS	4.1%	2.54E-01	0.063	2.54E-01

4.1.3 Functional connectome

The pedigree-based heritability (h^2) was estimated for each of the 300 functional connectivity extracted from SmPSS set of ROIs. In order to take into account the multiple tests, FDR correction on the p values was applied. This revealed 217 FCs with a significant pedigree-based heritabilities (Fig. 4.1, Table B.1), ranging from 11.4% for the F2p↔F3td to 48.7% for the

F3tv↔F3orb FCs.

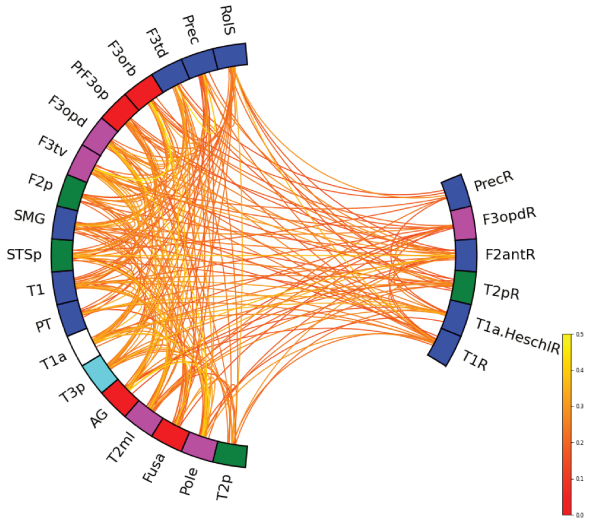

Figure 4.1 – **Pedigree-based heritabilities of brain functional connectivities extracted using SmPSS ROIs.** Circle plot where all 25 regions are represented (19 ROIs on the left represent the left hemisphere and 6 ROIs on the right represent the right hemisphere) illustrating the FCs with significant pedigree-based heritability after false discovery rate correction at $p < 0.05$. Each link between two regions represents an endophenotype. The intensity of the color between two regions represents the pedigree-based heritability of an endophenotype as defined by the color bar. Please refer to Table B.1 for all pedigree-based heritability values.

4.2 SNP-based heritability of neuroimaging endophenotypes: a general population study

Using GCTA, genomic-relatedness-based restricted maximum-likelihood (GREML) analyses were performed to estimate the SNP-based heritabilities of each endophenotypes. These ones were pre-residualised controlling for covariates including sex, genotype array type, age, recruitment site, and ten genetic principal components provided by UK Biobank. In addition, we performed a rank-based inverse-normal transformation of the residualised endophenotypes to ensure that the inputs are normally distributed. To account for multiple tests, a 0.05 threshold on False Discovery Rate (FDR) adjusted p-values was applied.

4.2.1 Functional connectome

The SNP-based heritability of the resting-state functional connectome was investigated using two set of ROIs introduced in the chapter 2.2.1. These are presented below.

4.2.1.1 Functional connectivity extracted using OcSS ROIs

The single-nucleotide polymorphism (SNP)-based heritability (h^2) was estimated for each of the 15 functional connectivity extracted from the OcSS set of ROIs. In order to take into account the multiple tests, FDR correction on the p values was applied. This revealed 14 FCs

with a significant SNP-based heritabilities (Fig. 4.2, Table B.2), ranging from 4.9% for the IFGtri↔pSTS to 12% for the IFGtri↔IFGorb FCs.

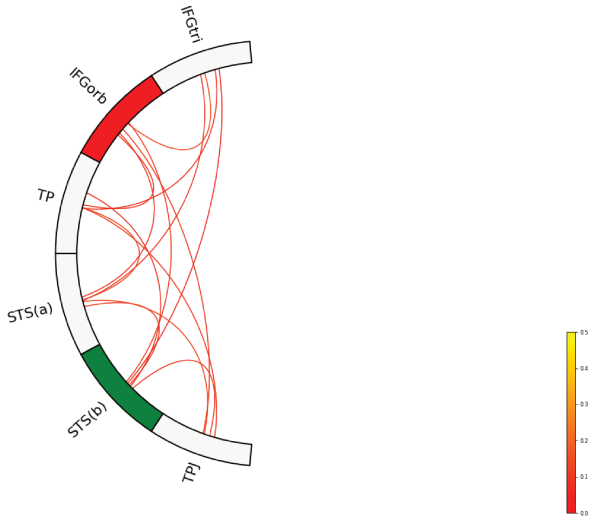

Figure 4.2 – **SNP-based heritabilities of brain functional connectivities extracted using OcSS ROIs.** Circle plot where all 6 regions are represented (6 ROIs on the left represent the left hemisphere. No region in the right hemisphere are included in OcSS ROIs.) illustrating the FCs with significant SNP-based heritability after false discovery rate correction at $p < 0.05$. Each link between two regions represents an endophenotype. The intensity of the color between two regions represents the SNP-based heritability of an endophenotype as defined by the color bar. Please refer to Table B.2 for all SNP-based heritability values.

4.2.1.2 Functional connectivity extracted using SmPSS ROIs

The single-nucleotide polymorphism (SNP)-based heritability (h^2) was estimated for each of the 300 functional connectivity extracted from SmPSS set of ROIs. In order to take into account the multiple tests, a FDR correction on the p-values was applied. This revealed 142 FCs with a significant SNP-based heritabilities (Fig. 4.3, Table B.3), ranging from 3.5% for the SMG↔T1 to 14.3% for the SMG↔F3opd FCs.

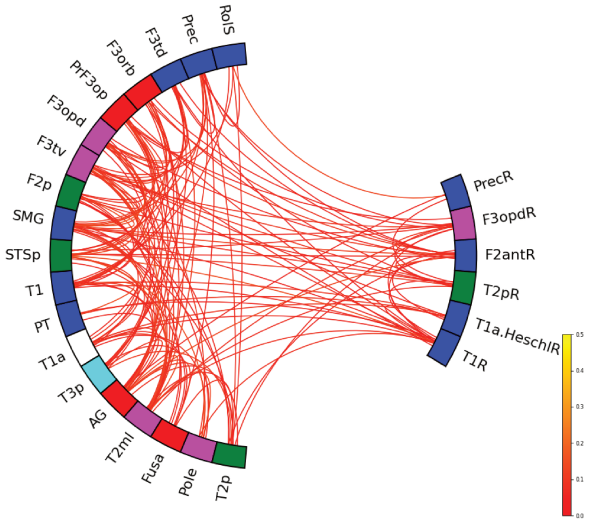

Figure 4.3 – **SNP-based heritabilities of brain functional connectivities extracted using SmPSS ROIs.** Circle plot where all 25 regions are represented (19 ROIs on the left represent the left hemisphere and 6 ROIs on the right represent the right hemisphere) illustrating the FCs with significant SNP-based heritability after false discovery rate correction at $p < 0.05$. Each link between two regions represents an endophenotype. The intensity of the color between two regions represents the SNP-based heritability of an endophenotype as defined by the color bar. Please refer to Table B.3 for all SNP-based heritability values.

4.2.2 Anatomical connectome

The single-nucleotide polymorphism (SNP)-based heritability (h^2) was estimated for each of the 315 bilateral bundles extracted measures of brain anatomical connectivity. All but two ACs (313) showed significant SNP-based heritability (False discovery rate (FDR)-corrected $p < 0.05$) (Table B.4), ranging from 3.8% for the left fronto Insular tract number 4 measured with OD to 62.7% for the corpus callosum measured with ICVF.

4.3 Discussion

A pivotal question in biology is the heritability of a particular trait. It provides a quantitative estimation of its association with a set of genetic markers and thus, informs us about the richness of its contribution in the trait of interest. We observed a hierarchy of language heritability estimates from the Human Connectome Project (twin study) with 19.4-71.7% for language-behavioural scores, 11.4-48.7% for resting-state FC, and 14.4-34.9% for language-task activations. In terms of heritability ranking, the resting-state functional connectivity edges show low levels of heritability compared to behavioural scores. This observation was also made regarding structural features such as cortical or white matter tracts features (in UKB [Elliott et al., 2018]). Overall, we show evidence that human language is, to some extent, under genetic control. Furthermore, we observed a discrepancy between both SNP-based and Pedigree-based heritabilities. The possible origins of these discrepancies will be further discussed.

4.4 Are heritability estimates inflated in twin studies?

We estimated the heritability of human language considering differents endophenotypes. These ones displayed a substantial genetic influence. We noticed a discrepancy between heritability estimates depending on the cohort used, with higher estimates using the HCP compared to the UK Biobank. For the sake of clarity, we focus here on the heritability estimates of the brain functional connectivities extracted using SmPSS ROIs.

The origin of this discrepancy may be related to differences in either the design parameters of the analyses, or the cohorts' environmental conditions which differ significantly. As regards the design parameters like the length of the rsfMRI used to compute the FC, global effects can be seen in Fig. 4.4 which highlights the heritability differences. This figure also reports the global minor differences in heritability estimates when using SOLAR or GCTA in a same cohort (HCP) for which both genotyping and pedigree information were available.

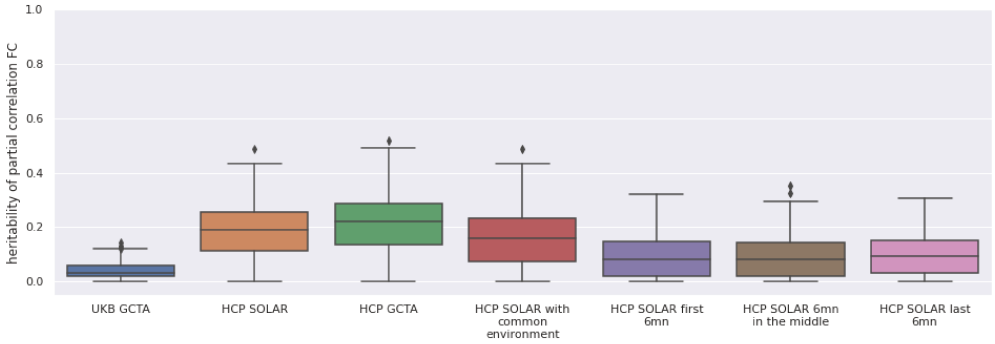

Figure 4.4 – **Comparison of heritabilities estimated according to different design parameters.** The endophenotypes extracted using SmPSS ROIs. Boxplots 1 and 2 display the heritability distributions estimated on UKB (using GCTA) and HCP (using SOLAR) respectively. Boxplot 3 : HCP-FCs using GCTA. Boxplot 4 : HCP-FCs using GCTA and considering the household effect. Boxplots 5 to 7 : HCP (using SOLAR) on rsfMRI sessions with the same duration as in UBK (6 min).

In order to shed lights on the origin of the observed heritability gap, we attempted to rule out a certain number of hypotheses supposed to be at the origin of these discrepancies. **First**,

we investigated whether the observed gap is due to the difference of genetic information (pedigree/genotyping data) between both cohorts. As both genetic information are available in the HCP cohort, we computed the heritability of FCs using pedigree in one hand and using the genotyping data in an other hand. We observed that the heritability computed on HCP genotyped SNPs are slightly higher than those obtained with pedigrees (See Fig.4.4). Although, these estimations are highly correlated ($r = 0.97, p = 1.1e-209$, Fig.4.5c), it is noteworthy that the SNP-based heritability estimation does not capture all genetic information. Indeed, only common SNPs are considered in our analysis. Rare SNPs variants, epigenetic variations, copy number variation are not modelised in the analysis. Additionally, genotype-based heritability with GCTA assume no shared environment. In practice, this is achieved by using unrelated individual. As HCP cohort is composed of twins and siblings, this HCP-GCTA analysis do not follow that standard and its derived results can be biased. These results should be taken with caution. Furthermore, while SNP-based GCTA heritability captures the SNP heritability, pedigree-based SOLAR heritability captures a much broader version of the heritability including for example non-additive effect [Manolio et al., 2009]. Starting from this observation, the comparison between both estimates became hard to do and irrelevant.

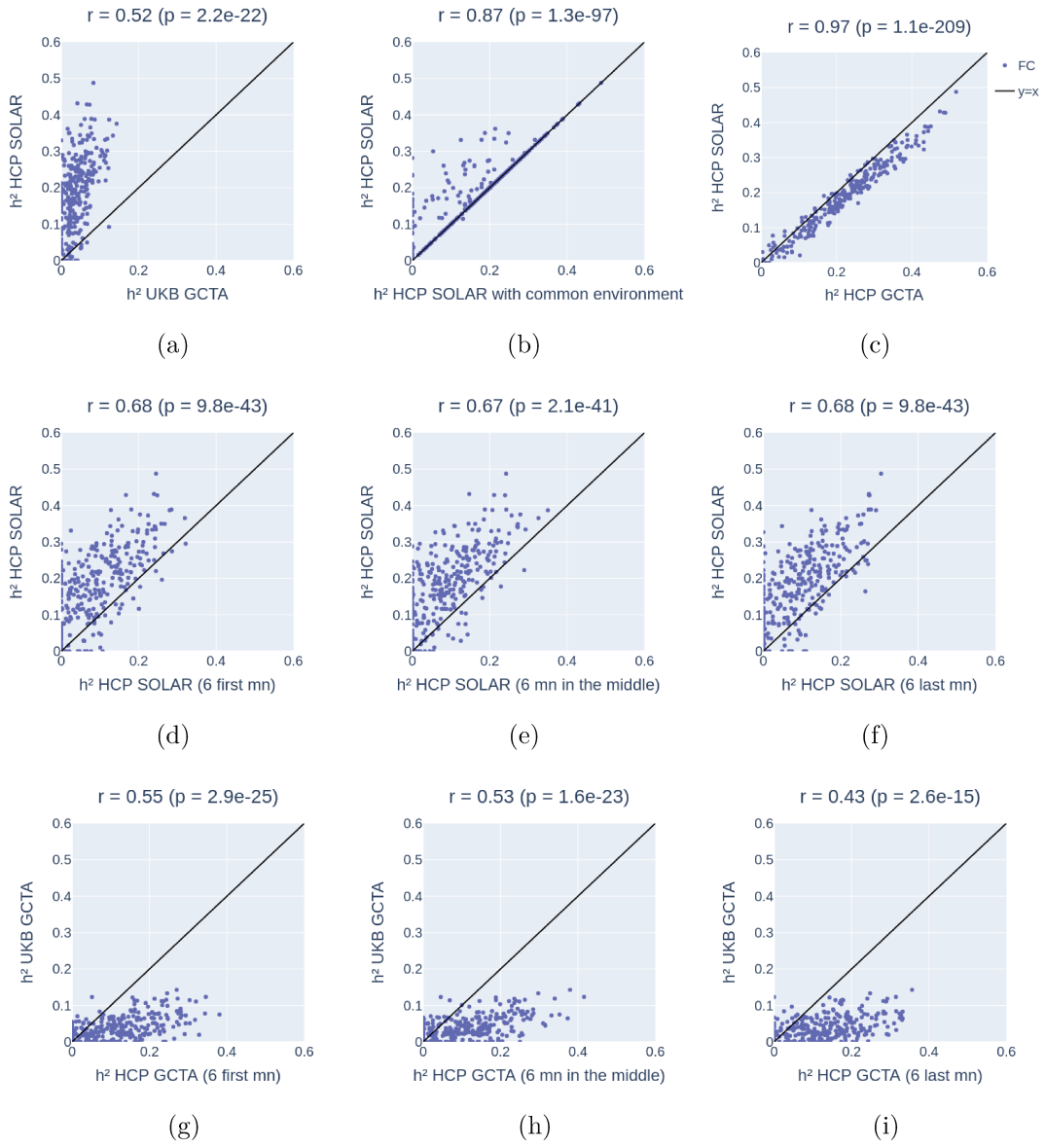

Figure 4.5 – Comparison between heritabilities obtained with SOLAR on HCP (concatenation of the 4 runs) and the ones obtained with : (a) GCTA on HCP, (b) SOLAR on HCP taking into account the shared environment, (c) GCTA on UKB, (d) SOLAR on HCP (6 first minutes of the signal), (e) SOLAR on HCP (6 minutes in the middle of the signal), (f) SOLAR on HCP (6 last minutes of the signal)

Second, we took into account the shared environment effect in the HCP cohort and found that the heritability estimations remained highly similar ($r = 0.87, p = 1.3\text{e}{-97}$) to the ones estimated without modeling the shared environment (See Fig.4.5b). These results could, to some extent, be compared to the adoption studies presented in chapter 1.6.1. The adoption studies compare adopted children's linguistic abilities with those of their adopted and biological relatives. Taken as a whole, these studies suggest that genetic factors affect language abilities. This observation is in line with our findings. However, this results should be taken with caution. One question arises: To what extent the household feature capture the environment variable

and to what extent, should we compare it to adoption studies which are certainly more relevant for the estimation of the human language environment part?

Third, as highlighted by [Elliott et al., 2019], long resting-state time series allow a better estimation of intrinsic connectivity and thus higher estimates of heritability. The resting-state time series last longer in HCP compared to UKB. We thus cut the time series the HCP's participants and considered the 6 first minutes, the 6 minutes in the middle and finally the 6 last minutes as shown in the Fig.4.6. We calculated resting-state FC endophenotypes and estimated their heritabilities. As in [Elliott et al., 2019], we observe that the values of $h2$ are higher for the whole uncut sessions compared to the 6-minute sessions in HCP (See Fig.4.5d, 4.5e, 4.5f). This suggest that long resting-state fMRI time series improve the reliability of intrinsic connectivity estimates and subsequently, it better captures inter-individual differences.

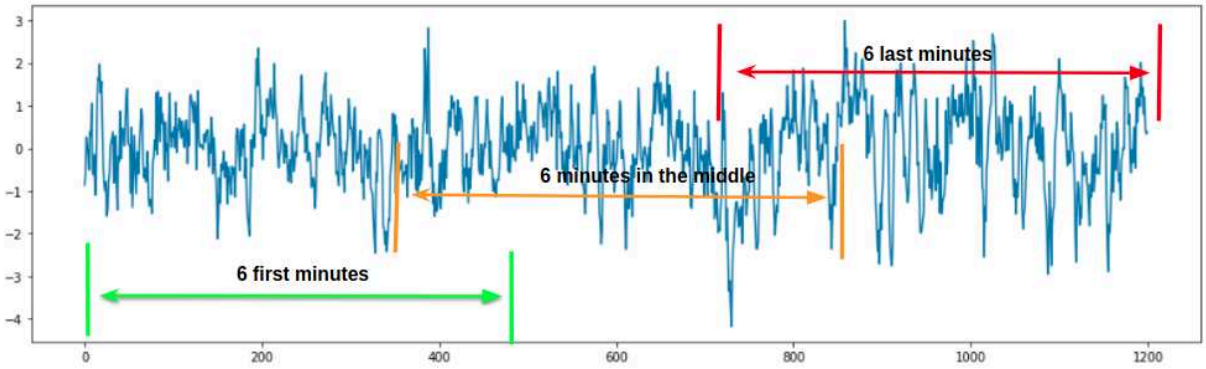

Figure 4.6 – Different cut of the resting-state time serie (6 minutes) obtained from HCP cohort.

Fourth, we compared the heritability of FC obtained from HCP cohort (6 first minutes, 6 minutes in the middle and 6 last minutes) using genotyping data (GCTA [Yang et al., 2011]) with the heritability of FC obtained from UKB cohort (6 minutes) using genotyping data as well (GCTA [Yang et al., 2011]). Although the session lengths are now comparable, a significant discrepancy between h_2 values remains (See Fig.4.5g, 4.5h, 4.5i). Nevertheless, the overall pattern remains correlated: UKB/HCP-(6 first minutes) $r = 0.55, p = 2.9e-25$; UKB/HCP-(6 minutes in the middle) $r = 0.53, p = 1.6e-23$; UKB/HCP-(6 last minutes) $r = 0.43, p = 2.6e-15$. One potential explanation of this observed gap concerns the age of the participants in each cohort. Contrary to UK Biobank which constitutes a relatively old sample (mean age=54 $\pm$7.45 years), participants in HCP cohort are younger (mean age=29 $\pm$3.56 years) and thus, the influence of the environmental factors may differ. A growing body of literature examines changes in heritability estimates over time [Bergen et al., 2007]. For example [Bouchard, 2013] show evidence that the heritability of IQ increases with age. It reaches an asymptote at about 0.80 at 18˘20 years of age and continuing at that level well into adulthood. Furthermore, the heritability of IQ appears to diminish with advancing age. In a sample of adult twins (aged from 27 to 59) and older cohort (aged from 60 to 94), a decrease of verbal and performance IQ heritability measures was observed with 70%, 73% and 56% and 60% respectively [Finkel and McGue, 1998]. [Bergen et al., 2007] suggests that beyond the tumultuous formative years, environmental effects may

begin to accumulate and form a larger proportion of the total phenotypic variance. Too little research has been done to deduce the overall pattern of heritability changes in later adulthood. Future studies that cover different developmental stages; i.e. adolescence and late adulthood, will inform us whether the observed heritability reflect some age-related specificity.

Overall, these different hypotheses contributed to explain the gap observed between both SNP-based and pedigree-based human language heritability estimates. The results obtained are in line with [Le Guen et al., 2019] work that used surface area and cortical thickness as endophenotypes. Although these different hypotheses helped to explain the observed discrepancy between the two heritability estimates, this experimental design does not allow us to present a definitive answer that would explain this phenomenon.

4.5 Conclusion

We observed significant heritabilities of the language (endo)phenotypes. These heritabilities display a large range of values depending on the trait considered but also the design of the cohort: twin versus general population cohorts. This work emphasises that human language brain organisation is under relatively strong genetic control. We found lower levels of SNP heritability for functional connectivity compared to heritability estimated in twin cohorts. This is a frequently voiced concern and typical of many traits in the literature [Elliott et al., 2018, Yang et al., 2015]. It may results from upward bias in twin study estimates due to gene–gene and gene–environment interactions [Purcell, 2002, Zuk et al., 2012], and/or downward bias of SNP heritability due to uncaptured rare genetic variation.

* * *
* *
*

Chapter 5

Shared genetic variance between language-related performance, language-brain activations and language functional connectivity

Chapter Outline

5.1 Shared heritability between both resting-state functional connectivity and neural activations 91
5.2 Shared heritability between both resting-state functional connectivity and language-related scores 92
5.3 Shared heritability between both task activations and language-related scores 92
5.4 Discussion 93

In the previous chapter, we estimated the human language heritability in both psychometric and imaging approaches. We used two large-scale resources currently available, namely the Human Connectome Project (HCP) and the UK Biobank (UKB) introduced in the chapter 2.1 to contribute to the study of language heritability. We observed a hierarchy of language heritability estimates from the Human Connectome Project (twin study) with 19.4-71.7% for language-behavioural scores, 11.4-48.7% for resting-state FC, and 14.4-34.9% for language-task activations. In terms of heritability ranking, the resting-state functional connectivity edges show low levels of heritability compared to behavioural scores. This observation was also made regarding structural features such as cortical or white matter tracts features (in UKB [Elliott et al., 2018]).

Although functional MR imaging is recognised to produce valuable endophenotypes [Elliott et al., 2018], resting-state FCs between language regions represent remote measures of language as the participants are not engaged in any language task-experiments and simply stay at rest. As stated in the chapter 1.3.2.1, previous works reported that resting-state derived endophenotypes are correlated with behavioural language processing [Cheema et al., 2021, Cross et al., 2021, Koyama et al., 2011, Stevens et al., 2017]. However, with the current release, no behavioural language scores were provided in the UK Biobank cohort. We were thus unable to confirm the observed correlations between resting-state FC endophenotypes and language behavioural scores.

In this chapter, we want to take advantage of the Human Connectome Project cohort which comprises language-related scores, language task-based fMRI data as well as resting-state fMRI data to calibrate the relevance of the resting-state image derived endophenotypes in the human language context through a bivariate heritability study. To do so, we performed bivariate genetic analyses to quantify the shared genetic influence between human language measure. In this chapter, we use pedigree and psychometric measures (chapter 3.1) and MRI data including neural activation measured in language task fMRI experiment (see chapter 3.2), functional connectivity estimated in resting-state fMRI (see chapter 3.3) from the Human Connectome Project (HCP) cohorts introduced in the chapter 2.1. We restricted our analysis to a small number of cognitive performance scores measured during the MRI session and considered the most representative of the human language. We used the average of accuracy of both conditions (STORY and MATH) in the language task to characterise the individual performance. Regarding the NIH behavioural scores, the working memory, the oral reading recognition, and the vocabulary comprehension scores were further considered in this analysis. All of these features are well detailed in the chapter 3. A large number of endophenotypes are derived from these three modalities. This methodological choice aims to reduce the number of tests to be performed and alleviates the correction for multiple tests. Furthermore, and for the sake of multiple corrections, we first conducted a (endo)phenotypic correlation to quantify the relationship between the human language performances (scores), and the two functional traits derived from the imaging. The significant (endo)phenotype pairs were subjected to a bivariate genetic analysis. The latter one quantify the shared genetic part taken in the correlation of these (endo)phenotypes pairs. As covariates, the sex, age, the ethnicity (Hispanic or not), and the first four principal components

of the principal component analysis of the genetic data were considered. Furthermore, to define significantly phenotypically and genetically correlated (endo)phenotypes, a 0.05 threshold on False Discovery Rate (FDR) adjusted p-values was applied to account for multiple testing on the paired (endo)phenotypes for both pheonotypic and genotypic correlation analysis.

5.1 Shared heritability between both resting-state functional connectivity and neural activations

We computed the endophenotypic correlation between resting-state functional connectivity (300 FCs) and neural activations (25). Table C.1 summarises the endophenotypic correlation and their associated p-values. P-values correction for multiple testing revealed 215 among 7500 = 300∗25 paired FCs-neural activations endophenotypes ranging from $r = -0.34, p_{FDR} = 4.76\text{e}{-19}$ for the PrF3op↔SMG with PrF3op to $r = 0.11, p_{FDR} = 4.95\text{e}{-02}$ for the F3td↔RolS with F3td. Next, we performed a bivariate genetic analysis using these 215 paired endophenotypes. The shared genetic variance estimates for these endophenotypes are presented in the Table 5.1 P-values correction for multiple testing revealed 12 among 215 significantly correlated endophenotypes pairs ranging from $rg = 0.89, p_{FDR} = 3.19\text{e}{-2}$ for the T1↔F2antR with T1 to $rg = 0.48, p_{FDR} = 3.19\text{e}{-02}$ for the Pole↔AG with AG.

Table 5.1 – **Shared heritabilities between both resting-state functional connectivity and neural activations.** Bold rows represents pairs of endophenotypes with significant shared heritability after false discovery rate correction at $p < 0.05$. For the sake of readability, only significant results are displayed. Pearson Correlation between pairs of endophenotypes are also shown. The asterisk represent significant endophenotypic correlation after false discovery rate correction at $p < 0.05$. Table C.1 summarises the endophenotypic correlation and their associated p-values.

Endophenotype 1	Endophenotype 2	Endophenotypic correlation	Genetic correlation	P value	SE	FDR P value
F2p↔SMG	**F3td**	0.128*	100.0%	1.03E-03	Not Computable	3.19E-02
F3td↔T3p	**F3td**	-0.115*	-100.0%	2.16E-03	Not Computable	3.84E-02
T1↔F2antR	**T1**	-0.177*	-89.0%	1.51E-03	0.376	3.19E-02
Prec↔F2antR	**PrF3op**	-0.124*	-76.6%	6.29E-04	0.242	3.19E-02
T2ml↔F3opdR	**T2ml**	-0.137*	-74.9%	9.93E-04	0.263	3.19E-02
Pole↔F3opd	**F3opd**	0.254*	74.4%	1.10E-04	0.173	2.35E-02
F3opd↔SMG	**F3opd**	-0.238*	-65.2%	4.15E-04	0.172	3.19E-02
Fusa↔T3p	**PT**	0.137*	57.4%	1.22E-03	0.176	3.19E-02
T1↔T1a.HeschlR	**T1**	0.197*	53.6%	1.64E-03	0.172	3.19E-02
PT↔T1	**T1R**	0.181*	50.2%	1.36E-03	0.148	3.19E-02
AG↔F3orb	**AG**	0.149*	49.6%	1.37E-03	0.154	3.19E-02
Pole↔AG	**AG**	0.154*	48.2%	7.46E-04	0.138	3.19E-02

5.2 Shared heritability between both resting-state functional connectivity and language-related scores

We computed the endophenotypic correlation between human language performances (4 language-related scores), and the functional connectivity estimated in resting-state fMRI (300 FCs). Table C.2 summarises the endophenotypic correlation and their associated p-values. None of the $1200 = 300 * 4$ pairs FCs-language-related scores endophenotypes passed the correction for multiple testing.

5.3 Shared heritability between both task activations and language-related scores

We computed the endophenotypic correlation between human language performances (4 language-related scores) and neural activations (25). Table C.3 summarises the endophenotypic correlation and their associated p-values. P-values correction for multiple testing revealed 28 among $100 = 25 * 4$ pairs FCs-neural activations endophenotypes ranging from $r = 0.24, p_{FDR} =$ 1.09e−09 for the vocabulary comprehension and Pole to $r = 0.09, p_{FDR} =$ 3.78e−02 for the oral reading recognition and PT. Next, we performed a bivariate genetic analysis using these 28 pairs of endophenotypes. The shared genetic variance estimates for these endophenotypes are presented in the Table 5.2. P-values correction for multiple testing revealed 23 among 28 significantly correlated endophenotypes pairs ranging from $rg = 0.61, p_{FDR} =$ 4.05e−4 for the Language task accuracy and the temporal pole to $rg = 0.26, p_{FDR} =$ 2e−02 for the vocabulary comprehension and T2ml.

Table 5.2 – **Shared heritabilities between both task activations and language-related scores.** Bold rows represents pairs of endophenotypes with significant shared heritability after false discovery rate correction at $p < 0.05$. For the sake of readability, only significant results are displayed. Pearson Correlation between pairs of endophenotypes are also shown. The asterisk represent significant endophenotypic correlation after false discovery rate correction at $p < 0.05$. Table C.3 summarises the endophenotypic correlation and their associated p-values.

Endophenotype 1	Endophenotype 2	Endophenotypic correlation	Genetic correlation	P value	SE	FDR P value
Pole	**Language task overall accuracy**	0.217*	61.8%	7.23E-05	0.155	4.05E-04
STSp	**Language task overall accuracy**	0.130*	61.1%	2.18E-04	0.175	8.72E-04
T1R	**Working Memory**	0.147*	59.3%	5.83E-06	0.134	8.16E-05
Pole	**Working Memory**	0.148*	57.0%	3.23E-05	0.142	2.26E-04
Pole	**Vocabulary Comprehension**	0.239*	56.3%	7.36E-07	0.112	2.06E-05
T1R	**Language task overall accuracy**	0.095*	53.3%	5.67E-04	0.167	1.30E-03
T2ml	**Working Memory**	0.145*	53.0%	2.41E-05	0.125	2.25E-04
PT	**Working Memory**	0.115*	50.9%	4.75E-04	0.146	1.23E-03
T2ml	**Language task overall accuracy**	0.142*	50.8%	3.83E-04	0.143	1.19E-03
STSp	**Working Memory**	0.133*	49.9%	4.82E-04	0.145	1.23E-03
T1a	**Language task overall accuracy**	0.175*	49.0%	2.27E-03	0.162	4.24E-03
STSp	**Vocabulary Comprehension**	0.183*	44.8%	3.48E-04	0.131	1.19E-03
Pole	**Oral reading recognition**	0.176*	41.8%	1.15E-04	0.108	5.36E-04
T1	**Language task overall accuracy**	0.093*	39.6%	3.82E-03	0.139	6.69E-03
T1a	**Working Memory**	0.142*	35.6%	1.04E-02	0.132	1.46E-02
T1R	**Vocabulary Comprehension**	0.105*	34.9%	1.78E-03	0.115	3.56E-03
T2ml	**Oral reading recognition**	0.142*	34.8%	6.02E-04	0.103	1.30E-03
T1	**Working Memory**	0.113*	34.7%	4.59E-03	0.122	7.14E-03
STSp	**Oral reading recognition**	0.108*	31.2%	6.97E-03	0.120	1.03E-02
T1R	**Oral reading recognition**	0.165*	30.0%	4.12E-03	0.000	6.79E-03
T1a	**Vocabulary Comprehension**	0.138*	29.9%	1.31E-02	0.122	1.74E-02
T1a.HeschlR	**Working Memory**	0.093*	28.0%	3.45E-02	0.132	4.21E-02
T2ml	**Vocabulary Comprehension**	0.126*	26.4%	1.58E-02	0.110	2.01E-02

5.4 Discussion

In the previous chapter, we showed that language related psychometric measures and image derived phenotypes are heritable. Although resting state fMRI data are reported as heritable, little is known about their relation to the language-related cognitive process. In this chapter, we address this question regarding the shared genetics between these ones and direct measures of language as cognitive process. To do so, we estimated phenotypic correlations between cognitive abilities, neural activations and task-free data in language. Moreover, we estimated the genetic proportion in these phenotypic correlations. Hence, we showed a shared aetiology between resting-state functional connectivity and neural activations. This work advocate for the existence of a link between resting-state and task-based data both phenotypically and genetically regarding human language brain organisation.

* * *
* *
*

Chapter 6

The genetic architecture of human language functional connectome

Chapter Outline

6.1 Multivariate genome-wide association analysis 97
6.2 Unraveling the genome: Evaluation of results from mvGWAS study of human language 107
6.3 Limitations 121
6.4 Conclusions 122

In the chapter 3, we exhibited different (endo)phenotypes including resting-state functional connectome regarding human language traits. In the chapter 4, we brought out that resting-state FC are, to some extent, under genetic control. This reinforce our belief that resting state FC endophenotypes capture inter-individual variation in brain function, and thus, are worthy targets for more in-depth genetic analysis. To date, no gene discovery experiments have been reported using resting-state functional MRI derived traits. Our study is therefore an attempt to fill this observed gap in the literature and to verify the relevance of task-free paradigm for the study of complex cognitive trait such as language.

Notwithstanding that rsfMRI FC are heritable, they are reported as showing the lowest levels of SNP heritability among available IDPs in UKB [Elliott et al., 2018]. In a massively univariate framework, it would be really difficult to disentangle the genetic associations with each FC signal and reach genome-wide statistical significance. Language-related brain regions share information across components and scales that support language, and genetic variants are supposed to have distributed effect across regions. Contrary to the massive univariate approach, multivariate GWASes have the advantage of leveraging the distributed nature of genetic effects and the presence of pleiotropy across modalities and is thus, more consistent with biology. Therefore, we consider globally this synergistic system and perform a multivariate approach with MOSTest [van der Meer et al., 2020]. This method introduced in the chapter 2.6 considers the distributed nature of genetic signals shared across brain regions and aggregates effects across spatially distributed traits of interest.

As mentioned in the chapter 2.2.1, in this thesis, two sets of regions of interest were employed for defining the language network. The first one named -Ocss- is defined based on the probabilistic activation map of a single fMRI contrast and includes the perisylvian regions which cover both Broca and Wernicke's areas. The second one named -SmPSS- represents a more extended language network and is a results of a meta-analysis regrouping and analysing a significant number of scientific reports. The latter one offers a more general view of the language regions, a rich interpretation of the regions' classification regarding language components (phonology, semantic and syntax) and more importantly, it offers potentially a more consensual set of ROIs within the neuroscientific community. In the chapter 4, we estimated the human language heritability using both resting-state functional connectivity extracted these two sets of ROIs. In this chapter, the same experimental design was applied to these two sets of endophenotypes. The obtained results will be compared to each other and will allow us to judge how representative the SmPSS set of ROIs actually is. Therefore, we performed a multivariate genetic association of the significantly heritable FC endophenotypes of each set separately. These consists on 142 FCs and 14 FCs extracted from both SmPSS and OcSS ROIs (see chapter 4.2.1). The results from these analyses were subjected to a replication study in an independent sample (N=4,754). Additionally, as the connections between different language regions are ensured by the white matter fiber bundles [Catani and Forkel, 2019, Catani et al., 2005], we hypothesised that the hit SNPs associated with the hit FCs could be associated with neuroanatomical white matter tracts that supports the information transmission between the regions that compose these hit-FCs. Therefore, we tested the potential associations of the hit SNPs with the following white matter bundles: the corpus callosum, the left frontal aslant tract, the left arcuate anterior/long/posterior segment,

the left inferior fronto-occipital fasciculus, the left uncinate tract (See Chapter 2.2.2 for more details). We used the endophenotypes resulting from the TBSS analysis described in the chapter 3·4·

6.1 Multivariate genome-wide association analysis

We performed a multivariate genome-wide association studies (mvGWAS) between the filtered imputed genotypes and the two sets of significantly heritable endophenotypes highlighted in the chapter 4.2.1.2, using the Multivariate Omnibus Statistical Test (MOSTest) [van der Meer et al., 2020]. As stated in the chapter 2.6, all endophenotypes were pre-residualised with covariates including sex, genotype array type, age, recruitment site, and ten first genetic principal components provided by UK Biobank. In addition, MOSTest performs a rank-based inverse-normal transformation of the residualised endophenotypes to ensure that the inputs are normally distributed. The distributions across the participants of all endophenotypes were visually inspected before and after covariate adjustment. MOSTest generated multivariate summary statistics that capture the significance of the association across all heritable language endophenotypes. To account for multiple testing over the whole genome, statistically significant SNPs were considered as those reaching the genome-wide threshold $p = 5e{-}8$.

GWAS using FCs derived from SmPSS set of ROIs. Concerning the FCs derived using SmPSS ROIs, we performed a mvGWAS with the 142 FCs with significant SNP-based heritability. This analysis tested each SNP separately for its simultaneous association with the 142 FCs and yielded 4566 significant SNPs at a genomic threshold, distributed on chromosomes 2, 3, 5, 6, 10, 11, 14, 15, 17, 18 and 22. FUMA [Watanabe et al., 2017] software was used to analyse mvGWAS results and identified lead SNPs at each associated locus. Considering the genome-wide significance threshold $p = 5e{-}8$, there were 20 distinct genomic loci distributed on the 11 chromosomes, associated with different aspects of language FC (Fig.6.1a, Table 6.1 and Supplementary Fig. 6.2, 6.3, 6.1b, and 6.5) and represented by 20 lead SNPs.

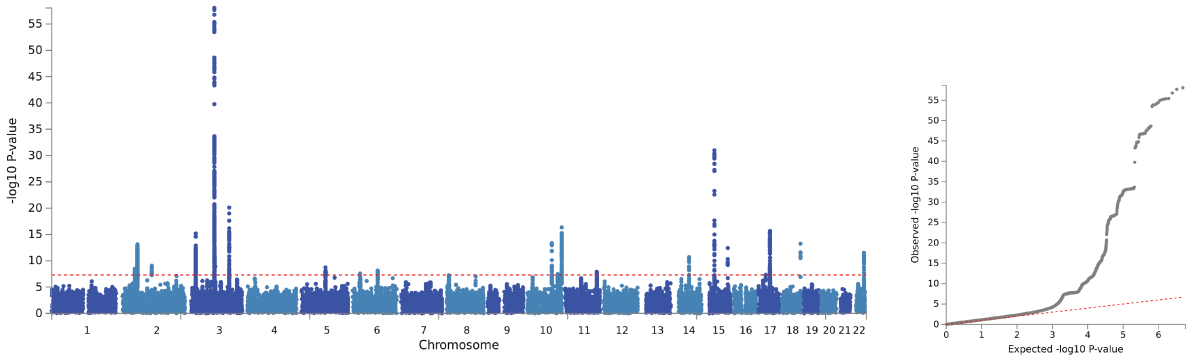

Figure 6.1 – **Multivariate GWAS analysis of the SmPSS resting state functional connectivity in 32,186 participants.** Manhattan plot for multivariate GWAS accross 142 FCs. The red dashed line indicates the genome-wide significance threshold $p = 5e{-}8$. The Quantile-quantile plot is also shown.

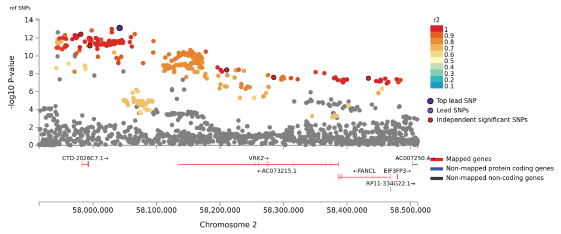

lead SNP: rs2717046

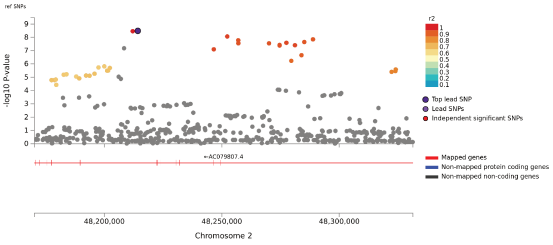

lead SNP: rs62141276

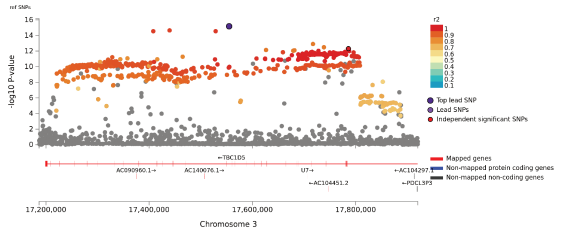

lead SNP: rs67851870

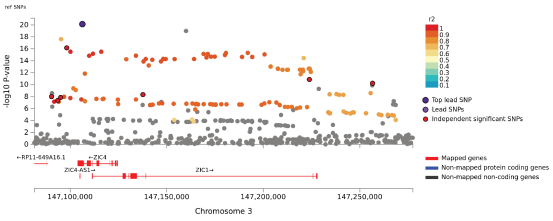

lead SNP: rs2279829

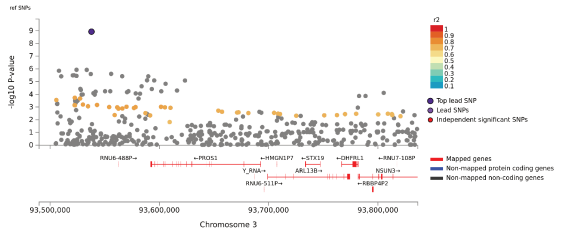

lead SNP: rs62266110

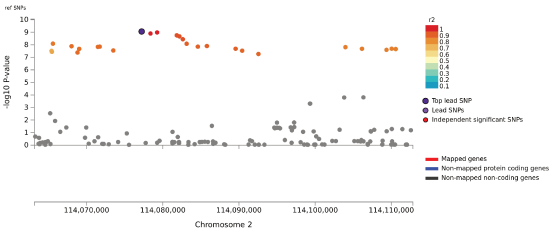

lead SNP: rs62158166

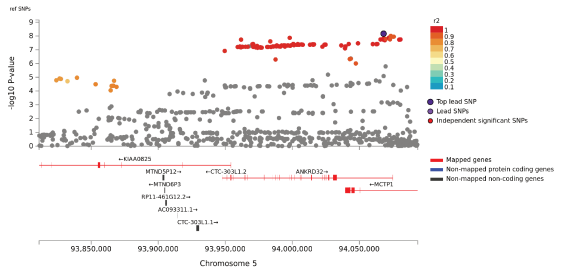

lead SNP: 5:94068140_AC_A

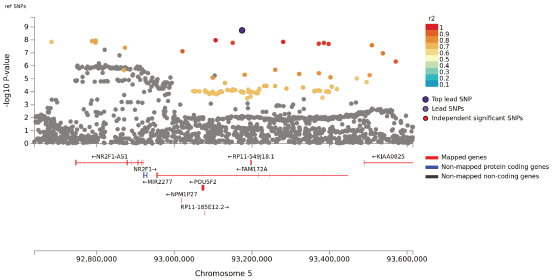

lead SNP: rs145120402

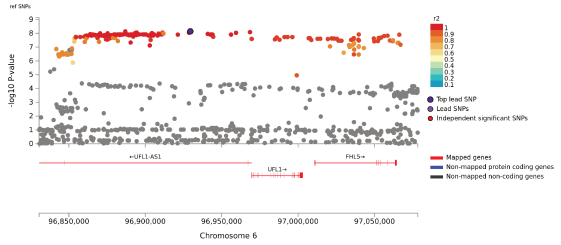

lead SNP: rs4262195

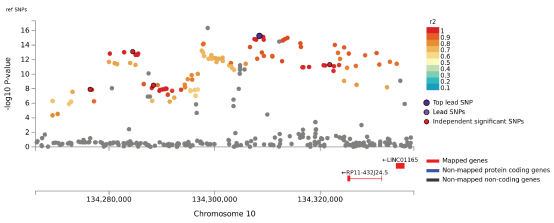

lead SNP: rs11146399

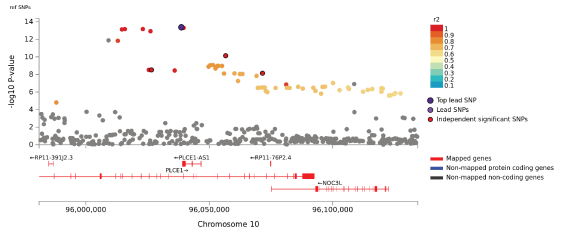

lead SNP: rs11187838

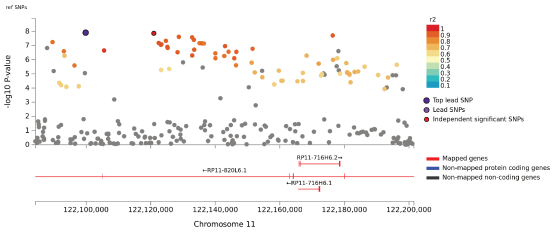

lead SNP: rs11218557

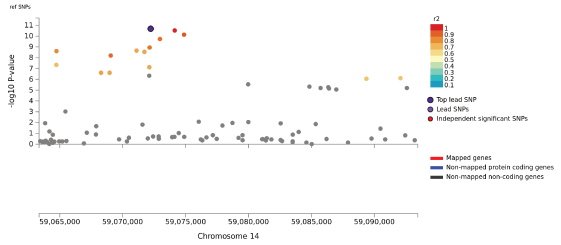

lead SNP: rs186347

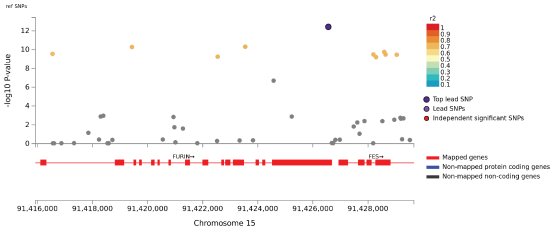

lead SNP: rs4702

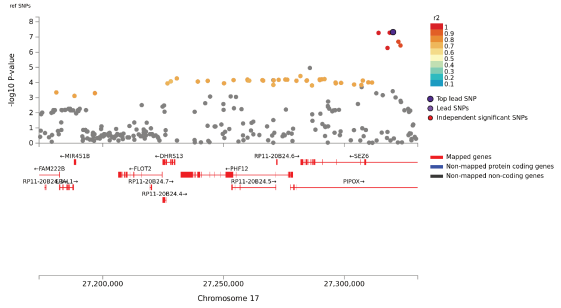

lead SNP: rs34039488

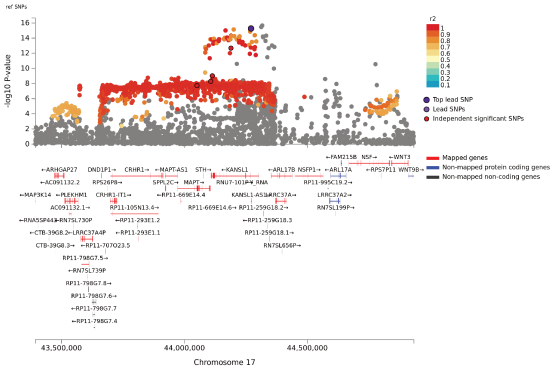

lead SNP: 17:44270659_G_A

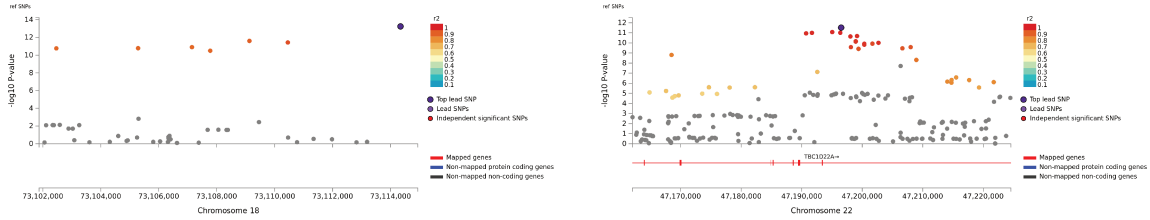

lead SNP: rs7234875 lead SNP: rs2542028

Figure 6.2 – Locus Zoom of the significant loci identified by the multiariate GWAS for functional connectivity.

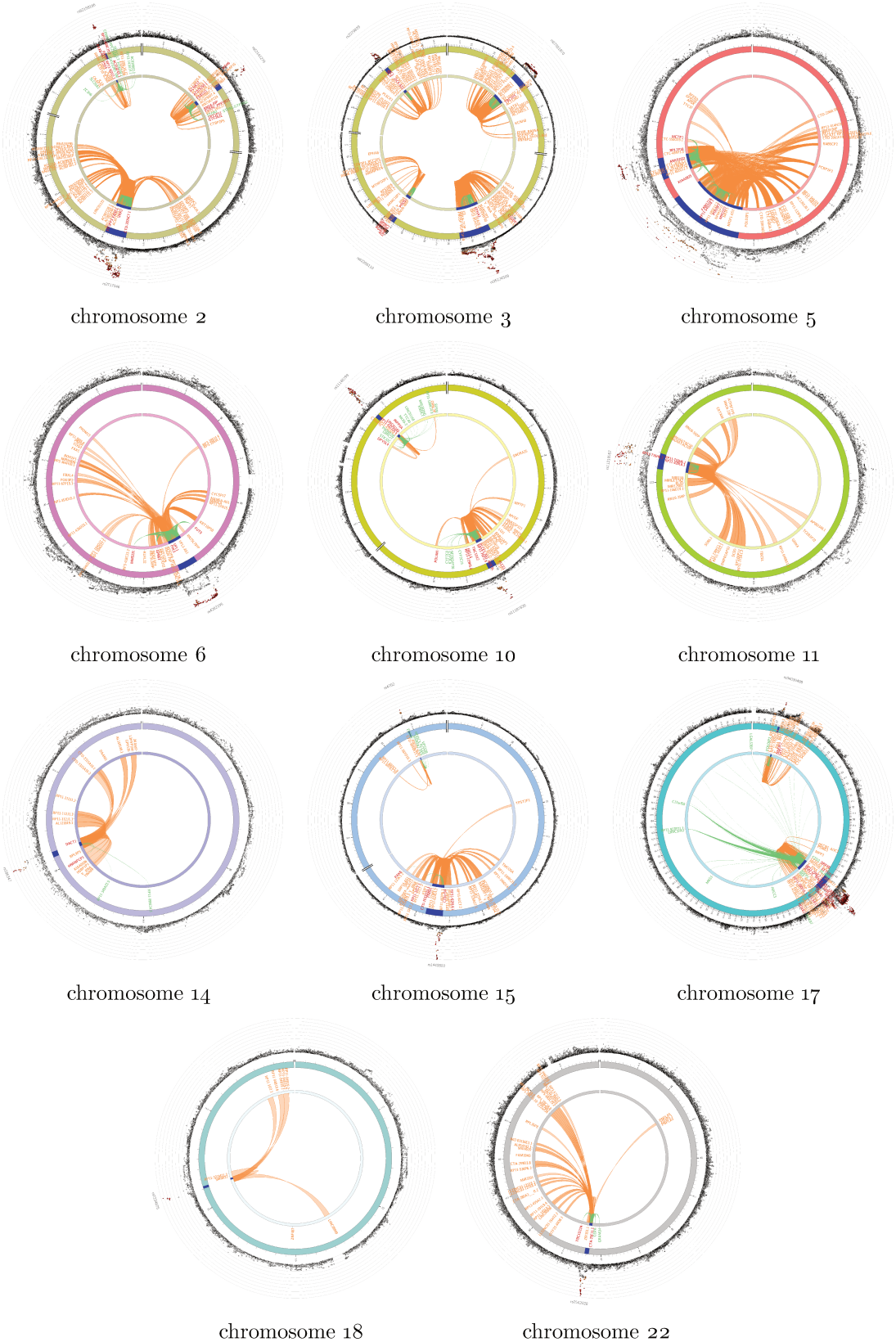

Figure 6.3 – **Genomic loci, eQTL associations and chromatin interactions identified via multivariate GWAS for functional connectivity.** Circos plot representing the genomic risk loci, and the genes associated with the loci by chromatin interactions and eQTLs. From outer layer to inner layer: Manhattan plot. Genomic risk loci are in blue. Genes mapped by chromatin interaction are in orange. Genes mapped by eQTL are in green. Genes mapped by both are in red. Chromatin interaction and eQTLs links follows the same color coding presented above.

GWAS using FCs derived from OcSS set of ROIs. Concerning the FCs derived using OcSS ROIs, we performed a multivariate genome-wide association study with the 14 heritable FCs. This analysis yielded 125 significant SNPs at a genomic threshold, distributed on chromosomes 3, 10, 14. FUMA identified 4 distinct genomic loci distributed on the 3 chromosomes, associated with different aspects of brain language cognitive activities (Fig.6.4, Table 6.2) and represented by 4 lead SNPs.

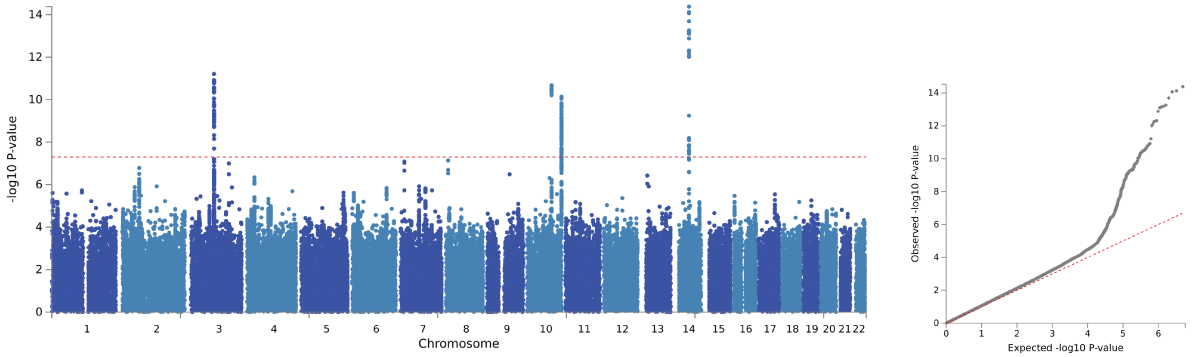

Figure 6.4 – Multivariate GWAS analysis of the OcSS resting state functional connectivity in 32,186 participants. Manhattan plot for multivariate GWAS accross 14 FCs. The red dashed line indicates the genome-wide significance threshold $p = 5e{-}8$. The Quantile-quantile plot is also shown.

Validation of lead SNPs associated with rsfMRI FCs. The multivariate genome-wide association results were replicated in an independent non-British sample considering the nominal significance threshold $p < 0.05$. Following the same pre-processing steps as for the primary sample, the non-British replication sample consists in 4,754 individuals with a mean age of 53 years ($\pm$7.55) and 2,601 female.

Concerning the **-SmPSS-FCs**, three lead SNPs out of twenty were replicated at the nominal significance level ($p < 5e{-}2$) on multivariate test in the independent non-British replication dataset: $rs1440802(p = 9.58e{-}3)$, $rs35124509(p = 3.25e{-}3)$, $rs11187838(p = 2.92e{-}2)$. Table 6.1 summarises these results. Moreover, these lead SNP showed association at $p < 0.05$ on univariate testing of all but three specific central traits identified in the discovery mvGWAS.

Table 6.1 – **Genomic loci associated with heritable language functional connectivities (SmPSS ROIs) using MOSTest.** Lead SNP: ID of the lead SNPs within each locus. Position: position of the SNP in the hg19 human reference genome. mvgwasP discovery -British-: MOSTest association P value obtained using the discovery sample. mvgwasP replication -non British-: MOSTest association P value obtained using the independent replication sample. Functionnal category: Functional consequence of the SNP on the gene obtained from ANNOVAR. 'Central' phenotypes: the phenotypes that contributed most to the multivariate association considering the genome-wide association threshold ($p = 5e - 8$).

Genomic Locus	Lead SNP	Chr	Position	Functional Category	non effect allele	effect allele	MAF	mvgwasP (discovery -British-)	mvgwasP (replication -non British-)	Nearest Gene	'central' phenotypes
1	rs62141276	2	48214217	ncRNA intronic	A	G	0.367	$p = 3.26e{-9}$	$p = 0.27$	*AC079807.4*	-
2	rs2717046	2	58041936	intergenic	T	C	0.380	$p = 7.50e{-14}$	$p = 0.95$	*CTD-2026C7.1*	-
3	rs62158166	2	114077218	intergenic	C	G	0.223	$p = 8.69e{-10}$	$p = 0.38$	*PAX8*	RolS↔PrecR
4	rs67851870	3	17554860	intronic	G	A	0.322	$p = 6.57e{-16}$	$p = 0.35$	*TBC1D5*	-
5	**rs35124509**	**3**	**89521693**	**exonic**	**C**	**T**	**0.401**	$p = 8.95e{-59}$	$p = 3.25e{-3}$	***EPHA3***	**AG↔F3orb,pSTS↔Pole, Pole↔T2ml,T1a↔STSp STSp↔F3orb,SMG↔T3p, AG↔STSp,F2p↔AG, T2ml↔SMG**
6	rs62266110	3	93537923	intergenic	A	G	0.319	$p = 1.17e{-09}$	$p = 0.93$	*RNU6-488P*	-
7	rs2279829	3	147106319	UTR3	T	C	0.212	$p = 7.57e{-21}$	$p = 0.68$	*ZIC4*	T2ml↔PrF3op,Prec↔F3opd, F2p↔STSp,SMG↔F2antR,
8	rs145120402	5	93174765	intronic	C	A	0.0433	$p = 1.83e{-9}$	$p = 0.10$	*FAM172A*	-
9	5:94068140_AC_A	5	94068140	intronic	A	AC	0.209	$p = 6.79e{-9}$	$p = 0.30$	*ANKRD32:MCTP1*	-
10	rs4262195	6	96929475	ncRNA intronic	C	T	0.181	$p = 7.19e{-9}$	$p = 0.70$	*UFL1-AS1*	-
11	**rs11187838**	**10**	**96038686**	**intronic**	**A**	**G**	**0.435**	$p = 4.29e{-14}$	$p = 2.92e{-2}$	***PLCE1***	-
12	rs11146399	10	134308479	intergenic	T	C	0.457	$p = 5.50e{-16}$	$p = 0.28$	*RP11-432J24.5*	RolS↔PrecR
13	rs11218557	11	122099839	ncRNA intronic	C	T	0.4579	$p = 1.24e{-8}$	$p = 0.77$	*RP11-820L6.1*	-
14	rs186347	14	59072226	intergenic	T	G	0.458	$p = 2.08e{-11}$	$p = 0.92$	*DACT1*	Pole↔T2ml
15	**rs1440802**	**15**	**39635124**	**ncRNA intronic**	**C**	**T**	**0.090**	$p = 1e{-31}$	$p = 9.58e{-3}$	***RP11-624L4.1***	**Prec↔F3opd, PrecR↔RolS**
16	rs4702	15	91426560	UTR3	A	G	0.442	$p = 3.77e{-13}$	$p = 0.42$	*FURIN*	-
17	rs34039488	17	27320232	intronic	A	G	0.162	$p = 4.74e{-8}$	$p = 0.46$	*PIPOX:SEZ6*	-
18	17:44270659_G_A	17	44270659	intronic	A	G	0.399	$p = 5.36e{-16}$	$p = 0.45$	*KANSL1*	-
19	rs7234875	18	73114340	intergenic	C	T	0.399	$p = 5.71e{-14}$	$p = 0.82$	*RP11-321M21.3*	F3tv↔SMG
20	rs2542028	22	47196524	intronic	G	A	0.268	$p = 3.06e{-12}$	$p = 0.60$	*TBC1D22A*	-

Concerning the **-OcSS-FCs**, one lead SNP was replicated at the nominal significance level ($p <$ 5e−2) on multivariate test in the independent non-British replication dataset ($rs7917322(p =$ 3.16e−2)) while the lead SNP $rs7650184(p =$ 6.43e−2) showed a tentative association in the multivariate level. Table 6.2 summarises these results.

Table 6.2 – **Genomic loci associated with heritable language functional connectivities (OcSS ROIs) using MOSTest.** Lead SNP: ID of the lead SNPs within each locus. Position: position of the SNP in the hg19 human reference genome. mvgwasP discovery -British-: MOSTest association P value obtained using the discovery sample. mvgwasP replication -non British-: MOSTest association P value obtained using the independent replication sample. Functionnal category: Functional consequence of the SNP on the gene obtained from ANNOVAR. 'Central' phenotypes: the phenotypes that contributed most to the multivariate association considering the genome-wide association threshold ($5e-8$).

Genomic Locus	Lead SNP	Chr	Position	Functional Category	non effect allele	effect allele	MAF	mvgwasP (discovery -British-)	mvgwasP (replication -non British-)	Nearest Gene	'central' phenotypes
1	rs35124509	3	3p11	exonic	C	T	0.4018	6.125755e-12	3.74e-1	*EPHA3*	-
2	rs11187838	10	10q23.33	intronic	A	G	0.4354	2.122796e-11	5.64e-2	*PLCE1*	TP↔aSTS
3	rs67221163	10	10q26.3	intergenic	G	C	0.4547	1.841408e-10	4.65e-1	*RP11-432J24.5*	-
4	rs160459	14	14q23	intergenic	C	A	0.4588	4.155101e-15	3.59e-4	*DACT1*	TP↔pSTS

The obtained results regarding the multivariate genome-wide association study with the 14 heritable FCs -OcSS- represented by 4 distinct genomic loci distributed on the 3 chromosomes are included in the results obtained from the multivariate genome-wide association study with the 142 heritable FCs -SmPSS-. In the following, for the sake of readability, we will only present the results of the FCs from this set ROIs.

Regional effect. Such a multivariate approach has the advantage of leveraging the distributed nature of genetic effects and the presence of pleiotropy across endophenotypes. Loci respectively identified by MOSTest as associated with several FCs made clear that these SNPs have distributed effects, often with mixed directions, across regions and FCs. Fig. 6.1 shows the FCs associations with each of the twenty lead SNPs loci.

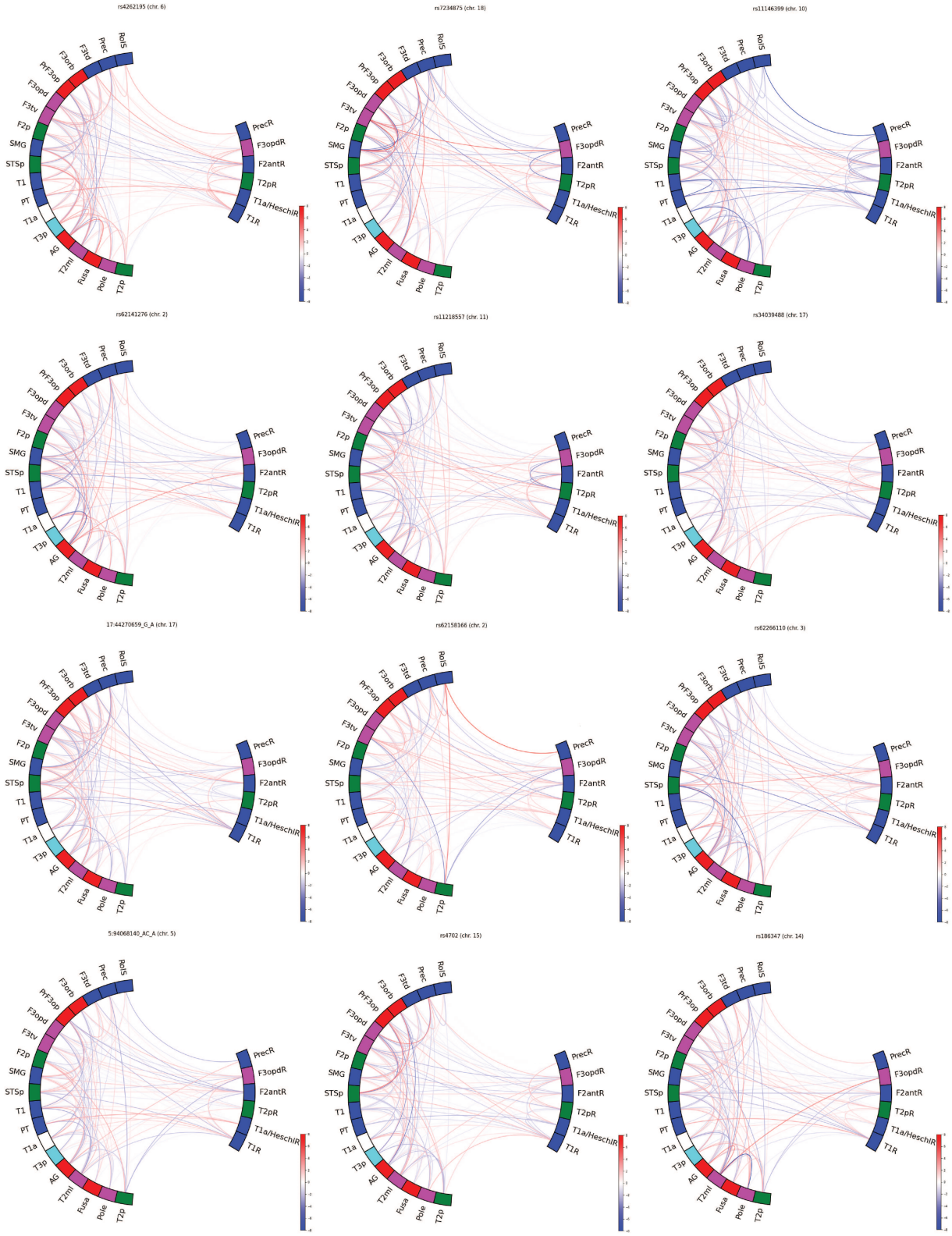
rs4262195 (chr. 6)
rs7234875 (chr. 18)
rs11146399 (chr. 10)
rs62141276 (chr. 2)
rs11218557 (chr. 11)
rs34039488 (chr. 17)
17:44270659_G_A (chr. 17)
rs62158166 (chr. 2)
rs62266110 (chr. 3)
5:94068140_AC_A (chr. 5)
rs4702 (chr. 15)
rs186347 (chr. 14)
RolS
Prec
F3td
F3orb
PrF3op
F3opd
F3tv
F2p
SMG
STSp
T1
PT
T1a
T3p
AG
T2mi
Fusa
Pole
T2p
PrecR
F3opdR
F2antR
T2pR
T1a/HeschlR
T1R

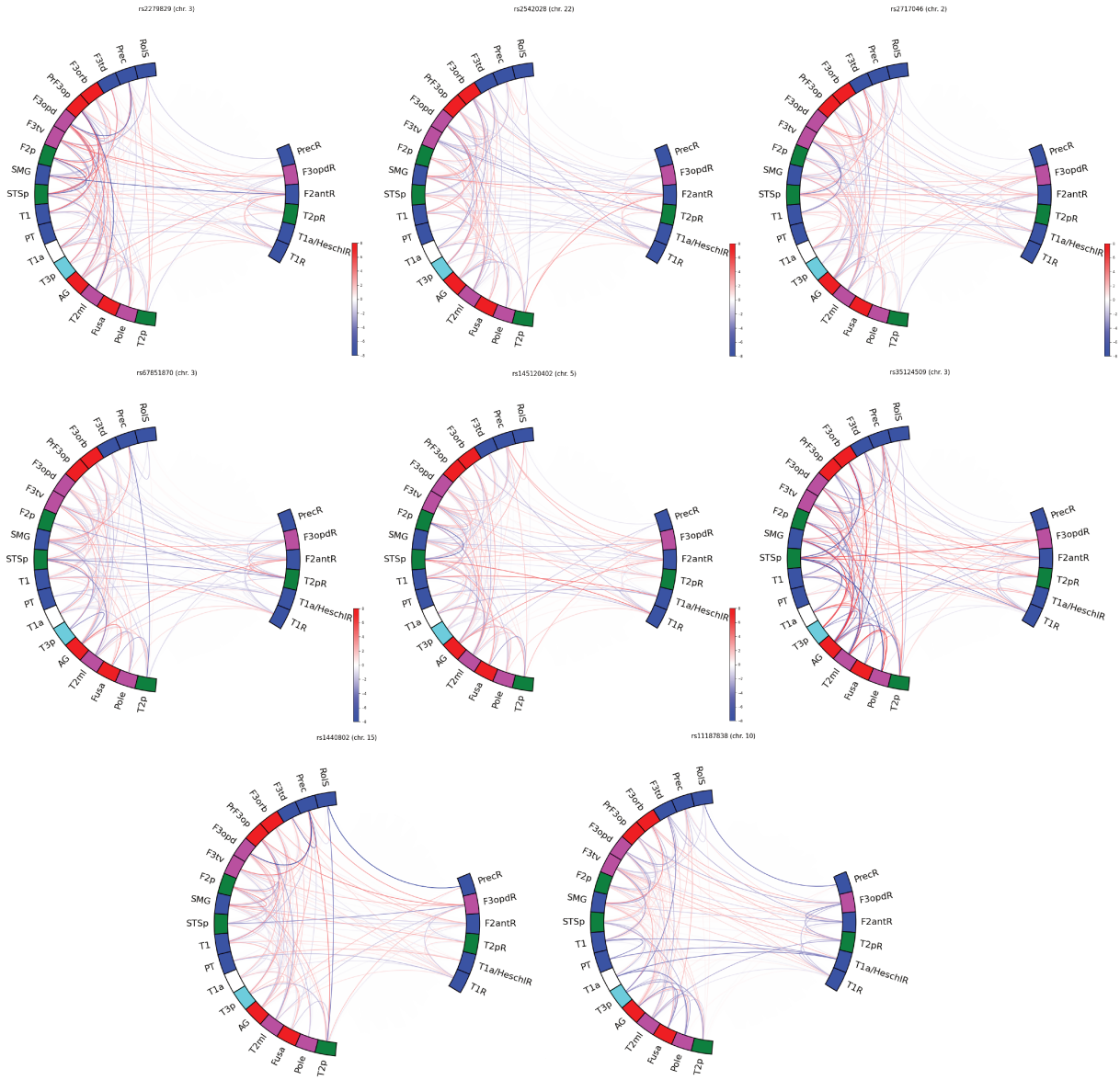

Figure 6.5 – **Regional effects.** Circle plot where all 25 regions are represented (19 ROIs on the left represent the left hemisphere and 6 ROIs on the right represent the right hemisphere) illustrating the lead SNPs identified from the multivariate GWAS for functional connectivity. Each link between two regions represents an endophenotype. The intensity of the color between two regions represents the Z-values from the univariate GWAS for each FCs as defined by the color bar. The absolute Z-values scaling is clipped at 8 ($p = 1.2\text{e}{-15}$). Positif effects of carrying the minor allele are shown in red, and negative in blue.

6.2 Unraveling the genome: Evaluation of results from mvGWAS study of human language

In order to interpret this wealth of results, we proceed as follow:

- First, for each lead SNP, we defined the 'central' endophenotypes that contributed the most in the multivariate association by using the individual univariate summary statistics performed by MOSTest and by considering the genome-wide significance threshold ($p < 5e-8$) (Supplementary Table 6.1).
- Second, the SNP-based genetic correlation was estimated (using GCTA [Lee et al., 2012] software) for each pair of central FCs associated to each genetic loci.
- Third, we hypothesised that the genetic variants significantly associated with the language FCs could be associated with neuroanatomical tracts that support the information transmission between language areas. Therefore, we tested the potential associations between the hit SNPs with the average values of dMRI relevant white matter tracts.

In what follows, we will review the associations that were replicated which includes these three genomic loci: $15q14$, $3p11.1$ and $10q23.33$.

6.2.1 *Perceptual motor* interactions process driven by *THBS1* gene

Identification of 'central' endophenotypes associated with $15q14$ genomic risk region. On $15q14$, the lead SNP rs1440802 had two central FCs (that contributed the most in the multivariate association, see 6.2). The minor allele was associated with the partial correlation between:

(i) The precentral gyrus and the dorsal pars opercularis (Prec↔F3opd). Both connected regions are in the left frontal lobe, and are labelled with a phonological linguistic component (Prec) and multi-labelled with semantic and sentence language processing (F3opd).

(ii) The (PrecR↔RolS) corresponds to the partial correlation between the precentral gyrus and the Rolandic sulcus. Both regions are identified in the right and left frontal lobes respectively, and are labelled as phonological linguistic component (Fig. 6.6a and Supplementary Table 6.1).

These edges have previously been described in FC studies dedicated to language and more specifically in the perceptual motor interactions [Fridriksson et al., 2009, Nishitani and Hari, 2000, Schwartz et al., 2008, 2012, Turner et al., 2009].

SNP-based genetic correlation of the 'central' endophenotypes.
Both (Prec↔F3opd) and (PrecR↔RolS) 'central' endophenotypes displays a non-significant genetic correlation ($r_G = 16.9 \pm 0.13$, $p = 9.80e-02, N = 32,186$). Table 6.3 reports genetic correlations for the 'central' endophenotypes identified in the three replicated genomic loci.

Table 6.3 – **The SNP-based genetic correlation analysis was estimated using GCTA software, for each pair of central FCs associated to** $15q14$**,** $3p11.1$ **or** $10q23.33$ **genetic loci.** Bold phenotypes represents pair of FCs with significant genetic correlation after false discovery rate correction at $p < 0.05$.

Endophenotype 1	Endophenotype 2	P value	rG	SE	FDR P value
T1a↔STSp	**Pole↔STSp**	2.29E-05	54.8%	0.132	8.47E-04
SMG↔T3p	**AG↔STSp**	9.78E-05	65.6%	0.192	1.81E-03
STSp↔F3orb	**Pole↔STSp**	2.21E-04	40.4%	0.111	2.72E-03
AG↔F3orb	**T2ml↔SMG**	1.01E-03	-46.9%	0.158	9.39E-03
AG↔F3orb	**SMG↔T3p**	3.76E-03	53.6%	0.211	1.39E-02
Pole↔T2ml	**STSp↔F3orb**	3.25E-03	-31.4%	0.113	1.39E-02
AG↔F3orb	**T1a↔STSp**	2.84E-03	-52.5%	0.196	1.39E-02
Pole↔T2ml	**AG↔STSp**	2.85E-03	36.2%	0.132	1.39E-02
Pole↔T2ml	**T2ml↔SMG**	2.52E-03	-30.5%	0.109	1.39E-02
Pole↔T2ml	**Pole↔STSp**	3.53E-03	-28.7%	0.099	1.39E-02
AG↔F3orb	**Pole↔STSp**	6.34E-03	-36.5%	0.150	1.80E-02
Pole↔T2ml	**SMG↔T3p**	6.81E-03	35.1%	0.146	1.80E-02
F2p↔AG	**AG↔STSp**	6.39E-03	54.5%	0.250	1.80E-02
SMG↔T3p	**STSp↔F3orb**	5.53E-03	-39.6%	0.160	1.80E-02
F2p↔AG	**T1a↔STSp**	1.07E-02	-51.2%	0.225	2.58E-02
AG↔F3orb	**STSp↔F3orb**	1.12E-02	-38.2%	0.142	2.58E-02
T1a↔STSp	**STSp↔F3orb**	1.21E-02	32.9%	0.153	2.63E-02
AG↔F3orb	**F2p↔AG**	1.39E-02	53.5%	0.243	2.85E-02
Pole↔STSp	**T2ml↔SMG**	1.68E-02	22.9%	0.109	3.16E-02
T1a↔STSp	**SMG↔T3p**	1.71E-02	-38.3%	0.187	3.16E-02
F2p↔AG	**T2ml↔SMG**	2.40E-02	-34.9%	0.180	4.04E-02
SMG↔T3p	**T2ml↔SMG**	2.33E-02	-29.0%	0.144	4.04E-02
STSp↔F3orb	T2ml↔SMG	3.98E-02	20.7%	0.120	6.40E-02
AG↔STSp	T2ml↔SMG	4.84E-02	-22.3%	0.137	7.46E-02
T1a↔STSp	T2ml↔SMG	5.60E-02	21.9%	0.137	8.28E-02
SMG↔T3p	Pole↔STSp	6.05E-02	-21.8%	0.142	8.61E-02
AG↔STSp	Pole↔STSp	7.06E-02	-19.3%	0.127	9.68E-02
AG↔STSp	STSp↔F3orb	8.66E-02	-19.6%	0.139	1.14E-01
F2p↔AG	SMG↔T3p	9.02E-02	31.1%	0.232	1.15E-01
Prec↔F3opd	RolS↔PrecR	9.80E-02	16.9%	0.131	1.21E-01
Pole↔T2ml	T1a↔STSp	1.08E-01	-16.6%	0.135	1.29E-01
AG↔F3orb	AG↔STSp	1.91E-01	16.0%	0.184	2.21E-01
F2p↔AG	Pole↔STSp	2.08E-01	14.0%	0.176	2.33E-01
Pole↔T2ml	F2p↔AG	2.15E-01	-13.7%	0.176	2.34E-01
T1a↔STSp	AG↔STSp	2.22E-01	-12.8%	0.164	2.34E-01
F2p↔AG	STSp↔F3orb	3.88E-01	5.4%	0.189	3.99E-01
Pole↔T2ml	AG↔F3orb	4.56E-01	1.6%	0.148	4.56E-01

Validation of lead SNPs using diffusion imaging derived endophenotypes. we tested the potential associations between the hit SNPs with the average values of dMRI relevant white matter tracts; 3 white matter tracts to be tested with locus on $15q14$: the white matter tracts linking the regions of the (Prec↔F3opd) consists of the *i)* arcuate anterior segment fasciculus

(AF) dorsal pathway [Catani et al., 2005], *ii)* the frontal aslant tract (FAT) which is reported as connecting Broca's region (BA44/45) with dorsal medial frontal areas including supplementary and pre-supplementary motor area (BA6) [Catani and Forkel, 2019, Rojkova et al., 2016] while the anatomical connectivity underlying the (PrecR↔RolS) FC endophenotype consists of *iii)* the corpus callosum which interconnects both hemispheres.

The MO measured in the FAT and the OD measured in the anterior segment of AF are associated with the rs1440802 SNP with $p = 3.33\text{e}{-6}$ and $p = 2.47\text{e}{-65}$, respectively. The corpus callosum exhibits no significant association (See Table 6.4).

Table 6.4 – **Univariate associations of 2 lead SNPs with diffusion MRI indices.** Bold phenotypes represents tracts significantly associated with the lead SNP after Bonferroni correction ($p = 6.94e-4(0.05/(3*9+5*9))$)

CHR	SNP	Endophenotype	Metric	Beta	P	Z
15	rs1440802	Corpus callosum	L3	-0.034427736	0.0128030706756605	-2.4892006
		Corpus callosum	ISOVF	-0.03349917	0.015433186438535	-2.422051
		Corpus callosum	FA	0.032574	0.0185153496000616	2.3551476
		Corpus callosum	MD	-0.0320895	0.0203348456808069	-2.3201115
		Corpus callosum	L2	-0.03150293	0.0227447878217582	-2.2776945
		Corpus callosum	L1	-0.024891464	0.0719201471926044	-1.7996233
		Corpus callosum	ICVF	0.020728022	0.1339805874968674	1.4985878
		Corpus callosum	MO	-0.007192162	0.6030911735857749	-0.5199604
		Corpus callosum	OD	-0.0071261316	0.6064225847816228	-0.51518667
		Frontal Aslant Tract Left	MO	-0.064280435	3.3395836340833396e-06	-4.6487465
		Frontal Aslant Tract Left	OD	0.05600727	5.119567913113231e-05	4.0501003
		Frontal Aslant Tract Left	L1	-0.05497112	7.0339389362849 84e-05	-3.9751348
		Frontal Aslant Tract Left	ISOVF	-0.03451673	0.0125731467908473	-2.4956362
		Frontal Aslant Tract Left	MD	-0.030007247	0.030041806799683	-2.1695387
		Frontal Aslant Tract Left	L3	-0.019929217	0.1496320442788888	-1.4408324
		Frontal Aslant Tract Left	ICVF	0.009302874	0.5012290542417216	0.6725572
		Frontal Aslant Tract Left	FA	-0.00893621	0.5182478779915272	-0.6460486
		Frontal Aslant Tract Left	L2	-0.0038335118	0.7816691369948107	-0.27714452
		Arcuate Anterior Segment Left	OD	-0.23503968	2.4731891328416e-65	-17.070208
		Arcuate Anterior Segment Left	MO	0.20940934	3.8547792195026 59e-52	15.194348
		Arcuate Anterior Segment Left	FA	0.14841966	5.9536747488 80915e-27	10.749573
		Arcuate Anterior Segment Left	L2	-0.14630064	3.1249679699971 89e-26	-10.595551
		Arcuate Anterior Segment Left	L1	0.10824838	4.7482438237844 88e-15	7.833407
		Arcuate Anterior Segment Left	L3	-0.048699692	0.000429210896869	-3.5214393
		Arcuate Anterior Segment Left	ISOVF	-0.04646888	0.000779221912092	-3.360072
		Arcuate Anterior Segment Left	MD	-0.03227475	0.0196215356697533	-2.3335073
		Arcuate Anterior Segment Left	ICVF	0.01887147	0.1724557985221415	1.3643552
3	rs35124509	**Inferior Fronto Occipital fasciculus Left**	MO	0.041906517	2.4978217518578 74e-07	5.1578646
		Inferior Fronto Occipital fasciculus Left	OD	-0.032216765	7.3528721895411 01e-05	-3.9645689
		Inferior Fronto Occipital fasciculus Left	L1	0.020603567	0.0112419137853251	2.5350878
		Inferior Fronto Occipital fasciculus Left	FA	0.011022241	0.1750699434483398	1.3560919
		Inferior Fronto Occipital fasciculus Left	MD	0.008882381	0.2744777383394011	1.0928088
		Inferior Fronto Occipital fasciculus Left	ISOVF	0.004858134	0.5500444614237823	0.5976935
		Inferior Fronto Occipital fasciculus Left	L2	-0.0047178925	0.5616182288559746	-0.58043957
		Inferior Fronto Occipital fasciculus Left	L3	0.004688471	0.5640612077910263	0.5768198
		Inferior Fronto Occipital fasciculus Left	ICVF	-0.0037015	0.6488269473186558	-0.45539242
		Uncinate Left	MO	0.04215374	2.1220118223943872e-07	5.1883187
		Uncinate Left	OD	-0.023885116	0.003293203051305	-2.9389555
		Uncinate Left	L1	0.022804746	0.0050162697429167	2.8059871
		Uncinate Left	FA	0.0124250045	0.1263415538835854	1.528689
		Uncinate Left	MD	0.009754712	0.2300860378190222	1.2001373
		Uncinate Left	ICVF	-0.008374233	0.3028745596840176	-1.0302886
		Uncinate Left	L3	0.0072252634	0.3740427072882268	0.88892627
		Uncinate Left	L2	-0.0059861178	0.4614441477476281	-0.73647094
		Uncinate Left	ISOVF	-0.00015708078	0.9845814785319852	-0.019325454
		Arcuate Anterior Segment Left	MO	-0.023604663	0.0036791304163527	-2.904438
		Arcuate Anterior Segment Left	L2	0.02263006	0.0053612311006976	2.784488
		Arcuate Anterior Segment Left	FA	-0.016705215	0.0398443764601674	-2.0553586
		Arcuate Anterior Segment Left	ISOVF	0.012345138	0.1287972035080454	1.5188621
		Arcuate Anterior Segment Left	MD	0.010159739	0.2113101729791165	1.2499709
		Arcuate Anterior Segment Left	ICVF	-0.010145878	0.2119338859324724	-1.2482654
		Arcuate Anterior Segment Left	L3	0.007130031	0.3803728653956867	0.8772095
		Arcuate Anterior Segment Left	OD	0.0058026165	0.4752924638259838	0.7138944
		Arcuate Anterior Segment Left	L1	-0.00077840226	0.9237065215197204	-0.095765874
		Arcuate Long Segment Left	OD	-0.036813475	5.882222834891848e-06	-4.530579
		Arcuate Long Segment Left	L1	0.020133851	0.0132387238045088	2.477282
		Arcuate Long Segment Left	MO	0.014724737	0.0700387951827605	1.8116597
		Arcuate Long Segment Left	MD	0.012832667	0.1143707059249424	1.578849
		Arcuate Long Segment Left	ISOVF	0.012217956	0.1327840217022739	1.5032134
		Arcuate Long Segment Left	L3	0.007494609	0.3564947860978851	0.9220648
		Arcuate Long Segment Left	ICVF	-0.006647461	0.4134499954108012	-0.8178375
		Arcuate Long Segment Left	FA	0.003683449	0.6504251731527789	0.4531716
		Arcuate Long Segment Left	L2	0.0017721133	0.827412710308558	0.21802105

CHR	SNP	Endophenotype	Metric	Beta	P	Z
		Arcuate Posterior Segment Left	L3	0.041222345	3.903850074370563e-07	5.0735874
		Arcuate Posterior Segment Left	ICVF	-0.038005184	2.90620129195227e-06	-4.67734
		Arcuate Posterior Segment Left	MD	0.036748115	6.110479990305916e-06	4.52253
		Arcuate Posterior Segment Left	FA	-0.03642834	7.3549024549896465e-06	-4.4831505
		Arcuate Posterior Segment Left	L2	0.030796966	0.0001507877719798	3.7897685
		Arcuate Posterior Segment Left	L1	0.021983918	0.0068311464928437	2.7049656
		Arcuate Posterior Segment Left	MO	0.016925715	0.0372975642974694	2.0824919
		Arcuate Posterior Segment Left	ISOVF	0.014387828	0.0766931917480869	1.7702038
		Arcuate Posterior Segment Left	OD	0.00464435	0.5677342741085722	0.5713915

Functional annotation: Locus in $15q14$ associated to (Prec↔F3opd) and (PrecR↔RolS) endophenotypes. Four independent SNPs were identified in locus $15q14$ (rs1440802, rs11629938, rs773225188, rs34680120) (Fig. 6.6c). Regarding eQTL annotations, we explored tissue-specific gene expression resources, including both brain tissues and blood - considered as a good proxy when brain tissues are not available [Qi et al., 2018]. Significant results were obtained:

- The four independant SNPs are cis-eQTL of *THBS1* gene in eQTLGen, BIOSQTL and GTEx/v8 . Additionally, rs34680120 is eQTL of *RP11-37C7.1* gene ($p_{adj} < 1.02e{-3}$) in PsychENCODE and eQTL of *CTD-2033D15.1* gene ($p_{adj} < 6.0e{-6}$) in BIOSQTL; see Fig.6.6c. Overall, the variants of this genomic risk region are found 72 times as eQTL of genes from different data sources.

- Based on the human gene expression data from the Brainspan database, we found that *THBS1* gene has relatively high mRNA expression during early mid-prenatal to late prenatal stages, from 16 to 37 post-conceptional weeks; see Fig. 6.6e.

- Indirect predictions might be added from the following annotation. For instance, *RASGRP1*, identified by chromatin interaction mapping and which also appears to be under control of temporal expression during neurodevelopment, is reported as over-expressed in the perisylvian language areas [Johnson et al., 2009] and as up-regulated in the dorsal striatum [Cirnaru et al., 2020].

Fig. 6.6 summarises these results, found by mvGWAS, associated to (Prec↔F3opd) and (PrecR↔RolS) FC endophenotypes. These pinpoint *THBS1* as the possible gene underlying this association signal.

Locus regulating *THBS1* associated with the *perceptual motor* interactions process In our results, a locus in $15q14$ was associated with the precentral-opercularis FC (Prec↔F3opd) and the precentral-Rolandic FC endophenotypes (PrecR↔RolS). In the literature, the L|R Prec regions in the ventral precentral gyrus are both associated with phonology language component and considered relevant for pharynx and tongue fine-movement coordination in the human and non-human primates [Belyk and Brown, 2017, Kumar et al., 2016, Vigneau et al., 2006]. RolS in the dorsal Rolandic sulcus is attributed to the phonology component and matches the mouth primary motor area but also the perception of syllables [Fadiga et al., 2002, Vigneau et al., 2006, Wilson et al., 2004]. F3opd in the dorsal pars opercularis (BA44/45) is associated with

semantic/sentence processing. The motor theory of speech perception has been quite an old debate [Flinker et al., 2015, Galantucci et al., 2006, Liberman and Mattingly, 1985, Schwartz et al., 2008, Whalen, 2019]. In this study, we report a locus in 15q14 (lead SNP rs1440802) associated with both this FC between the motor and Broca's areas and the frontal aslant tract connecting directly (pre)supplementary motor area with the opercular part of inferior frontal gyrus [Catani et al., 2012, Vergani et al., 2014], in line with this perception–motor link.
SNPs in high LD with rs1440802 in the genomic region have already been linked to several other structural features (surface area and cortical thickness) including primary motor cortex, primary somatosensory cortex [Elliott et al., 2018, van der Meer et al., 2020], supramarginal, and pars opercularis [van der Meer et al., 2020], supporting a common genetic influence of the sensory-motor interaction.
The lead SNP rs1440802 and SNPs in LD that we have shown to be associated with both (Prec↔F3opd) and (PrecR↔RolS) are found to be eQTL of *THBS1* gene in the blood with high confidence. The thrombospondin-1 protein encoded by *THBS1* gene is a member of the thrombospondin family, a glycoprotein expressed in the extracellular matrix. It has been implicated in synaptogenesis [Christopherson et al., 2005] and regulates the differentiation and proliferation of neural progenitor cells [Lu and Kipnis, 2010], and has been involved in human neocortical evolution [Cáceres et al., 2003, 2007]. Other members of the thrombospondin's family, *THBS2* and *THBS4*, have been shown to be over-expressed in the adult human cerebral cortex compared to chimpanzees and macaques [Cáceres et al., 2007]. Their increased expression suggests that human brain might display distinctive features involving enhanced synaptic plasticity in adulthood which may contribute to cognitive and linguistic abilities [Sherwood et al., 2008]. From a developmental point of view, *THBS1* appears to be under control of temporal expression during development, as revealed by BrainSpan data (See Fig. 6.6e. *THBS1* expression was studied from the longitudinal transcriptomic profile resource of the developing human brain (18, 19, 21, 23 weeks of gestation) [Johnson et al., 2009]. Its expression is reported as over-expressed in the neocortex, including the perisylvian language areas, compared to phylogenetically older parts of the brain such as the striatum, thalamus and cerebellum [Johnson et al., 2009]. Thrombospondin-1 have also been linked to Autism spectrum disorder [Lu et al., 2014], Alzheimer's disease [Ko et al., 2015], and Schizophrenia [Park et al., 2012].

Taken together, these results indicate that *THBS1*, modulated by a lead SNP in the 15q14 locus, could be prioritised in the study of key genes playing a role in the functional connectivity part of the *perceptual motor* interaction required for language, and with the anatomical connectivity that supports their interactions.

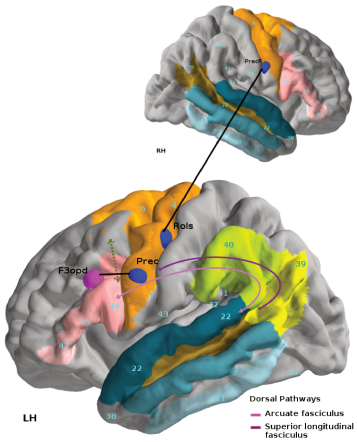
RH
RolS
Prec
F3opd
LH
Dorsal Pathways
Arcuate fasciculus
Superior longitudinal fasciculus

A)

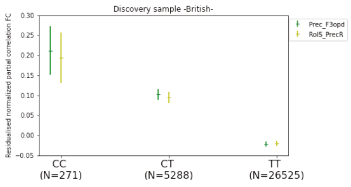
Discovery sample -British-
Prec_F3opd
RolS_PrecR
CC
(N=271)
CT
(N=5288)
TT
(N=26525)

B)

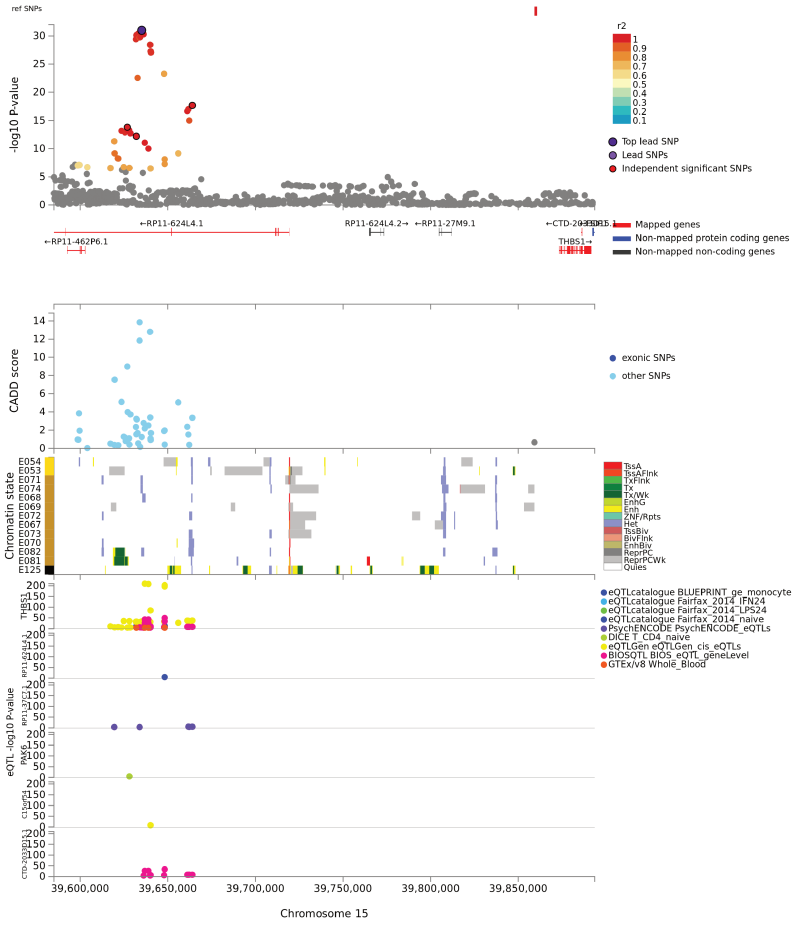
ref SNPs
-log10 P-value
r2
Top lead SNP
Lead SNPs
Independent significant SNPs
Mapped genes
Non-mapped protein coding genes
Non-mapped non-coding genes
CADD score
exonic SNPs
other SNPs
Chromatin state
eQTL -log10 P-value
Chromosome 15

C)

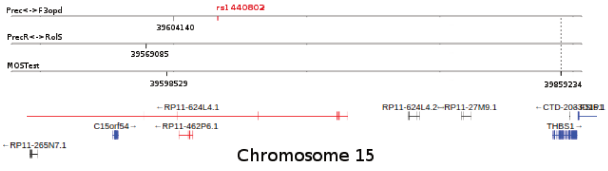
Prec<->F3opd
PrecR<->RolS
MOSTest
Chromosome 15

D)

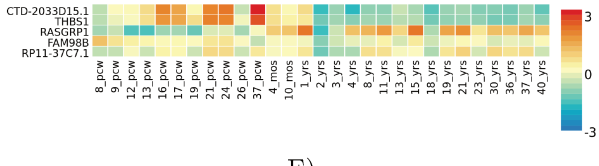
CTD-2033D15.1
THBS1
RASGRP1
FAM98B
RP11-37C7.1

E)

Figure 6.6 – **Main results for the** 15q14 **locus.** A) The two pairs of ROIs that forms the endpoints of the associated FCs reported as black bold lines. B) Effect sizes of the SNP rs1440802 for the two connections: (Prec↔F3opd) FC in green and (PrecR↔RolS) FC in yellow. C) Locus Zoom of the genomic region identified by the mvGWAS. Chromatin state of the genomic region. Brain tissue name abbreviations are the following; E054:Ganglion Eminence derived primary cultured neurospheres, E053: Cortex derived primary cultured neurospheres, E071: Brain Hippocampus Middle, E074: Brain Substantia Nigra, E068: Brain Anterior Caudate, E069: Brain Cingulate Gyrus, E072: Brain Inferior Temporal Lobe, E067:Brain Angular Gyrus, E073: Brain Dorsolateral Prefrontal Cortex, E070: Brain Germinal Matrix, E082: Fetal Brain Female, E081: Fetal Brain Male, E125: NH-A Astrocytes Primary Cells. The state abbreviations are the following; TssA: active transcription start site (TSS), TssFlnk: Flanking Active TSS, TxFlnk: Transcription at gene 5′ and 3′, Tx: Strong transcription, TxWk: Weak transcription, EnhG: Genic enhancers, Enh: Enhancers, ZNF/Rpts: ZNF genes & repeats, Het: Heterochromatin, TssBiv: Bivalent/Poised TSS, BivFlnk: Flanking Bivalent TSS/Enh, EnhBiv: Bivalent Enhancer, ReprPC: Repressed PolyComb, ReprPCWk: Weak Repressed PolyComb, Quies: Quiescent/Low. Expression quantitative trait loci (eQTL) associations (data source: eQTLGen [Võsa et al., 2018], PsychENCODE[Wang et al., 2018], DICE [Schmiedel et al., 2018], BIOS QTL browser [Zhernakova et al., 2017], GTEx/v8 [Consortium et al., 2017], eQTLcatalogue). D) Overlap of the genomic region risk region identified from FUMA for MOSTest results, (Prec↔F3opd) and (PrecR↔RolS). E) Gene expression from BrainSpan for the interesting genes prioritised by FUMA.

6.2.2 *Fronto-temporal semantic network* driven by *EPHA3* gene

Identification of 'central' endophenotypes associated with 3p11.1 **genomic risk region.** On 3p11.1, the lead SNP rs35124509 had nine central FCs (that contributed the most in the multivariate association, see 6.2). The minor allele was associated with the partial correlation between:

- the left posterior part of the superior temporal sulcus and the left temporal pole (Pole↔STSp),
- the left temporal pole and the lateral/middle part of the middle temporal gyrus (Pole↔T2ml),
- the angular gyrus and the pars orbitalis of the left inferior frontal gyrus (AG↔F3orb),
- the anterior part of the Superior temporal gyrus and the left posterior part of the superior temporal sulcus (T1a↔STSp),
- the left posterior part of the superior temporal sulcus and the pars orbitalis of the left inferior frontal gyrus (STSp↔F3orb),
- the supramarginal gyrus and the posterior part of the left inferior temporal gyrus (SMG↔T3p),
- the angular gyrus and the left posterior part of the superior temporal sulcus (AG↔STSp),
- the Posterior part of the middle frontal gyrus and the angular gyrus (F2p↔AG),
- the lateral/middle part of the middle temporal gyrus and the supramarginal gyrus (T2ml↔SMG)

See also Fig. 6.7a and Supplementary Table 6.1. These connected regions are located across the left parieto-fronto-temporal lobe, and are mainly labelled as semantic language processing. These edges have previously been described in FC studies dedicated to language and especially to the semantic component. This component typically includes the inferior frontal gyrus, the left temporal cortex (i.e. temporal pole, middle temporal gyrus, fusiform gyrus) and the left angular gyrus [Binder et al., 2009, Jackson et al., 2016, Vigneau et al., 2006]. At the univariate level, these loci associated to central endophenotypes display an important overlap; See Fig 6.7d.

SNP-based genetic correlation of the 'central' endophenotypes.

The SNP-based genetic correlation was estimated for each pair of central FCs associated to $3p11.1$ genetic loci, indicating overlapping genetic contributions among several FCs (Table 6.3). A negative genetic correlation between some FCs has been observed which indicates that variants can have antagonistic effects on the co-activations of these regions.

Validation of lead SNPs using diffusion imaging derived endophenotypes.
We tested the potential associations between the hit SNPs with the average values of dMRI relevant white matter tracts; 5 white matter tracts, to be tested with locus on $3p11.1$, were selected according to the nine central endophenotypes associated with the $3p11.1$ locus. The anatomical connectivity underlying these connections consists of the *i)* inferior fronto-occipital fasciculus (IFOF) which connects the inferior frontal regions with the temporal and occipital cortex [Forkel et al., 2014], *ii)* uncinate fasciculus (UF) which is reported to connect the anterior temporal lobe to the orbital region and part of the inferior frontal [Catani and De Schotten, 2008, Catani and Forkel, 2019, Friederici, 2017, Vigneau et al., 2006], and *iii)* arcuate long segment fasciculus (AF), *iv)* anterior segment of arcuate fasciculus, *v)*posterior segment of arcuate fasciculus [Catani et al., 2005].
The MO measured in the IFOF and UF is associated with the rs35124509 SNPs with $p = 2.49e{-}7$ and $p = 2.12e{-}7$, respectively. Both long and posterior segment of AF are associated with rs35124509 SNPs with $p = 5.88e{-}6$ (OD) and $p = 3.90e{-}7(L3)$, while the anterior segment of AF exhibits no significant association (See Table 6.4).

Functional annotation: Locus in $3p11.1$ associated to semantic-language related endophenotypes.
Fourteen independent SNPs were identified in locus $3p11.1$ (Fig. 6.7c).

- The rs35124509 SNP is a non-synonymous variant within exon 16 of *EPHA3* protein-coding gene. The subregion around rs35124509 and rs113141104 has its chromatin state annotated as (weak) actively-transcribed states (Tx, TxWk) in the brain tissues, specifically in the Brain Germinal Matrix, the Ganglion Eminence derived primary cultured neurospheres, and in the Fetal Brain Female.

- Concerning the subregion around rs6551410, it has its chromatin state annotated as Weak transcription (TxWk) in the Fetal Brain Female, enhancer (enh) in the Brain Germinal Matrix and Repressed PolyComb (ReprPC) in both the Ganglion Eminence and Cortex derived primary cultured neurospheres. Additionally, the subregion around rs6551407 has its chromatin state annotated as Weak transcription (TxWk) in the Brain Germinal Matrix, Fetal Brain Male and Fetal Brain Male. Overall, this reveals a genomic region involved in fine regulation mechanisms of brain development.

- Considering the rs35124509 SNP and variants in linkage disequilibrium (LD) with it in the genomic risk region, we scrutinised CADD and RDB scores, precise genomic positions and risk prediction, and we noticed some remarkable SNPs. We observed two exonic variants: *i)* The SNP rs1054750 ($LD_{rs35124509}$ $r^2 > 0.99$, $p_{mvGWAS} = 6.65e-34$) is a synonymous variant within exon 16 of *EPHA3*. *ii)* the already mentioned non-synonymous lead SNP

rs35124509 ($p_{mvGWAS} = 8.95e-59$), the minor allele results in a substitution in the protein from tryptophan (W) residue (large size and aromatic) into an arginine (R) (large size and basic) at position 924 (W924R, p.Trp924Arg) in the Sterile Alpha Motif (SAM) domain. This SNP is not predicted to alter protein function (Polyphen-2 = "benign") but is predicted to be potentially a regulatory element by several tools (RDB score = 3*a*, CADD = 22.3 - when $\text{CADD}_{thresh} = 12.37$ for deleterious effect as suggested by Kircher et al. [2014])

- Moreover, we observed eight SNP (rs28623022, rs7650184, rs7650466, rs73139147, rs3762717, rs73139144, rs73139148, rs566480002) ($LD_{rs35124509}$ $r^2 > 0.73$, $p_{mvGWAS} < 4.46e-20$) located in 3'-UTR of *EPHA3* which could affect its expression by modulating miRNA binding [Popp et al., 2016].

- The hit-SNP rs35124509 and the rest of highlighted SNPs act as eQTL for *EPHA3* in different tissues including brain cerebellum ($p_{FDR} < 5e{-}2$ in GTEx/v8 data source).

Fig. 6.7 summarises the functional annotations in 3*p*11.1 associated to multiple FC endophenotypes in semantic component of language. These functional characterization supports *EPHA3* as a possible gene with a key role in language development in humans.

Locus in *EPHA3* associated with the fronto-temporal semantic network In our results, a locus in 3*p*11.1 is found associated with nine fronto-parietal-temporal endophenotypes. In the literature, The angular gyrus (AG) has been shown to activate during functional imaging tasks probing semantics and involved in conceptual knowledge [Vigneau et al., 2006]. F3orb in the pars orbitalis in the inferior frontal gyrus is labelled semantic for its involvement in semantic retrieval in spoken and sign language [Rönnberg et al., 2004]. It has also been associated with categorisation, association, and word generation tasks [Booth et al., 2002, Gurd et al., 2002, Noppeney and Price, 2004]. The temporal pole region, located in the anterior temporal lobe, is associated with semantic and sentence processing [Vigneau et al., 2006] and the posterior superior temporal sulcus (pSTS) is reported to be implicated in syntactic complexity [Constable et al., 2004] but also process the semantic integration of complex linguistic material [Vigneau et al., 2006]. Both pSTS and the angular gyrus overlap with the Geschwind's territory (See Fig. 2.2). The lateral/middle part of the middle temporal gyrus is devoted to verbal knowledge [Vigneau et al., 2006]. These regions and their corresponding endophenotypes fit rather well with the *fronto-temporal semantic system* described in [Vigneau et al., 2006] facilitating the association of integrated input messages with internal knowledge. The anterior part of the superior temporal gyrus and the posterior part of the inferior temporal gyrus are phonological–semantic interface areas processing. [Vigneau et al., 2006] propose that these ones are transitional zones between the perception and semantic integration of language stimuli and are crucial during the development of language.
SNPs of this genomic region in high LD with the lead SNP rs35124509 have already been found associated with: rsfMRI ICA functional connectivity (edge 387, 383, 399, and ICA-features 3); see [Elliott et al., 2018]. The ICA maps used for these FC estimations partially-overlap

semantic language areas including the angular gyrus, the most anterior part of the STS, the anterior fusiform gyrus, the lateral-middle part of T2, the ventral part of the pars triangularis and the pars orbitalis of the left inferior frontal gyrus. Regarding cognitive traits, this locus was associated to intelligence [Savage et al., 2018]. Finally, other SNPs, in strong LD with the lead SNP rs35124509, consistently act as an eQTL of *EPHA3* in brain tissues.
The ephrin type-A receptor 3 protein encoded by *EPHA3* gene belongs to the ephrin receptor family that can bind the ephrins subfamily of the tyrosine kinase protein family. EPH receptors and their ligands were found to play important roles in multiple developmental processes, including tissue morphogenesis, embryogenesis, neurogenesis, vascular network formation, neural crest cell migration, axon fasciculation, axon guidance, and topographic neural map formation [Gerstmann and Zimmer, 2018, Gibson and Ma, 2011, Pasquale, 2008]. EPHA3 binds predominantly EFNA5 and plays a role in the segregation of motor and sensory axons during neuromuscular circuit development [Lawrenson et al., 2002]. In [Johnson et al., 2009], *EPHA3* is reported as over-expressed in the fetal rhesus macaque monkey neocortex (NCTX) and especially in the occipital lobe compared to the other NCTX areas. Noticeably, its ligand *EFNA5* is over-expressed in perisylvian areas and is located in a human accelerated conserved non-coding sequence (haCNS704) [Johnson et al., 2009]. EPH receptors have been linked to neurodevelopmental disorders, including schizophrenia [Zhang et al., 2010] and autism spectrum disorder [Casey et al., 2012]. Moreover, in [Rudov et al., 2013], *EPHA3* is found *in silico*, as putative gene implicated in dyspraxia, dyslexia and specific language impairment (SLI). Finally, we observed that *EPHA3* is expressed in the human brain, in a consistent manner across developmental stages from early prenatal to late-mid prenatal (8-24 pcw, BrainSpan ; see Fig. 6.7e.

Taken together, these results indicate that *EPHA3* in the 3*p*11.1 locus, could be prioritised in the study of key genes playing a role in the *fronto-temporal semantic* network, and with the anatomical connectivity support of this network.

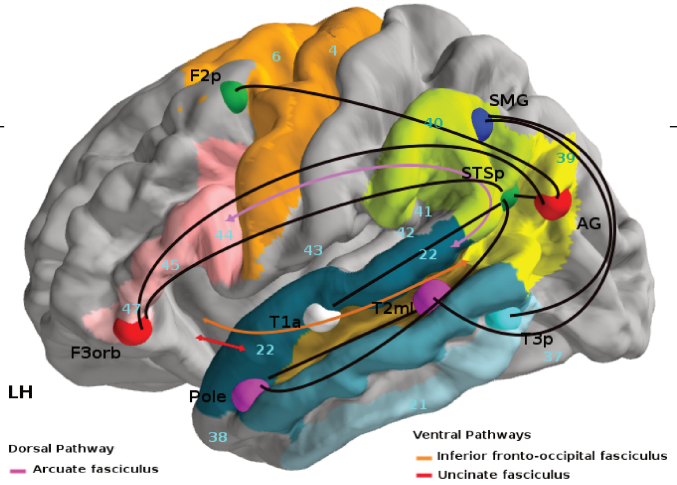
F2p
SMG
STSp
AG
T1a
T2ml
T3p
F3orb
Pole
LH
Dorsal Pathway
Arcuate fasciculus
Ventral Pathways
Inferior fronto-occipital fasciculus
Uncinate fasciculus

A)

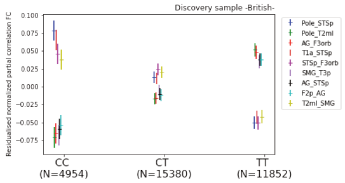
Discovery sample -British-
CC (N=4954)
CT (N=15380)
TT (N=11852)

B)

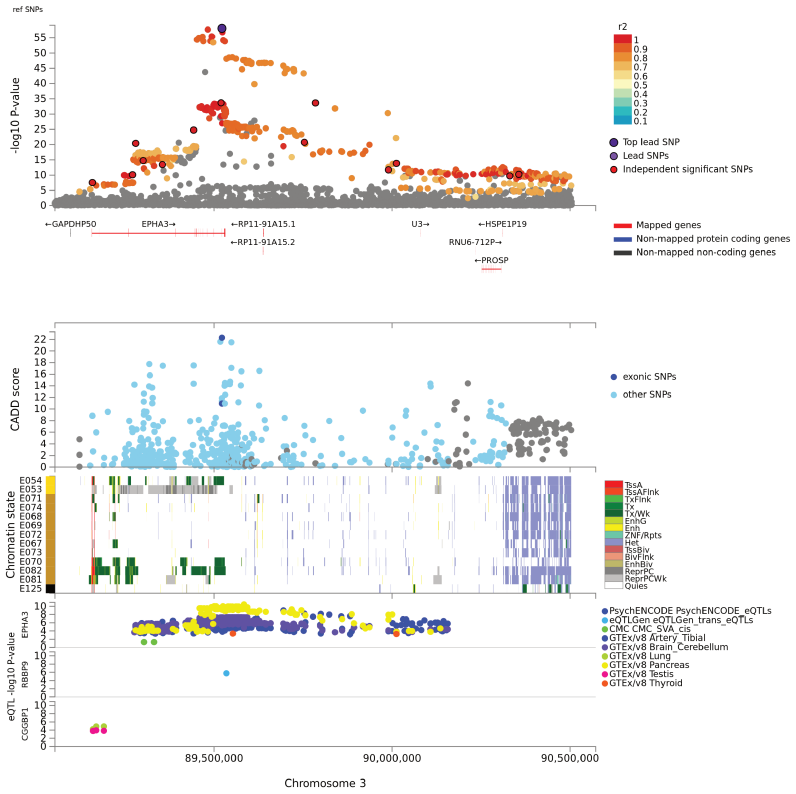
-log10 P-value
r2
Top lead SNP
Lead SNPs
Independent significant SNPs
Mapped genes
Non-mapped protein coding genes
Non-mapped non-coding genes
CADD score
exonic SNPs
other SNPs
Chromatin state
eQTL -log10 P-value
PsychENCODE PsychENCODE_eQTLs
eQTLGen eQTLGen_trans_eQTLs
CMC CMC_SVA_cis
GTEx/v8 Artery_Tibial
GTEx/v8 Brain_Cerebellum
GTEx/v8 Lung
GTEx/v8 Pancreas
GTEx/v8 Testis
GTEx/v8 Thyroid
89,500,000
90,000,000
90,500,000
Chromosome 3

C)

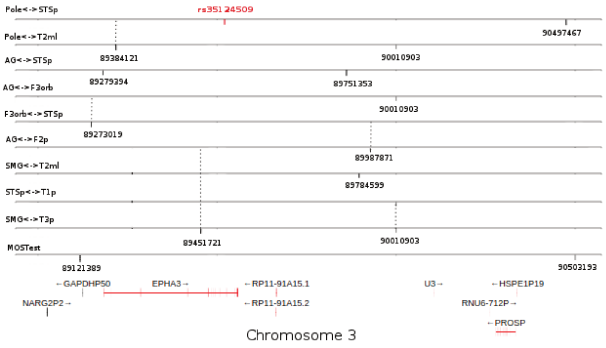
Pole<->STSp
Pole<->T2ml
AG<->STSp
AG<->F3orb
F3orb<->STSp
AG<->F2p
SMG<->T2ml
STSp<->T1p
SMG<->T3p
MOStest
rs35124509
Chromosome 3

D)

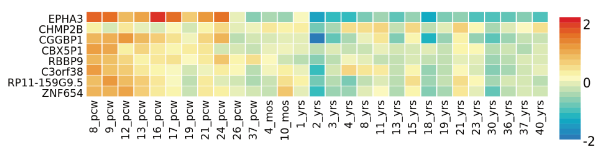
EPHA3
CHMP2B
CGGBP1
CBX5P1
RBBP9
C3orf38
RP11-159G9.5
ZNF654

E)

Figure 6.7 – **Main results for the** 3*p*11.1 **locus.** A) The pairs of ROIs that forms the endpoints of the associated FCs reported as black bold lines. B) Effect sizes of the SNP rs35124509 for the nine connections: (AG↔F3orb), (Pole↔STSp), (Pole↔T2ml), (T1a↔STSp), (STSp↔F3orb), (SMG↔T3p), (AG↔STSp), (F2p↔AG) and (T2ml↔SMG) FCs. C) Locus Zoom of the genomic region identified by the mvGWAS. Chromatin state of the genomic region. Brain tissue name abbreviations are the following; E054:Ganglion Eminence derived primary cultured neurospheres, E053: Cortex derived primary cultured neurospheres, E071: Brain Hippocampus Middle, E074: Brain Substantia Nigra, E068: Brain Anterior Caudate, E069: Brain Cingulate Gyrus, E072: Brain Inferior Temporal Lobe, E067:Brain Angular Gyrus, E073: Brain Dorsolateral Prefrontal Cortex, E070: Brain Germinal Matrix, E082: Fetal Brain Female, E081: Fetal Brain Male, E125: NH-A Astrocytes Primary Cells. The state abbreviations are the following; TssA: active transcription start site (TSS), TssFlnk: Flanking Active TSS, TxFlnk: Transcription at gene 5′ and 3′, Tx: Strong transcription, TxWk: Weak transcription, EnhG: Genic enhancers, Enh: Enhancers, ZNF/Rpts: ZNF genes & repeats, Het: Heterochromatin, TssBiv: Bivalent/Poised TSS, BivFlnk: Flanking Bivalent TSS/Enh, EnhBiv: Bivalent Enhancer, ReprPC: Repressed PolyComb, ReprPCWk: Weak Repressed PolyComb, Quies: Quiescent/Low. Expression quantitative trait loci (eQTL) associations (data source: eQTLGen [Võsa et al., 2018], PsychENCODE[Wang et al., 2018], DICE [Schmiedel et al., 2018], BIOS QTL browser [Zhernakova et al., 2017], GTEx/v8 [Consortium et al., 2017], eQTLcatalogue). D) Overlap of the genomic region risk region identified from FUMA for MOSTest results and the nine FCs mentioned above. E) Gene expression from BrainSpan for the interesting genes prioritised by FUMA.

6.2.3 PrecR↔RolS and T1a↔T1a/HeschlR endophenotypes driven by *PLCE1*, *NOC3L* and *HELLS* genes

Identification of 'central' endophenotypes associated with 10*q*23.33 **genomic risk region.**

A locus in 10*q*23.33 was highlighted by the mvGWAS. At the univariate level, no endophenotype reached the genome-wide significance threshold for the lead SNP in this locus (rs11187838). Consequently, we did not perform the genetic correlation study, nor perform a *post hoc* study on potential supporting anatomical tracts from dMRI data.

Functional annotation: Locus in 10*q*23.33 **associated to PrecR↔RolS T1a↔T1a/HeschlR endophenotypes.** Four independent SNPs were identified in locus 10*q*23.33 (rs11187838, rs17109875, rs11187844, rs20772180).

- The subregion around all four SNPs has its chromatin state annotated as (weak) actively-transcribed states (Tx, TxWk) in the brain tissues, specifically in the ganglion eminence and cortex derived primary cultured neurospheres, hippocampus (middle), substantia nigra, anterior caudate, angular gyrus, Dorsolateral/Prefrontal cortex, brain germinal matrix, fetal brain female/male and NH-A astrocytes primary cells.
- Two exonic variants are noteworthy: The rs2274224 ($LD_{rs11187838}$ $r^2 > 0.99$, $p_{mvGWAS} = 5.04e-14$) and rs11187895 ($LD_{rs17109875}$ $r^2 > 0.6$, $p_{mvGWAS} = 3.08e-7$) SNPs are nonsynonymous SNV within exon 19 of *PLCE1* and exon 11 of *NOC3L* and are both not predicted to alter protein function (Polyphen-2="benign") but are predicted to have a deleterious effect (CADD = 17.35, CADD = 19.24).
- Moreover, we observed three SNP (rs11187870, rs11187877, rs145707916) ($LD_{rs17109875}$ $r^2 > 0.66$, $p_{mvGWAS} < 7.546e-7$) located in 3'-UTR of *PLCE1:NOC3L*.
- Regarding eQTL annotations, the variants in the 10*q*23.33 locus act as eQTL for *HELLS*, *NOC3L* and *PLCE1* genes in different brain tissues including brain cerebellum, brain cerebellar hemisphere, Brain nucleus accumbens basal ganglia, hippocampus ($p_{FDR} < 5e{-}2$ in GTEx/v8 data source).

These functional characterisation highlight these three genes (*HELLS*, *NOC3L* and *PLCE1*) that may influence the FCs related to language processing in humans.

Locus regulating *PLCE1*, *NOC3L* and *HELLS* associated with PrecR↔RolS and T1a↔T1a.HeschlR.

A locus in 10q23.33 was highlighted by the mvGWAS. At the univariate level, no endophenotype reached the genome-wide significance threshold. But looking at the suggestive threshold $p = 1e-5$, we pinpoint putative 'central' endophenotypes to aid interpretation of the processes underlying this association signal. Two bilateral fronto-temporal endophenotypes were the most associated to rs111878 38: the precentral-Rolandic FC endophenotypes (PrecR↔RolS, $p = 1.85e-07$) and the right anterior part of the superior temporal gyrus (T1aR) overlapping Heschl's gyrus (T1a/HeschlR) and its homotopic areas of LH primary auditory regions (T1a↔T1a/HeschlR, $p = 9.61e-06$). All these regions participate in an elementary audio–motor loop involved in both comprehension and production of syllables forming a bilateral fronto-temporal network activated by the auditory representation of speech sounds [Vigneau et al., 2006, 2011]. SNPs of this genomic region in high LD with the lead rs11187838 act as an eQTL of *HELLS*, *NOC3L*, *PLCE1* genes in multiple brain tissues The *HELLS* gene encodes the lymphoid-specific helicase (Lsh), a member of the SNF2 helicase family of chromatin remodeling proteins. Patients with a genetic mutation of *HELLS* present psychomotor retardation including slow cognitive, motor development and psychomotor impairment [Thijssen et al., 2015]. The Lsh protein might play a role as epigenetic regulator in neural cells [Han et al., 2017]. Finally, we observed that the three genes (*NOC3L*, *PLCE1*, *HELLS*) are expressed in the human brain, across developmental stages from early prenatal to early mid prenatal (8-17 pcw, BrainSpan).

Taken together, these results indicate that the three highlighted genes (*PLCE1*, *NOC3L* and *HELLS*) in the 10q23.33 locus, as potential candidates in the study of key genes playing a role in the *bilateral fronto-temporal auditory-motor* network.

6.3 Limitations

Although functional MR imaging is recognised to produce valuable endophenotypes [Elliott et al., 2018], resting-state FC represent remote measures of language as the participants are not engaged in any language task-experiments and simply stay at rest. Yet, as stated in the introduction 1.3.2.1, previous works reported that resting-state derived endophenotypes are correlated with behavioural language processing [Cheema et al., 2021, Cross et al., 2021, Koyama et al., 2011, Stevens et al., 2017]. However, with the UK Biobank release at hand in this study, no behavioural language scores were provided. We were thus unable to check the correlations between our resting-state FC endophenotypes and language behavioural scores. Moreover, we observed a hierarchy of language heritability estimates from the Human Connectome Project (twin study) with 18-72% for language-behavioural scores, 11.6-34.6% for language-task activations [Le Guen et al., 2018] and 11.6-49.8% for resting-state FC, making resting-state FC not the most suitable endophenotype for an association study about language.

The lack of a large, age-matched replication sample represents one major limitation of the present study in the sense that we could not reproduce all our results.

Multivariate methods display a modest improvement in power as compared to univariate approach, and sometimes display lower power. Additionally, the results are less straightforward to interpret. We have addressed this issue by assessing each of the prioritized loci at the univariate level, to pinpoint at central endophenotypes that are contributing the most to the multivariate signal. Such a complex trait as language may be driven by a lot of interacting genes, a multivariate approach on the SNPs side is highly desired to uncover relevant gene pathways in language development and processing.

Compared to structural endophenotypes, the FCs have low amplitude which hinders the study in terms of statistical power. This observation constitute another limitation that is somehow surpassed when working on large scale cohorts and using multivariate approaches.

Another potential limitation is the UK Biobank dataset in which this study is based. It should be noted that the UKB constitutes a relatively old sample. Future studies in other developmental stages (i.e. children, adolescent, young-adult) will inform us whether the observed associations are stable across development, or whether they reflect some age-related specificity.

6.4 Conclusions

In this study, we extracted language endophenotypes from rsfMRI acquisitions in the largest imaging-genetic cohort on general population to date. To make these endophenotypes as closer as possible to language function in the brain, we adopted a ROI-based approach for FC estimation with language ROIs derived from an comprehensive meta-analysis of tbfMRI studies on language. This approach makes the endophenotypes comparable across individuals and thus suitable for an association study. After filtering on heritability significance, we performed a multivariate GWAS technique in order to take advantage of the correlation structure among rsfMRI FC and uncover potential pleiotropic loci.
Thereby, we highlighted potential key genes related to language processing including *EPHA3* gene in the 3p11.1 locus with a role in the *fronto-temporal semantic* network, *THBS1* gene, modulated by the 15q14 locus, associated with the functional connectivity part of the *perceptual motor* interaction required for language, and *PLCE1* gene in the 10q23.33 locus with a potential role in the *bilateral fronto-temporal auditory-motor* network. These genes could be prioritized to study language in suitable genetic model.
Furthermore, two results that have not shown significant association in the replication sample, have been reported in previous works; a 3q24 locus in *ZIC4* which is involved in visual and auditory pathway development [Horng et al., 2009] has been associated with brain assymetry [Sha et al., 2021]; a 14q23.1 locus near *DACT1* has been reported to be associate with the STAP [Le Guen et al., 2018] and superior temporal sulcus surface area [Sha et al., 2021]. Altogether, theses results provide an novel insight into the genetic architecture of the language in humans.
A growing number of works claim that language studies should consider task-free fMRI data in general population in order to really focus on the neurobiological organization of language and how it supports natural language, i.e. as it is used in everyday life [Hasson et al., 2018]. On a clinical side, such research settings are highly desirable as there is a need to map language areas in patients unable to perform language tasks [Branco et al., 2016, Klingbeil et al., 2019, Park et al., 2020, Ramage et al., 2020]. By validating our findings in rsfMRI FC endophenotypes with dMRI-derived endophenotypes, we tried to provide both a functional and structural connectome point of view of the language organisation in the brain.

Finally, recent imaging-genetic approaches such as multivariate GWAS, allowed us to increase in statistical power and circumvent the small effect sizes of these original endophenotypes. We believe that such approaches are really promising and will broadly disseminate in the imaging-genetic field and beyond. With the presented approach, we tried to contribute to these innovative trends and to pave the way to other alternative task-free approaches to study natural language and its genetic underpinnings.

* * *
* *
*

Chapter 7

The genetic architecture of anatomical connectivity in human language

Chapter Outline

7.1 Multivariate genome-wide association studies 124
7.2 Validation of lead SNPs associated with ACs. 128
7.3 Functional annotations of genomic loci associated with language 133
7.4 Discussion 139

In the chapter 6, we used resting-state fMRI in a discovery sample of 32,186 healthy volunteers from the UK Biobank [Sudlow et al., 2015], the compiled information of a large-scale meta-analysis on language components [Vigneau et al., 2006, 2011] and performed a multivariate genetic association of human language functional connectome endophenotypes filtered based on heritability significance presented in the chapter 4.

In the present chapter, the same experimental design is implemented regarding anatomical connectivity (AC) as it can be measured from dMRI. Using the significantly heritable AC endophenotypes, we performed a multivariate genome-wide association study on 31.775 participants from UK Biobank. Briefly, these ACs endophenotypes consists on nine measures (MD, FA, ICVF, ISOVF, L1, L2, L3, MO, OD) of the following bilateral white matter tracts: arcuate anterior/long/posterior segment, the frontal aslant tract, the frontal inferior longitudinal, the frontal superior longitudinal, fronto insular tract 1 to 5, the inferior fronto occipital fasciculus, inferior longitudinal, superior londgitudinal fasciculus I-III, uncinate and the corpus callosum.

The results from this analysis were subjected to a replication study in an independent sample (N=4,672). Finally, these results were functionally annotated and compared with genes identified as language-related in the literature.

7.1 Multivariate genome-wide association studies

We performed a multivariate genome-wide association studies (mvGWAS) between the filtered imputed genotypes and the set of significantly heritable endophenotypes ACs highlighted in the chapter 4.2.2, using the Multivariate Omnibus Statistical Test (MOSTest) [van der Meer et al., 2020].

As described in the Chapter 2.6, all endophenotypes were pre-residualised with covariates including sex, genotype array type, age, recruitment site, and ten first genetic principal components provided by UK Biobank. In addition, MOSTest performs a rank-based inverse-normal transformation of the residualised endophenotypes to ensure that the inputs are normally distributed. The distributions across the participants of all endophenotypes were visually inspected before and after covariate adjustment. MOSTest generated multivariate summary statistics that capture the significance of the association across all heritable language endophenotypes. To account for multiple testing over the whole genome, statistically significant SNPs were considered as those reaching the genome-wide threshold $p = 5e{-}8$.

More specifically, we performed a mvGWAS with the 313 ACs with significant SNP-based heritability. This analysis tested each SNP separately for its simultaneous association with the 313 ACs and yielded 34,881 significant SNPs at a genomic threshold, distributed on all autosomal chromosomes.

FUMA [Watanabe et al., 2017] software was used to analyse mvGWAS results and identify lead SNPs at each associated locus. Considering the genome-wide significance threshold $p = 5e{-}8$, there were 285 distinct genomic loci distributed on 21 chromosomes, associated with different aspects of brain-language AC and represented by 367 lead SNPs. (Fig.7.1, 7.2, Table 7.1).

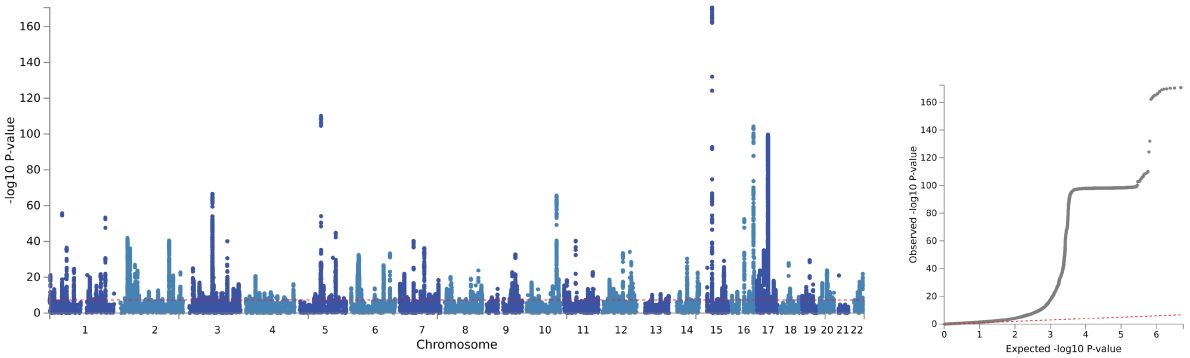

Figure 7.1 – **Multivariate GWAS analysis of the anatomical connectivity in 31,753 participants.** Manhattan plot for multivariate GWAS accross 313 FCs. The red dashed line indicates the genome-wide significance threshold $p = 5e{-}8$. The Quantile-quantile plot is also shown.

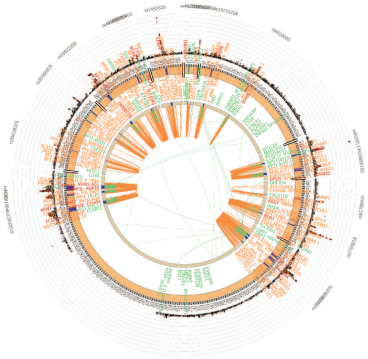

chromosome 1

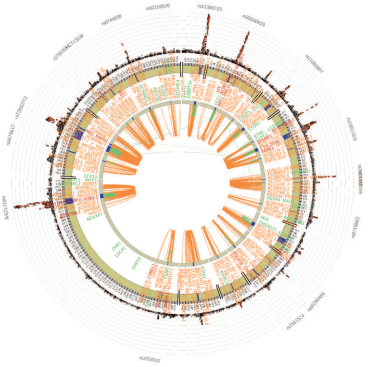

chromosome 2

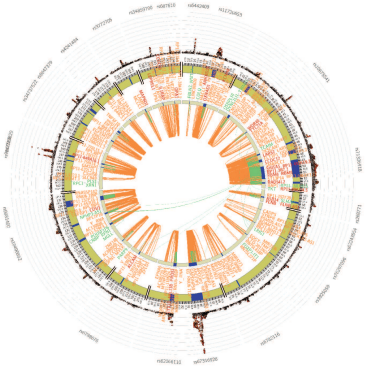

chromosome 3

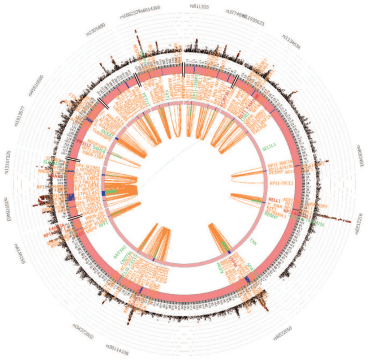

chromosome 4

chromosome 5

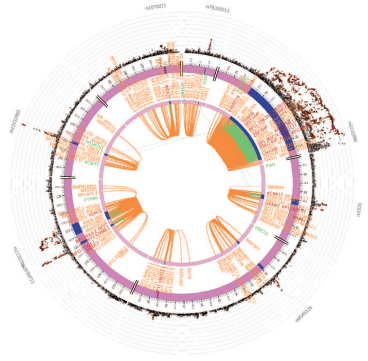

chromosome 6

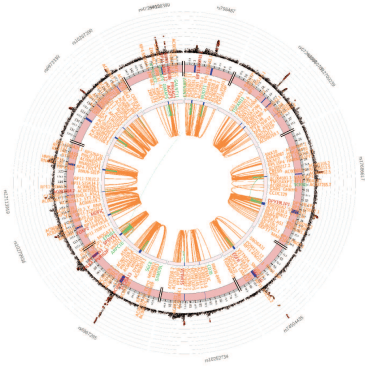

chromosome 7

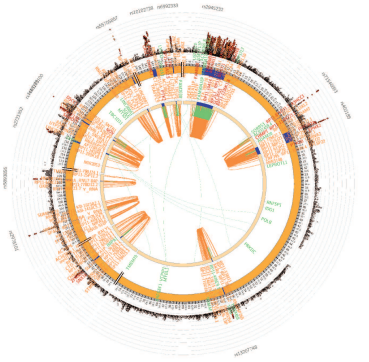

chromosome 8

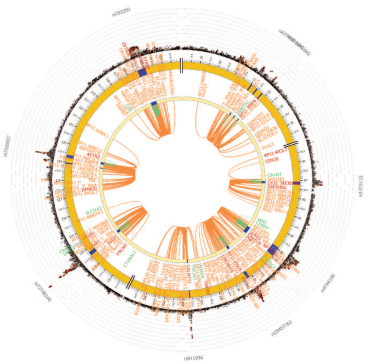

chromosome 9

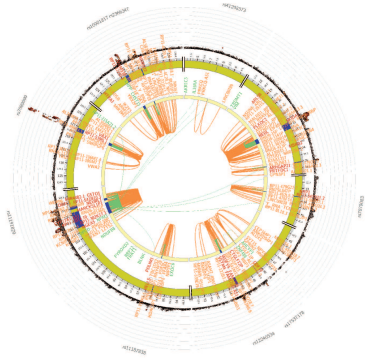

chromosome 10

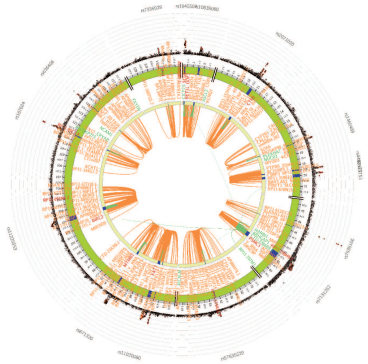

chromosome 11

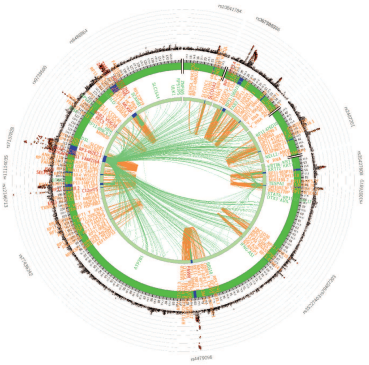

chromosome 12

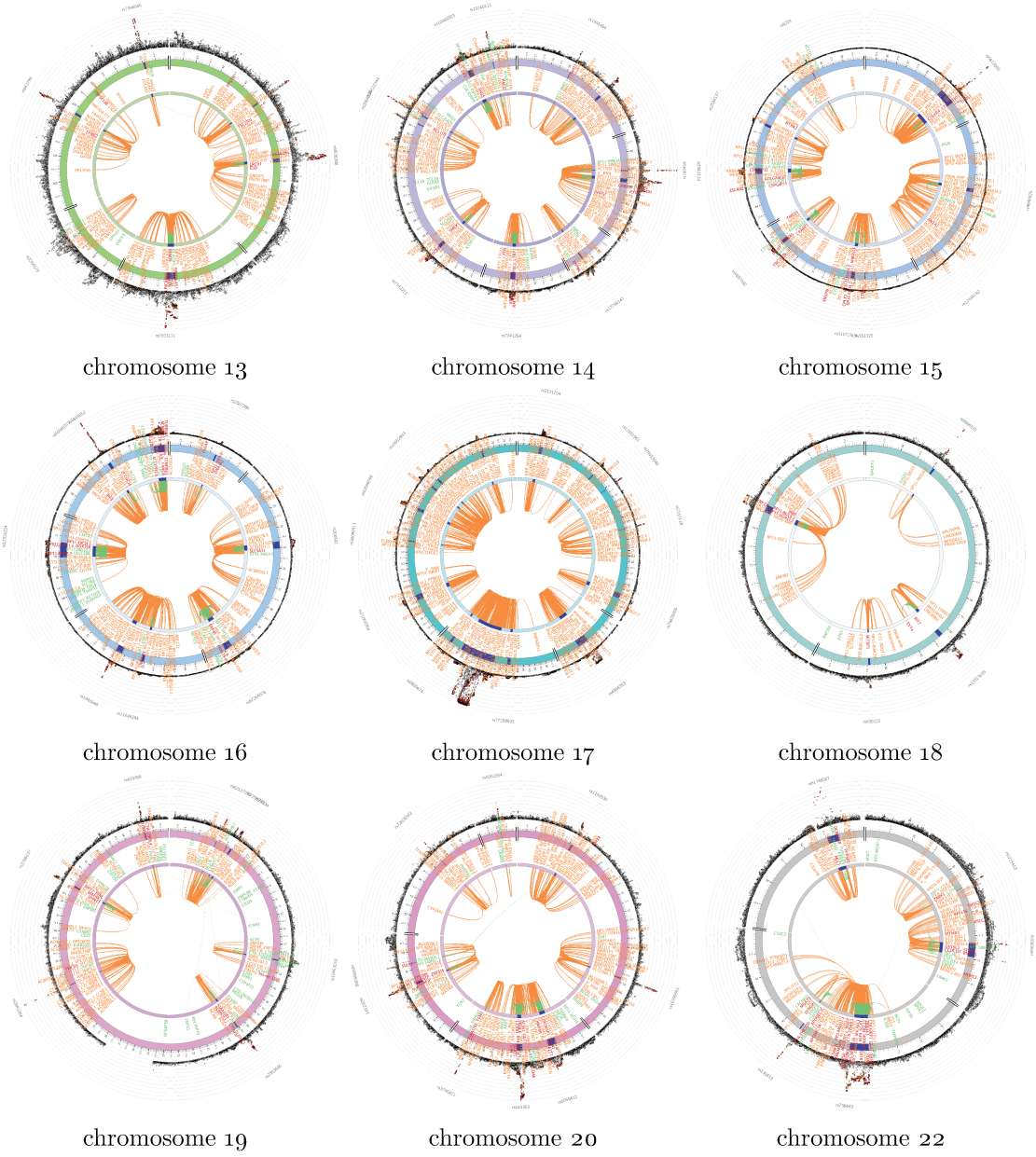

Figure 7.2 – **Genomic loci, eQTL associations and chromatin interactions identified via multivariate GWAS for anatomical connectivity.** Circos plot representing the genomic risk loci, and the genes associated with the loci by chromatin interactions and eQTLs. From outer layer to inner layer: Manhattan plot. Genomic risk loci are in blue. Genes mapped by chromatin interaction are in orange. Genes mapped by eQTL are in green. Genes mapped by both are in red. Chromatin interaction and eQTLs links follows the same color coding presented above. Due to a high number of genes identified using eQTLs mapping (361) and chromatin interaction (874), the chromosome 17 circos plot represent only chromatin interaction.

7.2 Validation of lead SNPs associated with ACs.

The multivariate genome-wide association results were replicated in an independent non-British sample considering the nominal significance threshold $p < 0.05$. Following the same pre-processing steps as for the primary sample, the non-British replication sample consists in 4,672 individuals with a mean age of 53 years ($\pm$7.55) and 2,572 female.
Seventy-one lead SNPs (out of the 367 unveiled by the discovery study) were replicated at the nominal significance level ($p < 5e{-}2$) on multivariate test in the independent non-British replication dataset. Table 7.1 summarises these results.

Table 7.1 – **Genomic loci associated with heritable language anatomical connectivities using MOSTest.** Lead SNP: ID of the lead SNPs within each locus. Position: position of the SNP in the hg19 human reference genome. mvgwasP discovery -British-: MOSTest association P value obtained using the discovery sample. mvgwasP replication -non British-: MOSTest association P value obtained using the independent replication sample. Functional category: Functional consequence of the SNP on the gene obtained from ANNOVAR. 'Central' endophenotypes: number of the endophenotypes that contributed most to the multivariate association considering the genome-wide association threshold ($5e-8$). 'Central' endophenotypes can be appreciated in the Table D.1.

Genomic Locus	Lead SNP	Chr	Position	Functional Category	non effect allele	effect allele	MAF	mvgwasP (discovery -British-)	mvgwasP (replication -non British-)	Nearest Gene	'central' endophenotypes
1	rs4970394	1	962891	intronic	T	C	0.421	4.01E-09	1.68E-01	AGRN	-
2	rs13303058	1	2005909	intronic	T	C	0.037	6.05E-10	1.43E-01	PRKCZ	-
3	rs11580768	1	2799480	intergenic	T	C	0.459	2.03E-21	4.12E-01	RP11-740P5.3	-
4	rs10779704	1	8693537	intronic	C	A	0.371	2.43E-08	3.57E-01	RERE	-
5	rs4920605	1	17315425	ncRNA intronic	A	G	0.431	5.07E-14	3.78E-01	RP1-37C10.3:ATP13A2	-
6	rs6658111	1	47980916	intergenic	G	T	0.360	2.01E-56	4.27E-02	AL356458.1	1
7	rs10888700	1	51086337	intronic	C	T	0.433	1.31E-10	4.33E-01	FAF1	-
8	rs61788401	1	59317534	ncRNA intronic	A	T	0.109	3.63E-14	2.67E-01	LINC01135	1
9	1:64228261 CCTCT C	1	64228261	intergenic	C	CCTCT	0.168	6.33E-12	6.04E-01	ROR1	-
10	rs2780818	1	65307994	intronic	G	T	0.223	3.43E-37	6.94E-04	JAK1	40
11	rs59679370	1	92922490	intergenic	T	C	0.197	4.81E-08	3.87E-01	GFI1	-
12	rs3767967	1	94002233	intronic	G	A	0.391	2.00E-25	1.71E-02	FNBP1L	3
13	rs114088373	1	95709197	ncRNA intronic	T	C	0.017	2.26E-08	3.22E-01	TMEM56-RWDD3:RWDD3:RP11-57H12.5	-
14	rs6693567	1	150510660	intergenic	T	C	0.265	1.65E-09	1.21E-01	RP11-54A4.2	-
14	rs72992015	1	150842696	intronic	T	C	0.212	3.47E-13	3.01E-01	ARNT	-
15	rs3841064	1	153919858	upstream:downstream	AC	A	0.491	1.14E-12	4.69E-02	CRTC2	4
16	rs4745	1	155106227	exonic	T	A	0.479	1.20E-20	1.60E-01	EFNA1	1
16	rs72704130	1	155207030	intronic	A	G	0.029	4.53E-10	6.66E-01	GBA	-
16	rs372518691	1	155856347	intergenic	C	CT	0.318	1.57E-12	7.94E-01	SYT11	-
17	rs35039375	1	171516863	intronic	G	A	0.091	1.67E-08	3.57E-01	PRRC2C	-
18	1:178770951 AAGGG A	1	178770951	intronic	A	AAGGG	0.429	8.46E-12	2.57E-01	RALGPS2	-
19	rs35306826	1	180956936	intronic	A	T	0.408	6.65E-16	3.00E-03	STX6	1
20	rs10922200	1	197321440	intronic	T	C	0.110	2.17E-22	1.33E-01	CRB1	18
20	rs17641524	1	197704717	exonic	T	C	0.209	1.16E-12	3.48E-02	DENND1B	-
21	rs4950982	1	205078247	intronic	C	T	0.122	2.02E-09	1.08E-01	RBBP5	-
22	rs1772159	1	205759195	UTR3	A	G	0.399	3.57E-10	2.32E-01	SLC41A1	-
23	rs2480403	1	206614441	intronic	C	T	0.203	1.14E-10	4.97E-01	SRGAP2	-
24	rs1452628	1	215139887	intergenic	T	A	0.385	4.97E-54	9.96E-03	RP11-323K10.1	59
24	rs2601645	1	215185552	intronic	T	C	0.084	2.12E-21	6.34E-02	KCNK2	16
25	rs11386753	2	27148654	intronic	CT	C	0.385	1.04E-42	1.99E-03	DPYSL5	3
25	rs41288789	2	27167617	exonic	A	G	0.051	8.28E-09	8.12E-01	DPYSL5	-
26	rs35050623	2	37063240	intergenic	CT	C	0.462	7.04E-37	2.08E-01	AC007382.1	2
27	2:42278500 GGGGCCCCCAGGCCTTGGAT G	2	42278500	intronic	G	GGGGCCCCC AGGCCTTGGAT	0.234	1.74E-14	9.75E-02	PKDCC	-
28	rs11891807	2	48288816	ncRNA intronic	G	T	0.385	2.29E-16	5.22E-02	AC079807.4	1
29	2:56116193 TTGATTCTTGGCCTCCCTCCC T	2	56116193	intronic	T	TTGATTCTTGG CCTCCCTCCC	0.090	1.13E-27	2.69E-03	EFEMP1	8
30	rs200493119	2	58154132	intronic	CG	C	0.399	2.04E-18	3.64E-01	VRK2	-
31	rs13011022	2	60626822	intergenic	A	G	0.409	1.55E-11	8.67E-02	AC007381.2	-
32	rs7600385	2	65984026	ncRNA intronic	T	A	0.401	2.03E-24	2.78E-02	AC074391.1	2
33	rs11688599	2	66756550	intronic	T	C	0.320	3.63E-08	2.92E-01	MEIS1	-
34	rs6719862	2	71958862	intergenic	G	A	0.375	1.62E-10	6.97E-01	DYSF	-
35	rs143238565	2	98430405	intronic	TA	T	0.076	2.26E-08	6.92E-01	TMEM131	-
36	rs60240458	2	109949227	intronic	C	A	0.488	1.37E-12	8.10E-02	SH3RF3	-
37	rs7581524	2	113234316	intergenic	T	C	0.275	3.44E-08	7.36E-01	TTL	-
38	rs36860848	2	119755965	intergenic	A	G	0.014	4.33E-08	6.75E-01	MARCO	-
39	rs144495495	2	145692649	ncRNA intronic	CAT	C	0.250	2.36E-13	4.22E-01	TEX41	9
40	rs1558957	2	162890175	intronic	C	T	0.411	1.97E-08	3.07E-01	DPP4	-
41	rs56136540	2	187501682	intronic	A	G	0.404	7.32E-16	2.60E-01	ITGAV	-
41	rs62172376	2	188289174	ncRNA intronic	A	C	0.303	2.99E-41	6.17E-03	AC007319.1:CALCRL	-
42	rs4675617	2	200342749	intergenic	G	A	0.161	5.07E-12	5.38E-01	SATB2-AS1	-
43	rs343449435	2	203619455	intronic	A	C	0.034	2.03E-09	6.95E-01	FAM117B	4
43	rs72932772	2	203682304	intronic	G	C	0.129	1.05E-21	5.23E-02	ICA1L	10
43	rs113796732	2	204323814	intronic	C	G	0.039	2.50E-12	3.13E-02	RAPH1	-
44	rs142787179	2	204840948	intergenic	C	G	0.028	5.42E-09	7.51E-01	ICOS	-
45	rs7593551	2	225231713	intergenic	C	T	0.299	3.17E-08	8.04E-01	FAM124B	-
46	rs1156040	2	227057413	intergenic	A	G	0.133	6.60E-10	2.97E-01	AC068138.1	-
46	rs2713536	2	227163642	intergenic	T	C	0.363	2.93E-10	5.08E-01	AC068138.1	-
47	rs6749936	2	232055684	intergenic	T	C	0.211	2.23E-23	1.12E-02	ARMC9	21
48	rs62189826	2	237501894	intergenic	C	T	0.181	9.16E-09	8.97E-01	ACKR3	-
49	rs13079464	3	13822439	intergenic	C	G	0.467	7.77E-12	3.48E-01	LINC00620	4
49	rs6442409	3	13835087	intergenic	C	T	0.343	1.20E-25	2.94E-01	WNT7A	107
50	rs11720653	3	17439510	intronic	C	T	0.316	1.04E-18	1.95E-01	TBC1D5	1
51	rs111710612	3	33577384	intronic	C	A	0.018	4.70E-08	6.36E-01	CLASP2	-
51	3:33846846 CA C	3	33846846	intronic	C	CA	0.342	2.90E-08	7.07E-01	PDCD6IP	-
52	rs142003765	3	39479611	intergenic	G	A	0.020	1.26E-09	8.81E-02	AC099332.1	8
52	rs10675541	3	39510286	intronic	TAC	T	0.480	2.16E-16	3.10E-01	MOBP	5
53	3:45795731 CTCTT C	3	45795731	intergenic	C	CTCTT	0.104	2.21E-11	2.18E-01	SLC6A20	-
54	3:47312635 AAAAAAG A	3	47312635	intronic	A	AAAAAAG	0.402	5.85E-09	9.80E-02	KIF9	-
55	rs59623077	3	49106542	intronic	TA	T	0.336	6.27E-09	8.95E-01	QRICH1	1
55	rs7627910	3	49971831	intergenic	C	T	0.458	2.73E-08	8.03E-01	MON1A	-
55	rs71326918	3	50174844	ncRNA intronic	A	C	0.110	6.40E-12	5.53E-02	RP11-493K19.3	-

Genomic Locus	Lead SNP	Chr	Position	Functional Category	non effect allele	effect allele	MAF	mvgwasP (discovery -British-)	mvgwasP (replication -non British-)	Nearest Gene	'central' endophenotypes
55	rs9832454	3	50217558	intronic	T	C	0.089	1.35E-11	5.60E-03	SEMA3F	1
55	rs62260798	3	50274278	intronic	T	C	0.080	4.74E-08	9.39E-01	GNAI2	-
56	rs762174010	3	52572841	intronic	T	TTTG	0.453	1.26E-10	6.46E-01	SMIM4	-
57	rs268771	3	57937992	intergenic	T	C	0.435	1.13E-09	6.99E-01	PPIAP16	-
58	rs62243554	3	62568709	intronic	T	A	0.339	5.43E-09	2.23E-01	CADPS	-
59	rs76207096	3	66044816	intergenic	A	C	0.303	2.77E-09	6.57E-02	MAGI1	-
60	rs3925059	3	69463714	intronic	G	C	0.319	2.46E-09	7.16E-01	FRMD4B	-
61	rs6782116	3	77176032	intronic	T	C	0.427	1.55E-09	1.80E-01	ROBO2	-
61	rs553398120	3	77340010	intronic	C	A	0.421	5.46E-09	8.86E-01	ROBO2	-
62	rs10638977	3	88781746	intergenic	AAC	A	0.499	8.44E-12	1.64E-01	NDUFA5P5	-
62	rs58378065	3	88943830	intergenic	AT	A	0.190	1.50E-08	8.65E-01	NARG2P2	-
62	3:89257759 AGAAG A	3	89257759	intronic	A	AGAAG	0.290	2.56E-08	3.31E-02	EPHA3	-
62	rs67316928	3	89482234	intronic	C	T	0.398	2.94E-67	3.17E-05	EPHA3	1
63	rs62266110	3	93537923	intergenic	A	G	0.319	1.33E-20	1.39E-01	RNU6-488P	-
64	rs6788676	3	104674040	intergenic	A	G	0.355	6.95E-12	1.76E-01	ALCAM	-
65	rs373566812	3	124462488	intronic	AAAAT	A	0.165	1.02E-11	7.18E-01	UMPS	3
66	rs747333548	3	129568656	intronic	TAC	T	0.082	9.17E-12	2.32E-01	TMCC1	-
67	rs10490862	3	132160713	intronic	G	A	0.120	4.45E-09	5.03E-01	DNAJC13	-
68	rs9881400	3	135861666	intronic	T	G	0.265	1.43E-09	8.39E-02	PPP2R3A	-
69	rs36008198	3	146362717	intergenic	TGTA	T	0.394	4.23E-09	1.09E-01	PLSCR5	-
69	rs9847565	3	146369166	intergenic	G	C	0.462	9.03E-28	6.43E-02	PLSCR5	-
70	rs62275311	3	147034001	ncRNA intronic	C	A	0.245	4.95E-20	2.74E-02	RP11-649A16.1	1
70	rs2279829	3	147106319	UTR3	T	C	0.212	7.46E-41	2.42E-02	ZIC4	-
71	rs34737522	3	168892763	intronic	CT	C	0.144	2.67E-08	6.56E-01	MECOM	-
72	3:170987040 ACTCT A	3	170987040	intronic	A	ACTCT	0.455	2.71E-14	7.93E-02	TNIK	2
73	rs16856586	3	171436724	intronic	A	G	0.302	1.42E-09	8.16E-01	PLD1	-
73	rs9647379	3	171785168	intronic	C	G	0.410	5.56E-12	2.28E-01	FNDC3B	28
74	rs4241484	3	177316085	ncRNA intronic	A	C	0.406	2.40E-12	6.99E-01	LINC00578	-
75	rs3772705	3	183388403	intronic	G	A	0.255	2.84E-13	6.43E-01	KLHL24	25
76	rs34859790	3	190652830	intergenic	T	C	0.384	7.78E-17	3.23E-01	GMNC	-
77	rs687610	3	193515781	intergenic	G	C	0.426	1.54E-12	2.74E-02	RP11-528A4.3	1
78	rs811316	4	1689377	intergenic	C	T	0.190	1.23E-08	6.53E-01	FAM53A	-
79	rs3774893	4	5887388	intronic	C	A	0.418	2.87E-08	5.41E-01	CRMP1	-
80	rs11930623	4	7931682	intronic	C	A	0.405	4.95E-08	2.20E-01	AFAP1	-
81	rs1134634	4	15603069	UTR3	C	G	0.415	4.61E-10	3.81E-01	CC2D2A	-
82	4:20318933 GA G	4	20318933	intronic	G	GA	0.062	8.34E-09	6.02E-01	SLIT2	-
83	rs4692493	4	30949606	intronic	T	A	0.495	1.08E-08	6.54E-02	PCDH7	-
84	rs6812216	4	38651939	ncRNA intronic	A	G	0.354	2.24E-21	3.35E-01	RP11-617D20.1:AC021860.1	-
85	rs10032190	4	53734940	intergenic	A	C	0.243	3.20E-08	6.83E-01	RASL11B	-
85	rs6822050	4	53943333	intronic	A	G	0.273	6.88E-12	2.35E-01	SCFD2	61
86	rs36114335	4	73319708	intronic	AT	A	0.350	1.59E-11	4.62E-01	ADAMTS3	-
87	rs34272002	4	77657959	intronic	CAG	C	0.385	2.39E-08	4.06E-01	SHROOM3	-
88	rs4148155	4	89054667	intronic	G	A	0.114	4.35E-09	8.15E-01	ABCG2	-
89	4:96797672 TA T	4	96797672	intergenic	T	TA	0.099	4.26E-08	3.10E-01	RNU6-1059P	-
90	rs35976463	4	97926008	intergenic	CATG	C	0.316	2.24E-12	6.82E-01	COX7A2P2	10
90	rs62315846	4	98455696	ncRNA intronic	G	A	0.135	2.15E-09	5.51E-02	STPG2:RP11-681L8.1	-
91	rs13107325	4	103188709	exonic	T	C	0.076	3.20E-10	1.30E-01	SLC39A8	1
92	rs1913577	4	119297657	intergenic	G	A	0.365	2.13E-09	4.93E-01	PRSS12	-
93	rs45510500	4	123179900	exonic	T	C	0.056	3.91E-10	3.13E-03	KIAA1109	-
94	4:149409090 CAG C	4	149409090	intergenic	C	CAG	0.465	1.70E-09	8.38E-01	RP11-655B23.1	-
95	rs2305980	4	151171269	intronic	A	T	0.257	1.74E-09	2.73E-01	DCLK2	-
96	rs1882325	4	185126789	intronic	T	G	0.350	7.55E-17	1.30E-01	ENPP6	30
97	rs6814390	4	187385465	ncRNA intronic	A	G	0.161	1.94E-08	2.12E-01	F11-AS1:RP11-215A19.2	-
98	rs6450402	5	56040390	intergenic	T	A	0.226	1.26E-08	5.12E-01	AC008940.1	-
99	rs72755166	5	59982433	intronic	G	A	0.134	3.85E-10	2.60E-01	DEPDC1B	-
99	rs4604142	5	60642595	intronic	T	C	0.499	2.71E-11	4.09E-01	ZSWIM6	-
100	rs34592828	5	75996909	exonic	A	G	0.045	6.33E-10	4.43E-01	IQGAP2:CTD-2384B11.2	1
101	rs145824047	5	81800313	intergenic	A	G	0.396	4.50E-10	8.02E-01	CTD-2015A6.1	2
101	rs752021310	5	81866998	intergenic	C	CTAAT	0.447	3.20E-23	8.87E-03	CTD-2015A6.2	2
102	rs11749904	5	82782530	intronic	C	T	0.380	6.09E-29	4.43E-02	VCAN	145
102	rs160184	5	82822037	intronic	G	A	0.480	4.03E-25	3.63E-02	VCAN	140
102	rs309588	5	82852578	ncRNA intronic	T	A	0.204	5.16E-28	1.55E-01	VCAN:VCAN-AS1	55
102	rs10052710	5	82860025	ncRNA intronic	G	T	0.195	7.72E-111	6.11E-06	VCAN:VCAN-AS1	203
103	rs6882046	5	87968864	ncRNA exonic	G	A	0.262	4.02E-12	5.02E-01	LINC00461	-
104	rs17669337	5	92187932	intergenic	T	C	0.412	4.08E-08	3.21E-01	CTC-458G6.4	-
105	rs73135321	5	92928643	intronic	A	G	0.093	3.45E-09	6.63E-01	NR2F1	-
105	rs115136616	5	93021116	intronic	T	C	0.047	6.85E-16	1.73E-01	FAM172A	1
106	rs2974619	5	114470013	intronic	G	T	0.400	1.90E-09	1.11E-01	TRIM36	-
107	rs111353435	5	116608074	intergenic	AAGAT	A	0.330	7.03E-10	1.46E-01	RPL35AP15	-
108	rs7729285	5	122754416	intronic	G	A	0.431	9.63E-11	2.12E-02	CEP120	1
109	rs10037401	5	139568762	intronic	T	A	0.208	1.48E-24	8.21E-03	CYSTM1	-
109	rs4150210	5	139721913	intronic	A	T	0.259	1.79E-45	3.91E-03	HBEGF	38
110	rs12518238	5	151259002	intronic	A	G	0.250	1.62E-09	3.86E-01	GLRA1	-
111	rs6555969	5	171128464	intergenic	C	T	0.320	4.50E-09	2.17E-01	AC011410.1	-
112	rs79318212	6	1365244	intergenic	G	A	0.106	1.45E-14	5.92E-01	RP4-668J24.2	28
113	rs940404	6	25343444	intronic	A	T	0.068	4.17E-08	1.84E-02	LRRC16A	-
113	rs1800562	6	26093141	exonic	A	G	0.078	1.83E-10	5.26E-02	HFE	2
113	rs146863150	6	26408472	intronic	CATAT	C	0.103	7.93E-22	5.93E-04	BTN3A1	17
113	rs34196306	6	27425644	intronic	C	G	0.104	1.17E-27	1.29E-03	ZNF184	32
113	rs71546548	6	27493970	intergenic	TTTCTTA	T	0.010	1.41E-13	8.72E-01	HNRNPA1P1	15
113	rs34676049	6	28453618	intergenic	G	T	0.108	1.93E-28	4.67E-04	GPX6	40
113	rs3131856	6	29607101	intergenic	C	T	0.121	4.75E-33	7.66E-04	SUMO2P1	55
114	rs1520	6	39526867	intronic	G	A	0.374	6.46E-14	9.02E-01	KIF6	-
114	rs9380899	6	39794806	intronic	G	C	0.271	8.76E-12	5.17E-01	DAAM2	13
115	rs9345125	6	92002653	intergenic	G	A	0.171	1.90E-14	2.68E-01	RP1-177I10.1	-
116	rs770637388	6	98561749	ncRNA intronic	C	CAATTT	0.486	2.91E-08	1.82E-02	RP11-436D23.1	-
117	rs3799711	6	126075313	intronic	C	T	0.480	2.29E-27	3.15E-01	HEY2	1
118	rs75343521	6	126732511	intergenic	T	C	0.041	8.00E-09	2.25E-01	CENPW	-
118	rs1120786	6	126808637	intergenic	G	T	0.451	2.50E-22	4.85E-01	MIR588	2
119	rs12192990	6	151021978	intronic	G	C	0.412	5.37E-34	3.98E-01	PLEKHG1	1
120	rs1078211	6	170201300	ncRNA exonic	C	T	0.403	1.51E-08	1.99E-01	LINC00574	-
121	rs201865165	7	1087676	intronic	C	CA	0.422	1.27E-08	9.37E-01	C7orf50:GPR146	-
122	rs798487	7	2802943	intronic	A	G	0.297	4.19E-17	1.46E-01	AMZ1:GNA12	8
123	rs67248060	7	18899163	intronic	T	C	0.366	1.33E-22	4.78E-01	HDAC9	15
124	rs10950739	7	19628139	intergenic	A	G	0.374	4.38E-10	8.63E-01	AC007091.1	-
125	rs12700239	7	20865979	upstream	A	C	0.211	6.75E-09	4.69E-01	RPL23P8	-

Genomic Locus	Lead SNP	Chr	Position	Functional Category	non effect allele	effect allele	MAF	mvgwasP (discovery -British-)	mvgwasP (replication -non British-)	Nearest Gene	'central' endophenotypes
126	rs17686617	7	29346518	intronic	T	C	0.313	1.36E-09	1.94E-01	CHN2	2
127	7:33344749 TAA T	7	33344749	intronic	T	TAA	0.304	1.02E-08	4.20E-01	BBS9	-
128	rs74504435	7	54949256	intergenic	G	A	0.094	5.65E-41	1.26E-01	SNORA73	67
128	rs10244020	7	55108994	intronic	C	T	0.472	1.02E-10	1.83E-01	EGFR	16
129	rs10252734	7	81418596	intergenic	G	T	0.400	5.23E-12	2.30E-01	HGF	1
130	rs761326546	7	83628746	intronic	T	TAATTA	0.212	6.84E-13	2.51E-01	SEMA3A	-
131	rs6967285	7	96200086	nan	C	T	0.308	6.42E-37	3.87E-02	SHFM1	2
132	7:99965328 GA G	7	99965328	ncRNA exonic	G	GA	0.189	1.71E-08	2.09E-01	STAG3L5P-PVRIG2P-PILRB:PILRB:PILRA	-
133	rs10279936	7	114147217	intronic	A	C	0.491	4.01E-11	2.96E-01	FOXP2	-
134	rs12113919	7	117612315	intergenic	G	C	0.410	4.78E-11	4.22E-01	AC003084.2	-
135	rs566523025	7	120759189	intronic	CT	C	0.365	4.06E-09	1.19E-02	CPED1	-
136	7:132558516 TATC T	7	132558516	intronic	T	TATC	0.253	3.12E-08	3.40E-01	CHCHD3	-
137	rs6973339	7	134388544	intergenic	T	G	0.358	2.90E-10	3.26E-01	AC009276.4	7
138	rs10267280	7	137111423	intronic	T	C	0.366	2.71E-09	4.83E-01	DGKI	-
139	rs4725995	7	150819169	intronic	T	C	0.305	3.86E-19	3.41E-01	AGAP3	10
140	rs4128399	7	151498679	intronic	C	T	0.160	8.29E-19	2.19E-03	PRKAG2	23
141	rs2945232	8	8098038	ncRNA exonic	C	T	0.472	3.23E-14	7.48E-01	FAM86B3P:ALG1L13P	-
141	rs4075359	8	9487813	intronic	C	T	0.377	1.73E-13	7.90E-02	TNKS	2
141	rs10108511	8	11435516	ncRNA intronic	C	T	0.469	6.75E-14	6.52E-01	LINC00208	-
142	rs71548883	8	23101514	intronic	CT	C	0.384	8.31E-21	3.02E-01	CHMP7	1
143	rs17055142	8	26201601	intronic	T	C	0.076	4.76E-10	6.70E-02	PPP2R2A	-
143	rs11421016	8	26327197	intronic	GA	G	0.174	3.05E-10	2.17E-01	BNIP3L	-
143	rs565497548	8	26452540	intronic	A	AAATC	0.000	2.33E-14	1.77E-02	DPYSL2	-
143	rs403185	8	26476721	intronic	G	A	0.408	1.84E-17	5.67E-02	DPYSL2	1
144	rs13207748	8	57185107	intergenic	A	G	0.219	1.50E-08	6.04E-01	RP11-140I16.2	-
145	8:82719186 TA T	8	82719186	ncRNA intronic	T	TA	0.414	1.62E-08	2.21E-01	RP13-923O23.6:SNX16	-
146	rs2978101	8	101679224	intergenic	G	T	0.461	7.07E-20	2.26E-02	SNX31	36
147	rs5893855	8	108394765	intronic	GA	G	0.421	2.00E-12	6.38E-02	ANGPT1	-
148	rs2721952	8	116645056	intronic	T	C	0.401	1.02E-10	1.16E-02	TRPS1	-
149	rs7463176	8	119957625	intronic	G	A	0.455	2.24E-09	5.54E-01	TNFRSF11B	-
150	rs10283100	8	120596023	exonic	G	A	0.060	3.68E-16	2.47E-03	ENPP2	19
150	rs1992721	8	120597417	intronic	G	A	0.283	2.72E-09	7.31E-01	ENPP2	-
151	rs55705857	8	130645692	ncRNA intronic	G	A	0.058	1.60E-24	8.28E-01	CCDC26	81
152	rs45613837	8	141744917	intronic	A	G	0.452	2.94E-14	6.80E-01	PTK2	-
152	rs10102728	8	142205964	downstream	A	G	0.409	3.98E-16	4.91E-02	DENND3	2
153	rs6992333	8	144993377	exonic	G	A	0.430	3.58E-11	1.96E-01	PLEC	1
154	rs679038	9	22029080	ncRNA intronic	A	G	0.421	1.68E-08	1.62E-01	RP11-145E5.5:CDKN2B-AS1	14
155	rs693370	9	22446297	upstream	A	G	0.118	1.86E-09	6.32E-01	DMRTA1	-
156	rs842842	9	22767821	ncRNA intronic	C	A	0.421	2.53E-08	3.74E-01	RP11-399D6.2: RP11-370B11.3	-
157	rs1329733	9	92208227	intergenic	G	A	0.480	1.04E-08	6.07E-01	GADD45G	-
158	rs4744186	9	95932546	intergenic	T	C	0.431	2.93E-11	5.89E-02	WNK2	1
158	rs10992828	9	96415368	intronic	A	G	0.272	3.54E-08	8.46E-01	PHF2	-
159	rs28457763	9	98260514	intronic	A	G	0.328	8.49E-14	2.38E-01	PTCH1	-
160	rs911934	9	101637477	intergenic	G	T	0.313	1.75E-23	6.15E-01	RP11-92C4.3	3
161	rs10980607	9	113638375	intronic	T	C	0.216	8.06E-12	5.46E-01	LPAR1	25
161	rs72748148	9	113677241	intronic	A	G	0.214	1.93E-33	2.41E-02	LPAR1	59
162	9:118957629 AAAG A	9	118957629	intronic	A	AAAG	0.424	1.55E-08	3.09E-02	PAPPA	3
163	rs7030607	9	119245183	intronic	A	G	0.354	7.46E-16	7.30E-02	ASTN2	1
164	rs783200	9	125857032	intronic	A	G	0.136	2.58E-10	2.17E-01	RABGAP1	-
165	rs41298373	10	7622009	exonic	A	G	0.100	9.46E-11	9.34E-02	ITIH5	-
166	10:21878831 TCCCTTC T	10	21878831	intronic	T	TCCCTTC	0.298	8.21E-18	1.16E-01	MLLT10	-
167	rs774455421	10	25041543	intergenic	G	GAGACAGTCAAGTC	0.352	2.01E-09	2.43E-01	ARHGAP21	10
168	rs7079083	10	33676655	intergenic	T	A	0.291	5.05E-09	6.41E-01	RP11-90B22.1	-
169	rs17537178	10	48442894	intergenic	G	A	0.267	3.61E-10	2.84E-01	GDF10	1
170	rs12240534	10	50318141	intronic	T	C	0.349	3.28E-10	1.67E-01	VSTM4	1
171	rs11187838	10	96038686	intronic	A	G	0.435	6.80E-12	2.43E-01	PLCE1	-
172	rs3740405	10	103908080	intronic	A	G	0.454	4.10E-08	6.11E-01	PPRC1	-
172	rs758741000	10	104299191	intronic	A	ATTGT	0.319	1.10E-15	7.39E-01	SUFU	-
172	rs1163084	10	105039048	intronic	C	T	0.456	2.15E-15	1.09E-01	INA	6
173	rs11394128	10	105454037	intronic	TG	T	0.485	3.49E-09	3.10E-01	SH3PXD2A	44
173	rs11191829	10	105614452	intronic	T	G	0.353	3.25E-13	1.84E-01	SH3PXD2A	8
174	rs7089699	10	118692698	intronic	G	A	0.249	2.67E-66	9.69E-03	KIAA1598	3
175	rs10901817	10	126443404	intronic	T	A	0.427	1.26E-19	5.77E-01	RP11-12J10.3:METTL10	2
176	rs2366347	10	127674508	intronic	A	G	0.421	1.04E-11	6.53E-02	FANK1	-
177	rs1045502	11	252818	UTR3	A	G	0.086	1.81E-14	4.19E-01	PSMD13	7
178	rs10835060	11	1488143	intergenic	G	T	0.191	2.50E-09	3.98E-01	MOB2	-
179	rs2071020	11	10478228	intronic	T	C	0.452	4.99E-19	7.47E-01	AMPD3	23
179	rs4442541	11	10669172	intronic	G	A	0.311	5.91E-12	2.23E-03	MRVI1	-
180	rs1468489	11	17022894	intronic	C	T	0.378	7.34E-09	9.20E-01	PLEKHA7	-
181	rs4488177	11	19454969	intronic	A	C	0.343	2.59E-12	1.49E-01	NAV2	-
182	rs2585753	11	19895756	intronic	G	C	0.226	1.52E-11	4.18E-03	NAV2	5
182	rs35891966	11	20129311	exonic	A	G	0.071	3.87E-08	2.17E-01	NAV2	-
183	rs7935166	11	44636547	intronic	A	G	0.133	4.43E-41	3.00E-01	CD82	89
184	rs7131262	11	47836302	intronic	A	T	0.288	1.44E-09	2.19E-01	NUP160	-
185	rs57630229	11	82409631	ncRNA intronic	A	G	0.113	4.35E-08	3.58E-01	RP11-179A16.1	15
186	rs777407913	11	91968738	intergenic	C	CTATT	0.181	3.96E-14	3.68E-03	RPL7AP57	-
187	11:92504928 TA T	11	92504928	intronic	T	TA	0.329	5.33E-10	1.15E-01	FAT3	-
187	rs11020080	11	92578985	intronic	A	G	0.387	9.29E-12	7.11E-02	FAT3	2
188	rs671320	11	95578780	intronic	T	G	0.465	2.40E-12	6.32E-01	MTMR2	-
189	rs11225553	11	102989206	intronic	G	A	0.076	3.24E-08	6.80E-01	DYNC2H1	-
190	rs167684	11	110962880	ncRNA exonic	G	A	0.314	1.38E-23	7.87E-02	RP11-89C3.4	-
191	rs636406	11	114031092	intronic	G	C	0.358	2.80E-09	6.12E-01	ZBTB16	2
192	rs7936928	11	130279168	intronic	C	T	0.395	1.40E-09	4.03E-01	ADAMTS8	-
193	rs10841784	12	21441577	intronic	C	T	0.283	9.57E-09	5.77E-01	SLCO1A2	1
194	rs2075378	12	27788021	exonic	A	G	0.355	2.20E-19	6.03E-01	PPFIBP1	-
195	rs7305286	12	28282047	intergenic	G	A	0.307	3.24E-17	4.99E-04	CCDC91	1
196	12:32495060 GTA G	12	32495060	intronic	G	GTA	0.210	5.34E-11	2.20E-01	BICD1	-
197	rs2407281	12	43609752	intergenic	C	T	0.253	2.92E-14	1.35E-01	RP11-118A3.1	-
198	rs35427608	12	53826327	intergenic	AT	A	0.177	4.60E-11	8.43E-01	AMHR2	-
199	rs10876870	12	56478002	intronic	C	A	0.425	4.56E-09	2.20E-01	ERBB3	1
200	rs79487293	12	65905126	ncRNA intronic	T	C	0.325	5.11E-10	5.89E-01	RP11-230G5.2	-
201	rs35227403	12	68216239	intergenic	A	T	0.057	1.45E-09	2.06E-01	RP11-43N5.1	-
202	rs4479056	12	79938856	ncRNA intronic	A	G	0.307	3.57E-34	3.65E-01	RP11-359M6.1	4
203	rs77436242	12	99640159	exonic	C	G	0.048	3.03E-10	5.36E-01	ANKS1B	1
204	rs12146713	12	106476805	intronic	C	T	0.096	7.00E-35	1.99E-01	NUAK1	8
205	rs536700128	12	107063485	intronic	GA	G	0.243	1.13E-13	3.57E-01	RP11-144F15.1:RFX4	2
206	rs111140335	12	109102983	intronic	A	T	0.438	1.01E-08	8.17E-01	CORO1C	1
207	rs7137828	12	111932800	intronic	T	C	0.484	2.99E-29	6.03E-01	ATXN2	2
207	rs10219716	12	112503474	ncRNA exonic	A	T	0.085	1.60E-09	3.98E-01	NAA25:RP1-267L14.3	1
208	rs9739560	12	118461574	intronic	A	T	0.417	3.29E-17	1.33E-01	RFC5	33
209	rs6488864	12	123618362	intronic	C	G	0.199	5.66E-11	4.31E-01	PITPNM2	-
210	13:44887065 AT A	13	44887065	intergenic	A	AT	0.250	2.04E-08	1.66E-02	SERP2	-
211	rs9526208	13	47208767	intronic	G	A	0.245	7.67E-11	4.92E-02	LRCH1	-
212	rs6563121	13	80175000	intergenic	C	T	0.478	2.38E-11	8.49E-01	LINC01068	-
213	rs2254579	13	101045359	intronic	C	G	0.429	1.30E-08	1.46E-01	PCCA	-

Genomic Locus	Lead SNP	Chr	Position	Functional Category	non effect allele	effect allele	MAF	mvgwasP (discovery -British-)	mvgwasP (replication -non British-)	Nearest Gene	'central' endophenotypes
214	rs943799	13	107724282	intergenic	A	G	0.484	2.34E-09	2.70E-01	AL445204.1	-
215	rs11838776	13	111040681	intronic	A	G	0.277	3.42E-10	2.91E-03	COL4A2	1
215	rs7996686	13	111093237	intronic	G	A	0.429	2.89E-10	1.48E-01	COL4A2	-
216	rs1955454	14	29226194	ncRNA intronic	G	T	0.438	2.24E-11	1.32E-01	RP11-966I7.1	-
217	14:31370483 TA T	14	31370483	intronic	T	TA	0.450	1.93E-12	2.91E-01	STRN3	-
218	rs160459	14	59074136	intergenic	C	A	0.459	4.19E-31	5.26E-01	DACT1	7
219	14:59631075 GTTGT G	14	59631075	intergenic	G	GTTGT	0.120	1.60E-19	4.58E-01	CTD-2315A10.1	-
219	rs17833810	14	59697746	intronic	G	A	0.432	1.79E-09	9.85E-01	DAAM1	-
220	rs17756147	14	69036127	intronic	A	G	0.246	2.17E-08	1.99E-01	RAD51B	-
221	rs7141254	14	75190527	intronic	T	G	0.459	4.12E-08	2.77E-01	FCF1	-
222	rs7142211	14	91910995	intergenic	A	G	0.443	4.74E-08	4.17E-01	SMEK1	1
223	rs12895055	14	99712794	intronic	T	C	0.437	1.10E-09	1.40E-01	BCL11B	-
223	rs2664299	14	99742187	intergenic	C	T	0.420	1.36E-10	4.81E-01	BCL11B	-
224	rs11846963	14	100271376	intronic	C	T	0.403	8.38E-11	8.04E-01	EML1	-
224	rs35522344	14	100283856	intronic	T	C	0.382	2.60E-23	3.21E-01	EML1	1
225	rs12889303	14	104161666	intronic	A	G	0.312	2.80E-08	8.48E-01	KLC1	-
226	rs10140111	14	105644282	ncRNA intronic	G	C	0.384	5.59E-17	1.16E-02	RP11-44N21.4:NUDT14	-
227	rs2929686	15	39085781	intergenic	T	C	0.387	7.99E-10	6.86E-01	RP11-326N17.1	-
227	rs716980	15	39374094	ncRNA intronic	C	T	0.493	6.98E-11	3.94E-01	RP11-624L4.1	-
227	rs12907993	15	39590057	ncRNA intronic	G	A	0.466	1.00E-10	5.06E-01	RP11-624L4.1	-
227	rs5812099	15	39633877	ncRNA intronic	AG	A	0.090	2.15E-171	2.63E-06	RP11-624L4.1	9
228	rs4646625	15	58256296	intronic	T	C	0.463	3.16E-08	6.10E-03	ALDH1A2	-
229	rs12438742	15	61947280	ncRNA intronic	G	C	0.429	1.36E-08	2.57E-01	RP11-507B12.1	6
230	rs351175	15	74528985	UTR5	G	T	0.281	1.35E-08	2.11E-01	CCDC33	-
231	rs11072509	15	75114374	ncRNA intronic	G	C	0.266	4.59E-08	6.90E-01	LMAN1L:RP11-414J4.2	-
232	rs4887098	15	79057950	intronic	C	G	0.429	7.08E-14	3.27E-02	ADAMTS7	-
233	rs2342118	15	85693016	intergenic	A	G	0.325	7.28E-30	1.84E-03	PDE8A	6
234	rs2584137	15	87988620	ncRNA intronic	G	A	0.371	2.60E-10	4.34E-01	RP11-648K4.2	-
235	rs6224	15	91423543	intronic	T	G	0.475	9.79E-16	6.63E-01	FURIN	1
236	rs2387280	16	4339684	intergenic	T	A	0.247	2.19E-10	2.98E-02	TFAP4	-
237	rs200541	16	24733141	intergenic	G	A	0.196	1.55E-12	2.86E-01	TNRC6A	-
237	rs72770483	16	24926314	intergenic	G	T	0.065	1.03E-08	8.15E-02	SLC5A11	-
238	rs67264578	16	30879395	intronic	A	G	0.264	4.94E-08	8.05E-01	BCL7C	-
239	rs11649294	16	50091335	ncRNA intronic	T	C	0.205	3.75E-08	9.06E-01	RP11-429P3.3	-
240	16:51185924 TA T	16	51185924	upstream	T	TA	0.203	1.11E-08	8.61E-01	SALL1	-
240	rs1948948	16	51442679	intergenic	T	C	0.438	3.49E-53	5.03E-04	RP11-437L7.1	95
240	16:51495932 CAA C	16	51495932	intergenic	C	CAA	0.362	1.21E-08	5.29E-02	RP11-437L7.1	4
241	rs12325224	16	70675363	intronic	T	C	0.441	8.68E-13	3.18E-02	IL34	-
242	rs55845372	16	86606321	intergenic	C	T	0.188	1.25E-09	4.79E-03	FOXL1	1
243	rs4843552	16	87233516	intergenic	A	G	0.422	6.18E-105	1.00E-05	C16orf95	45
243	rs4060100	16	87302354	ncRNA intronic	A	C	0.299	2.12E-08	2.25E-01	C16orf95:RP11-178L8.5	-
244	rs9939914	16	89939929	upstream	C	T	0.237	1.36E-12	7.84E-02	TCF25	-
244	rs111398992	16	89992613	intronic	T	G	0.131	1.17E-31	9.85E-04	TUBB3:TUBB3	6
245	rs2131704	17	1970898	intronic	T	C	0.425	8.01E-19	6.48E-03	SMG6	10
245	rs11078865	17	2109109	intronic	A	T	0.371	1.11E-12	1.74E-01	SMG6	3
246	rs12451961	17	7351479	intronic	G	A	0.362	6.65E-13	4.45E-01	CHRNB1	-
247	rs76653948	17	9151562	intergenic	G	C	0.177	1.03E-21	8.99E-02	STX8	-
248	rs7210118	17	13047713	intergenic	T	C	0.414	1.54E-24	6.24E-02	RP11-488L1.1	3
249	rs79626005	17	19210026	intronic	A	G	0.080	7.45E-10	3.47E-01	EPN2	-
250	rs4994353	17	28386280	intronic	A	T	0.443	9.63E-36	9.98E-02	EFCAB5	6
251	rs77259033	17	41351400	intronic	A	T	0.324	3.36E-08	6.25E-01	NBR1	-
252	rs9898671	17	42935321	intronic	A	G	0.161	1.30E-21	1.05E-01	EFTUD2	76
252	17:42986266 AAAGG A	17	42986266	intronic	A	AAAGG	0.116	2.36E-10	1.85E-01	GFAP	-
252	rs12936234	17	43177951	intronic	C	T	0.350	8.59E-26	4.26E-01	NMT1	86
252	rs113448888	17	44108482	UTR3	AGCCCTCT	A	0.224	2.09E-100	9.42E-05	KANSL1	93
252	17:44259690 T G	17	44259690	intronic	G	T	0.186	2.32E-42	3.85E-01	KANSL1	-
252	rs62074125	17	44852612	intronic	C	A	0.257	3.84E-27	5.19E-02	WNT3	-
252	rs33933653	17	44888742	intronic	T	C	0.265	2.22E-10	3.07E-01	WNT3	-
252	rs56325564	17	45766771	intergenic	A	G	0.480	6.03E-12	5.02E-01	KPNB1	-
253	rs9889674	17	47010008	ncRNA intronic	A	G	0.265	1.78E-08	5.76E-01	SNF8:AC091133.1	-
254	rs11869269	17	57800388	intronic	A	G	0.157	1.21E-09	8.66E-01	VMP1	-
255	rs36090413	17	62984671	intergenic	C	G	0.081	3.35E-10	1.56E-01	AMZ2P1	1
256	rs62086046	17	65982943	intergenic	T	C	0.204	8.58E-19	3.20E-02	BPTF	68
257	17:68282406 GA G	17	68282406	intergenic	G	GA	0.243	1.56E-12	3.10E-01	CTD-2378E21.1	-
258	rs10652863	17	69179642	ncRNA intronic	CAG	C	0.418	4.98E-08	7.49E-01	CASC17	-
259	rs770068798	17	73866798	intergenic	G	GT	0.183	1.36E-13	4.55E-02	TRIM47	16
260	rs9966170	18	35029506	intronic	G	A	0.360	1.24E-28	5.40E-01	CELF4	1
261	rs13313639	18	40318077	intergenic	A	G	0.277	2.05E-14	8.55E-01	RIT2	-
262	rs630122	18	42429610	intronic	C	G	0.315	1.97E-09	3.95E-01	SETBP1	-
263	18:74537564 TA T	18	74537564	intronic	T	TA	0.171	9.73E-10	2.54E-01	ZNF236	-
264	rs62127993	19	3298646	ncRNA intronic	A	G	0.135	2.58E-10	3.58E-01	AC010649.1	2
265	rs7256295	19	4071814	intergenic	A	G	0.223	6.17E-09	9.02E-01	ZBTB7A	3
266	rs73234	19	4394310	intronic	C	G	0.456	9.25E-09	3.11E-01	SH3GL1	-
267	rs10403210	19	13103638	intergenic	C	T	0.466	4.69E-08	4.17E-02	NFIX	1
268	rs2303696	19	18548884	UTR5	C	T	0.379	2.82E-15	1.16E-01	ISYNA1	-
269	rs2043294	19	32207820	intergenic	T	A	0.178	2.72E-30	3.92E-01	RNA5SP471	-
270	rs37866837	19	39172042	intronic	C	G	0.476	8.88E-10	6.20E-02	ACTN4	-
271	rs429358	19	45411941	exonic	C	T	0.156	1.20E-16	5.37E-02	APOE	11
272	rs1159530	20	7103709	ncRNA intronic	C	G	0.324	3.66E-09	5.44E-01	RP4-764O22.1	-
273	rs16996551	20	15773571	intronic	T	C	0.371	1.94E-17	1.99E-01	MACROD2	-
274	rs6059412	20	32280829	intergenic	T	G	0.292	3.32E-09	5.99E-01	E2F1	-
275	rs143383	20	34025983	UTR5	G	A	0.363	1.31E-24	2.93E-03	GDF5	-
276	rs3746471	20	36841914	exonic	A	G	0.467	4.17E-17	2.22E-01	KIAA1755	-
277	rs202393	20	45195738	intronic	C	T	0.160	1.77E-12	4.82E-01	SLC13A3	23
277	rs2694896	20	45237143	intronic	G	A	0.385	4.95E-08	3.64E-01	SLC13A3	13
277	rs6011998	20	45269867	intronic	T	C	0.042	9.31E-10	3.66E-01	SLC13A3	9
278	rs66806308	20	46360465	intronic	T	C	0.209	4.12E-08	7.45E-01	SULF2	-
279	rs72626592	20	55528415	intergenic	T	C	0.036	1.58E-09	3.84E-01	AL117380.2	1
280	rs6062264	20	61154871	intronic	T	C	0.279	2.12E-08	4.59E-01	C20orf166	13
281	rs3215453	22	29453442	UTR3	TA	T	0.482	3.90E-08	4.45E-01	ZNRF3	-
282	rs9608859	22	30667277	intergenic	C	T	0.437	2.31E-12	5.74E-01	OSM	27
282	rs2267161	22	30953295	exonic	T	C	0.306	2.46E-12	2.57E-02	GAL3ST1	47
283	rs5750482	22	38117943	intronic	C	T	0.373	4.18E-09	4.13E-01	NOL12:TRIOBP	-
283	rs738443	22	38458681	ncRNA intronic	A	G	0.381	3.31E-18	4.80E-01	PICK1:RP5-1039K5.13	46
284	rs130653	22	39642740	intergenic	T	A	0.236	1.05E-15	4.71E-03	PDGFB	-
285	rs61748567	22	50685332	exonic	A	G	0.017	1.39E-22	3.23E-01	HDAC10:MAPK12	5

7.3 Functional annotations of genomic loci associated with language

To further link human language AC-associated SNPs to genes, the MAGMA software was used to perform genome-wide gene-based association analysis based on the results from mvGWAS (see chapter 2.7 for more details about the gene-based association analysis). A total of 981 genes attained the Bonferroni-corrected significance threshold $p = 2.61\text{e}{-6}(0.05/19,157)$ (Fig. 7.3). Overall, among the genes identified by positional mapping, eQTL mapping and/or chromatin interaction mapping, we found that:

- Fourteen of these genes were previously associated with language FC presented in chapter 6: *AC079807.4*, *CTD-2026C7.1*, *TBC1D5*, *EPHA3*, *RNU6-488P*, *ZIC4*, *FAM172A*, *PLCE1*, *DACT1*, *RP11-624L4.1*, *FURIN*, *KANSL1*, *PIPOX*, *SEZ6*.

- Twenty of these genes have been reported to be associate with left-right asymmetry [Sha et al., 2021]: *AL356458.1*, *MAPRE3*, *CGREF1*, *ZIC4*, *FAM13A*, *NR2F1*, *NCOA7*, *BBS9*, *GALNT12*, *ITIH5*, *DACT1*, *DAAM1*, *SPIRE2*, *TUBB3*, *CRHR1*, *MAPT*, *KANSL1*, *LRRC37A2*, *ARL17A*, *MACROD2*.

- *DCDC2*, *KIAA0319*, and *ACOT13* were associate with dyslexia [Deffenbacher et al., 2004, Eicher et al., 2016, Kaplan et al., 2002], *CNTNAP2* and *FOXP2* were associated with language impairment [Fisher et al., 1998, Vernes et al., 2008].

- Nine other gene were associated with reading and language traits: *FGF18* [Field et al., 2013], *COL4A2* [Skeide et al., 2016], *SETBP1* [Perdue et al., 2019], *ROBO2*, *INSC*, *CAND1*, and *DAPK3* [St Pourcain et al., 2014], .

Please refer to chapter 1.6 for details on these associations. For the proteins encoded by 944 genes (944 out of the 981 genes code for proteins), there were 2007 known pairwise interactions in the STRING database [Szklarczyk et al., 2017], compared with 1391 interactions expected for a random set of this size from the whole proteome ($p = 1.0\text{e}{-16}$). This observation supports the validity of our mvGWAS association findings, as random associations would not lead to such functional clustering. (Fig. 7.4).

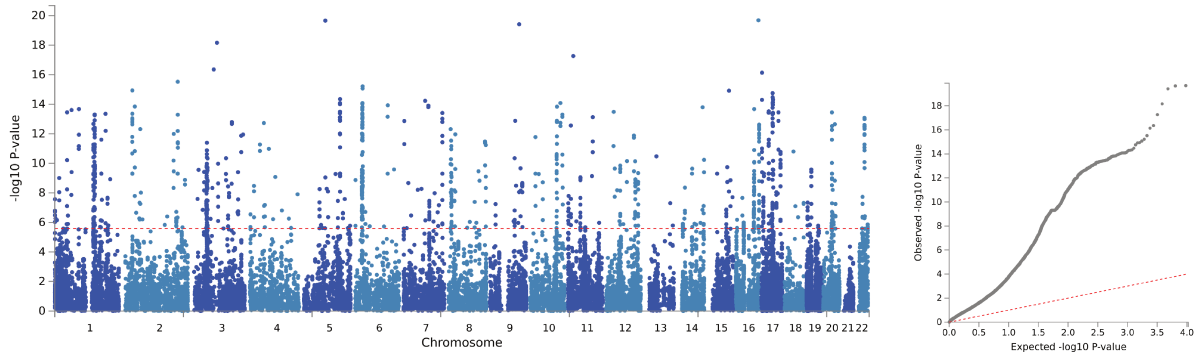

Figure 7.3 – **Genome-wide gene-based association analysis of the anatomical connectivity in 31,753 participants.** genome-wide gene-based association analysis of 313 ACs using mvGWAS results as input. Input SNPs were mapped to 19,157 protein coding genes. The red dashed line indicates the Bonferroni-corrected significance threshold for gene-based analysis $p = 2.61\text{e}{-6}(0.05/19,157)$. The Quantile-quantile plot is also shown.

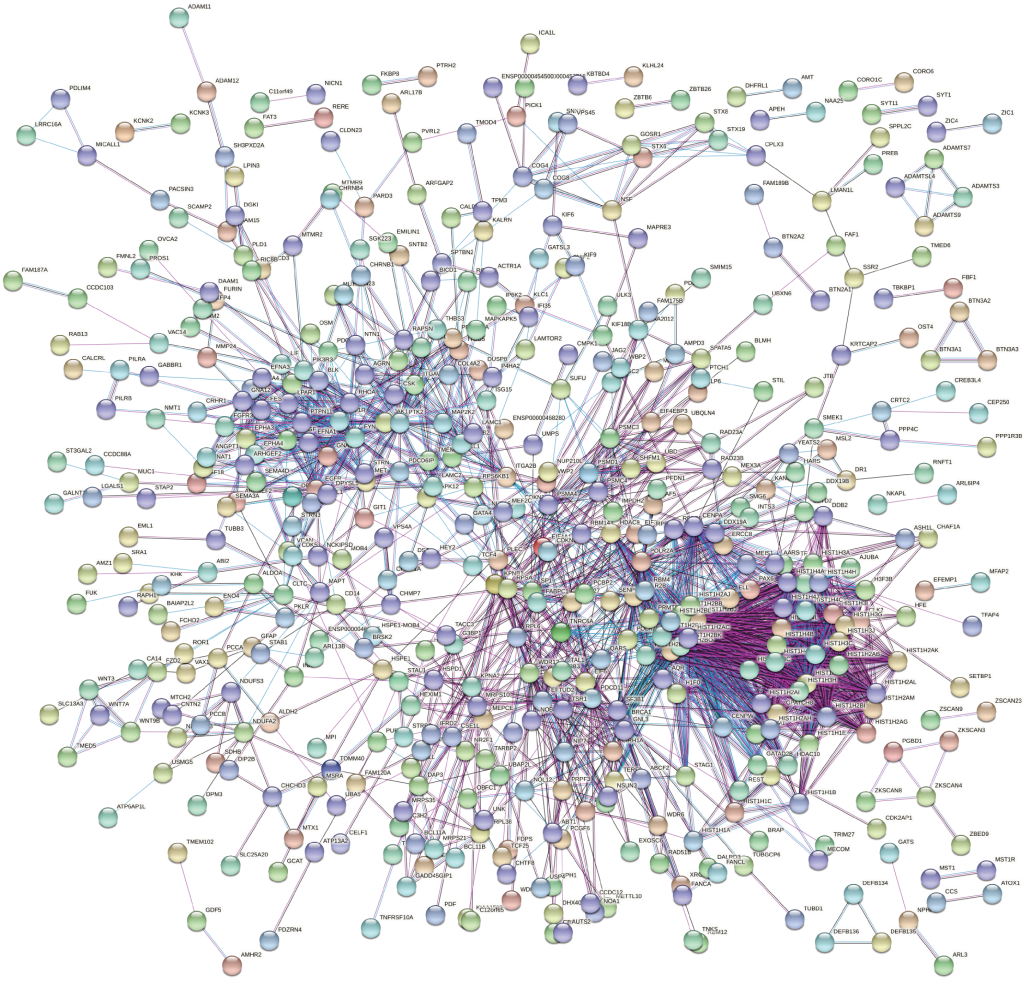

Figure 7.4 – **Human language AC-associated genes integrated into a protein–protein interaction network.** Proteins are represented by nodes. Edges between nodes represent different types of protein–protein interactions according to the STRING [Szklarczyk et al., 2017] database (chapter 2.8), including known interactions (turquoise and dark purple represent interactions identified by curated databases and biological experiments, respectively) and interactions determined by co-expression. Coloured nodes represent the queried proteins. Only at least medium-confidence (> 0.4) links were retained, and disconnected proteins are not shown.

In order to obtain a broader biological context of these gene-level results, we conducted a gene-set analysis using MAGMA [de Leeuw et al., 2015] as implemented in FUMA platform [Watanabe et al., 2017]. We identified ninety-one biological system associated with human language AC differences (Table 7.2).

Table 7.2 – **MAGMA gene-set analysis.** Gene-set attaining statistical significance following Bonferroni control for multiple test.

Gene-set Name	Number of genes in gene set	Beta	SE of Beta	P value
GO bp:go neurogenesis	1515	0.246	0.066	2.01E-16
GO bp:go neuron differentiation	1277	0.248	0.062	1.62E-14
GO bp:go cell part morphogenesis	639	0.343	0.062	5.16E-14
GO bp:go cellular component morphogenesis	1061	0.260	0.060	1.16E-13
GO bp:go cell morphogenesis involved in differentiation	688	0.323	0.060	1.25E-13
GO bp:go cell morphogenesis involved in neuron differentiation	546	0.356	0.059	7.06E-13
GO bp:go regulation of cell development	875	0.268	0.056	1.94E-12
GO bp:go regulation of cell differentiation	1723	0.197	0.056	2.28E-12
GO bp:go neuron projection guidance	264	0.481	0.056	8.21E-12
Curated gene sets:dacosta uv response via ercc3 dn	837	0.265	0.054	1.49E-11
GO bp:go regulation of anatomical structure morphogenesis	995	0.239	0.053	3.20E-11
GO bp:go regulation of nervous system development	857	0.254	0.053	4.33E-11
GO bp:go central nervous system development	918	0.250	0.053	4.49E-11
GO bp:go neuron development	1037	0.232	0.052	6.86E-11
GO bp:go cell projection organization	1433	0.196	0.052	9.73E-11
GO bp:go axon development	478	0.332	0.052	1.43E-10
GO bp:go cytoskeleton organization	1221	0.206	0.050	1.85E-10
GO bp:go regulation of neuron differentiation	613	0.287	0.050	2.34E-10
GO bp:go negative regulation of transcription by rna polymerase ii	777	0.253	0.050	4.27E-10
Curated gene sets:kegg axon guidance	124	0.624	0.050	6.39E-10
GO bp:go negative regulation of developmental process	896	0.236	0.050	6.64E-10
GO cc:go cell substrate junction	390	0.339	0.048	8.03E-10
GO bp:go taxis	610	0.291	0.051	1.27E-09
GO bp:go negative regulation of biosynthetic process	1452	0.182	0.048	1.69E-09
GO bp:go embryo development	949	0.225	0.049	1.89E-09
GO bp:go negative regulation of nervous system development	287	0.392	0.048	2.27E-09
Curated gene sets:reactome axon guidance	533	0.285	0.047	2.83E-09
GO bp:go protein phosphorylation	1830	0.163	0.048	3.06E-09
GO bp:go tube development	960	0.218	0.047	3.24E-09
GO bp:go negative regulation of multicellular organismal process	1118	0.200	0.047	3.39E-09
Curated gene sets:dacosta uv response via ercc3 common dn	453	0.309	0.047	5.04E-09
GO bp:go negative regulation of cell differentiation	675	0.253	0.047	5.07E-09
GO bp:go tube morphogenesis	781	0.235	0.046	5.79E-09
GO bp:go regulation of cell morphogenesis	448	0.304	0.046	6.82E-09
GO bp:go head development	726	0.244	0.047	7.51E-09
GO bp:go positive regulation of biosynthetic process	1858	0.157	0.046	8.25E-09
GO bp:go locomotion	1693	0.164	0.047	8.85E-09
GO cc:go anchoring junction	526	0.277	0.045	9.00E-09
GO bp:go negative regulation of rna biosynthetic process	1170	0.187	0.045	1.81E-08
GO bp:go regulation of phosphorus metabolic process	1563	0.166	0.045	1.82E-08
Curated gene sets:kegg pathways in cancer	318	0.324	0.041	3.03E-08
GO bp:go negative regulation of cell development	310	0.346	0.044	3.41E-08
GO bp:go regulation of intracellular signal transduction	1695	0.155	0.044	4.54E-08
Curated gene sets:charafe breast cancer luminal vs mesenchymal dn	442	0.290	0.044	5.68E-08
GO bp:go regulation of cell projection organization	628	0.231	0.041	7.01E-08
Curated gene sets:cui tcf21 targets 2 dn	791	0.214	0.043	7.97E-08
GO bp:go animal organ morphogenesis	1002	0.193	0.043	8.63E-08
GO bp:go positive regulation of signaling	1707	0.148	0.042	1.08E-07
GO bp:go positive regulation of developmental process	1269	0.167	0.041	1.35E-07
Curated gene sets:gobert oligodendrocyte differentiation dn	1023	0.186	0.042	1.42E-07
GO bp:go positive regulation of rna biosynthetic process	1518	0.156	0.042	1.51E-07
Curated gene sets:reactome semaphorin interactions	61	0.675	0.038	1.56E-07
GO bp:go regulation of protein modification process	1700	0.147	0.042	1.57E-07

Gene-set Name	Number of genes in gene set	Beta	SE of Beta	P value
GO bp:go cardiovascular system development	669	0.227	0.042	1.70E-07
GO bp:go positive regulation of gene expression	1837	0.142	0.042	1.70E-07
GO mf:go gtpase binding	502	0.261	0.042	2.06E-07
Curated gene sets:blalock alzheimers disease up	1569	0.146	0.040	2.68E-07
GO bp:go cell surface receptor signaling pathway involved in cell cell signaling	582	0.234	0.040	2.87E-07
GO bp:go regulation of neuron projection development	460	0.260	0.040	3.29E-07
Curated gene sets:pid fak pathway	57	0.708	0.039	3.63E-07
GO bp:go positive regulation of cellular component organization	1126	0.170	0.040	3.66E-07
Curated gene sets:martinez response to trabectedin dn	265	0.344	0.040	3.78E-07
GO bp:go cell cell signaling by wnt	486	0.249	0.039	4.05E-07
GO bp:go embryonic organ development	411	0.280	0.041	4.90E-07
GO bp:go developmental growth	604	0.223	0.039	5.10E-07
GO mf:go small gtpase binding	409	0.277	0.040	5.18E-07
GO bp:go embryo development ending in birth or egg hatching	603	0.226	0.040	6.05E-07
GO bp:go positive regulation of cell development	501	0.242	0.039	6.15E-07
GO bp:go negative regulation of neuron differentiation	210	0.374	0.039	7.23E-07
GO bp:go circulatory system development	1000	0.177	0.039	7.38E-07
GO bp:go regulation of cytoskeleton organization	490	0.242	0.038	8.39E-07
GO bp:go cell motility	1475	0.147	0.039	9.08E-07
GO bp:go pattern specification process	420	0.274	0.040	1.02E-06
GO mf:go cytoskeletal protein binding	905	0.177	0.038	1.07E-06
Curated gene sets:ikeda mir30 targets up	110	0.542	0.041	1.08E-06
GO bp:go pulmonary valve morphogenesis	16	1.179	0.034	1.09E-06
GO bp:go small gtpase mediated signal transduction	521	0.235	0.038	1.27E-06
Curated gene sets:lim mammary luminal mature dn	93	0.570	0.040	1.37E-06
GO bp:go positive regulation of intracellular signal transduction	943	0.178	0.039	1.55E-06
Curated gene sets:reactome crmps in sema3a signaling	15	1.244	0.035	1.59E-06
Curated gene sets:reactome diseases of signal transduction	376	0.267	0.037	1.61E-06
GO bp:go negative regulation of cellular component organization	638	0.210	0.038	1.63E-06
Curated gene sets:vanharanta uterine fibroid up	40	0.852	0.039	1.71E-06
Curated gene sets:graessmann apoptosis by doxorubicin dn	1638	0.137	0.038	1.71E-06
Curated gene sets:reactome developmental biology	1073	0.177	0.041	1.82E-06
Curated gene sets:nikolsky breast cancer 16q24 amplicon	53	1.174	0.062	2.00E-06
GO bp:go artery development	84	0.554	0.037	2.26E-06
GO bp:go anatomical structure formation involved in morphogenesis	1034	0.165	0.037	2.38E-06
GO bp:go forebrain development	362	0.273	0.037	2.72E-06
GO bp:go regulation of cell morphogenesis involved in differentiation	276	0.312	0.037	2.76E-06
GO mf:go rho gtpase binding	159	0.403	0.037	2.97E-06

We also conducted a gene-expression analysis using data from the BrainSpan [Miller et al., 2014] database, from either 29 age groups or 11 defined general developmental stages of brain samples. We found relatively higher mRNA expression of human language AC associated genes during early-prenatal ($p = 1.94e{-}6$), early–mid-prenatal ($p = 3.59e{-}9$), Late mid-prenatal ($p = 3.11e{-}6$), Late prenatal ($p = 1.07e{-}7$), from 9 ($p = 4.32e{-}7$) to 21 ($p = 1.73e{-}5$) post-conceptional weeks (FDR-corrected p values < 0.05) (Fig. 7.5a, 7.5b).

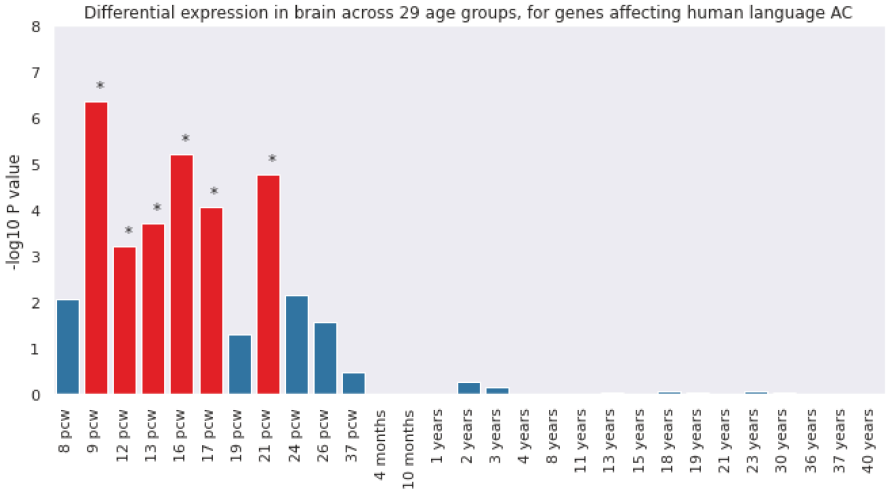

A)

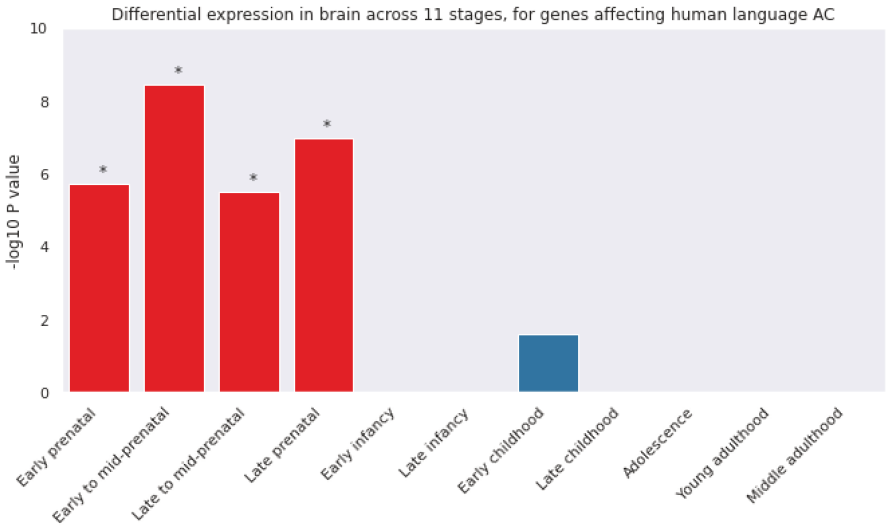

B)

Figure 7.5 – **MAGMA gene-property analysis.** A) Relation between gene-based association with human language AC and relatively higher mRNA expression in the human brain at particular ages, using BrainSpan data from 29 age groups. Asterisks indicate significant age groups meeting $p < 0.05$ with FDR correction. pcw: post-conceptional weeks. B) Relation between gene-based association with human language AC and relatively higher mRNA expression in the human brain at particular ages, using BrainSpan data from 11 developmental stages. Asterisks indicate significant groups meeting $p < 0.05$ with FDR correction.

7.4 Discussion

In this study, we extracted language endophenotypes, namely the anatomical connectivities, from diffusion-weighted acquisitions in the largest imaging-genetic cohort in general population to date. We targeted language white matter tract identified by [Rojkova et al., 2016]. After filtering on heritability significance, we performed a multivariate GWAS in order to take advantage of the correlation structure among AC endophenotypes and uncover potential pleiotropic loci. This analysis identified 285 distinct genetic loci associated with different aspects of adult humain brain anatomical connectivity.

Thereby we highlighted potential key genes related to language processing including ones that were previously associated with language impairment through candidate genes and linkage analysis.
Altogether, theses results provide an novel insight into the genetic architecture of the language in humans. Functional annotation implicated genes particularly involved in different brain organisation including neurogenesis and neuron differentiation as well as in prenatal brain development. Overall, this preliminary study, which highly call for replication, brings interesting leads regarding the molecular foundation of human brain anatomical connectivity.

* * *
* *
*

General Conclusions

Human language is a complex trait. Different types of genetic variants are expected to affect its variability. This thesis aimed to bring a modest contribution by proposing the genetic underpinning of individual differences in image derived language-related endophenotypes.

Summary

In chapter 4, we provided an in-depth study of human language heritability of the phenotypes that we chose carefully. In particular, we evaluated the heritability of both psychometric and MRI derived endophenotypes on two large-scale resources currently available; the Human Connectome Project (HCP) and the UK Biobank (UKB) using state-of-the-art approaches. These endophenotypes include resting-state functional pairwise interaction, structural connectivity and, language-brain activation. From the Human Connectome Project, we observed a hierarchy of language heritability estimates with 19.4-71.7% for language-behavioural scores, 11.4-48.7% for resting-state FC, and 14.4-34.9% for language-task activations. In terms of heritability ranking, the resting-state functional connectivity edges show low levels of heritability compared to behavioural scores and structural features in both general population and twin based studies. This observations are consistent with heritabilities obtained on general population by [Elliott et al., 2018] who reported low levels of SNP heritability for the resting-state FC edges compared to structural and diffusion MRI endophenotypes. Regarding inter-cohort variability, we observed, in line with the literature, higher values of heritability in pedigree studies compared to SNP-based heritability study. The possible origins of these discrepancies were investigated according to an experimental design that takes into account dissimilarities between both cohort with no success.

We were particularly interested by the resting-state data and its relevance for studying specific brain functions such as language. This type of data offers multiple advantages as it is paradigm free and as such it is easier to implement in very large cohorts like the UK Biobank. It has certain interests over task-based design, specially when one knows that certain populations have difficulties to engage in specific tasks. Although resting state fMRI data are reported as heritable, little is known about their relation to the language-related cognitive process.

In chapter 5, we address this question regarding the shared genetics between these ones and direct measures of language as cognitive process. To do so, we estimated both phenotypic and genetic correlations and between cognitive abilities, neural activations and task-free data in language. To this end, we took advantage of the Human Connectome Project cohort which comprises language-related scores, language task-based fMRI data as well as resting-state fMRI data. The results show a shared aetiology between resting-state functional connectivity and neural activations. This work advocates for the existence of a link between resting-state and task-based data both phenotypically and genetically regarding human language brain organisation.

In chapter 6, we contributed to enlighten the genetic architecture of language functional connectivity by exhibiting potential key genes related to language processing. We extracted language endophenotypes from rsfMRI acquisitions in the largest imaging-genetic cohort on general population to date (UK Biobank). To make these endophenotypes as closer as possible to language function in the brain, we adopted an ROI-based approach for FC estimation with language ROIs derived from an comprehensive meta-analysis of tbfMRI studies on language. This approach makes the endophenotypes comparable across individuals and thus suitable for an association study. After filtering on heritability significance, we performed a multivariate GWAS technique in order to take advantage of the correlation structure among rsfMRI FC and uncover potential pleiotropic loci. Thereby, we highlighted potential key genes related to language processing including:

- *EPHA3* gene in the 3p11.1 locus with a role in the *fronto-temporal semantic* network,
- *THBS1* gene, modulated by the 15q14 locus, associated with the functional connectivity part of the *perceptual motor* interaction required for language, and
- *PLCE1* gene in the 10q23.33 locus with a potential role in the *bilateral fronto-temporal auditory-motor* network.

These genes could be prioritised to study language in suitable genetic model. A growing number of works claims that language studies should consider task-free fMRI data in general population in order to focus on the neurobiological organisation of language and how it supports natural language, i.e. as it is used in everyday life [Hasson et al., 2018]. On a clinical side, such research settings are highly desirable as there is a need to map language areas in patients unable to perform language tasks [Branco et al., 2016, Klingbeil et al., 2019, Park et al., 2020, Ramage et al., 2020]. By validating our findings in rsfMRI FC endophenotypes with dMRI-derived endophenotypes, we tried to provide both a functional and structural connectome point of view of the language organisation in the brain. Finally, recent imaging-genetic approaches such as multivariate GWAS, allowed us to increase in statistical power and circumvent the small effect sizes of these original endophenotypes. We believe that such approaches are promising and will broadly disseminate in the imaging-genetic field and beyond. With the presented approach, we tried to contribute to these innovative trends and to pave the way to other alternative task-free approaches to study natural language and its genetic underpinnings.

In chapter 7, we adopted a similar experimental design than the one presented in the chapter 6 to study the genetic architecture of anatomical connectivity. We extracted language endophenotypes from diffusion-weighed acquisitions using UK Biobank cohort. We adopted a ROI-based approach for AC estimation with well-known language white matter tracts. After filtering on heritability significance, we performed a multivariate GWAS technique in order to take advantage of the correlation structure among structural connectivity and uncover potential pleiotropic loci. Thereby, we highlighted potential key genes related to language processing. These genes could be prioritised to study language in suitable genetic model. The findings suggested new candidates genes which connect with biological pathways that are already suspected to be important for human brain-language. Overall, theses results provide a novel insight into the genetic architecture of the language in humans.

Discussion, limitations

An integrative approach. We have followed an integrative approach in our study of language genetic architecture. First, by validating our findings in rsfMRI FC endophenotypes with dMRI-derived endophenotypes, we tried to provide both a functional and structural connectome point of view of the language organisation in the brain. Second, we used recent imaging-genetic association approaches such as multivariate GWAS, that allowed us to increase in statistical power and circumvent the small effect sizes of these original endophenotypes. We believe that such approaches are promising and will broadly disseminate in the imaging-genetic field and beyond. With the presented approach, we tried to contribute to these innovative trends and to pave the way to other alternative task-free approaches to study natural language and its genetic underpinnings.

A study in general population. We conducted our study on a general population cohort by selecting state-of-the-art language (endo)phenotypes. We believe it provides an interesting alternative framework to studies based on language impairment. General population cohorts provide a wealth of measurements that make possible to develop (endo)phenotypes of interest, including for complex cognitive processes. This approach offers a promising alternative to case-control paradigm.

Conclusion

Language is a central component of human life. Understanding how we are able to acquire and use this highly complex trait has required the development of numerous language descriptions at multiple levels. On the one hand, we leveraged well characterised language processing scores and intermediate phenotypes. On the other hand, we applied association methods to identify genes that relate to the behavioural differences, and understand how they impact the development and function of the brain by looking at the cellular function of the proteins they encode and the biological pathways in which they are involved. In order to build a comprehensive account

of the human language, it will be necessary to integrate the results from the different strategies undertaken and levels of description.

In this thesis, we approached the question of the genetic basis of human language using the state-of-art genomic strategies: by highlighting the brain inter-individual variability and evaluate the role of common SNPs regarding the whole genome with no *a priori* on potential candidate genes. We related these investigations to current knowledge in language-related cognitive performance and to molecular mechanisms known to occur in brain and development. The findings from this thesis provide new entry-points for future work bridging the gap between our genetic make-up and human language processing.

* * *
* *
*

Appendices

Appendix A

A.1 Population structure of Human connectome project data

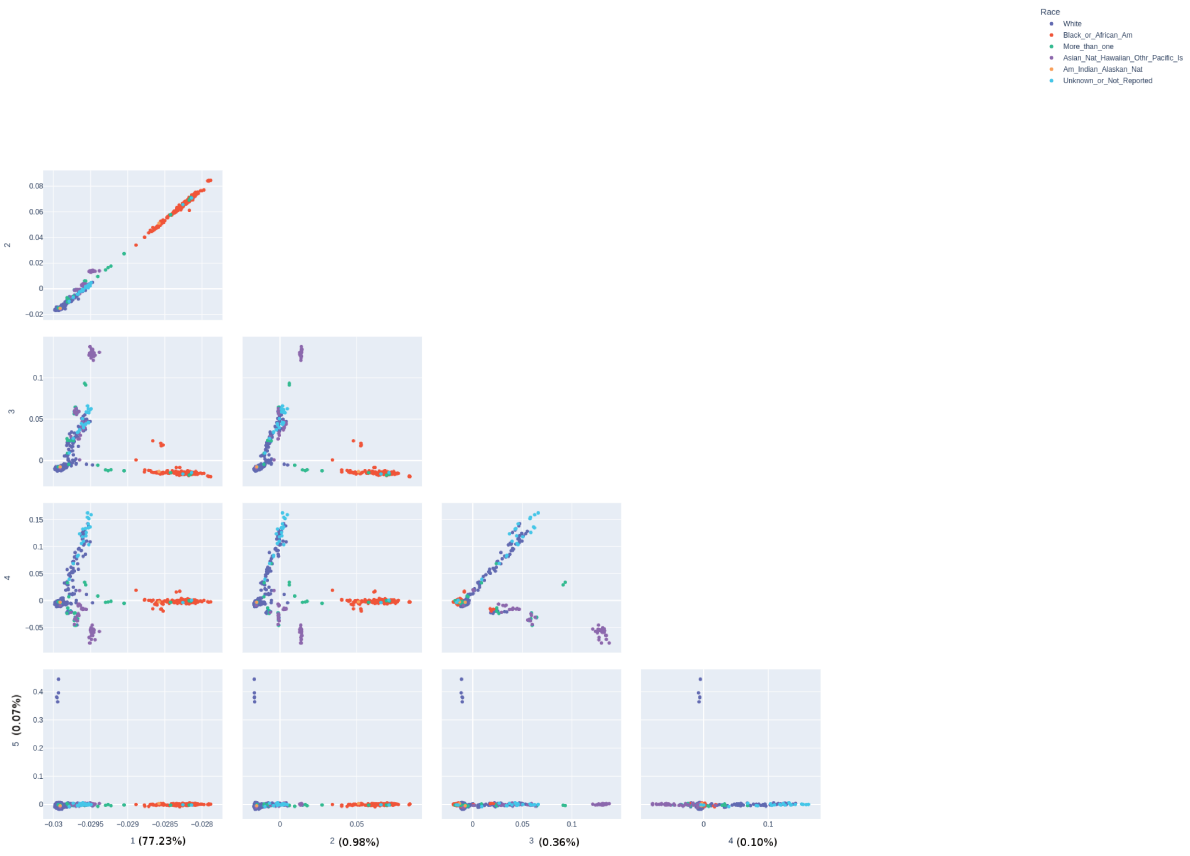

Figure A.1 – **Overview of the first five principal components of the principal component analysis of the genotype data.** We can observe that the fifth principal component separate individual from the white ethnicity.

Appendix B

B.1 Pedigree-based heritability of behavioural and neuroimaging (endo)phenotypes: a twin study

Table B.1 – **Heritabilities of brain functional connectivities extracted using SmSSPAs ROIs.** Bold phenotypes represents FCs with significant heritability after false discovery rate correction at $p < 0.05$.

Endophenotype	heritability	P value	SE	FDR P value
F3tv↔F3orb	48.8%	1.61E-13	0.060	4.82E-11
Pole↔AG	42.9%	1.19E-10	0.066	1.79E-08
Prec↔F3td	43.2%	5.69E-10	0.066	5.69E-08
T2ml↔STSp	38.7%	2.79E-09	0.064	1.96E-07
AG↔F3orb	38.9%	3.93E-09	0.066	1.96E-07
STSp↔F2antR	37.3%	3.48E-09	0.063	1.96E-07
F3opd↔SMG	37.6%	4.68E-09	0.064	2.00E-07
Fusa↔AG	38.8%	5.36E-09	0.068	2.01E-07
T1a↔STSp	34.0%	8.89E-09	0.059	2.96E-07
T3p↔F2antR	36.2%	1.27E-08	0.063	3.82E-07
PT↔T1a	35.0%	1.79E-08	0.061	4.89E-07
AG↔T1a	34.9%	2.00E-08	0.063	5.00E-07
Pole↔F3opd	42.8%	3.29E-08	0.077	7.58E-07
Pole↔T1a	38.9%	4.57E-08	0.072	9.79E-07
Prec↔F3opd	33.4%	1.00E-07	0.063	1.87E-06
T2ml↔F3orb	36.6%	1.00E-07	0.069	1.87E-06
T2p↔RolS	33.1%	2.00E-07	0.064	3.53E-06
PT↔T1a.HeschlR	33.2%	3.00E-07	0.066	5.00E-06
F3tv↔F3td	32.3%	4.00E-07	0.067	5.71E-06
PT↔T1	33.4%	4.00E-07	0.067	5.71E-06
AG↔F2antR	33.2%	4.00E-07	0.068	5.71E-06
RolS↔T1R	35.0%	5.00E-07	0.069	6.52E-06
Pole↔F3tv	33.4%	5.00E-07	0.067	6.52E-06
Fusa↔T3p	34.4%	6.00E-07	0.070	7.50E-06
AG↔F3tv	34.3%	7.00E-07	0.073	8.08E-06
T1a↔T1a.HeschlR	34.4%	7.00E-07	0.072	8.08E-06
Pole↔T1	32.7%	8.00E-07	0.068	8.89E-06
F3td↔T3p	32.4%	1.00E-06	0.068	1.03E-05
T1a↔F3td	33.0%	1.00E-06	0.070	1.03E-05
F3tv↔F2antR	29.5%	1.20E-06	0.063	1.20E-05
PT↔F3tv	29.0%	1.80E-06	0.063	1.74E-05
F3opd↔T2pR	28.2%	2.50E-06	0.062	2.34E-05
Pole↔T2ml	30.2%	2.60E-06	0.067	2.36E-05
F3opd↔T3p	30.0%	2.70E-06	0.065	2.38E-05
T1↔F3tv	30.9%	2.90E-06	0.068	2.49E-05
T2ml↔SMG	28.6%	3.90E-06	0.065	3.24E-05
F3tv↔SMG	30.3%	4.00E-06	0.069	3.24E-05
F3opd↔AG	29.7%	4.20E-06	0.068	3.32E-05
Pole↔F3orb	31.7%	4.60E-06	0.071	3.45E-05
PrF3op↔SMG	28.9%	4.60E-06	0.065	3.45E-05
Prec↔AG	29.6%	6.10E-06	0.068	4.46E-05
F3td↔F3orb	29.5%	8.80E-06	0.071	6.29E-05

Endophenotype	heritability	P value	SE	FDR P value
F3tv↔STSp	29.0%	1.08E-05	0.069	7.53E-05
F3opdR↔T2pR	27.7%	1.11E-05	0.066	7.57E-05
T1↔T1a.HeschIR	29.4%	1.43E-05	0.071	9.53E-05
PrF3op↔F3tv	29.7%	1.57E-05	0.074	9.65E-05
T1a↔T2pR	28.5%	1.64E-05	0.070	9.65E-05
Prec↔F2antR	25.0%	1.61E-05	0.062	9.65E-05
Fusa↔T2p	28.8%	1.61E-05	0.070	9.65E-05
T2ml↔T1	29.1%	1.58E-05	0.071	9.65E-05
F2p↔STSp	26.8%	1.57E-05	0.065	9.65E-05
RolS↔PrecR	27.4%	1.69E-05	0.066	9.75E-05
T1↔T2p	27.9%	1.78E-05	0.069	1.01E-04
T2p↔F2antR	27.4%	1.86E-05	0.070	1.03E-04
Pole↔F3td	27.3%	1.96E-05	0.068	1.07E-04
PrF3op↔T3p	27.3%	2.49E-05	0.069	1.33E-04
Pole↔T1R	28.1%	2.78E-05	0.070	1.46E-04
T2ml↔T1a.HeschIR	26.1%	2.88E-05	0.066	1.49E-04
F2p↔PrF3op	26.9%	3.29E-05	0.069	1.64E-04
T1↔T3p	26.1%	3.27E-05	0.066	1.64E-04
Fusa↔T1a	27.4%	3.72E-05	0.070	1.80E-04
F3opd↔F3orb	28.5%	3.70E-05	0.072	1.80E-04
F3td↔F2antR	26.1%	3.86E-05	0.067	1.84E-04
SMG↔F3opdR	25.0%	3.97E-05	0.065	1.84E-04
AG↔STSp	23.6%	3.99E-05	0.061	1.84E-04
STSp↔F3td	27.5%	4.19E-05	0.071	1.88E-04
F2p↔F3tv	26.8%	4.13E-05	0.070	1.88E-04
T2p↔T3p	24.9%	4.67E-05	0.065	2.06E-04
Pole↔Fusa	27.8%	4.76E-05	0.074	2.06E-04
F3opd↔F2antR	25.6%	4.81E-05	0.067	2.06E-04
F3opd↔T2ml	25.9%	4.97E-05	0.068	2.10E-04
STSp↔F3orb	28.7%	5.42E-05	0.077	2.26E-04
T3p↔F3orb	23.9%	5.75E-05	0.064	2.36E-04
STSp↔SMG	25.5%	6.14E-05	0.069	2.49E-04
F2p↔F3orb	26.0%	7.07E-05	0.069	2.83E-04
SMG↔F3orb	26.9%	7.45E-05	0.073	2.94E-04
T1a↔T3p	23.3%	8.05E-05	0.062	3.14E-04
T1↔RolS	24.6%	8.51E-05	0.067	3.27E-04
PrF3op↔T1a	27.7%	9.91E-05	0.075	3.76E-04
F3opd↔F3tv	25.2%	1.03E-04	0.071	3.86E-04
F2antR↔T1a.HeschIR	24.4%	1.06E-04	0.067	3.92E-04
T1a↔T2p	23.7%	1.20E-04	0.066	4.39E-04

Endophenotype	heritability	P value	SE	FDR P value
T1↔T1a	23.7%	1.23E-04	0.066	4.40E-04
T2ml↔F3tv	26.4%	1.24E-04	0.073	4.40E-04
Pole↔STSp	25.4%	1.25E-04	0.070	4.40E-04
T1a↔RolS	25.3%	1.29E-04	0.070	4.44E-04
SMG↔F3td	23.6%	1.28E-04	0.067	4.44E-04
Prec↔SMG	24.1%	2.08E-04	0.070	7.09E-04
F2p↔SMG	25.5%	2.27E-04	0.073	7.65E-04
F3opd↔F3td	24.4%	2.39E-04	0.070	7.97E-04
T1a↔T1R	24.5%	2.68E-04	0.072	8.85E-04
T3p↔T2pR	21.9%	2.83E-04	0.065	9.14E-04
T3p↔RolS	23.6%	2.80E-04	0.070	9.14E-04
AG↔SMG	22.0%	2.93E-04	0.067	9.34E-04
PrF3op↔T1R	24.3%	3.16E-04	0.072	9.99E-04
STSp↔T2pR	24.6%	3.84E-04	0.076	1.20E-03
T1↔PrF3op	21.9%	3.91E-04	0.067	1.21E-03
F3opd↔T1	21.4%	4.07E-04	0.065	1.24E-03
T2pR↔T1R	23.1%	4.40E-04	0.071	1.33E-03
Prec↔F2p	21.2%	4.67E-04	0.066	1.40E-03
F3tv↔T1a.HeschlR	23.3%	5.03E-04	0.074	1.49E-03
T2ml↔AG	22.0%	5.08E-04	0.068	1.49E-03
F3opd↔STSp	24.1%	5.40E-04	0.075	1.57E-03
T1↔Fusa	23.0%	5.53E-04	0.072	1.58E-03
T2ml↔T1a	21.6%	5.53E-04	0.067	1.58E-03
T1↔T1R	23.2%	6.11E-04	0.073	1.73E-03
T2ml↔PrF3op	23.2%	6.30E-04	0.074	1.77E-03
Prec↔T1	20.7%	6.70E-04	0.066	1.86E-03
F3tv↔RolS	21.8%	6.89E-04	0.070	1.90E-03
T2p↔F3td	21.1%	7.00E-04	0.068	1.91E-03
T1↔T2pR	22.3%	7.08E-04	0.071	1.91E-03
PrF3op↔RolS	20.0%	7.18E-04	0.064	1.92E-03
F2p↔T2ml	24.1%	7.35E-04	0.078	1.94E-03
Prec↔T2p	21.5%	7.36E-04	0.069	1.94E-03
AG↔T3p	22.4%	7.73E-04	0.073	2.02E-03
PT↔T1R	21.8%	7.91E-04	0.070	2.05E-03
SMG↔T2p	20.5%	8.25E-04	0.068	2.10E-03
AG↔F3td	22.5%	8.38E-04	0.074	2.10E-03
T2ml↔RolS	21.2%	8.42E-04	0.069	2.10E-03
T1↔STSp	21.8%	8.39E-04	0.070	2.10E-03
SMG↔T3p	19.6%	8.82E-04	0.064	2.19E-03
F3tv↔T1R	20.1%	9.19E-04	0.066	2.26E-03

Endophenotype	heritability	P value	SE	FDR P value
T2ml↔F3td	21.4%	9.77E-04	0.071	2.36E-03
Prec↔RolS	22.3%	9.75E-04	0.073	2.36E-03
SMG↔F2antR	21.7%	1.01E-03	0.073	2.42E-03
F3orb↔F2antR	21.7%	1.02E-03	0.073	2.44E-03
PT↔F2antR	18.9%	1.05E-03	0.064	2.48E-03
T2ml↔T2pR	22.2%	1.11E-03	0.075	2.60E-03
F3orb↔F3opdR	18.4%	1.12E-03	0.061	2.61E-03
SMG↔T1a.HeschlR	19.7%	1.16E-03	0.067	2.64E-03
T1a↔SMG	19.5%	1.15E-03	0.066	2.64E-03
AG↔RolS	20.5%	1.16E-03	0.070	2.64E-03
PrF3op↔T2pR	21.9%	1.26E-03	0.075	2.84E-03
F3opd↔T2p	21.3%	1.27E-03	0.073	2.84E-03
T2p↔T1a.HeschlR	19.5%	1.29E-03	0.067	2.87E-03
Prec↔T1R	20.1%	1.33E-03	0.068	2.94E-03
F3opd↔F2p	20.2%	1.35E-03	0.069	2.95E-03
F2p↔Fusa	19.1%	1.40E-03	0.066	3.03E-03
F2p↔T1a	22.8%	1.64E-03	0.079	3.55E-03
T2ml↔PrecR	21.1%	1.71E-03	0.074	3.66E-03
Fusa↔F3tv	20.9%	1.98E-03	0.076	4.22E-03
T1a↔F2antR	20.0%	2.01E-03	0.072	4.24E-03
Pole↔PrF3op	19.1%	2.03E-03	0.069	4.25E-03
F3opd↔T1R	18.5%	2.07E-03	0.067	4.32E-03
T1↔AG	19.0%	2.12E-03	0.068	4.38E-03
SMG↔RolS	18.3%	2.17E-03	0.067	4.42E-03
Fusa↔SMG	19.3%	2.16E-03	0.069	4.42E-03
Pole↔T2pR	20.6%	2.27E-03	0.074	4.60E-03
AG↔T2p	18.9%	2.42E-03	0.069	4.88E-03
PrF3op↔F3orb	19.9%	2.56E-03	0.074	5.12E-03
F2p↔T1	18.6%	2.62E-03	0.069	5.21E-03
T1↔SMG	17.0%	2.68E-03	0.063	5.29E-03
Pole↔F2p	17.8%	3.01E-03	0.067	5.91E-03
Fusa↔F3td	18.8%	3.13E-03	0.070	6.05E-03
F3opd↔RolS	19.7%	3.11E-03	0.074	6.05E-03
T2ml↔Fusa	17.7%	3.17E-03	0.066	6.10E-03
T1↔F3orb	17.8%	3.31E-03	0.067	6.32E-03
Pole↔T2p	18.3%	3.40E-03	0.069	6.45E-03
Fusa↔F3orb	18.5%	3.42E-03	0.072	6.45E-03
Pole↔T3p	19.3%	3.61E-03	0.074	6.77E-03
F3orb↔T1R	16.9%	3.79E-03	0.065	7.06E-03
Pole↔PT	16.7%	4.13E-03	0.065	7.64E-03
Prec↔STSp	19.6%	4.40E-03	0.076	8.10E-03
F2antR↔T1R	16.2%	4.61E-03	0.065	8.38E-03

Endophenotype	heritability	P value	SE	FDR P value
PT↔RolS	17.1%	4.58E-03	0.068	8.38E-03
T2p↔T1R	19.5%	4.74E-03	0.077	8.57E-03
T2ml↔T3p	16.8%	4.78E-03	0.067	8.59E-03
T2ml↔F2antR	16.4%	4.90E-03	0.066	8.75E-03
RolS↔T1a.HeschIR	17.5%	5.02E-03	0.069	8.90E-03
Prec↔T2ml	16.9%	5.06E-03	0.068	8.92E-03
STSp↔T3p	15.5%	5.25E-03	0.063	9.20E-03
Prec↔T1a	16.7%	5.36E-03	0.068	9.34E-03
F3opd↔PrF3op	18.2%	5.40E-03	0.074	9.37E-03
F3tv↔PrecR	16.9%	5.65E-03	0.068	9.74E-03
F3tv↔F3opdR	17.7%	6.12E-03	0.072	1.04E-02
F2p↔F2antR	16.2%	6.11E-03	0.067	1.04E-02
Prec↔PT	15.4%	6.42E-03	0.064	1.09E-02
RolS↔T2pR	17.1%	6.71E-03	0.071	1.13E-02
T2ml↔F3opdR	15.8%	6.84E-03	0.067	1.15E-02
F3opd↔T1a	19.5%	7.00E-03	0.082	1.17E-02
Fusa↔STSp	17.0%	7.22E-03	0.071	1.19E-02
T1↔F3opdR	16.0%	7.19E-03	0.067	1.19E-02
T1a↔F3opdR	15.6%	7.85E-03	0.066	1.28E-02
STSp↔T1a.HeschIR	16.5%	7.82E-03	0.070	1.28E-02
F3opdR↔T1R	15.3%	8.58E-03	0.065	1.39E-02
AG↔T1R	15.5%	9.44E-03	0.069	1.52E-02
T1a.HeschIR↔PrecR	15.1%	9.74E-03	0.067	1.56E-02
T1↔F3td	15.2%	9.85E-03	0.066	1.57E-02
Prec↔T2pR	16.2%	1.02E-02	0.071	1.63E-02
Prec↔Fusa	16.0%	1.03E-02	0.071	1.63E-02
F3td↔PrecR	13.8%	1.29E-02	0.064	2.03E-02
STSp↔PrecR	15.3%	1.32E-02	0.072	2.06E-02
AG↔T1a.HeschIR	15.5%	1.32E-02	0.072	2.06E-02
F2p↔T1R	15.1%	1.40E-02	0.071	2.17E-02
F3opdR↔F2antR	14.7%	1.49E-02	0.069	2.27E-02
Fusa↔PrF3op	13.4%	1.48E-02	0.063	2.27E-02
PrF3op↔STSp	14.5%	1.49E-02	0.069	2.27E-02
Pole↔F2antR	15.5%	1.54E-02	0.074	2.33E-02
F3orb↔PrecR	14.5%	1.56E-02	0.069	2.36E-02
SMG↔T2pR	14.0%	1.65E-02	0.068	2.48E-02
PrF3op↔F2antR	15.0%	1.67E-02	0.072	2.49E-02
PrF3op↔F3opdR	15.9%	1.72E-02	0.077	2.56E-02
F3td↔T2pR	14.3%	1.73E-02	0.070	2.56E-02
PT↔Fusa	13.4%	1.84E-02	0.066	2.71E-02

Endophenotype	heritability	P value	SE	FDR P value
AG↔T2pR	14.7%	1.94E-02	0.073	2.83E-02
Pole↔T1a.HeschlR	14.4%	2.12E-02	0.073	3.08E-02
Fusa↔F3opdR	13.0%	2.30E-02	0.067	3.33E-02
SMG↔T1R	12.9%	2.60E-02	0.068	3.75E-02
PT↔STSp	12.5%	2.66E-02	0.066	3.82E-02
Prec↔T3p	12.8%	2.69E-02	0.069	3.85E-02
RolS↔F2antR	13.7%	2.92E-02	0.074	4.15E-02
AG↔F3opdR	11.6%	2.98E-02	0.063	4.21E-02
F3tv↔T2pR	12.9%	3.00E-02	0.071	4.23E-02
F2p↔F3td	11.5%	3.08E-02	0.063	4.32E-02
Prec↔F3orb	11.7%	3.10E-02	0.064	4.33E-02
T2ml↔T2p	11.6%	3.21E-02	0.065	4.46E-02
STSp↔RolS	11.8%	3.25E-02	0.066	4.49E-02
PrF3op↔F3td	11.9%	3.95E-02	0.070	5.44E-02
PT↔AG	10.7%	4.27E-02	0.066	5.85E-02
F2p↔AG	11.6%	4.39E-02	0.070	5.99E-02
PT↔T2p	11.7%	4.47E-02	0.071	6.04E-02
F3tv↔T2p	11.9%	4.45E-02	0.072	6.04E-02
T1a.HeschlR↔T1R	12.6%	4.61E-02	0.077	6.18E-02
T1↔PrecR	11.9%	4.61E-02	0.072	6.18E-02
Fusa↔T1a.HeschlR	10.6%	4.66E-02	0.065	6.22E-02
F2p↔RolS	11.3%	4.98E-02	0.070	6.62E-02
STSp↔T2p	11.3%	5.01E-02	0.071	6.62E-02
T3p↔T1R	10.7%	5.07E-02	0.066	6.67E-02
Pole↔SMG	11.4%	5.14E-02	0.072	6.74E-02
T2pR↔T1a.HeschlR	9.4%	5.25E-02	0.059	6.85E-02
T2ml↔T1R	10.2%	6.83E-02	0.070	8.87E-02
F3tv↔T1a	10.4%	7.18E-02	0.073	9.29E-02
Prec↔T1a.HeschlR	9.5%	7.62E-02	0.068	9.81E-02
Prec↔PrF3op	9.8%	7.72E-02	0.071	9.90E-02
T1↔F2antR	9.2%	8.23E-02	0.068	1.05E-01
F2p↔T2pR	9.3%	8.61E-02	0.070	1.09E-01
PrF3op↔AG	10.1%	8.67E-02	0.076	1.10E-01
Fusa↔T2pR	9.0%	8.77E-02	0.067	1.11E-01
Prec↔Pole	8.9%	9.24E-02	0.069	1.16E-01
Fusa↔RolS	10.1%	9.31E-02	0.079	1.16E-01
F3orb↔T1a.HeschlR	8.4%	9.77E-02	0.067	1.22E-01
STSp↔T1R	9.3%	1.02E-01	0.074	1.25E-01
T2p↔F3orb	7.6%	1.01E-01	0.062	1.25E-01

Endophenotype	heritability	P value	SE	FDR P value
T3p↔F3opdR	7.7%	1.02E-01	0.062	1.26E-01
F2antR↔T2pR	7.7%	1.08E-01	0.063	1.32E-01
F2p↔T1a.HeschlR	7.9%	1.17E-01	0.068	1.43E-01
T1a↔F3orb	7.4%	1.20E-01	0.065	1.46E-01
F3tv↔T3p	8.4%	1.22E-01	0.074	1.47E-01
AG↔PrecR	7.7%	1.26E-01	0.068	1.51E-01
PT↔F3td	7.1%	1.35E-01	0.066	1.62E-01
PT↔PrF3op	8.2%	1.37E-01	0.076	1.63E-01
PrF3op↔T2p	7.4%	1.37E-01	0.069	1.63E-01
Pole↔F3opdR	7.5%	1.36E-01	0.070	1.63E-01
Fusa↔T1R	7.0%	1.50E-01	0.069	1.77E-01
F3orb↔RolS	7.4%	1.55E-01	0.074	1.82E-01
STSp↔F3opdR	6.2%	1.57E-01	0.062	1.83E-01
F3opd↔T1a.HeschlR	5.8%	1.76E-01	0.064	2.06E-01
F3td↔RolS	5.7%	1.81E-01	0.064	2.11E-01
PT↔T3p	4.7%	2.29E-01	0.065	2.65E-01
Prec↔F3tv	5.0%	2.30E-01	0.068	2.66E-01
PT↔F3opdR	4.6%	2.36E-01	0.065	2.71E-01
RolS↔F3opdR	4.9%	2.42E-01	0.071	2.77E-01
F3td↔T1R	4.5%	2.49E-01	0.067	2.84E-01
Prec↔PrecR	4.6%	2.52E-01	0.069	2.87E-01
F3orb↔T2pR	4.4%	2.62E-01	0.070	2.96E-01
Fusa↔F2antR	3.9%	2.73E-01	0.065	3.08E-01
Prec↔F3opdR	3.6%	2.95E-01	0.068	3.30E-01
F3opd↔Fusa	3.7%	2.95E-01	0.069	3.30E-01
T2p↔F3opdR	3.3%	2.96E-01	0.063	3.30E-01
PT↔T2ml	3.5%	3.01E-01	0.068	3.34E-01
T1a↔PrecR	3.2%	3.09E-01	0.065	3.42E-01
T2p↔T2pR	3.0%	3.26E-01	0.068	3.60E-01
T3p↔T1a.HeschlR	2.8%	3.30E-01	0.065	3.63E-01
F3opdR↔T1a.HeschlR	2.9%	3.35E-01	0.068	3.67E-01
F3opd↔F3opdR	2.9%	3.38E-01	0.071	3.68E-01
PT↔F3orb	2.1%	3.79E-01	0.069	4.12E-01
PT↔F3opd	1.9%	3.86E-01	0.066	4.18E-01
PT↔SMG	1.7%	3.89E-01	0.059	4.20E-01
T1R↔PrecR	1.6%	4.03E-01	0.064	4.33E-01
F2p↔F3opdR	1.0%	4.34E-01	0.063	4.65E-01
PrF3op↔PrecR	1.0%	4.37E-01	0.064	4.66E-01
F2antR↔PrecR	0.0%	5.00E-01	0.000	5.00E-01
Fusa↔PrecR	0.0%	5.00E-01	0.000	5.00E-01

Endophenotype	heritability	P value	SE	FDR P value
F2p↔PrecR	0.0%	5.00E-01	0.000	5.00E-01
PrF3op↔T1a.HeschlR	0.0%	5.00E-01	0.000	5.00E-01
PT↔F2p	0.0%	5.00E-01	0.000	5.00E-01
Pole↔RolS	0.0%	5.00E-01	0.000	5.00E-01
F3td↔T1a.HeschlR	0.0%	5.00E-01	0.000	5.00E-01
F3opdR↔PrecR	0.0%	5.00E-01	0.000	5.00E-01
Pole↔PrecR	0.0%	5.00E-01	0.000	5.00E-01
F3opd↔PrecR	0.0%	5.00E-01	0.000	5.00E-01
SMG↔PrecR	0.0%	5.00E-01	0.000	5.00E-01
F3td↔F3opdR	0.0%	5.00E-01	0.000	5.00E-01
T2p↔PrecR	0.0%	5.00E-01	0.000	5.00E-01
T2pR↔PrecR	0.0%	5.00E-01	0.000	5.00E-01
F2p↔T2p	0.0%	5.00E-01	0.000	5.00E-01
T3p↔PrecR	0.0%	5.00E-01	0.000	5.00E-01
PT↔T2pR	0.0%	5.00E-01	0.000	5.00E-01
PT↔PrecR	0.0%	5.00E-01	0.000	5.00E-01
F2p↔T3p	0.0%	5.00E-01	0.000	5.00E-01

B.2 SNP-based heritability of neuroimaging endophenotypes: a general population study

Table B.2 – **Heritabilities of brain functional connectivities extracted using OcSS ROIs.** Bold phenotypes represents FCs with significant heritability after false discovery rate correction at $p<0.05$.

Endophenotype	heritability	P value	SE	FDR P value
IFGtri↔IFGorb	12.0%	1.01E-12	0.018	1.52E-11
aSTS↔TPJ	11.4%	3.07E-11	0.018	2.30E-10
TP↔aSTS	11.0%	1.04E-10	0.018	5.20E-10
IFGorb↔pSTS	8.9%	1.65E-07	0.018	6.18E-07
TP↔TPJ	8.3%	1.02E-06	0.018	2.19E-06
IFGorb↔TPJ	8.3%	8.84E-07	0.018	2.19E-06
aSTS↔pSTS	8.3%	1.00E-06	0.018	2.19E-06
IFGorb↔TP	8.0%	2.41E-06	0.018	4.51E-06
pSTS↔TPJ	7.9%	2.83E-06	0.018	4.72E-06
IFGorb↔aSTS	7.2%	8.42E-06	0.017	1.26E-05
IFGtri↔aSTS	7.1%	1.69E-05	0.017	2.31E-05
IFGtri↔TP	6.3%	1.16E-04	0.017	1.45E-04
TP↔pSTS	5.3%	1.06E-03	0.018	1.22E-03
IFGtri↔pSTS	4.9%	2.05E-03	0.017	2.20E-03
IFGtri↔TPJ	2.0%	1.22E-01	0.017	1.22E-01

Table B.3 – **Heritabilities of brain functional connectivities extracted using SmPSS ROIs.** Bold phenotypes represents FCs with significant heritability after false discovery rate correction at p<0.05.

Endophenotype	heritability	P value	SE	FDR P value
F3opd↔SMG	14.3%	3.89E-16	0.018	1.17E-13
AG↔F3tv	13.3%	9.99E-15	0.018	1.50E-12
T2ml↔STSp	12.4%	5.04E-13	0.018	5.04E-11
STSp↔T1R	12.3%	7.60E-13	0.018	5.70E-11
Pole↔STSp	12.2%	1.05E-12	0.018	6.27E-11
Pole↔T2ml	11.9%	2.14E-12	0.018	1.07E-10
PT↔T1	11.9%	4.90E-12	0.018	2.10E-10
F2p↔STSp	11.6%	1.32E-11	0.018	4.95E-10
T2ml↔SMG	11.2%	2.75E-11	0.018	8.26E-10
T2ml↔AG	11.5%	2.62E-11	0.018	8.26E-10
AG↔F2antR	11.3%	3.87E-11	0.018	1.06E-09
PrF3op↔SMG	11.4%	5.13E-11	0.018	1.28E-09
F3tv↔STSp	11.2%	9.27E-11	0.018	2.14E-09
RolS↔PrecR	11.1%	2.27E-10	0.018	4.87E-09
PrF3op↔F3tv	10.7%	9.50E-10	0.018	1.90E-08
F3tv↔SMG	10.4%	1.93E-09	0.018	3.61E-08
F2p↔SMG	9.9%	2.84E-09	0.018	5.01E-08
STSp↔F3orb	10.1%	3.71E-09	0.018	6.18E-08
SMG↔F2antR	9.7%	1.32E-08	0.018	2.08E-07
T1↔F3tv	9.1%	1.40E-07	0.018	2.10E-06
Fusa↔AG	8.7%	1.79E-07	0.018	2.56E-06
F3opd↔F3td	8.9%	1.89E-07	0.018	2.58E-06
T2p↔T3p	8.4%	3.86E-07	0.018	5.04E-06
Prec↔F3opd	8.5%	4.82E-07	0.018	6.03E-06
T2ml↔F3tv	8.3%	5.64E-07	0.018	6.76E-06
SMG↔F3orb	8.4%	6.25E-07	0.018	7.21E-06
Prec↔SMG	8.4%	6.54E-07	0.018	7.27E-06
F3tv↔F3orb	8.3%	1.04E-06	0.018	1.11E-05
SMG↔F3td	8.2%	1.80E-06	0.018	1.80E-05
T2ml↔F3td	8.1%	1.79E-06	0.018	1.80E-05
AG↔T1a	7.8%	2.55E-06	0.018	2.47E-05
F3opd↔T2ml	7.8%	2.66E-06	0.018	2.50E-05
AG↔SMG	8.0%	2.88E-06	0.018	2.54E-05
F3tv↔F2antR	7.8%	2.80E-06	0.018	2.54E-05
Pole↔T1a	7.8%	3.00E-06	0.018	2.58E-05

Endophenotype	heritability	P value	SE	FDR P value
T1↔PrF3op	7.7%	4.74E-06	0.018	3.95E-05
AG↔STSp	7.7%	4.98E-06	0.018	4.04E-05
F3opd↔STSp	7.7%	5.28E-06	0.018	4.17E-05
PrF3op↔T3p	7.4%	6.48E-06	0.018	4.98E-05
PrF3op↔F2antR	7.5%	7.05E-06	0.018	5.28E-05
T2ml↔F3orb	7.5%	9.05E-06	0.018	6.62E-05
T1a↔STSp	7.3%	1.07E-05	0.018	7.62E-05
F3opdR↔F2antR	7.3%	1.13E-05	0.018	7.87E-05
Pole↔F3opd	7.3%	1.55E-05	0.018	1.06E-04
AG↔T3p	7.1%	1.86E-05	0.018	1.24E-04
STSp↔T2pR	7.0%	2.38E-05	0.018	1.55E-04
F3opd↔PrF3op	6.9%	3.25E-05	0.018	2.08E-04
T1↔T1a/HeschlR	6.9%	3.60E-05	0.018	2.25E-04
Prec↔AG	6.9%	4.14E-05	0.018	2.54E-04
F3tv↔T2pR	6.7%	4.25E-05	0.018	2.54E-04
T1a↔T1a/HeschlR	6.8%	4.32E-05	0.018	2.54E-04
PrF3op↔AG	6.7%	4.52E-05	0.018	2.60E-04
T1↔T1a	6.8%	5.09E-05	0.018	2.88E-04
Prec↔F3tv	6.7%	5.59E-05	0.018	3.10E-04
Pole↔AG	6.6%	5.71E-05	0.018	3.11E-04
F3opd↔AG	6.5%	6.10E-05	0.017	3.27E-04
F3tv↔F3opdR	6.6%	6.29E-05	0.018	3.31E-04
F3orb↔F2antR	6.6%	7.82E-05	0.018	3.85E-04
PT↔T1a/HeschlR	6.6%	7.74E-05	0.018	3.85E-04
SMG↔T3p	6.7%	7.78E-05	0.018	3.85E-04
T1a↔SMG	6.5%	7.59E-05	0.018	3.85E-04
Prec↔T1	6.5%	8.27E-05	0.018	4.00E-04
Prec↔T2p	6.5%	8.48E-05	0.018	4.04E-04
PrF3op↔STSp	6.5%	9.15E-05	0.018	4.29E-04
T2ml↔PrF3op	6.4%	1.32E-04	0.018	6.11E-04
Fusa↔T2p	6.3%	1.39E-04	0.018	6.30E-04
F3opd↔T3p	6.3%	1.74E-04	0.018	7.78E-04
T2ml↔T1R	6.1%	1.93E-04	0.018	8.53E-04
F2p↔F3tv	6.1%	2.04E-04	0.018	8.84E-04
T2ml↔F3opdR	6.2%	2.06E-04	0.018	8.84E-04
F3opd↔F2p	6.0%	2.13E-04	0.017	8.99E-04
T2ml↔T1a	6.2%	2.18E-04	0.018	9.07E-04
Pole↔T1R	6.2%	2.33E-04	0.018	9.59E-04
SMG↔T2pR	5.9%	2.42E-04	0.017	9.70E-04
AG↔F3orb	6.0%	2.43E-04	0.018	9.70E-04
AG↔T2p	6.0%	2.63E-04	0.018	1.04E-03
STSp↔F3opdR	5.5%	6.15E-04	0.017	2.40E-03
F2p↔T2ml	5.7%	6.92E-04	0.018	2.66E-03
T2p↔RolS	5.6%	7.09E-04	0.018	2.69E-03
T3p↔F3orb	5.5%	7.21E-04	0.017	2.70E-03
T1a.HeschlR↔T1R	5.5%	8.11E-04	0.018	3.01E-03
F3tv↔RolS	5.5%	1.01E-03	0.018	3.65E-03
F3orb↔T2pR	5.2%	1.01E-03	0.017	3.65E-03
T2ml↔T2pR	5.3%	1.08E-03	0.018	3.84E-03

Endophenotype	heritability	P value	SE	FDR P value
F3tv↔T1R	5.3%	1.14E-03	0.018	4.03E-03
F3td↔T3p	5.3%	1.18E-03	0.018	4.07E-03
T2p↔F3opdR	5.0%	1.18E-03	0.017	4.07E-03
F3opd↔F3orb	5.2%	1.34E-03	0.017	4.58E-03
F2p↔PrF3op	5.1%	1.46E-03	0.017	4.92E-03
F3tv↔T2p	5.2%	1.52E-03	0.018	5.02E-03
T1↔RolS	5.2%	1.51E-03	0.018	5.02E-03
Prec↔F3opdR	5.2%	1.59E-03	0.018	5.18E-03
T1↔AG	5.1%	1.62E-03	0.017	5.23E-03
STSp↔F3td	5.2%	1.72E-03	0.018	5.37E-03
F3tv↔T1a/HeschIR	5.1%	1.70E-03	0.018	5.37E-03
STSp↔F2antR	5.1%	1.71E-03	0.018	5.37E-03
F3tv↔T3p	5.0%	2.11E-03	0.018	6.53E-03
Fusa↔T3p	4.9%	2.37E-03	0.017	7.26E-03
Prec↔Fusa	5.0%	2.61E-03	0.018	7.90E-03
F3opdR↔T2pR	4.7%	2.96E-03	0.017	8.87E-03
F3tv↔F3td	4.7%	3.13E-03	0.018	9.22E-03
F3opdR↔T1R	4.7%	3.11E-03	0.017	9.22E-03
SMG↔F3opdR	4.6%	3.45E-03	0.017	1.01E-02
F3orb↔F3opdR	4.4%	3.88E-03	0.017	1.12E-02
Fusa↔STSp	4.6%	4.18E-03	0.018	1.18E-02
T1↔T1R	4.6%	4.15E-03	0.017	1.18E-02
F3td↔F2antR	4.4%	4.60E-03	0.017	1.29E-02
PrF3op↔T1R	4.6%	4.70E-03	0.018	1.30E-02
F2antR↔T2pR	4.5%	4.88E-03	0.018	1.34E-02
T1↔F3orb	4.5%	4.97E-03	0.017	1.36E-02
Prec↔RolS	4.5%	5.65E-03	0.018	1.53E-02
F2p↔AG	4.5%	5.93E-03	0.018	1.59E-02
T1a↔F3orb	4.4%	6.00E-03	0.018	1.59E-02
T1a↔T1R	4.3%	6.51E-03	0.017	1.71E-02
PT↔T1R	4.2%	6.84E-03	0.017	1.78E-02
T2pR↔PrecR	4.2%	7.83E-03	0.018	2.02E-02
Pole↔F2p	4.1%	8.14E-03	0.017	2.09E-02
F3opd↔F2antR	4.1%	8.40E-03	0.017	2.13E-02
Prec↔F3td	4.2%	9.12E-03	0.018	2.30E-02
SMG↔T2p	4.0%	9.78E-03	0.017	2.44E-02
PT↔AG	4.1%	9.95E-03	0.018	2.47E-02
PrF3op↔F3opdR	4.0%	1.04E-02	0.018	2.55E-02
PrF3op↔F3td	3.9%	1.15E-02	0.017	2.77E-02
Fusa↔T1a	4.0%	1.14E-02	0.018	2.77E-02
T2pR↔T1R	3.8%	1.35E-02	0.017	3.24E-02
T2p↔F2antR	3.9%	1.39E-02	0.018	3.32E-02
T2ml↔T2p	3.6%	1.41E-02	0.017	3.34E-02
T2ml↔T1	3.8%	1.45E-02	0.017	3.39E-02
F2antR↔T1a/HeschIR	3.9%	1.50E-02	0.018	3.48E-02
F3opd↔T1R	3.8%	1.60E-02	0.018	3.69E-02
F3td↔T1R	3.7%	1.70E-02	0.017	3.88E-02
F3opd↔T1	3.7%	1.74E-02	0.018	3.92E-02

Endophenotype	heritability	P value	SE	FDR P value
F3opd↔T1a	3.6%	1.73E-02	0.017	3.92E-02
F2p↔T2p	3.6%	1.79E-02	0.017	4.01E-02
Prec↔F2antR	3.6%	1.85E-02	0.017	4.11E-02
Fusa↔SMG	3.6%	1.93E-02	0.017	4.24E-02
AG↔PrecR	3.7%	1.94E-02	0.018	4.24E-02
SMG↔T1R	3.5%	1.95E-02	0.017	4.24E-02
F2antR↔T1R	3.6%	2.02E-02	0.018	4.36E-02
F2p↔T2pR	3.5%	2.17E-02	0.018	4.65E-02
T1↔SMG	3.5%	2.30E-02	0.017	4.89E-02
F2p↔T1	3.5%	2.33E-02	0.018	4.93E-02
STSp↔SMG	3.4%	2.50E-02	0.018	5.25E-02
F2p↔T1a	3.4%	2.54E-02	0.017	5.29E-02
F3tv↔T1a	3.3%	2.57E-02	0.017	5.32E-02
Prec↔T3p	3.4%	2.63E-02	0.018	5.40E-02
T2ml↔F2antR	3.3%	2.81E-02	0.017	5.73E-02
Pole↔F3orb	3.2%	2.90E-02	0.017	5.89E-02
F3opd↔T2pR	3.2%	3.22E-02	0.017	6.49E-02
Prec↔F3orb	3.0%	3.68E-02	0.017	7.35E-02
PrF3op↔T2pR	3.1%	3.70E-02	0.017	7.35E-02
RolS↔F3opdR	3.1%	3.77E-02	0.017	7.44E-02
PT↔RolS	3.1%	3.82E-02	0.017	7.47E-02
AG↔T1R	3.1%	3.86E-02	0.017	7.47E-02
T1a↔RolS	3.1%	3.85E-02	0.018	7.47E-02
PrF3op↔T2p	3.0%	4.08E-02	0.017	7.85E-02
Pole↔PT	2.9%	4.16E-02	0.017	7.95E-02
PT↔F2antR	2.9%	4.30E-02	0.017	8.17E-02
T1↔PrecR	3.0%	4.34E-02	0.017	8.18E-02
Pole↔PrF3op	2.9%	4.44E-02	0.017	8.32E-02
RolS↔F2antR	3.0%	4.48E-02	0.017	8.36E-02
T1↔T2p	2.9%	4.76E-02	0.017	8.82E-02
Pole↔T1	2.9%	4.83E-02	0.017	8.90E-02
PrF3op↔PrecR	2.8%	5.01E-02	0.017	9.17E-02
F3opd↔RolS	2.8%	5.17E-02	0.017	9.39E-02
Pole↔F3tv	2.8%	5.21E-02	0.017	9.42E-02
T1↔T2pR	2.8%	5.50E-02	0.017	9.88E-02
Pole↔T2p	2.7%	5.84E-02	0.017	1.04E-01
F2p↔F2antR	2.7%	5.99E-02	0.017	1.06E-01
T1↔F2antR	2.6%	6.18E-02	0.017	1.09E-01
PT↔T2ml	2.7%	6.21E-02	0.018	1.09E-01
F3tv↔PrecR	2.7%	6.39E-02	0.017	1.10E-01
T2ml↔T1a.HeschlR	2.6%	6.36E-02	0.017	1.10E-01
AG↔F3td	2.6%	6.35E-02	0.017	1.10E-01
T2p↔T1R	2.6%	6.86E-02	0.017	1.18E-01
PT↔T2pR	2.5%	7.04E-02	0.017	1.20E-01
F3opd↔F3tv	2.5%	7.24E-02	0.017	1.23E-01

Endophenotype	heritability	P value	SE	FDR P value
F2p↔T1R	2.5%	7.45E-02	0.017	1.26E-01
AG↔RolS	2.5%	7.69E-02	0.017	1.29E-01
STSp↔T3p	2.5%	7.91E-02	0.018	1.31E-01
T2ml↔T3p	2.5%	7.91E-02	0.017	1.31E-01
F2p↔F3opdR	2.4%	7.97E-02	0.017	1.31E-01
T1↔STSp	2.4%	8.26E-02	0.017	1.35E-01
T3p↔T2pR	2.4%	8.40E-02	0.017	1.37E-01
Fusa↔PrF3op	2.3%	8.76E-02	0.017	1.42E-01
STSp↔T2p	2.3%	8.88E-02	0.017	1.43E-01
T1↔Fusa	2.4%	8.93E-02	0.018	1.43E-01
T3p↔RolS	2.3%	9.24E-02	0.017	1.46E-01
AG↔T2pR	2.3%	9.26E-02	0.017	1.46E-01
Prec↔PrF3op	2.3%	9.17E-02	0.017	1.46E-01
Fusa↔T1a.HeschlR	2.3%	9.17E-02	0.018	1.46E-01
T3p↔F3opdR	2.2%	9.38E-02	0.017	1.47E-01
Prec↔STSp	2.2%	9.65E-02	0.017	1.50E-01
T2ml↔RolS	2.3%	9.88E-02	0.018	1.53E-01
T1a↔F2antR	2.2%	1.03E-01	0.017	1.59E-01
SMG↔PrecR	2.1%	1.04E-01	0.017	1.60E-01
Prec↔T1a	2.1%	1.05E-01	0.017	1.60E-01
PT↔STSp	2.2%	1.05E-01	0.018	1.60E-01
PT↔T2p	2.1%	1.06E-01	0.017	1.60E-01
T3p↔T1R	2.1%	1.07E-01	0.017	1.60E-01
T1↔F3opdR	2.1%	1.12E-01	0.017	1.67E-01
F3td↔T2pR	2.1%	1.14E-01	0.017	1.67E-01
PT↔T1a	2.1%	1.13E-01	0.018	1.67E-01
F3opdR↔PrecR	2.1%	1.14E-01	0.017	1.67E-01
T1a↔F3opdR	2.1%	1.14E-01	0.017	1.67E-01
Fusa↔F3tv	2.0%	1.19E-01	0.017	1.71E-01
F3orb↔T1R	2.1%	1.19E-01	0.018	1.71E-01
PT↔F3opd	2.0%	1.18E-01	0.017	1.71E-01
PrF3op↔F3orb	2.1%	1.18E-01	0.017	1.71E-01
F3orb↔RolS	2.0%	1.24E-01	0.017	1.78E-01
Fusa↔F2antR	2.0%	1.25E-01	0.017	1.78E-01
F3opd↔F3opdR	2.0%	1.27E-01	0.018	1.79E-01
F2p↔T3p	2.0%	1.27E-01	0.017	1.79E-01
Fusa↔T1R	2.0%	1.28E-01	0.017	1.79E-01
F3td↔F3orb	2.0%	1.29E-01	0.018	1.80E-01
RolS↔T1R	1.9%	1.30E-01	0.017	1.81E-01
F3td↔F3opdR	2.0%	1.31E-01	0.018	1.81E-01
F2p↔F3orb	1.9%	1.32E-01	0.017	1.82E-01
Fusa↔RolS	1.9%	1.33E-01	0.017	1.83E-01
F3orb↔T1a.HeschlR	1.9%	1.35E-01	0.017	1.84E-01
T1a↔T2p	1.9%	1.39E-01	0.017	1.88E-01
T1R↔PrecR	1.8%	1.42E-01	0.017	1.92E-01
Prec↔T1a.HeschlR	1.8%	1.50E-01	0.017	2.01E-01
Pole↔SMG	1.8%	1.53E-01	0.017	2.03E-01
SMG↔T1a.HeschlR	1.8%	1.53E-01	0.017	2.03E-01
Prec↔T2ml	1.8%	1.52E-01	0.017	2.03E-01

Endophenotype	heritability	P value	SE	FDR P value
Pole↔T1a.HeschlR	1.8%	1.55E-01	0.017	2.05E-01
RolS↔T1a.HeschlR	1.8%	1.57E-01	0.017	2.07E-01
T2p↔F3orb	1.7%	1.68E-01	0.017	2.20E-01
T2p↔T2pR	1.6%	1.71E-01	0.017	2.22E-01
T3p↔F2antR	1.7%	1.72E-01	0.017	2.22E-01
F3opd↔T2p	1.7%	1.72E-01	0.017	2.22E-01
Pole↔RolS	1.6%	1.77E-01	0.017	2.28E-01
F2antR↔PrecR	1.5%	1.99E-01	0.017	2.55E-01
STSp↔T1a.HeschlR	1.3%	2.35E-01	0.017	2.99E-01
STSp↔RolS	1.2%	2.37E-01	0.017	3.02E-01
Prec↔PrecR	1.3%	2.38E-01	0.017	3.02E-01
Fusa↔F3orb	1.2%	2.41E-01	0.017	3.04E-01
Pole↔T2pR	1.1%	2.52E-01	0.017	3.17E-01
T3p↔PrecR	1.0%	2.76E-01	0.017	3.45E-01
Fusa↔F3td	1.0%	2.82E-01	0.017	3.51E-01
T2pR↔T1a.HeschlR	1.0%	2.86E-01	0.017	3.55E-01
T1a↔T3p	1.0%	2.89E-01	0.017	3.56E-01
Pole↔PrecR	1.0%	2.89E-01	0.017	3.56E-01
Pole↔F3td	0.9%	3.04E-01	0.017	3.72E-01
T2p↔F3td	0.9%	3.06E-01	0.017	3.73E-01
Fusa↔F3opdR	0.9%	3.08E-01	0.017	3.74E-01
Pole↔Fusa	0.8%	3.29E-01	0.017	3.98E-01
T1↔T3p	0.7%	3.34E-01	0.017	4.02E-01
Fusa↔PrecR	0.7%	3.45E-01	0.017	4.15E-01
Pole↔F2antR	0.6%	3.60E-01	0.017	4.30E-01
Prec↔Pole	0.6%	3.64E-01	0.017	4.31E-01
PrF3op↔T1a	0.6%	3.62E-01	0.017	4.31E-01
PT↔SMG	0.6%	3.70E-01	0.017	4.37E-01
T2p↔T1a.HeschlR	0.5%	3.91E-01	0.017	4.60E-01
PT↔F3tv	0.3%	4.26E-01	0.017	4.99E-01
Pole↔F3opdR	0.0%	5.00E-01	0.017	5.00E-01
STSp↔PrecR	0.0%	5.00E-01	0.017	5.00E-01
T1a↔PrecR	0.0%	5.00E-01	0.017	5.00E-01
F2p↔T1a.HeschlR	0.0%	5.00E-01	0.017	5.00E-01
Fusa↔T2pR	0.2%	4.46E-01	0.017	5.00E-01
F3td↔PrecR	0.0%	5.00E-01	0.017	5.00E-01
T2ml↔Fusa	0.0%	5.00E-01	0.017	5.00E-01
PT↔F2p	0.0%	5.00E-01	0.017	5.00E-01
PT↔F3opdR	0.0%	5.00E-01	0.017	5.00E-01
PT↔F3orb	0.0%	5.00E-01	0.017	5.00E-01
F3td↔RolS	0.0%	5.00E-01	0.017	5.00E-01
Prec↔T2pR	0.2%	4.50E-01	0.017	5.00E-01
PrF3op↔RolS	0.0%	5.00E-01	0.017	5.00E-01
F3orb↔PrecR	0.0%	5.00E-01	0.017	5.00E-01
AG↔F3opdR	0.0%	5.00E-01	0.017	5.00E-01
T1a↔T2pR	0.2%	4.65E-01	0.017	5.00E-01
F2p↔PrecR	0.0%	5.00E-01	0.017	5.00E-01
PrF3op↔T1a.HeschlR	0.0%	5.00E-01	0.017	5.00E-01

Endophenotype	heritability	P value	SE	FDR P value
F2p↔RolS	0.0%	5.00E-01	0.017	5.00E-01
F2p↔Fusa	0.0%	5.00E-01	0.017	5.00E-01
F3opdR↔T1a.HeschlR	0.3%	4.35E-01	0.017	5.00E-01
T1a↔F3td	0.0%	5.00E-01	0.017	5.00E-01
Prec↔T1R	0.0%	4.99E-01	0.017	5.00E-01
T2p↔PrecR	0.0%	5.00E-01	0.017	5.00E-01
T1a.HeschlR↔PrecR	0.0%	5.00E-01	0.017	5.00E-01
T2ml↔PrecR	0.0%	5.00E-01	0.017	5.00E-01
F3opd↔T1a.HeschlR	0.0%	5.00E-01	0.017	5.00E-01
PT↔Fusa	0.0%	5.00E-01	0.017	5.00E-01
SMG↔RolS	0.0%	5.00E-01	0.017	5.00E-01
Pole↔T3p	0.0%	5.00E-01	0.017	5.00E-01
AG↔T1a.HeschlR	0.0%	4.99E-01	0.017	5.00E-01
F3opd↔PrecR	0.0%	5.00E-01	0.017	5.00E-01
PT↔T3p	0.0%	5.00E-01	0.017	5.00E-01
PT↔F3td	0.0%	5.00E-01	0.018	5.00E-01
RolS↔T2pR	0.0%	5.00E-01	0.017	5.00E-01
PT↔PrecR	0.0%	5.00E-01	0.017	5.00E-01
T1↔F3td	0.0%	5.00E-01	0.017	5.00E-01
F2p↔F3td	0.0%	5.00E-01	0.017	5.00E-01
Prec↔F2p	0.0%	5.00E-01	0.017	5.00E-01
T3p↔T1a.HeschlR	0.0%	5.00E-01	0.017	5.00E-01
F3opd↔Fusa	0.0%	5.00E-01	0.017	5.00E-01
PT↔PrF3op	0.0%	5.00E-01	0.017	5.00E-01
Prec↔PT	0.0%	5.00E-01	0.017	5.00E-01
F3td↔T1a.HeschlR	0.0%	5.00E-01	0.017	5.00E-01

Table B.4 – **Heritabilities of brain anatomical connectivities.** Bold phenotypes represents ACs with significant heritability after false discovery rate correction at p<0.05.

Category	Endophenotype	h2(%)	P value	SE	FDR P value
ICVF	**Corpus callosum**	62.7%	1.98E-272	0.018	6.22E-270
ICVF	**Arcuate Long Segment Left**	60.5%	2.43E-251	0.018	3.82E-249
ICVF	**Superior Londgitudinal Fasciculus I Right**	60.2%	8.83E-251	0.018	9.27E-249
ICVF	**Superior Londgitudinal Fasciculus I Left**	60.0%	3.88E-250	0.018	3.06E-248
ICVF	**Inferior Fronto Occipital fasciculus Left**	59.9%	1.27E-247	0.018	8.00E-246
ICVF	**Superior Londgitudinal Fasciculus II Left**	59.7%	3.42E-243	0.018	1.80E-241
ICVF	**Superior Londgitudinal Fasciculus III Left**	58.5%	9.02E-243	0.018	4.06E-241
ICVF	**Inferior Longitudinal Left**	59.1%	4.71E-241	0.018	1.86E-239
ICVF	**Superior Londgitudinal Fasciculus III Right**	58.2%	2.31E-240	0.018	8.08E-239
ICVF	**Superior Londgitudinal Fasciculus II Right**	58.4%	3.33E-235	0.018	1.05E-233
ICVF	**Arcuate Long Segment Right**	58.1%	8.32E-233	0.018	2.38E-231
ICVF	**Arcuate Anterior Segment Right**	57.6%	2.22E-232	0.018	5.82E-231
ICVF	**Arcuate Posterior Segment Left**	57.5%	2.49E-232	0.018	6.03E-231
ICVF	**Inferior Fronto Occipital fasciculus Right**	58.0%	9.51E-231	0.018	2.14E-229
ICVF	**Frontal Aslant Tract Right**	57.2%	3.18E-230	0.018	6.69E-229
ICVF	**Frontal Aslant Tract Left**	57.2%	3.65E-230	0.018	7.19E-229
ICVF	**Inferior Longitudinal Right**	57.5%	2.17E-226	0.018	4.03E-225
ICVF	**Arcuate Posterior Segment Right**	56.9%	3.10E-224	0.018	5.43E-223
ICVF	**Uncinate Left**	54.1%	7.06E-208	0.018	1.17E-206
ICVF	**Arcuate Anterior Segment Left**	53.2%	1.08E-201	0.018	1.70E-200
ICVF	**Uncinate Right**	51.3%	2.79E-187	0.018	4.19E-186
FA	**Corpus callosum**	50.8%	2.19E-181	0.018	3.14E-180
L3	**Inferior Fronto Occipital fasciculus Left**	50.3%	1.17E-177	0.018	1.60E-176
FA	**Arcuate Long Segment Left**	49.9%	1.68E-174	0.018	2.20E-173
L3	**Arcuate Long Segment Left**	49.9%	7.05E-174	0.018	8.89E-173
MD	**Arcuate Long Segment Left**	49.7%	1.10E-172	0.018	1.33E-171
FA	**Inferior Fronto Occipital fasciculus Left**	49.3%	3.77E-172	0.018	4.40E-171
ICVF	**Frontal Inferior longitudinal Right**	49.0%	2.44E-171	0.018	2.75E-170
L3	**Inferior Fronto Occipital fasciculus Right**	48.5%	3.99E-166	0.018	4.33E-165
FA	**Inferior Fronto Occipital fasciculus Right**	48.4%	4.71E-166	0.018	4.95E-165
FA	**Arcuate Anterior Segment Right**	47.5%	2.21E-164	0.018	2.24E-163
FA	**Superior Londgitudinal Fasciculus III Right**	47.7%	2.96E-164	0.018	2.91E-163
MD	**Inferior Fronto Occipital fasciculus Left**	48.4%	3.67E-164	0.018	3.51E-163

Category	Endophenotype	h2(%)	P value	SE	FDR P value
L3	**Corpus callosum**	48.0%	1.06E-163	0.018	9.83E-163
MD	**Superior Londgitudinal Fasciculus III Left**	47.1%	4.72E-158	0.018	4.25E-157
L3	**Superior Londgitudinal Fasciculus II Left**	47.7%	6.38E-157	0.018	5.58E-156
L2	**Superior Londgitudinal Fasciculus III Left**	46.7%	7.14E-156	0.018	6.08E-155
FA	**Superior Londgitudinal Fasciculus II Left**	47.8%	3.25E-155	0.018	2.69E-154
L2	**Inferior Fronto Occipital fasciculus Left**	46.7%	2.02E-154	0.018	1.63E-153
L2	**Arcuate Long Segment Left**	46.6%	2.47E-153	0.018	1.94E-152
L3	**Superior Londgitudinal Fasciculus III Right**	45.9%	8.16E-153	0.018	6.27E-152
L3	**Superior Londgitudinal Fasciculus III Left**	45.9%	1.30E-151	0.018	9.76E-151
L2	**Superior Londgitudinal Fasciculus III Right**	45.7%	1.98E-151	0.018	1.45E-150
L3	**Inferior Longitudinal Right**	46.3%	4.84E-151	0.018	3.47E-150
FA	**Superior Londgitudinal Fasciculus III Left**	45.5%	4.01E-150	0.018	2.80E-149
MD	**Superior Londgitudinal Fasciculus II Left**	46.1%	1.44E-149	0.018	9.85E-149
MD	**Superior Londgitudinal Fasciculus III Right**	45.4%	5.65E-149	0.018	3.79E-148
L3	**Arcuate Anterior Segment Right**	45.2%	1.35E-147	0.018	8.86E-147
L2	**Corpus callosum**	45.2%	1.69E-146	0.018	1.08E-145
FA	**Superior Londgitudinal Fasciculus II Right**	45.1%	1.39E-142	0.018	8.74E-142
L2	**Arcuate Anterior Segment Right**	44.3%	1.72E-142	0.018	1.06E-141
MD	**Arcuate Anterior Segment Right**	44.6%	8.39E-142	0.018	5.08E-141
MD	**Corpus callosum**	44.5%	5.43E-141	0.018	3.23E-140
FA	**Inferior Longitudinal Right**	45.0%	7.60E-141	0.018	4.43E-140
L2	**Superior Londgitudinal Fasciculus II Left**	44.9%	1.61E-140	0.018	9.22E-140
L3	**Inferior Longitudinal Left**	44.3%	2.83E-138	0.018	1.59E-137
OD	**Fronto Insular tract3 Right**	43.6%	1.19E-136	0.018	6.59E-136
L3	**Arcuate Long Segment Right**	43.8%	1.49E-136	0.018	8.10E-136
ICVF	**Fronto Insular tract2 Right**	43.2%	4.63E-136	0.018	2.47E-135
MD	**Arcuate Long Segment Right**	43.7%	1.73E-135	0.018	9.06E-135
ICVF	**Frontal Superior Longitudinal Right**	44.2%	8.28E-135	0.018	4.28E-134
FA	**Superior Londgitudinal Fasciculus I Left**	43.7%	5.33E-134	0.018	2.71E-133
ICVF	**Fronto Insular tract4 Right**	43.1%	1.26E-132	0.018	6.30E-132
L3	**Superior Londgitudinal Fasciculus II Right**	43.3%	2.01E-132	0.018	9.87E-132
L1	**Inferior Fronto Occipital fasciculus Left**	43.4%	3.46E-132	0.018	1.68E-131
L1	**Superior Londgitudinal Fasciculus III Left**	43.5%	3.68E-132	0.018	1.76E-131
MD	**Inferior Fronto Occipital fasciculus Right**	43.1%	2.28E-131	0.018	1.07E-130
L2	**Inferior Fronto Occipital fasciculus Right**	43.0%	7.82E-131	0.018	3.62E-130
FA	**Uncinate Left**	43.4%	1.23E-130	0.018	5.61E-130
ICVF	**Fronto Insular tract3 Right**	41.9%	1.94E-128	0.018	8.74E-128
L3	**Superior Londgitudinal Fasciculus I Right**	42.9%	3.34E-128	0.018	1.48E-127
L2	**Superior Londgitudinal Fasciculus II Right**	42.5%	6.81E-128	0.018	2.98E-127
L1	**Superior Londgitudinal Fasciculus III Right**	42.2%	1.50E-126	0.018	6.47E-126
L3	**Superior Londgitudinal Fasciculus I Left**	42.1%	2.40E-126	0.018	1.02E-125
L3	**Frontal Aslant Tract Left**	41.7%	3.00E-125	0.018	1.26E-124
FA	**Superior Londgitudinal Fasciculus I Right**	42.5%	1.11E-123	0.018	4.61E-123
MD	**Superior Londgitudinal Fasciculus II Right**	41.3%	8.72E-122	0.018	3.57E-121
MD	**Arcuate Posterior Segment Right**	41.6%	9.44E-122	0.018	3.81E-121
MD	**Frontal Aslant Tract Left**	41.1%	1.15E-121	0.018	4.60E-121
FA	**Frontal Aslant Tract Left**	41.4%	1.67E-121	0.018	6.57E-121
FA	**Arcuate Long Segment Right**	41.3%	3.32E-121	0.018	1.29E-120
MD	**Inferior Longitudinal Left**	41.6%	1.24E-120	0.018	4.76E-120
L3	**Uncinate Left**	41.5%	2.92E-120	0.018	1.11E-119
MD	**Arcuate Posterior Segment Left**	41.2%	4.10E-120	0.018	1.54E-119

Category	Endophenotype	h2(%)	P value	SE	FDR P value
FA	**Inferior Longitudinal Left**	41.4%	1.20E-118	0.018	4.46E-118
ICVF	**Frontal Inferior longitudinal Left**	41.6%	5.12E-118	0.018	1.87E-117
L2	**Arcuate Long Segment Right**	40.6%	1.19E-117	0.018	4.32E-117
ICVF	**Fronto Insular tract5 Right**	40.6%	3.48E-117	0.018	1.24E-116
FA	**Uncinate Right**	40.5%	2.22E-116	0.018	7.86E-116
MD	**Inferior Longitudinal Right**	40.5%	3.73E-116	0.018	1.30E-115
L2	**Uncinate Left**	40.9%	2.62E-115	0.018	9.09E-115
L2	**Frontal Aslant Tract Left**	40.4%	5.63E-115	0.018	1.93E-114
L3	**Uncinate Right**	40.2%	7.38E-115	0.018	2.50E-114
L1	**Arcuate Anterior Segment Right**	40.6%	8.19E-114	0.019	2.74E-113
L2	**Inferior Longitudinal Left**	40.7%	1.22E-113	0.018	4.03E-113
OD	**Arcuate Anterior Segment Right**	40.6%	1.91E-113	0.019	6.28E-113
L2	**Inferior Longitudinal Right**	40.3%	2.63E-113	0.018	8.53E-113
ICVF	**Frontal Superior Longitudinal Left**	40.3%	3.28E-113	0.018	1.06E-112
L1	**Corpus callosum**	40.2%	8.26E-113	0.018	2.63E-112
L1	**Arcuate Long Segment Left**	40.1%	5.00E-112	0.019	1.57E-111
L1	**Superior Londgitudinal Fasciculus II Left**	39.0%	8.17E-112	0.018	2.55E-111
L1	**Frontal Aslant Tract Left**	39.2%	1.17E-111	0.018	3.62E-111
L2	**Superior Londgitudinal Fasciculus I Left**	39.2%	6.85E-111	0.018	2.10E-110
L2	**Arcuate Posterior Segment Left**	39.5%	3.09E-110	0.018	9.36E-110
L3	**Arcuate Posterior Segment Right**	39.5%	1.04E-109	0.018	3.11E-109
OD	**Inferior Fronto Occipital fasciculus Left**	39.7%	1.26E-109	0.018	3.75E-109
ICVF	**Fronto Insular tract1 Right**	38.9%	1.41E-109	0.018	4.15E-109
MD	**Arcuate Anterior Segment Left**	38.9%	4.95E-109	0.018	1.44E-108
MD	**Frontal Aslant Tract Right**	38.4%	4.90E-106	0.018	1.42E-105
MD	**Superior Londgitudinal Fasciculus I Left**	38.4%	8.92E-106	0.018	2.55E-105
L2	**Arcuate Anterior Segment Left**	38.3%	8.60E-105	0.018	2.44E-104
MO	**Frontal Aslant Tract Left**	38.2%	1.31E-104	0.018	3.68E-104
L1	**Frontal Aslant Tract Right**	37.9%	8.94E-104	0.018	2.49E-103
MD	**Superior Londgitudinal Fasciculus I Right**	38.2%	1.09E-103	0.018	3.02E-103
L3	**Frontal Aslant Tract Right**	37.5%	1.15E-101	0.018	3.14E-101
FA	**Frontal Aslant Tract Right**	37.7%	1.58E-101	0.018	4.30E-101
ISOVF	**Superior Londgitudinal Fasciculus III Right**	37.4%	4.45E-101	0.018	1.20E-100
L2	**Frontal Aslant Tract Right**	37.5%	7.79E-100	0.018	2.08E-99
OD	**Superior Londgitudinal Fasciculus II Left**	37.0%	3.27E-99	0.018	8.65E-99
ISOVF	**Superior Londgitudinal Fasciculus III Left**	37.4%	4.02E-99	0.018	1.06E-98
ISOVF	**Inferior Fronto Occipital fasciculus Left**	37.2%	3.35E-98	0.018	8.73E-98
MD	**Uncinate Left**	37.4%	3.92E-98	0.018	1.01E-97
L2	**Superior Londgitudinal Fasciculus I Right**	36.8%	1.46E-97	0.018	3.73E-97
MO	**Frontal Aslant Tract Right**	37.2%	6.74E-97	0.018	1.71E-96
L2	**Uncinate Right**	36.2%	8.87E-96	0.018	2.23E-95
MD	**Frontal Inferior longitudinal Right**	36.4%	1.53E-95	0.018	3.84E-95
MO	**Arcuate Anterior Segment Right**	36.8%	7.11E-95	0.018	1.76E-94
L1	**Inferior Fronto Occipital fasciculus Right**	36.1%	2.09E-94	0.018	5.14E-94
MO	**Fronto Insular tract3 Right**	35.7%	2.48E-92	0.018	6.05E-92

Category	Endophenotype	h2(%)	P value	SE	FDR P value
OD	**Fronto Insular tract4 Right**	33.9%	3.86E-91	0.018	9.36E-91
MO	**Corpus callosum**	36.3%	5.82E-91	0.019	1.40E-90
L3	**Arcuate Posterior Segment Left**	35.5%	7.21E-91	0.018	1.72E-90
L1	**Superior Londgitudinal Fasciculus II Right**	35.5%	1.59E-90	0.018	3.77E-90
MO	**Superior Londgitudinal Fasciculus I Left**	36.1%	5.44E-90	0.019	1.28E-89
OD	**Inferior Fronto Occipital fasciculus Right**	35.5%	7.26E-90	0.018	1.69E-89
MD	**Uncinate Right**	35.1%	4.39E-89	0.018	1.02E-88
L2	**Arcuate Posterior Segment Right**	35.3%	6.57E-89	0.018	1.51E-88
L3	**Arcuate Anterior Segment Left**	35.0%	6.94E-89	0.018	1.58E-88
FA	**Arcuate Anterior Segment Left**	34.9%	1.50E-88	0.018	3.39E-88
OD	**Fronto Insular tract5 Right**	34.9%	1.76E-88	0.018	3.97E-88
OD	**Corpus callosum**	35.7%	7.24E-88	0.019	1.62E-87
ISOVF	**Superior Londgitudinal Fasciculus II Left**	34.8%	3.75E-87	0.018	8.32E-87
ICVF	**Fronto Insular tract3 Left**	34.6%	3.27E-86	0.018	7.20E-86
OD	**Arcuate Long Segment Left**	35.2%	8.03E-86	0.019	1.76E-85
OD	**Superior Londgitudinal Fasciculus II Right**	34.5%	8.32E-86	0.018	1.81E-85
ISOVF	**Inferior Fronto Occipital fasciculus Right**	34.5%	5.23E-85	0.018	1.13E-84
MO	**Inferior Fronto Occipital fasciculus Left**	35.2%	1.90E-84	0.019	4.07E-84
ISOVF	**Arcuate Long Segment Left**	33.9%	1.45E-83	0.018	3.09E-83
OD	**Superior Londgitudinal Fasciculus III Right**	34.4%	1.40E-82	0.019	2.96E-82
FA	**Arcuate Posterior Segment Right**	34.0%	1.24E-81	0.018	2.61E-81
MO	**Inferior Fronto Occipital fasciculus Right**	33.6%	2.08E-81	0.018	4.34E-81
L1	**Arcuate Anterior Segment Left**	33.6%	4.18E-81	0.018	8.67E-81
FA	**Fronto Insular tract3 Right**	33.8%	4.51E-81	0.018	9.28E-81
FA	**Arcuate Posterior Segment Left**	33.4%	3.82E-80	0.018	7.81E-80
L3	**Frontal Inferior longitudinal Right**	33.2%	4.60E-80	0.018	9.35E-80
OD	**Superior Londgitudinal Fasciculus III Left**	33.5%	6.95E-80	0.018	1.40E-79
L1	**Arcuate Long Segment Right**	33.2%	4.86E-79	0.018	9.74E-79
MO	**Superior Londgitudinal Fasciculus I Right**	33.7%	1.38E-78	0.019	2.75E-78
L1	**Superior Londgitudinal Fasciculus I Left**	33.3%	1.55E-77	0.019	3.06E-77
MO	**Fronto Insular tract4 Right**	32.0%	2.35E-77	0.018	4.63E-77
MO	**Arcuate Long Segment Left**	33.5%	4.15E-77	0.019	8.11E-77
L1	**Inferior Longitudinal Left**	32.7%	2.66E-76	0.019	5.17E-76
L2	**Frontal Inferior longitudinal Right**	32.6%	3.57E-76	0.018	6.89E-76
FA	**Fronto Insular tract1 Right**	32.9%	6.36E-76	0.019	1.22E-75
L1	**Superior Londgitudinal Fasciculus I Right**	32.8%	2.06E-75	0.019	3.93E-75
ISOVF	**Inferior Longitudinal Right**	32.6%	4.96E-75	0.018	9.41E-75
L1	**Inferior Longitudinal Right**	32.0%	6.02E-75	0.018	1.14E-74
L1	**Arcuate Posterior Segment Right**	32.1%	2.07E-74	0.018	3.89E-74
OD	**Frontal Aslant Tract Left**	31.6%	6.70E-74	0.018	1.25E-73
L1	**Fronto Insular tract4 Right**	30.9%	3.72E-73	0.018	6.90E-73
FA	**Fronto Insular tract5 Right**	32.0%	2.34E-72	0.019	4.31E-72
L2	**Fronto Insular tract2 Right**	31.3%	7.82E-71	0.018	1.43E-70
ISOVF	**Corpus callosum**	31.1%	1.04E-70	0.018	1.89E-70
L1	**Fronto Insular tract3 Right**	30.9%	1.12E-70	0.018	2.02E-70
ISOVF	**Arcuate Anterior Segment Right**	30.7%	7.18E-70	0.018	1.29E-69
MO	**Superior Londgitudinal Fasciculus III Left**	31.0%	2.41E-69	0.018	4.32E-69
OD	**Superior Londgitudinal Fasciculus I Left**	31.7%	1.60E-68	0.019	2.85E-68
FA	**Fronto Insular tract2 Right**	30.7%	2.05E-68	0.018	3.64E-68

Category	Endophenotype	h2(%)	P value	SE	FDR P value
L1	**Arcuate Posterior Segment Left**	30.8%	1.63E-67	0.019	2.86E-67
FA	**Fronto Insular tract4 Right**	30.3%	4.18E-67	0.018	7.31E-67
L1	**Uncinate Left**	30.1%	2.55E-65	0.018	4.43E-65
L1	**Fronto Insular tract5 Right**	29.7%	2.63E-65	0.018	4.55E-65
FA	**Frontal Inferior longitudinal Right**	29.9%	1.05E-64	0.018	1.80E-64
L3	**Fronto Insular tract2 Right**	29.8%	8.16E-64	0.018	1.40E-63
ISOVF	**Superior Londgitudinal Fasciculus II Right**	29.4%	3.10E-63	0.018	5.27E-63
MD	**Fronto Insular tract2 Right**	29.7%	4.33E-63	0.018	7.34E-63
L1	**Frontal Inferior longitudinal Right**	29.1%	6.48E-61	0.018	1.09E-60
ISOVF	**Inferior Longitudinal Left**	29.6%	9.60E-61	0.019	1.61E-60
ISOVF	**Frontal Aslant Tract Right**	28.7%	8.42E-60	0.018	1.40E-59
MO	**Superior Londgitudinal Fasciculus III Right**	28.6%	5.78E-59	0.018	9.58E-59
ICVF	**Fronto Insular tract2 Left**	28.3%	1.18E-58	0.018	1.94E-58
OD	**Frontal Aslant Tract Right**	28.1%	1.78E-58	0.018	2.93E-58
ICVF	**Fronto Insular tract5 Left**	28.3%	1.97E-58	0.018	3.21E-58
L1	**Fronto Insular tract2 Right**	28.4%	1.72E-57	0.018	2.79E-57
L2	**Fronto Insular tract1 Right**	27.7%	1.11E-56	0.018	1.79E-56
OD	**Superior Londgitudinal Fasciculus I Right**	28.8%	1.23E-56	0.019	1.97E-56
L3	**Fronto Insular tract5 Right**	28.1%	1.64E-56	0.018	2.62E-56
L1	**Uncinate Right**	27.9%	2.26E-56	0.018	3.59E-56
ISOVF	**Frontal Aslant Tract Left**	27.6%	1.20E-55	0.018	1.89E-55
ISOVF	**Superior Londgitudinal Fasciculus I Right**	27.3%	6.06E-55	0.018	9.54E-55
L3	**Fronto Insular tract1 Left**	27.2%	8.22E-55	0.018	1.29E-54
OD	**Uncinate Left**	27.3%	3.24E-54	0.018	5.06E-54
ISOVF	**Arcuate Anterior Segment Left**	27.6%	4.03E-54	0.019	6.26E-54
MD	**Fronto Insular tract5 Right**	26.7%	1.07E-52	0.018	1.65E-52
ISOVF	**Arcuate Long Segment Right**	26.4%	2.03E-52	0.018	3.12E-52
ISOVF	**Arcuate Posterior Segment Right**	26.6%	4.34E-52	0.018	6.64E-52
MO	**Arcuate Long Segment Right**	26.6%	5.05E-52	0.018	7.68E-52
L2	**Fronto Insular tract3 Right**	26.5%	4.07E-51	0.018	6.16E-51
ISOVF	**Frontal Inferior longitudinal Right**	26.5%	8.12E-51	0.018	1.22E-50
MD	**Frontal Inferior longitudinal Left**	26.3%	2.22E-50	0.018	3.33E-50
L1	**Fronto Insular tract1 Right**	25.8%	7.51E-50	0.018	1.12E-49
OD	**Arcuate Long Segment Right**	26.1%	8.86E-50	0.018	1.32E-49
ISOVF	**Arcuate Posterior Segment Left**	25.8%	1.28E-49	0.018	1.90E-49
MO	**Fronto Insular tract5 Right**	26.0%	2.02E-49	0.018	2.98E-49
L3	**Fronto Insular tract3 Right**	26.1%	2.24E-49	0.018	3.29E-49
MD	**Fronto Insular tract1 Left**	25.9%	4.53E-49	0.018	6.61E-49
L2	**Fronto Insular tract1 Left**	25.8%	2.61E-47	0.019	3.79E-47
OD	**Fronto Insular tract1 Right**	25.6%	2.64E-47	0.018	3.82E-47
MD	**Fronto Insular tract3 Right**	25.2%	4.80E-47	0.018	6.91E-47
ISOVF	**Uncinate Left**	25.3%	1.29E-46	0.018	1.85E-46
FA	**Fronto Insular tract2 Left**	25.2%	2.10E-46	0.018	2.99E-46
L2	**Fronto Insular tract5 Right**	24.9%	6.80E-46	0.018	9.64E-46
ISOVF	**Superior Londgitudinal Fasciculus I Left**	24.6%	2.37E-45	0.018	3.35E-45
MO	**Inferior Longitudinal Left**	24.6%	7.19E-45	0.018	1.01E-44
L3	**Fronto Insular tract1 Right**	24.6%	7.60E-45	0.018	1.06E-44
MO	**Inferior Longitudinal Right**	24.5%	1.27E-44	0.018	1.77E-44

Category	Endophenotype	h2(%)	P value	SE	FDR P value
OD	**Fronto Insular tract2 Left**	24.7%	1.01E-43	0.018	1.40E-43
MD	**Fronto Insular tract1 Right**	24.1%	1.29E-43	0.018	1.79E-43
ISOVF	**Fronto Insular tract3 Right**	24.4%	2.15E-43	0.018	2.96E-43
L3	**Fronto Insular tract4 Right**	24.2%	2.09E-42	0.018	2.86E-42
MD	**Fronto Insular tract4 Right**	23.8%	5.62E-42	0.018	7.66E-42
ICVF	**Fronto Insular tract1 Left**	23.4%	1.34E-41	0.018	1.83E-41
MO	**Superior Londgitudinal Fasciculus II Right**	23.8%	1.46E-40	0.019	1.98E-40
OD	**Uncinate Right**	23.9%	2.10E-40	0.019	2.83E-40
L2	**Fronto Insular tract4 Right**	23.4%	7.97E-40	0.018	1.07E-39
ISOVF	**Fronto Insular tract5 Right**	22.6%	9.59E-39	0.018	1.28E-38
OD	**Inferior Longitudinal Right**	22.9%	1.08E-38	0.018	1.44E-38
MO	**Uncinate Left**	23.1%	6.46E-38	0.019	8.54E-38
L3	**Frontal Inferior longitudinal Left**	22.6%	7.22E-38	0.018	9.51E-38
MO	**Fronto Insular tract1 Right**	22.1%	4.62E-37	0.018	6.07E-37
MO	**Arcuate Anterior Segment Left**	22.5%	2.62E-36	0.018	3.43E-36
ISOVF	**Fronto Insular tract2 Right**	22.1%	8.41E-36	0.018	1.10E-35
L1	**Fronto Insular tract2 Left**	22.0%	3.28E-35	0.018	4.26E-35
MD	**Fronto Insular tract3 Left**	21.7%	3.94E-35	0.018	5.08E-35
MO	**Fronto Insular tract2 Right**	21.6%	3.66E-34	0.018	4.70E-34
L2	**Fronto Insular tract2 Left**	21.0%	1.03E-33	0.018	1.31E-33
OD	**Fronto Insular tract2 Right**	21.3%	2.35E-33	0.018	2.99E-33
OD	**Arcuate Anterior Segment Left**	20.7%	8.73E-32	0.018	1.11E-31
MO	**Fronto Insular tract2 Left**	20.5%	9.99E-32	0.018	1.26E-31
L1	**Fronto Insular tract1 Left**	20.4%	1.68E-31	0.018	2.12E-31
L2	**Fronto Insular tract3 Left**	20.2%	1.83E-31	0.018	2.30E-31
OD	**Inferior Longitudinal Left**	20.5%	6.13E-31	0.018	7.67E-31
L1	**Frontal Superior Longitudinal Right**	20.3%	1.60E-30	0.018	1.99E-30
MO	**Uncinate Right**	20.4%	2.28E-30	0.018	2.82E-30
ICVF	**Fronto Insular tract4 Left**	19.3%	1.52E-28	0.018	1.88E-28
L2	**Frontal Inferior longitudinal Left**	19.1%	8.21E-28	0.018	1.01E-27
ISOVF	**Fronto Insular tract1 Right**	19.0%	2.23E-26	0.018	2.74E-26
MO	**Superior Londgitudinal Fasciculus II Left**	18.8%	3.85E-26	0.018	4.71E-26
L1	**Frontal Inferior longitudinal Left**	18.8%	4.64E-26	0.018	5.64E-26
FA	**Fronto Insular tract1 Left**	18.3%	1.26E-25	0.018	1.52E-25
OD	**Arcuate Posterior Segment Right**	17.7%	3.83E-24	0.018	4.63E-24
ISOVF	**Uncinate Right**	17.4%	1.69E-23	0.018	2.03E-23
L1	**Fronto Insular tract5 Left**	17.2%	4.10E-23	0.018	4.91E-23
MD	**Fronto Insular tract5 Left**	16.8%	2.27E-22	0.018	2.71E-22
L1	**Frontal Superior Longitudinal Left**	16.8%	4.69E-22	0.018	5.58E-22
FA	**Frontal Superior Longitudinal Left**	16.6%	5.85E-21	0.018	6.92E-21
MD	**Frontal Superior Longitudinal Left**	16.2%	1.14E-20	0.018	1.34E-20
L2	**Frontal Superior Longitudinal Left**	16.3%	1.15E-20	0.018	1.35E-20
MO	**Frontal Superior Longitudinal Right**	16.5%	1.94E-20	0.018	2.27E-20
L3	**Fronto Insular tract3 Left**	16.0%	3.22E-20	0.018	3.76E-20
ISOVF	**Fronto Insular tract4 Right**	15.9%	3.61E-20	0.018	4.19E-20
OD	**Arcuate Posterior Segment Left**	16.0%	7.37E-20	0.018	8.54E-20

Category	Endophenotype	h2(%)	P value	SE	FDR P value
FA	**Frontal Superior Longitudinal Right**	16.1%	9.29E-20	0.018	1.07E-19
MD	**Frontal Superior Longitudinal Right**	16.0%	1.29E-19	0.018	1.48E-19
FA	**Frontal Inferior longitudinal Left**	15.9%	1.48E-19	0.018	1.70E-19
MO	**Frontal Inferior longitudinal Right**	16.2%	2.13E-19	0.018	2.43E-19
L3	**Fronto Insular tract5 Left**	15.5%	3.38E-19	0.018	3.84E-19
OD	**Fronto Insular tract5 Left**	15.4%	4.01E-19	0.018	4.55E-19
L3	**Fronto Insular tract2 Left**	15.6%	8.86E-19	0.018	1.00E-18
ISOVF	**Fronto Insular tract1 Left**	16.6%	2.63E-18	0.020	2.96E-18
MO	**Fronto Insular tract5 Left**	15.2%	3.72E-18	0.018	4.17E-18
ISOVF	**Frontal Inferior longitudinal Left**	14.8%	1.05E-17	0.018	1.18E-17
L2	**Fronto Insular tract5 Left**	14.5%	2.77E-17	0.018	3.08E-17
L3	**Frontal Superior Longitudinal Left**	14.4%	1.91E-16	0.018	2.12E-16
OD	**Frontal Inferior longitudinal Right**	14.6%	2.52E-16	0.018	2.79E-16
L3	**Frontal Superior Longitudinal Right**	14.3%	4.46E-16	0.018	4.91E-16
FA	**Fronto Insular tract5 Left**	14.0%	9.77E-16	0.018	1.07E-15
L2	**Frontal Superior Longitudinal Right**	13.9%	3.32E-15	0.018	3.63E-15
MD	**Fronto Insular tract2 Left**	13.7%	4.41E-15	0.018	4.81E-15
ISOVF	**Fronto Insular tract3 Left**	12.7%	3.71E-13	0.018	4.03E-13
ISOVF	**Frontal Superior Longitudinal Left**	12.5%	4.07E-13	0.018	4.40E-13
L1	**Fronto Insular tract3 Left**	12.2%	2.93E-12	0.018	3.16E-12
MO	**Frontal Superior Longitudinal Left**	11.9%	1.06E-11	0.018	1.14E-11
MO	**Arcuate Posterior Segment Right**	11.5%	2.07E-11	0.018	2.21E-11
FA	**Fronto Insular tract3 Left**	11.3%	6.24E-11	0.018	6.67E-11
ISOVF	**Frontal Superior Longitudinal Right**	11.2%	1.26E-10	0.018	1.35E-10
MD	**Fronto Insular tract4 Left**	11.0%	1.58E-10	0.018	1.68E-10
MO	**Frontal Inferior longitudinal Left**	10.7%	7.56E-10	0.018	7.99E-10
OD	**Fronto Insular tract1 Left**	10.0%	3.73E-09	0.018	3.93E-09
L3	**Fronto Insular tract4 Left**	10.0%	4.41E-09	0.018	4.63E-09
OD	**Frontal Superior Longitudinal Left**	10.0%	4.77E-09	0.018	4.99E-09
OD	**Frontal Superior Longitudinal Right**	9.9%	5.58E-09	0.018	5.82E-09
L2	**Fronto Insular tract4 Left**	9.7%	1.30E-08	0.018	1.35E-08
ISOVF	**Fronto Insular tract2 Left**	11.2%	2.77E-08	0.022	2.87E-08
MO	**Arcuate Posterior Segment Left**	9.3%	7.79E-08	0.018	8.05E-08
ISOVF	**Fronto Insular tract5 Left**	11.1%	8.78E-08	0.022	9.04E-08
MO	**Fronto Insular tract3 Left**	8.0%	2.24E-06	0.018	2.30E-06
FA	**Fronto Insular tract4 Left**	6.6%	7.15E-05	0.018	7.31E-05
OD	**Frontal Inferior longitudinal Left**	6.7%	7.78E-05	0.018	7.93E-05
L1	**Fronto Insular tract4 Left**	6.6%	8.26E-05	0.018	8.39E-05
OD	**Fronto Insular tract3 Left**	6.6%	8.39E-05	0.018	8.50E-05
MO	**Fronto Insular tract1 Left**	6.4%	1.47E-04	0.018	1.49E-04
OD	**Fronto Insular tract4 Left**	3.8%	1.32E-02	0.018	1.33E-02
MO	Fronto Insular tract4 Left	2.9%	5.05E-02	0.018	5.07E-02
ISOVF	Fronto Insular tract4 Left	2.4%	8.67E-02	0.018	8.67E-02

Appendix C

C.1 (Endo)phenotypic correlation between both resting-state functional connectivity and neural activations

Table C.1 – **Pearson Correlation between both resting-state functional connectivity and neural activations.** Bold values represents pairs of endophenotypes with significant correlation after false discovery rate correction at $p < 0.05$.

Endophenotype	PrF3op	T2ml	F3td	T1R	F3opd	F2p	T1a	F2antR	T1a.HeschlR	AG	STSp	T1	PT	F3orb	Pole	Prec	F3opdR	F3tv	T2pR	SMG	T2p	RolS	Fusa	PrecR	T3p
PrF3op↔SMG	**-0.341***	0.047	0.055	0.046	0.099	-0.034	0.028	0.042	-0.026	-0.046	0.014	0.024	-0.001	0.0	-0.008	-0.005	0.019	0.009	-0.013	0.004	0.003	-0.031	-0.013	0.003	-0.004
Pole↔PrF3op	**0.323***	-0.031	-0.027	-0.074	-0.096	0.008	-0.032	-0.018	0.002	0.034	-0.019	-0.041	-0.011	0.01	-0.017	-0.005	-0.064	0.025	0.002	0.015	-0.006	0.064	0.037	-0.018	-0.032
Pole↔T2ml	-0.012	**0.303***	0.013	**0.116***	-0.007	0.048	0.066	-0.018	0.079	0.026	-0.024	**0.114***	0.1	0.009	**0.16***	0.026	0.003	0.009	0.085	-0.021	0.0	0.012	0.049	-0.013	0.004
T2ml↔F3td	-0.024	-0.028	**0.28***	0.013	**0.143***	-0.01	-0.001	0.101	-0.003	0.032	0.058	0.005	-0.018	0.058	0.024	0.042	0.082	-0.01	-0.007	0.056	0.042	0.031	-0.001	0.019	0.043
PrF3op↔STSp	**0.261***	-0.012	-0.08	0.007	**-0.128***	-0.038	-0.012	-0.021	0.014	0.017	-0.039	-0.017	0.023	0.014	-0.025	0.024	-0.066	0.054	0.021	0.027	-0.025	0.074	0.019	0.064	-0.019
T1a↔T1R	0.063	0.058	0.075	**0.256***	0.07	0.01	**0.169***	0.064	**0.115***	0.016	0.051	0.098	0.073	0.047	0.109	0.064	0.108	0.008	0.103	-0.001	0.019	0.03	0.079	0.062	0.06
Pole↔F3opd	-0.041	-0.032	**0.153***	-0.005	**0.254***	-0.11	-0.042	0.077	-0.055	-0.024	-0.032	0.015	-0.061	0.005	-0.057	0.057	0.087	-0.102	-0.025	-0.002	0.009	0.028	-0.019	0.04	0.048
Pole↔F2p	-0.005	-0.026	-0.001	-0.005	-0.026	**0.251***	0.017	0.058	0.087	-0.009	-0.022	-0.011	-0.01	0.031	-0.027	-0.038	-0.011	0.101	-0.003	0.053	-0.021	0.07	0.013	0.03	0.0
SMG↔F3td	0.064	-0.014	**-0.249***	-0.039	-0.111	-0.037	0.031	**-0.126***	-0.012	0.021	-0.029	-0.042	0.017	0.012	0.023	-0.068	-0.037	0.033	-0.012	-0.008	-0.048	-0.009	-0.041	0.011	-0.047
F3opd↔SMG	0.062	-0.011	-0.107	-0.093	**-0.238***	**0.121***	0.023	-0.056	0.031	0.001	-0.001	-0.034	-0.005	-0.015	-0.023	-0.013	**-0.117***	0.101	0.037	0.028	0.035	0.065	0.001	0.025	0.01
PrF3op↔F3tv	**0.181***	0.105	0.028	0.02	0.018	**0.234***	0.033	0.034	0.035	0.088	0.105	0.028	0.042	0.086	0.097	0.001	0.052	0.05	0.017	0.051	0.071	0.051	0.092	0.04	0.071
F2p↔SMG	0.038	0.006	**0.128***	0.095	**0.173***	**-0.229***	-0.06	0.087	-0.005	-0.042	0.043	0.014	-0.02	0.004	-0.012	0.092	0.087	-0.014	0.033	-0.062	-0.052	-0.026	-0.042	-0.056	-0.002
T1a↔T1a.HeschlR	0.015	0.036	0.001	0.061	0.049	0.03	**0.228***	-0.05	**0.219***	0.062	0.038	0.025	-0.032	0.014	**0.144***	0.06	0.028	0.022	0.035	0.002	0.016	0.013	0.045	0.015	0.041
PrF3op↔T1a	**0.228***	-0.015	-0.04	-0.008	-0.055	-0.069	0.047	-0.026	0.04	0.014	-0.048	0.008	0.014	0.032	-0.034	0.058	-0.036	0.035	0.027	-0.017	-0.041	0.006	0.021	-0.005	-0.016
SMG↔F2antR	0.042	0.064	-0.077	-0.058	-0.019	0.056	0.041	**-0.227***	0.014	0.027	0.025	-0.022	0.023	0.015	0.088	-0.059	-0.02	0.028	-0.028	-0.089	-0.0	0.026	-0.008	-0.003	-0.004
PrF3op↔T2pR	**-0.226***	-0.039	0.044	0.01	0.053	-0.095	-0.045	-0.008	-0.02	-0.045	-0.022	0.004	0.025	-0.04	-0.014	0.001	0.025	-0.035	-0.046	-0.016	0.019	-0.011	0.003	0.042	0.025
F3opd↔T2ml	-0.077	0.012	**0.12***	0.046	**0.22***	-0.05	-0.009	0.035	-0.007	-0.058	0.009	0.034	0.009	0.016	-0.001	-0.002	0.085	-0.087	-0.049	-0.02	-0.007	-0.017	-0.007	0.035	-0.006
PT↔T1a	0.082	0.049	0.034	0.03	0.085	0.026	**0.21***	0.008	0.075	0.04	0.041	-0.017	**0.143***	0.011	**0.138***	0.086	0.057	-0.033	0.056	-0.021	0.033	0.011	0.034	0.025	0.02
T2ml↔RolS	0.054	**0.21***	0.01	0.033	0.044	0.04	-0.005	0.031	0.016	0.082	0.018	-0.066	-0.035	0.069	0.021	0.05	0.029	0.042	0.06	0.052	0.078	**0.115***	0.025	0.068	0.047
AG↔F3tv	-0.029	-0.103	0.047	-0.006	0.087	0.026	-0.069	0.063	-0.063	**-0.209***	0.047	0.004	-0.015	-0.058	-0.007	-0.009	0.048	-0.044	-0.007	-0.052	-0.02	-0.056	-0.023	-0.016	0.009
F3opd↔T1a	0.008	-0.004	**0.116***	0.109	**0.209***	-0.052	-0.001	0.093	0.068	0.049	0.044	0.096	0.026	0.012	-0.001	0.041	0.113	-0.028	0.009	-0.037	**0.116***	0.077	0.071	0.088	0.098
T2ml↔PrF3op	**0.207***	-0.029	-0.104	**-0.118***	**-0.158***	-0.036	-0.041	-0.031	-0.042	-0.01	-0.059	-0.076	-0.054	-0.011	-0.038	-0.027	-0.073	0.018	-0.036	-0.025	-0.004	0.028	-0.019	-0.035	-0.012
Prec↔F3tv	-0.051	0.065	**0.153***	0.03	**0.207***	-0.017	-0.012	0.041	0.0	-0.015	0.047	0.051	0.033	0.042	0.032	0.062	0.048	-0.025	-0.034	0.018	-0.007	0.002	0.009	-0.013	0.002
Pole↔F2antR	-0.018	0.056	0.112	0.059	0.086	0.016	0.044	**0.201***	0.018	0.062	0.071	0.031	0.047	0.066	-0.005	0.106	0.045	-0.003	0.06	0.005	0.073	0.047	0.064	0.041	0.05
Pole↔STSp	-0.036	-0.069	0.026	0.008	0.01	0.002	0.051	-0.025	0.047	-0.081	**0.201***	-0.036	0.024	-0.056	0.004	-0.035	0.001	0.002	0.005	-0.036	0.017	-0.013	-0.028	0.025	0.012
T1↔T1a.HeschlR	0.002	**0.118***	-0.057	0.1	0.013	0.086	0.083	-0.072	0.08	0.05	0.047	**0.197***	**0.115***	0.01	**0.134***	0.005	-0.009	-0.002	0.01	0.004	0.021	0.016	0.053	0.06	-0.005
T2ml↔T1a	0.011	**0.196***	0.007	0.017	-0.056	0.056	**0.115***	-0.002	0.067	-0.05	-0.031	0.006	-0.001	-0.009	0.032	-0.029	-0.013	-0.013	0.061	0.013	-0.047	-0.018	-0.01	0.021	-0.002
RolS↔T1R	0.079	0.085	0.038	**0.195***	0.041	0.002	-0.024	0.063	0.034	0.057	0.01	-0.027	-0.015	-0.008	-0.027	0.032	0.069	0.003	0.076	0.064	-0.025	0.041	0.032	0.011	0.022
Pole↔F3td	-0.071	0.017	**0.192***	0.056	0.04	-0.039	0.002	0.079	-0.019	0.021	0.025	0.045	0.012	-0.045	-0.006	0.022	0.024	-0.081	-0.006	-0.044	0.019	-0.03	0.057	-0.041	-0.001
PrF3op↔T1R	**0.192***	-0.002	-0.006	-0.041	-0.072	0.081	-0.017	-0.035	-0.003	0.045	-0.021	-0.041	-0.037	0.013	-0.032	-0.042	-0.067	-0.008	0.017	0.012	-0.012	0.023	0.059	-0.037	-0.005
T2ml↔STSp	0.0	0.077	-0.012	0.062	0.015	0.008	0.01	-0.032	0.032	0.017	**0.186***	**0.129***	**0.142***	-0.045	0.022	0.013	-0.0	-0.003	0.006	-0.056	0.021	0.033	0.038	-0.013	0.015
F2p↔STSp	-0.021	0.081	-0.018	0.009	0.004	0.078	**0.185***	-0.052	**0.13***	-0.006	0.082	0.035	0.068	-0.048	0.074	0.015	0.03	0.041	0.029	0.02	0.095	0.099	0.059	0.055	0.074
F2p↔T2ml	-0.065	0.021	0.004	-0.03	0.032	**0.185***	0.02	0.009	-0.042	-0.046	-0.045	0.043	0.07	0.055	0.086	-0.068	-0.006	0.022	-0.032	0.004	-0.065	0.028	-0.022	-0.025	-0.038
PT↔T1a.HeschlR	0.038	0.074	0.053	0.067	0.091	0.063	**0.145***	0.01	**0.185***	0.038	0.111	0.041	**0.182***	0.027	**0.112***	0.06	0.093	0.022	0.068	0.022	0.017	0.003	0.025	0.023	0.018
T2ml↔T1R	-0.016	0.037	0.022	**0.184***	-0.026	0.014	-0.035	0.073	0.047	-0.057	-0.02	-0.013	-0.065	0.003	0.038	0.013	0.1	0.004	0.099	0.017	-0.036	0.003	0.044	0.028	-0.015
PT↔T1	0.042	**0.136***	0.062	**0.181***	0.063	0.04	0.111	0.02	**0.184***	0.083	0.102	**0.151***	**0.171***	0.052	**0.146***	0.062	**0.141***	0.061	0.093	0.015	0.107	0.06	0.087	0.026	0.089
T1a.HeschlR↔T1R	0.031	0.071	0.023	**0.182***	0.005	0.037	0.057	-0.019	**0.115***	0.042	0.037	0.033	0.046	-0.009	0.1	0.035	0.009	-0.005	0.067	-0.049	0.004	-0.002	0.043	-0.024	0.027
AG↔T1R	-0.007	-0.072	0.003	**-0.179***	-0.029	-0.045	-0.051	-0.039	-0.083	0.014	-0.065	-0.039	-0.006	-0.03	-0.103	-0.03	-0.082	-0.023	-0.067	0.06	0.001	-0.005	-0.046	-0.048	0.005
F3opd↔F2antR	-0.047	-0.064	-0.031	0.011	**-0.174***	-0.024	-0.07	**0.178***	-0.026	-0.036	-0.069	-0.077	-0.002	-0.027	-0.042	0.019	0.035	-0.011	0.028	0.017	-0.033	-0.037	0.007	0.021	-0.015
PT↔T1R	0.041	0.045	0.048	**0.178***	0.036	-0.018	0.045	0.053	0.082	0.084	-0.003	-0.011	0.099	-0.001	0.044	0.059	0.037	-0.035	0.099	0.015	0.041	-0.025	0.069	0.027	0.028
T1↔F2antR	0.001	-0.028	-0.041	-0.069	-0.03	-0.049	-0.083	-0.103	-0.013	0.002	-0.013	**-0.177***	-0.061	0.024	0.013	-0.039	0.034	0.049	0.008	0.038	0.012	-0.002	-0.006	-0.024	-0.001
F2antR↔T1R	-0.016	-0.081	0.068	**-0.175***	0.05	-0.041	-0.047	**0.12***	-0.049	-0.003	-0.03	0.005	-0.035	-0.023	-0.05	0.005	-0.028	-0.004	-0.084	-0.009	0.026	0.011	-0.027	0.002	0.009
F3td↔F2antR	0.02	-0.043	**-0.175***	0.007	-0.052	-0.005	0.06	-0.092	0.047	0.021	0.05	0.029	0.021	-0.013	0.019	0.019	-0.012	0.019	-0.005	0.004	0.01	-0.005	-0.037	0.032	-0.008
T2ml↔F2antR	-0.006	**-0.173***	0.07	0.023	0.039	-0.029	0.055	**0.174***	0.046	0.021	0.065	-0.008	0.001	-0.061	0.03	-0.004	0.058	-0.03	0.01	-0.05	0.012	0.013	-0.021	0.033	0.028
AG↔F2antR	-0.039	-0.044	0.058	0.017	0.061	0.019	-0.082	0.085	-0.036	**-0.173***	0.027	0.001	-0.029	-0.026	-0.076	0.025	0.056	-0.035	-0.019	-0.01	0.006	-0.011	0.011	-0.004	0.029
AG↔T1a	0.002	0.058	-0.035	0.06	-0.071	-0.03	-0.083	0.011	-0.078	**0.172***	0.001	-0.02	-0.005	-0.004	0.014	-0.008	-0.049	-0.001	-0.016	-0.019	-0.006	0.011	-0.018	-0.001	-0.056
Prec↔F3opd	0.054	0.006	**-0.119***	-0.042	**-0.172***	0.016	0.03	-0.065	0.008	0.012	-0.045	0.012	0.021	-0.056	-0.024	-0.014	-0.076	0.052	-0.034	-0.023	-0.014	0.027	0.011	-0.016	-0.023
PrF3op↔F2antR	**-0.17***	0.0	0.065	0.026	0.049	0.003	-0.05	**0.136***	-0.032	-0.044	-0.004	-0.057	-0.072	0.047	-0.01	-0.049	0.048	-0.052	-0.07	-0.079	-0.037	-0.072	-0.026	0.019	-0.004
T2ml↔T1	-0.094	**-0.128***	-0.056	-0.101	-0.06	-0.099	-0.006	-0.045	-0.06	**-0.127***	-0.056	0.015	**-0.152***	**-0.169***	**-0.147***	-0.11	-0.046	-0.104	-0.056	-0.037	-0.029	-0.064	-0.089	-0.054	0.004
Pole↔T1a	-0.009	0.05	-0.034	-0.044	0.009	0.057	**0.167***	-0.049	0.041	0.072	0.035	0.046	0.035	0.054	**0.169***	-0.021	0.03	0.071	0.007	-0.0	0.023	-0.006	0.046	-0.001	0.041
PrF3op↔T3p	**-0.143***	0.049	0.112	0.069	**0.168***	-0.032	0.033	0.057	0.007	0.006	0.065	0.101	0.082	0.034	0.031	0.026	0.079	-0.012	0.015	-0.018	0.059	-0.021	0.03	0.005	0.026
Prec↔F3td	0.01	-0.001	**-0.168***	-0.02	-0.06	0.006	0.051	-0.088	0.016	-0.001	0.033	-0.016	-0.024	-0.005	0.018	**-0.116***	-0.028	-0.009	-0.019	-0.028	0.004	-0.038	-0.043	-0.055	-0.024
Prec↔T3p	0.035	0.037	-0.018	0.009	0.01	0.097	0.031	-0.085	0.074	-0.004	0.018	0.009	-0.013	-0.077	-0.002	**-0.166***	-0.042	-0.058	-0.011	-0.067	-0.003	0.004	-0.017	0.025	-0.059
F3opdR↔F2antR	0.063	**0.128***	0.014	0.089	0.051	0.056	**0.166***	0.0	0.09	0.037	0.076	**0.138***	**0.115***	0.034	0.108	0.074	-0.035	0.046	0.063	0.037	-0.004	0.056	0.033	0.051	0.022
T2ml↔AG	0.031	**-0.166***	-0.046	-0.029	-0.063	-0.053	-0.012	0.005	0.002	**0.117***	-0.096	-0.083	-0.082	0.015	-0.039	-0.003	-0.032	0.001	-0.034	0.038	-0.017	-0.013	-0.004	0.017	-0.013
T1↔T1a	0.005	0.055	-0.016	0.085	-0.004	-0.029	0.105	0.0	0.036	0.017	0.037	**0.163***	-0.016	0.008	0.096	0.023	-0.008	-0.008	0.006	-0.057	0.01	0.018	0.025	0.071	0.026
F3opd↔T1R	-0.045	-0.014	0.06	**0.163***	**0.135***	-0.085	-0.01	0.083	0.024	0.018	-0.024	0.043	0.048	-0.0	0.003	0.046	0.079	-0.083	0.077	0.002	0.04	0.008	0.003	0.038	0.043
PT↔STSp	-0.096	-0.1	-0.081	-0.078	-0.107	-0.077	**-0.162***	0.044	**-0.116***	-0.038	-0.097	-0.046	-0.058	-0.041	-0.087	-0.051	-0.06	-0.066	-0.016	-0.025	-0.03	-0.052	-0.044	-0.049	0.0
PT↔RolS	0.037	0.002	0.045	-0.096	0.037	0.017	0.026	-0.02	-0.044	-0.014	0.04	-0.03	**0.162***	0.054	0.053	-0.021	0.019	0.031	-0.094	-0.021	-0.005	0.017	0.007	-0.025	-0.035
F3opd↔STSp	0.005	-0.032	0.101	0.054	**0.159***	-0.031	-0.079	0.105	-0.042	-0.072	0.031	-0.013	-0.057	0.021	-0.073	0.004	0.097	-0.055	0.041	0.034	0.032	-0.008	-0.023	0.01	0.034
Fusa↔T3p	0.052	**0.122***	-0.024	**0.158***	0.059	0.017	**0.159***	-0.04	**0.153***	**0.137***	**0.125***	**0.139***	**0.137***	0.013	**0.145***	0.067	0.095	0.006	0.07	0.004	0.041	0.068	-0.003	0.08	0.025
F3tv↔F3opdR	-0.0	0.016	**0.157***	0.074	**0.128***	0.001	-0.057	0.103	0.012	0.012	0.043	0.073	0.062	0.036	-0.033	0.11	0.09	-0.014	-0.014	0.071	0.018	0.028	-0.002	0.063	0.052
F3tv↔T1R	0.048	0.041	**-0.124***	**-0.156***	-0.059	0.025	0.056	-0.101	-0.01	0.039	0.034	0.026	0.057	-0.003	-0.032	-0.043	-0.111	0.071	**-0.121***	0.004	-0.036	-0.003	-0.029	-0.038	-0.067
T1↔T1R	0.059	0.113	-0.013	0.023	0.032	0.0	**0.116***	-0.045	**0.133***	0.11	0.096	**0.156***	**0.117***	-0.037	0.025	0.029	-0.026	0.007	-0.023	-0.024	0.069	0.031	-0.025	0.024	0.061
Pole↔AG	0.022	-0.001	-0.059	0.034	-0.078	-0.056	-0.047	0.013	0.016	**0.154***	**-0.115***	-0.018	-0.056	-0.008	-0.093	0.02	-0.056	-0.046	0.018	0.011	-0.028	-0.019	0.021	-0.001	-0.039
STSp↔F3td	-0.036	0.02	**0.151***	0.022	0.071	-0.06	-0.086	0.11	-0.051	0.004	-0.07	0.04	0.027	0.001	-0.024	0.068	0.023	-0.017	-0.024	0.016	-0.013	-0.002	0.022	0.024	0.001
F3td↔T1R	0.058	0.07	**0.151***	-0.005	0.063	0.051	0.005	-0.031	0.001	0.049	0.044	-0.008	0.021	0.008	0.044	0.049	-0.05	-0.013	-0.018	0.013	0.019	-0.013	0.001	-0.012	0.015
T2p↔T1a.HeschlR	-0.043	-0.093	-0.039	-0.088	-0.058	-0.037	**-0.125***	-0.051	-0.072	**-0.151***	-0.091	-0.093	-0.104	-0.037	**-0.149***	-0.087	-0.033	-0.026	-0.07	-0.008	-0.091	-0.043	-0.102	-0.048	-0.088
F3opd↔T1	-0.009	0.023	0.091	0.064	**0.122***	0.006	0.082	0.094	0.018	0.015	0.024	**0.149***	0.061	0.001	0.078	0.045	0.066	0.016	0.049	-0.034	0.043	0.022	0.022	0.079	0.063
AG↔F3orb	-0.018	0.062	0.001	0.012	-0.006	-0.036	0.005	-0.011	-0.009	**0.149***	-0.031	-0.031	-0.029	-0.005	-0.059	-0.029	-0.026	-0.094	0.002	0.028	-0.004	-0.042	0.037	-0.012	-0.005
STSp↔F2antR	0.023	0.05	0.049	0.055	0.02	-0.029	-0.025	0.086	0.025	**0.121***	**-0.147***	0.011	-0.012	0.043	-0.012	-0.001	-0.048	-0.052	0.013	0.016	-0.038	-0.009	-0.001	-0.023	-0.032

Endophenotype	PrF3op	T2ml	F3td	T1R	F3opd	F2p	T1a	F2antR	T1a.HeschlR	AG	STSp	T1	PT	F3orb	Pole	Prec	F3opdR	F3tv	T2pR	SMG	T2p	RolS	Fusa	PrecR	T3p
T2p↔F2antR	0.009	0.009	-0.053	-0.075	-0.058	0.03	-0.014	**-0.147***	-0.079	-0.006	-0.032	0.006	0.023	-0.026	0.018	0.0	-0.077	0.015	-0.048	-0.016	-0.055	0.01	-0.001	-0.072	-0.046
Prec↔SMG	0.049	0.028	-0.054	0.037	0.001	0.025	0.026	-0.037	-0.005	0.04	-0.014	0.003	0.018	-0.022	0.024	**-0.146***	0.029	-0.03	0.044	0.105	-0.033	0.014	-0.038	0.025	-0.031
SMG↔T1R	-0.011	0.0	-0.01	**-0.146***	0.004	-0.02	-0.001	-0.027	-0.058	0.028	0.005	-0.077	-0.082	-0.006	-0.021	0.037	-0.026	0.031	-0.06	-0.032	0.071	-0.019	0.019	-0.001	0.019
Prec↔T1	-0.05	-0.02	0.055	0.05	0.063	-0.074	-0.026	0.065	-0.021	-0.047	0.013	-0.006	0.044	0.017	-0.012	**0.143***	0.049	0.022	-0.026	0.007	0.049	0.011	-0.005	0.001	0.008
AG↔T3p	0.011	-0.017	0.033	-0.031	0.057	0.017	-0.045	0.029	0.003	**-0.142***	-0.047	-0.048	0.005	0.004	-0.028	0.015	0.041	0.007	-0.013	-0.004	-0.007	-0.005	0.057	-0.013	-0.0
Pole↔T1R	-0.11	-0.041	-0.045	**0.141***	-0.061	-0.027	-0.07	0.029	-0.034	-0.089	-0.048	-0.019	-0.019	-0.015	0.055	-0.049	0.049	-0.027	0.055	-0.007	-0.053	-0.06	-0.017	-0.003	-0.041
Prec↔PrF3op	**-0.14***	0.047	0.022	0.054	0.056	-0.03	0.034	-0.016	-0.03	-0.042	0.042	0.036	0.005	-0.032	0.038	-0.044	-0.022	-0.007	0.014	-0.026	-0.065	-0.07	-0.038	0.007	-0.058
STSp↔SMG	-0.056	0.033	-0.031	-0.066	-0.055	-0.015	0.05	-0.077	-0.025	0.041	**-0.14***	-0.054	-0.061	-0.014	0.03	-0.071	-0.105	-0.052	-0.074	-0.097	-0.049	-0.038	0.0	-0.01	-0.049
Prec↔Pole	-0.007	0.016	0.008	0.052	-0.015	-0.021	0.041	0.018	-0.046	0.056	0.052	0.002	0.007	0.023	0.101	**0.138***	-0.017	-0.008	0.017	-0.012	0.004	-0.0	0.028	0.012	0.004
T2ml↔F3opdR	-0.0	**-0.137***	-0.051	-0.035	-0.046	-0.051	-0.038	0.079	-0.037	-0.011	-0.042	-0.102	-0.106	-0.021	-0.065	-0.0	**0.127***	-0.009	0.023	0.004	0.01	0.001	0.018	0.011	-0.025
Fusa↔T2p	0.065	0.045	-0.024	0.026	0.052	0.022	**0.136***	0.008	0.07	0.077	0.008	0.089	0.055	-0.005	0.077	0.05	0.048	0.013	-0.031	0.039	0.052	0.053	0.057	0.06	0.064
T1a↔STSp	-0.071	-0.058	0.054	-0.065	0.038	0.052	-0.064	-0.003	-0.059	**-0.135***	**0.114***	-0.036	-0.031	-0.025	-0.014	-0.016	-0.022	0.023	-0.02	0.011	0.02	-0.032	-0.021	0.01	0.009
T2ml↔T1a.HeschlR	-0.017	0.041	0.012	-0.023	-0.024	0.01	-0.063	0.023	0.043	0.021	-0.053	**-0.134***	-0.031	-0.037	-0.054	0.036	0.059	0.007	0.035	0.04	0.022	0.002	-0.025	0.106	-0.018
F2p↔AG	0.046	0.039	-0.047	0.047	-0.027	**-0.117***	-0.001	-0.007	-0.017	**0.134***	-0.01	-0.038	-0.002	0.011	0.004	-0.019	0.008	-0.048	0.009	0.019	-0.029	-0.008	0.044	-0.003	-0.023
Prec↔T2ml	0.033	-0.038	-0.067	-0.081	**-0.132***	-0.095	-0.051	-0.026	-0.069	-0.043	-0.058	**-0.117***	-0.048	-0.022	-0.102	**0.131***	-0.035	-0.039	-0.042	-0.012	-0.066	-0.023	-0.063	-0.019	-0.078
F3opd↔F2p	**0.13***	0.029	0.046	-0.018	0.06	0.076	0.007	-0.064	-0.012	0.053	0.031	0.014	0.029	0.038	0.023	0.023	0.026	-0.029	-0.025	0.013	-0.047	0.013	0.031	0.022	0.002
Pole↔F3tv	-0.022	0.043	-0.058	-0.056	-0.069	0.039	0.042	-0.097	0.018	0.036	-0.01	-0.034	-0.003	0.044	0.017	-0.013	-0.049	**0.13***	-0.019	0.05	0.08	0.013	0.013	0.006	0.021
T2ml↔SMG	0.048	**-0.13***	0.067	-0.011	0.094	0.047	-0.029	0.05	0.006	-0.032	0.098	0.104	0.089	0.067	-0.042	0.033	0.028	0.064	0.012	0.04	0.039	0.027	0.007	-0.026	0.04
F3tv↔F2antR	0.083	0.067	0.067	0.06	**0.115***	0.037	0.058	**-0.13***	0.029	0.045	0.054	0.088	0.078	0.059	0.037	0.031	0.015	0.023	0.05	0.078	0.069	0.111	0.052	0.022	0.046
F2p↔F2antR	-0.019	-0.004	-0.002	-0.001	-0.017	**-0.129***	0.011	0.099	0.0	-0.037	-0.06	-0.04	-0.028	-0.039	-0.003	0.042	0.027	-0.025	0.015	-0.072	-0.033	-0.004	-0.046	0.005	-0.016
Pole↔T3p	-0.019	-0.001	-0.005	0.054	0.022	0.019	**0.129***	-0.026	0.063	0.023	0.084	0.05	**0.125***	0.059	0.078	0.035	0.05	0.076	0.052	0.012	0.022	0.081	-0.008	0.098	0.063
F3tv↔STSp	-0.006	0.057	-0.041	0.049	-0.068	-0.02	0.002	-0.045	0.03	0.112	**-0.128***	0.014	-0.013	0.011	0.024	-0.004	-0.065	0.02	-0.006	0.036	-0.031	-0.011	-0.016	0.015	-0.058
T1↔F3orb	-0.061	**-0.128***	-0.069	-0.048	-0.083	-0.022	-0.05	-0.0	-0.056	-0.078	-0.068	0.019	-0.029	-0.084	-0.079	-0.042	-0.056	-0.044	-0.038	-0.058	-0.067	-0.048	-0.076	-0.049	-0.046
AG↔STSp	0.04	**0.128***	0.02	0.091	0.048	0.06	0.06	0.037	0.071	**0.12***	-0.0	0.056	0.051	0.055	0.086	0.018	0.095	0.037	0.07	0.042	0.053	-0.016	0.038	-0.009	0.064
F3tv↔SMG	0.081	0.068	0.113	0.075	**0.127***	-0.035	0.008	0.104	-0.04	0.066	0.083	0.033	0.005	0.033	0.084	0.054	0.079	**-0.118***	0.055	-0.103	0.017	-0.024	0.047	-0.049	0.036
Pole↔T2pR	-0.009	0.074	-0.018	0.049	-0.053	-0.015	0.052	-0.02	0.042	0.02	0.024	-0.002	0.01	-0.004	0.049	-0.028	-0.011	-0.021	**0.126***	-0.017	0.016	-0.026	-0.037	0.018	-0.018
PrF3op↔RolS	**0.126***	0.03	0.051	0.006	0.093	0.03	-0.06	-0.019	-0.041	0.049	0.014	0.025	0.015	0.006	0.015	0.044	-0.019	-0.026	-0.016	0.023	0.014	0.054	0.019	-0.026	0.052
Prec↔T1a	0.017	0.017	0.039	-0.03	-0.019	0.004	0.051	0.019	-0.018	0.08	0.047	0.043	0.022	0.048	0.068	**0.124***	-0.039	-0.004	-0.01	-0.005	-0.005	0.026	0.031	0.004	0.007
T2ml↔F3tv	-0.043	0.014	**-0.124***	-0.027	-0.104	0.032	0.061	**-0.12***	0.063	0.029	0.011	-0.052	-0.019	0.004	0.025	-0.049	-0.091	0.111	-0.084	-0.024	-0.005	-0.033	0.028	-0.024	-0.023
Prec↔F2antR	**-0.124***	0.015	-0.045	0.015	0.023	-0.014	0.011	-0.031	0.024	-0.028	-0.033	-0.028	-0.009	0.013	-0.073	-0.1	0.036	-0.035	0.022	0.026	0.019	-0.047	-0.009	-0.027	0.001
Fusa↔STSp	-0.037	**-0.119***	-0.024	-0.048	-0.038	-0.017	-0.1	0.006	-0.018	-0.079	**-0.123***	-0.041	-0.019	-0.033	-0.069	-0.008	-0.035	0.018	-0.065	-0.018	-0.045	0.006	-0.051	-0.029	-0.049
F3opd↔AG	0.024	0.055	-0.07	-0.063	**-0.123***	0.058	0.102	-0.098	0.025	0.068	0.007	-0.024	0.042	0.025	-0.009	-0.019	-0.039	0.052	-0.005	-0.035	0.002	0.019	0.026	-0.008	-0.041
PT↔T2pR	0.015	-0.025	0.018	**-0.123***	0.005	0.056	-0.066	-0.057	-0.065	-0.016	0.008	-0.027	-0.029	0.016	-0.026	-0.004	-0.017	0.03	-0.086	0.008	-0.024	0.005	-0.047	-0.038	-0.039
F3tv↔T1a.HeschlR	-0.021	-0.044	-0.033	0.007	-0.053	-0.026	-0.078	0.005	**-0.122***	-0.017	-0.071	-0.061	-0.039	-0.051	0.013	-0.037	0.025	-0.026	0.026	-0.002	0.015	-0.017	0.037	-0.014	0.024
T3p↔F3opdR	-0.012	-0.05	-0.024	-0.035	-0.048	-0.014	0.014	-0.02	-0.02	-0.031	-0.017	-0.07	-0.004	-0.02	0.009	-0.045	**-0.122***	0.005	0.03	-0.033	-0.029	-0.026	-0.033	0.0	-0.025
SMG↔F3opdR	0.041	0.018	0.017	-0.023	-0.038	0.05	0.024	0.041	0.007	0.041	-0.048	0.021	0.012	0.043	-0.051	-0.035	-0.112	0.06	0.043	**0.121***	0.002	0.039	0.046	0.023	-0.021
F3orb↔T2pR	-0.042	-0.023	-0.036	0.038	-0.033	-0.024	-0.017	-0.028	-0.033	-0.04	-0.052	-0.002	-0.029	-0.084	-0.049	-0.011	-0.015	-0.035	**0.121***	-0.027	-0.022	-0.003	-0.011	0.006	-0.008
F3opd↔F3orb	0.002	0.093	0.073	0.072	**0.12***	0.059	0.047	0.022	0.036	0.052	0.08	0.063	0.01	0.044	0.077	0.029	0.04	-0.033	0.024	0.011	0.002	-0.002	0.072	0.016	0.052
AG↔T1a.HeschlR	-0.017	0.001	-0.066	-0.005	-0.058	-0.013	-0.006	-0.017	-0.053	-0.081	-0.048	-0.042	-0.046	-0.042	0.003	-0.096	-0.087	-0.07	-0.074	**-0.12***	-0.107	-0.038	-0.035	0.003	-0.104
F3opdR↔T1R	-0.01	-0.025	-0.002	-0.098	0.05	0.021	-0.002	-0.008	-0.024	-0.03	0.022	-0.038	-0.005	0.015	0.062	0.032	**0.118***	0.004	-0.073	0.003	0.004	-0.012	-0.024	0.017	0.02
F2p↔T1a	-0.05	-0.055	-0.046	-0.073	**-0.118***	0.084	-0.061	0.008	-0.009	-0.043	-0.075	-0.018	-0.048	-0.009	-0.069	-0.053	-0.037	0.047	-0.012	0.008	-0.031	-0.013	-0.014	0.013	-0.043
PrF3op↔F3td	**-0.116***	0.053	0.107	0.019	**0.117***	-0.052	0.013	0.021	-0.019	-0.002	-0.018	0.039	0.036	0.047	0.01	0.058	0.023	0.033	-0.009	0.019	0.035	0.039	0.013	-0.002	0.051
F2p↔T2pR	0.004	-0.039	0.019	0.004	-0.03	**-0.117***	-0.027	0.005	-0.051	-0.067	-0.081	-0.038	-0.013	-0.038	-0.036	-0.008	0.011	-0.033	-0.063	-0.024	-0.039	-0.036	-0.024	-0.058	-0.058
T1a↔T2pR	0.003	-0.017	-0.008	0.033	-0.052	-0.025	-0.071	0.069	-0.013	-0.001	-0.01	-0.029	-0.003	0.018	0.032	0.034	0.026	0.061	**0.117***	0.01	0.027	0.007	0.007	-0.005	-0.005
F3opd↔T1a.HeschlR	-0.001	0.001	-0.049	**-0.116***	-0.021	-0.006	0.023	-0.073	0.003	0.049	0.037	-0.024	-0.018	0.037	-0.007	-0.023	-0.066	0.003	-0.088	0.001	-0.005	-0.003	-0.026	-0.02	-0.012
Fusa↔AG	-0.022	0.028	0.025	0.016	0.05	0.058	0.046	-0.011	-0.001	**-0.116***	0.098	0.055	0.013	-0.004	0.031	-0.045	0.027	-0.015	0.026	-0.012	0.015	0.008	-0.046	-0.02	-0.005
RolS↔T1a.HeschlR	-0.021	**-0.116***	0.01	-0.079	-0.032	-0.053	-0.021	-0.011	0.033	-0.028	-0.059	-0.098	-0.105	-0.057	-0.102	-0.032	0.004	0.005	-0.05	0.03	0.011	-0.008	-0.017	-0.066	-0.0
F3td↔T3p	0.068	0.052	**-0.115***	-0.029	-0.04	0.093	0.071	-0.074	0.067	0.029	0.062	0.04	0.024	0.006	0.031	-0.051	0.007	0.058	-0.009	-0.023	0.038	0.027	0.009	0.008	0.026
F2p↔T1	0.022	0.003	-0.009	-0.014	-0.022	**0.115***	-0.014	-0.0	-0.058	0.036	0.068	0.07	-0.035	-0.002	0.019	0.007	0.019	0.03	0.01	0.03	0.044	-0.007	0.004	0.009	0.035
PT↔F3tv	-0.025	-0.101	0.005	-0.099	-0.031	-0.033	-0.07	-0.001	-0.091	-0.057	-0.027	-0.003	**-0.114***	-0.023	-0.055	-0.047	0.004	0.03	-0.035	-0.09	0.027	-0.011	-0.032	-0.057	0.015
T2ml↔T2pR	-0.021	**-0.114***	-0.004	0.024	0.014	-0.034	0.012	-0.056	0.008	-0.034	-0.029	0.029	0.044	-0.017	0.05	-0.021	-0.026	-0.028	0.022	-0.025	-0.028	-0.026	-0.073	-0.055	-0.045
PT↔PrF3op	**-0.114***	-0.027	-0.055	0.019	-0.015	-0.039	-0.027	-0.073	-0.036	-0.026	-0.024	-0.008	0.032	-0.07	-0.003	-0.031	-0.064	0.014	-0.041	-0.051	-0.011	-0.004	-0.031	0.018	-0.031
F3td↔RolS	-0.008	-0.007	**0.113***	0.053	0.03	-0.025	-0.106	0.106	-0.034	-0.028	-0.047	0.027	0.016	-0.029	-0.099	0.019	0.047	-0.011	0.068	0.027	-0.018	-0.013	-0.015	0.034	0.043
T2p↔T3p	0.016	0.041	-0.024	0.047	-0.032	-0.021	0.078	-0.07	0.074	0.052	0.077	0.015	0.066	-0.005	0.112	0.04	-0.001	-0.054	-0.009	-0.025	0.013	-0.005	-0.019	-0.014	-0.013
F2p↔F3orb	-0.005	0.004	-0.038	0.021	-0.001	0.089	0.113	-0.012	0.083	0.003	0.049	0.035	0.059	0.005	0.072	0.01	0.008	0.075	-0.001	-0.025	0.037	0.046	-0.039	0.017	0.001
AG↔F3td	-0.028	-0.066	-0.112	-0.033	-0.053	-0.03	0.024	-0.01	0.028	-0.04	-0.015	-0.032	-0.013	-0.038	-0.021	-0.04	-0.004	-0.002	0.004	-0.048	0.014	-0.018	-0.065	0.004	0.01
Prec↔PT	-0.078	0.023	0.028	-0.061	-0.044	-0.012	-0.026	0.113	-0.026	-0.018	-0.045	-0.015	-0.016	0.001	-0.023	-0.032	-0.054	-0.008	-0.053	-0.054	0.026	-0.064	-0.024	0.019	0.008
SMG↔T2pR	-0.003	0.049	0.085	-0.024	0.106	0.044	-0.062	0.017	0.006	0.029	0.034	-0.008	-0.022	0.049	-0.006	0.001	0.019	-0.002	-0.112	0.088	0.002	0.017	-0.034	0.001	0.027
STSp↔F3orb	0.024	-0.034	0.014	-0.066	0.001	0.028	0.054	-0.022	0.021	-0.021	0.112	0.013	0.027	0.016	-0.012	-0.004	-0.015	0.045	-0.025	0.012	0.073	0.017	0.013	-0.017	0.074
PT↔Fusa	-0.072	0.026	-0.049	-0.026	-0.043	-0.112	0.026	-0.041	0.018	-0.032	-0.073	0.026	0.023	-0.045	-0.026	-0.047	-0.074	-0.032	-0.052	-0.059	-0.047	-0.062	-0.079	0.018	-0.057
F3opd↔RolS	-0.017	0.021	0.013	-0.024	0.112	-0.069	-0.003	0.007	0.014	0.009	0.003	0.009	0.007	0.056	0.022	0.042	0.029	-0.012	0.006	0.002	0.001	0.109	0.005	0.022	0.021
T3p↔RolS	-0.077	-0.059	0.022	-0.111	-0.012	-0.034	-0.005	-0.022	-0.093	-0.029	0.021	-0.037	-0.043	0.086	0.025	0.043	0.005	0.109	0.002	0.023	-0.018	-0.019	-0.015	-0.015	-0.007
T2ml↔F3orb	0.0	0.098	-0.088	0.072	-0.035	0.025	0.044	-0.046	0.023	0.005	0.058	0.064	0.111	0.088	0.076	-0.029	-0.0	-0.009	0.049	-0.029	0.008	0.011	0.092	0.023	-0.0
F3tv↔T3p	0.037	-0.035	-0.067	-0.076	-0.097	-0.016	-0.018	0.008	-0.092	-0.013	-0.041	-0.111	-0.084	-0.059	-0.089	-0.037	-0.069	-0.031	-0.054	-0.004	-0.069	-0.013	-0.02	0.003	-0.026
T1a↔F3opdR	-0.025	0.092	-0.061	0.008	-0.042	0.003	0.02	-0.084	0.039	0.015	0.042	-0.025	0.012	-0.057	0.076	0.018	0.111	-0.035	0.007	0.053	0.015	0.005	-0.025	-0.007	0.016
RolS↔PrecR	-0.019	0.105	-0.023	0.075	0.015	0.016	0.105	-0.04	0.049	0.024	0.054	0.074	0.022	0.021	0.11	-0.017	-0.049	-0.014	0.037	-0.013	-0.006	-0.033	-0.002	-0.065	0.0
F3opd↔PrF3op	-0.104	-0.031	-0.038	-0.015	0.04	-0.083	0.056	-0.11	0.059	-0.046	0.027	-0.014	0.006	-0.029	0.04	-0.031	0.015	-0.027	-0.044	-0.028	-0.03	-0.052	-0.062	-0.074	-0.045
PT↔F2antR	-0.001	0.011	-0.059	-0.016	-0.081	0.006	0.016	-0.041	0.008	-0.026	-0.003	-0.016	-0.11	-0.023	-0.012	-0.016	0.006	0.035	0.051	0.028	0.031	-0.02	0.022	-0.009	0.037
PT↔F3opdR	-0.049	-0.106	-0.031	-0.026	-0.037	-0.039	-0.073	0.051	-0.067	-0.048	-0.097	-0.01	-0.078	-0.06	-0.11	-0.06	-0.015	-0.049	0.007	0.007	0.008	-0.059	-0.016	-0.021	-0.057
PT↔T2ml	0.055	0.045	0.091	0.029	0.048	0.06	-0.004	0.074	0.044	0.106	0.006	-0.06	0.085	0.041	0.004	0.077	0.036	0.06	0.047	0.109	0.063	0.034	0.04	0.056	0.047
T1↔T3p	0.034	-0.009	-0.021	-0.01	-0.045	-0.03	-0.106	0.028	-0.064	0.024	-0.043	-0.091	-0.052	0.004	-0.109	0.033	-0.007	0.037	-0.015	0.065	-0.047	0.009	-0.009	-0.016	-0.038
PT↔AG	0.02	0.033	0.005	-0.031	0.018	0.041	0.108	-0.022	0.065	-0.041	0.06	0.077	-0.005	0.032	0.048	-0.013	-0.011	0.029	-0.013	-0.033	-0.043	0.011	0.014	-0.033	-0.003
STSp↔F3opdR	-0.055	0.037	-0.09	0.015	-0.037	-0.029	-0.041	-0.078	-0.029	-0.013	-0.042	-0.051	-0.013	-0.038	-0.023	0.007	0.035	-0.045	-0.036	-0.012	-0.099	-0.013	-0.108	-0.011	-0.086
F2p↔Fusa	0.027	-0.108	0.017	-0.042	-0.015	-0.054	-0.077	0.01	-0.01	-0.002	0.0	0.012	0.052	-0.01	-0.076	0.036	0.012	0.019	0.014	0.047	0.072	0.053	0.036	0.065	0.065
T1a↔RolS	-0.051	-0.04	0.025	-0.107	0.003	0.007	0.068	0.021	-0.038	-0.013	-0.055	-0.044	-0.072	0.002	-0.08	-0.014	-0.072	0.032	-0.036	0.047	-0.001	-0.031	0.008	0.004	0.028
F3tv↔T1a	0.001	0.018	-0.079	-0.024	-0.107	-0.013	0.043	-0.097	0.008	0.002	-0.001	-0.032	-0.052	0.03	0.01	0.005	-0.016	0.027	0.013	-0.008	-0.001	-0.023	0.013	-0.04	0.029
Prec↔T1R	-0.015	0.017	0.035	0.107	-0.027	-0.028	-0.05	0.054	0.026	0.003	0.037	-0.042	-0.032	0.023	0.015	0.106	0.035	-0.013	0.078	0.036	-0.011	0.011	0.03	0.029	0.014
AG↔SMG	0.006	-0.038	0.061	0.014	0.084	0.035	-0.044	0.063	0.019	-0.095	0.057	0.017	0.047	0.012	0.018	0.027	0.106	0.014	0.04	0.058	0.046	0.022	0.022	-0.001	0.075
Fusa↔F3orb	0.085	0.013	0.106	0.011	0.094	0.01	0.013	0.074	-0.013	-0.054	0.011	0.035	0.042	-0.012	0.004	0.032	0.025	-0.015	-0.003	0.018	-0.054	0.033	-0.023	0.053	-0.044
F2p↔F3td	0.067	0.09	0.086	0.038	0.068	-0.004	0.038	0.066	-0.004	0.072	0.078	0.052	0.033	0.062	0.05	0.106	0.076	-0.002	0.005	0.055	-0.012	0.03	0.028	0.084	0.063
STSp↔T2pR	0.025	0.095	-0.017	0.076	-0.029	0.031	0.06	-0.075	0.034	-0.005	-0.01	0.007	-0.015	-0.048	0.018	-0.037	-0.09	-0.068	0.106	-0.037	-0.03	-0.05	-0.004	-0.041	-0.007
SMG↔RolS	-0.037	-0.046	-0.027	-0.023	-0.04	-0.043	-0.039	-0.021	-0.052	-0.018	-0.084	-0.044	-0.032	-0.012	-0.042	0.043	-0.039	0.015	-0.038	0.105	-0.004	-0.071	-0.039	-0.022	-0.023
T1↔PrF3op	0.1	-0.003	0.025	-0.01	0.014	0.104	0.011	0.035	0.011	0.021	0.034	0.077	0.008	0.019	-0.031	-0.014	0.012	-0.05	0.011	0.032	0.012	0.017	0.029	0.026	0.06
F3opd↔F3td	0.06	0.05	0.078	0.02	-0.015	0.086	0.104	-0.052	0.058	0.009	0.084	0.06	-0.005	-0.007	0.073	-0.036	-0.006	0.043	-0.006	0.033	0.032	0.019	0.032	-0.011	0.044
Pole↔SMG	-0.041	-0.028	-0.045	-0.082	-0.064	0.018	-0.013	-0.006	-0.03	-0.035	-0.009	-0.003	0.033	0.021	-0.088	-0.021	-0.065	0.051	-0.036	0.104	0.033	-0.021	-0.025	-0.014	-0.009
T2p↔T2pR	-0.052	-0.029	-0.07	-0.051	-0.076	-0.052	0.01	-0.103	0.009	-0.005	0.023	-0.037	-0.064	-0.053	0.038	-0.033	-0.064	-0.037	-0.024	-0.103	0.012	-0.046	-0.005	-0.054	-0.071
Pole↔F3opdR	-0.084	-0.014	-0.032	-0.08	-0.023	-0.078	-0.043	-0.076	-0.04	-0.042	-0.049	-0.077	-0.062	-0.099	-0.059	-0.012	0.044	-0.103	-0.058	-0.093	-0.001	-0.035	-0.042	-0.059	-0.027
F3tv↔F3orb	-0.036	0.014	-0.085	-0.002	-0.063	-0.007	0.037	-0.102	0.059	-0.022	-0.006	0.046	0.014	-0.073	0.068	-0.012	-0.032	0.056	-0.049	-0.06	-0.002	0.004	-0.026	-0.021	-0.044
Prec↔STSp	-0.023	-0.047	-0.009	-0.004	-0.045	-0.042	-0.052	0.016	-0.043	-0.016	-0.03	0.009	-0.011	0.007	0.011	0.102	-0.005	0.019	-0.037	-0.035	-0.056	-0.01	-0.022	-0.016	-0.043
PrF3op↔T2p	0.06	0.035	0.06	0.058	0.065	0.102	0.006	0.054	0.004	0.053	0.044	0.055	0.012	0.026	0.002	-0.029	-0.004	-0.017	0.007	-0.009	0.024	0.0	0.077	0.037	0.025
SMG↔T3p	0.018	0.078	-0.019	0.04	0.017	-0.047	0.001	-0.006	-0.052	0.102	-0.006	-0.017	-0.034	-0.012	0.063	-0.02	0.001	-0.086	0.019	0.086	0.058	-0.057	0.023	-0.004	-0.017
PT↔PrecR	-0.046	-0.049	-0.025	-0.102	-0.083	-0.036	-0.035	-0.012	-0.071	-0.033	-0.032	-0.052	-0.056	-0.007	-0.052	-0.066	-0.075	-0.043	-0.017	-0.044	0.008	-0.024	0.01	-0.025	-0.044
RolS↔F2antR	-0.001	-0.01	-0.035	-0.064	-0.083	-0.003	0.022	0.049	-0.053	-0.042	-0.062	-0.03	-0.048	-0.032	0.004	-0.027	-0.055	-0.022	-0.071	-0.062	-0.025	-0.102	0.013	-0.064	-0.023
F3td↔F3opdR	0.092	-0.002	0.095	-0.052	0.048	0.004	-0.093	0.029	-0.101	0.013	-0.012	0.018	-0.019	0.04	-0.061	0.09	-0.054	0.026	0.012	0.056	-0.007	0.028	-0.01	0.007	0.022
Fusa↔T1a	-0.012	-0.023	-0.011	0.041	0.015	-0.042	-0.101	0.018	-0.052	-0.048	-0.0	-0.001	-0.005	-0.048	0.017	-0.042	0.016	-0.014	-0.034	-0.039	-0.018	-0.019	-0.002	-0.025	-0.007
Prec↔RolS	0.012	0.021	0.027	0.03	0.007	0.047	0.027	-0.008	0.014	0.012	0.079	0.022	0.048	0.034	0.1	0.08	0.033	0.006	-0.001	-0.024	0.017	0.014	0.003	0.037	0.019
T3p↔T1R	-0.045	-0.043	-0.068	-0.055	-0.058	-0.035	0.048	-0.019	0.002	-0.076	0.017	-0.074	-0.075	-0.017	0.092	-0.033	-0.028	-0.0	-0.013	-0.099	-0.069	-0.045	-0.066	0.004	-0.036
PT↔F2p	0.072	0.013	0.042	0.068	0.054	-0.07	-0.016	0.011	0.018	0.032	0.031	-0.013	0.081	0.041	0.01	0.013	0.018	-0.02	0.099	-0.032	-0.011	0.004	-0.024	0.007	-0.029
T1↔F3opdR	-0.002	0.029	0.042	0.028	0.048	0.047	0.052	0.009	0.055	0.067	0.052	0.005	0.051	0.08	0.014	0.044	0.073	0.031	0.001	0.042	0.099	0.017	0.077	0.057	0.056
F3orb↔F3opdR	0.072	0.004	-0.001	0.0	0.04	-0.032	-0.032	0.048	-0.046	-0.03	-0.004	-0.033	-0.049	-0.012	-0.046	0.087	0.096	0.052	0.038	0.012	0.018	0.098	0.003	0.005	0.057
Fusa↔PrF3op	-0.075	-0.012	0.009	0.067	0.03	-0.097	0.029	-0.045	0.044	0.008	-0.017	0.021	-0.004	-0.025	0.01	0.039	0.038	-0.007	0.044	-0.071	-0.01	-0.018	0.009	0.028	-0.021
F2p↔F3tv	-0.096	-0.002	-0.022	0.03	0.007	0.021	0.04	-0.009	0.031	-0.026	-0.004	0.013	0.0	-0.006	0.002	0.001	-0.038	0.0	0.037	0.032	0.027	-0.021	0.002	0.015	0.015
F3td↔F3orb	-0.02	0.025	0.031	0.038	0.005	-0.035	-0.008	-0.027	0.029	-0.028	-0.025	-0.02	-0.013	-0.043	0.026	-0.069	-0.031	-0.096	-0.073	-0.011	-0.052	-0.07	-0.042	-0.052	-0.029
PrF3op↔F3opdR	-0.06	-0.031	0.015	0.037	0.015	-0.052	0.003	-0.015	0.013	-0.049	-0.012	0.011	-0.059	-0.033	0.035	-0.047	-0.003	-0.038	-0.013	-0.045	-0.036	-0.083	-0.036	-0.096	-0.034
T2ml↔Fusa	0.033	-0.015	0.04	-0.082	0.024	0.041	-0.055	0.022	-0.075	-0.025	0.032	-0.081	-0.063	0.096	0.012	0.053	-0.073	0.014	-0.064	0.026	-0.028	-0.05	0.024	-0.003	0.025
T1↔STSp	0.006	-0.096	-0.033	-0.052	0.024	-0.036	-0.027	0.005	-0.039	-0.01	-0.088	0.008	-0.027	0.029	0.017	-0.018	-0.011	-0.016	-0.046	-0.037	-0.087	-0.044	-0.033	-0.08	-0.044
Prec↔Fusa	0.016	-0.021	-0.013	-0.046	-0.041	-0.035	0.047	0.01	0.008	-0.002	-0.023	-0.02	-0.014	-0.014	-0.009	-0.095	0.011	-0.014	-0.01	-0.071	-0.006	-0.019	0.014	-0.034	-0.003
F2p↔T1R	-0.034	-0.07	0.011	0.006	-0.03	0.067	-0.05	0.036	-0.037	-0.031	-0.038	-0.011	-0.035	0.008	-0.028	-0.022	0.004	0.056	0.018	0.039	0.061	0.011	0.095	0.024	0.028
T2p↔F3orb	-0.033	-0.095	0.007	-0.073	-0.03	-0.021	-0.081	0.011	-0.046	-0.062	-0.013	-0.03	-0.052	-0.015	-0.051	-0.014	-0.038	-0.007	-0.049	0.008	-0.012	-0.027	-0.032	-0.051	-0.007
T1↔T2p	0.075	0.04	0.044	-0.03	0.04	0.032	-0.008	0.009	-0.033	0.094	0.017	-0.06	-0.043	0.008	0.012	0.045	0.064	0.039	0.031	0.082	0.044	0.039	0.03	0.023	0.071
T1↔AG	-0.048	-0.022	0.038	0.008	0.006	0.002	0.014	-0.094	0.051	-0.064	0.035	-0.039	0.041	0.035	0.015	0.03	0.023	0.023	0.021	0.039	0.046	0.079	0.013	0.035	0.003
T2p↔F3opdR	0.019	0.022	0.034	0.088	-0.001	0.014	0.039	0.036	0.094	0.02	0.019	0.049	0.04	-0.021	-0.034	-0.009	-0.035	-0.034	0.023	0.01	-0.018	-0.041	-0.025	0.011	0.006
Pole↔T2p	-0.026	0.033	0.033	0.027	0.023	0.038	0.043	0.029	0.063	0.019	0.073	0.039	0.094	0.023	0.092	0.016	0.015	-0.009	-0.013	0.032	0.024	-0.035	0.07	0.05	0.019
Fusa↔RolS	-0.011	-0.02	-0.046	-0.024	-0.024	0.029	0.016	0.036	0.002	0.093	-0.007	0.058	0.01	0.024	-0.004	0.053	0.008	0.083	-0.033	0.067	0.05	0.044	0.004	0.054	0.021
T2pR↔PrecR	-0.019	-0.02	-0.008	-0.065	-0.037	-0.083	-0.066	-0.06	-0.046	-0.017	-0.044	-0.035	-0.014	-0.093	-0.038	0.021	-0.054	-0.02	-0.034	-0.03	-0.056	-0.021	-0.057	-0.009	-0.046
SMG↔T1a.HeschlR	-0.023	0.041	-0.018	0.037	-0.019	-0.017	0.018	-0.034	-0.007	-0.014	-0.041	0.093	0.02	-0.066	0.025	0.0	-0.077	-0.026	-0.008	-0.034	-0.01	-0.001	-0.054	0.012	-0.021
T3p↔F3orb	-0.004	0.069	0.093	0.062	0.031	0.078	-0.001	-0.019	0.017	0.026	0.051	0.062	-0.022	0.032	0.05	0.035	-0.004	-0.007	0.091	0.02	0.065	0.011	0.081	-0.021	0.03

Endophenotype	PrF3op	T2ml	F3td	T1R	F3opd	F2p	T1a	F2antR	T1a.HeschlR	AG	STSp	T1	PT	F3orb	Pole	Prec	F3opdR	F3tv	T2pR	SMG	T2p	RolS	Fusa	PrecR	T3p
PT↔F3orb	0.0	0.004	0.033	0.035	0.03	-0.022	-0.003	0.058	0.015	0.009	0.01	-0.071	0.002	0.026	0.035	0.055	0.038	-0.028	0.058	0.093	0.01	-0.001	0.044	0.049	0.011
SMG↔F3orb	-0.01	-0.093	-0.019	-0.021	-0.022	-0.028	-0.06	-0.008	0.014	-0.006	-0.042	-0.064	-0.02	-0.066	-0.023	0.013	0.024	0.082	-0.023	0.047	0.003	0.009	-0.031	0.038	0.01
STSp↔T1R	-0.07	-0.071	-0.055	-0.066	-0.03	-0.019	-0.009	-0.054	-0.092	-0.058	0.019	0.031	-0.007	0.006	0.038	-0.056	-0.042	-0.013	-0.089	-0.02	-0.079	-0.034	-0.034	-0.062	-0.071
Fusa↔SMG	0.078	0.005	0.07	0.063	0.084	0.039	-0.027	0.015	0.02	0.071	0.008	-0.001	0.013	0.059	0.051	0.092	0.041	0.066	0.021	0.058	0.011	0.067	-0.002	0.082	-0.009
Prec↔AG	0.015	-0.022	0.03	-0.044	0.076	0.091	-0.011	0.053	-0.037	-0.036	0.023	-0.024	-0.002	0.01	0.027	-0.038	0.038	0.035	0.042	0.063	0.092	0.03	0.021	-0.001	0.081
F3opdR↔T2pR	0.033	0.059	-0.027	-0.005	-0.04	0.059	0.087	-0.006	0.012	0.043	0.056	0.021	-0.007	0.039	0.078	-0.057	-0.091	0.048	-0.049	0.015	0.037	0.015	0.044	-0.013	-0.007
T1a↔PrecR	0.051	0.003	-0.018	-0.091	0.002	-0.062	0.023	-0.008	-0.073	-0.047	-0.015	-0.04	-0.051	0.007	-0.021	-0.006	-0.038	0.054	-0.051	-0.011	-0.016	0.009	-0.01	-0.012	-0.014
T1↔F3tv	-0.013	-0.037	-0.012	0.017	-0.016	-0.041	0.033	0.052	0.049	0.033	0.015	-0.091	0.024	0.012	0.022	-0.002	0.065	0.013	0.059	0.02	-0.003	0.045	0.017	-0.018	0.017
STSp↔T3p	-0.003	-0.012	-0.068	-0.054	-0.091	0.03	-0.075	-0.015	-0.03	0.01	-0.056	-0.032	-0.046	-0.022	-0.012	-0.048	-0.069	-0.013	0.027	0.02	-0.08	-0.076	-0.065	-0.044	-0.03
F2antR↔T1a.HeschlR	0.044	0.015	-0.007	0.007	-0.007	0.041	-0.024	-0.083	-0.091	-0.013	-0.033	0.004	-0.005	0.012	0.005	0.008	-0.024	-0.008	0.008	0.011	0.034	-0.005	0.02	0.031	0.038
Pole↔PT	0.001	-0.081	-0.028	-0.054	-0.027	-0.049	-0.082	0.003	-0.058	-0.021	-0.046	-0.049	0.091	0.022	-0.003	-0.011	-0.018	-0.021	-0.063	-0.019	-0.006	-0.007	-0.052	-0.025	-0.056
Fusa↔F2antR	-0.022	0.007	-0.031	0.053	-0.024	-0.032	-0.091	0.022	-0.009	-0.007	-0.069	-0.042	-0.01	0.039	-0.059	-0.003	-0.014	-0.038	-0.023	-0.027	-0.05	-0.032	-0.061	-0.01	-0.023
RolS↔T2pR	-0.004	-0.079	-0.06	-0.035	-0.062	-0.081	-0.051	-0.074	-0.047	-0.082	-0.09	-0.03	-0.047	-0.033	0.018	-0.028	-0.003	-0.029	-0.051	-0.064	-0.06	-0.045	-0.031	-0.046	0.003
F2p↔T3p	-0.002	-0.017	0.002	-0.029	-0.021	-0.059	-0.026	0.011	-0.042	-0.016	-0.069	-0.005	-0.054	-0.057	-0.063	-0.019	-0.005	-0.09	-0.025	-0.065	-0.01	-0.035	-0.028	-0.037	0.011
PrF3op↔F3orb	0.09	0.005	-0.036	-0.0	-0.025	-0.029	-0.026	0.023	0.012	0.001	-0.02	-0.06	-0.029	0.054	-0.012	0.017	-0.017	0.03	0.036	-0.007	0.016	0.055	-0.02	0.011	-0.013
T1a↔SMG	0.009	-0.006	-0.089	-0.025	-0.08	0.014	-0.011	-0.062	0.036	-0.03	-0.045	0.004	-0.021	-0.022	-0.045	-0.012	-0.068	0.011	-0.061	0.019	-0.026	-0.0	-0.047	0.02	-0.019
Prec↔F3orb	-0.028	-0.007	0.032	-0.017	-0.042	-0.068	-0.046	0.017	-0.068	-0.038	-0.052	-0.089	-0.068	0.035	-0.026	0.019	-0.03	-0.047	-0.002	-0.009	-0.065	-0.057	-0.074	-0.023	-0.042
F3tv↔PrecR	-0.037	-0.017	0.018	-0.089	-0.012	0.014	0.029	-0.002	-0.036	0.007	0.037	0.001	-0.032	0.001	-0.003	-0.019	-0.006	-0.03	-0.04	-0.02	0.012	-0.071	0.001	-0.032	0.021
F3opd↔T3p	0.002	0.014	0.008	0.038	-0.082	0.013	-0.042	0.02	0.011	0.046	-0.032	0.089	0.072	-0.033	-0.006	0.085	-0.031	0.039	0.004	0.028	0.052	0.055	0.053	-0.005	0.026
STSp↔PrecR	-0.046	0.008	-0.043	0.016	-0.003	0.002	0.033	-0.043	0.046	-0.029	0.088	-0.002	0.026	-0.038	0.029	-0.038	-0.02	-0.012	0.004	0.007	0.032	0.009	-0.006	-0.015	-0.006
STSp↔RolS	0.033	-0.065	0.002	-0.012	-0.009	0.037	-0.04	0.061	0.006	-0.023	0.088	0.031	-0.007	0.001	0.009	-0.032	0.076	0.03	-0.016	-0.045	0.014	-0.022	0.003	0.023	0.002
Fusa↔PrecR	-0.035	-0.054	0.012	0.036	-0.005	-0.049	-0.043	-0.011	-0.014	-0.006	-0.087	0.017	-0.02	-0.009	-0.047	0.009	0.037	0.005	-0.003	-0.035	-0.0	0.02	0.048	0.026	0.036
Fusa↔F3opdR	-0.007	-0.006	-0.025	-0.003	-0.065	0.059	0.015	-0.016	-0.037	0.034	0.025	-0.043	-0.048	0.019	0.008	-0.049	-0.087	0.033	0.076	-0.031	-0.021	-0.01	-0.038	0.014	0.0
Prec↔F2p	0.086	0.016	-0.031	0.004	-0.071	0.026	-0.027	0.002	0.024	0.052	-0.0	0.016	-0.028	0.014	-0.052	-0.006	-0.013	0.004	0.005	0.006	-0.022	-0.006	0.026	0.007	0.018
Pole↔F3orb	-0.016	-0.002	-0.014	-0.0	-0.015	0.026	0.014	-0.003	0.016	0.015	-0.026	-0.011	-0.027	0.086	0.0	0.026	-0.008	0.026	-0.011	0.01	-0.027	-0.005	-0.051	-0.046	-0.004
F3orb↔F2antR	0.045	-0.004	0.073	0.071	0.042	-0.085	-0.031	0.023	0.054	-0.046	-0.039	0.026	-0.003	-0.084	-0.023	0.024	0.074	0.001	0.037	0.004	-0.027	-0.011	-0.003	0.033	-0.018
AG↔T2pR	-0.03	0.068	0.047	0.064	0.049	-0.027	0.017	0.045	0.04	0.034	0.035	0.085	0.068	0.003	0.006	0.02	0.05	-0.009	-0.04	-0.023	0.039	0.051	0.01	0.046	0.026
T1a↔F3td	-0.055	0.024	0.084	0.057	0.023	0.009	-0.037	0.041	-0.011	-0.059	-0.034	-0.034	-0.018	-0.034	-0.014	0.003	0.034	-0.056	0.052	-0.008	-0.012	-0.02	-0.02	0.014	-0.021
F3tv↔RolS	0.001	0.041	-0.052	0.041	-0.055	-0.02	0.084	-0.058	0.037	0.006	0.004	0.026	0.014	0.003	0.031	-0.034	-0.004	0.012	0.061	-0.04	0.011	0.043	-0.015	0.079	-0.0
T3p↔T1a.HeschlR	0.013	-0.006	0.025	0.033	0.044	-0.007	0.014	0.083	0.068	-0.011	0.008	0.027	0.025	-0.011	-0.024	-0.013	0.03	-0.031	-0.0	-0.067	-0.02	0.03	-0.008	-0.02	-0.01
T1a↔T3p	0.01	-0.004	0.024	0.015	0.014	-0.042	0.039	-0.025	0.022	-0.037	0.002	0.04	0.083	0.013	0.015	0.015	0.01	0.031	0.007	-0.012	-0.022	0.046	0.002	0.03	-0.013
F3opd↔T2pR	0.026	-0.034	-0.049	-0.002	-0.073	0.082	-0.019	-0.018	0.007	0.013	-0.019	-0.028	-0.005	-0.033	0.009	0.042	-0.002	0.045	0.057	0.027	0.015	0.068	-0.013	0.065	-0.009
F2antR↔T2pR	0.022	0.055	-0.017	0.034	0.0	0.053	0.073	-0.009	0.047	-0.049	0.025	0.044	0.061	-0.065	0.027	-0.062	0.03	-0.032	-0.082	-0.014	-0.021	-0.046	-0.051	-0.052	-0.023
F3td↔T1a.HeschlR	0.016	-0.033	-0.057	0.008	-0.038	-0.025	-0.004	-0.051	0.02	-0.017	-0.029	-0.015	-0.026	-0.014	-0.046	-0.028	-0.009	0.008	-0.038	-0.005	0.004	-0.005	-0.082	-0.003	-0.038
F3opd↔T2p	-0.018	-0.077	-0.019	-0.028	-0.031	-0.059	-0.071	0.039	-0.027	-0.02	-0.08	-0.073	-0.082	-0.017	-0.026	-0.005	-0.027	-0.072	0.001	-0.015	-0.01	-0.025	-0.008	-0.03	0.038
F2p↔PrF3op	-0.021	0.019	0.017	0.035	0.042	0.082	0.017	0.027	0.006	-0.015	-0.008	0.008	0.022	0.036	0.057	0.012	0.024	0.036	-0.019	0.024	-0.015	-0.001	-0.016	-0.032	0.015
T3p↔PrecR	-0.005	-0.082	-0.046	-0.033	-0.071	-0.018	-0.025	-0.035	0.016	-0.081	-0.046	-0.042	-0.032	-0.024	-0.061	-0.039	-0.018	-0.009	-0.031	-0.08	0.01	-0.007	-0.023	0.015	-0.062
Fusa↔T1R	-0.026	0.048	0.001	-0.022	-0.008	0.023	0.036	-0.029	-0.013	0.061	0.051	0.014	0.033	0.02	0.003	0.027	0.002	0.024	0.003	0.036	0.015	0.012	-0.014	0.053	0.082
Prec↔T2p	0.057	0.001	0.037	-0.012	0.004	0.039	-0.039	0.012	-0.023	0.081	0.046	0.02	0.001	0.022	-0.02	-0.001	0.02	-0.009	0.021	-0.014	0.064	0.032	0.059	-0.05	-0.001
T1↔PrecR	-0.03	-0.041	0.003	0.022	-0.06	-0.025	-0.066	0.014	-0.019	-0.061	-0.062	0.02	-0.031	-0.024	-0.045	-0.016	-0.011	-0.033	-0.052	-0.028	-0.081	-0.036	-0.027	0.004	-0.07
T2ml↔T2p	-0.021	0.071	0.029	0.014	0.045	0.047	0.01	0.027	-0.044	-0.011	0.002	-0.047	-0.051	-0.005	-0.021	0.001	0.029	0.046	0.031	0.068	0.081	-0.032	0.025	0.034	0.063
T3p↔T2pR	0.032	0.049	0.028	-0.002	0.064	0.015	0.073	-0.007	0.053	0.014	0.065	0.051	0.027	0.02	0.075	0.059	0.078	0.001	-0.043	0.027	0.042	-0.014	0.034	0.028	0.081
PrF3op↔PrecR	-0.0	-0.002	0.029	0.038	0.007	-0.013	-0.005	0.031	0.072	0.045	0.039	0.064	0.053	0.014	-0.02	0.031	0.032	0.081	-0.025	0.021	0.01	0.031	0.005	0.016	-0.002
Pole↔T1	-0.045	-0.08	0.079	-0.055	0.046	-0.05	0.009	0.016	-0.076	-0.064	-0.039	0.062	-0.027	-0.019	-0.044	-0.005	-0.024	-0.011	-0.037	-0.025	0.027	0.017	0.001	-0.021	0.029
T1a↔F3orb	-0.08	-0.065	-0.012	-0.063	-0.046	0.002	-0.038	0.063	-0.048	-0.027	-0.038	-0.066	-0.021	0.028	0.003	-0.066	-0.041	-0.044	-0.056	0.008	-0.032	-0.028	-0.035	-0.06	-0.059
F3opdR↔T1a.HeschlR	-0.003	-0.01	0.026	-0.013	0.048	0.017	-0.043	0.01	-0.065	-0.023	-0.013	-0.001	0.001	0.055	-0.016	0.033	0.029	0.023	0.077	0.027	-0.011	0.003	-0.0	0.01	-0.014
T1a↔F2antR	0.014	0.068	-0.03	0.03	-0.01	0.038	-0.031	0.076	-0.0	0.023	0.01	0.005	0.021	0.043	0.02	0.067	-0.022	-0.067	-0.024	-0.03	-0.052	-0.0	-0.025	-0.016	-0.02
F3orb↔T1a.HeschlR	-0.007	-0.031	0.03	-0.016	0.018	0.017	0.024	0.035	0.069	-0.003	-0.02	0.076	-0.013	-0.027	-0.012	0.014	0.031	-0.021	0.02	0.011	0.042	-0.03	0.005	0.011	0.009
F3orb↔PrecR	0.061	0.003	0.075	0.006	0.022	0.025	-0.014	0.051	-0.002	0.004	-0.0	0.045	0.071	0.074	-0.012	0.045	0.033	0.039	0.011	0.055	0.048	0.01	0.005	-0.014	0.045
PrF3op↔T1a.HeschlR	-0.039	-0.019	0.014	-0.063	0.007	-0.029	-0.028	-0.008	-0.075	-0.006	0.004	-0.01	0.002	-0.001	-0.057	-0.003	-0.049	0.011	-0.03	0.052	-0.015	-0.075	0.002	0.002	-0.007
T2p↔F3td	0.005	-0.005	-0.009	-0.003	-0.009	0.017	-0.026	0.051	-0.075	0.024	0.021	0.028	-0.002	-0.001	-0.005	0.017	0.012	0.012	0.039	-0.017	0.009	0.036	0.023	-0.022	-0.01
F2p↔PrecR	0.035	-0.043	-0.05	-0.01	-0.012	-0.018	-0.046	0.014	-0.069	-0.052	-0.035	-0.04	-0.067	-0.075	-0.011	-0.057	0.001	-0.074	0.013	-0.029	-0.057	-0.052	-0.055	-0.0	-0.016
T2p↔T1R	-0.04	-0.009	-0.016	0.012	0.024	-0.046	0.051	-0.002	0.074	0.025	-0.039	-0.036	-0.023	-0.033	0.051	0.016	0.032	-0.032	-0.004	-0.026	0.04	-0.02	-0.006	0.029	-0.023
Fusa↔T1a.HeschlR	0.009	-0.014	-0.055	-0.013	-0.013	-0.035	0.021	-0.006	0.013	-0.018	-0.023	0.014	0.059	0.016	-0.048	0.013	0.065	0.027	-0.011	0.074	0.018	0.049	0.006	0.016	-0.001
F3orb↔T1R	-0.029	0.011	-0.038	-0.017	-0.021	0.012	-0.007	-0.058	-0.074	-0.032	-0.019	0.042	0.033	0.025	0.001	-0.054	-0.047	0.007	-0.031	-0.019	-0.039	0.041	-0.036	-0.019	-0.03
Fusa↔T2pR	0.035	0.023	-0.008	0.061	0.05	0.02	0.039	0.01	0.047	0.071	0.074	0.041	0.057	0.006	0.07	0.067	0.042	-0.025	0.04	0.008	0.015	0.014	0.01	-0.008	0.033
T2ml↔T3p	0.029	-0.015	0.02	-0.059	0.01	0.04	0.03	-0.028	0.009	-0.047	-0.007	0.011	-0.002	0.005	0.012	-0.011	0.005	0.063	-0.056	-0.031	0.01	-0.019	-0.011	-0.045	0.073
Pole↔RolS	-0.007	-0.035	-0.02	-0.022	-0.035	0.033	-0.06	0.036	-0.035	-0.005	-0.002	-0.049	0.044	-0.031	-0.01	-0.013	-0.015	-0.034	-0.016	0.073	0.022	0.011	0.016	-0.018	-0.01
T1a↔T2p	0.024	-0.061	0.014	-0.073	0.026	-0.025	0.073	-0.024	0.018	-0.046	0.005	-0.048	-0.034	0.034	-0.054	-0.012	-0.009	0.02	-0.061	0.004	0.028	-0.007	0.026	0.024	0.036
F3td↔T2pR	0.006	-0.004	-0.023	-0.031	-0.032	-0.01	0.016	0.035	0.001	-0.037	0.001	-0.018	0.022	0.029	-0.027	-0.012	0.029	0.027	0.022	0.019	0.014	-0.014	-0.01	0.073	0.018
F3opd↔F3opdR	0.018	0.003	-0.028	0.051	-0.033	0.016	0.042	0.023	0.073	0.01	-0.017	0.041	0.001	0.028	0.042	-0.015	0.065	0.031	0.027	-0.057	0.036	0.03	0.035	0.047	0.025
F3opdR↔PrecR	-0.072	-0.013	-0.01	0.006	-0.016	-0.021	-0.015	-0.008	-0.025	-0.028	-0.022	-0.028	-0.001	-0.005	-0.066	-0.016	-0.033	-0.062	-0.006	-0.046	-0.001	-0.043	0.006	-0.007	-0.009
T2pR↔T1R	-0.004	0.019	0.005	-0.014	-0.011	0.072	0.061	0.007	0.06	0.02	-0.012	0.002	-0.014	0.007	0.066	0.015	0.042	-0.023	0.051	-0.014	0.055	-0.047	0.003	-0.032	0.062
F2p↔F3opdR	0.009	0.002	-0.057	-0.051	-0.072	0.049	0.016	-0.041	-0.011	-0.02	-0.032	-0.048	-0.009	-0.027	-0.03	-0.045	-0.005	0.006	-0.023	0.001	0.003	0.002	-0.02	-0.068	-0.015
Pole↔PrecR	-0.041	-0.01	0.03	-0.017	0.012	0.037	-0.003	0.043	0.033	0.028	-0.008	-0.008	-0.015	-0.004	0.009	0.005	0.009	0.009	-0.009	-0.024	0.071	0.011	0.072	0.028	0.054
SMG↔T2p	0.027	0.023	-0.03	-0.024	-0.018	-0.002	0.057	-0.028	0.042	0.018	-0.058	0.055	0.045	-0.015	0.049	0.04	0.017	0.013	-0.026	0.045	-0.072	0.04	-0.001	0.06	-0.043
F3tv↔T2p	-0.005	-0.009	0.017	0.058	-0.028	-0.019	-0.044	0.072	-0.004	-0.008	-0.051	0.02	-0.037	-0.013	-0.041	-0.039	0.003	-0.025	0.055	-0.019	-0.039	-0.004	-0.01	0.002	-0.041
T1R↔PrecR	0.007	-0.025	0.071	0.06	0.051	0.024	-0.012	0.061	-0.005	0.024	-0.001	0.013	-0.035	0.036	-0.017	0.032	-0.003	0.037	-0.016	0.031	0.012	0.037	0.042	0.041	0.026
PT↔F3opd	0.034	-0.034	-0.02	0.001	-0.022	-0.015	-0.008	-0.071	0.026	-0.024	0.005	-0.056	0.033	0.029	0.062	0.021	-0.034	-0.01	-0.032	-0.04	-0.028	0.002	-0.007	-0.055	-0.049
PrF3op↔AG	-0.05	0.023	0.032	0.008	0.054	-0.032	-0.04	0.056	-0.023	-0.002	-0.002	-0.014	-0.071	0.021	0.027	0.031	0.053	-0.01	-0.023	0.053	-0.028	-0.063	-0.015	-0.017	-0.007
T1a.HeschlR↔PrecR	0.008	0.04	-0.023	0.005	-0.024	-0.005	0.071	-0.001	0.06	-0.03	0.006	0.001	-0.033	0.005	0.062	-0.026	0.016	0.026	-0.024	-0.005	-0.027	-0.002	-0.0	-0.036	0.007
T3p↔F2antR	0.023	0.01	-0.07	-0.057	-0.029	0.031	-0.032	-0.071	-0.017	-0.003	-0.0	-0.037	-0.008	0.006	-0.061	-0.018	-0.011	-0.028	-0.034	0.042	-0.025	-0.053	-0.027	-0.005	-0.009
F2antR↔PrecR	0.036	0.04	0.0	-0.013	0.024	0.07	0.052	0.069	-0.006	0.056	0.005	0.021	0.009	0.023	0.06	0.001	0.036	0.011	0.009	-0.003	0.01	0.009	0.032	-0.022	0.005
Fusa↔F3tv	0.018	0.009	-0.031	-0.024	0.027	-0.022	0.032	-0.066	0.015	0.06	0.017	0.024	-0.025	-0.014	0.017	0.01	0.035	0.012	0.014	-0.02	0.07	0.015	0.022	0.031	0.042
Fusa↔F3td	-0.002	0.011	-0.017	-0.045	0.012	0.013	-0.008	-0.026	-0.027	-0.012	-0.025	-0.015	-0.009	0.009	-0.002	-0.07	-0.006	0.005	-0.038	-0.047	0.008	0.011	0.02	-0.056	0.013
SMG↔PrecR	0.052	0.027	-0.016	0.002	0.025	-0.006	0.043	0.013	0.011	0.039	0.027	0.023	0.007	0.003	0.032	0.03	0.042	0.001	-0.006	-0.024	0.069	0.028	0.029	-0.01	0.027
T1↔T2pR	0.034	-0.01	0.008	-0.018	-0.021	-0.028	-0.019	0.018	-0.015	0.013	0.02	-0.028	-0.025	-0.0	-0.069	-0.008	-0.034	0.008	-0.023	0.015	-0.025	-0.005	0.026	-0.015	-0.021
F3opd↔F3tv	-0.015	-0.044	-0.036	-0.029	-0.062	-0.041	-0.03	0.05	-0.014	0.008	-0.069	-0.015	0.021	-0.03	-0.048	0.001	-0.027	0.031	0.039	0.027	0.033	-0.015	-0.003	-0.038	-0.015
F3opd↔PrecR	-0.017	-0.016	0.024	-0.006	0.015	-0.01	-0.032	0.022	-0.006	0.012	-0.014	-0.013	0.001	-0.023	-0.069	0.007	-0.003	-0.043	0.031	-0.0	-0.019	-0.034	-0.042	0.003	0.0
PT↔F3td	0.021	-0.012	-0.069	0.002	-0.067	-0.005	0.023	-0.022	0.057	0.003	0.007	0.026	0.005	-0.002	0.004	-0.037	0.002	0.068	-0.013	0.007	-0.038	0.006	-0.013	0.005	0.0
Prec↔PrecR	0.029	0.019	-0.049	-0.005	0.013	0.02	0.058	-0.043	-0.031	0.055	0.053	0.017	-0.04	-0.01	0.069	-0.008	-0.043	-0.004	-0.007	0.004	0.028	0.0	0.058	-0.014	0.001
T1↔SMG	0.009	-0.021	-0.003	-0.005	-0.042	0.002	-0.043	0.032	-0.043	0.04	0.023	-0.068	-0.02	0.048	-0.045	0.023	0.022	0.056	0.048	0.016	0.014	-0.028	0.019	-0.043	-0.013
AG↔F3opdR	-0.044	-0.029	0.023	-0.054	-0.005	0.004	-0.015	-0.043	-0.051	-0.068	-0.001	-0.017	-0.005	0.001	-0.012	-0.066	-0.056	-0.015	0.0	-0.064	0.001	-0.005	0.002	-0.018	0.021
T2ml↔PrecR	-0.023	-0.008	0.048	-0.024	0.052	0.067	-0.058	0.025	-0.029	-0.022	-0.053	-0.025	-0.04	0.049	0.006	-0.023	0.017	-0.006	-0.025	0.048	-0.003	-0.057	-0.026	-0.018	0.036
PT↔T2p	0.035	-0.004	0.006	-0.067	-0.01	0.03	-0.009	-0.05	-0.044	-0.017	-0.038	0.017	0.006	0.008	-0.051	0.006	-0.039	0.058	0.031	-0.021	0.018	0.012	0.03	-0.02	0.023
F2p↔T1a.HeschlR	0.042	0.008	0.048	-0.066	0.021	-0.007	-0.017	0.017	-0.023	0.036	-0.014	-0.03	-0.013	0.016	-0.043	0.044	-0.039	-0.011	-0.011	0.015	0.022	-0.025	-0.051	-0.028	0.018
Pole↔Fusa	-0.003	-0.027	-0.016	-0.006	-0.018	-0.039	0.034	-0.023	0.01	-0.027	0.025	0.035	-0.023	-0.024	-0.003	-0.014	0.061	-0.038	-0.006	-0.013	0.014	-0.014	0.031	0.004	0.066
F3tv↔T2pR	0.016	-0.012	-0.025	-0.025	-0.031	-0.066	0.032	0.054	-0.003	0.035	-0.01	-0.018	-0.049	0.012	-0.054	-0.02	-0.011	-0.015	-0.033	-0.038	0.019	-0.021	0.028	-0.014	0.023
T1↔Fusa	0.007	0.021	-0.007	-0.007	0.025	-0.027	0.044	-0.049	0.023	0.066	-0.029	-0.015	0.039	0.04	0.019	0.013	-0.011	0.005	-0.017	0.017	0.039	0.034	0.019	0.02	0.033
PT↔T3p	-0.001	-0.009	0.029	-0.011	0.019	-0.023	-0.015	0.04	-0.008	0.015	0.008	-0.015	-0.031	0.004	-0.019	-0.023	0.038	0.005	0.016	-0.018	0.026	0.025	0.0	-0.018	0.065
AG↔PrecR	0.02	0.024	0.01	-0.003	0.019	-0.041	-0.022	-0.032	-0.03	0.064	-0.045	0.028	0.015	-0.021	-0.022	0.007	-0.058	-0.026	0.002	0.003	-0.033	0.039	-0.044	0.049	-0.035
Pole↔T1a.HeschlR	0.023	-0.047	0.028	-0.042	0.008	-0.045	-0.039	0.029	0.025	-0.032	-0.019	-0.064	0.001	0.01	0.008	0.003	0.05	0.039	-0.029	-0.004	0.016	0.014	-0.015	0.044	0.018
T2p↔RolS	-0.023	0.056	-0.023	0.015	0.021	0.004	0.042	-0.051	0.052	-0.043	0.009	0.032	0.049	-0.045	0.058	-0.014	0.017	0.033	-0.06	0.026	-0.042	-0.03	-0.005	0.017	-0.064
T1↔RolS	0.024	0.056	-0.028	0.035	-0.021	0.058	-0.042	-0.016	0.004	0.013	0.001	0.061	0.006	0.037	0.01	-0.002	0.001	-0.02	-0.024	0.014	-0.056	0.018	-0.049	-0.008	-0.0
RolS↔F3opdR	-0.061	-0.015	-0.027	0.039	-0.011	-0.051	0.023	0.013	0.056	0.039	0.007	0.031	-0.014	0.001	0.052	-0.023	-0.003	-0.023	0.013	-0.03	0.012	-0.061	0.006	-0.016	0.037
Prec↔F3opdR	0.02	-0.042	0.014	0.024	-0.001	0.024	0.039	-0.038	0.036	0.019	0.008	0.05	0.05	0.016	0.06	-0.047	-0.036	0.031	0.031	-0.024	-0.007	0.024	0.027	0.003	0.003
AG↔T2p	-0.06	-0.038	0.02	0.003	0.012	-0.037	0.044	-0.015	-0.008	-0.056	-0.016	0.056	0.015	-0.0	0.029	0.03	-0.009	0.007	0.031	-0.03	0.007	0.048	-0.029	-0.011	0.025
Prec↔T2pR	0.051	-0.038	0.006	-0.012	0.005	0.034	-0.009	0.06	0.039	-0.008	0.029	-0.027	-0.016	0.047	-0.018	-0.056	0.054	0.055	0.02	0.042	0.027	0.0	0.019	0.034	0.005
Prec↔T1a.HeschlR	-0.004	-0.043	-0.02	-0.023	-0.049	0.002	0.008	0.025	0.059	0.009	0.004	-0.009	-0.033	-0.003	-0.025	-0.039	0.033	0.024	-0.034	0.002	0.016	0.017	0.057	0.042	-0.023
AG↔RolS	-0.036	-0.056	0.001	0.048	-0.028	-0.041	0.031	-0.002	0.036	-0.027	-0.03	0.033	0.054	-0.002	-0.033	0.028	-0.057	-0.011	-0.012	-0.008	-0.01	-0.02	-0.02	0.024	-0.035
F3orb↔RolS	0.039	-0.009	0.037	-0.057	-0.015	0.015	-0.035	0.017	-0.03	0.022	-0.026	0.028	0.024	0.017	-0.057	0.048	-0.021	-0.04	-0.023	-0.017	-0.007	0.053	-0.014	0.049	0.013
F2p↔T2p	-0.013	-0.047	-0.017	-0.057	-0.016	0.042	0.023	-0.029	0.023	-0.041	0.047	-0.036	-0.019	0.039	0.003	-0.011	-0.034	-0.01	-0.027	-0.008	0.01	-0.025	-0.018	0.003	-0.03
PT↔SMG	0.024	-0.039	0.004	0.024	-0.009	-0.006	-0.03	0.018	-0.021	0.001	-0.031	-0.049	-0.056	-0.021	-0.029	-0.035	0.002	-0.034	0.008	0.007	-0.017	-0.031	0.045	0.031	0.017
F2p↔RolS	0.032	-0.026	-0.005	-0.036	-0.012	0.044	-0.004	-0.026	-0.028	0.038	0.0	-0.025	0.031	0.003	0.025	-0.016	-0.043	-0.055	-0.051	-0.049	0.012	-0.04	-0.02	-0.042	0.031
F3td↔PrecR	0.036	-0.015	0.012	-0.039	-0.016	-0.0	-0.043	0.007	0.0	0.023	0.019	-0.009	-0.012	0.019	0.006	0.005	0.027	0.055	0.013	0.046	0.007	0.039	0.032	-0.002	0.03
F3opd↔Fusa	-0.025	0.025	-0.016	0.045	-0.049	0.005	-0.006	0.0	0.017	-0.025	-0.016	0.012	0.013	-0.033	0.019	0.027	-0.054	-0.012	-0.009	-0.007	-0.017	0.007	0.032	-0.034	-0.031
STSp↔T1a.HeschlR	-0.032	-0.022	-0.05	-0.02	-0.039	-0.05	-0.036	0.004	-0.025	0.0	-0.005	0.04	0.031	0.02	0.002	-0.011	0.005	0.054	0.027	0.009	0.014	0.041	0.018	-0.01	0.015
T1↔F3td	-0.001	0.027	0.024	0.002	-0.004	0.008	0.003	0.051	0.025	-0.007	-0.028	-0.01	0.003	-0.011	-0.002	0.008	-0.041	-0.025	0.03	-0.022	0.048	-0.033	0.028	0.007	-0.015
T2pR↔T1a.HeschlR	0.018	-0.044	0.005	-0.014	0.004	0.006	-0.017	0.013	-0.038	-0.025	0.027	-0.011	-0.022	-0.015	0.021	0.001	0.027	0.007	0.045	0.02	-0.026	0.004	0.005	-0.05	0.022
T2p↔PrecR	0.04	-0.009	-0.044	-0.003	-0.018	0.016	-0.005	-0.034	0.001	0.003	-0.01	0.031	0.014	0.027	-0.0	0.004	0.005	0.026	-0.029	-0.007	0.037	0.028	0.02	0.009	0.005
STSp↔T2p	0.002	0.028	-0.022	-0.014	-0.012	-0.019	-0.044	0.031	0.014	0.014	0.013	-0.008	0.016	0.015	-0.019	0.012	-0.01	-0.01	-0.025	-0.002	-0.038	-0.041	-0.027	0.015	-0.021
F3tv↔F3td	-0.015	0.003	-0.025	-0.002	0.009	0.003	0.025	-0.007	-0.02	0.035	0.03	-0.013	0.014	-0.023	0.015	0.039	-0.011	-0.038	0.039	-0.007	-0.013	-0.016	0.017	-0.036	-0.026

C.2 (Endo)phenotypic correlation between both resting-state functional connectivity and language-related scores

Table C.2 – **Pearson Correlation between both resting-state functional connectivity and language-related scores.** No significant correlation was observed after false discovery rate correction at $p < 0.05$.

Endophenotype	Language task overall accuracy			Working Memory			Oral reading recognition			Vocabulary Comprehension		
	r	p value	FDR p value	r	p value	FDR p value	r	p value	FDR p value	r	p value	FDR p value
PT↔PrF3op	0.111	1.77E-03	1.76E-01	0.051	1.49E-01	5.74E-01	0.137	1.13E-04	1.36E-01	0.123	5.34E-04	1.49E-01
F3td↔RolS	-0.122	6.22E-04	1.49E-01	0.018	6.17E-01	8.95E-01	-0.032	3.63E-01	7.77E-01	-0.001	9.85E-01	9.93E-01
T2ml↔T1a.HeschlR	-0.080	2.44E-02	3.29E-01	-0.040	2.59E-01	6.96E-01	-0.126	4.07E-04	1.49E-01	-0.049	1.69E-01	6.00E-01
PrF3op↔T3p	0.055	1.21E-01	5.45E-01	0.024	4.98E-01	8.69E-01	0.129	2.75E-04	1.49E-01	0.035	3.22E-01	7.57E-01
F3td↔F3orb	0.108	2.31E-03	1.76E-01	0.033	3.50E-01	7.74E-01	0.089	1.22E-02	2.98E-01	0.088	1.35E-02	2.98E-01
F3opdR↔T1a.HeschlR	0.009	7.92E-01	9.49E-01	0.032	3.73E-01	7.82E-01	0.109	2.29E-03	1.76E-01	0.059	9.69E-02	4.78E-01
T1↔T3p	-0.040	2.66E-01	6.96E-01	-0.009	8.11E-01	9.49E-01	-0.100	5.09E-03	2.61E-01	-0.111	1.81E-03	1.76E-01
SMG↔F3orb	-0.044	2.16E-01	6.44E-01	-0.013	7.20E-01	9.31E-01	-0.109	2.19E-03	1.76E-01	-0.069	5.43E-02	4.03E-01
F2p↔T2ml	0.102	4.07E-03	2.44E-01	0.023	5.25E-01	8.80E-01	0.108	2.35E-03	1.76E-01	0.038	2.84E-01	7.12E-01
T3p↔F3orb	0.090	1.18E-02	2.98E-01	0.041	2.51E-01	6.91E-01	0.109	2.25E-03	1.76E-01	0.083	1.92E-02	3.03E-01
Fusa↔F3orb	0.022	5.44E-01	8.80E-01	0.034	3.46E-01	7.73E-01	0.111	1.84E-03	1.76E-01	0.066	6.56E-02	4.15E-01
Fusa↔RolS	-0.048	1.79E-01	6.13E-01	-0.047	1.86E-01	6.13E-01	-0.111	1.78E-03	1.76E-01	-0.088	1.33E-02	2.98E-01
T1↔T1a.HeschlR	0.111	1.80E-03	1.76E-01	0.033	3.52E-01	7.74E-01	0.100	5.04E-03	2.61E-01	0.040	2.59E-01	6.96E-01
F2p↔AG	0.043	2.31E-01	6.67E-01	0.110	2.07E-03	1.76E-01	0.024	5.00E-01	8.69E-01	0.006	8.63E-01	9.69E-01
T1↔T1a	0.106	2.87E-03	2.03E-01	0.073	4.07E-02	3.89E-01	0.068	5.81E-02	4.03E-01	0.057	1.13E-01	5.27E-01
F3opdR↔F2antR	0.103	3.96E-03	2.44E-01	0.053	1.34E-01	5.64E-01	0.047	1.83E-01	6.13E-01	0.030	3.96E-01	7.97E-01
Pole↔T2ml	0.102	4.00E-03	2.44E-01	0.039	2.76E-01	7.09E-01	0.059	9.93E-02	4.85E-01	-0.054	1.29E-01	5.52E-01
Pole↔PrecR	-0.061	8.70E-02	4.56E-01	-0.100	4.91E-03	2.61E-01	-0.087	1.40E-02	2.98E-01	-0.050	1.58E-01	5.85E-01
T3p↔F2antR	-0.053	1.39E-01	5.67E-01	-0.047	1.85E-01	6.13E-01	-0.099	5.29E-03	2.61E-01	-0.097	6.22E-03	2.66E-01
T1↔F3orb	-0.048	1.76E-01	6.09E-01	0.003	9.42E-01	9.77E-01	-0.080	2.39E-02	3.29E-01	-0.099	5.43E-03	2.61E-01
T2ml↔F3tv	0.098	5.94E-03	2.64E-01	0.009	8.03E-01	9.49E-01	0.018	6.14E-01	8.95E-01	0.057	1.12E-01	5.27E-01
AG↔T1R	-0.098	5.91E-03	2.64E-01	-0.072	4.36E-02	3.89E-01	-0.087	1.40E-02	2.98E-01	-0.078	2.86E-02	3.35E-01
T2ml↔STSp	0.077	3.00E-02	3.36E-01	-0.014	6.87E-01	9.15E-01	0.097	6.61E-03	2.73E-01	0.052	1.46E-01	5.71E-01
T1↔AG	-0.063	7.64E-02	4.36E-01	-0.089	1.26E-02	2.98E-01	-0.085	1.67E-02	3.00E-01	-0.026	4.71E-01	8.59E-01
Pole↔F3td	-0.012	7.44E-01	9.43E-01	0.026	4.65E-01	8.55E-01	0.028	4.36E-01	8.33E-01	0.089	1.20E-02	2.98E-01
F3tv↔STSp	0.044	2.20E-01	6.51E-01	0.090	1.14E-02	2.98E-01	0.022	5.36E-01	8.80E-01	0.033	3.57E-01	7.76E-01
F3tv↔F3opdR	-0.088	1.31E-02	2.98E-01	-0.079	2.75E-02	3.35E-01	-0.061	8.48E-02	4.51E-01	-0.033	3.50E-01	7.74E-01
SMG↔F3opdR	0.093	9.18E-03	2.98E-01	0.062	8.18E-02	4.45E-01	0.020	5.75E-01	8.83E-01	0.002	9.62E-01	9.81E-01
Pole↔T1a.HeschlR	-0.043	2.28E-01	6.64E-01	-0.043	2.23E-01	6.54E-01	-0.090	1.18E-02	2.98E-01	-0.011	7.57E-01	9.46E-01
Fusa↔SMG	-0.024	4.99E-01	8.69E-01	0.016	6.54E-01	8.99E-01	0.072	4.34E-02	3.89E-01	0.090	1.10E-02	2.98E-01
PT↔T1a	0.053	1.39E-01	5.67E-01	0.092	1.01E-02	2.98E-01	0.033	3.59E-01	7.76E-01	-0.005	8.83E-01	9.71E-01
AG↔F3orb	0.020	5.68E-01	8.83E-01	0.020	5.76E-01	8.83E-01	0.090	1.14E-02	2.98E-01	0.028	4.37E-01	8.33E-01
Prec↔SMG	0.003	9.33E-01	9.77E-01	0.037	3.03E-01	7.36E-01	0.091	1.06E-02	2.98E-01	0.089	1.28E-02	2.98E-01
T3p↔T1a.HeschlR	-0.033	3.50E-01	7.74E-01	0.021	5.62E-01	8.83E-01	0.087	1.41E-02	2.98E-01	0.050	1.63E-01	5.94E-01
F2p↔T1	0.039	2.73E-01	7.09E-01	0.039	2.70E-01	7.04E-01	-0.095	7.53E-03	2.98E-01	-0.014	6.97E-01	9.22E-01
F3opd↔F2antR	-0.079	2.71E-02	3.35E-01	0.006	8.75E-01	9.70E-01	-0.052	1.45E-01	5.71E-01	-0.091	1.02E-02	2.98E-01
F3opd↔F3orb	0.061	8.50E-02	4.51E-01	0.024	5.07E-01	8.73E-01	0.087	1.46E-02	2.99E-01	0.089	1.27E-02	2.98E-01
F3opd↔F2p	0.040	2.63E-01	6.96E-01	-0.090	1.17E-02	2.98E-01	0.035	3.20E-01	7.57E-01	0.036	3.13E-01	7.52E-01
PrF3op↔RolS	-0.050	1.59E-01	5.86E-01	-0.087	1.41E-02	2.98E-01	-0.034	3.34E-01	7.64E-01	-0.027	4.53E-01	8.48E-01
RolS↔T2pR	0.035	3.32E-01	7.63E-01	0.007	8.46E-01	9.64E-01	0.093	8.80E-03	2.98E-01	0.043	2.31E-01	6.67E-01
T2ml↔T1a	-0.010	7.69E-01	9.49E-01	0.009	7.93E-01	9.49E-01	-0.064	7.20E-02	4.29E-01	-0.092	9.45E-03	2.98E-01
T2ml↔F3td	-0.015	6.76E-01	9.09E-01	0.011	7.54E-01	9.46E-01	0.048	1.78E-01	6.12E-01	0.088	1.30E-02	2.98E-01
Prec↔F3orb	-0.074	3.72E-02	3.83E-01	-0.007	8.38E-01	9.62E-01	-0.090	1.11E-02	2.98E-01	-0.047	1.89E-01	6.14E-01
T1a↔T1R	0.033	3.53E-01	7.74E-01	0.089	1.28E-02	2.98E-01	0.068	5.68E-02	4.03E-01	0.051	1.54E-01	5.82E-01
F3opd↔T3p	0.065	6.80E-02	4.23E-01	0.073	3.94E-02	3.89E-01	0.087	1.47E-02	2.99E-01	0.020	5.84E-01	8.84E-01
T1a.HeschlR↔T1R	0.037	2.93E-01	7.27E-01	0.086	1.59E-02	3.00E-01	0.056	1.13E-01	5.27E-01	0.049	1.69E-01	6.00E-01
F3opd↔T2pR	0.010	7.73E-01	9.49E-01	-0.012	7.42E-01	9.41E-01	-0.062	8.17E-02	4.45E-01	-0.085	1.69E-02	3.00E-01
F3opd↔T1a	0.033	3.51E-01	7.74E-01	0.007	8.53E-01	9.64E-01	0.085	1.76E-02	3.00E-01	0.062	8.39E-02	4.51E-01
Prec↔PrF3op	0.085	1.74E-02	3.00E-01	0.042	2.41E-01	6.80E-01	0.036	3.16E-01	7.54E-01	0.022	5.36E-01	8.80E-01
Prec↔F2p	-0.014	7.05E-01	9.26E-01	-0.070	4.82E-02	4.03E-01	-0.023	5.14E-01	8.77E-01	-0.084	1.81E-02	3.00E-01
T2ml↔PrecR	-0.033	3.58E-01	7.76E-01	0.084	1.84E-02	3.00E-01	-0.026	4.63E-01	8.55E-01	-0.053	1.38E-01	5.67E-01
T2ml↔F2antR	-0.011	7.59E-01	9.46E-01	-0.085	1.74E-02	3.00E-01	0.004	9.16E-01	9.74E-01	0.035	3.32E-01	7.63E-01
AG↔F3opdR	-0.085	1.65E-02	3.00E-01	-0.057	1.07E-01	5.12E-01	-0.056	1.19E-01	5.40E-01	-0.035	3.28E-01	7.63E-01
AG↔F3tv	0.027	4.51E-01	8.48E-01	-0.032	3.75E-01	7.82E-01	0.086	1.55E-02	3.00E-01	-0.006	8.71E-01	9.69E-01
AG↔F3td	0.004	9.12E-01	9.74E-01	-0.056	1.13E-01	5.27E-01	-0.083	1.99E-02	3.11E-01	-0.084	1.84E-02	3.00E-01
T1a↔T2pR	0.086	1.55E-02	3.00E-01	0.026	4.60E-01	8.54E-01	0.066	6.31E-02	4.11E-01	0.045	2.04E-01	6.31E-01
SMG↔PrecR	0.077	3.15E-02	3.47E-01	0.038	2.84E-01	7.12E-01	0.015	6.75E-01	9.09E-01	0.084	1.81E-02	3.00E-01
F2antR↔T1R	0.052	1.48E-01	5.73E-01	-0.013	7.23E-01	9.33E-01	0.085	1.73E-02	3.00E-01	0.066	6.47E-02	4.13E-01

Endophenotype	Language task overall accuracy			Working Memory			Oral reading recognition			Vocabulary Comprehension		
	r	p value	FDR p value	r	p value	FDR p value	r	p value	FDR p value	r	p value	FDR p value
Prec↔T2pR	-0.084	1.85E-02	3.00E-01	-0.061	8.48E-02	4.51E-01	-0.002	9.51E-01	9.79E-01	-0.006	8.71E-01	9.69E-01
T2p↔T2pR	-0.026	4.73E-01	8.59E-01	-0.040	2.62E-01	6.96E-01	-0.084	1.89E-02	3.03E-01	-0.017	6.28E-01	8.95E-01
T1↔F2antR	-0.017	6.38E-01	8.97E-01	-0.001	9.78E-01	9.90E-01	0.031	3.89E-01	7.95E-01	0.081	2.37E-02	3.29E-01
T1a↔PrecR	-0.009	8.11E-01	9.49E-01	-0.018	6.14E-01	8.95E-01	0.045	2.06E-01	6.31E-01	0.081	2.22E-02	3.29E-01
F3opdR↔T1R	0.031	3.88E-01	7.95E-01	-0.080	2.43E-02	3.29E-01	0.009	7.93E-01	9.49E-01	0.029	4.18E-01	8.16E-01
PrF3op↔T2p	-0.039	2.74E-01	7.09E-01	-0.069	5.31E-02	4.03E-01	0.082	2.17E-02	3.29E-01	0.047	1.86E-01	6.13E-01
T1a↔STSp	-0.073	4.12E-02	3.89E-01	-0.081	2.27E-02	3.29E-01	-0.025	4.76E-01	8.62E-01	-0.035	3.20E-01	7.57E-01
T1↔PrecR	-0.022	5.40E-01	8.80E-01	-0.082	2.17E-02	3.29E-01	-0.043	2.32E-01	6.68E-01	-0.078	2.92E-02	3.35E-01
F2p↔T1a	-0.066	6.35E-02	4.11E-01	-0.038	2.89E-01	7.20E-01	-0.080	2.39E-02	3.29E-01	-0.020	5.69E-01	8.83E-01
SMG↔T1a.HeschlR	0.022	5.33E-01	8.80E-01	0.080	2.44E-02	3.29E-01	0.044	2.13E-01	6.40E-01	0.016	6.62E-01	9.01E-01
Fusa↔F3opdR	-0.051	1.55E-01	5.82E-01	-0.002	9.58E-01	9.79E-01	-0.080	2.47E-02	3.29E-01	-0.068	5.71E-02	4.03E-01
T1↔F3tv	-0.081	2.28E-02	3.29E-01	-0.069	5.34E-02	4.03E-01	-0.001	9.83E-01	9.93E-01	-0.060	9.32E-02	4.70E-01
PT↔RolS	-0.082	2.20E-02	3.29E-01	0.006	8.70E-01	9.69E-01	-0.043	2.26E-01	6.61E-01	0.009	8.07E-01	9.49E-01
PT↔F3tv	-0.018	6.08E-01	8.95E-01	-0.030	4.05E-01	8.03E-01	-0.078	2.88E-02	3.35E-01	-0.080	2.56E-02	3.35E-01
T1a↔F3td	0.078	2.90E-02	3.35E-01	0.051	1.56E-01	5.82E-01	0.017	6.24E-01	8.95E-01	0.058	1.02E-01	4.94E-01
Fusa↔F3td	0.044	2.18E-01	6.49E-01	-0.009	7.94E-01	9.49E-01	0.078	2.77E-02	3.35E-01	0.009	7.97E-01	9.49E-01
Fusa↔F2antR	-0.079	2.72E-02	3.35E-01	-0.024	5.08E-01	8.74E-01	-0.043	2.31E-01	6.67E-01	-0.046	1.99E-01	6.28E-01
T1↔STSp	0.015	6.76E-01	9.09E-01	0.079	2.75E-02	3.35E-01	0.068	5.69E-02	4.03E-01	0.068	5.56E-02	4.03E-01
F2p↔RolS	0.005	8.98E-01	9.72E-01	-0.030	4.03E-01	8.02E-01	-0.078	2.92E-02	3.35E-01	-0.064	7.46E-02	4.33E-01
Pole↔F3opdR	-0.078	2.89E-02	3.35E-01	-0.021	5.49E-01	8.80E-01	-0.048	1.74E-01	6.08E-01	0.010	7.89E-01	9.49E-01
RolS↔F2antR	0.036	3.19E-01	7.57E-01	0.035	3.30E-01	7.63E-01	-0.040	2.63E-01	6.96E-01	0.078	2.90E-02	3.35E-01
F3opd↔SMG	-0.025	4.90E-01	8.68E-01	-0.048	1.74E-01	6.08E-01	-0.078	2.96E-02	3.35E-01	-0.053	1.38E-01	5.67E-01
T1a↔T1a.HeschlR	0.079	2.75E-02	3.35E-01	0.066	6.50E-02	4.13E-01	0.031	3.81E-01	7.88E-01	0.011	7.68E-01	9.49E-01
F2p↔F3tv	-0.009	7.94E-01	9.49E-01	0.078	2.96E-02	3.35E-01	0.001	9.74E-01	9.89E-01	0.060	9.29E-02	4.70E-01
Prec↔PrecR	-0.020	5.81E-01	8.83E-01	-0.030	3.98E-01	7.99E-01	0.076	3.24E-02	3.47E-01	0.073	4.04E-02	3.89E-01
PT↔F2antR	-0.028	4.35E-01	8.33E-01	-0.022	5.36E-01	8.80E-01	-0.074	3.74E-02	3.83E-01	-0.076	3.21E-02	3.47E-01
F3opd↔PrecR	0.007	8.47E-01	9.64E-01	-0.004	9.08E-01	9.74E-01	-0.076	3.21E-02	3.47E-01	-0.017	6.30E-01	8.95E-01
PrF3op↔F3opdR	0.076	3.23E-02	3.47E-01	0.052	1.46E-01	5.71E-01	0.027	4.43E-01	8.41E-01	-0.021	5.59E-01	8.83E-01
Fusa↔STSp	-0.052	1.44E-01	5.71E-01	-0.066	6.50E-02	4.13E-01	-0.065	7.03E-02	4.27E-01	-0.075	3.48E-02	3.65E-01
PT↔F3td	-0.019	6.03E-01	8.94E-01	-0.075	3.50E-02	3.65E-01	-0.074	3.77E-02	3.83E-01	-0.022	5.30E-01	8.80E-01
F3opd↔AG	-0.013	7.07E-01	9.27E-01	-0.013	7.17E-01	9.31E-01	-0.075	3.49E-02	3.65E-01	-0.024	5.02E-01	8.70E-01
STSp↔F3opdR	-0.074	3.91E-02	3.89E-01	-0.024	4.94E-01	8.69E-01	-0.011	7.60E-01	9.46E-01	-0.011	7.68E-01	9.49E-01
F3opd↔T2ml	-0.073	4.15E-02	3.89E-01	0.020	5.71E-01	8.83E-01	0.034	3.36E-01	7.65E-01	0.034	3.43E-01	7.70E-01
F3opd↔STSp	-0.073	4.02E-02	3.89E-01	-0.055	1.23E-01	5.47E-01	-0.022	5.38E-01	8.80E-01	-0.040	2.64E-01	6.96E-01
Pole↔PrF3op	-0.073	4.06E-02	3.89E-01	-0.025	4.88E-01	8.67E-01	-0.004	9.11E-01	9.74E-01	-0.025	4.82E-01	8.66E-01
PrF3op↔F3orb	-0.055	1.24E-01	5.47E-01	-0.025	4.86E-01	8.67E-01	-0.073	4.02E-02	3.89E-01	-0.021	5.52E-01	8.82E-01
Pole↔F3tv	0.006	8.68E-01	9.69E-01	0.073	4.13E-02	3.89E-01	0.017	6.25E-01	8.95E-01	0.010	7.78E-01	9.49E-01
F3orb↔T1R	-0.026	4.63E-01	8.55E-01	-0.063	7.78E-02	4.36E-01	-0.021	5.65E-01	8.83E-01	-0.072	4.28E-02	3.89E-01
RolS↔F3opdR	0.054	1.28E-01	5.49E-01	0.072	4.31E-02	3.89E-01	-0.020	5.66E-01	8.83E-01	0.014	6.93E-01	9.20E-01
T2ml↔F3orb	0.020	5.81E-01	8.83E-01	0.063	7.88E-02	4.40E-01	0.072	4.34E-02	3.89E-01	0.041	2.55E-01	6.95E-01
PT↔STSp	-0.072	4.32E-02	3.89E-01	0.021	5.65E-01	8.83E-01	-0.049	1.68E-01	6.00E-01	-0.016	6.53E-01	8.99E-01
T1↔T1R	-0.006	8.66E-01	9.69E-01	0.072	4.41E-02	3.89E-01	-0.026	4.64E-01	8.55E-01	0.005	8.86E-01	9.71E-01
T1a↔SMG	0.005	8.79E-01	9.71E-01	0.013	7.09E-01	9.27E-01	-0.072	4.40E-02	3.89E-01	-0.044	2.19E-01	6.49E-01
F3opd↔F3tv	-0.037	2.98E-01	7.28E-01	0.017	6.26E-01	8.95E-01	0.071	4.60E-02	4.02E-01	0.059	9.92E-02	4.85E-01
SMG↔T3p	0.036	3.12E-01	7.52E-01	0.063	7.57E-02	4.35E-01	0.071	4.66E-02	4.02E-01	0.061	8.74E-02	4.56E-01
PT↔T1a.HeschlR	0.064	7.37E-02	4.29E-01	0.031	3.89E-01	7.95E-01	0.067	6.20E-02	4.11E-01	0.071	4.66E-02	4.02E-01
Prec↔F2antR	-0.019	5.96E-01	8.89E-01	0.046	1.97E-01	6.28E-01	-0.069	5.27E-02	4.03E-01	-0.025	4.84E-01	8.66E-01
F3opd↔PrF3op	0.071	4.77E-02	4.03E-01	0.007	8.38E-01	9.62E-01	0.016	6.44E-01	8.98E-01	0.009	7.93E-01	9.49E-01
Pole↔SMG	-0.008	8.23E-01	9.54E-01	0.009	7.91E-01	9.49E-01	-0.068	5.74E-02	4.03E-01	-0.069	5.26E-02	4.03E-01
F3opdR↔T2pR	0.070	4.99E-02	4.03E-01	0.003	9.29E-01	9.77E-01	0.043	2.28E-01	6.64E-01	0.039	2.73E-01	7.09E-01
T2ml↔T1R	0.022	5.45E-01	8.80E-01	-0.007	8.51E-01	9.64E-01	-0.009	8.09E-01	9.49E-01	-0.068	5.59E-02	4.03E-01
PT↔PrecR	-0.047	1.91E-01	6.15E-01	-0.068	5.61E-02	4.03E-01	-0.041	2.54E-01	6.92E-01	0.000	9.90E-01	9.95E-01
F2p↔F3td	0.069	5.42E-02	4.03E-01	0.003	9.40E-01	9.77E-01	-0.033	3.50E-01	7.74E-01	-0.002	9.56E-01	9.79E-01
T2p↔F3orb	-0.054	1.27E-01	5.49E-01	-0.038	2.83E-01	7.12E-01	-0.069	5.38E-02	4.03E-01	-0.052	1.41E-01	5.71E-01
PrF3op↔STSp	-0.068	5.64E-02	4.03E-01	-0.027	4.45E-01	8.42E-01	-0.042	2.42E-01	6.82E-01	-0.020	5.81E-01	8.83E-01
Pole↔T1	-0.050	1.64E-01	5.94E-01	-0.068	5.54E-02	4.03E-01	-0.003	9.44E-01	9.77E-01	0.020	5.73E-01	8.83E-01
Pole↔AG	0.011	7.49E-01	9.45E-01	0.015	6.81E-01	9.13E-01	0.001	9.89E-01	9.95E-01	0.069	5.41E-02	4.03E-01
T2ml↔T2pR	0.014	6.96E-01	9.22E-01	0.023	5.12E-01	8.75E-01	0.040	2.63E-01	6.96E-01	0.069	5.40E-02	4.03E-01
PrF3op↔T1R	-0.020	5.71E-01	8.83E-01	-0.070	5.11E-02	4.03E-01	-0.067	6.19E-02	4.11E-01	-0.057	1.08E-01	5.12E-01
T1↔F3opdR	-0.068	5.53E-02	4.03E-01	0.013	7.09E-01	9.27E-01	-0.011	7.52E-01	9.46E-01	0.039	2.80E-01	7.12E-01
T2p↔T1a.HeschlR	-0.020	5.77E-01	8.83E-01	-0.069	5.23E-02	4.03E-01	-0.035	3.32E-01	7.63E-01	-0.064	7.08E-02	4.27E-01
T1a↔RolS	0.049	1.68E-01	6.00E-01	0.020	5.72E-01	8.83E-01	0.070	4.95E-02	4.03E-01	0.055	1.23E-01	5.47E-01
T2ml↔T2p	-0.017	6.30E-01	8.95E-01	-0.012	7.35E-01	9.39E-01	-0.069	5.38E-02	4.03E-01	-0.020	5.68E-01	8.83E-01
Fusa↔F3tv	-0.071	4.76E-02	4.03E-01	0.025	4.81E-01	8.66E-01	-0.061	8.64E-02	4.56E-01	-0.062	8.21E-02	4.45E-01
PrF3op↔F2antR	-0.066	6.37E-02	4.11E-01	-0.068	5.67E-02	4.03E-01	-0.047	1.90E-01	6.14E-01	-0.010	7.76E-01	9.49E-01
F3td↔F3opdR	-0.070	4.94E-02	4.03E-01	-0.025	4.87E-01	8.67E-01	0.034	3.41E-01	7.67E-01	0.002	9.48E-01	9.77E-01
Fusa↔T1a.HeschlR	-0.039	2.75E-01	7.09E-01	-0.070	5.01E-02	4.03E-01	-0.045	2.06E-01	6.31E-01	-0.035	3.27E-01	7.63E-01
F3orb↔RolS	-0.010	7.79E-01	9.49E-01	0.014	6.98E-01	9.22E-01	-0.070	4.99E-02	4.03E-01	-0.040	2.64E-01	6.96E-01
F3tv↔T2pR	-0.064	7.27E-02	4.29E-01	0.028	4.36E-01	8.33E-01	-0.068	5.68E-02	4.03E-01	0.015	6.64E-01	9.01E-01
T2p↔F3opdR	0.011	7.66E-01	9.49E-01	0.068	5.80E-02	4.03E-01	0.003	9.29E-01	9.77E-01	-0.008	8.30E-01	9.57E-01
STSp↔T3p	0.017	6.40E-01	8.97E-01	-0.018	6.22E-01	8.95E-01	-0.067	5.92E-02	4.08E-01	-0.021	5.64E-01	8.83E-01

Endophenotype	Language task overall accuracy			Working Memory			Oral reading recognition			Vocabulary Comprehension		
	r	p value	FDR p value	r	p value	FDR p value	r	p value	FDR p value	r	p value	FDR p value
AG↔T1a.HeschlR	0.006	8.76E-01	9.71E-01	0.048	1.82E-01	6.13E-01	0.067	5.96E-02	4.09E-01	0.050	1.63E-01	5.94E-01
T2ml↔PrF3op	0.001	9.70E-01	9.85E-01	-0.006	8.63E-01	9.69E-01	-0.067	6.00E-02	4.09E-01	-0.034	3.34E-01	7.64E-01
F3tv↔SMG	-0.030	4.00E-01	7.99E-01	-0.035	3.20E-01	7.57E-01	0.046	2.01E-01	6.31E-01	0.067	6.08E-02	4.11E-01
T1a↔F3orb	0.013	7.06E-01	9.27E-01	-0.066	6.28E-02	4.11E-01	0.042	2.39E-01	6.78E-01	0.045	2.09E-01	6.34E-01
F3tv↔T1R	0.066	6.22E-02	4.11E-01	-0.013	7.20E-01	9.31E-01	-0.002	9.58E-01	9.79E-01	-0.010	7.89E-01	9.49E-01
SMG↔RolS	0.011	7.60E-01	9.46E-01	0.010	7.86E-01	9.49E-01	-0.067	6.17E-02	4.11E-01	-0.064	7.16E-02	4.29E-01
T2ml↔AG	-0.066	6.32E-02	4.11E-01	0.028	4.27E-01	8.24E-01	-0.009	7.99E-01	9.49E-01	0.025	4.78E-01	8.64E-01
AG↔T2pR	-0.003	9.43E-01	9.77E-01	0.015	6.78E-01	9.11E-01	0.065	6.76E-02	4.23E-01	0.012	7.37E-01	9.39E-01
AG↔STSp	0.036	3.12E-01	7.52E-01	0.065	6.77E-02	4.23E-01	0.026	4.67E-01	8.55E-01	-0.013	7.15E-01	9.31E-01
F2p↔F3orb	0.065	6.92E-02	4.26E-01	0.048	1.80E-01	6.13E-01	0.045	2.05E-01	6.31E-01	0.030	4.05E-01	8.03E-01
Fusa↔T2pR	0.021	5.65E-01	8.83E-01	0.065	6.90E-02	4.26E-01	0.018	6.08E-01	8.95E-01	-0.015	6.72E-01	9.07E-01
T2p↔RolS	0.018	6.10E-01	8.95E-01	0.022	5.37E-01	8.80E-01	0.064	7.07E-02	4.27E-01	0.035	3.23E-01	7.58E-01
F3tv↔T1a.HeschlR	-0.041	2.48E-01	6.87E-01	-0.065	7.02E-02	4.27E-01	0.051	1.49E-01	5.75E-01	0.027	4.57E-01	8.52E-01
RolS↔T1R	0.004	9.10E-01	9.74E-01	0.064	7.33E-02	4.29E-01	0.048	1.75E-01	6.08E-01	0.063	7.74E-02	4.36E-01
T1↔RolS	0.064	7.37E-02	4.29E-01	0.061	8.90E-02	4.60E-01	-0.004	9.17E-01	9.74E-01	-0.019	5.94E-01	8.89E-01
PT↔T2pR	-0.017	6.26E-01	8.95E-01	-0.064	7.24E-02	4.29E-01	-0.002	9.47E-01	9.77E-01	-0.005	8.85E-01	9.71E-01
AG↔F2antR	0.063	7.54E-02	4.35E-01	-0.029	4.11E-01	8.08E-01	0.004	9.15E-01	9.74E-01	-0.024	4.94E-01	8.69E-01
F2p↔T2pR	0.052	1.43E-01	5.71E-01	-0.022	5.30E-01	8.80E-01	0.063	7.74E-02	4.36E-01	0.006	8.64E-01	9.69E-01
Fusa↔AG	-0.018	6.10E-01	8.95E-01	-0.063	7.73E-02	4.36E-01	0.033	3.61E-01	7.76E-01	-0.013	7.16E-01	9.31E-01
T3p↔T1R	0.040	2.58E-01	6.96E-01	0.027	4.48E-01	8.46E-01	-0.014	6.98E-01	9.22E-01	0.062	7.99E-02	4.44E-01
PT↔T2p	-0.047	1.89E-01	6.14E-01	-0.027	4.54E-01	8.48E-01	-0.062	8.19E-02	4.45E-01	-0.041	2.54E-01	6.92E-01
Pole↔T3p	-0.008	8.18E-01	9.51E-01	-0.009	8.02E-01	9.49E-01	-0.062	8.06E-02	4.45E-01	-0.018	6.11E-01	8.95E-01
F3opd↔Fusa	0.062	8.24E-02	4.45E-01	0.037	3.03E-01	7.36E-01	0.041	2.50E-01	6.89E-01	0.005	8.97E-01	9.72E-01
RolS↔PrecR	0.047	1.86E-01	6.13E-01	0.041	2.51E-01	6.91E-01	0.061	8.77E-02	4.56E-01	0.020	5.83E-01	8.83E-01
T2pR↔T1R	0.061	8.77E-02	4.56E-01	-0.035	3.28E-01	7.63E-01	-0.040	2.65E-01	6.96E-01	-0.056	1.14E-01	5.27E-01
PrF3op↔T1a.HeschlR	0.002	9.53E-01	9.79E-01	-0.017	6.41E-01	8.98E-01	-0.022	5.34E-01	8.80E-01	-0.061	8.96E-02	4.61E-01
F3opd↔T1a.HeschlR	0.018	6.19E-01	8.95E-01	0.060	9.06E-02	4.62E-01	-0.012	7.27E-01	9.35E-01	0.012	7.42E-01	9.41E-01
F2p↔SMG	0.003	9.35E-01	9.77E-01	-0.005	8.79E-01	9.71E-01	0.060	9.04E-02	4.62E-01	-0.022	5.38E-01	8.80E-01
PrF3op↔F3td	0.044	2.13E-01	6.40E-01	0.059	9.65E-02	4.78E-01	-0.047	1.89E-01	6.14E-01	-0.060	9.25E-02	4.70E-01
F3td↔T2pR	-0.010	7.89E-01	9.49E-01	0.017	6.42E-01	8.98E-01	-0.037	2.95E-01	7.28E-01	-0.059	9.67E-02	4.78E-01
T1↔Fusa	-0.010	7.74E-01	9.49E-01	0.059	9.57E-02	4.78E-01	-0.027	4.55E-01	8.49E-01	-0.024	4.99E-01	8.69E-01
STSp↔F3td	-0.059	9.57E-02	4.78E-01	-0.029	4.15E-01	8.12E-01	-0.022	5.40E-01	8.80E-01	-0.009	8.02E-01	9.49E-01
Pole↔F3orb	0.039	2.80E-01	7.12E-01	0.018	6.19E-01	8.95E-01	0.059	9.95E-02	4.85E-01	0.046	1.99E-01	6.28E-01
F2p↔T3p	0.022	5.35E-01	8.80E-01	-0.058	1.03E-01	5.00E-01	-0.012	7.30E-01	9.36E-01	-0.003	9.39E-01	9.77E-01
F2p↔PrecR	-0.058	1.05E-01	5.05E-01	-0.023	5.19E-01	8.77E-01	-0.012	7.29E-01	9.36E-01	0.013	7.16E-01	9.31E-01
F2p↔STSp	0.015	6.83E-01	9.13E-01	-0.005	8.88E-01	9.71E-01	0.006	8.72E-01	9.69E-01	0.058	1.07E-01	5.12E-01
F3tv↔T2p	0.011	7.49E-01	9.45E-01	-0.009	7.98E-01	9.49E-01	0.057	1.10E-01	5.24E-01	0.021	5.52E-01	8.82E-01
F2antR↔PrecR	-0.008	8.18E-01	9.51E-01	-0.052	1.46E-01	5.71E-01	-0.054	1.32E-01	5.61E-01	-0.057	1.13E-01	5.27E-01
SMG↔T2pR	-0.041	2.47E-01	6.86E-01	-0.056	1.15E-01	5.27E-01	-0.034	3.36E-01	7.65E-01	0.009	8.12E-01	9.49E-01
STSp↔SMG	0.056	1.14E-01	5.27E-01	0.023	5.11E-01	8.75E-01	0.008	8.23E-01	9.54E-01	0.013	7.18E-01	9.31E-01
T2ml↔F3opdR	-0.049	1.73E-01	6.08E-01	-0.042	2.37E-01	6.78E-01	-0.056	1.18E-01	5.39E-01	-0.015	6.83E-01	9.13E-01
F3opd↔F3td	0.055	1.26E-01	5.49E-01	0.020	5.67E-01	8.83E-01	0.056	1.19E-01	5.40E-01	0.045	2.10E-01	6.34E-01
STSp↔F3orb	0.005	8.92E-01	9.72E-01	-0.019	5.94E-01	8.89E-01	-0.055	1.21E-01	5.45E-01	-0.036	3.11E-01	7.52E-01
PT↔T1R	-0.037	2.96E-01	7.28E-01	0.055	1.23E-01	5.47E-01	0.032	3.72E-01	7.82E-01	0.052	1.45E-01	5.71E-01
STSp↔T1a.HeschlR	-0.011	7.55E-01	9.46E-01	-0.042	2.44E-01	6.83E-01	-0.035	3.32E-01	7.63E-01	-0.055	1.24E-01	5.47E-01
AG↔SMG	-0.011	7.59E-01	9.46E-01	-0.031	3.91E-01	7.95E-01	-0.021	5.65E-01	8.83E-01	-0.055	1.23E-01	5.47E-01
PT↔F3orb	-0.055	1.26E-01	5.49E-01	0.002	9.65E-01	9.82E-01	-0.021	5.58E-01	8.83E-01	0.017	6.39E-01	8.97E-01
PT↔T1	0.032	3.75E-01	7.82E-01	0.019	5.91E-01	8.87E-01	0.054	1.27E-01	5.49E-01	-0.006	8.56E-01	9.66E-01
Fusa↔T1a	0.054	1.27E-01	5.49E-01	0.007	8.43E-01	9.64E-01	0.031	3.91E-01	7.95E-01	0.004	9.01E-01	9.73E-01
F3orb↔PrecR	-0.002	9.60E-01	9.80E-01	-0.055	1.25E-01	5.49E-01	-0.008	8.30E-01	9.57E-01	0.007	8.41E-01	9.63E-01
PT↔F3opdR	-0.032	3.73E-01	7.82E-01	0.020	5.80E-01	8.83E-01	-0.002	9.45E-01	9.77E-01	-0.054	1.28E-01	5.50E-01
T2p↔F2antR	0.021	5.56E-01	8.83E-01	0.048	1.77E-01	6.10E-01	0.021	5.48E-01	8.80E-01	0.054	1.32E-01	5.61E-01
F2p↔Fusa	-0.053	1.37E-01	5.67E-01	-0.038	2.87E-01	7.16E-01	-0.054	1.33E-01	5.63E-01	-0.035	3.24E-01	7.58E-01
Pole↔F3opd	0.007	8.38E-01	9.62E-01	0.053	1.36E-01	5.67E-01	-0.005	8.91E-01	9.72E-01	0.012	7.31E-01	9.36E-01
F3td↔PrecR	0.053	1.37E-01	5.67E-01	0.031	3.84E-01	7.93E-01	-0.019	6.02E-01	8.93E-01	-0.033	3.51E-01	7.74E-01
F3tv↔T1a	0.053	1.36E-01	5.67E-01	0.040	2.67E-01	6.98E-01	0.009	8.11E-01	9.49E-01	0.004	9.18E-01	9.74E-01
T2ml↔Fusa	-0.047	1.87E-01	6.13E-01	-0.002	9.45E-01	9.77E-01	-0.036	3.17E-01	7.56E-01	0.053	1.37E-01	5.67E-01
T1a.HeschlR↔PrecR	0.033	3.61E-01	7.76E-01	0.022	5.45E-01	8.80E-01	0.052	1.46E-01	5.71E-01	0.022	5.47E-01	8.80E-01
F3td↔T1a.HeschlR	-0.026	4.69E-01	8.57E-01	-0.003	9.37E-01	9.77E-01	0.010	7.87E-01	9.49E-01	0.052	1.44E-01	5.71E-01
T2p↔T1R	-0.034	3.45E-01	7.73E-01	0.024	4.95E-01	8.69E-01	-0.052	1.42E-01	5.71E-01	-0.041	2.48E-01	6.87E-01
Pole↔T2p	0.020	5.81E-01	8.83E-01	0.052	1.46E-01	5.71E-01	0.002	9.47E-01	9.77E-01	0.016	6.60E-01	9.00E-01
T2p↔T3p	0.010	7.72E-01	9.49E-01	-0.052	1.45E-01	5.71E-01	-0.029	4.08E-01	8.04E-01	-0.004	9.01E-01	9.73E-01
F3tv↔F3orb	0.052	1.45E-01	5.71E-01	0.018	6.23E-01	8.95E-01	-0.016	6.58E-01	8.99E-01	-0.015	6.79E-01	9.12E-01
T1a↔T2p	-0.024	4.96E-01	8.69E-01	0.052	1.48E-01	5.73E-01	-0.002	9.55E-01	9.79E-01	-0.017	6.35E-01	8.97E-01
Prec↔STSp	0.008	8.27E-01	9.55E-01	-0.051	1.50E-01	5.76E-01	0.013	7.10E-01	9.29E-01	-0.006	8.67E-01	9.69E-01
T1a↔F2antR	0.005	8.83E-01	9.71E-01	0.051	1.54E-01	5.82E-01	0.012	7.39E-01	9.39E-01	0.032	3.64E-01	7.77E-01
PrF3op↔AG	0.051	1.55E-01	5.82E-01	0.035	3.20E-01	7.57E-01	-0.003	9.22E-01	9.76E-01	-0.021	5.51E-01	8.82E-01
T2pR↔T1a.HeschlR	-0.025	4.84E-01	8.66E-01	-0.023	5.17E-01	8.77E-01	0.051	1.54E-01	5.82E-01	0.023	5.11E-01	8.75E-01
SMG↔F2antR	-0.009	8.08E-01	9.49E-01	-0.034	3.40E-01	7.67E-01	-0.051	1.56E-01	5.82E-01	-0.018	6.09E-01	8.95E-01
T2ml↔T1	-0.025	4.79E-01	8.65E-01	-0.029	4.20E-01	8.19E-01	-0.051	1.54E-01	5.82E-01	-0.027	4.48E-01	8.46E-01

Endophenotype	Language task overall accuracy			Working Memory			Oral reading recognition			Vocabulary Comprehension		
	r	p value	FDR p value	r	p value	FDR p value	r	p value	FDR p value	r	p value	FDR p value
F3tv↔PrecR	0.051	1.55E-01	5.82E-01	-0.037	2.98E-01	7.28E-01	0.012	7.37E-01	9.39E-01	0.019	5.87E-01	8.85E-01
Prec↔T1a.HeschlR	0.012	7.38E-01	9.39E-01	0.005	8.95E-01	9.72E-01	-0.050	1.57E-01	5.84E-01	-0.006	8.69E-01	9.69E-01
F3orb↔F2antR	0.034	3.45E-01	7.73E-01	-0.050	1.59E-01	5.86E-01	0.045	2.05E-01	6.31E-01	-0.015	6.65E-01	9.01E-01
T1↔T2p	0.050	1.60E-01	5.87E-01	0.024	5.06E-01	8.73E-01	-0.017	6.36E-01	8.97E-01	-0.026	4.67E-01	8.55E-01
PT↔Fusa	-0.004	9.18E-01	9.74E-01	-0.030	3.97E-01	7.98E-01	-0.050	1.63E-01	5.94E-01	-0.048	1.78E-01	6.12E-01
Pole↔Fusa	-0.024	5.02E-01	8.70E-01	-0.006	8.60E-01	9.69E-01	-0.050	1.64E-01	5.94E-01	-0.034	3.38E-01	7.65E-01
Prec↔T2ml	-0.036	3.13E-01	7.52E-01	-0.049	1.66E-01	5.97E-01	-0.021	5.65E-01	8.83E-01	-0.016	6.54E-01	8.99E-01
PT↔T3p	-0.011	7.48E-01	9.45E-01	0.016	6.61E-01	9.00E-01	0.007	8.46E-01	9.64E-01	-0.049	1.67E-01	6.00E-01
Fusa↔T2p	-0.015	6.64E-01	9.01E-01	0.045	2.06E-01	6.31E-01	-0.044	2.22E-01	6.54E-01	-0.049	1.72E-01	6.08E-01
Prec↔Fusa	-0.009	7.93E-01	9.49E-01	0.025	4.81E-01	8.66E-01	0.018	6.14E-01	8.95E-01	0.049	1.74E-01	6.08E-01
STSp↔T1R	0.048	1.75E-01	6.08E-01	-0.022	5.42E-01	8.80E-01	-0.007	8.35E-01	9.62E-01	0.011	7.55E-01	9.46E-01
F2p↔T2p	-0.048	1.75E-01	6.08E-01	-0.000	9.99E-01	9.99E-01	-0.026	4.61E-01	8.55E-01	0.040	2.62E-01	6.96E-01
T2p↔PrecR	-0.047	1.84E-01	6.13E-01	-0.016	6.44E-01	8.98E-01	-0.016	6.49E-01	8.99E-01	-0.022	5.37E-01	8.80E-01
PrF3op↔F3tv	-0.016	6.52E-01	8.99E-01	0.004	9.17E-01	9.74E-01	0.026	4.74E-01	8.60E-01	0.047	1.86E-01	6.13E-01
Fusa↔PrecR	-0.011	7.67E-01	9.49E-01	-0.047	1.83E-01	6.13E-01	-0.008	8.18E-01	9.51E-01	-0.017	6.25E-01	8.95E-01
T2ml↔SMG	-0.019	5.87E-01	8.85E-01	0.030	3.93E-01	7.95E-01	-0.032	3.74E-01	7.82E-01	-0.047	1.84E-01	6.13E-01
Prec↔F3td	0.004	9.04E-01	9.74E-01	-0.003	9.32E-01	9.77E-01	0.009	8.02E-01	9.49E-01	0.048	1.83E-01	6.13E-01
Pole↔F2antR	0.014	6.92E-01	9.20E-01	0.048	1.81E-01	6.13E-01	0.035	3.21E-01	7.57E-01	0.008	8.23E-01	9.54E-01
F3orb↔T1a.HeschlR	0.004	9.03E-01	9.74E-01	-0.020	5.79E-01	8.83E-01	-0.047	1.83E-01	6.13E-01	-0.030	4.01E-01	7.99E-01
AG↔T1a	0.032	3.75E-01	7.82E-01	0.047	1.89E-01	6.14E-01	0.019	5.90E-01	8.87E-01	0.045	2.07E-01	6.31E-01
F2p↔F3opdR	0.033	3.59E-01	7.76E-01	0.003	9.33E-01	9.77E-01	0.047	1.91E-01	6.15E-01	-0.016	6.55E-01	8.99E-01
STSp↔F2antR	0.009	8.03E-01	9.49E-01	0.046	1.92E-01	6.17E-01	0.046	2.01E-01	6.31E-01	0.009	7.98E-01	9.49E-01
F2p↔PrF3op	0.000	9.95E-01	9.98E-01	0.046	1.94E-01	6.20E-01	-0.014	7.01E-01	9.24E-01	0.010	7.72E-01	9.49E-01
PT↔F3opd	-0.016	6.53E-01	8.99E-01	-0.029	4.09E-01	8.04E-01	-0.046	1.95E-01	6.22E-01	-0.039	2.80E-01	7.12E-01
STSp↔T2p	-0.045	2.03E-01	6.31E-01	0.016	6.52E-01	8.99E-01	-0.046	1.98E-01	6.28E-01	-0.040	2.58E-01	6.96E-01
SMG↔F3td	0.046	1.99E-01	6.28E-01	-0.017	6.39E-01	8.97E-01	0.032	3.70E-01	7.82E-01	-0.016	6.59E-01	8.99E-01
Pole↔F2p	-0.045	2.05E-01	6.31E-01	-0.013	7.20E-01	9.31E-01	-0.010	7.85E-01	9.49E-01	-0.002	9.58E-01	9.79E-01
Pole↔T1R	0.045	2.06E-01	6.31E-01	-0.005	8.85E-01	9.71E-01	0.040	2.65E-01	6.96E-01	0.022	5.40E-01	8.80E-01
PrF3op↔SMG	0.021	5.63E-01	8.83E-01	0.045	2.08E-01	6.33E-01	-0.010	7.76E-01	9.49E-01	-0.023	5.24E-01	8.80E-01
F3opd↔T1R	-0.033	3.55E-01	7.76E-01	0.033	3.61E-01	7.76E-01	0.041	2.50E-01	6.89E-01	0.045	2.09E-01	6.34E-01
Pole↔STSp	-0.015	6.72E-01	9.07E-01	-0.045	2.10E-01	6.34E-01	-0.022	5.30E-01	8.80E-01	0.007	8.51E-01	9.64E-01
Fusa↔PrF3op	0.044	2.15E-01	6.43E-01	0.002	9.66E-01	9.82E-01	0.042	2.37E-01	6.78E-01	0.018	6.23E-01	8.95E-01
PT↔AG	0.003	9.24E-01	9.76E-01	0.006	8.61E-01	9.69E-01	0.033	3.61E-01	7.76E-01	0.044	2.21E-01	6.53E-01
Prec↔F3opd	0.043	2.23E-01	6.54E-01	0.008	8.13E-01	9.49E-01	-0.024	4.98E-01	8.69E-01	-0.021	5.62E-01	8.83E-01
F3td↔T1R	-0.002	9.53E-01	9.79E-01	0.020	5.68E-01	8.83E-01	0.020	5.72E-01	8.83E-01	0.043	2.30E-01	6.67E-01
T2pR↔PrecR	-0.042	2.37E-01	6.78E-01	0.023	5.14E-01	8.77E-01	-0.029	4.13E-01	8.10E-01	-0.005	8.87E-01	9.71E-01
T1a↔F3opdR	0.042	2.39E-01	6.78E-01	0.038	2.86E-01	7.15E-01	0.003	9.40E-01	9.77E-01	0.002	9.55E-01	9.79E-01
PrF3op↔PrecR	0.022	5.33E-01	8.80E-01	-0.003	9.42E-01	9.77E-01	0.031	3.86E-01	7.94E-01	-0.042	2.40E-01	6.78E-01
F2antR↔T1a.HeschlR	-0.033	3.57E-01	7.76E-01	-0.003	9.24E-01	9.76E-01	-0.026	4.65E-01	8.55E-01	-0.042	2.40E-01	6.78E-01
PT↔F2p	-0.017	6.34E-01	8.97E-01	0.022	5.44E-01	8.80E-01	0.042	2.43E-01	6.82E-01	0.003	9.34E-01	9.77E-01
T3p↔PrecR	-0.041	2.45E-01	6.85E-01	-0.022	5.45E-01	8.80E-01	-0.021	5.48E-01	8.80E-01	-0.007	8.41E-01	9.63E-01
RolS↔T1a.HeschlR	0.041	2.45E-01	6.85E-01	-0.032	3.69E-01	7.81E-01	0.016	6.49E-01	8.99E-01	0.014	6.96E-01	9.22E-01
Prec↔PT	0.041	2.52E-01	6.91E-01	0.030	3.93E-01	7.95E-01	-0.017	6.30E-01	8.95E-01	-0.010	7.75E-01	9.49E-01
F3tv↔F2antR	-0.007	8.52E-01	9.64E-01	0.040	2.63E-01	6.96E-01	0.032	3.75E-01	7.82E-01	0.027	4.53E-01	8.48E-01
SMG↔T1R	0.040	2.57E-01	6.96E-01	0.004	9.09E-01	9.74E-01	-0.006	8.68E-01	9.69E-01	0.022	5.40E-01	8.80E-01
F3tv↔F3td	-0.040	2.63E-01	6.96E-01	-0.015	6.83E-01	9.13E-01	-0.003	9.41E-01	9.77E-01	-0.021	5.49E-01	8.80E-01
F3orb↔T2pR	-0.004	9.16E-01	9.74E-01	0.039	2.75E-01	7.09E-01	0.033	3.55E-01	7.76E-01	-0.003	9.39E-01	9.77E-01
Pole↔T2pR	0.039	2.74E-01	7.09E-01	0.024	5.03E-01	8.70E-01	0.011	7.57E-01	9.46E-01	0.020	5.82E-01	8.83E-01
Prec↔F3tv	0.039	2.77E-01	7.09E-01	0.032	3.68E-01	7.81E-01	-0.029	4.19E-01	8.17E-01	-0.030	4.00E-01	7.99E-01
Prec↔T1R	-0.028	4.30E-01	8.26E-01	0.039	2.77E-01	7.09E-01	-0.017	6.27E-01	8.95E-01	-0.030	4.05E-01	8.03E-01
F3tv↔RolS	0.031	3.90E-01	7.95E-01	-0.016	6.52E-01	8.99E-01	-0.038	2.83E-01	7.12E-01	-0.018	6.08E-01	8.95E-01
Prec↔T2p	-0.021	5.54E-01	8.83E-01	-0.038	2.83E-01	7.12E-01	-0.005	8.87E-01	9.71E-01	-0.000	9.96E-01	9.98E-01
STSp↔T2pR	0.038	2.83E-01	7.12E-01	0.031	3.85E-01	7.94E-01	0.012	7.47E-01	9.45E-01	-0.002	9.57E-01	9.79E-01
T1↔T2pR	0.025	4.90E-01	8.68E-01	0.010	7.82E-01	9.49E-01	0.005	8.97E-01	9.72E-01	0.038	2.86E-01	7.15E-01
T2ml↔T3p	0.027	4.52E-01	8.48E-01	0.025	4.90E-01	8.68E-01	0.033	3.50E-01	7.74E-01	0.038	2.92E-01	7.25E-01
Prec↔Pole	-0.003	9.35E-01	9.77E-01	-0.009	7.93E-01	9.49E-01	0.018	6.11E-01	8.95E-01	0.037	2.94E-01	7.27E-01
T3p↔RolS	-0.037	2.96E-01	7.28E-01	-0.028	4.24E-01	8.20E-01	-0.035	3.29E-01	7.63E-01	-0.011	7.53E-01	9.46E-01
F3tv↔T3p	-0.024	5.07E-01	8.73E-01	-0.037	2.98E-01	7.28E-01	-0.029	4.23E-01	8.20E-01	0.030	4.08E-01	8.04E-01
PrF3op↔T1a	0.005	8.83E-01	9.71E-01	0.001	9.77E-01	9.90E-01	-0.037	3.00E-01	7.32E-01	0.003	9.35E-01	9.77E-01
AG↔RolS	-0.036	3.10E-01	7.52E-01	0.004	9.08E-01	9.74E-01	-0.009	8.00E-01	9.49E-01	0.016	6.44E-01	8.98E-01
F3opd↔RolS	-0.016	6.51E-01	8.99E-01	0.036	3.15E-01	7.54E-01	0.018	6.21E-01	8.95E-01	-0.019	6.01E-01	8.93E-01
F3opd↔T2p	0.022	5.41E-01	8.80E-01	0.033	3.50E-01	7.74E-01	-0.004	9.01E-01	9.73E-01	0.035	3.22E-01	7.57E-01
T1↔SMG	-0.035	3.31E-01	7.63E-01	-0.026	4.69E-01	8.57E-01	0.034	3.36E-01	7.65E-01	0.025	4.84E-01	8.66E-01
F3orb↔F3opdR	-0.016	6.57E-01	8.99E-01	0.001	9.84E-01	9.93E-01	-0.017	6.33E-01	8.97E-01	-0.034	3.38E-01	7.65E-01
T2ml↔RolS	0.008	8.22E-01	9.54E-01	0.034	3.38E-01	7.65E-01	0.004	9.08E-01	9.74E-01	-0.019	5.88E-01	8.85E-01
F3opd↔T1	-0.031	3.81E-01	7.88E-01	0.032	3.65E-01	7.77E-01	0.018	6.23E-01	8.95E-01	0.025	4.87E-01	8.67E-01
PT↔SMG	-0.028	4.30E-01	8.26E-01	0.032	3.65E-01	7.77E-01	-0.026	4.71E-01	8.58E-01	0.010	7.88E-01	9.49E-01
STSp↔RolS	-0.017	6.29E-01	8.95E-01	0.020	5.79E-01	8.83E-01	-0.005	8.81E-01	9.71E-01	-0.032	3.65E-01	7.77E-01
T1↔F3td	-0.032	3.67E-01	7.80E-01	0.019	5.99E-01	8.92E-01	-0.012	7.26E-01	9.35E-01	0.005	8.90E-01	9.72E-01

Endophenotype	Language task overall accuracy			Working Memory			Oral reading recognition			Vocabulary Comprehension		
	r	p value	FDR p value	r	p value	FDR p value	r	p value	FDR p value	r	p value	FDR p value
F3td↔F2antR	-0.011	7.61E-01	9.46E-01	0.002	9.48E-01	9.77E-01	-0.022	5.33E-01	8.80E-01	-0.032	3.69E-01	7.81E-01
F2p↔T1a.HeschlR	0.020	5.81E-01	8.83E-01	-0.031	3.77E-01	7.85E-01	0.010	7.82E-01	9.49E-01	0.002	9.63E-01	9.81E-01
T3p↔T2pR	-0.019	5.92E-01	8.87E-01	-0.031	3.80E-01	7.88E-01	0.008	8.13E-01	9.49E-01	-0.009	8.06E-01	9.49E-01
Fusa↔T1R	-0.010	7.79E-01	9.49E-01	0.003	9.27E-01	9.77E-01	-0.031	3.86E-01	7.94E-01	-0.030	3.94E-01	7.95E-01
Pole↔RolS	-0.028	4.40E-01	8.38E-01	-0.006	8.59E-01	9.69E-01	-0.030	3.94E-01	7.95E-01	-0.014	6.86E-01	9.14E-01
AG↔T3p	-0.030	3.94E-01	7.95E-01	-0.018	6.08E-01	8.95E-01	-0.009	8.06E-01	9.49E-01	-0.007	8.51E-01	9.64E-01
F2p↔F2antR	-0.000	9.97E-01	9.98E-01	-0.024	5.09E-01	8.74E-01	-0.007	8.46E-01	9.64E-01	-0.030	3.99E-01	7.99E-01
AG↔PrecR	-0.004	9.00E-01	9.73E-01	0.024	4.93E-01	8.69E-01	0.029	4.09E-01	8.04E-01	-0.020	5.74E-01	8.83E-01
T3p↔F3opdR	-0.000	9.91E-01	9.96E-01	0.001	9.85E-01	9.93E-01	-0.029	4.22E-01	8.19E-01	-0.010	7.82E-01	9.49E-01
F2p↔T1R	-0.009	7.93E-01	9.49E-01	0.001	9.77E-01	9.90E-01	-0.005	8.92E-01	9.72E-01	-0.029	4.22E-01	8.19E-01
Pole↔T1a	0.014	7.03E-01	9.25E-01	-0.001	9.87E-01	9.93E-01	0.029	4.23E-01	8.19E-01	0.014	6.91E-01	9.20E-01
F3opdR↔PrecR	-0.009	8.01E-01	9.49E-01	0.019	6.03E-01	8.94E-01	0.028	4.30E-01	8.26E-01	-0.002	9.62E-01	9.81E-01
Prec↔T1	0.009	8.11E-01	9.49E-01	0.027	4.41E-01	8.39E-01	0.024	4.96E-01	8.69E-01	-0.026	4.59E-01	8.54E-01
Prec↔T1a	0.018	6.20E-01	8.95E-01	0.024	5.04E-01	8.72E-01	0.027	4.44E-01	8.42E-01	0.022	5.32E-01	8.80E-01
PT↔T2ml	-0.015	6.66E-01	9.02E-01	-0.027	4.54E-01	8.48E-01	0.006	8.73E-01	9.69E-01	0.022	5.46E-01	8.80E-01
Prec↔F3opdR	0.010	7.79E-01	9.49E-01	-0.019	5.96E-01	8.89E-01	0.026	4.65E-01	8.55E-01	0.006	8.69E-01	9.69E-01
T1a↔T3p	-0.003	9.24E-01	9.76E-01	0.023	5.17E-01	8.77E-01	0.008	8.16E-01	9.51E-01	0.025	4.76E-01	8.62E-01
F3opd↔F3opdR	0.024	4.93E-01	8.69E-01	0.004	9.07E-01	9.74E-01	-0.000	9.97E-01	9.98E-01	-0.012	7.32E-01	9.37E-01
Pole↔PT	-0.005	8.95E-01	9.72E-01	0.013	7.17E-01	9.31E-01	-0.023	5.19E-01	8.77E-01	0.003	9.44E-01	9.77E-01
Prec↔RolS	-0.018	6.14E-01	8.95E-01	-0.023	5.19E-01	8.77E-01	0.016	6.58E-01	8.99E-01	0.016	6.63E-01	9.01E-01
PrF3op↔T2pR	0.016	6.49E-01	8.99E-01	0.023	5.18E-01	8.77E-01	-0.022	5.38E-01	8.80E-01	-0.009	8.09E-01	9.49E-01
SMG↔T2p	0.017	6.37E-01	8.97E-01	-0.004	9.15E-01	9.74E-01	0.003	9.35E-01	9.77E-01	-0.022	5.32E-01	8.80E-01
T1R↔PrecR	-0.019	5.88E-01	8.85E-01	-0.019	5.96E-01	8.89E-01	-0.007	8.46E-01	9.64E-01	-0.022	5.42E-01	8.80E-01
AG↔T2p	-0.004	9.14E-01	9.74E-01	-0.020	5.69E-01	8.83E-01	0.021	5.64E-01	8.83E-01	0.007	8.37E-01	9.62E-01
F2antR↔T2pR	0.006	8.62E-01	9.69E-01	-0.021	5.65E-01	8.83E-01	0.011	7.55E-01	9.46E-01	-0.005	8.98E-01	9.72E-01
T1↔PrF3op	0.017	6.35E-01	8.97E-01	-0.018	6.13E-01	8.95E-01	0.008	8.27E-01	9.55E-01	0.003	9.23E-01	9.76E-01
STSp↔PrecR	0.011	7.67E-01	9.49E-01	-0.012	7.38E-01	9.39E-01	-0.018	6.16E-01	8.95E-01	-0.001	9.79E-01	9.90E-01
Prec↔T3p	0.017	6.32E-01	8.97E-01	0.013	7.20E-01	9.31E-01	0.005	8.80E-01	9.71E-01	-0.009	8.03E-01	9.49E-01
F3td↔T3p	0.015	6.84E-01	9.14E-01	-0.007	8.50E-01	9.64E-01	0.013	7.25E-01	9.34E-01	-0.016	6.52E-01	8.99E-01
T2p↔F3td	-0.016	6.57E-01	8.99E-01	0.011	7.54E-01	9.46E-01	0.008	8.25E-01	9.55E-01	0.013	7.20E-01	9.31E-01
Prec↔AG	-0.012	7.31E-01	9.36E-01	-0.010	7.72E-01	9.49E-01	-0.005	8.83E-01	9.71E-01	0.014	7.01E-01	9.24E-01
Fusa↔T3p	-0.007	8.47E-01	9.64E-01	0.007	8.53E-01	9.64E-01	-0.001	9.75E-01	9.89E-01	0.005	8.98E-01	9.72E-01

C.3 (Endo)phenotypic correlation between both task activations and language-related scores

Table C.3 – **Pearson Correlation between both task activations and language-related scores.** Significant correlation was observed after false discovery rate correction at $p < 0.05$.

Endophenotype	Language task overall accuracy			Working Memory			Oral reading recognition			Vocabulary Comprehension		
	r	p value	FDR p value	r	p value	FDR p value	r	p value	FDR p value	r	p value	FDR p value
Pole	0.217	7.56E-10	3.78E-08	0.148	3.13E-05	4.15E-04	0.176	6.28E-07	1.57E-05	0.239	1.10E-11	1.10E-09
STSp	0.130	2.47E-04	1.65E-03	0.133	1.87E-04	1.34E-03	0.108	2.38E-03	1.13E-02	0.183	2.31E-07	7.70E-06
T1a	0.175	8.10E-07	1.62E-05	0.142	6.29E-05	5.57E-04	0.101	4.61E-03	2.01E-02	0.138	9.82E-05	7.55E-04
T1R	0.095	7.85E-03	3.14E-02	0.147	3.32E-05	4.15E-04	0.165	3.05E-06	5.08E-05	0.105	3.07E-03	1.39E-02
T2ml	0.142	6.68E-05	5.57E-04	0.145	4.62E-05	5.13E-04	0.142	6.68E-05	5.57E-04	0.126	3.87E-04	2.42E-03
T1a.HeschlR	0.119	8.22E-04	4.83E-03	0.093	9.37E-03	3.47E-02	0.085	1.64E-02	5.42E-02	0.046	1.95E-01	3.82E-01
PT	0.058	1.03E-01	2.58E-01	0.115	1.17E-03	6.48E-03	0.091	1.06E-02	3.79E-02	0.055	1.20E-01	2.83E-01
SMG	-0.114	1.37E-03	7.19E-03	-0.020	5.77E-01	6.76E-01	-0.030	4.00E-01	5.27E-01	-0.048	1.81E-01	3.61E-01
T1	0.093	8.65E-03	3.33E-02	0.113	1.49E-03	7.43E-03	0.077	3.03E-02	8.92E-02	0.040	2.68E-01	4.79E-01
AG	0.030	3.99E-01	5.27E-01	0.082	2.11E-02	6.61E-02	0.055	1.22E-01	2.83E-01	0.100	5.09E-03	2.12E-02
F2antR	-0.087	1.51E-02	5.20E-02	-0.027	4.52E-01	5.58E-01	-0.019	5.89E-01	6.77E-01	-0.073	4.01E-02	1.11E-01
Fusa	0.028	4.25E-01	5.45E-01	0.048	1.74E-01	3.61E-01	0.085	1.68E-02	5.42E-02	0.063	7.92E-02	2.08E-01
F3orb	0.010	7.84E-01	8.43E-01	0.077	3.01E-02	8.92E-02	0.038	2.81E-01	4.94E-01	0.036	3.19E-01	5.02E-01
F3opd	-0.026	4.66E-01	5.69E-01	0.035	3.29E-01	5.06E-01	0.075	3.49E-02	9.98E-02	0.032	3.70E-01	5.27E-01
T2pR	-0.065	6.80E-02	1.84E-01	0.030	4.00E-01	5.27E-01	0.061	8.77E-02	2.25E-01	-0.016	6.58E-01	7.39E-01
F2p	0.045	2.10E-01	4.03E-01	0.056	1.18E-01	2.83E-01	0.031	3.79E-01	5.27E-01	0.053	1.36E-01	3.10E-01
T2p	-0.052	1.46E-01	3.24E-01	0.050	1.57E-01	3.41E-01	-0.020	5.81E-01	6.76E-01	0.004	9.02E-01	9.20E-01
F3td	-0.048	1.78E-01	3.61E-01	0.030	4.08E-01	5.30E-01	0.031	3.89E-01	5.27E-01	0.037	3.03E-01	5.02E-01
T3p	0.007	8.35E-01	8.79E-01	0.049	1.71E-01	3.61E-01	0.035	3.21E-01	5.02E-01	0.016	6.54E-01	7.39E-01
RolS	-0.043	2.25E-01	4.25E-01	0.043	2.31E-01	4.28E-01	0.025	4.85E-01	5.85E-01	-0.011	7.54E-01	8.19E-01
Prec	-0.009	7.97E-01	8.48E-01	0.040	2.66E-01	4.79E-01	0.038	2.91E-01	4.96E-01	0.005	8.98E-01	9.20E-01
F3opdR	-0.036	3.19E-01	5.02E-01	-0.034	3.39E-01	5.13E-01	0.028	4.40E-01	5.58E-01	-0.038	2.92E-01	4.96E-01
PrF3op	-0.002	9.53E-01	9.63E-01	0.036	3.09E-01	5.02E-01	0.031	3.79E-01	5.27E-01	-0.006	8.66E-01	9.03E-01
F3tv	-0.020	5.73E-01	6.76E-01	0.034	3.44E-01	5.13E-01	-0.000	9.90E-01	9.90E-01	-0.014	6.92E-01	7.61E-01
PrecR	-0.032	3.64E-01	5.27E-01	0.027	4.48E-01	5.58E-01	-0.030	3.94E-01	5.27E-01	-0.014	6.88E-01	7.61E-01

Appendix D

D.1 Genomic loci associated with heritable language anatomical connectivities using MOSTest

Table D.1 – **Genomic loci associated with heritable language anatomical connectivities using MOSTest.** Lead SNP: ID of the lead SNPs within each locus. Position: position of the SNP in the hg19 human reference genome. mvgwasP discovery -British-: MOSTest association P value obtained using the discovery sample. mvgwasP replication -non British-: MOSTest association P value obtained using the independent replication sample. Functionnal category: Functional consequence of the SNP on the gene obtained from ANNOVAR. 'Central' phenotypes: the phenotypes that contributed most to the multivariate association considering the genome-wide association threshold ($5e-8$).

Genomic Locus	Lead SNP	chr	Position	Functional category	Non-effect allele	Effect allele	MAF	mvgwasP (discovery -British-)	mvgwasP (replication -non British-)	Nearest gene	Central endophenotypes	univariate P value	univariate Z
6	rs6658111	1	47980916	intergenic	G	T	0.360	2.01E-56	4.27E-02	AL356458.1	MO Fronto Insular tract5 Right	6.73E-16	-8.075324
8	rs61788401	1	59317534	ncRNA intronic	A	T	0.109	3.63E-14	2.67E-01	LINC01135	L3 Superior Londgitudinal Fasciculus II Left	3.63E-08	5.507745
10	rs2780818	1	65307994	intronic	G	T	0.223	3.43E-37	6.94E-04	JAK1	ICVF Fronto Insular tract4 Right	2.97E-15	-7.891989
10	rs2780818	1	65307994	intronic	G	T	0.223	3.43E-37	6.94E-04	JAK1	ICVF Superior Londgitudinal Fasciculus II Right	7.30E-12	-6.851627
10	rs2780818	1	65307994	intronic	G	T	0.223	3.43E-37	6.94E-04	JAK1	ICVF Arcuate Anterior Segment Right	7.20E-20	-9.124649
10	rs2780818	1	65307994	intronic	G	T	0.223	3.43E-37	6.94E-04	JAK1	ICVF Fronto Insular tract3 Right	2.23E-14	-7.636839
10	rs2780818	1	65307994	intronic	G	T	0.223	3.43E-37	6.94E-04	JAK1	MD Arcuate Anterior Segment Right	3.25E-08	5.527584
10	rs2780818	1	65307994	intronic	G	T	0.223	3.43E-37	6.94E-04	JAK1	ICVF Arcuate Long Segment Left	3.78E-20	-9.194018
10	rs2780818	1	65307994	intronic	G	T	0.223	3.43E-37	6.94E-04	JAK1	ICVF Fronto Insular tract5 Right	2.27E-13	-7.331844
10	rs2780818	1	65307994	intronic	G	T	0.223	3.43E-37	6.94E-04	JAK1	ICVF Inferior Fronto Occipital fasciculus Right	4.40E-08	-5.473817
10	rs2780818	1	65307994	intronic	G	T	0.223	3.43E-37	6.94E-04	JAK1	FA Arcuate Long Segment Left	1.07E-08	-5.718978
10	rs2780818	1	65307994	intronic	G	T	0.223	3.43E-37	6.94E-04	JAK1	ICVF Corpus callosum	9.13E-09	-5.746152
10	rs2780818	1	65307994	intronic	G	T	0.223	3.43E-37	6.94E-04	JAK1	ICVF Arcuate Posterior Segment Right	1.14E-14	-7.722946
10	rs2780818	1	65307994	intronic	G	T	0.223	3.43E-37	6.94E-04	JAK1	ICVF Fronto Insular tract3 Left	6.26E-12	-6.873663
10	rs2780818	1	65307994	intronic	G	T	0.223	3.43E-37	6.94E-04	JAK1	MD Superior Londgitudinal Fasciculus III Left	1.56E-08	5.655382
10	rs2780818	1	65307994	intronic	G	T	0.223	3.43E-37	6.94E-04	JAK1	ICVF Inferior Fronto Occipital fasciculus Left	1.02E-10	-6.463870
10	rs2780818	1	65307994	intronic	G	T	0.223	3.43E-37	6.94E-04	JAK1	ICVF Frontal Aslant Tract Right	4.30E-15	-7.845731
10	rs2780818	1	65307994	intronic	G	T	0.223	3.43E-37	6.94E-04	JAK1	ICVF Frontal Inferior longitudinal Left	1.59E-08	-5.651815
10	rs2780818	1	65307994	intronic	G	T	0.223	3.43E-37	6.94E-04	JAK1	ICVF Superior Londgitudinal Fasciculus II Left	9.41E-11	-6.476183
10	rs2780818	1	65307994	intronic	G	T	0.223	3.43E-37	6.94E-04	JAK1	L3 Arcuate Long Segment Left	2.25E-08	5.591641
10	rs2780818	1	65307994	intronic	G	T	0.223	3.43E-37	6.94E-04	JAK1	ICVF Frontal Aslant Tract Left	2.36E-17	-8.474467
10	rs2780818	1	65307994	intronic	G	T	0.223	3.43E-37	6.94E-04	JAK1	ICVF Superior Londgitudinal Fasciculus III Right	4.41E-17	-8.401499
10	rs2780818	1	65307994	intronic	G	T	0.223	3.43E-37	6.94E-04	JAK1	ICVF Arcuate Posterior Segment Left	1.40E-18	-8.797344
10	rs2780818	1	65307994	intronic	G	T	0.223	3.43E-37	6.94E-04	JAK1	ICVF Fronto Insular tract5 Left	3.02E-13	-7.293440
10	rs2780818	1	65307994	intronic	G	T	0.223	3.43E-37	6.94E-04	JAK1	ICVF Arcuate Long Segment Right	1.38E-13	-7.398095
10	rs2780818	1	65307994	intronic	G	T	0.223	3.43E-37	6.94E-04	JAK1	ICVF Inferior Longitudinal Right	8.61E-09	-5.756002
10	rs2780818	1	65307994	intronic	G	T	0.223	3.43E-37	6.94E-04	JAK1	ICVF Fronto Insular tract2 Left	1.25E-09	-6.073372
10	rs2780818	1	65307994	intronic	G	T	0.223	3.43E-37	6.94E-04	JAK1	MD Arcuate Posterior Segment Left	4.36E-08	5.475430
10	rs2780818	1	65307994	intronic	G	T	0.223	3.43E-37	6.94E-04	JAK1	ICVF Arcuate Anterior Segment Left	5.75E-14	-7.513694
10	rs2780818	1	65307994	intronic	G	T	0.223	3.43E-37	6.94E-04	JAK1	ICVF Superior Londgitudinal Fasciculus I Right	4.46E-09	-5.866297
10	rs2780818	1	65307994	intronic	G	T	0.223	3.43E-37	6.94E-04	JAK1	L2 Arcuate Long Segment Left	3.25E-11	6.634737
10	rs2780818	1	65307994	intronic	G	T	0.223	3.43E-37	6.94E-04	JAK1	ICVF Superior Londgitudinal Fasciculus I Left	8.36E-11	-6.493977
10	rs2780818	1	65307994	intronic	G	T	0.223	3.43E-37	6.94E-04	JAK1	ISOVF Fronto Insular tract3 Right	2.53E-08	-5.571125
10	rs2780818	1	65307994	intronic	G	T	0.223	3.43E-37	6.94E-04	JAK1	MD Arcuate Long Segment Left	2.06E-10	6.356944
10	rs2780818	1	65307994	intronic	G	T	0.223	3.43E-37	6.94E-04	JAK1	ICVF Uncinate Right	1.09E-12	-7.118951
10	rs2780818	1	65307994	intronic	G	T	0.223	3.43E-37	6.94E-04	JAK1	ICVF Uncinate Left	4.15E-12	-6.931883
10	rs2780818	1	65307994	intronic	G	T	0.223	3.43E-37	6.94E-04	JAK1	ICVF Inferior Longitudinal Left	6.95E-10	-6.167145
10	rs2780818	1	65307994	intronic	G	T	0.223	3.43E-37	6.94E-04	JAK1	ICVF Superior Londgitudinal Fasciculus III Left	4.35E-19	-8.927577
10	rs2780818	1	65307994	intronic	G	T	0.223	3.43E-37	6.94E-04	JAK1	ISOVF Fronto Insular tract4 Right	8.08E-09	-5.766822
10	rs2780818	1	65307994	intronic	G	T	0.223	3.43E-37	6.94E-04	JAK1	L3 Arcuate Anterior Segment Right	3.64E-08	5.507350
10	rs2780818	1	65307994	intronic	G	T	0.223	3.43E-37	6.94E-04	JAK1	L2 Arcuate Posterior Segment Left	2.30E-08	5.587950
10	rs2780818	1	65307994	intronic	G	T	0.223	3.43E-37	6.94E-04	JAK1	ICVF Frontal Inferior longitudinal Right	1.59E-16	-8.249888
12	rs3767967	1	94002233	intronic	G	A	0.391	2.00E-25	1.71E-02	FNBP1L	OD Superior Londgitudinal Fasciculus II Right	1.57E-08	-5.654032
12	rs3767967	1	94002233	intronic	G	A	0.391	2.00E-25	1.71E-02	FNBP1L	MO Superior Londgitudinal Fasciculus I Left	2.42E-08	-5.579175
12	rs3767967	1	94002233	intronic	G	A	0.391	2.00E-25	1.71E-02	FNBP1L	OD Superior Londgitudinal Fasciculus II Left	9.73E-09	-5.735333
15	rs3841064	1	153919858	upstream:downstream	AC	A	0.491	1.14E-12	4.69E-02	CRTC2	ICVF Arcuate Posterior Segment Right	5.62E-09	5.827759
15	rs3841064	1	153919858	upstream:downstream	AC	A	0.491	1.14E-12	4.69E-02	CRTC2	ICVF Arcuate Posterior Segment Left	3.06E-10	6.295846
15	rs3841064	1	153919858	upstream:downstream	AC	A	0.491	1.14E-12	4.69E-02	CRTC2	ICVF Arcuate Anterior Segment Left	9.69E-09	5.736030
15	rs3841064	1	153919858	upstream:downstream	AC	A	0.491	1.14E-12	4.69E-02	CRTC2	ICVF Superior Londgitudinal Fasciculus III Left	3.22E-08	5.529218
16	rs4745	1	155106227	exonic	T	A	0.479	1.20E-20	1.60E-01	EFNA1	OD Fronto Insular tract3 Right	1.82E-08	-5.628755
19	rs35306826	1	1809569936	intronic	A	T	0.408	6.65E-16	3.00E-03	STX6	ICVF Uncinate Right	2.07E-09	-5.992424
20	rs10922200	1	197321440	intronic	T	C	0.110	2.17E-22	1.33E-01	CRB1	FA Inferior Fronto Occipital fasciculus Right	4.81E-08	-5.458275
20	rs10922200	1	197321440	intronic	T	C	0.110	2.17E-22	1.33E-01	CRB1	FA Uncinate Right	2.04E-08	-5.608183
20	rs10922200	1	197321440	intronic	T	C	0.110	2.17E-22	1.33E-01	CRB1	FA Inferior Fronto Occipital fasciculus Left	3.92E-08	-5.494500
20	rs10922200	1	197321440	intronic	T	C	0.110	2.17E-22	1.33E-01	CRB1	FA Uncinate Left	5.57E-09	-5.829170
20	rs10922200	1	197321440	intronic	T	C	0.110	2.17E-22	1.33E-01	CRB1	FA Arcuate Anterior Segment Right	1.55E-09	-6.039372
20	rs10922200	1	197321440	intronic	T	C	0.110	2.17E-22	1.33E-01	CRB1	FA Fronto Insular tract4 Right	1.31E-10	-6.425766
20	rs10922200	1	197321440	intronic	T	C	0.110	2.17E-22	1.33E-01	CRB1	FA Arcuate Long Segment Left	1.32E-10	-6.425243
20	rs10922200	1	197321440	intronic	T	C	0.110	2.17E-22	1.33E-01	CRB1	MO Inferior Fronto Occipital fasciculus Right	2.80E-10	-6.309694
20	rs10922200	1	197321440	intronic	T	C	0.110	2.17E-22	1.33E-01	CRB1	OD Arcuate Long Segment Left	3.43E-13	7.276474
20	rs10922200	1	197321440	intronic	T	C	0.110	2.17E-22	1.33E-01	CRB1	OD Inferior Fronto Occipital fasciculus Left	5.87E-09	5.820496
20	rs10922200	1	197321440	intronic	T	C	0.110	2.17E-22	1.33E-01	CRB1	FA Arcuate Long Segment Right	1.93E-10	-6.367021
20	rs10922200	1	197321440	intronic	T	C	0.110	2.17E-22	1.33E-01	CRB1	OD Superior Londgitudinal Fasciculus III Right	5.92E-09	5.818894
20	rs10922200	1	197321440	intronic	T	C	0.110	2.17E-22	1.33E-01	CRB1	FA Fronto Insular tract3 Right	3.68E-11	-6.616588
20	rs10922200	1	197321440	intronic	T	C	0.110	2.17E-22	1.33E-01	CRB1	OD Arcuate Long Segment Right	5.15E-13	7.221302
20	rs10922200	1	197321440	intronic	T	C	0.110	2.17E-22	1.33E-01	CRB1	OD Arcuate Anterior Segment Right	2.32E-11	6.684432
20	rs10922200	1	197321440	intronic	T	C	0.110	2.17E-22	1.33E-01	CRB1	OD Fronto Insular tract4 Right	9.50E-09	5.739337
20	rs10922200	1	197321440	intronic	T	C	0.110	2.17E-22	1.33E-01	CRB1	OD Inferior Fronto Occipital fasciculus Right	4.51E-11	6.586259
20	rs10922200	1	197321440	intronic	T	C	0.110	2.17E-22	1.33E-01	CRB1	OD Fronto Insular tract3 Right	3.92E-13	7.258305
24	rs1452628	1	215139887	intergenic	T	A	0.385	4.97E-54	9.96E-03	RP11-323K10.1	ISOVF Frontal Aslant Tract Left	1.16E-15	8.008297
24	rs1452628	1	215139887	intergenic	T	A	0.385	4.97E-54	9.96E-03	RP11-323K10.1	L1 Arcuate Anterior Segment Right	2.59E-08	5.567129
24	rs1452628	1	215139887	intergenic	T	A	0.385	4.97E-54	9.96E-03	RP11-323K10.1	ISOVF Inferior Fronto Occipital fasciculus Left	1.31E-09	6.066640
24	rs1452628	1	215139887	intergenic	T	A	0.385	4.97E-54	9.96E-03	RP11-323K10.1	ISOVF Superior Londgitudinal Fasciculus II Right	2.43E-14	7.625774
24	rs1452628	1	215139887	intergenic	T	A	0.385	4.97E-54	9.96E-03	RP11-323K10.1	MO Frontal Aslant Tract Left	3.53E-08	5.512863
24	rs1452628	1	215139887	intergenic	T	A	0.385	4.97E-54	9.96E-03	RP11-323K10.1	MD Arcuate Anterior Segment Right	1.44E-09	6.050839
24	rs1452628	1	215139887	intergenic	T	A	0.385	4.97E-54	9.96E-03	RP11-323K10.1	L1 Frontal Superior Longitudinal Right	8.31E-14	7.465263
24	rs1452628	1	215139887	intergenic	T	A	0.385	4.97E-54	9.96E-03	RP11-323K10.1	ISOVF Frontal Inferior longitudinal Right	1.21E-15	8.003749
24	rs1452628	1	215139887	intergenic	T	A	0.385	4.97E-54	9.96E-03	RP11-323K10.1	MD Frontal Aslant Tract Right	2.98E-10	6.299814

Genomic Locus	Lead SNP	chr	Position	Functional category	Non-effect allele	Effect allele	MAF	mvgwasP (discovery -British-)	mvgwasP (replication -non British-)	Nearest gene	Central endophenotypes	univariate P value	univariate Z
24	rs1452628	1	215139887	intergenic	T	A	0.385	4.97E-54	9.96E-03	RP11-323K10.1	ISOVF Inferior Longitudinal Right	1.01E-13	7.439071
24	rs1452628	1	215139887	intergenic	T	A	0.385	4.97E-54	9.96E-03	RP11-323K10.1	ISOVF Superior Londgitudinal Fasciculus III Left	3.00E-17	8.446710
24	rs1452628	1	215139887	intergenic	T	A	0.385	4.97E-54	9.96E-03	RP11-323K10.1	OD Frontal Aslant Tract Left	1.59E-09	-6.035381
24	rs1452628	1	215139887	intergenic	T	A	0.385	4.97E-54	9.96E-03	RP11-323K10.1	ISOVF Arcuate Anterior Segment Left	6.40E-17	8.357630
24	rs1452628	1	215139887	intergenic	T	A	0.385	4.97E-54	9.96E-03	RP11-323K10.1	L3 Frontal Aslant Tract Left	3.08E-08	5.536681
24	rs1452628	1	215139887	intergenic	T	A	0.385	4.97E-54	9.96E-03	RP11-323K10.1	OD Corpus callosum	1.39E-08	-5.675166
24	rs1452628	1	215139887	intergenic	T	A	0.385	4.97E-54	9.96E-03	RP11-323K10.1	ISOVF Arcuate Posterior Segment Left	3.92E-20	9.190332
24	rs1452628	1	215139887	intergenic	T	A	0.385	4.97E-54	9.96E-03	RP11-323K10.1	L1 Arcuate Anterior Segment Left	8.60E-10	6.133483
24	rs1452628	1	215139887	intergenic	T	A	0.385	4.97E-54	9.96E-03	RP11-323K10.1	L3 Superior Londgitudinal Fasciculus III Right	7.96E-11	6.501320
24	rs1452628	1	215139887	intergenic	T	A	0.385	4.97E-54	9.96E-03	RP11-323K10.1	ISOVF Frontal Superior Longitudinal Right	8.57E-12	6.828709
24	rs1452628	1	215139887	intergenic	T	A	0.385	4.97E-54	9.96E-03	RP11-323K10.1	ISOVF Inferior Longitudinal Left	3.09E-14	7.594427
24	rs1452628	1	215139887	intergenic	T	A	0.385	4.97E-54	9.96E-03	RP11-323K10.1	ISOVF Frontal Aslant Tract Right	4.80E-15	7.832073
24	rs1452628	1	215139887	intergenic	T	A	0.385	4.97E-54	9.96E-03	RP11-323K10.1	OD Superior Londgitudinal Fasciculus I Left	2.06E-10	-6.356845
24	rs1452628	1	215139887	intergenic	T	A	0.385	4.97E-54	9.96E-03	RP11-323K10.1	MD Superior Londgitudinal Fasciculus III Left	1.60E-12	7.065431
24	rs1452628	1	215139887	intergenic	T	A	0.385	4.97E-54	9.96E-03	RP11-323K10.1	OD Superior Londgitudinal Fasciculus I Right	1.67E-13	-7.373076
24	rs1452628	1	215139887	intergenic	T	A	0.385	4.97E-54	9.96E-03	RP11-323K10.1	ISOVF Arcuate Long Segment Left	4.61E-12	6.916993
24	rs1452628	1	215139887	intergenic	T	A	0.385	4.97E-54	9.96E-03	RP11-323K10.1	L1 Arcuate Posterior Segment Left	9.64E-10	6.115220
24	rs1452628	1	215139887	intergenic	T	A	0.385	4.97E-54	9.96E-03	RP11-323K10.1	ISOVF Superior Londgitudinal Fasciculus II Left	4.55E-13	7.238041
24	rs1452628	1	215139887	intergenic	T	A	0.385	4.97E-54	9.96E-03	RP11-323K10.1	L2 Superior Londgitudinal Fasciculus III Right	3.47E-10	6.276107
24	rs1452628	1	215139887	intergenic	T	A	0.385	4.97E-54	9.96E-03	RP11-323K10.1	L3 Superior Londgitudinal Fasciculus III Left	2.01E-10	6.360294
24	rs1452628	1	215139887	intergenic	T	A	0.385	4.97E-54	9.96E-03	RP11-323K10.1	ISOVF Superior Londgitudinal Fasciculus I Left	1.42E-12	7.082466
24	rs1452628	1	215139887	intergenic	T	A	0.385	4.97E-54	9.96E-03	RP11-323K10.1	MO Frontal Aslant Tract Right	4.87E-08	5.456051
24	rs1452628	1	215139887	intergenic	T	A	0.385	4.97E-54	9.96E-03	RP11-323K10.1	ISOVF Superior Londgitudinal Fasciculus I Right	8.46E-10	6.136037
24	rs1452628	1	215139887	intergenic	T	A	0.385	4.97E-54	9.96E-03	RP11-323K10.1	L2 Superior Londgitudinal Fasciculus III Left	2.75E-08	5.556904
24	rs1452628	1	215139887	intergenic	T	A	0.385	4.97E-54	9.96E-03	RP11-323K10.1	MD Frontal Aslant Tract Left	1.15E-11	6.786115
24	rs1452628	1	215139887	intergenic	T	A	0.385	4.97E-54	9.96E-03	RP11-323K10.1	L1 Superior Londgitudinal Fasciculus II Right	4.54E-08	5.468581
24	rs1452628	1	215139887	intergenic	T	A	0.385	4.97E-54	9.96E-03	RP11-323K10.1	MD Arcuate Anterior Segment Left	1.26E-11	6.761146
24	rs1452628	1	215139887	intergenic	T	A	0.385	4.97E-54	9.96E-03	RP11-323K10.1	MD Frontal Inferior longitudinal Left	1.04E-08	5.723423
24	rs1452628	1	215139887	intergenic	T	A	0.385	4.97E-54	9.96E-03	RP11-323K10.1	L1 Superior Londgitudinal Fasciculus III Right	1.33E-13	7.402864
24	rs1452628	1	215139887	intergenic	T	A	0.385	4.97E-54	9.96E-03	RP11-323K10.1	L1 Frontal Aslant Tract Left	5.29E-18	8.646900
24	rs1452628	1	215139887	intergenic	T	A	0.385	4.97E-54	9.96E-03	RP11-323K10.1	MD Frontal Inferior longitudinal Right	4.11E-10	6.249785
24	rs1452628	1	215139887	intergenic	T	A	0.385	4.97E-54	9.96E-03	RP11-323K10.1	MD Arcuate Posterior Segment Left	1.06E-08	5.720891
24	rs1452628	1	215139887	intergenic	T	A	0.385	4.97E-54	9.96E-03	RP11-323K10.1	L1 Frontal Inferior longitudinal Right	3.03E-10	6.296993
24	rs1452628	1	215139887	intergenic	T	A	0.385	4.97E-54	9.96E-03	RP11-323K10.1	L1 Superior Londgitudinal Fasciculus I Right	8.39E-16	8.048415
24	rs1452628	1	215139887	intergenic	T	A	0.385	4.97E-54	9.96E-03	RP11-323K10.1	ISOVF Corpus callosum	3.11E-17	8.442507
24	rs1452628	1	215139887	intergenic	T	A	0.385	4.97E-54	9.96E-03	RP11-323K10.1	L3 Arcuate Anterior Segment Left	1.23E-08	5.696193
24	rs1452628	1	215139887	intergenic	T	A	0.385	4.97E-54	9.96E-03	RP11-323K10.1	ISOVF Frontal Inferior longitudinal Left	2.31E-09	5.974366
24	rs1452628	1	215139887	intergenic	T	A	0.385	4.97E-54	9.96E-03	RP11-323K10.1	ISOVF Arcuate Anterior Segment Right	1.07E-12	7.121270
24	rs1452628	1	215139887	intergenic	T	A	0.385	4.97E-54	9.96E-03	RP11-323K10.1	L2 Arcuate Anterior Segment Left	2.34E-09	5.972572
24	rs1452628	1	215139887	intergenic	T	A	0.385	4.97E-54	9.96E-03	RP11-323K10.1	L1 Superior Londgitudinal Fasciculus III Left	9.17E-15	7.750299
24	rs1452628	1	215139887	intergenic	T	A	0.385	4.97E-54	9.96E-03	RP11-323K10.1	L1 Frontal Aslant Tract Right	1.73E-15	7.959599
24	rs1452628	1	215139887	intergenic	T	A	0.385	4.97E-54	9.96E-03	RP11-323K10.1	ISOVF Superior Londgitudinal Fasciculus III Right	1.87E-17	8.501368
24	rs1452628	1	215139887	intergenic	T	A	0.385	4.97E-54	9.96E-03	RP11-323K10.1	L1 Corpus callosum	1.08E-12	7.119446
24	rs1452628	1	215139887	intergenic	T	A	0.385	4.97E-54	9.96E-03	RP11-323K10.1	ISOVF Arcuate Long Segment Right	4.37E-12	6.924797
24	rs1452628	1	215139887	intergenic	T	A	0.385	4.97E-54	9.96E-03	RP11-323K10.1	ISOVF Arcuate Posterior Segment Right	1.32E-14	7.704352
24	rs1452628	1	215139887	intergenic	T	A	0.385	4.97E-54	9.96E-03	RP11-323K10.1	MD Superior Londgitudinal Fasciculus III Right	2.29E-12	7.015655
24	rs1452628	1	215139887	intergenic	T	A	0.385	4.97E-54	9.96E-03	RP11-323K10.1	L3 Frontal Inferior longitudinal Right	4.93E-08	5.453957
24	rs1452628	1	215139887	intergenic	T	A	0.385	4.97E-54	9.96E-03	RP11-323K10.1	MO Superior Londgitudinal Fasciculus I Right	1.65E-08	5.645088
24	rs1452628	1	215139887	intergenic	T	A	0.385	4.97E-54	9.96E-03	RP11-323K10.1	L3 Arcuate Anterior Segment Right	1.33E-08	5.682268
24	rs1452628	1	215139887	intergenic	T	A	0.385	4.97E-54	9.96E-03	RP11-323K10.1	L1 Superior Londgitudinal Fasciculus I Left	9.47E-15	7.746150
24	rs2601645	1	215185552	intronic	T	C	0.084	2.12E-21	6.34E-02	KCNK2	ISOVF Inferior Longitudinal Right	2.15E-08	5.599845
24	rs2601645	1	215185552	intronic	T	C	0.084	2.12E-21	6.34E-02	KCNK2	ISOVF Superior Londgitudinal Fasciculus III Left	1.29E-10	6.428596
24	rs2601645	1	215185552	intronic	T	C	0.084	2.12E-21	6.34E-02	KCNK2	ISOVF Arcuate Anterior Segment Left	1.09E-12	7.118477
24	rs2601645	1	215185552	intronic	T	C	0.084	2.12E-21	6.34E-02	KCNK2	ISOVF Arcuate Posterior Segment Left	6.76E-11	6.525994
24	rs2601645	1	215185552	intronic	T	C	0.084	2.12E-21	6.34E-02	KCNK2	L3 Superior Londgitudinal Fasciculus III Right	2.23E-08	5.593048
24	rs2601645	1	215185552	intronic	T	C	0.084	2.12E-21	6.34E-02	KCNK2	ISOVF Inferior Longitudinal Left	3.95E-11	6.605793
24	rs2601645	1	215185552	intronic	T	C	0.084	2.12E-21	6.34E-02	KCNK2	MD Superior Londgitudinal Fasciculus III Left	3.63E-09	5.900043
24	rs2601645	1	215185552	intronic	T	C	0.084	2.12E-21	6.34E-02	KCNK2	ISOVF Arcuate Long Segment Left	8.14E-09	5.766537
24	rs2601645	1	215185552	intronic	T	C	0.084	2.12E-21	6.34E-02	KCNK2	MD Arcuate Anterior Segment Left	3.63E-09	5.900351
24	rs2601645	1	215185552	intronic	T	C	0.084	2.12E-21	6.34E-02	KCNK2	L1 Superior Londgitudinal Fasciculus III Right	4.96E-09	5.848653
24	rs2601645	1	215185552	intronic	T	C	0.084	2.12E-21	6.34E-02	KCNK2	L1 Frontal Aslant Tract Left	1.56E-10	6.399594
24	rs2601645	1	215185552	intronic	T	C	0.084	2.12E-21	6.34E-02	KCNK2	L2 Arcuate Anterior Segment Left	4.99E-08	5.451683
24	rs2601645	1	215185552	intronic	T	C	0.084	2.12E-21	6.34E-02	KCNK2	L1 Superior Londgitudinal Fasciculus III Left	1.99E-11	6.706575
24	rs2601645	1	215185552	intronic	T	C	0.084	2.12E-21	6.34E-02	KCNK2	L1 Frontal Aslant Tract Right	2.78E-09	5.943946
24	rs2601645	1	215185552	intronic	T	C	0.084	2.12E-21	6.34E-02	KCNK2	ISOVF Superior Londgitudinal Fasciculus III Right	7.56E-09	5.777919
24	rs2601645	1	215185552	intronic	T	C	0.084	2.12E-21	6.34E-02	KCNK2	MD Superior Londgitudinal Fasciculus III Right	6.26E-09	5.809792
25	rs11386753	2	27148654	intronic	CT	C	0.384	1.04E-42	1.99E-03	DPYSL5	OD Superior Londgitudinal Fasciculus II Right	2.75E-13	7.305951
25	rs11386753	2	27148654	intronic	CT	C	0.384	1.04E-42	1.99E-03	DPYSL5	MO Superior Londgitudinal Fasciculus I Left	6.45E-11	6.533017
25	rs11386753	2	27148654	intronic	CT	C	0.384	1.04E-42	1.99E-03	DPYSL5	OD Superior Londgitudinal Fasciculus II Left	6.83E-10	6.170080
26	rs35050623	2	37063240	intergenic	CT	C	0.462	7.04E-37	2.08E-01	ACo07382.1	OD Frontal Superior Longitudinal Right	4.34E-08	-5.476237
26	rs35050623	2	37063240	intergenic	CT	C	0.462	7.04E-37	2.08E-01	ACo07382.1	OD Superior Londgitudinal Fasciculus II Left	4.48E-08	-5.470685
28	rs11891807	2	48288816	ncRNA intronic	G	T	0.385	2.29E-16	5.22E-02	ACo79807.4	MO Fronto Insular tract4 Right	2.43E-08	-5.578464
29	2:56116193 TTGATTCTTGGCCTCCCTCCC T	2	56116193	intronic	T	TTGATTCTTGGCCTCCCTCCC	0.090	1.13E-27	2.69E-03	EFEMP1	ISOVF Fronto Insular tract1 Left	3.79E-08	5.500390
29	2:56116193 TTGATTCTTGGCCTCCCTCCC T	2	56116193	intronic	T	TTGATTCTTGGCCTCCCTCCC	0.090	1.13E-27	2.69E-03	EFEMP1	L1 Fronto Insular tract1 Left	1.87E-09	6.008724
29	2:56116193 TTGATTCTTGGCCTCCCTCCC T	2	56116193	intronic	T	TTGATTCTTGGCCTCCCTCCC	0.090	1.13E-27	2.69E-03	EFEMP1	MD Fronto Insular tract1 Left	1.53E-13	7.384537
29	2:56116193 TTGATTCTTGGCCTCCCTCCC T	2	56116193	intronic	T	TTGATTCTTGGCCTCCCTCCC	0.090	1.13E-27	2.69E-03	EFEMP1	ISOVF Uncinate Left	3.26E-13	7.281168
29	2:56116193 TTGATTCTTGGCCTCCCTCCC T	2	56116193	intronic	T	TTGATTCTTGGCCTCCCTCCC	0.090	1.13E-27	2.69E-03	EFEMP1	ICVF Fronto Insular tract1 Left	1.04E-09	6.103828
29	2:56116193 TTGATTCTTGGCCTCCCTCCC T	2	56116193	intronic	T	TTGATTCTTGGCCTCCCTCCC	0.090	1.13E-27	2.69E-03	EFEMP1	L2 Fronto Insular tract1 Left	1.31E-13	7.404875
29	2:56116193 TTGATTCTTGGCCTCCCTCCC T	2	56116193	intronic	T	TTGATTCTTGGCCTCCCTCCC	0.090	1.13E-27	2.69E-03	EFEMP1	L3 Fronto Insular tract1 Left	1.02E-13	7.437878
29	2:56116193 TTGATTCTTGGCCTCCCTCCC T	2	56116193	intronic	T	TTGATTCTTGGCCTCCCTCCC	0.090	1.13E-27	2.69E-03	EFEMP1	ISOVF Fronto Insular tract2 Right	1.25E-13	7.411435
32	rs7600385	2	65984026	ncRNA intronic	T	A	0.401	2.03E-24	2.78E-02	ACo74391.1	L1 Frontal Inferior longitudinal Left	2.28E-11	-6.686608
32	rs7600385	2	65984026	ncRNA intronic	T	A	0.401	2.03E-24	2.78E-02	ACo74391.1	MO Frontal Inferior longitudinal Left	2.70E-15	-7.903943
39	rs144495495	2	145692649	ncRNA intronic	CAT	C	0.250	2.36E-13	4.22E-01	TEX41	MD Superior Londgitudinal Fasciculus II Right	2.65E-09	5.952180
39	rs144495495	2	145692649	ncRNA intronic	CAT	C	0.250	2.36E-13	4.22E-01	TEX41	L1 Arcuate Anterior Segment Left	1.13E-08	5.719963
39	rs144495495	2	145692649	ncRNA intronic	CAT	C	0.250	2.36E-13	4.22E-01	TEX41	L1 Superior Londgitudinal Fasciculus II Left	2.86E-09	5.939562
39	rs144495495	2	145692649	ncRNA intronic	CAT	C	0.250	2.36E-13	4.22E-01	TEX41	L1 Superior Londgitudinal Fasciculus II Right	2.94E-09	5.934713
39	rs144495495	2	145692649	ncRNA intronic	CAT	C	0.250	2.36E-13	4.22E-01	TEX41	L2 Superior Londgitudinal Fasciculus I Right	7.22E-09	5.785624
39	rs144495495	2	145692649	ncRNA intronic	CAT	C	0.250	2.36E-13	4.22E-01	TEX41	MD Superior Londgitudinal Fasciculus I Right	5.56E-11	6.555018
39	rs144495495	2	145692649	ncRNA intronic	CAT	C	0.250	2.36E-13	4.22E-01	TEX41	L2 Frontal Aslant Tract Right	1.34E-09	6.062982
39	rs144495495	2	145692649	ncRNA intronic	CAT	C	0.250	2.36E-13	4.22E-01	TEX41	L3 Superior Londgitudinal Fasciculus I Right	1.08E-10	6.485701
39	rs144495495	2	145692649	ncRNA intronic	CAT	C	0.250	2.36E-13	4.22E-01	TEX41	MD Superior Londgitudinal Fasciculus I Left	1.43E-08	5.669349
43	rs34349435	2	203619455	intronic	A	C	0.034	2.03E-09	6.95E-01	FAM117B	MO Arcuate Anterior Segment Right	8.19E-09	5.764498
43	rs34349435	2	203619455	intronic	A	C	0.034	2.03E-09	6.95E-01	FAM117B	L1 Arcuate Long Segment Right	2.41E-08	5.579761
43	rs34349435	2	203619455	intronic	A	C	0.034	2.03E-09	6.95E-01	FAM117B	OD Arcuate Long Segment Right	4.41E-12	-6.923501
43	rs34349435	2	203619455	intronic	A	C	0.034	2.03E-09	6.95E-01	FAM117B	OD Arcuate Anterior Segment Right	4.52E-11	-6.586003
43	rs72932772	2	203682304	intronic	G	C	0.129	1.05E-21	5.23E-02	ICA1L	FA Inferior Fronto Occipital fasciculus Left	2.50E-08	-5.573346
43	rs72932772	2	203682304	intronic	G	C	0.129	1.05E-21	5.23E-02	ICA1L	MO Corpus callosum	2.44E-08	-5.577649
43	rs72932772	2	203682304	intronic	G	C	0.129	1.05E-21	5.23E-02	ICA1L	L1 Fronto Insular tract4 Right	1.23E-12	7.101592
43	rs72932772	2	203682304	intronic	G	C	0.129	1.05E-21	5.23E-02	ICA1L	MD Fronto Insular tract3 Right	6.29E-09	5.808813
43	rs72932772	2	203682304	intronic	G	C	0.129	1.05E-21	5.23E-02	ICA1L	L3 Fronto Insular tract4 Right	9.06E-10	6.125165
43	rs72932772	2	203682304	intronic	G	C	0.129	1.05E-21	5.23E-02	ICA1L	L1 Fronto Insular tract3 Right	5.37E-12	6.895494
43	rs72932772	2	203682304	intronic	G	C	0.129	1.05E-21	5.23E-02	ICA1L	MD Fronto Insular tract4 Right	2.12E-12	7.026515
43	rs72932772	2	203682304	intronic	G	C	0.129	1.05E-21	5.23E-02	ICA1L	ISOVF Fronto Insular tract3 Right	1.37E-11	6.761320
43	rs72932772	2	203682304	intronic	G	C	0.129	1.05E-21	5.23E-02	ICA1L	ISOVF Fronto Insular tract4 Right	1.20E-08	5.699535
43	rs72932772	2	203682304	intronic	G	C	0.129	1.05E-21	5.23E-02	ICA1L	L1 Fronto Insular tract5 Right	1.60E-08	5.649974
47	rs6749936	2	232055684	intergenic	T	C	0.212	2.23E-23	1.12E-02	ARMC9	L3 Fronto Insular tract5 Right	1.26E-12	-7.098208
47	rs6749936	2	232055684	intergenic	T	C	0.212	2.23E-23	1.12E-02	ARMC9	L3 Fronto Insular tract2 Right	5.18E-09	-5.841266
47	rs6749936	2	232055684	intergenic	T	C	0.212	2.23E-23	1.12E-02	ARMC9	MD Fronto Insular tract5 Right	1.32E-12	-7.092039
47	rs6749936	2	232055684	intergenic	T	C	0.212	2.23E-23	1.12E-02	ARMC9	L3 Fronto Insular tract1 Right	4.48E-08	-5.470622
47	rs6749936	2	232055684	intergenic	T	C	0.212	2.23E-23	1.12E-02	ARMC9	MD Fronto Insular tract3 Right	5.09E-09	-5.844257
47	rs6749936	2	232055684	intergenic	T	C	0.212	2.23E-23	1.12E-02	ARMC9	L3 Fronto Insular tract4 Right	7.85E-09	-5.771605
47	rs6749936	2	232055684	intergenic	T	C	0.212	2.23E-23	1.12E-02	ARMC9	L1 Fronto Insular tract3 Right	2.98E-08	-5.542322
47	rs6749936	2	232055684	intergenic	T	C	0.212	2.23E-23	1.12E-02	ARMC9	L3 Fronto Insular tract5 Left	3.38E-12	-6.961144
47	rs6749936	2	232055684	intergenic	T	C	0.212	2.23E-23	1.12E-02	ARMC9	MD Fronto Insular tract2 Left	4.47E-08	-5.471256
47	rs6749936	2	232055684	intergenic	T	C	0.212	2.23E-23	1.12E-02	ARMC9	MD Fronto Insular tract5 Left	2.86E-10	-6.306627
47	rs6749936	2	232055684	intergenic	T	C	0.212	2.23E-23	1.12E-02	ARMC9	L1 Uncinate Left	4.06E-10	-6.251702
47	rs6749936	2	232055684	intergenic	T	C	0.212	2.23E-23	1.12E-02	ARMC9	L2 Fronto Insular tract5 Right	4.59E-10	-6.232387
47	rs6749936	2	232055684	intergenic	T	C	0.212	2.23E-23	1.12E-02	ARMC9	MD Fronto Insular tract4 Right	1.28E-09	-6.069391
47	rs6749936	2	232055684	intergenic	T	C	0.212	2.23E-23	1.12E-02	ARMC9	L2 Uncinate Left	5.81E-10	-6.195512
47	rs6749936	2	232055684	intergenic	T	C	0.212	2.23E-23	1.12E-02	ARMC9	L3 Uncinate Left	1.11E-10	-6.451729
47	rs6749936	2	232055684	intergenic	T	C	0.212	2.23E-23	1.12E-02	ARMC9	MD Fronto Insular tract1 Right	1.59E-08	-5.651320
47	rs6749936	2	232055684	intergenic	T	C	0.212	2.23E-23	1.12E-02	ARMC9	L2 Fronto Insular tract4 Right	2.95E-08	-5.544120
47	rs6749936	2	232055684	intergenic	T	C	0.212	2.23E-23	1.12E-02	ARMC9	MD Fronto Insular tract2 Right	2.16E-09	-5.985281
47	rs6749936	2	232055684	intergenic	T	C	0.212	2.23E-23	1.12E-02	ARMC9	L3 Fronto Insular tract3 Right	1.26E-08	-5.691340
47	rs6749936	2	232055684	intergenic	T	C	0.212	2.23E-23	1.12E-02	ARMC9	MD Uncinate Left	3.07E-12	-6.974633
47	rs6749936	2	232055684	intergenic	T	C	0.212	2.23E-23	1.12E-02	ARMC9	L1 Fronto Insular tract5 Right	8.28E-10	-6.139431
49	rs13079464	3	13822439	intergenic	C	G	0.467	7.77E-12	3.48E-01	LINCo0620	L3 Superior Londgitudinal Fasciculus II Left	4.95E-08	-5.453202
49	rs13079464	3	13822439	intergenic	C	G	0.467	7.77E-12	3.48E-01	LINCo0620	MD Superior Londgitudinal Fasciculus II Left	8.88E-09	-5.750763
49	rs13079464	3	13822439	intergenic	C	G	0.467	7.77E-12	3.48E-01	LINCo0620	L2 Superior Londgitudinal Fasciculus I Left	2.73E-08	-5.558016
49	rs13079464	3	13822439	intergenic	C	G	0.467	7.77E-12	3.48E-01	LINCo0620	L1 Corpus callosum	7.50E-09	-5.779351
49	rs6442409	3	13835087	intergenic	C	T	0.343	1.20E-25	2.94E-01	WNT7A	L3 Superior Londgitudinal Fasciculus II Left	9.22E-12	-6.818191
49	rs6442409	3	13835087	intergenic	C	T	0.343	1.20E-25	2.94E-01	WNT7A	MD Inferior Longitudinal Left	2.59E-13	-7.314134
49	rs6442409	3	13835087	intergenic	C	T	0.343	1.20E-25	2.94E-01	WNT7A	ICVF Fronto Insular tract4 Right	3.14E-09	5.924016
49	rs6442409	3	13835087	intergenic	C	T	0.343	1.20E-25	2.94E-01	WNT7A	MD Superior Londgitudinal Fasciculus II Right	3.23E-14	-7.588907

Genomic Locus	Lead SNP	chr	Position	Functional category	Non-effect allele	Effect allele	MAF	mvgwasP (discovery -British-)	mvgwasP (replication -non British-)	Nearest gene	Central endophenotypes	univariate P value	univariate Z
49	rs6442409	3	13835087	intergenic	C	T	0.343	1.20E-25	2.94E-01	WNT7A	L1 Inferior Longitudinal Left	1.42E-10	-6.414158
49	rs6442409	3	13835087	intergenic	C	T	0.343	1.20E-25	2.94E-01	WNT7A	ICVF Superior Londgitudinal Fasciculus II Right	3.84E-12	6.942855
49	rs6442409	3	13835087	intergenic	C	T	0.343	1.20E-25	2.94E-01	WNT7A	ICVF Arcuate Anterior Segment Right	3.75E-10	6.264164
49	rs6442409	3	13835087	intergenic	C	T	0.343	1.20E-25	2.94E-01	WNT7A	ICVF Fronto Insular tract3 Right	1.48E-10	6.407570
49	rs6442409	3	13835087	intergenic	C	T	0.343	1.20E-25	2.94E-01	WNT7A	MD Arcuate Anterior Segment Right	5.12E-09	-5.843240
49	rs6442409	3	13835087	intergenic	C	T	0.343	1.20E-25	2.94E-01	WNT7A	L2 Inferior Longitudinal Left	5.94E-14	-7.509462
49	rs6442409	3	13835087	intergenic	C	T	0.343	1.20E-25	2.94E-01	WNT7A	MD Inferior Longitudinal Right	5.96E-12	-6.880593
49	rs6442409	3	13835087	intergenic	C	T	0.343	1.20E-25	2.94E-01	WNT7A	L1 Inferior Fronto Occipital fasciculus Left	1.05E-09	-6.101993
49	rs6442409	3	13835087	intergenic	C	T	0.343	1.20E-25	2.94E-01	WNT7A	ICVF Arcuate Long Segment Left	4.42E-10	6.238554
49	rs6442409	3	13835087	intergenic	C	T	0.343	1.20E-25	2.94E-01	WNT7A	MD Frontal Aslant Tract Right	5.20E-09	-5.840553
49	rs6442409	3	13835087	intergenic	C	T	0.343	1.20E-25	2.94E-01	WNT7A	L3 Superior Londgitudinal Fasciculus I Left	5.08E-13	-7.223186
49	rs6442409	3	13835087	intergenic	C	T	0.343	1.20E-25	2.94E-01	WNT7A	ICVF Fronto Insular tract2 Right	5.25E-11	6.563652
49	rs6442409	3	13835087	intergenic	C	T	0.343	1.20E-25	2.94E-01	WNT7A	ICVF Fronto Insular tract5 Right	1.35E-09	6.060788
49	rs6442409	3	13835087	intergenic	C	T	0.343	1.20E-25	2.94E-01	WNT7A	FA Superior Londgitudinal Fasciculus I Left	2.35E-09	5.971554
49	rs6442409	3	13835087	intergenic	C	T	0.343	1.20E-25	2.94E-01	WNT7A	L3 Frontal Aslant Tract Left	2.40E-09	-5.968352
49	rs6442409	3	13835087	intergenic	C	T	0.343	1.20E-25	2.94E-01	WNT7A	ICVF Inferior Fronto Occipital fasciculus Right	9.89E-11	6.468648
49	rs6442409	3	13835087	intergenic	C	T	0.343	1.20E-25	2.94E-01	WNT7A	MD Uncinate Right	6.25E-12	-6.873877
49	rs6442409	3	13835087	intergenic	C	T	0.343	1.20E-25	2.94E-01	WNT7A	MD Inferior Fronto Occipital fasciculus Right	8.72E-13	-7.149285
49	rs6442409	3	13835087	intergenic	C	T	0.343	1.20E-25	2.94E-01	WNT7A	ICVF Corpus callosum	2.25E-11	6.689113
49	rs6442409	3	13835087	intergenic	C	T	0.343	1.20E-25	2.94E-01	WNT7A	L3 Superior Londgitudinal Fasciculus III Right	1.79E-09	-6.016055
49	rs6442409	3	13835087	intergenic	C	T	0.343	1.20E-25	2.94E-01	WNT7A	ICVF Arcuate Posterior Segment Right	6.25E-09	5.809952
49	rs6442409	3	13835087	intergenic	C	T	0.343	1.20E-25	2.94E-01	WNT7A	MD Corpus callosum	5.30E-12	-6.897253
49	rs6442409	3	13835087	intergenic	C	T	0.343	1.20E-25	2.94E-01	WNT7A	L2 Inferior Fronto Occipital fasciculus Right	6.57E-10	-6.176125
49	rs6442409	3	13835087	intergenic	C	T	0.343	1.20E-25	2.94E-01	WNT7A	L1 Arcuate Long Segment Right	3.81E-08	-5.499589
49	rs6442409	3	13835087	intergenic	C	T	0.343	1.20E-25	2.94E-01	WNT7A	L3 Arcuate Posterior Segment Right	4.01E-08	-5.490439
49	rs6442409	3	13835087	intergenic	C	T	0.343	1.20E-25	2.94E-01	WNT7A	ICVF Fronto Insular tract3 Left	2.69E-09	5.949629
49	rs6442409	3	13835087	intergenic	C	T	0.343	1.20E-25	2.94E-01	WNT7A	MD Superior Londgitudinal Fasciculus III Left	1.35E-10	-6.421772
49	rs6442409	3	13835087	intergenic	C	T	0.343	1.20E-25	2.94E-01	WNT7A	ICVF Inferior Fronto Occipital fasciculus Left	3.46E-12	6.957512
49	rs6442409	3	13835087	intergenic	C	T	0.343	1.20E-25	2.94E-01	WNT7A	L1 Superior Londgitudinal Fasciculus II Left	2.71E-09	-5.948241
49	rs6442409	3	13835087	intergenic	C	T	0.343	1.20E-25	2.94E-01	WNT7A	ICVF Frontal Aslant Tract Right	2.32E-12	7.013661
49	rs6442409	3	13835087	intergenic	C	T	0.343	1.20E-25	2.94E-01	WNT7A	L1 Inferior Fronto Occipital fasciculus Right	9.22E-11	-6.479284
49	rs6442409	3	13835087	intergenic	C	T	0.343	1.20E-25	2.94E-01	WNT7A	ICVF Frontal Superior Longitudinal Left	2.74E-08	5.556999
49	rs6442409	3	13835087	intergenic	C	T	0.343	1.20E-25	2.94E-01	WNT7A	L1 Arcuate Posterior Segment Left	4.00E-13	-7.255522
49	rs6442409	3	13835087	intergenic	C	T	0.343	1.20E-25	2.94E-01	WNT7A	MD Fronto Insular tract2 Left	1.15E-10	-6.445209
49	rs6442409	3	13835087	intergenic	C	T	0.343	1.20E-25	2.94E-01	WNT7A	MD Arcuate Posterior Segment Right	3.28E-12	-6.965255
49	rs6442409	3	13835087	intergenic	C	T	0.343	1.20E-25	2.94E-01	WNT7A	FA Superior Londgitudinal Fasciculus II Right	2.02E-08	5.609972
49	rs6442409	3	13835087	intergenic	C	T	0.343	1.20E-25	2.94E-01	WNT7A	L2 Uncinate Right	4.23E-08	-5.480942
49	rs6442409	3	13835087	intergenic	C	T	0.343	1.20E-25	2.94E-01	WNT7A	L2 Corpus callosum	5.73E-10	-6.197547
49	rs6442409	3	13835087	intergenic	C	T	0.343	1.20E-25	2.94E-01	WNT7A	L1 Uncinate Left	1.03E-12	-7.125875
49	rs6442409	3	13835087	intergenic	C	T	0.343	1.20E-25	2.94E-01	WNT7A	L2 Superior Londgitudinal Fasciculus III Right	7.51E-12	-6.847624
49	rs6442409	3	13835087	intergenic	C	T	0.343	1.20E-25	2.94E-01	WNT7A	L3 Superior Londgitudinal Fasciculus III Left	6.73E-09	-5.797503
49	rs6442409	3	13835087	intergenic	C	T	0.343	1.20E-25	2.94E-01	WNT7A	L1 Uncinate Right	2.78E-11	-6.657625
49	rs6442409	3	13835087	intergenic	C	T	0.343	1.20E-25	2.94E-01	WNT7A	ICVF Superior Londgitudinal Fasciculus II Left	1.89E-11	6.714385
49	rs6442409	3	13835087	intergenic	C	T	0.343	1.20E-25	2.94E-01	WNT7A	L3 Inferior Fronto Occipital fasciculus Right	3.78E-10	-6.262762
49	rs6442409	3	13835087	intergenic	C	T	0.343	1.20E-25	2.94E-01	WNT7A	L2 Frontal Aslant Tract Left	2.95E-11	-6.649022
49	rs6442409	3	13835087	intergenic	C	T	0.343	1.20E-25	2.94E-01	WNT7A	L2 Superior Londgitudinal Fasciculus III Left	1.15E-10	-6.445393
49	rs6442409	3	13835087	intergenic	C	T	0.343	1.20E-25	2.94E-01	WNT7A	L3 Inferior Fronto Occipital fasciculus Left	4.56E-09	-5.862525
49	rs6442409	3	13835087	intergenic	C	T	0.343	1.20E-25	2.94E-01	WNT7A	L3 Arcuate Long Segment Left	1.50E-08	-5.661758
49	rs6442409	3	13835087	intergenic	C	T	0.343	1.20E-25	2.94E-01	WNT7A	ICVF Frontal Aslant Tract Left	3.11E-14	7.593450
49	rs6442409	3	13835087	intergenic	C	T	0.343	1.20E-25	2.94E-01	WNT7A	MD Frontal Aslant Tract Left	4.84E-11	-6.575894
49	rs6442409	3	13835087	intergenic	C	T	0.343	1.20E-25	2.94E-01	WNT7A	L1 Superior Londgitudinal Fasciculus II Right	1.56E-10	-6.399763
49	rs6442409	3	13835087	intergenic	C	T	0.343	1.20E-25	2.94E-01	WNT7A	ICVF Superior Londgitudinal Fasciculus III Right	2.84E-13	7.301674
49	rs6442409	3	13835087	intergenic	C	T	0.343	1.20E-25	2.94E-01	WNT7A	L2 Superior Londgitudinal Fasciculus II Right	1.11E-12	-7.116329
49	rs6442409	3	13835087	intergenic	C	T	0.343	1.20E-25	2.94E-01	WNT7A	ICVF Frontal Superior Longitudinal Right	1.34E-10	6.422650
49	rs6442409	3	13835087	intergenic	C	T	0.343	1.20E-25	2.94E-01	WNT7A	MD Arcuate Anterior Segment Left	1.52E-09	-6.041865
49	rs6442409	3	13835087	intergenic	C	T	0.343	1.20E-25	2.94E-01	WNT7A	L3 Arcuate Posterior Segment Left	1.77E-11	-6.724194
49	rs6442409	3	13835087	intergenic	C	T	0.343	1.20E-25	2.94E-01	WNT7A	L1 Superior Londgitudinal Fasciculus III Right	1.26E-10	-6.431617
49	rs6442409	3	13835087	intergenic	C	T	0.343	1.20E-25	2.94E-01	WNT7A	MD Superior Londgitudinal Fasciculus II Left	5.73E-13	-7.206804
49	rs6442409	3	13835087	intergenic	C	T	0.343	1.20E-25	2.94E-01	WNT7A	L1 Frontal Aslant Tract Left	1.94E-08	-5.616839
49	rs6442409	3	13835087	intergenic	C	T	0.343	1.20E-25	2.94E-01	WNT7A	L2 Inferior Fronto Occipital fasciculus Left	1.10E-10	-6.451918
49	rs6442409	3	13835087	intergenic	C	T	0.343	1.20E-25	2.94E-01	WNT7A	ICVF Arcuate Posterior Segment Left	2.04E-12	7.031511
49	rs6442409	3	13835087	intergenic	C	T	0.343	1.20E-25	2.94E-01	WNT7A	L2 Uncinate Left	4.26E-11	-6.594731
49	rs6442409	3	13835087	intergenic	C	T	0.343	1.20E-25	2.94E-01	WNT7A	ICVF Arcuate Long Segment Right	3.52E-08	5.513313
49	rs6442409	3	13835087	intergenic	C	T	0.343	1.20E-25	2.94E-01	WNT7A	L3 Inferior Longitudinal Left	1.03E-09	-6.104600
49	rs6442409	3	13835087	intergenic	C	T	0.343	1.20E-25	2.94E-01	WNT7A	L3 Corpus callosum	7.20E-09	-5.786267
49	rs6442409	3	13835087	intergenic	C	T	0.343	1.20E-25	2.94E-01	WNT7A	L3 Uncinate Left	1.34E-10	-6.422321
49	rs6442409	3	13835087	intergenic	C	T	0.343	1.20E-25	2.94E-01	WNT7A	ICVF Inferior Longitudinal Right	2.30E-10	6.339963
49	rs6442409	3	13835087	intergenic	C	T	0.343	1.20E-25	2.94E-01	WNT7A	ICVF Fronto Insular tract2 Left	1.18E-12	7.108204
49	rs6442409	3	13835087	intergenic	C	T	0.343	1.20E-25	2.94E-01	WNT7A	L2 Superior Londgitudinal Fasciculus I Right	1.74E-12	-7.053910
49	rs6442409	3	13835087	intergenic	C	T	0.343	1.20E-25	2.94E-01	WNT7A	L2 Superior Londgitudinal Fasciculus I Left	1.34E-13	-7.402627
49	rs6442409	3	13835087	intergenic	C	T	0.343	1.20E-25	2.94E-01	WNT7A	L1 Inferior Longitudinal Right	5.46E-11	-6.557708
49	rs6442409	3	13835087	intergenic	C	T	0.343	1.20E-25	2.94E-01	WNT7A	MD Arcuate Posterior Segment Left	2.44E-16	-8.198103
49	rs6442409	3	13835087	intergenic	C	T	0.343	1.20E-25	2.94E-01	WNT7A	ICVF Arcuate Anterior Segment Left	1.38E-10	6.418407
49	rs6442409	3	13835087	intergenic	C	T	0.343	1.20E-25	2.94E-01	WNT7A	ICVF Superior Londgitudinal Fasciculus I Right	1.28E-15	7.996247
49	rs6442409	3	13835087	intergenic	C	T	0.343	1.20E-25	2.94E-01	WNT7A	MD Superior Londgitudinal Fasciculus I Right	1.69E-13	-7.371610
49	rs6442409	3	13835087	intergenic	C	T	0.343	1.20E-25	2.94E-01	WNT7A	MD Arcuate Long Segment Right	2.14E-10	-6.350957
49	rs6442409	3	13835087	intergenic	C	T	0.343	1.20E-25	2.94E-01	WNT7A	L3 Uncinate Right	1.27E-10	-6.431300
49	rs6442409	3	13835087	intergenic	C	T	0.343	1.20E-25	2.94E-01	WNT7A	ICVF Fronto Insular tract1 Right	7.18E-13	7.176040
49	rs6442409	3	13835087	intergenic	C	T	0.343	1.20E-25	2.94E-01	WNT7A	L2 Arcuate Long Segment Left	3.16E-08	-5.532600
49	rs6442409	3	13835087	intergenic	C	T	0.343	1.20E-25	2.94E-01	WNT7A	ICVF Superior Londgitudinal Fasciculus I Left	4.68E-15	7.835254
49	rs6442409	3	13835087	intergenic	C	T	0.343	1.20E-25	2.94E-01	WNT7A	L2 Frontal Aslant Tract Right	1.73E-09	-6.020910
49	rs6442409	3	13835087	intergenic	C	T	0.343	1.20E-25	2.94E-01	WNT7A	FA Superior Londgitudinal Fasciculus I Right	1.27E-08	5.690551
49	rs6442409	3	13835087	intergenic	C	T	0.343	1.20E-25	2.94E-01	WNT7A	L2 Inferior Longitudinal Right	7.60E-11	-6.508347
49	rs6442409	3	13835087	intergenic	C	T	0.343	1.20E-25	2.94E-01	WNT7A	L1 Arcuate Posterior Segment Right	2.07E-10	-6.356286
49	rs6442409	3	13835087	intergenic	C	T	0.343	1.20E-25	2.94E-01	WNT7A	L2 Arcuate Anterior Segment Left	6.30E-10	-6.182678
49	rs6442409	3	13835087	intergenic	C	T	0.343	1.20E-25	2.94E-01	WNT7A	L1 Superior Londgitudinal Fasciculus III Left	1.75E-08	-5.634974
49	rs6442409	3	13835087	intergenic	C	T	0.343	1.20E-25	2.94E-01	WNT7A	L3 Superior Londgitudinal Fasciculus II Right	2.09E-13	-7.342730
49	rs6442409	3	13835087	intergenic	C	T	0.343	1.20E-25	2.94E-01	WNT7A	L1 Corpus callosum	4.11E-15	-7.851513
49	rs6442409	3	13835087	intergenic	C	T	0.343	1.20E-25	2.94E-01	WNT7A	MD Arcuate Long Segment Left	2.07E-11	-6.701220
49	rs6442409	3	13835087	intergenic	C	T	0.343	1.20E-25	2.94E-01	WNT7A	ICVF Uncinate Right	3.46E-13	7.275126
49	rs6442409	3	13835087	intergenic	C	T	0.343	1.20E-25	2.94E-01	WNT7A	L3 Superior Londgitudinal Fasciculus I Right	5.67E-12	-6.887785
49	rs6442409	3	13835087	intergenic	C	T	0.343	1.20E-25	2.94E-01	WNT7A	ICVF Uncinate Left	5.96E-16	8.090064
49	rs6442409	3	13835087	intergenic	C	T	0.343	1.20E-25	2.94E-01	WNT7A	ICVF Inferior Longitudinal Left	3.50E-11	6.623824
49	rs6442409	3	13835087	intergenic	C	T	0.343	1.20E-25	2.94E-01	WNT7A	ICVF Superior Londgitudinal Fasciculus III Left	1.19E-12	7.106960
49	rs6442409	3	13835087	intergenic	C	T	0.343	1.20E-25	2.94E-01	WNT7A	L3 Inferior Longitudinal Right	1.78E-09	-6.016874
49	rs6442409	3	13835087	intergenic	C	T	0.343	1.20E-25	2.94E-01	WNT7A	MD Uncinate Left	5.32E-14	-7.523776
49	rs6442409	3	13835087	intergenic	C	T	0.343	1.20E-25	2.94E-01	WNT7A	L2 Arcuate Posterior Segment Right	3.10E-10	-6.293810
49	rs6442409	3	13835087	intergenic	C	T	0.343	1.20E-25	2.94E-01	WNT7A	L2 Superior Londgitudinal Fasciculus II Left	1.32E-11	-6.766603
49	rs6442409	3	13835087	intergenic	C	T	0.343	1.20E-25	2.94E-01	WNT7A	MD Superior Londgitudinal Fasciculus III Right	1.52E-11	-6.745635
49	rs6442409	3	13835087	intergenic	C	T	0.343	1.20E-25	2.94E-01	WNT7A	MD Inferior Fronto Occipital fasciculus Left	1.01E-11	-6.805088
49	rs6442409	3	13835087	intergenic	C	T	0.343	1.20E-25	2.94E-01	WNT7A	L2 Arcuate Posterior Segment Left	1.07E-13	-7.431660
49	rs6442409	3	13835087	intergenic	C	T	0.343	1.20E-25	2.94E-01	WNT7A	ICVF Frontal Inferior longitudinal Right	1.33E-10	6.423744
49	rs6442409	3	13835087	intergenic	C	T	0.343	1.20E-25	2.94E-01	WNT7A	MD Superior Londgitudinal Fasciculus I Left	2.71E-14	-7.611477
50	rs11720653	3	17439510	intronic	C	T	0.316	1.04E-18	1.95E-01	TBC1D5	MO Inferior Longitudinal Right	2.03E-08	5.609236
52	rs142003765	3	39479611	intergenic	G	A	0.020	1.26E-09	8.81E-02	AC099332.1	FA Inferior Fronto Occipital fasciculus Left	1.43E-08	5.670050
52	rs142003765	3	39479611	intergenic	G	A	0.020	1.26E-09	8.81E-02	AC099332.1	OD Corpus callosum	4.87E-11	-6.574736
52	rs142003765	3	39479611	intergenic	G	A	0.020	1.26E-09	8.81E-02	AC099332.1	OD Superior Londgitudinal Fasciculus III Left	4.36E-09	-5.869843
52	rs142003765	3	39479611	intergenic	G	A	0.020	1.26E-09	8.81E-02	AC099332.1	OD Inferior Fronto Occipital fasciculus Left	8.10E-10	-6.143033
52	rs142003765	3	39479611	intergenic	G	A	0.020	1.26E-09	8.81E-02	AC099332.1	OD Superior Londgitudinal Fasciculus III Right	7.67E-13	-7.166841
52	rs142003765	3	39479611	intergenic	G	A	0.020	1.26E-09	8.81E-02	AC099332.1	FA Corpus callosum	2.31E-09	5.974270
52	rs142003765	3	39479611	intergenic	G	A	0.020	1.26E-09	8.81E-02	AC099332.1	OD Arcuate Anterior Segment Left	1.88E-08	-5.622957
52	rs142003765	3	39479611	intergenic	G	A	0.020	1.26E-09	8.81E-02	AC099332.1	OD Arcuate Anterior Segment Right	3.35E-08	-5.522076
52	rs10675541	3	39510286	intronic	TAC	T	0.480	2.16E-16	3.10E-01	MOBP	OD Corpus callosum	1.67E-08	5.642831
52	rs10675541	3	39510286	intronic	TAC	T	0.480	2.16E-16	3.10E-01	MOBP	OD Superior Londgitudinal Fasciculus III Left	6.57E-09	5.801588
52	rs10675541	3	39510286	intronic	TAC	T	0.480	2.16E-16	3.10E-01	MOBP	OD Inferior Fronto Occipital fasciculus Left	1.33E-08	5.682229
52	rs10675541	3	39510286	intronic	TAC	T	0.480	2.16E-16	3.10E-01	MOBP	OD Superior Londgitudinal Fasciculus III Right	5.97E-11	6.544439
52	rs10675541	3	39510286	intronic	TAC	T	0.480	2.16E-16	3.10E-01	MOBP	OD Arcuate Anterior Segment Right	3.07E-08	5.537203
55	rs59623077	3	49106542	intronic	TA	T	0.336	6.27E-09	8.95E-01	QRICH1	FA Fronto Insular tract1 Right	1.97E-08	-5.614360
55	rs9832454	3	50217558	intronic	T	C	0.089	1.35E-11	5.60E-03	SEMA3F	ICVF Fronto Insular tract2 Left	1.81E-10	6.376559
62	rs67316928	3	89482234	intronic	C	T	0.398	2.94E-67	3.17E-05	EPHA3	OD Superior Londgitudinal Fasciculus II Left	3.25E-08	-5.527406
65	rs373566812	3	124462488	intronic	AAAAT	A	0.165	1.02E-11	7.18E-01	UMPS	ISOVF Superior Londgitudinal Fasciculus II Right	3.98E-11	6.604634
65	rs373566812	3	124462488	intronic	AAAAT	A	0.165	1.02E-11	7.18E-01	UMPS	ISOVF Arcuate Posterior Segment Left	8.43E-09	5.759549
65	rs373566812	3	124462488	intronic	AAAAT	A	0.165	1.02E-11	7.18E-01	UMPS	ISOVF Superior Londgitudinal Fasciculus II Left	1.31E-10	6.426407
70	rs62275311	3	147034001	ncRNA intronic	C	A	0.245	4.95E-20	2.74E-02	RP11-649A16.1	ISOVF Corpus callosum	8.36E-10	-6.137961

Genomic Locus	Lead SNP	chr	Position	Functional category	Non-effect allele	Effect allele	MAF	mvgwasP (discovery -British-)	mvgwasP (replication -non British-)	Nearest gene	Central endophenotypes	univariate P value	univariate Z
72	3:170987040 ACTCT A	3	170987040	intronic	A	ACTCT	0.455	2.71E-14	7.93E-02	TNIK	OD Fronto Insular tract4 Right	9.33E-09	5.742494
72	3:170987040 ACTCT A	3	170987040	intronic	A	ACTCT	0.455	2.71E-14	7.93E-02	TNIK	OD Fronto Insular tract3 Right	4.13E-08	5.485095
73	rs9647379	3	171785168	intronic	C	G	0.410	5.56E-12	2.28E-01	FNDC3B	L3 Frontal Aslant Tract Right	1.48E-09	-6.046996
73	rs9647379	3	171785168	intronic	C	G	0.410	5.56E-12	2.28E-01	FNDC3B	ISOVF Frontal Aslant Tract Left	1.46E-08	-5.665789
73	rs9647379	3	171785168	intronic	C	G	0.410	5.56E-12	2.28E-01	FNDC3B	MD Arcuate Anterior Segment Right	5.12E-10	-6.215248
73	rs9647379	3	171785168	intronic	C	G	0.410	5.56E-12	2.28E-01	FNDC3B	L2 Inferior Longitudinal Left	3.91E-08	-5.494767
73	rs9647379	3	171785168	intronic	C	G	0.410	5.56E-12	2.28E-01	FNDC3B	MD Frontal Aslant Tract Right	6.12E-10	-6.187278
73	rs9647379	3	171785168	intronic	C	G	0.410	5.56E-12	2.28E-01	FNDC3B	ISOVF Superior Londgitudinal Fasciculus III Left	8.37E-11	-6.493747
73	rs9647379	3	171785168	intronic	C	G	0.410	5.56E-12	2.28E-01	FNDC3B	ISOVF Arcuate Anterior Segment Left	3.13E-09	-5.924591
73	rs9647379	3	171785168	intronic	C	G	0.410	5.56E-12	2.28E-01	FNDC3B	L3 Frontal Aslant Tract Left	1.07E-08	-5.719064
73	rs9647379	3	171785168	intronic	C	G	0.410	5.56E-12	2.28E-01	FNDC3B	ISOVF Frontal Aslant Tract Right	2.16E-08	-5.598414
73	rs9647379	3	171785168	intronic	C	G	0.410	5.56E-12	2.28E-01	FNDC3B	MD Superior Londgitudinal Fasciculus III Left	2.64E-09	-5.952408
73	rs9647379	3	171785168	intronic	C	G	0.410	5.56E-12	2.28E-01	FNDC3B	L2 Superior Londgitudinal Fasciculus III Right	1.18E-09	-6.083558
73	rs9647379	3	171785168	intronic	C	G	0.410	5.56E-12	2.28E-01	FNDC3B	L2 Frontal Aslant Tract Left	1.05E-09	-6.101431
73	rs9647379	3	171785168	intronic	C	G	0.410	5.56E-12	2.28E-01	FNDC3B	L2 Superior Londgitudinal Fasciculus III Left	4.87E-09	-5.851703
73	rs9647379	3	171785168	intronic	C	G	0.410	5.56E-12	2.28E-01	FNDC3B	L2 Arcuate Anterior Segment Right	3.96E-10	-6.255507
73	rs9647379	3	171785168	intronic	C	G	0.410	5.56E-12	2.28E-01	FNDC3B	L3 Inferior Fronto Occipital fasciculus Left	2.24E-08	-5.592626
73	rs9647379	3	171785168	intronic	C	G	0.410	5.56E-12	2.28E-01	FNDC3B	MD Frontal Aslant Tract Left	1.29E-09	-6.068114
73	rs9647379	3	171785168	intronic	C	G	0.410	5.56E-12	2.28E-01	FNDC3B	MD Arcuate Anterior Segment Left	1.51E-09	-6.043451
73	rs9647379	3	171785168	intronic	C	G	0.410	5.56E-12	2.28E-01	FNDC3B	L2 Inferior Fronto Occipital fasciculus Left	3.13E-08	-5.533811
73	rs9647379	3	171785168	intronic	C	G	0.410	5.56E-12	2.28E-01	FNDC3B	MD Fronto Insular tract3 Left	9.09E-09	-5.746821
73	rs9647379	3	171785168	intronic	C	G	0.410	5.56E-12	2.28E-01	FNDC3B	MD Superior Londgitudinal Fasciculus I Right	4.85E-08	-5.456874
73	rs9647379	3	171785168	intronic	C	G	0.410	5.56E-12	2.28E-01	FNDC3B	ISOVF Arcuate Anterior Segment Right	1.67E-10	-6.389048
73	rs9647379	3	171785168	intronic	C	G	0.410	5.56E-12	2.28E-01	FNDC3B	L2 Frontal Aslant Tract Right	1.00E-08	-5.730239
73	rs9647379	3	171785168	intronic	C	G	0.410	5.56E-12	2.28E-01	FNDC3B	L2 Arcuate Anterior Segment Left	6.54E-10	-6.176943
73	rs9647379	3	171785168	intronic	C	G	0.410	5.56E-12	2.28E-01	FNDC3B	L1 Superior Londgitudinal Fasciculus III Left	2.81E-08	-5.553056
73	rs9647379	3	171785168	intronic	C	G	0.410	5.56E-12	2.28E-01	FNDC3B	ISOVF Superior Londgitudinal Fasciculus III Right	1.59E-09	-6.034471
73	rs9647379	3	171785168	intronic	C	G	0.410	5.56E-12	2.28E-01	FNDC3B	L3 Superior Londgitudinal Fasciculus I Right	3.74E-09	-5.895467
73	rs9647379	3	171785168	intronic	C	G	0.410	5.56E-12	2.28E-01	FNDC3B	MD Superior Londgitudinal Fasciculus III Right	5.35E-09	-5.835794
73	rs9647379	3	171785168	intronic	C	G	0.410	5.56E-12	2.28E-01	FNDC3B	L3 Arcuate Anterior Segment Right	2.19E-08	-5.596156
75	rs3772705	3	183388403	intronic	G	A	0.255	2.84E-13	6.43E-01	KLHL24	L1 Arcuate Anterior Segment Right	1.40E-10	6.415792
75	rs3772705	3	183388403	intronic	G	A	0.255	2.84E-13	6.43E-01	KLHL24	ICVF Superior Londgitudinal Fasciculus II Right	1.99E-10	-6.362051
75	rs3772705	3	183388403	intronic	G	A	0.255	2.84E-13	6.43E-01	KLHL24	ICVF Arcuate Anterior Segment Right	1.02E-08	-5.726704
75	rs3772705	3	183388403	intronic	G	A	0.255	2.84E-13	6.43E-01	KLHL24	L1 Inferior Fronto Occipital fasciculus Left	4.43E-08	5.472603
75	rs3772705	3	183388403	intronic	G	A	0.255	2.84E-13	6.43E-01	KLHL24	ICVF Arcuate Long Segment Left	6.82E-10	-6.170280
75	rs3772705	3	183388403	intronic	G	A	0.255	2.84E-13	6.43E-01	KLHL24	ICVF Inferior Fronto Occipital fasciculus Right	1.66E-11	-6.733381
75	rs3772705	3	183388403	intronic	G	A	0.255	2.84E-13	6.43E-01	KLHL24	MD Inferior Fronto Occipital fasciculus Right	3.83E-08	5.498678
75	rs3772705	3	183388403	intronic	G	A	0.255	2.84E-13	6.43E-01	KLHL24	ICVF Corpus callosum	8.00E-10	-6.144987
75	rs3772705	3	183388403	intronic	G	A	0.255	2.84E-13	6.43E-01	KLHL24	ICVF Arcuate Posterior Segment Right	7.11E-10	-6.163619
75	rs3772705	3	183388403	intronic	G	A	0.255	2.84E-13	6.43E-01	KLHL24	MD Corpus callosum	4.13E-08	5.485329
75	rs3772705	3	183388403	intronic	G	A	0.255	2.84E-13	6.43E-01	KLHL24	ICVF Inferior Fronto Occipital fasciculus Left	4.51E-11	-6.586364
75	rs3772705	3	183388403	intronic	G	A	0.255	2.84E-13	6.43E-01	KLHL24	ICVF Superior Londgitudinal Fasciculus II Left	1.42E-09	-6.052866
75	rs3772705	3	183388403	intronic	G	A	0.255	2.84E-13	6.43E-01	KLHL24	L1 Arcuate Long Segment Left	1.68E-10	6.388323
75	rs3772705	3	183388403	intronic	G	A	0.255	2.84E-13	6.43E-01	KLHL24	L1 Superior Londgitudinal Fasciculus II Right	2.78E-08	5.554889
75	rs3772705	3	183388403	intronic	G	A	0.255	2.84E-13	6.43E-01	KLHL24	ICVF Superior Londgitudinal Fasciculus III Right	6.04E-09	-5.815685
75	rs3772705	3	183388403	intronic	G	A	0.255	2.84E-13	6.43E-01	KLHL24	L1 Superior Londgitudinal Fasciculus III Right	6.93E-09	5.792699
75	rs3772705	3	183388403	intronic	G	A	0.255	2.84E-13	6.43E-01	KLHL24	ICVF Arcuate Posterior Segment Left	8.88E-10	-6.128355
75	rs3772705	3	183388403	intronic	G	A	0.255	2.84E-13	6.43E-01	KLHL24	ICVF Arcuate Long Segment Right	5.53E-10	-6.203224
75	rs3772705	3	183388403	intronic	G	A	0.255	2.84E-13	6.43E-01	KLHL24	ICVF Inferior Longitudinal Right	2.40E-10	-6.333359
75	rs3772705	3	183388403	intronic	G	A	0.255	2.84E-13	6.43E-01	KLHL24	ICVF Superior Londgitudinal Fasciculus I Right	3.27E-09	-5.917310
75	rs3772705	3	183388403	intronic	G	A	0.255	2.84E-13	6.43E-01	KLHL24	ICVF Superior Londgitudinal Fasciculus I Left	8.02E-10	-6.144571
75	rs3772705	3	183388403	intronic	G	A	0.255	2.84E-13	6.43E-01	KLHL24	L1 Corpus callosum	1.70E-08	5.640440
75	rs3772705	3	183388403	intronic	G	A	0.255	2.84E-13	6.43E-01	KLHL24	ICVF Inferior Longitudinal Left	2.77E-09	-5.944915
75	rs3772705	3	183388403	intronic	G	A	0.255	2.84E-13	6.43E-01	KLHL24	ICVF Superior Londgitudinal Fasciculus III Left	1.28E-08	-5.688848
75	rs3772705	3	183388403	intronic	G	A	0.255	2.84E-13	6.43E-01	KLHL24	MD Inferior Fronto Occipital fasciculus Left	2.46E-09	5.964393
77	rs6871610	3	193515781	intergenic	G	C	0.426	1.54E-12	2.74E-02	RP11-528A4.3	ISOVF Superior Londgitudinal Fasciculus II Left	3.99E-08	-5.491078
85	rs6822050	4	53943333	intronic	A	G	0.273	6.88E-12	2.35E-01	SCFD2	L3 Superior Londgitudinal Fasciculus II Left	1.35E-08	-5.679882
85	rs6822050	4	53943333	intronic	A	G	0.273	6.88E-12	2.35E-01	SCFD2	MD Inferior Longitudinal Left	1.19E-10	-6.440017
85	rs6822050	4	53943333	intronic	A	G	0.273	6.88E-12	2.35E-01	SCFD2	ICVF Fronto Insular tract4 Right	2.73E-08	5.557798
85	rs6822050	4	53943333	intronic	A	G	0.273	6.88E-12	2.35E-01	SCFD2	ICVF Superior Londgitudinal Fasciculus II Right	5.45E-17	8.376554
85	rs6822050	4	53943333	intronic	A	G	0.273	6.88E-12	2.35E-01	SCFD2	ICVF Arcuate Anterior Segment Right	1.06E-21	9.570958
85	rs6822050	4	53943333	intronic	A	G	0.273	6.88E-12	2.35E-01	SCFD2	MD Arcuate Anterior Segment Right	3.17E-10	-6.290227
85	rs6822050	4	53943333	intronic	A	G	0.273	6.88E-12	2.35E-01	SCFD2	L2 Inferior Longitudinal Left	4.11E-09	-5.879709
85	rs6822050	4	53943333	intronic	A	G	0.273	6.88E-12	2.35E-01	SCFD2	MD Inferior Longitudinal Right	5.09E-09	-5.844186
85	rs6822050	4	53943333	intronic	A	G	0.273	6.88E-12	2.35E-01	SCFD2	ICVF Arcuate Long Segment Left	5.01E-19	8.912072
85	rs6822050	4	53943333	intronic	A	G	0.273	6.88E-12	2.35E-01	SCFD2	ICVF Fronto Insular tract2 Right	4.51E-08	5.469481
85	rs6822050	4	53943333	intronic	A	G	0.273	6.88E-12	2.35E-01	SCFD2	ICVF Inferior Fronto Occipital fasciculus Right	2.47E-13	7.320707
85	rs6822050	4	53943333	intronic	A	G	0.273	6.88E-12	2.35E-01	SCFD2	MD Inferior Fronto Occipital fasciculus Right	1.71E-08	-5.639318
85	rs6822050	4	53943333	intronic	A	G	0.273	6.88E-12	2.35E-01	SCFD2	ICVF Corpus callosum	8.24E-17	8.327737
85	rs6822050	4	53943333	intronic	A	G	0.273	6.88E-12	2.35E-01	SCFD2	L3 Superior Londgitudinal Fasciculus III Right	6.55E-09	-5.802008
85	rs6822050	4	53943333	intronic	A	G	0.273	6.88E-12	2.35E-01	SCFD2	ICVF Arcuate Posterior Segment Right	6.37E-20	9.137876
85	rs6822050	4	53943333	intronic	A	G	0.273	6.88E-12	2.35E-01	SCFD2	L3 Arcuate Posterior Segment Right	6.31E-09	-5.808250
85	rs6822050	4	53943333	intronic	A	G	0.273	6.88E-12	2.35E-01	SCFD2	ICVF Fronto Insular tract3 Left	1.07E-08	5.719064
85	rs6822050	4	53943333	intronic	A	G	0.273	6.88E-12	2.35E-01	SCFD2	MD Superior Londgitudinal Fasciculus III Left	3.19E-08	-5.530655
85	rs6822050	4	53943333	intronic	A	G	0.273	6.88E-12	2.35E-01	SCFD2	ICVF Inferior Fronto Occipital fasciculus Left	6.23E-14	7.503160
85	rs6822050	4	53943333	intronic	A	G	0.273	6.88E-12	2.35E-01	SCFD2	ICVF Frontal Aslant Tract Right	3.33E-18	8.699588
85	rs6822050	4	53943333	intronic	A	G	0.273	6.88E-12	2.35E-01	SCFD2	ICVF Frontal Superior Longitudinal Left	5.70E-10	6.198491
85	rs6822050	4	53943333	intronic	A	G	0.273	6.88E-12	2.35E-01	SCFD2	MD Arcuate Posterior Segment Right	6.65E-11	-6.528347
85	rs6822050	4	53943333	intronic	A	G	0.273	6.88E-12	2.35E-01	SCFD2	L2 Corpus callosum	5.91E-09	-5.819223
85	rs6822050	4	53943333	intronic	A	G	0.273	6.88E-12	2.35E-01	SCFD2	ICVF Superior Londgitudinal Fasciculus II Left	3.43E-16	8.157308
85	rs6822050	4	53943333	intronic	A	G	0.273	6.88E-12	2.35E-01	SCFD2	L3 Inferior Fronto Occipital fasciculus Right	3.32E-09	-5.915186
85	rs6822050	4	53943333	intronic	A	G	0.273	6.88E-12	2.35E-01	SCFD2	L3 Arcuate Long Segment Left	3.52E-10	-6.273889
85	rs6822050	4	53943333	intronic	A	G	0.273	6.88E-12	2.35E-01	SCFD2	L1 Arcuate Long Segment Left	3.40E-08	-5.519341
85	rs6822050	4	53943333	intronic	A	G	0.273	6.88E-12	2.35E-01	SCFD2	ICVF Frontal Aslant Tract Left	1.35E-14	7.700957
85	rs6822050	4	53943333	intronic	A	G	0.273	6.88E-12	2.35E-01	SCFD2	ICVF Superior Londgitudinal Fasciculus III Right	5.43E-18	8.643922
85	rs6822050	4	53943333	intronic	A	G	0.273	6.88E-12	2.35E-01	SCFD2	ICVF Frontal Superior Longitudinal Right	1.79E-13	7.363934
85	rs6822050	4	53943333	intronic	A	G	0.273	6.88E-12	2.35E-01	SCFD2	MD Arcuate Anterior Segment Left	3.43E-08	-5.518034
85	rs6822050	4	53943333	intronic	A	G	0.273	6.88E-12	2.35E-01	SCFD2	L2 Inferior Fronto Occipital fasciculus Left	2.64E-08	-5.563686
85	rs6822050	4	53943333	intronic	A	G	0.273	6.88E-12	2.35E-01	SCFD2	ICVF Arcuate Posterior Segment Left	2.93E-19	8.971474
85	rs6822050	4	53943333	intronic	A	G	0.273	6.88E-12	2.35E-01	SCFD2	ICVF Arcuate Long Segment Right	9.06E-19	8.846117
85	rs6822050	4	53943333	intronic	A	G	0.273	6.88E-12	2.35E-01	SCFD2	L3 Inferior Longitudinal Left	5.49E-11	-6.556984
85	rs6822050	4	53943333	intronic	A	G	0.273	6.88E-12	2.35E-01	SCFD2	L3 Corpus callosum	3.06E-08	-5.537822
85	rs6822050	4	53943333	intronic	A	G	0.273	6.88E-12	2.35E-01	SCFD2	ICVF Inferior Longitudinal Right	8.35E-16	8.048997
85	rs6822050	4	53943333	intronic	A	G	0.273	6.88E-12	2.35E-01	SCFD2	L3 Arcuate Long Segment Right	7.69E-11	-6.506509
85	rs6822050	4	53943333	intronic	A	G	0.273	6.88E-12	2.35E-01	SCFD2	L2 Superior Londgitudinal Fasciculus I Right	8.85E-09	-5.751443
85	rs6822050	4	53943333	intronic	A	G	0.273	6.88E-12	2.35E-01	SCFD2	FA Corpus callosum	4.09E-09	5.880587
85	rs6822050	4	53943333	intronic	A	G	0.273	6.88E-12	2.35E-01	SCFD2	L2 Superior Londgitudinal Fasciculus I Left	1.38E-08	-5.675894
85	rs6822050	4	53943333	intronic	A	G	0.273	6.88E-12	2.35E-01	SCFD2	MD Arcuate Posterior Segment Left	1.61E-10	-6.394432
85	rs6822050	4	53943333	intronic	A	G	0.273	6.88E-12	2.35E-01	SCFD2	ICVF Arcuate Anterior Segment Left	2.55E-20	9.236247
85	rs6822050	4	53943333	intronic	A	G	0.273	6.88E-12	2.35E-01	SCFD2	ICVF Superior Londgitudinal Fasciculus I Right	8.67E-17	8.321706
85	rs6822050	4	53943333	intronic	A	G	0.273	6.88E-12	2.35E-01	SCFD2	MD Arcuate Long Segment Right	2.30E-10	-6.340171
85	rs6822050	4	53943333	intronic	A	G	0.273	6.88E-12	2.35E-01	SCFD2	ICVF Fronto Insular tract1 Right	1.54E-10	6.401436
85	rs6822050	4	53943333	intronic	A	G	0.273	6.88E-12	2.35E-01	SCFD2	ICVF Superior Londgitudinal Fasciculus I Left	2.11E-16	8.215701
85	rs6822050	4	53943333	intronic	A	G	0.273	6.88E-12	2.35E-01	SCFD2	FA Superior Londgitudinal Fasciculus I Right	2.10E-09	5.989819
85	rs6822050	4	53943333	intronic	A	G	0.273	6.88E-12	2.35E-01	SCFD2	L3 Superior Londgitudinal Fasciculus II Right	4.35E-09	-5.870284
85	rs6822050	4	53943333	intronic	A	G	0.273	6.88E-12	2.35E-01	SCFD2	MD Arcuate Long Segment Left	2.57E-11	-6.669134
85	rs6822050	4	53943333	intronic	A	G	0.273	6.88E-12	2.35E-01	SCFD2	ICVF Uncinate Right	9.01E-13	7.144845
85	rs6822050	4	53943333	intronic	A	G	0.273	6.88E-12	2.35E-01	SCFD2	L3 Superior Londgitudinal Fasciculus I Right	2.71E-08	-5.559108
85	rs6822050	4	53943333	intronic	A	G	0.273	6.88E-12	2.35E-01	SCFD2	ICVF Uncinate Left	3.38E-16	8.159055
85	rs6822050	4	53943333	intronic	A	G	0.273	6.88E-12	2.35E-01	SCFD2	ICVF Inferior Longitudinal Left	5.48E-18	8.642989
85	rs6822050	4	53943333	intronic	A	G	0.273	6.88E-12	2.35E-01	SCFD2	ICVF Superior Londgitudinal Fasciculus III Left	7.87E-18	8.601525
85	rs6822050	4	53943333	intronic	A	G	0.273	6.88E-12	2.35E-01	SCFD2	L3 Inferior Longitudinal Right	7.52E-10	-6.154802
85	rs6822050	4	53943333	intronic	A	G	0.273	6.88E-12	2.35E-01	SCFD2	L2 Arcuate Posterior Segment Right	3.74E-10	-6.264559
85	rs6822050	4	53943333	intronic	A	G	0.273	6.88E-12	2.35E-01	SCFD2	MD Superior Londgitudinal Fasciculus III Right	2.15E-08	-5.599760
85	rs6822050	4	53943333	intronic	A	G	0.273	6.88E-12	2.35E-01	SCFD2	L3 Arcuate Anterior Segment Right	6.94E-12	-6.858903
85	rs6822050	4	53943333	intronic	A	G	0.273	6.88E-12	2.35E-01	SCFD2	L2 Arcuate Posterior Segment Left	2.32E-11	-6.684406
85	rs6822050	4	53943333	intronic	A	G	0.273	6.88E-12	2.35E-01	SCFD2	ICVF Frontal Inferior longitudinal Right	5.18E-15	7.822496
90	rs35976463	4	97926008	intergenic	CATG	C	0.316	2.24E-12	6.82E-01	COX7A2P2	OD Fronto Insular tract1 Right	4.26E-11	-6.594594
90	rs35976463	4	97926008	intergenic	CATG	C	0.316	2.24E-12	6.82E-01	COX7A2P2	FA Inferior Fronto Occipital fasciculus Left	8.45E-09	5.759177
90	rs35976463	4	97926008	intergenic	CATG	C	0.316	2.24E-12	6.82E-01	COX7A2P2	FA Uncinate Left	4.75E-10	6.227113
90	rs35976463	4	97926008	intergenic	CATG	C	0.316	2.24E-12	6.82E-01	COX7A2P2	L2 Fronto Insular tract2 Right	3.56E-08	-5.511461
90	rs35976463	4	97926008	intergenic	CATG	C	0.316	2.24E-12	6.82E-01	COX7A2P2	FA Fronto Insular tract1 Right	1.25E-15	7.999852
90	rs35976463	4	97926008	intergenic	CATG	C	0.316	2.24E-12	6.82E-01	COX7A2P2	OD Fronto Insular tract2 Right	6.21E-09	-5.810925
90	rs35976463	4	97926008	intergenic	CATG	C	0.316	2.24E-12	6.82E-01	COX7A2P2	FA Fronto Insular tract2 Right	2.73E-15	7.902532
90	rs35976463	4	97926008	intergenic	CATG	C	0.316	2.24E-12	6.82E-01	COX7A2P2	OD Inferior Fronto Occipital fasciculus Left	4.80E-10	-6.225518
90	rs35976463	4	97926008	intergenic	CATG	C	0.316	2.24E-12	6.82E-01	COX7A2P2	MO Inferior Fronto Occipital fasciculus Left	4.85E-09	5.852124
90	rs35976463	4	97926008	intergenic	CATG	C	0.316	2.24E-12	6.82E-01	COX7A2P2	L2 Fronto Insular tract1 Right	3.50E-08	-5.514365
91	rs13107325	4	103188709	exonic	T	C	0.076	3.20E-10	1.30E-01	SLC39A8	ICVF Superior Londgitudinal Fasciculus II Right	2.23E-08	5.593429

Genomic Locus	Lead SNP	chr	Position	Functional category	Non-effect allele	Effect allele	MAF	mvgwasP (discovery -British-)	mvgwasP (replication -non British-)	Nearest gene	Central endophenotypes	univariate P value	univariate Z
96	rs1882325	4	185126789	intronic	T	G	0.350	7.55E-17	1.30E-01	ENPP6	ISOVF Frontal Aslant Tract Left	8.22E-15	-7.764066
96	rs1882325	4	185126789	intronic	T	G	0.350	7.55E-17	1.30E-01	ENPP6	ISOVF Inferior Fronto Occipital fasciculus Left	5.78E-19	-8.896224
96	rs1882325	4	185126789	intronic	T	G	0.350	7.55E-17	1.30E-01	ENPP6	ISOVF Superior Londgitudinal Fasciculus II Right	9.29E-16	-8.035886
96	rs1882325	4	185126789	intronic	T	G	0.350	7.55E-17	1.30E-01	ENPP6	L1 Inferior Longitudinal Left	5.33E-10	-6.209028
96	rs1882325	4	185126789	intronic	T	G	0.350	7.55E-17	1.30E-01	ENPP6	ISOVF Frontal Inferior longitudinal Right	6.92E-11	-6.522459
96	rs1882325	4	185126789	intronic	T	G	0.350	7.55E-17	1.30E-01	ENPP6	ISOVF Inferior Longitudinal Right	4.66E-16	-8.120021
96	rs1882325	4	185126789	intronic	T	G	0.350	7.55E-17	1.30E-01	ENPP6	ISOVF Superior Londgitudinal Fasciculus III Left	1.24E-16	-8.279063
96	rs1882325	4	185126789	intronic	T	G	0.350	7.55E-17	1.30E-01	ENPP6	ISOVF Arcuate Anterior Segment Left	7.53E-13	-7.169408
96	rs1882325	4	185126789	intronic	T	G	0.350	7.55E-17	1.30E-01	ENPP6	ISOVF Arcuate Posterior Segment Left	3.25E-13	-7.283655
96	rs1882325	4	185126789	intronic	T	G	0.350	7.55E-17	1.30E-01	ENPP6	ISOVF Uncinate Left	4.55E-08	-5.468247
96	rs1882325	4	185126789	intronic	T	G	0.350	7.55E-17	1.30E-01	ENPP6	ISOVF Frontal Superior Longitudinal Right	2.35E-08	-5.584337
96	rs1882325	4	185126789	intronic	T	G	0.350	7.55E-17	1.30E-01	ENPP6	ISOVF Inferior Fronto Occipital fasciculus Right	3.24E-17	-8.437657
96	rs1882325	4	185126789	intronic	T	G	0.350	7.55E-17	1.30E-01	ENPP6	ISOVF Inferior Longitudinal Left	4.13E-18	-8.675029
96	rs1882325	4	185126789	intronic	T	G	0.350	7.55E-17	1.30E-01	ENPP6	ISOVF Frontal Aslant Tract Right	1.90E-19	-9.018783
96	rs1882325	4	185126789	intronic	T	G	0.350	7.55E-17	1.30E-01	ENPP6	L1 Inferior Fronto Occipital fasciculus Right	1.61E-08	-5.649119
96	rs1882325	4	185126789	intronic	T	G	0.350	7.55E-17	1.30E-01	ENPP6	ISOVF Arcuate Long Segment Left	5.35E-19	-8.904707
96	rs1882325	4	185126789	intronic	T	G	0.350	7.55E-17	1.30E-01	ENPP6	MD Arcuate Posterior Segment Right	2.37E-08	-5.582730
96	rs1882325	4	185126789	intronic	T	G	0.350	7.55E-17	1.30E-01	ENPP6	ISOVF Superior Londgitudinal Fasciculus II Left	1.56E-15	-7.971976
96	rs1882325	4	185126789	intronic	T	G	0.350	7.55E-17	1.30E-01	ENPP6	ISOVF Superior Londgitudinal Fasciculus I Left	1.43E-12	-7.081019
96	rs1882325	4	185126789	intronic	T	G	0.350	7.55E-17	1.30E-01	ENPP6	ISOVF Superior Londgitudinal Fasciculus I Right	7.86E-14	-7.472712
96	rs1882325	4	185126789	intronic	T	G	0.350	7.55E-17	1.30E-01	ENPP6	L1 Superior Londgitudinal Fasciculus I Right	2.75E-10	-6.312001
96	rs1882325	4	185126789	intronic	T	G	0.350	7.55E-17	1.30E-01	ENPP6	ISOVF Corpus callosum	4.64E-19	-8.920562
96	rs1882325	4	185126789	intronic	T	G	0.350	7.55E-17	1.30E-01	ENPP6	MD Superior Londgitudinal Fasciculus I Right	1.41E-08	-5.671943
96	rs1882325	4	185126789	intronic	T	G	0.350	7.55E-17	1.30E-01	ENPP6	ISOVF Arcuate Anterior Segment Right	7.61E-20	-9.118536
96	rs1882325	4	185126789	intronic	T	G	0.350	7.55E-17	1.30E-01	ENPP6	L1 Arcuate Posterior Segment Right	1.25E-09	-6.073356
96	rs1882325	4	185126789	intronic	T	G	0.350	7.55E-17	1.30E-01	ENPP6	ISOVF Superior Londgitudinal Fasciculus III Right	7.53E-22	-9.606162
96	rs1882325	4	185126789	intronic	T	G	0.350	7.55E-17	1.30E-01	ENPP6	L1 Corpus callosum	1.96E-12	-7.037331
96	rs1882325	4	185126789	intronic	T	G	0.350	7.55E-17	1.30E-01	ENPP6	ISOVF Arcuate Long Segment Right	6.50E-24	-10.083985
96	rs1882325	4	185126789	intronic	T	G	0.350	7.55E-17	1.30E-01	ENPP6	ISOVF Arcuate Posterior Segment Right	9.36E-21	-9.343050
96	rs1882325	4	185126789	intronic	T	G	0.350	7.55E-17	1.30E-01	ENPP6	L1 Superior Londgitudinal Fasciculus I Left	1.42E-09	-6.053075
100	rs34592828	5	75996909	exonic	A	G	0.045	6.33E-10	4.43E-01	IQGAP2:CTD-2384B11.2	L3 Fronto Insular tract1 Left	4.57E-08	5.467468
101	rs145824047	5	81800313	intergenic	A	G	0.396	4.50E-10	8.02E-01	CTD-2015A6.1	L2 Superior Londgitudinal Fasciculus I Left	2.38E-09	5.969787
101	rs145824047	5	81800313	intergenic	A	G	0.396	4.50E-10	8.02E-01	CTD-2015A6.1	ICVF Superior Londgitudinal Fasciculus I Right	2.65E-08	-5.563281
101	rs7520021310	5	81866998	intergenic	C	CTAAT	0.447	3.20E-23	8.87E-03	CTD-2015A6.2	L2 Superior Londgitudinal Fasciculus I Left	4.93E-09	-5.849502
101	rs7520021310	5	81866998	intergenic	C	CTAAT	0.447	3.20E-23	8.87E-03	CTD-2015A6.2	OD Superior Londgitudinal Fasciculus II Left	1.78E-09	6.016626
102	rs11749904	5	82782530	intronic	C	T	0.380	6.09E-29	4.43E-02	VCAN	L3 Superior Londgitudinal Fasciculus II Left	1.96E-23	-9.975102
102	rs11749904	5	82782530	intronic	C	T	0.380	6.09E-29	4.43E-02	VCAN	MD Inferior Longitudinal Left	6.81E-27	-10.737232
102	rs11749904	5	82782530	intronic	C	T	0.380	6.09E-29	4.43E-02	VCAN	ICVF Fronto Insular tract4 Right	1.06E-19	9.082184
102	rs11749904	5	82782530	intronic	C	T	0.380	6.09E-29	4.43E-02	VCAN	L3 Frontal Aslant Tract Right	8.37E-17	-8.325912
102	rs11749904	5	82782530	intronic	C	T	0.380	6.09E-29	4.43E-02	VCAN	FA Inferior Fronto Occipital fasciculus Right	1.43E-17	8.532678
102	rs11749904	5	82782530	intronic	C	T	0.380	6.09E-29	4.43E-02	VCAN	L1 Arcuate Anterior Segment Right	2.42E-13	-7.323442
102	rs11749904	5	82782530	intronic	C	T	0.380	6.09E-29	4.43E-02	VCAN	FA Superior Londgitudinal Fasciculus III Right	1.28E-17	8.545063
102	rs11749904	5	82782530	intronic	C	T	0.380	6.09E-29	4.43E-02	VCAN	MD Superior Londgitudinal Fasciculus II Right	4.83E-20	-9.167744
102	rs11749904	5	82782530	intronic	C	T	0.380	6.09E-29	4.43E-02	VCAN	FA Uncinate Right	9.19E-12	6.818681
102	rs11749904	5	82782530	intronic	C	T	0.380	6.09E-29	4.43E-02	VCAN	L2 Frontal Inferior longitudinal Right	5.28E-12	-6.897765
102	rs11749904	5	82782530	intronic	C	T	0.380	6.09E-29	4.43E-02	VCAN	L1 Inferior Longitudinal Left	6.09E-17	-8.363389
102	rs11749904	5	82782530	intronic	C	T	0.380	6.09E-29	4.43E-02	VCAN	ICVF Superior Londgitudinal Fasciculus II Right	3.21E-43	13.783430
102	rs11749904	5	82782530	intronic	C	T	0.380	6.09E-29	4.43E-02	VCAN	FA Inferior Longitudinal Left	2.89E-19	8.972650
102	rs11749904	5	82782530	intronic	C	T	0.380	6.09E-29	4.43E-02	VCAN	FA Inferior Fronto Occipital fasciculus Left	2.36E-18	8.738840
102	rs11749904	5	82782530	intronic	C	T	0.380	6.09E-29	4.43E-02	VCAN	FA Frontal Aslant Tract Left	1.03E-14	7.735723
102	rs11749904	5	82782530	intronic	C	T	0.380	6.09E-29	4.43E-02	VCAN	ICVF Arcuate Anterior Segment Right	4.01E-43	13.767352
102	rs11749904	5	82782530	intronic	C	T	0.380	6.09E-29	4.43E-02	VCAN	FA Uncinate Left	4.05E-13	7.253748
102	rs11749904	5	82782530	intronic	C	T	0.380	6.09E-29	4.43E-02	VCAN	ICVF Fronto Insular tract3 Right	9.78E-17	8.307416
102	rs11749904	5	82782530	intronic	C	T	0.380	6.09E-29	4.43E-02	VCAN	MD Arcuate Anterior Segment Right	1.07E-18	-8.827836
102	rs11749904	5	82782530	intronic	C	T	0.380	6.09E-29	4.43E-02	VCAN	L2 Inferior Longitudinal Left	1.91E-25	-10.424755
102	rs11749904	5	82782530	intronic	C	T	0.380	6.09E-29	4.43E-02	VCAN	MD Inferior Longitudinal Right	1.07E-28	-11.113815
102	rs11749904	5	82782530	intronic	C	T	0.380	6.09E-29	4.43E-02	VCAN	L1 Inferior Fronto Occipital fasciculus Left	9.57E-20	-9.093740
102	rs11749904	5	82782530	intronic	C	T	0.380	6.09E-29	4.43E-02	VCAN	ICVF Arcuate Long Segment Left	1.71E-44	13.993418
102	rs11749904	5	82782530	intronic	C	T	0.380	6.09E-29	4.43E-02	VCAN	MD Frontal Aslant Tract Right	3.48E-17	-8.429308
102	rs11749904	5	82782530	intronic	C	T	0.380	6.09E-29	4.43E-02	VCAN	L3 Superior Londgitudinal Fasciculus I Left	1.44E-23	-10.005901
102	rs11749904	5	82782530	intronic	C	T	0.380	6.09E-29	4.43E-02	VCAN	ICVF Fronto Insular tract2 Right	1.73E-16	8.239398
102	rs11749904	5	82782530	intronic	C	T	0.380	6.09E-29	4.43E-02	VCAN	ICVF Fronto Insular tract5 Right	3.65E-16	8.149803
102	rs11749904	5	82782530	intronic	C	T	0.380	6.09E-29	4.43E-02	VCAN	FA Arcuate Anterior Segment Right	3.08E-12	6.973879
102	rs11749904	5	82782530	intronic	C	T	0.380	6.09E-29	4.43E-02	VCAN	FA Superior Londgitudinal Fasciculus I Left	5.51E-21	9.398876
102	rs11749904	5	82782530	intronic	C	T	0.380	6.09E-29	4.43E-02	VCAN	L3 Frontal Aslant Tract Left	2.63E-15	-7.907178
102	rs11749904	5	82782530	intronic	C	T	0.380	6.09E-29	4.43E-02	VCAN	ICVF Inferior Fronto Occipital fasciculus Right	2.74E-45	14.123123
102	rs11749904	5	82782530	intronic	C	T	0.380	6.09E-29	4.43E-02	VCAN	L1 Arcuate Anterior Segment Left	1.68E-13	-7.371795
102	rs11749904	5	82782530	intronic	C	T	0.380	6.09E-29	4.43E-02	VCAN	FA Arcuate Long Segment Left	3.62E-11	6.618973
102	rs11749904	5	82782530	intronic	C	T	0.380	6.09E-29	4.43E-02	VCAN	MD Uncinate Right	8.52E-21	-9.353032
102	rs11749904	5	82782530	intronic	C	T	0.380	6.09E-29	4.43E-02	VCAN	MD Inferior Fronto Occipital fasciculus Right	8.71E-30	-11.335894
102	rs11749904	5	82782530	intronic	C	T	0.380	6.09E-29	4.43E-02	VCAN	ICVF Corpus callosum	1.80E-48	14.630109
102	rs11749904	5	82782530	intronic	C	T	0.380	6.09E-29	4.43E-02	VCAN	L3 Superior Londgitudinal Fasciculus III Right	2.70E-19	-8.980335
102	rs11749904	5	82782530	intronic	C	T	0.380	6.09E-29	4.43E-02	VCAN	ICVF Arcuate Posterior Segment Right	6.08E-38	12.876784
102	rs11749904	5	82782530	intronic	C	T	0.380	6.09E-29	4.43E-02	VCAN	FA Frontal Inferior longitudinal Right	5.11E-10	6.215768
102	rs11749904	5	82782530	intronic	C	T	0.380	6.09E-29	4.43E-02	VCAN	MD Corpus callosum	3.20E-25	-10.375750
102	rs11749904	5	82782530	intronic	C	T	0.380	6.09E-29	4.43E-02	VCAN	L2 Inferior Fronto Occipital fasciculus Right	1.10E-23	-10.032299
102	rs11749904	5	82782530	intronic	C	T	0.380	6.09E-29	4.43E-02	VCAN	L1 Arcuate Long Segment Right	1.86E-16	-8.230978
102	rs11749904	5	82782530	intronic	C	T	0.380	6.09E-29	4.43E-02	VCAN	L3 Arcuate Posterior Segment Right	2.24E-18	-8.744312
102	rs11749904	5	82782530	intronic	C	T	0.380	6.09E-29	4.43E-02	VCAN	ICVF Fronto Insular tract3 Left	1.98E-17	8.494888
102	rs11749904	5	82782530	intronic	C	T	0.380	6.09E-29	4.43E-02	VCAN	FA Superior Londgitudinal Fasciculus III Left	2.53E-13	7.317192
102	rs11749904	5	82782530	intronic	C	T	0.380	6.09E-29	4.43E-02	VCAN	MD Superior Londgitudinal Fasciculus III Left	5.10E-20	-9.161869
102	rs11749904	5	82782530	intronic	C	T	0.380	6.09E-29	4.43E-02	VCAN	ICVF Inferior Fronto Occipital fasciculus Left	4.38E-46	14.251594
102	rs11749904	5	82782530	intronic	C	T	0.380	6.09E-29	4.43E-02	VCAN	L1 Superior Londgitudinal Fasciculus II Left	1.94E-10	-6.365670
102	rs11749904	5	82782530	intronic	C	T	0.380	6.09E-29	4.43E-02	VCAN	ICVF Frontal Aslant Tract Right	2.08E-43	13.814543
102	rs11749904	5	82782530	intronic	C	T	0.380	6.09E-29	4.43E-02	VCAN	L1 Inferior Fronto Occipital fasciculus Right	3.66E-18	-8.688868
102	rs11749904	5	82782530	intronic	C	T	0.380	6.09E-29	4.43E-02	VCAN	ICVF Frontal Superior Longitudinal Left	8.61E-25	10.280711
102	rs11749904	5	82782530	intronic	C	T	0.380	6.09E-29	4.43E-02	VCAN	L1 Arcuate Posterior Segment Left	2.53E-17	-8.466628
102	rs11749904	5	82782530	intronic	C	T	0.380	6.09E-29	4.43E-02	VCAN	MD Arcuate Posterior Segment Right	3.23E-25	-10.374780
102	rs11749904	5	82782530	intronic	C	T	0.380	6.09E-29	4.43E-02	VCAN	FA Superior Londgitudinal Fasciculus II Right	1.05E-16	8.299360
102	rs11749904	5	82782530	intronic	C	T	0.380	6.09E-29	4.43E-02	VCAN	L2 Uncinate Right	7.57E-18	-8.606000
102	rs11749904	5	82782530	intronic	C	T	0.380	6.09E-29	4.43E-02	VCAN	L2 Corpus callosum	2.15E-25	-10.413692
102	rs11749904	5	82782530	intronic	C	T	0.380	6.09E-29	4.43E-02	VCAN	L1 Uncinate Left	4.38E-10	-6.239670
102	rs11749904	5	82782530	intronic	C	T	0.380	6.09E-29	4.43E-02	VCAN	L2 Superior Londgitudinal Fasciculus III Right	8.03E-17	-8.330781
102	rs11749904	5	82782530	intronic	C	T	0.380	6.09E-29	4.43E-02	VCAN	L3 Superior Londgitudinal Fasciculus III Left	6.47E-18	-8.623889
102	rs11749904	5	82782530	intronic	C	T	0.380	6.09E-29	4.43E-02	VCAN	L1 Uncinate Right	4.90E-13	-7.228138
102	rs11749904	5	82782530	intronic	C	T	0.380	6.09E-29	4.43E-02	VCAN	ICVF Frontal Inferior longitudinal Left	3.24E-23	9.925058
102	rs11749904	5	82782530	intronic	C	T	0.380	6.09E-29	4.43E-02	VCAN	ICVF Superior Londgitudinal Fasciculus II Left	1.53E-45	14.164145
102	rs11749904	5	82782530	intronic	C	T	0.380	6.09E-29	4.43E-02	VCAN	L3 Inferior Fronto Occipital fasciculus Right	6.57E-28	-10.951076
102	rs11749904	5	82782530	intronic	C	T	0.380	6.09E-29	4.43E-02	VCAN	L2 Frontal Aslant Tract Left	3.16E-17	-8.440378
102	rs11749904	5	82782530	intronic	C	T	0.380	6.09E-29	4.43E-02	VCAN	FA Frontal Superior Longitudinal Right	1.49E-10	6.406352
102	rs11749904	5	82782530	intronic	C	T	0.380	6.09E-29	4.43E-02	VCAN	L2 Superior Londgitudinal Fasciculus III Left	8.88E-16	-8.041473

Genomic Locus	Lead SNP	chr	Position	Functional category	Non-effect allele	Effect allele	MAF	mvgwasP (discovery -British-)	mvgwasP (replication -non British-)	Nearest gene	Central endophenotypes	univariate P value	univariate Z
102	rs11749904	5	82782530	intronic	C	T	0.380	6.09E-29	4.43E-02	VCAN	FA Arcuate Anterior Segment Left	7.21E-11	6.516128
102	rs11749904	5	82782530	intronic	C	T	0.380	6.09E-29	4.43E-02	VCAN	L2 Arcuate Anterior Segment Right	3.49E-10	-6.275274
102	rs11749904	5	82782530	intronic	C	T	0.380	6.09E-29	4.43E-02	VCAN	L3 Inferior Fronto Occipital fasciculus Left	9.52E-28	-10.917384
102	rs11749904	5	82782530	intronic	C	T	0.380	6.09E-29	4.43E-02	VCAN	L3 Arcuate Long Segment Left	4.44E-23	-9.893455
102	rs11749904	5	82782530	intronic	C	T	0.380	6.09E-29	4.43E-02	VCAN	L1 Arcuate Long Segment Left	7.09E-19	-8.873440
102	rs11749904	5	82782530	intronic	C	T	0.380	6.09E-29	4.43E-02	VCAN	ICVF Frontal Aslant Tract Left	4.04E-40	13.258209
102	rs11749904	5	82782530	intronic	C	T	0.380	6.09E-29	4.43E-02	VCAN	MD Frontal Aslant Tract Left	1.27E-16	-8.275975
102	rs11749904	5	82782530	intronic	C	T	0.380	6.09E-29	4.43E-02	VCAN	L1 Superior Londgitudinal Fasciculus II Right	9.00E-11	-6.482926
102	rs11749904	5	82782530	intronic	C	T	0.380	6.09E-29	4.43E-02	VCAN	ICVF Superior Londgitudinal Fasciculus III Right	1.77E-42	13.659461
102	rs11749904	5	82782530	intronic	C	T	0.380	6.09E-29	4.43E-02	VCAN	L2 Superior Londgitudinal Fasciculus II Right	1.07E-18	-8.828012
102	rs11749904	5	82782530	intronic	C	T	0.380	6.09E-29	4.43E-02	VCAN	ICVF Frontal Superior Longitudinal Right	2.19E-35	12.414077
102	rs11749904	5	82782530	intronic	C	T	0.380	6.09E-29	4.43E-02	VCAN	MD Arcuate Anterior Segment Left	1.68E-17	-8.514318
102	rs11749904	5	82782530	intronic	C	T	0.380	6.09E-29	4.43E-02	VCAN	L3 Arcuate Posterior Segment Left	3.13E-14	-7.592898
102	rs11749904	5	82782530	intronic	C	T	0.380	6.09E-29	4.43E-02	VCAN	L1 Superior Londgitudinal Fasciculus III Right	1.14E-14	-7.722874
102	rs11749904	5	82782530	intronic	C	T	0.380	6.09E-29	4.43E-02	VCAN	MD Superior Londgitudinal Fasciculus II Left	3.25E-22	-9.692440
102	rs11749904	5	82782530	intronic	C	T	0.380	6.09E-29	4.43E-02	VCAN	FA Frontal Aslant Tract Right	1.44E-17	8.531560
102	rs11749904	5	82782530	intronic	C	T	0.380	6.09E-29	4.43E-02	VCAN	L1 Frontal Aslant Tract Left	4.55E-10	-6.233906
102	rs11749904	5	82782530	intronic	C	T	0.380	6.09E-29	4.43E-02	VCAN	L2 Inferior Fronto Occipital fasciculus Left	1.72E-23	-9.988109
102	rs11749904	5	82782530	intronic	C	T	0.380	6.09E-29	4.43E-02	VCAN	ICVF Arcuate Posterior Segment Left	9.39E-37	12.663724
102	rs11749904	5	82782530	intronic	C	T	0.380	6.09E-29	4.43E-02	VCAN	L2 Uncinate Left	1.40E-17	-8.534760
102	rs11749904	5	82782530	intronic	C	T	0.380	6.09E-29	4.43E-02	VCAN	FA Arcuate Long Segment Right	2.54E-10	6.324656
102	rs11749904	5	82782530	intronic	C	T	0.380	6.09E-29	4.43E-02	VCAN	ICVF Fronto Insular tract5 Left	1.76E-21	9.518091
102	rs11749904	5	82782530	intronic	C	T	0.380	6.09E-29	4.43E-02	VCAN	ICVF Arcuate Long Segment Right	1.12E-41	13.524638
102	rs11749904	5	82782530	intronic	C	T	0.380	6.09E-29	4.43E-02	VCAN	L3 Inferior Longitudinal Left	6.22E-25	-10.311986
102	rs11749904	5	82782530	intronic	C	T	0.380	6.09E-29	4.43E-02	VCAN	L3 Corpus callosum	9.70E-24	-10.044636
102	rs11749904	5	82782530	intronic	C	T	0.380	6.09E-29	4.43E-02	VCAN	L3 Uncinate Left	5.77E-20	-9.148559
102	rs11749904	5	82782530	intronic	C	T	0.380	6.09E-29	4.43E-02	VCAN	ICVF Inferior Longitudinal Right	1.08E-46	14.349357
102	rs11749904	5	82782530	intronic	C	T	0.380	6.09E-29	4.43E-02	VCAN	L3 Arcuate Long Segment Right	1.52E-21	-9.533713
102	rs11749904	5	82782530	intronic	C	T	0.380	6.09E-29	4.43E-02	VCAN	FA Arcuate Posterior Segment Left	1.48E-08	5.664306
102	rs11749904	5	82782530	intronic	C	T	0.380	6.09E-29	4.43E-02	VCAN	ICVF Fronto Insular tract2 Left	4.38E-12	6.924223
102	rs11749904	5	82782530	intronic	C	T	0.380	6.09E-29	4.43E-02	VCAN	L2 Superior Londgitudinal Fasciculus I Right	5.05E-24	-10.108881
102	rs11749904	5	82782530	intronic	C	T	0.380	6.09E-29	4.43E-02	VCAN	FA Corpus callosum	3.92E-22	9.673302
102	rs11749904	5	82782530	intronic	C	T	0.380	6.09E-29	4.43E-02	VCAN	L2 Superior Londgitudinal Fasciculus I Left	8.83E-23	-9.824556
102	rs11749904	5	82782530	intronic	C	T	0.380	6.09E-29	4.43E-02	VCAN	OD Arcuate Long Segment Right	1.70E-09	6.024277
102	rs11749904	5	82782530	intronic	C	T	0.380	6.09E-29	4.43E-02	VCAN	MD Frontal Inferior longitudinal Right	1.90E-09	-6.006486
102	rs11749904	5	82782530	intronic	C	T	0.380	6.09E-29	4.43E-02	VCAN	L1 Inferior Longitudinal Right	2.28E-18	-8.742265
102	rs11749904	5	82782530	intronic	C	T	0.380	6.09E-29	4.43E-02	VCAN	MD Arcuate Posterior Segment Left	3.22E-21	-9.455477
102	rs11749904	5	82782530	intronic	C	T	0.380	6.09E-29	4.43E-02	VCAN	ICVF Arcuate Anterior Segment Left	5.34E-39	13.063247
102	rs11749904	5	82782530	intronic	C	T	0.380	6.09E-29	4.43E-02	VCAN	L3 Arcuate Anterior Segment Left	2.64E-13	-7.311471
102	rs11749904	5	82782530	intronic	C	T	0.380	6.09E-29	4.43E-02	VCAN	ICVF Superior Londgitudinal Fasciculus I Right	5.11E-50	14.870634
102	rs11749904	5	82782530	intronic	C	T	0.380	6.09E-29	4.43E-02	VCAN	FA Arcuate Posterior Segment Right	1.77E-09	6.017361
102	rs11749904	5	82782530	intronic	C	T	0.380	6.09E-29	4.43E-02	VCAN	FA Inferior Longitudinal Right	2.97E-21	9.463958
102	rs11749904	5	82782530	intronic	C	T	0.380	6.09E-29	4.43E-02	VCAN	MD Superior Londgitudinal Fasciculus I Right	1.14E-21	-9.562940
102	rs11749904	5	82782530	intronic	C	T	0.380	6.09E-29	4.43E-02	VCAN	MD Arcuate Long Segment Right	2.36E-24	-10.182992
102	rs11749904	5	82782530	intronic	C	T	0.380	6.09E-29	4.43E-02	VCAN	L3 Uncinate Right	2.11E-22	-9.736150
102	rs11749904	5	82782530	intronic	C	T	0.380	6.09E-29	4.43E-02	VCAN	ICVF Fronto Insular tract1 Right	3.87E-22	9.674549
102	rs11749904	5	82782530	intronic	C	T	0.380	6.09E-29	4.43E-02	VCAN	L2 Arcuate Long Segment Left	8.95E-11	-6.483729
102	rs11749904	5	82782530	intronic	C	T	0.380	6.09E-29	4.43E-02	VCAN	ICVF Superior Londgitudinal Fasciculus I Left	1.90E-50	14.936710
102	rs11749904	5	82782530	intronic	C	T	0.380	6.09E-29	4.43E-02	VCAN	L2 Frontal Aslant Tract Right	6.09E-20	-9.142730
102	rs11749904	5	82782530	intronic	C	T	0.380	6.09E-29	4.43E-02	VCAN	FA Superior Londgitudinal Fasciculus I Right	2.46E-25	10.400744
102	rs11749904	5	82782530	intronic	C	T	0.380	6.09E-29	4.43E-02	VCAN	L2 Arcuate Long Segment Right	1.61E-13	-7.377843
102	rs11749904	5	82782530	intronic	C	T	0.380	6.09E-29	4.43E-02	VCAN	FA Superior Londgitudinal Fasciculus II Left	1.74E-19	9.028315
102	rs11749904	5	82782530	intronic	C	T	0.380	6.09E-29	4.43E-02	VCAN	L2 Inferior Longitudinal Right	1.11E-27	-10.903403
102	rs11749904	5	82782530	intronic	C	T	0.380	6.09E-29	4.43E-02	VCAN	L1 Arcuate Posterior Segment Right	1.70E-18	-8.775296
102	rs11749904	5	82782530	intronic	C	T	0.380	6.09E-29	4.43E-02	VCAN	L2 Arcuate Anterior Segment Left	1.55E-13	-7.383214
102	rs11749904	5	82782530	intronic	C	T	0.380	6.09E-29	4.43E-02	VCAN	L1 Superior Londgitudinal Fasciculus III Left	6.40E-17	-8.357634
102	rs11749904	5	82782530	intronic	C	T	0.380	6.09E-29	4.43E-02	VCAN	L3 Superior Londgitudinal Fasciculus II Right	3.74E-21	-9.439771
102	rs11749904	5	82782530	intronic	C	T	0.380	6.09E-29	4.43E-02	VCAN	L1 Frontal Aslant Tract Right	1.23E-08	-5.695006
102	rs11749904	5	82782530	intronic	C	T	0.380	6.09E-29	4.43E-02	VCAN	L1 Corpus callosum	9.53E-19	-8.840494
102	rs11749904	5	82782530	intronic	C	T	0.380	6.09E-29	4.43E-02	VCAN	MD Arcuate Long Segment Left	6.36E-25	-10.309780
102	rs11749904	5	82782530	intronic	C	T	0.380	6.09E-29	4.43E-02	VCAN	ICVF Uncinate Right	5.67E-34	12.151007
102	rs11749904	5	82782530	intronic	C	T	0.380	6.09E-29	4.43E-02	VCAN	L3 Superior Londgitudinal Fasciculus I Right	1.06E-25	-10.480289
102	rs11749904	5	82782530	intronic	C	T	0.380	6.09E-29	4.43E-02	VCAN	ICVF Uncinate Left	5.57E-35	12.339237
102	rs11749904	5	82782530	intronic	C	T	0.380	6.09E-29	4.43E-02	VCAN	ICVF Inferior Longitudinal Left	3.03E-46	14.277367
102	rs11749904	5	82782530	intronic	C	T	0.380	6.09E-29	4.43E-02	VCAN	ICVF Superior Londgitudinal Fasciculus III Left	5.59E-40	13.233906
102	rs11749904	5	82782530	intronic	C	T	0.380	6.09E-29	4.43E-02	VCAN	L3 Inferior Longitudinal Right	5.12E-28	-10.973555
102	rs11749904	5	82782530	intronic	C	T	0.380	6.09E-29	4.43E-02	VCAN	MD Uncinate Left	1.97E-18	-8.758834
102	rs11749904	5	82782530	intronic	C	T	0.380	6.09E-29	4.43E-02	VCAN	L2 Frontal Superior Longitudinal Right	2.20E-09	-5.982425
102	rs11749904	5	82782530	intronic	C	T	0.380	6.09E-29	4.43E-02	VCAN	L2 Arcuate Posterior Segment Right	9.99E-20	-9.089033
102	rs11749904	5	82782530	intronic	C	T	0.380	6.09E-29	4.43E-02	VCAN	L2 Superior Londgitudinal Fasciculus II Left	6.26E-21	-9.385589
102	rs11749904	5	82782530	intronic	C	T	0.380	6.09E-29	4.43E-02	VCAN	MD Superior Londgitudinal Fasciculus III Right	9.65E-19	-8.839089
102	rs11749904	5	82782530	intronic	C	T	0.380	6.09E-29	4.43E-02	VCAN	L3 Frontal Inferior longitudinal Right	3.96E-08	-5.492809
102	rs11749904	5	82782530	intronic	C	T	0.380	6.09E-29	4.43E-02	VCAN	MD Inferior Fronto Occipital fasciculus Left	1.39E-29	-11.294734
102	rs11749904	5	82782530	intronic	C	T	0.380	6.09E-29	4.43E-02	VCAN	MD Frontal Superior Longitudinal Right	3.86E-08	-5.497014
102	rs11749904	5	82782530	intronic	C	T	0.380	6.09E-29	4.43E-02	VCAN	L3 Arcuate Anterior Segment Right	9.69E-20	-9.092389
102	rs11749904	5	82782530	intronic	C	T	0.380	6.09E-29	4.43E-02	VCAN	L2 Arcuate Posterior Segment Left	1.83E-16	-8.232991
102	rs11749904	5	82782530	intronic	C	T	0.380	6.09E-29	4.43E-02	VCAN	ICVF Frontal Inferior longitudinal Right	2.05E-30	11.461794
102	rs11749904	5	82782530	intronic	C	T	0.380	6.09E-29	4.43E-02	VCAN	MD Superior Londgitudinal Fasciculus I Left	2.18E-22	-9.733031
102	rs11749904	5	82782530	intronic	C	T	0.380	6.09E-29	4.43E-02	VCAN	L1 Superior Londgitudinal Fasciculus I Left	2.14E-08	-5.599967
102	rs160184	5	82822037	intronic	G	A	0.480	4.03E-25	3.63E-02	VCAN	L3 Superior Londgitudinal Fasciculus II Left	5.44E-09	5.833135
102	rs160184	5	82822037	intronic	G	A	0.480	4.03E-25	3.63E-02	VCAN	MD Inferior Longitudinal Left	6.57E-14	7.496263

Genomic Locus	Lead SNP	chr	Position	Functional category	Non-effect allele	Effect allele	MAF	mvgwasP (discovery -British-)	mvgwasP (replication -non British-)	Nearest gene	Central endophenotypes	univariate P value	univariate Z
102	rs160184	5	82822037	intronic	G	A	0.480	4.03E-25	3.63E-02	VCAN	ICVF Fronto Insular tract4 Right	3.64E-32	-11.805896
102	rs160184	5	82822037	intronic	G	A	0.480	4.03E-25	3.63E-02	VCAN	L3 Frontal Aslant Tract Right	3.32E-11	6.631745
102	rs160184	5	82822037	intronic	G	A	0.480	4.03E-25	3.63E-02	VCAN	L3 Fronto Insular tract5 Right	3.33E-12	6.962911
102	rs160184	5	82822037	intronic	G	A	0.480	4.03E-25	3.63E-02	VCAN	FA Inferior Fronto Occipital fasciculus Right	1.37E-11	-6.760879
102	rs160184	5	82822037	intronic	G	A	0.480	4.03E-25	3.63E-02	VCAN	FA Superior Londgitudinal Fasciculus III Right	5.92E-11	-6.545660
102	rs160184	5	82822037	intronic	G	A	0.480	4.03E-25	3.63E-02	VCAN	MD Superior Londgitudinal Fasciculus II Right	2.00E-09	5.998050
102	rs160184	5	82822037	intronic	G	A	0.480	4.03E-25	3.63E-02	VCAN	FA Uncinate Right	4.18E-10	-6.247190
102	rs160184	5	82822037	intronic	G	A	0.480	4.03E-25	3.63E-02	VCAN	L1 Inferior Longitudinal Left	3.41E-10	6.278886
102	rs160184	5	82822037	intronic	G	A	0.480	4.03E-25	3.63E-02	VCAN	ICVF Superior Londgitudinal Fasciculus II Right	1.12E-23	-10.030157
102	rs160184	5	82822037	intronic	G	A	0.480	4.03E-25	3.63E-02	VCAN	L3 Fronto Insular tract2 Right	4.37E-08	5.475121
102	rs160184	5	82822037	intronic	G	A	0.480	4.03E-25	3.63E-02	VCAN	FA Inferior Longitudinal Left	6.47E-09	-5.804067
102	rs160184	5	82822037	intronic	G	A	0.480	4.03E-25	3.63E-02	VCAN	FA Inferior Fronto Occipital fasciculus Left	6.05E-11	-6.542565
102	rs160184	5	82822037	intronic	G	A	0.480	4.03E-25	3.63E-02	VCAN	FA Frontal Aslant Tract Left	8.54E-11	-6.490825
102	rs160184	5	82822037	intronic	G	A	0.480	4.03E-25	3.63E-02	VCAN	ICVF Arcuate Anterior Segment Right	5.51E-25	-10.323584
102	rs160184	5	82822037	intronic	G	A	0.480	4.03E-25	3.63E-02	VCAN	FA Uncinate Left	7.25E-16	-8.066150
102	rs160184	5	82822037	intronic	G	A	0.480	4.03E-25	3.63E-02	VCAN	ICVF Fronto Insular tract3 Right	1.94E-29	-11.265423
102	rs160184	5	82822037	intronic	G	A	0.480	4.03E-25	3.63E-02	VCAN	MD Arcuate Anterior Segment Right	9.75E-12	6.810189
102	rs160184	5	82822037	intronic	G	A	0.480	4.03E-25	3.63E-02	VCAN	L2 Inferior Longitudinal Left	3.20E-12	6.968825
102	rs160184	5	82822037	intronic	G	A	0.480	4.03E-25	3.63E-02	VCAN	MD Inferior Longitudinal Right	6.96E-13	7.180310
102	rs160184	5	82822037	intronic	G	A	0.480	4.03E-25	3.63E-02	VCAN	L1 Inferior Fronto Occipital fasciculus Left	3.68E-13	7.266737
102	rs160184	5	82822037	intronic	G	A	0.480	4.03E-25	3.63E-02	VCAN	ICVF Arcuate Long Segment Left	1.73E-24	-10.213161
102	rs160184	5	82822037	intronic	G	A	0.480	4.03E-25	3.63E-02	VCAN	MD Frontal Aslant Tract Right	2.51E-12	7.002939
102	rs160184	5	82822037	intronic	G	A	0.480	4.03E-25	3.63E-02	VCAN	ISOVF Inferior Longitudinal Right	6.05E-09	-5.815480
102	rs160184	5	82822037	intronic	G	A	0.480	4.03E-25	3.63E-02	VCAN	L3 Superior Londgitudinal Fasciculus I Left	3.88E-13	7.259639
102	rs160184	5	82822037	intronic	G	A	0.480	4.03E-25	3.63E-02	VCAN	L1 Fronto Insular tract4 Right	1.90E-09	6.005892
102	rs160184	5	82822037	intronic	G	A	0.480	4.03E-25	3.63E-02	VCAN	ICVF Fronto Insular tract2 Right	9.65E-22	-9.580606
102	rs160184	5	82822037	intronic	G	A	0.480	4.03E-25	3.63E-02	VCAN	ICVF Fronto Insular tract5 Right	3.38E-24	-10.148181
102	rs160184	5	82822037	intronic	G	A	0.480	4.03E-25	3.63E-02	VCAN	FA Arcuate Anterior Segment Right	2.98E-08	-5.542577
102	rs160184	5	82822037	intronic	G	A	0.480	4.03E-25	3.63E-02	VCAN	MD Fronto Insular tract5 Right	2.11E-10	6.353067
102	rs160184	5	82822037	intronic	G	A	0.480	4.03E-25	3.63E-02	VCAN	FA Superior Londgitudinal Fasciculus I Left	5.35E-13	-7.216068
102	rs160184	5	82822037	intronic	G	A	0.480	4.03E-25	3.63E-02	VCAN	L3 Frontal Aslant Tract Left	1.87E-11	6.715763
102	rs160184	5	82822037	intronic	G	A	0.480	4.03E-25	3.63E-02	VCAN	FA Fronto Insular tract4 Right	2.65E-08	-5.563005
102	rs160184	5	82822037	intronic	G	A	0.480	4.03E-25	3.63E-02	VCAN	ICVF Inferior Fronto Occipital fasciculus Right	3.77E-25	-10.359923
102	rs160184	5	82822037	intronic	G	A	0.480	4.03E-25	3.63E-02	VCAN	L1 Arcuate Anterior Segment Left	1.43E-11	6.754910
102	rs160184	5	82822037	intronic	G	A	0.480	4.03E-25	3.63E-02	VCAN	FA Arcuate Long Segment Left	3.68E-09	-5.898117
102	rs160184	5	82822037	intronic	G	A	0.480	4.03E-25	3.63E-02	VCAN	MD Uncinate Right	2.35E-20	9.245185
102	rs160184	5	82822037	intronic	G	A	0.480	4.03E-25	3.63E-02	VCAN	L3 Fronto Insular tract1 Right	2.24E-09	5.979323
102	rs160184	5	82822037	intronic	G	A	0.480	4.03E-25	3.63E-02	VCAN	MD Inferior Fronto Occipital fasciculus Right	9.32E-14	7.450224
102	rs160184	5	82822037	intronic	G	A	0.480	4.03E-25	3.63E-02	VCAN	ICVF Corpus callosum	4.33E-30	-11.396921
102	rs160184	5	82822037	intronic	G	A	0.480	4.03E-25	3.63E-02	VCAN	L3 Superior Londgitudinal Fasciculus III Right	1.98E-13	7.350119
102	rs160184	5	82822037	intronic	G	A	0.480	4.03E-25	3.63E-02	VCAN	ICVF Arcuate Posterior Segment Right	5.77E-23	-9.867319
102	rs160184	5	82822037	intronic	G	A	0.480	4.03E-25	3.63E-02	VCAN	MD Corpus callosum	2.57E-15	7.910342
102	rs160184	5	82822037	intronic	G	A	0.480	4.03E-25	3.63E-02	VCAN	MD Fronto Insular tract3 Right	1.20E-10	6.439869
102	rs160184	5	82822037	intronic	G	A	0.480	4.03E-25	3.63E-02	VCAN	L2 Inferior Fronto Occipital fasciculus Right	4.88E-12	6.908957
102	rs160184	5	82822037	intronic	G	A	0.480	4.03E-25	3.63E-02	VCAN	L3 Fronto Insular tract4 Right	1.41E-14	7.695473
102	rs160184	5	82822037	intronic	G	A	0.480	4.03E-25	3.63E-02	VCAN	L3 Arcuate Posterior Segment Right	3.98E-08	5.491571
102	rs160184	5	82822037	intronic	G	A	0.480	4.03E-25	3.63E-02	VCAN	ICVF Fronto Insular tract3 Left	1.06E-23	-10.035687
102	rs160184	5	82822037	intronic	G	A	0.480	4.03E-25	3.63E-02	VCAN	FA Superior Londgitudinal Fasciculus III Left	4.73E-12	-6.913438
102	rs160184	5	82822037	intronic	G	A	0.480	4.03E-25	3.63E-02	VCAN	MD Superior Londgitudinal Fasciculus III Left	3.70E-16	8.148023
102	rs160184	5	82822037	intronic	G	A	0.480	4.03E-25	3.63E-02	VCAN	ICVF Inferior Fronto Occipital fasciculus Left	9.73E-30	-11.326238
102	rs160184	5	82822037	intronic	G	A	0.480	4.03E-25	3.63E-02	VCAN	ICVF Frontal Aslant Tract Right	6.36E-28	-10.953925
102	rs160184	5	82822037	intronic	G	A	0.480	4.03E-25	3.63E-02	VCAN	ICVF Frontal Superior Longitudinal Left	3.24E-17	-8.437509
102	rs160184	5	82822037	intronic	G	A	0.480	4.03E-25	3.63E-02	VCAN	L3 Fronto Insular tract5 Left	4.89E-09	5.850868
102	rs160184	5	82822037	intronic	G	A	0.480	4.03E-25	3.63E-02	VCAN	MD Arcuate Posterior Segment Right	2.72E-10	6.313945
102	rs160184	5	82822037	intronic	G	A	0.480	4.03E-25	3.63E-02	VCAN	L2 Uncinate Right	1.28E-16	8.275255
102	rs160184	5	82822037	intronic	G	A	0.480	4.03E-25	3.63E-02	VCAN	L2 Corpus callosum	2.65E-15	7.906340
102	rs160184	5	82822037	intronic	G	A	0.480	4.03E-25	3.63E-02	VCAN	MD Fronto Insular tract5 Left	7.21E-10	6.161482
102	rs160184	5	82822037	intronic	G	A	0.480	4.03E-25	3.63E-02	VCAN	L1 Uncinate Left	4.80E-12	6.911254
102	rs160184	5	82822037	intronic	G	A	0.480	4.03E-25	3.63E-02	VCAN	L2 Superior Londgitudinal Fasciculus III Right	2.85E-12	6.985002
102	rs160184	5	82822037	intronic	G	A	0.480	4.03E-25	3.63E-02	VCAN	L3 Superior Londgitudinal Fasciculus III Left	3.41E-15	7.874987
102	rs160184	5	82822037	intronic	G	A	0.480	4.03E-25	3.63E-02	VCAN	L1 Uncinate Right	1.57E-14	7.681912
102	rs160184	5	82822037	intronic	G	A	0.480	4.03E-25	3.63E-02	VCAN	ICVF Frontal Inferior longitudinal Left	3.69E-14	-7.571394
102	rs160184	5	82822037	intronic	G	A	0.480	4.03E-25	3.63E-02	VCAN	ICVF Superior Londgitudinal Fasciculus II Left	7.24E-24	-10.073487
102	rs160184	5	82822037	intronic	G	A	0.480	4.03E-25	3.63E-02	VCAN	L3 Inferior Fronto Occipital fasciculus Right	3.78E-15	7.861915
102	rs160184	5	82822037	intronic	G	A	0.480	4.03E-25	3.63E-02	VCAN	L2 Frontal Aslant Tract Left	1.67E-14	7.674138
102	rs160184	5	82822037	intronic	G	A	0.480	4.03E-25	3.63E-02	VCAN	ICVF Fronto Insular tract1 Left	4.34E-09	-5.870851
102	rs160184	5	82822037	intronic	G	A	0.480	4.03E-25	3.63E-02	VCAN	L2 Superior Londgitudinal Fasciculus III Left	1.70E-14	7.671690
102	rs160184	5	82822037	intronic	G	A	0.480	4.03E-25	3.63E-02	VCAN	L2 Arcuate Anterior Segment Right	6.70E-09	5.798346
102	rs160184	5	82822037	intronic	G	A	0.480	4.03E-25	3.63E-02	VCAN	L3 Inferior Fronto Occipital fasciculus Left	2.66E-17	8.460688
102	rs160184	5	82822037	intronic	G	A	0.480	4.03E-25	3.63E-02	VCAN	L3 Arcuate Long Segment Left	2.17E-13	7.337708
102	rs160184	5	82822037	intronic	G	A	0.480	4.03E-25	3.63E-02	VCAN	ICVF Frontal Aslant Tract Left	1.50E-25	-10.447966
102	rs160184	5	82822037	intronic	G	A	0.480	4.03E-25	3.63E-02	VCAN	MD Frontal Aslant Tract Left	8.09E-13	7.159550
102	rs160184	5	82822037	intronic	G	A	0.480	4.03E-25	3.63E-02	VCAN	MD Fronto Insular tract4 Right	3.34E-14	7.584461
102	rs160184	5	82822037	intronic	G	A	0.480	4.03E-25	3.63E-02	VCAN	ICVF Superior Londgitudinal Fasciculus III Right	2.23E-27	-10.839948
102	rs160184	5	82822037	intronic	G	A	0.480	4.03E-25	3.63E-02	VCAN	L2 Superior Londgitudinal Fasciculus II Right	1.13E-09	6.089697
102	rs160184	5	82822037	intronic	G	A	0.480	4.03E-25	3.63E-02	VCAN	ICVF Frontal Superior Longitudinal Right	2.14E-27	-10.843346
102	rs160184	5	82822037	intronic	G	A	0.480	4.03E-25	3.63E-02	VCAN	MD Arcuate Anterior Segment Left	3.94E-14	7.562991
102	rs160184	5	82822037	intronic	G	A	0.480	4.03E-25	3.63E-02	VCAN	L3 Arcuate Posterior Segment Left	2.50E-10	6.327145
102	rs160184	5	82822037	intronic	G	A	0.480	4.03E-25	3.63E-02	VCAN	L1 Superior Londgitudinal Fasciculus III Right	4.70E-12	6.914465
102	rs160184	5	82822037	intronic	G	A	0.480	4.03E-25	3.63E-02	VCAN	MD Superior Londgitudinal Fasciculus II Left	2.25E-10	6.343008
102	rs160184	5	82822037	intronic	G	A	0.480	4.03E-25	3.63E-02	VCAN	FA Frontal Aslant Tract Right	6.03E-10	-6.189584
102	rs160184	5	82822037	intronic	G	A	0.480	4.03E-25	3.63E-02	VCAN	L2 Inferior Fronto Occipital fasciculus Left	1.20E-13	7.417331
102	rs160184	5	82822037	intronic	G	A	0.480	4.03E-25	3.63E-02	VCAN	ICVF Arcuate Posterior Segment Left	1.31E-27	-10.888193
102	rs160184	5	82822037	intronic	G	A	0.480	4.03E-25	3.63E-02	VCAN	L2 Uncinate Left	1.07E-21	9.569963
102	rs160184	5	82822037	intronic	G	A	0.480	4.03E-25	3.63E-02	VCAN	ICVF Fronto Insular tract5 Left	6.46E-26	-10.527410
102	rs160184	5	82822037	intronic	G	A	0.480	4.03E-25	3.63E-02	VCAN	ICVF Arcuate Long Segment Right	2.41E-22	-9.722781
102	rs160184	5	82822037	intronic	G	A	0.480	4.03E-25	3.63E-02	VCAN	L3 Inferior Longitudinal Left	1.00E-12	7.129914
102	rs160184	5	82822037	intronic	G	A	0.480	4.03E-25	3.63E-02	VCAN	MD Fronto Insular tract3 Left	2.13E-08	5.600923
102	rs160184	5	82822037	intronic	G	A	0.480	4.03E-25	3.63E-02	VCAN	L3 Corpus callosum	1.98E-14	7.651601
102	rs160184	5	82822037	intronic	G	A	0.480	4.03E-25	3.63E-02	VCAN	L3 Uncinate Left	2.37E-24	10.182705
102	rs160184	5	82822037	intronic	G	A	0.480	4.03E-25	3.63E-02	VCAN	ICVF Inferior Longitudinal Right	1.24E-26	-10.682055
102	rs160184	5	82822037	intronic	G	A	0.480	4.03E-25	3.63E-02	VCAN	L3 Arcuate Long Segment Right	1.31E-09	6.065665
102	rs160184	5	82822037	intronic	G	A	0.480	4.03E-25	3.63E-02	VCAN	FA Arcuate Posterior Segment Left	2.76E-09	-5.945568
102	rs160184	5	82822037	intronic	G	A	0.480	4.03E-25	3.63E-02	VCAN	ICVF Fronto Insular tract2 Left	4.54E-18	-8.664315
102	rs160184	5	82822037	intronic	G	A	0.480	4.03E-25	3.63E-02	VCAN	L2 Superior Londgitudinal Fasciculus I Right	3.34E-14	7.584520
102	rs160184	5	82822037	intronic	G	A	0.480	4.03E-25	3.63E-02	VCAN	FA Corpus callosum	7.41E-13	-7.171730
102	rs160184	5	82822037	intronic	G	A	0.480	4.03E-25	3.63E-02	VCAN	L2 Superior Londgitudinal Fasciculus I Left	1.12E-13	7.426331
102	rs160184	5	82822037	intronic	G	A	0.480	4.03E-25	3.63E-02	VCAN	MD Frontal Inferior longitudinal Right	8.76E-09	5.753127
102	rs160184	5	82822037	intronic	G	A	0.480	4.03E-25	3.63E-02	VCAN	L1 Inferior Longitudinal Right	3.94E-08	5.493619
102	rs160184	5	82822037	intronic	G	A	0.480	4.03E-25	3.63E-02	VCAN	MD Arcuate Posterior Segment Left	3.01E-11	6.645898
102	rs160184	5	82822037	intronic	G	A	0.480	4.03E-25	3.63E-02	VCAN	ICVF Arcuate Anterior Segment Left	9.28E-27	-10.708550
102	rs160184	5	82822037	intronic	G	A	0.480	4.03E-25	3.63E-02	VCAN	L3 Arcuate Anterior Segment Left	6.58E-11	6.529891
102	rs160184	5	82822037	intronic	G	A	0.480	4.03E-25	3.63E-02	VCAN	ICVF Superior Londgitudinal Fasciculus I Right	7.62E-32	-11.743556
102	rs160184	5	82822037	intronic	G	A	0.480	4.03E-25	3.63E-02	VCAN	FA Inferior Longitudinal Right	7.23E-12	-6.852945
102	rs160184	5	82822037	intronic	G	A	0.480	4.03E-25	3.63E-02	VCAN	MD Superior Londgitudinal Fasciculus I Right	9.54E-15	7.745243
102	rs160184	5	82822037	intronic	G	A	0.480	4.03E-25	3.63E-02	VCAN	MD Arcuate Long Segment Right	1.43E-09	6.052309

Genomic Locus	Lead SNP	chr	Position	Functional category	Non-effect allele	Effect allele	MAF	mvgwasP (discovery -British-)	mvgwasP (replication -non British-)	Nearest gene	Central endophenotypes	univariate P value	univariate Z
102	rs160184	5	82822037	intronic	G	A	0.480	4.03E-25	3.63E-02	VCAN	MD Fronto Insular tract1 Right	1.34E-08	5.681118
102	rs160184	5	82822037	intronic	G	A	0.480	4.03E-25	3.63E-02	VCAN	L3 Uncinate Right	1.34E-20	9.305059
102	rs160184	5	82822037	intronic	G	A	0.480	4.03E-25	3.63E-02	VCAN	ICVF Fronto Insular tract1 Right	5.44E-25	-10.324912
102	rs160184	5	82822037	intronic	G	A	0.480	4.03E-25	3.63E-02	VCAN	L2 Arcuate Long Segment Left	5.10E-09	5.843830
102	rs160184	5	82822037	intronic	G	A	0.480	4.03E-25	3.63E-02	VCAN	ICVF Superior Londgitudinal Fasciculus I Left	1.04E-30	-11.520304
102	rs160184	5	82822037	intronic	G	A	0.480	4.03E-25	3.63E-02	VCAN	L2 Frontal Aslant Tract Right	2.73E-12	6.991090
102	rs160184	5	82822037	intronic	G	A	0.480	4.03E-25	3.63E-02	VCAN	FA Superior Londgitudinal Fasciculus I Right	1.80E-13	-7.362729
102	rs160184	5	82822037	intronic	G	A	0.480	4.03E-25	3.63E-02	VCAN	L2 Fronto Insular tract4 Right	1.00E-08	5.730159
102	rs160184	5	82822037	intronic	G	A	0.480	4.03E-25	3.63E-02	VCAN	L2 Inferior Longitudinal Right	1.08E-11	6.795993
102	rs160184	5	82822037	intronic	G	A	0.480	4.03E-25	3.63E-02	VCAN	L2 Arcuate Anterior Segment Left	1.58E-10	6.397387
102	rs160184	5	82822037	intronic	G	A	0.480	4.03E-25	3.63E-02	VCAN	L1 Superior Londgitudinal Fasciculus III Left	2.43E-11	6.677325
102	rs160184	5	82822037	intronic	G	A	0.480	4.03E-25	3.63E-02	VCAN	L3 Superior Londgitudinal Fasciculus II Right	1.28E-08	5.689141
102	rs160184	5	82822037	intronic	G	A	0.480	4.03E-25	3.63E-02	VCAN	L1 Frontal Aslant Tract Right	3.17E-08	5.531548
102	rs160184	5	82822037	intronic	G	A	0.480	4.03E-25	3.63E-02	VCAN	L1 Corpus callosum	1.09E-11	6.794672
102	rs160184	5	82822037	intronic	G	A	0.480	4.03E-25	3.63E-02	VCAN	MD Arcuate Long Segment Left	7.94E-14	7.471271
102	rs160184	5	82822037	intronic	G	A	0.480	4.03E-25	3.63E-02	VCAN	ICVF Uncinate Right	1.11E-38	-13.007257
102	rs160184	5	82822037	intronic	G	A	0.480	4.03E-25	3.63E-02	VCAN	ICVF Fronto Insular tract4 Left	1.73E-10	-6.383199
102	rs160184	5	82822037	intronic	G	A	0.480	4.03E-25	3.63E-02	VCAN	L3 Superior Londgitudinal Fasciculus I Right	4.23E-16	8.131766
102	rs160184	5	82822037	intronic	G	A	0.480	4.03E-25	3.63E-02	VCAN	ICVF Uncinate Left	1.88E-40	-13.315482
102	rs160184	5	82822037	intronic	G	A	0.480	4.03E-25	3.63E-02	VCAN	L3 Fronto Insular tract3 Right	1.90E-11	6.713418
102	rs160184	5	82822037	intronic	G	A	0.480	4.03E-25	3.63E-02	VCAN	ICVF Inferior Longitudinal Left	6.19E-28	-10.956462
102	rs160184	5	82822037	intronic	G	A	0.480	4.03E-25	3.63E-02	VCAN	ICVF Superior Londgitudinal Fasciculus III Left	5.91E-29	-11.167090
102	rs160184	5	82822037	intronic	G	A	0.480	4.03E-25	3.63E-02	VCAN	L3 Inferior Longitudinal Right	1.02E-14	7.736500
102	rs160184	5	82822037	intronic	G	A	0.480	4.03E-25	3.63E-02	VCAN	MD Uncinate Left	1.21E-22	9.792542
102	rs160184	5	82822037	intronic	G	A	0.480	4.03E-25	3.63E-02	VCAN	L2 Arcuate Posterior Segment Right	4.83E-09	5.852767
102	rs160184	5	82822037	intronic	G	A	0.480	4.03E-25	3.63E-02	VCAN	L2 Superior Londgitudinal Fasciculus II Left	3.05E-10	6.296238
102	rs160184	5	82822037	intronic	G	A	0.480	4.03E-25	3.63E-02	VCAN	MD Superior Londgitudinal Fasciculus III Right	9.78E-14	7.443781
102	rs160184	5	82822037	intronic	G	A	0.480	4.03E-25	3.63E-02	VCAN	MD Inferior Fronto Occipital fasciculus Left	5.30E-18	8.646753
102	rs160184	5	82822037	intronic	G	A	0.480	4.03E-25	3.63E-02	VCAN	L3 Arcuate Anterior Segment Right	3.29E-11	6.633151
102	rs160184	5	82822037	intronic	G	A	0.480	4.03E-25	3.63E-02	VCAN	L2 Arcuate Posterior Segment Left	9.51E-10	6.117467
102	rs160184	5	82822037	intronic	G	A	0.480	4.03E-25	3.63E-02	VCAN	ICVF Frontal Inferior longitudinal Right	8.71E-21	-9.350690
102	rs160184	5	82822037	intronic	G	A	0.480	4.03E-25	3.63E-02	VCAN	MD Superior Londgitudinal Fasciculus I Left	1.87E-12	7.043585
102	rs309588	5	82852578	ncRNA intronic	T	A	0.204	5.16E-28	1.55E-01	VCAN:VCAN-AS1	L3 Superior Londgitudinal Fasciculus II Left	3.80E-08	5.499868
102	rs309588	5	82852578	ncRNA intronic	T	A	0.204	5.16E-28	1.55E-01	VCAN:VCAN-AS1	MD Inferior Longitudinal Left	5.38E-11	6.559915
102	rs309588	5	82852578	ncRNA intronic	T	A	0.204	5.16E-28	1.55E-01	VCAN:VCAN-AS1	ICVF Fronto Insular tract4 Right	5.87E-11	-6.546986
102	rs309588	5	82852578	ncRNA intronic	T	A	0.204	5.16E-28	1.55E-01	VCAN:VCAN-AS1	L1 Inferior Longitudinal Left	1.07E-09	6.098036
102	rs309588	5	82852578	ncRNA intronic	T	A	0.204	5.16E-28	1.55E-01	VCAN:VCAN-AS1	ICVF Superior Londgitudinal Fasciculus II Right	1.34E-08	-5.680892
102	rs309588	5	82852578	ncRNA intronic	T	A	0.204	5.16E-28	1.55E-01	VCAN:VCAN-AS1	ICVF Fronto Insular tract3 Right	5.70E-09	-5.825353
102	rs309588	5	82852578	ncRNA intronic	T	A	0.204	5.16E-28	1.55E-01	VCAN:VCAN-AS1	L2 Inferior Longitudinal Left	1.50E-08	5.661298
102	rs309588	5	82852578	ncRNA intronic	T	A	0.204	5.16E-28	1.55E-01	VCAN:VCAN-AS1	MD Inferior Longitudinal Right	1.57E-10	6.398742
102	rs309588	5	82852578	ncRNA intronic	T	A	0.204	5.16E-28	1.55E-01	VCAN:VCAN-AS1	L1 Inferior Fronto Occipital fasciculus Left	2.11E-13	7.341875
102	rs309588	5	82852578	ncRNA intronic	T	A	0.204	5.16E-28	1.55E-01	VCAN:VCAN-AS1	ICVF Arcuate Long Segment Left	6.60E-09	-5.800691
102	rs309588	5	82852578	ncRNA intronic	T	A	0.204	5.16E-28	1.55E-01	VCAN:VCAN-AS1	ICVF Fronto Insular tract2 Right	2.60E-09	-5.955293
102	rs309588	5	82852578	ncRNA intronic	T	A	0.204	5.16E-28	1.55E-01	VCAN:VCAN-AS1	ICVF Fronto Insular tract5 Right	1.83E-10	-6.374661
102	rs309588	5	82852578	ncRNA intronic	T	A	0.204	5.16E-28	1.55E-01	VCAN:VCAN-AS1	ICVF Inferior Fronto Occipital fasciculus Right	3.51E-15	-7.871307
102	rs309588	5	82852578	ncRNA intronic	T	A	0.204	5.16E-28	1.55E-01	VCAN:VCAN-AS1	MD Uncinate Right	2.53E-10	6.325435
102	rs309588	5	82852578	ncRNA intronic	T	A	0.204	5.16E-28	1.55E-01	VCAN:VCAN-AS1	MD Inferior Fronto Occipital fasciculus Right	7.37E-12	6.850231
102	rs309588	5	82852578	ncRNA intronic	T	A	0.204	5.16E-28	1.55E-01	VCAN:VCAN-AS1	ICVF Corpus callosum	2.25E-13	-7.333056
102	rs309588	5	82852578	ncRNA intronic	T	A	0.204	5.16E-28	1.55E-01	VCAN:VCAN-AS1	ICVF Arcuate Posterior Segment Right	1.18E-10	-6.442358
102	rs309588	5	82852578	ncRNA intronic	T	A	0.204	5.16E-28	1.55E-01	VCAN:VCAN-AS1	MD Corpus callosum	9.29E-09	5.743138
102	rs309588	5	82852578	ncRNA intronic	T	A	0.204	5.16E-28	1.55E-01	VCAN:VCAN-AS1	ICVF Inferior Fronto Occipital fasciculus Left	2.23E-13	-7.334358
102	rs309588	5	82852578	ncRNA intronic	T	A	0.204	5.16E-28	1.55E-01	VCAN:VCAN-AS1	ICVF Frontal Aslant Tract Right	3.48E-09	-5.907264
102	rs309588	5	82852578	ncRNA intronic	T	A	0.204	5.16E-28	1.55E-01	VCAN:VCAN-AS1	L1 Inferior Fronto Occipital fasciculus Right	2.54E-10	6.324765
102	rs309588	5	82852578	ncRNA intronic	T	A	0.204	5.16E-28	1.55E-01	VCAN:VCAN-AS1	L2 Uncinate Right	2.02E-08	5.610667
102	rs309588	5	82852578	ncRNA intronic	T	A	0.204	5.16E-28	1.55E-01	VCAN:VCAN-AS1	L1 Uncinate Left	1.29E-08	5.687958
102	rs309588	5	82852578	ncRNA intronic	T	A	0.204	5.16E-28	1.55E-01	VCAN:VCAN-AS1	ICVF Superior Londgitudinal Fasciculus II Left	2.42E-09	-5.967026
102	rs309588	5	82852578	ncRNA intronic	T	A	0.204	5.16E-28	1.55E-01	VCAN:VCAN-AS1	L3 Inferior Fronto Occipital fasciculus Right	6.65E-11	6.528414
102	rs309588	5	82852578	ncRNA intronic	T	A	0.204	5.16E-28	1.55E-01	VCAN:VCAN-AS1	L1 Fronto Insular tract1 Right	8.49E-11	6.491628
102	rs309588	5	82852578	ncRNA intronic	T	A	0.204	5.16E-28	1.55E-01	VCAN:VCAN-AS1	L3 Inferior Fronto Occipital fasciculus Left	5.57E-11	6.554913
102	rs309588	5	82852578	ncRNA intronic	T	A	0.204	5.16E-28	1.55E-01	VCAN:VCAN-AS1	ICVF Frontal Aslant Tract Left	2.50E-08	-5.573475
102	rs309588	5	82852578	ncRNA intronic	T	A	0.204	5.16E-28	1.55E-01	VCAN:VCAN-AS1	ICVF Superior Londgitudinal Fasciculus III Right	2.45E-09	-5.964439
102	rs309588	5	82852578	ncRNA intronic	T	A	0.204	5.16E-28	1.55E-01	VCAN:VCAN-AS1	ICVF Arcuate Posterior Segment Left	5.50E-11	-6.556615
102	rs309588	5	82852578	ncRNA intronic	T	A	0.204	5.16E-28	1.55E-01	VCAN:VCAN-AS1	L2 Uncinate Left	9.57E-12	6.812799
102	rs309588	5	82852578	ncRNA intronic	T	A	0.204	5.16E-28	1.55E-01	VCAN:VCAN-AS1	ICVF Fronto Insular tract5 Left	9.30E-10	-6.121013
102	rs309588	5	82852578	ncRNA intronic	T	A	0.204	5.16E-28	1.55E-01	VCAN:VCAN-AS1	ICVF Arcuate Long Segment Right	6.57E-09	-5.801542
102	rs309588	5	82852578	ncRNA intronic	T	A	0.204	5.16E-28	1.55E-01	VCAN:VCAN-AS1	L3 Inferior Longitudinal Left	1.23E-09	6.076083
102	rs309588	5	82852578	ncRNA intronic	T	A	0.204	5.16E-28	1.55E-01	VCAN:VCAN-AS1	L3 Uncinate Left	1.37E-11	6.761474
102	rs309588	5	82852578	ncRNA intronic	T	A	0.204	5.16E-28	1.55E-01	VCAN:VCAN-AS1	ICVF Inferior Longitudinal Right	3.57E-16	-8.152479
102	rs309588	5	82852578	ncRNA intronic	T	A	0.204	5.16E-28	1.55E-01	VCAN:VCAN-AS1	L1 Inferior Longitudinal Right	4.21E-10	6.245884
102	rs309588	5	82852578	ncRNA intronic	T	A	0.204	5.16E-28	1.55E-01	VCAN:VCAN-AS1	L1 Fronto Insular tract2 Right	8.33E-11	6.494515
102	rs309588	5	82852578	ncRNA intronic	T	A	0.204	5.16E-28	1.55E-01	VCAN:VCAN-AS1	ICVF Arcuate Anterior Segment Left	1.53E-09	-6.040801
102	rs309588	5	82852578	ncRNA intronic	T	A	0.204	5.16E-28	1.55E-01	VCAN:VCAN-AS1	ICVF Superior Londgitudinal Fasciculus I Right	5.16E-10	-6.214298
102	rs309588	5	82852578	ncRNA intronic	T	A	0.204	5.16E-28	1.55E-01	VCAN:VCAN-AS1	L3 Uncinate Right	6.49E-11	6.532081
102	rs309588	5	82852578	ncRNA intronic	T	A	0.204	5.16E-28	1.55E-01	VCAN:VCAN-AS1	ICVF Superior Londgitudinal Fasciculus I Left	5.31E-11	-6.562049
102	rs309588	5	82852578	ncRNA intronic	T	A	0.204	5.16E-28	1.55E-01	VCAN:VCAN-AS1	FA Superior Londgitudinal Fasciculus II Left	6.42E-10	-6.179765
102	rs309588	5	82852578	ncRNA intronic	T	A	0.204	5.16E-28	1.55E-01	VCAN:VCAN-AS1	MO Fronto Insular tract1 Right	4.93E-08	5.453714
102	rs309588	5	82852578	ncRNA intronic	T	A	0.204	5.16E-28	1.55E-01	VCAN:VCAN-AS1	OD Fronto Insular tract3 Right	1.81E-08	-5.629376
102	rs309588	5	82852578	ncRNA intronic	T	A	0.204	5.16E-28	1.55E-01	VCAN:VCAN-AS1	MO Fronto Insular tract2 Right	3.31E-08	5.524145
102	rs309588	5	82852578	ncRNA intronic	T	A	0.204	5.16E-28	1.55E-01	VCAN:VCAN-AS1	L1 Corpus callosum	1.16E-10	6.444237
102	rs309588	5	82852578	ncRNA intronic	T	A	0.204	5.16E-28	1.55E-01	VCAN:VCAN-AS1	ICVF Uncinate Right	6.96E-14	-7.488548
102	rs309588	5	82852578	ncRNA intronic	T	A	0.204	5.16E-28	1.55E-01	VCAN:VCAN-AS1	ICVF Uncinate Left	2.54E-14	-7.619770
102	rs309588	5	82852578	ncRNA intronic	T	A	0.204	5.16E-28	1.55E-01	VCAN:VCAN-AS1	ICVF Inferior Longitudinal Left	3.92E-16	-8.140975
102	rs309588	5	82852578	ncRNA intronic	T	A	0.204	5.16E-28	1.55E-01	VCAN:VCAN-AS1	ICVF Superior Londgitudinal Fasciculus III Left	7.73E-09	-5.774191
102	rs309588	5	82852578	ncRNA intronic	T	A	0.204	5.16E-28	1.55E-01	VCAN:VCAN-AS1	L3 Inferior Longitudinal Right	5.93E-10	6.192230
102	rs309588	5	82852578	ncRNA intronic	T	A	0.204	5.16E-28	1.55E-01	VCAN:VCAN-AS1	MD Uncinate Left	1.09E-12	7.118211
102	rs309588	5	82852578	ncRNA intronic	T	A	0.204	5.16E-28	1.55E-01	VCAN:VCAN-AS1	L2 Superior Londgitudinal Fasciculus II Left	4.15E-08	5.484259
102	rs309588	5	82852578	ncRNA intronic	T	A	0.204	5.16E-28	1.55E-01	VCAN:VCAN-AS1	MD Inferior Fronto Occipital fasciculus Left	6.15E-13	7.197086
102	rs10052710	5	82860025	ncRNA intronic	G	T	0.195	7.72E-111	6.11E-06	VCAN:VCAN-AS1	L3 Superior Londgitudinal Fasciculus II Left	9.95E-31	-11.524289
102	rs10052710	5	82860025	ncRNA intronic	G	T	0.195	7.72E-111	6.11E-06	VCAN:VCAN-AS1	MD Inferior Longitudinal Left	4.33E-57	-15.923778
102	rs10052710	5	82860025	ncRNA intronic	G	T	0.195	7.72E-111	6.11E-06	VCAN:VCAN-AS1	ICVF Fronto Insular tract4 Right	5.07E-74	18.200966
102	rs10052710	5	82860025	ncRNA intronic	G	T	0.195	7.72E-111	6.11E-06	VCAN:VCAN-AS1	L3 Frontal Aslant Tract Right	3.50E-22	-9.684640
102	rs10052710	5	82860025	ncRNA intronic	G	T	0.195	7.72E-111	6.11E-06	VCAN:VCAN-AS1	L3 Fronto Insular tract5 Right	6.16E-16	-8.086042
102	rs10052710	5	82860025	ncRNA intronic	G	T	0.195	7.72E-111	6.11E-06	VCAN:VCAN-AS1	FA Inferior Fronto Occipital fasciculus Right	7.10E-35	12.319705
102	rs10052710	5	82860025	ncRNA intronic	G	T	0.195	7.72E-111	6.11E-06	VCAN:VCAN-AS1	L1 Arcuate Anterior Segment Right	3.82E-16	-8.144158
102	rs10052710	5	82860025	ncRNA intronic	G	T	0.195	7.72E-111	6.11E-06	VCAN:VCAN-AS1	L3 Frontal Inferior longitudinal Left	7.25E-12	-6.852562
102	rs10052710	5	82860025	ncRNA intronic	G	T	0.195	7.72E-111	6.11E-06	VCAN:VCAN-AS1	FA Superior Londgitudinal Fasciculus III Right	3.57E-27	10.796739
102	rs10052710	5	82860025	ncRNA intronic	G	T	0.195	7.72E-111	6.11E-06	VCAN:VCAN-AS1	MD Superior Londgitudinal Fasciculus II Right	7.10E-30	-11.353789
102	rs10052710	5	82860025	ncRNA intronic	G	T	0.195	7.72E-111	6.11E-06	VCAN:VCAN-AS1	FA Uncinate Right	6.00E-35	12.333212
102	rs10052710	5	82860025	ncRNA intronic	G	T	0.195	7.72E-111	6.11E-06	VCAN:VCAN-AS1	L2 Frontal Inferior longitudinal Left	2.69E-12	-6.992930
102	rs10052710	5	82860025	ncRNA intronic	G	T	0.195	7.72E-111	6.11E-06	VCAN:VCAN-AS1	L2 Frontal Inferior longitudinal Right	1.81E-18	-8.768569
102	rs10052710	5	82860025	ncRNA intronic	G	T	0.195	7.72E-111	6.11E-06	VCAN:VCAN-AS1	ISOVF Inferior Fronto Occipital fasciculus Left	3.24E-16	8.164154
102	rs10052710	5	82860025	ncRNA intronic	G	T	0.195	7.72E-111	6.11E-06	VCAN:VCAN-AS1	L1 Inferior Longitudinal Left	1.28E-37	-12.818955
102	rs10052710	5	82860025	ncRNA intronic	G	T	0.195	7.72E-111	6.11E-06	VCAN:VCAN-AS1	ICVF Superior Londgitudinal Fasciculus II Right	8.03E-67	17.269178

Genomic Locus	Lead SNP	chr	Position	Functional category	Non-effect allele	Effect allele	MAF	mvgwasP (discovery -British-)	mvgwasP (replication -non British-)	Nearest gene	Central endophenotypes	univariate P value	univariate Z
102	rs10052710	5	82860025	ncRNA intronic	G	T	0.195	7.72E-111	6.11E-06	VCAN:VCAN-AS1	L3 Fronto Insular tract2 Right	3.61E-14	-7.574321
102	rs10052710	5	82860025	ncRNA intronic	G	T	0.195	7.72E-111	6.11E-06	VCAN:VCAN-AS1	FA Inferior Longitudinal Left	1.36E-37	12.814352
102	rs10052710	5	82860025	ncRNA intronic	G	T	0.195	7.72E-111	6.11E-06	VCAN:VCAN-AS1	FA Inferior Fronto Occipital fasciculus Left	7.60E-37	12.680293
102	rs10052710	5	82860025	ncRNA intronic	G	T	0.195	7.72E-111	6.11E-06	VCAN:VCAN-AS1	FA Frontal Aslant Tract Left	8.62E-22	9.592198
102	rs10052710	5	82860025	ncRNA intronic	G	T	0.195	7.72E-111	6.11E-06	VCAN:VCAN-AS1	ICVF Arcuate Anterior Segment Right	8.33E-59	16.169107
102	rs10052710	5	82860025	ncRNA intronic	G	T	0.195	7.72E-111	6.11E-06	VCAN:VCAN-AS1	FA Uncinate Left	2.01E-36	12.603867
102	rs10052710	5	82860025	ncRNA intronic	G	T	0.195	7.72E-111	6.11E-06	VCAN:VCAN-AS1	ICVF Fronto Insular tract3 Right	2.95E-63	16.788730
102	rs10052710	5	82860025	ncRNA intronic	G	T	0.195	7.72E-111	6.11E-06	VCAN:VCAN-AS1	MD Arcuate Anterior Segment Right	3.49E-27	-10.798826
102	rs10052710	5	82860025	ncRNA intronic	G	T	0.195	7.72E-111	6.11E-06	VCAN:VCAN-AS1	L2 Inferior Longitudinal Left	3.98E-51	-15.040544
102	rs10052710	5	82860025	ncRNA intronic	G	T	0.195	7.72E-111	6.11E-06	VCAN:VCAN-AS1	MD Inferior Longitudinal Right	1.07E-51	-15.127479
102	rs10052710	5	82860025	ncRNA intronic	G	T	0.195	7.72E-111	6.11E-06	VCAN:VCAN-AS1	L1 Inferior Fronto Occipital fasciculus Left	5.34E-37	-12.708015
102	rs10052710	5	82860025	ncRNA intronic	G	T	0.195	7.72E-111	6.11E-06	VCAN:VCAN-AS1	ICVF Arcuate Long Segment Left	3.62E-59	16.220398
102	rs10052710	5	82860025	ncRNA intronic	G	T	0.195	7.72E-111	6.11E-06	VCAN:VCAN-AS1	MD Frontal Aslant Tract Right	2.65E-25	-10.393648
102	rs10052710	5	82860025	ncRNA intronic	G	T	0.195	7.72E-111	6.11E-06	VCAN:VCAN-AS1	ISOVF Inferior Longitudinal Right	4.67E-23	9.888535
102	rs10052710	5	82860025	ncRNA intronic	G	T	0.195	7.72E-111	6.11E-06	VCAN:VCAN-AS1	L3 Superior Londgitudinal Fasciculus I Left	6.34E-38	-12.873556
102	rs10052710	5	82860025	ncRNA intronic	G	T	0.195	7.72E-111	6.11E-06	VCAN:VCAN-AS1	L1 Fronto Insular tract4 Right	5.10E-11	-6.567859
102	rs10052710	5	82860025	ncRNA intronic	G	T	0.195	7.72E-111	6.11E-06	VCAN:VCAN-AS1	ICVF Fronto Insular tract2 Right	3.55E-50	14.895094
102	rs10052710	5	82860025	ncRNA intronic	G	T	0.195	7.72E-111	6.11E-06	VCAN:VCAN-AS1	ICVF Fronto Insular tract5 Right	1.87E-57	15.976378
102	rs10052710	5	82860025	ncRNA intronic	G	T	0.195	7.72E-111	6.11E-06	VCAN:VCAN-AS1	FA Arcuate Anterior Segment Right	3.91E-19	8.939611
102	rs10052710	5	82860025	ncRNA intronic	G	T	0.195	7.72E-111	6.11E-06	VCAN:VCAN-AS1	MD Fronto Insular tract5 Right	2.40E-13	-7.324107
102	rs10052710	5	82860025	ncRNA intronic	G	T	0.195	7.72E-111	6.11E-06	VCAN:VCAN-AS1	FA Superior Londgitudinal Fasciculus I Left	1.66E-29	11.279085
102	rs10052710	5	82860025	ncRNA intronic	G	T	0.195	7.72E-111	6.11E-06	VCAN:VCAN-AS1	L3 Frontal Aslant Tract Left	8.83E-26	-10.497878
102	rs10052710	5	82860025	ncRNA intronic	G	T	0.195	7.72E-111	6.11E-06	VCAN:VCAN-AS1	OD Corpus callosum	9.43E-18	8.580713
102	rs10052710	5	82860025	ncRNA intronic	G	T	0.195	7.72E-111	6.11E-06	VCAN:VCAN-AS1	FA Fronto Insular tract4 Right	1.13E-13	7.424574
102	rs10052710	5	82860025	ncRNA intronic	G	T	0.195	7.72E-111	6.11E-06	VCAN:VCAN-AS1	ICVF Inferior Fronto Occipital fasciculus Right	6.67E-92	20.332209
102	rs10052710	5	82860025	ncRNA intronic	G	T	0.195	7.72E-111	6.11E-06	VCAN:VCAN-AS1	L1 Arcuate Anterior Segment Left	2.49E-26	-10.616861
102	rs10052710	5	82860025	ncRNA intronic	G	T	0.195	7.72E-111	6.11E-06	VCAN:VCAN-AS1	FA Arcuate Long Segment Left	2.09E-20	9.257859
102	rs10052710	5	82860025	ncRNA intronic	G	T	0.195	7.72E-111	6.11E-06	VCAN:VCAN-AS1	MD Uncinate Right	2.10E-52	-15.233983
102	rs10052710	5	82860025	ncRNA intronic	G	T	0.195	7.72E-111	6.11E-06	VCAN:VCAN-AS1	ISOVF Uncinate Left	4.31E-10	6.242214
102	rs10052710	5	82860025	ncRNA intronic	G	T	0.195	7.72E-111	6.11E-06	VCAN:VCAN-AS1	L3 Fronto Insular tract1 Right	5.43E-12	-6.893733
102	rs10052710	5	82860025	ncRNA intronic	G	T	0.195	7.72E-111	6.11E-06	VCAN:VCAN-AS1	MD Inferior Fronto Occipital fasciculus Right	9.29E-54	-15.436575
102	rs10052710	5	82860025	ncRNA intronic	G	T	0.195	7.72E-111	6.11E-06	VCAN:VCAN-AS1	ICVF Corpus callosum	1.49E-90	20.179390
102	rs10052710	5	82860025	ncRNA intronic	G	T	0.195	7.72E-111	6.11E-06	VCAN:VCAN-AS1	L3 Superior Londgitudinal Fasciculus III Right	3.56E-28	-11.006467
102	rs10052710	5	82860025	ncRNA intronic	G	T	0.195	7.72E-111	6.11E-06	VCAN:VCAN-AS1	ISOVF Frontal Superior Longitudinal Right	4.98E-09	5.847708
102	rs10052710	5	82860025	ncRNA intronic	G	T	0.195	7.72E-111	6.11E-06	VCAN:VCAN-AS1	ICVF Arcuate Posterior Segment Right	1.05E-67	17.386177
102	rs10052710	5	82860025	ncRNA intronic	G	T	0.195	7.72E-111	6.11E-06	VCAN:VCAN-AS1	ISOVF Inferior Fronto Occipital fasciculus Right	3.11E-23	9.929254
102	rs10052710	5	82860025	ncRNA intronic	G	T	0.195	7.72E-111	6.11E-06	VCAN:VCAN-AS1	FA Frontal Inferior longitudinal Right	4.13E-14	7.556704
102	rs10052710	5	82860025	ncRNA intronic	G	T	0.195	7.72E-111	6.11E-06	VCAN:VCAN-AS1	MD Corpus callosum	3.88E-47	-14.419935
102	rs10052710	5	82860025	ncRNA intronic	G	T	0.195	7.72E-111	6.11E-06	VCAN:VCAN-AS1	MD Fronto Insular tract3 Right	6.23E-18	-8.628263
102	rs10052710	5	82860025	ncRNA intronic	G	T	0.195	7.72E-111	6.11E-06	VCAN:VCAN-AS1	ISOVF Inferior Longitudinal Left	1.95E-14	7.653767
102	rs10052710	5	82860025	ncRNA intronic	G	T	0.195	7.72E-111	6.11E-06	VCAN:VCAN-AS1	L2 Inferior Fronto Occipital fasciculus Right	1.73E-41	-13.492504
102	rs10052710	5	82860025	ncRNA intronic	G	T	0.195	7.72E-111	6.11E-06	VCAN:VCAN-AS1	L3 Fronto Insular tract4 Right	3.41E-22	-9.687356
102	rs10052710	5	82860025	ncRNA intronic	G	T	0.195	7.72E-111	6.11E-06	VCAN:VCAN-AS1	L1 Arcuate Long Segment Right	3.26E-17	-8.436820
102	rs10052710	5	82860025	ncRNA intronic	G	T	0.195	7.72E-111	6.11E-06	VCAN:VCAN-AS1	ISOVF Frontal Aslant Tract Right	1.24E-09	6.075617
102	rs10052710	5	82860025	ncRNA intronic	G	T	0.195	7.72E-111	6.11E-06	VCAN:VCAN-AS1	OD Arcuate Posterior Segment Right	2.55E-09	5.958035
102	rs10052710	5	82860025	ncRNA intronic	G	T	0.195	7.72E-111	6.11E-06	VCAN:VCAN-AS1	L3 Arcuate Posterior Segment Right	4.84E-28	-10.978763
102	rs10052710	5	82860025	ncRNA intronic	G	T	0.195	7.72E-111	6.11E-06	VCAN:VCAN-AS1	ICVF Fronto Insular tract3 Left	3.03E-46	14.277343
102	rs10052710	5	82860025	ncRNA intronic	G	T	0.195	7.72E-111	6.11E-06	VCAN:VCAN-AS1	FA Superior Londgitudinal Fasciculus III Left	3.07E-23	9.930523
102	rs10052710	5	82860025	ncRNA intronic	G	T	0.195	7.72E-111	6.11E-06	VCAN:VCAN-AS1	L2 Frontal Superior Longitudinal Left	1.14E-10	-6.447239
102	rs10052710	5	82860025	ncRNA intronic	G	T	0.195	7.72E-111	6.11E-06	VCAN:VCAN-AS1	MD Superior Londgitudinal Fasciculus III Left	1.18E-35	-12.463672
102	rs10052710	5	82860025	ncRNA intronic	G	T	0.195	7.72E-111	6.11E-06	VCAN:VCAN-AS1	ICVF Inferior Fronto Occipital fasciculus Left	6.32E-92	20.334910
102	rs10052710	5	82860025	ncRNA intronic	G	T	0.195	7.72E-111	6.11E-06	VCAN:VCAN-AS1	L1 Superior Londgitudinal Fasciculus II Left	9.86E-19	-8.836666
102	rs10052710	5	82860025	ncRNA intronic	G	T	0.195	7.72E-111	6.11E-06	VCAN:VCAN-AS1	L1 Fronto Insular tract3 Right	2.34E-14	-7.630382
102	rs10052710	5	82860025	ncRNA intronic	G	T	0.195	7.72E-111	6.11E-06	VCAN:VCAN-AS1	ICVF Frontal Aslant Tract Right	1.51E-66	17.232664
102	rs10052710	5	82860025	ncRNA intronic	G	T	0.195	7.72E-111	6.11E-06	VCAN:VCAN-AS1	L1 Inferior Fronto Occipital fasciculus Right	3.24E-31	-11.620692
102	rs10052710	5	82860025	ncRNA intronic	G	T	0.195	7.72E-111	6.11E-06	VCAN:VCAN-AS1	ICVF Frontal Superior Longitudinal Left	5.67E-47	14.393627
102	rs10052710	5	82860025	ncRNA intronic	G	T	0.195	7.72E-111	6.11E-06	VCAN:VCAN-AS1	L3 Fronto Insular tract5 Left	2.85E-09	-5.940084
102	rs10052710	5	82860025	ncRNA intronic	G	T	0.195	7.72E-111	6.11E-06	VCAN:VCAN-AS1	L1 Arcuate Posterior Segment Left	4.68E-22	-9.655101
102	rs10052710	5	82860025	ncRNA intronic	G	T	0.195	7.72E-111	6.11E-06	VCAN:VCAN-AS1	MD Fronto Insular tract2 Left	1.12E-14	-7.724849
102	rs10052710	5	82860025	ncRNA intronic	G	T	0.195	7.72E-111	6.11E-06	VCAN:VCAN-AS1	MD Arcuate Posterior Segment Right	4.19E-37	-12.726990
102	rs10052710	5	82860025	ncRNA intronic	G	T	0.195	7.72E-111	6.11E-06	VCAN:VCAN-AS1	FA Superior Londgitudinal Fasciculus II Right	1.42E-24	10.232062
102	rs10052710	5	82860025	ncRNA intronic	G	T	0.195	7.72E-111	6.11E-06	VCAN:VCAN-AS1	L2 Uncinate Right	6.87E-49	-14.695684
102	rs10052710	5	82860025	ncRNA intronic	G	T	0.195	7.72E-111	6.11E-06	VCAN:VCAN-AS1	L2 Corpus callosum	3.12E-45	-14.113869
102	rs10052710	5	82860025	ncRNA intronic	G	T	0.195	7.72E-111	6.11E-06	VCAN:VCAN-AS1	MD Fronto Insular tract5 Left	3.84E-08	-5.497972
102	rs10052710	5	82860025	ncRNA intronic	G	T	0.195	7.72E-111	6.11E-06	VCAN:VCAN-AS1	L1 Uncinate Left	2.28E-24	-10.186294
102	rs10052710	5	82860025	ncRNA intronic	G	T	0.195	7.72E-111	6.11E-06	VCAN:VCAN-AS1	L2 Superior Londgitudinal Fasciculus III Right	3.07E-31	-11.625057
102	rs10052710	5	82860025	ncRNA intronic	G	T	0.195	7.72E-111	6.11E-06	VCAN:VCAN-AS1	L3 Superior Londgitudinal Fasciculus III Left	5.75E-31	-11.571516
102	rs10052710	5	82860025	ncRNA intronic	G	T	0.195	7.72E-111	6.11E-06	VCAN:VCAN-AS1	FA Frontal Superior Longitudinal Left	2.92E-10	6.302974
102	rs10052710	5	82860025	ncRNA intronic	G	T	0.195	7.72E-111	6.11E-06	VCAN:VCAN-AS1	L1 Uncinate Right	2.91E-29	-11.229709
102	rs10052710	5	82860025	ncRNA intronic	G	T	0.195	7.72E-111	6.11E-06	VCAN:VCAN-AS1	ICVF Frontal Inferior longitudinal Left	3.49E-41	13.440660
102	rs10052710	5	82860025	ncRNA intronic	G	T	0.195	7.72E-111	6.11E-06	VCAN:VCAN-AS1	ICVF Superior Londgitudinal Fasciculus II Left	1.33E-65	17.106213
102	rs10052710	5	82860025	ncRNA intronic	G	T	0.195	7.72E-111	6.11E-06	VCAN:VCAN-AS1	L3 Inferior Fronto Occipital fasciculus Right	1.18E-54	-15.569282
102	rs10052710	5	82860025	ncRNA intronic	G	T	0.195	7.72E-111	6.11E-06	VCAN:VCAN-AS1	L2 Frontal Aslant Tract Left	4.00E-29	-11.201635
102	rs10052710	5	82860025	ncRNA intronic	G	T	0.195	7.72E-111	6.11E-06	VCAN:VCAN-AS1	ISOVF Superior Londgitudinal Fasciculus I Right	3.56E-08	5.511349
102	rs10052710	5	82860025	ncRNA intronic	G	T	0.195	7.72E-111	6.11E-06	VCAN:VCAN-AS1	L2 Fronto Insular tract5 Right	5.26E-09	-5.838574
102	rs10052710	5	82860025	ncRNA intronic	G	T	0.195	7.72E-111	6.11E-06	VCAN:VCAN-AS1	ICVF Fronto Insular tract1 Left	1.95E-13	7.352316
102	rs10052710	5	82860025	ncRNA intronic	G	T	0.195	7.72E-111	6.11E-06	VCAN:VCAN-AS1	L2 Superior Londgitudinal Fasciculus III Left	4.09E-32	-11.796055
102	rs10052710	5	82860025	ncRNA intronic	G	T	0.195	7.72E-111	6.11E-06	VCAN:VCAN-AS1	FA Arcuate Anterior Segment Left	1.68E-12	7.058530
102	rs10052710	5	82860025	ncRNA intronic	G	T	0.195	7.72E-111	6.11E-06	VCAN:VCAN-AS1	L2 Arcuate Anterior Segment Right	3.98E-21	-9.433104
102	rs10052710	5	82860025	ncRNA intronic	G	T	0.195	7.72E-111	6.11E-06	VCAN:VCAN-AS1	L1 Fronto Insular tract1 Right	2.03E-10	-6.359415
102	rs10052710	5	82860025	ncRNA intronic	G	T	0.195	7.72E-111	6.11E-06	VCAN:VCAN-AS1	L3 Inferior Fronto Occipital fasciculus Left	9.31E-56	-15.730744
102	rs10052710	5	82860025	ncRNA intronic	G	T	0.195	7.72E-111	6.11E-06	VCAN:VCAN-AS1	OD Inferior Longitudinal Left	7.83E-17	8.333814
102	rs10052710	5	82860025	ncRNA intronic	G	T	0.195	7.72E-111	6.11E-06	VCAN:VCAN-AS1	L3 Arcuate Long Segment Left	1.23E-32	-11.896969
102	rs10052710	5	82860025	ncRNA intronic	G	T	0.195	7.72E-111	6.11E-06	VCAN:VCAN-AS1	L1 Arcuate Long Segment Left	1.75E-21	-9.519097
102	rs10052710	5	82860025	ncRNA intronic	G	T	0.195	7.72E-111	6.11E-06	VCAN:VCAN-AS1	L3 Fronto Insular tract2 Left	9.92E-11	-6.468194
102	rs10052710	5	82860025	ncRNA intronic	G	T	0.195	7.72E-111	6.11E-06	VCAN:VCAN-AS1	ICVF Frontal Aslant Tract Left	1.99E-62	16.675030
102	rs10052710	5	82860025	ncRNA intronic	G	T	0.195	7.72E-111	6.11E-06	VCAN:VCAN-AS1	MD Frontal Aslant Tract Left	1.90E-28	-11.062854
102	rs10052710	5	82860025	ncRNA intronic	G	T	0.195	7.72E-111	6.11E-06	VCAN:VCAN-AS1	L1 Superior Londgitudinal Fasciculus II Right	3.61E-16	-8.151017
102	rs10052710	5	82860025	ncRNA intronic	G	T	0.195	7.72E-111	6.11E-06	VCAN:VCAN-AS1	MD Fronto Insular tract4 Right	1.52E-18	-8.788153
102	rs10052710	5	82860025	ncRNA intronic	G	T	0.195	7.72E-111	6.11E-06	VCAN:VCAN-AS1	MD Frontal Superior Longitudinal Left	3.52E-10	-6.273928
102	rs10052710	5	82860025	ncRNA intronic	G	T	0.195	7.72E-111	6.11E-06	VCAN:VCAN-AS1	L2 Fronto Insular tract3 Right	5.70E-10	-6.198460

Genomic Locus	Lead SNP	chr	Position	Functional category	Non-effect allele	Effect allele	MAF	mvgwasP (discovery -British-)	mvgwasP (replication -non British-)	Nearest gene	Central endophenotypes	univariate P value	univariate Z
102	rs10052710	5	82860025	ncRNA intronic	G	T	0.195	7.72E-111	6.11E-06	VCAN:VCAN-AS1	ICVF Superior Londgitudinal Fasciculus III Right	1.62E-66	17.228440
102	rs10052710	5	82860025	ncRNA intronic	G	T	0.195	7.72E-111	6.11E-06	VCAN:VCAN-AS1	L2 Superior Londgitudinal Fasciculus II Right	1.73E-29	-11.275508
102	rs10052710	5	82860025	ncRNA intronic	G	T	0.195	7.72E-111	6.11E-06	VCAN:VCAN-AS1	ICVF Frontal Superior Longitudinal Right	1.76E-53	15.395450
102	rs10052710	5	82860025	ncRNA intronic	G	T	0.195	7.72E-111	6.11E-06	VCAN:VCAN-AS1	OD Inferior Fronto Occipital fasciculus Left	7.85E-13	7.163734
102	rs10052710	5	82860025	ncRNA intronic	G	T	0.195	7.72E-111	6.11E-06	VCAN:VCAN-AS1	MD Arcuate Anterior Segment Left	1.00E-28	-11.119898
102	rs10052710	5	82860025	ncRNA intronic	G	T	0.195	7.72E-111	6.11E-06	VCAN:VCAN-AS1	L3 Arcuate Posterior Segment Left	1.11E-21	-9.565999
102	rs10052710	5	82860025	ncRNA intronic	G	T	0.195	7.72E-111	6.11E-06	VCAN:VCAN-AS1	ISOVF Uncinate Right	2.41E-09	5.967349
102	rs10052710	5	82860025	ncRNA intronic	G	T	0.195	7.72E-111	6.11E-06	VCAN:VCAN-AS1	MD Frontal Inferior longitudinal Left	1.15E-14	-7.721514
102	rs10052710	5	82860025	ncRNA intronic	G	T	0.195	7.72E-111	6.11E-06	VCAN:VCAN-AS1	L1 Superior Londgitudinal Fasciculus III Right	2.08E-23	-9.969208
102	rs10052710	5	82860025	ncRNA intronic	G	T	0.195	7.72E-111	6.11E-06	VCAN:VCAN-AS1	MD Superior Londgitudinal Fasciculus II Left	5.31E-33	-11.966718
102	rs10052710	5	82860025	ncRNA intronic	G	T	0.195	7.72E-111	6.11E-06	VCAN:VCAN-AS1	FA Frontal Aslant Tract Right	1.87E-20	9.269461
102	rs10052710	5	82860025	ncRNA intronic	G	T	0.195	7.72E-111	6.11E-06	VCAN:VCAN-AS1	L1 Frontal Aslant Tract Left	5.26E-18	-8.647552
102	rs10052710	5	82860025	ncRNA intronic	G	T	0.195	7.72E-111	6.11E-06	VCAN:VCAN-AS1	L2 Inferior Fronto Occipital fasciculus Left	6.45E-47	-14.384758
102	rs10052710	5	82860025	ncRNA intronic	G	T	0.195	7.72E-111	6.11E-06	VCAN:VCAN-AS1	ICVF Arcuate Posterior Segment Left	3.55E-64	16.913961
102	rs10052710	5	82860025	ncRNA intronic	G	T	0.195	7.72E-111	6.11E-06	VCAN:VCAN-AS1	L2 Uncinate Left	4.87E-50	-14.873906
102	rs10052710	5	82860025	ncRNA intronic	G	T	0.195	7.72E-111	6.11E-06	VCAN:VCAN-AS1	L2 Fronto Insular tract3 Left	5.99E-13	-7.200603
102	rs10052710	5	82860025	ncRNA intronic	G	T	0.195	7.72E-111	6.11E-06	VCAN:VCAN-AS1	FA Arcuate Long Segment Right	9.79E-21	9.338259
102	rs10052710	5	82860025	ncRNA intronic	G	T	0.195	7.72E-111	6.11E-06	VCAN:VCAN-AS1	ICVF Fronto Insular tract5 Left	2.50E-52	15.222791
102	rs10052710	5	82860025	ncRNA intronic	G	T	0.195	7.72E-111	6.11E-06	VCAN:VCAN-AS1	ICVF Arcuate Long Segment Right	2.12E-59	16.253178
102	rs10052710	5	82860025	ncRNA intronic	G	T	0.195	7.72E-111	6.11E-06	VCAN:VCAN-AS1	L3 Inferior Longitudinal Left	2.55E-54	-15.519731
102	rs10052710	5	82860025	ncRNA intronic	G	T	0.195	7.72E-111	6.11E-06	VCAN:VCAN-AS1	OD Superior Londgitudinal Fasciculus III Right	1.12E-08	5.711987
102	rs10052710	5	82860025	ncRNA intronic	G	T	0.195	7.72E-111	6.11E-06	VCAN:VCAN-AS1	MD Fronto Insular tract3 Left	5.77E-20	-9.148502
102	rs10052710	5	82860025	ncRNA intronic	G	T	0.195	7.72E-111	6.11E-06	VCAN:VCAN-AS1	L3 Corpus callosum	3.89E-43	-13.769543
102	rs10052710	5	82860025	ncRNA intronic	G	T	0.195	7.72E-111	6.11E-06	VCAN:VCAN-AS1	L3 Uncinate Left	1.35E-52	-15.263124
102	rs10052710	5	82860025	ncRNA intronic	G	T	0.195	7.72E-111	6.11E-06	VCAN:VCAN-AS1	ICVF Inferior Longitudinal Right	1.23E-95	20.749887
102	rs10052710	5	82860025	ncRNA intronic	G	T	0.195	7.72E-111	6.11E-06	VCAN:VCAN-AS1	L3 Arcuate Long Segment Right	3.69E-31	-11.609333
102	rs10052710	5	82860025	ncRNA intronic	G	T	0.195	7.72E-111	6.11E-06	VCAN:VCAN-AS1	FA Arcuate Posterior Segment Left	7.25E-15	7.780112
102	rs10052710	5	82860025	ncRNA intronic	G	T	0.195	7.72E-111	6.11E-06	VCAN:VCAN-AS1	ICVF Fronto Insular tract2 Left	6.99E-37	12.686869
102	rs10052710	5	82860025	ncRNA intronic	G	T	0.195	7.72E-111	6.11E-06	VCAN:VCAN-AS1	L2 Superior Londgitudinal Fasciculus I Right	2.15E-31	-11.655714
102	rs10052710	5	82860025	ncRNA intronic	G	T	0.195	7.72E-111	6.11E-06	VCAN:VCAN-AS1	FA Fronto Insular tract3 Right	3.71E-09	5.896633
102	rs10052710	5	82860025	ncRNA intronic	G	T	0.195	7.72E-111	6.11E-06	VCAN:VCAN-AS1	FA Corpus callosum	3.20E-38	12.926243
102	rs10052710	5	82860025	ncRNA intronic	G	T	0.195	7.72E-111	6.11E-06	VCAN:VCAN-AS1	L2 Superior Londgitudinal Fasciculus I Left	4.15E-31	-11.599427
102	rs10052710	5	82860025	ncRNA intronic	G	T	0.195	7.72E-111	6.11E-06	VCAN:VCAN-AS1	MD Frontal Inferior longitudinal Right	4.32E-19	-8.928500
102	rs10052710	5	82860025	ncRNA intronic	G	T	0.195	7.72E-111	6.11E-06	VCAN:VCAN-AS1	L1 Inferior Longitudinal Right	1.64E-33	-12.063662
102	rs10052710	5	82860025	ncRNA intronic	G	T	0.195	7.72E-111	6.11E-06	VCAN:VCAN-AS1	MD Arcuate Posterior Segment Left	7.96E-32	-11.739891
102	rs10052710	5	82860025	ncRNA intronic	G	T	0.195	7.72E-111	6.11E-06	VCAN:VCAN-AS1	L1 Frontal Inferior longitudinal Right	1.46E-09	-6.048654
102	rs10052710	5	82860025	ncRNA intronic	G	T	0.195	7.72E-111	6.11E-06	VCAN:VCAN-AS1	L1 Fronto Insular tract2 Right	2.28E-11	-6.687162
102	rs10052710	5	82860025	ncRNA intronic	G	T	0.195	7.72E-111	6.11E-06	VCAN:VCAN-AS1	ICVF Arcuate Anterior Segment Left	1.30E-68	17.505499
102	rs10052710	5	82860025	ncRNA intronic	G	T	0.195	7.72E-111	6.11E-06	VCAN:VCAN-AS1	OD Arcuate Anterior Segment Left	5.07E-09	5.844970
102	rs10052710	5	82860025	ncRNA intronic	G	T	0.195	7.72E-111	6.11E-06	VCAN:VCAN-AS1	L1 Superior Londgitudinal Fasciculus I Right	3.96E-16	-8.139924
102	rs10052710	5	82860025	ncRNA intronic	G	T	0.195	7.72E-111	6.11E-06	VCAN:VCAN-AS1	ISOVF Corpus callosum	5.18E-09	5.841244
102	rs10052710	5	82860025	ncRNA intronic	G	T	0.195	7.72E-111	6.11E-06	VCAN:VCAN-AS1	L3 Arcuate Anterior Segment Left	3.27E-19	-8.959343
102	rs10052710	5	82860025	ncRNA intronic	G	T	0.195	7.72E-111	6.11E-06	VCAN:VCAN-AS1	ICVF Superior Londgitudinal Fasciculus I Right	8.73E-88	19.861713
102	rs10052710	5	82860025	ncRNA intronic	G	T	0.195	7.72E-111	6.11E-06	VCAN:VCAN-AS1	FA Arcuate Posterior Segment Right	2.46E-15	7.915687
102	rs10052710	5	82860025	ncRNA intronic	G	T	0.195	7.72E-111	6.11E-06	VCAN:VCAN-AS1	FA Inferior Longitudinal Right	3.79E-41	13.434695
102	rs10052710	5	82860025	ncRNA intronic	G	T	0.195	7.72E-111	6.11E-06	VCAN:VCAN-AS1	OD Inferior Longitudinal Right	2.52E-14	7.620740
102	rs10052710	5	82860025	ncRNA intronic	G	T	0.195	7.72E-111	6.11E-06	VCAN:VCAN-AS1	MD Superior Londgitudinal Fasciculus I Right	2.55E-38	-12.943630
102	rs10052710	5	82860025	ncRNA intronic	G	T	0.195	7.72E-111	6.11E-06	VCAN:VCAN-AS1	FA Fronto Insular tract5 Right	1.18E-10	6.441556
102	rs10052710	5	82860025	ncRNA intronic	G	T	0.195	7.72E-111	6.11E-06	VCAN:VCAN-AS1	MD Arcuate Long Segment Right	6.07E-35	-12.332317
102	rs10052710	5	82860025	ncRNA intronic	G	T	0.195	7.72E-111	6.11E-06	VCAN:VCAN-AS1	OD Inferior Fronto Occipital fasciculus Right	1.04E-12	7.125738
102	rs10052710	5	82860025	ncRNA intronic	G	T	0.195	7.72E-111	6.11E-06	VCAN:VCAN-AS1	MD Fronto Insular tract1 Right	7.48E-13	-7.170331
102	rs10052710	5	82860025	ncRNA intronic	G	T	0.195	7.72E-111	6.11E-06	VCAN:VCAN-AS1	L3 Uncinate Right	2.50E-55	-15.667974
102	rs10052710	5	82860025	ncRNA intronic	G	T	0.195	7.72E-111	6.11E-06	VCAN:VCAN-AS1	ICVF Fronto Insular tract1 Right	2.25E-46	14.298014
102	rs10052710	5	82860025	ncRNA intronic	G	T	0.195	7.72E-111	6.11E-06	VCAN:VCAN-AS1	FA Frontal Inferior longitudinal Left	3.44E-08	5.517370
102	rs10052710	5	82860025	ncRNA intronic	G	T	0.195	7.72E-111	6.11E-06	VCAN:VCAN-AS1	L2 Arcuate Long Segment Left	4.73E-23	-9.887253
102	rs10052710	5	82860025	ncRNA intronic	G	T	0.195	7.72E-111	6.11E-06	VCAN:VCAN-AS1	ICVF Superior Londgitudinal Fasciculus I Left	1.28E-85	19.609669
102	rs10052710	5	82860025	ncRNA intronic	G	T	0.195	7.72E-111	6.11E-06	VCAN:VCAN-AS1	ISOVF Arcuate Anterior Segment Right	2.76E-08	5.555774
102	rs10052710	5	82860025	ncRNA intronic	G	T	0.195	7.72E-111	6.11E-06	VCAN:VCAN-AS1	L3 Frontal Superior Longitudinal Left	2.85E-08	-5.550447
102	rs10052710	5	82860025	ncRNA intronic	G	T	0.195	7.72E-111	6.11E-06	VCAN:VCAN-AS1	L2 Frontal Aslant Tract Right	4.98E-27	-10.765956
102	rs10052710	5	82860025	ncRNA intronic	G	T	0.195	7.72E-111	6.11E-06	VCAN:VCAN-AS1	FA Superior Londgitudinal Fasciculus I Right	2.80E-33	12.019693
102	rs10052710	5	82860025	ncRNA intronic	G	T	0.195	7.72E-111	6.11E-06	VCAN:VCAN-AS1	L2 Arcuate Long Segment Right	1.15E-25	-10.472967
102	rs10052710	5	82860025	ncRNA intronic	G	T	0.195	7.72E-111	6.11E-06	VCAN:VCAN-AS1	L2 Fronto Insular tract4 Right	6.62E-11	-6.529048
102	rs10052710	5	82860025	ncRNA intronic	G	T	0.195	7.72E-111	6.11E-06	VCAN:VCAN-AS1	FA Superior Londgitudinal Fasciculus II Left	1.32E-23	10.014218
102	rs10052710	5	82860025	ncRNA intronic	G	T	0.195	7.72E-111	6.11E-06	VCAN:VCAN-AS1	L1 Fronto Insular tract3 Left	1.02E-08	-5.727486
102	rs10052710	5	82860025	ncRNA intronic	G	T	0.195	7.72E-111	6.11E-06	VCAN:VCAN-AS1	L2 Inferior Longitudinal Right	1.51E-45	-14.164917
102	rs10052710	5	82860025	ncRNA intronic	G	T	0.195	7.72E-111	6.11E-06	VCAN:VCAN-AS1	L1 Arcuate Posterior Segment Right	1.54E-27	-10.873801
102	rs10052710	5	82860025	ncRNA intronic	G	T	0.195	7.72E-111	6.11E-06	VCAN:VCAN-AS1	L2 Arcuate Anterior Segment Left	2.60E-22	-9.715273
102	rs10052710	5	82860025	ncRNA intronic	G	T	0.195	7.72E-111	6.11E-06	VCAN:VCAN-AS1	L1 Superior Londgitudinal Fasciculus III Left	1.12E-27	-10.902361
102	rs10052710	5	82860025	ncRNA intronic	G	T	0.195	7.72E-111	6.11E-06	VCAN:VCAN-AS1	L3 Superior Londgitudinal Fasciculus II Right	5.09E-30	-11.382888
102	rs10052710	5	82860025	ncRNA intronic	G	T	0.195	7.72E-111	6.11E-06	VCAN:VCAN-AS1	L1 Frontal Aslant Tract Right	1.11E-15	-8.014571
102	rs10052710	5	82860025	ncRNA intronic	G	T	0.195	7.72E-111	6.11E-06	VCAN:VCAN-AS1	ISOVF Superior Londgitudinal Fasciculus III Right	2.04E-11	6.703276
102	rs10052710	5	82860025	ncRNA intronic	G	T	0.195	7.72E-111	6.11E-06	VCAN:VCAN-AS1	MD Fronto Insular tract2 Right	6.39E-13	-7.191925
102	rs10052710	5	82860025	ncRNA intronic	G	T	0.195	7.72E-111	6.11E-06	VCAN:VCAN-AS1	L1 Corpus callosum	4.50E-39	-13.076252
102	rs10052710	5	82860025	ncRNA intronic	G	T	0.195	7.72E-111	6.11E-06	VCAN:VCAN-AS1	MD Arcuate Long Segment Left	1.61E-36	-12.621229
102	rs10052710	5	82860025	ncRNA intronic	G	T	0.195	7.72E-111	6.11E-06	VCAN:VCAN-AS1	ICVF Uncinate Right	5.29E-94	20.568151
102	rs10052710	5	82860025	ncRNA intronic	G	T	0.195	7.72E-111	6.11E-06	VCAN:VCAN-AS1	ICVF Fronto Insular tract4 Left	8.55E-21	9.352638
102	rs10052710	5	82860025	ncRNA intronic	G	T	0.195	7.72E-111	6.11E-06	VCAN:VCAN-AS1	L3 Superior Londgitudinal Fasciculus I Right	1.34E-44	-14.010869
102	rs10052710	5	82860025	ncRNA intronic	G	T	0.195	7.72E-111	6.11E-06	VCAN:VCAN-AS1	ICVF Uncinate Left	2.47E-91	20.267982
102	rs10052710	5	82860025	ncRNA intronic	G	T	0.195	7.72E-111	6.11E-06	VCAN:VCAN-AS1	L3 Fronto Insular tract3 Right	1.23E-18	-8.811597
102	rs10052710	5	82860025	ncRNA intronic	G	T	0.195	7.72E-111	6.11E-06	VCAN:VCAN-AS1	ICVF Inferior Longitudinal Left	6.69E-100	21.216751
102	rs10052710	5	82860025	ncRNA intronic	G	T	0.195	7.72E-111	6.11E-06	VCAN:VCAN-AS1	ICVF Superior Londgitudinal Fasciculus III Left	8.01E-68	17.401705
102	rs10052710	5	82860025	ncRNA intronic	G	T	0.195	7.72E-111	6.11E-06	VCAN:VCAN-AS1	L3 Inferior Longitudinal Right	4.13E-55	-15.636162
102	rs10052710	5	82860025	ncRNA intronic	G	T	0.195	7.72E-111	6.11E-06	VCAN:VCAN-AS1	MD Uncinate Left	1.58E-49	-14.794776
102	rs10052710	5	82860025	ncRNA intronic	G	T	0.195	7.72E-111	6.11E-06	VCAN:VCAN-AS1	L2 Arcuate Posterior Segment Right	4.62E-27	-10.772937
102	rs10052710	5	82860025	ncRNA intronic	G	T	0.195	7.72E-111	6.11E-06	VCAN:VCAN-AS1	L2 Superior Londgitudinal Fasciculus II Left	8.13E-32	-11.738090
102	rs10052710	5	82860025	ncRNA intronic	G	T	0.195	7.72E-111	6.11E-06	VCAN:VCAN-AS1	ISOVF Arcuate Posterior Segment Right	4.76E-08	5.459866
102	rs10052710	5	82860025	ncRNA intronic	G	T	0.195	7.72E-111	6.11E-06	VCAN:VCAN-AS1	MD Superior Londgitudinal Fasciculus III Right	2.39E-30	-11.448662
102	rs10052710	5	82860025	ncRNA intronic	G	T	0.195	7.72E-111	6.11E-06	VCAN:VCAN-AS1	L3 Frontal Inferior longitudinal Right	1.68E-15	-7.962776
102	rs10052710	5	82860025	ncRNA intronic	G	T	0.195	7.72E-111	6.11E-06	VCAN:VCAN-AS1	L1 Fronto Insular tract5 Right	4.22E-08	-5.481237

Genomic Locus	Lead SNP	chr	Position	Functional category	Non-effect allele	Effect allele	MAF	mvgwasP (discovery -British-)	mvgwasP (replication -non British-)	Nearest gene	Central endophenotypes	univariate P value	univariate Z
102	rs10052710	5	82860025	ncRNA intronic	G	T	0.195	7.72E-111	6.11E-06	VCAN:VCAN-AS1	L3 Fronto Insular tract3 Left	8.32E-14	-7.465223
102	rs10052710	5	82860025	ncRNA intronic	G	T	0.195	7.72E-111	6.11E-06	VCAN:VCAN-AS1	MD Inferior Fronto Occipital fasciculus Left	7.15E-58	-16.036083
102	rs10052710	5	82860025	ncRNA intronic	G	T	0.195	7.72E-111	6.11E-06	VCAN:VCAN-AS1	L3 Arcuate Anterior Segment Right	9.03E-25	-10.276080
102	rs10052710	5	82860025	ncRNA intronic	G	T	0.195	7.72E-111	6.11E-06	VCAN:VCAN-AS1	L2 Arcuate Posterior Segment Left	6.89E-28	-10.946752
102	rs10052710	5	82860025	ncRNA intronic	G	T	0.195	7.72E-111	6.11E-06	VCAN:VCAN-AS1	ICVF Frontal Inferior longitudinal Right	2.96E-47	14.438477
102	rs10052710	5	82860025	ncRNA intronic	G	T	0.195	7.72E-111	6.11E-06	VCAN:VCAN-AS1	MD Superior Londgitudinal Fasciculus I Left	7.63E-36	-12.498301
102	rs10052710	5	82860025	ncRNA intronic	G	T	0.195	7.72E-111	6.11E-06	VCAN:VCAN-AS1	L1 Superior Londgitudinal Fasciculus I Left	7.89E-17	-8.332809
105	rs115136616	5	93021116	intronic	T	C	0.047	6.85E-16	1.73E-01	FAM172A	MO Inferior Fronto Occipital fasciculus Right	6.09E-10	6.188109
108	rs77729285	5	122754416	intronic	G	A	0.431	9.63E-11	2.12E-02	CEP120	OD Frontal Aslant Tract Left	4.21E-08	5.481863
109	rs4150210	5	139721913	intronic	A	T	0.259	1.79E-45	3.91E-03	HBEGF	ICVF Superior Londgitudinal Fasciculus II Right	4.29E-09	-5.872429
109	rs4150210	5	139721913	intronic	A	T	0.259	1.79E-45	3.91E-03	HBEGF	ICVF Arcuate Anterior Segment Right	1.31E-12	-7.093482
109	rs4150210	5	139721913	intronic	A	T	0.259	1.79E-45	3.91E-03	HBEGF	ICVF Arcuate Long Segment Left	1.90E-18	-8.763229
109	rs4150210	5	139721913	intronic	A	T	0.259	1.79E-45	3.91E-03	HBEGF	L3 Superior Londgitudinal Fasciculus I Left	1.08E-08	5.717267
109	rs4150210	5	139721913	intronic	A	T	0.259	1.79E-45	3.91E-03	HBEGF	ICVF Inferior Fronto Occipital fasciculus Right	1.54E-10	-6.401701
109	rs4150210	5	139721913	intronic	A	T	0.259	1.79E-45	3.91E-03	HBEGF	FA Arcuate Long Segment Left	8.72E-10	-6.131196
109	rs4150210	5	139721913	intronic	A	T	0.259	1.79E-45	3.91E-03	HBEGF	ICVF Corpus callosum	1.38E-19	-9.054096
109	rs4150210	5	139721913	intronic	A	T	0.259	1.79E-45	3.91E-03	HBEGF	ICVF Arcuate Posterior Segment Right	1.67E-15	-7.963845
109	rs4150210	5	139721913	intronic	A	T	0.259	1.79E-45	3.91E-03	HBEGF	MD Corpus callosum	1.92E-09	6.004444
109	rs4150210	5	139721913	intronic	A	T	0.259	1.79E-45	3.91E-03	HBEGF	L3 Arcuate Posterior Segment Right	2.70E-10	6.315022
109	rs4150210	5	139721913	intronic	A	T	0.259	1.79E-45	3.91E-03	HBEGF	ICVF Inferior Fronto Occipital fasciculus Left	4.05E-09	-5.882072
109	rs4150210	5	139721913	intronic	A	T	0.259	1.79E-45	3.91E-03	HBEGF	ICVF Frontal Aslant Tract Right	1.67E-08	-5.643236
109	rs4150210	5	139721913	intronic	A	T	0.259	1.79E-45	3.91E-03	HBEGF	MD Arcuate Posterior Segment Right	1.92E-09	6.004774
109	rs4150210	5	139721913	intronic	A	T	0.259	1.79E-45	3.91E-03	HBEGF	L2 Corpus callosum	8.33E-09	5.761588
109	rs4150210	5	139721913	intronic	A	T	0.259	1.79E-45	3.91E-03	HBEGF	L3 Superior Londgitudinal Fasciculus III Left	2.38E-08	5.582024
109	rs4150210	5	139721913	intronic	A	T	0.259	1.79E-45	3.91E-03	HBEGF	L3 Arcuate Long Segment Left	1.40E-12	7.084507
109	rs4150210	5	139721913	intronic	A	T	0.259	1.79E-45	3.91E-03	HBEGF	ICVF Frontal Aslant Tract Left	6.75E-09	-5.796974
109	rs4150210	5	139721913	intronic	A	T	0.259	1.79E-45	3.91E-03	HBEGF	ICVF Superior Londgitudinal Fasciculus III Right	8.18E-10	-6.141472
109	rs4150210	5	139721913	intronic	A	T	0.259	1.79E-45	3.91E-03	HBEGF	ICVF Frontal Superior Longitudinal Right	3.81E-08	-5.499387
109	rs4150210	5	139721913	intronic	A	T	0.259	1.79E-45	3.91E-03	HBEGF	ICVF Arcuate Posterior Segment Left	7.51E-15	-7.775621
109	rs4150210	5	139721913	intronic	A	T	0.259	1.79E-45	3.91E-03	HBEGF	ICVF Arcuate Long Segment Right	2.31E-16	-8.205026
109	rs4150210	5	139721913	intronic	A	T	0.259	1.79E-45	3.91E-03	HBEGF	L3 Corpus callosum	5.14E-10	6.214628
109	rs4150210	5	139721913	intronic	A	T	0.259	1.79E-45	3.91E-03	HBEGF	ICVF Inferior Longitudinal Right	8.70E-13	-7.149618
109	rs4150210	5	139721913	intronic	A	T	0.259	1.79E-45	3.91E-03	HBEGF	L3 Arcuate Long Segment Right	8.55E-11	6.490505
109	rs4150210	5	139721913	intronic	A	T	0.259	1.79E-45	3.91E-03	HBEGF	FA Corpus callosum	1.05E-08	-5.723085
109	rs4150210	5	139721913	intronic	A	T	0.259	1.79E-45	3.91E-03	HBEGF	MD Arcuate Posterior Segment Left	5.17E-09	5.841690
109	rs4150210	5	139721913	intronic	A	T	0.259	1.79E-45	3.91E-03	HBEGF	ICVF Arcuate Anterior Segment Left	2.94E-11	-6.649790
109	rs4150210	5	139721913	intronic	A	T	0.259	1.79E-45	3.91E-03	HBEGF	ICVF Superior Londgitudinal Fasciculus I Right	1.25E-10	-6.432976
109	rs4150210	5	139721913	intronic	A	T	0.259	1.79E-45	3.91E-03	HBEGF	FA Arcuate Posterior Segment Right	2.32E-08	-5.586520
109	rs4150210	5	139721913	intronic	A	T	0.259	1.79E-45	3.91E-03	HBEGF	FA Inferior Longitudinal Right	4.30E-08	-5.478195
109	rs4150210	5	139721913	intronic	A	T	0.259	1.79E-45	3.91E-03	HBEGF	MD Arcuate Long Segment Right	1.58E-09	6.035883
109	rs4150210	5	139721913	intronic	A	T	0.259	1.79E-45	3.91E-03	HBEGF	ICVF Superior Londgitudinal Fasciculus I Left	1.02E-11	-6.803649
109	rs4150210	5	139721913	intronic	A	T	0.259	1.79E-45	3.91E-03	HBEGF	MD Arcuate Long Segment Left	1.21E-10	6.438217
109	rs4150210	5	139721913	intronic	A	T	0.259	1.79E-45	3.91E-03	HBEGF	ICVF Inferior Longitudinal Left	1.23E-13	-7.413313
109	rs4150210	5	139721913	intronic	A	T	0.259	1.79E-45	3.91E-03	HBEGF	ICVF Superior Londgitudinal Fasciculus III Left	4.55E-13	-7.237987
109	rs4150210	5	139721913	intronic	A	T	0.259	1.79E-45	3.91E-03	HBEGF	L3 Inferior Longitudinal Right	2.04E-08	5.608463
109	rs4150210	5	139721913	intronic	A	T	0.259	1.79E-45	3.91E-03	HBEGF	ICVF Frontal Inferior longitudinal Right	4.43E-08	-5.472616
109	rs4150210	5	139721913	intronic	A	T	0.259	1.79E-45	3.91E-03	HBEGF	MD Superior Londgitudinal Fasciculus I Left	4.47E-08	5.471189
112	rs79318212	6	1365244	intergenic	G	A	0.106	1.45E-14	5.92E-01	RP4-668J24.2	ISOVF Frontal Aslant Tract Left	5.81E-10	-6.195533
112	rs79318212	6	1365244	intergenic	G	A	0.106	1.45E-14	5.92E-01	RP4-668J24.2	L3 Fronto Insular tract5 Right	6.77E-09	-5.796631
112	rs79318212	6	1365244	intergenic	G	A	0.106	1.45E-14	5.92E-01	RP4-668J24.2	L3 Frontal Inferior longitudinal Left	1.12E-08	-5.711693
112	rs79318212	6	1365244	intergenic	G	A	0.106	1.45E-14	5.92E-01	RP4-668J24.2	ISOVF Inferior Fronto Occipital fasciculus Left	9.14E-09	-5.746033
112	rs79318212	6	1365244	intergenic	G	A	0.106	1.45E-14	5.92E-01	RP4-668J24.2	ISOVF Superior Londgitudinal Fasciculus II Right	5.13E-12	-6.901921
112	rs79318212	6	1365244	intergenic	G	A	0.106	1.45E-14	5.92E-01	RP4-668J24.2	ISOVF Frontal Inferior longitudinal Right	3.38E-09	-5.912147
112	rs79318212	6	1365244	intergenic	G	A	0.106	1.45E-14	5.92E-01	RP4-668J24.2	ISOVF Inferior Longitudinal Right	1.12E-08	-5.712204
112	rs79318212	6	1365244	intergenic	G	A	0.106	1.45E-14	5.92E-01	RP4-668J24.2	ISOVF Superior Londgitudinal Fasciculus III Left	1.73E-13	-7.368442
112	rs79318212	6	1365244	intergenic	G	A	0.106	1.45E-14	5.92E-01	RP4-668J24.2	ISOVF Arcuate Anterior Segment Left	1.46E-09	-6.048258
112	rs79318212	6	1365244	intergenic	G	A	0.106	1.45E-14	5.92E-01	RP4-668J24.2	MD Fronto Insular tract5 Right	1.33E-11	-6.764804
112	rs79318212	6	1365244	intergenic	G	A	0.106	1.45E-14	5.92E-01	RP4-668J24.2	ISOVF Arcuate Posterior Segment Left	1.91E-09	-6.005233
112	rs79318212	6	1365244	intergenic	G	A	0.106	1.45E-14	5.92E-01	RP4-668J24.2	L3 Superior Londgitudinal Fasciculus III Right	9.49E-09	-5.739634
112	rs79318212	6	1365244	intergenic	G	A	0.106	1.45E-14	5.92E-01	RP4-668J24.2	ISOVF Inferior Longitudinal Left	2.28E-09	-5.976312
112	rs79318212	6	1365244	intergenic	G	A	0.106	1.45E-14	5.92E-01	RP4-668J24.2	ISOVF Frontal Aslant Tract Right	5.99E-09	-5.817113
112	rs79318212	6	1365244	intergenic	G	A	0.106	1.45E-14	5.92E-01	RP4-668J24.2	ISOVF Arcuate Long Segment Left	1.06E-08	-5.720895
112	rs79318212	6	1365244	intergenic	G	A	0.106	1.45E-14	5.92E-01	RP4-668J24.2	ISOVF Superior Londgitudinal Fasciculus II Left	6.80E-12	-6.861857
112	rs79318212	6	1365244	intergenic	G	A	0.106	1.45E-14	5.92E-01	RP4-668J24.2	L2 Fronto Insular tract5 Right	1.61E-10	-6.394204
112	rs79318212	6	1365244	intergenic	G	A	0.106	1.45E-14	5.92E-01	RP4-668J24.2	MD Frontal Inferior longitudinal Left	3.51E-09	-5.905781
112	rs79318212	6	1365244	intergenic	G	A	0.106	1.45E-14	5.92E-01	RP4-668J24.2	L1 Superior Londgitudinal Fasciculus III Right	3.13E-09	-5.924546
112	rs79318212	6	1365244	intergenic	G	A	0.106	1.45E-14	5.92E-01	RP4-668J24.2	ISOVF Corpus callosum	3.44E-08	-5.517474
112	rs79318212	6	1365244	intergenic	G	A	0.106	1.45E-14	5.92E-01	RP4-668J24.2	ISOVF Frontal Inferior longitudinal Left	1.15E-08	-5.706528
112	rs79318212	6	1365244	intergenic	G	A	0.106	1.45E-14	5.92E-01	RP4-668J24.2	ISOVF Arcuate Anterior Segment Right	1.38E-08	-5.676228
112	rs79318212	6	1365244	intergenic	G	A	0.106	1.45E-14	5.92E-01	RP4-668J24.2	L1 Frontal Aslant Tract Right	1.96E-08	-5.615074
112	rs79318212	6	1365244	intergenic	G	A	0.106	1.45E-14	5.92E-01	RP4-668J24.2	ISOVF Superior Londgitudinal Fasciculus III Right	4.30E-13	-7.245699
112	rs79318212	6	1365244	intergenic	G	A	0.106	1.45E-14	5.92E-01	RP4-668J24.2	ISOVF Arcuate Long Segment Right	5.58E-09	-5.828825
112	rs79318212	6	1365244	intergenic	G	A	0.106	1.45E-14	5.92E-01	RP4-668J24.2	ISOVF Arcuate Posterior Segment Right	1.80E-10	-6.377154
112	rs79318212	6	1365244	intergenic	G	A	0.106	1.45E-14	5.92E-01	RP4-668J24.2	MD Superior Londgitudinal Fasciculus III Right	2.56E-09	-5.957691
112	rs79318212	6	1365244	intergenic	G	A	0.106	1.45E-14	5.92E-01	RP4-668J24.2	L1 Fronto Insular tract5 Right	3.13E-09	-5.924638
113	rs1800562	6	26093141	exonic	A	G	0.078	1.83E-10	5.26E-02	HFE	ICVF Fronto Insular tract3 Right	2.35E-08	-5.584043
113	rs1800562	6	26093141	exonic	A	G	0.078	1.83E-10	5.26E-02	HFE	ICVF Fronto Insular tract5 Right	2.13E-10	-6.351889

Genomic Locus	Lead SNP	chr	Position	Functional category	Non-effect allele	Effect allele	MAF	mvgwasP (discovery -British-)	mvgwasP (replication -non British-)	Nearest gene	Central endophenotypes	univariate P value	univariate Z
113	rs146863150	6	26408472	intronic	CATAT	C	0.103	7.93E-22	5.93E-04	BTN3A1	ICVF Arcuate Anterior Segment Right	2.60E-08	-5.566167
113	rs146863150	6	26408472	intronic	CATAT	C	0.103	7.93E-22	5.93E-04	BTN3A1	L1 Fronto Insular tract4 Right	3.97E-13	7.256620
113	rs146863150	6	26408472	intronic	CATAT	C	0.103	7.93E-22	5.93E-04	BTN3A1	ICVF Inferior Fronto Occipital fasciculus Right	2.94E-09	-5.934977
113	rs146863150	6	26408472	intronic	CATAT	C	0.103	7.93E-22	5.93E-04	BTN3A1	MD Inferior Fronto Occipital fasciculus Right	3.93E-08	5.494021
113	rs146863150	6	26408472	intronic	CATAT	C	0.103	7.93E-22	5.93E-04	BTN3A1	ICVF Corpus callosum	3.76E-09	-5.894504
113	rs146863150	6	26408472	intronic	CATAT	C	0.103	7.93E-22	5.93E-04	BTN3A1	L1 Superior Londgitudinal Fasciculus II Left	2.21E-10	6.346283
113	rs146863150	6	26408472	intronic	CATAT	C	0.103	7.93E-22	5.93E-04	BTN3A1	L1 Fronto Insular tract3 Right	5.96E-10	6.191563
113	rs146863150	6	26408472	intronic	CATAT	C	0.103	7.93E-22	5.93E-04	BTN3A1	ICVF Frontal Aslant Tract Right	3.59E-08	-5.509742
113	rs146863150	6	26408472	intronic	CATAT	C	0.103	7.93E-22	5.93E-04	BTN3A1	L2 Corpus callosum	1.11E-08	5.713069
113	rs146863150	6	26408472	intronic	CATAT	C	0.103	7.93E-22	5.93E-04	BTN3A1	ICVF Superior Londgitudinal Fasciculus III Right	2.76E-08	-5.555774
113	rs146863150	6	26408472	intronic	CATAT	C	0.103	7.93E-22	5.93E-04	BTN3A1	ICVF Inferior Longitudinal Right	2.98E-08	-5.542630
113	rs146863150	6	26408472	intronic	CATAT	C	0.103	7.93E-22	5.93E-04	BTN3A1	L2 Superior Londgitudinal Fasciculus I Left	2.73E-08	5.557684
113	rs146863150	6	26408472	intronic	CATAT	C	0.103	7.93E-22	5.93E-04	BTN3A1	OD Fronto Insular tract4 Right	2.01E-13	-7.348413
113	rs146863150	6	26408472	intronic	CATAT	C	0.103	7.93E-22	5.93E-04	BTN3A1	MO Fronto Insular tract4 Right	1.01E-11	6.805337
113	rs146863150	6	26408472	intronic	CATAT	C	0.103	7.93E-22	5.93E-04	BTN3A1	OD Fronto Insular tract3 Right	2.07E-08	-5.605954
113	rs146863150	6	26408472	intronic	CATAT	C	0.103	7.93E-22	5.93E-04	BTN3A1	MD Inferior Fronto Occipital fasciculus Left	3.27E-08	5.526334
113	rs146863150	6	26408472	intronic	CATAT	C	0.103	7.93E-22	5.93E-04	BTN3A1	L2 Arcuate Posterior Segment Left	9.46E-09	5.740156
113	rs34196306	6	27425644	intronic	C	G	0.104	1.17E-27	1.29E-03	ZNF184	ICVF Arcuate Anterior Segment Right	7.21E-09	-5.785976
113	rs34196306	6	27425644	intronic	C	G	0.104	1.17E-27	1.29E-03	ZNF184	MD Inferior Longitudinal Right	4.20E-08	5.482432
113	rs34196306	6	27425644	intronic	C	G	0.104	1.17E-27	1.29E-03	ZNF184	MD Frontal Aslant Tract Right	3.30E-08	5.524620
113	rs34196306	6	27425644	intronic	C	G	0.104	1.17E-27	1.29E-03	ZNF184	L1 Fronto Insular tract4 Right	6.93E-14	7.489196
113	rs34196306	6	27425644	intronic	C	G	0.104	1.17E-27	1.29E-03	ZNF184	ICVF Fronto Insular tract2 Right	2.96E-08	-5.543756
113	rs34196306	6	27425644	intronic	C	G	0.104	1.17E-27	1.29E-03	ZNF184	ICVF Inferior Fronto Occipital fasciculus Right	1.26E-10	-6.431894
113	rs34196306	6	27425644	intronic	C	G	0.104	1.17E-27	1.29E-03	ZNF184	MD Inferior Fronto Occipital fasciculus Right	4.04E-09	5.882638
113	rs34196306	6	27425644	intronic	C	G	0.104	1.17E-27	1.29E-03	ZNF184	ICVF Corpus callosum	2.66E-10	-6.317386
113	rs34196306	6	27425644	intronic	C	G	0.104	1.17E-27	1.29E-03	ZNF184	L3 Superior Londgitudinal Fasciculus III Right	4.73E-08	5.461322
113	rs34196306	6	27425644	intronic	C	G	0.104	1.17E-27	1.29E-03	ZNF184	MD Corpus callosum	2.44E-08	5.577441
113	rs34196306	6	27425644	intronic	C	G	0.104	1.17E-27	1.29E-03	ZNF184	ICVF Inferior Fronto Occipital fasciculus Left	6.29E-09	-5.808930
113	rs34196306	6	27425644	intronic	C	G	0.104	1.17E-27	1.29E-03	ZNF184	L1 Superior Londgitudinal Fasciculus II Left	4.34E-12	6.925611
113	rs34196306	6	27425644	intronic	C	G	0.104	1.17E-27	1.29E-03	ZNF184	L1 Fronto Insular tract3 Right	1.28E-10	6.429275
113	rs34196306	6	27425644	intronic	C	G	0.104	1.17E-27	1.29E-03	ZNF184	ICVF Frontal Aslant Tract Right	5.54E-09	-5.830134
113	rs34196306	6	27425644	intronic	C	G	0.104	1.17E-27	1.29E-03	ZNF184	L2 Corpus callosum	1.50E-09	6.044187
113	rs34196306	6	27425644	intronic	C	G	0.104	1.17E-27	1.29E-03	ZNF184	L2 Superior Londgitudinal Fasciculus III Right	1.28E-08	5.688832
113	rs34196306	6	27425644	intronic	C	G	0.104	1.17E-27	1.29E-03	ZNF184	L3 Inferior Fronto Occipital fasciculus Right	1.00E-08	5.730438
113	rs34196306	6	27425644	intronic	C	G	0.104	1.17E-27	1.29E-03	ZNF184	ICVF Superior Londgitudinal Fasciculus III Right	7.95E-09	-5.769418
113	rs34196306	6	27425644	intronic	C	G	0.104	1.17E-27	1.29E-03	ZNF184	MD Superior Londgitudinal Fasciculus II Left	1.43E-08	5.670182
113	rs34196306	6	27425644	intronic	C	G	0.104	1.17E-27	1.29E-03	ZNF184	L3 Corpus callosum	3.16E-08	5.532312
113	rs34196306	6	27425644	intronic	C	G	0.104	1.17E-27	1.29E-03	ZNF184	ICVF Inferior Longitudinal Right	1.67E-09	-6.027422
113	rs34196306	6	27425644	intronic	C	G	0.104	1.17E-27	1.29E-03	ZNF184	L2 Superior Londgitudinal Fasciculus I Right	4.02E-08	5.489855
113	rs34196306	6	27425644	intronic	C	G	0.104	1.17E-27	1.29E-03	ZNF184	L2 Superior Londgitudinal Fasciculus I Left	3.33E-09	5.914402
113	rs34196306	6	27425644	intronic	C	G	0.104	1.17E-27	1.29E-03	ZNF184	OD Fronto Insular tract4 Right	1.34E-14	-7.701769
113	rs34196306	6	27425644	intronic	C	G	0.104	1.17E-27	1.29E-03	ZNF184	MO Fronto Insular tract4 Right	5.17E-13	7.220820
113	rs34196306	6	27425644	intronic	C	G	0.104	1.17E-27	1.29E-03	ZNF184	OD Fronto Insular tract3 Right	3.72E-08	-5.503509
113	rs34196306	6	27425644	intronic	C	G	0.104	1.17E-27	1.29E-03	ZNF184	ICVF Inferior Longitudinal Left	3.50E-08	-5.514405
113	rs34196306	6	27425644	intronic	C	G	0.104	1.17E-27	1.29E-03	ZNF184	MD Superior Londgitudinal Fasciculus III Right	2.15E-08	5.599325
113	rs34196306	6	27425644	intronic	C	G	0.104	1.17E-27	1.29E-03	ZNF184	OD Superior Londgitudinal Fasciculus II Left	4.95E-09	-5.848971
113	rs34196306	6	27425644	intronic	C	G	0.104	1.17E-27	1.29E-03	ZNF184	MD Inferior Fronto Occipital fasciculus Left	4.85E-09	5.852100
113	rs34196306	6	27425644	intronic	C	G	0.104	1.17E-27	1.29E-03	ZNF184	L3 Arcuate Anterior Segment Right	2.31E-08	5.586711
113	rs34196306	6	27425644	intronic	C	G	0.104	1.17E-27	1.29E-03	ZNF184	L2 Arcuate Posterior Segment Left	3.33E-09	5.914387
113	rs71546548	6	27493970	intergenic	TTTCTTA	T	0.010	1.41E-13	8.72E-01	HNRNPA1P1	L1 Fronto Insular tract4 Right	3.47E-12	6.957306
113	rs71546548	6	27493970	intergenic	TTTCTTA	T	0.010	1.41E-13	4.58E-03	HNRNPA1P1	L1 Fronto Insular tract4 Right	3.47E-12	6.957306
113	rs71546548	6	27493970	intergenic	TTTCTTA	T	0.010	1.41E-13	3.10E-01	HNRNPA1P1	L1 Fronto Insular tract4 Right	3.47E-12	6.957306
113	rs71546548	6	27493970	intergenic	TTTCTTA	T	0.010	1.41E-13	8.72E-01	HNRNPA1P1	L1 Superior Londgitudinal Fasciculus II Left	4.23E-08	5.480995
113	rs71546548	6	27493970	intergenic	TTTCTTA	T	0.010	1.41E-13	4.58E-03	HNRNPA1P1	L1 Superior Londgitudinal Fasciculus II Left	4.23E-08	5.480995
113	rs71546548	6	27493970	intergenic	TTTCTTA	T	0.010	1.41E-13	3.10E-01	HNRNPA1P1	L1 Superior Londgitudinal Fasciculus II Left	4.23E-08	5.480995
113	rs71546548	6	27493970	intergenic	TTTCTTA	T	0.010	1.41E-13	8.72E-01	HNRNPA1P1	L1 Fronto Insular tract3 Right	1.96E-08	5.615684
113	rs71546548	6	27493970	intergenic	TTTCTTA	T	0.010	1.41E-13	4.58E-03	HNRNPA1P1	L1 Fronto Insular tract3 Right	1.96E-08	5.615684
113	rs71546548	6	27493970	intergenic	TTTCTTA	T	0.010	1.41E-13	3.10E-01	HNRNPA1P1	L1 Fronto Insular tract3 Right	1.96E-08	5.615684
113	rs71546548	6	27493970	intergenic	TTTCTTA	T	0.010	1.41E-13	8.72E-01	HNRNPA1P1	OD Fronto Insular tract4 Right	4.03E-12	-6.936293
113	rs71546548	6	27493970	intergenic	TTTCTTA	T	0.010	1.41E-13	4.58E-03	HNRNPA1P1	OD Fronto Insular tract4 Right	4.03E-12	-6.936293
113	rs71546548	6	27493970	intergenic	TTTCTTA	T	0.010	1.41E-13	3.10E-01	HNRNPA1P1	OD Fronto Insular tract4 Right	4.03E-12	-6.936293
113	rs71546548	6	27493970	intergenic	TTTCTTA	T	0.010	1.41E-13	8.72E-01	HNRNPA1P1	MO Fronto Insular tract4 Right	1.21E-08	5.697879
113	rs71546548	6	27493970	intergenic	TTTCTTA	T	0.010	1.41E-13	4.58E-03	HNRNPA1P1	MO Fronto Insular tract4 Right	1.21E-08	5.697879
113	rs71546548	6	27493970	intergenic	TTTCTTA	T	0.010	1.41E-13	3.10E-01	HNRNPA1P1	MO Fronto Insular tract4 Right	1.21E-08	5.697879
113	rs34676049	6	28453618	intergenic	G	T	0.108	1.93E-28	4.67E-04	GPX6	MD Superior Londgitudinal Fasciculus II Right	2.04E-08	5.608634
113	rs34676049	6	28453618	intergenic	G	T	0.108	1.93E-28	4.67E-04	GPX6	L1 Inferior Longitudinal Left	3.49E-08	5.514751
113	rs34676049	6	28453618	intergenic	G	T	0.108	1.93E-28	4.67E-04	GPX6	ICVF Arcuate Anterior Segment Right	7.32E-09	-5.783392
113	rs34676049	6	28453618	intergenic	G	T	0.108	1.93E-28	4.67E-04	GPX6	MD Arcuate Anterior Segment Right	3.23E-08	5.528453
113	rs34676049	6	28453618	intergenic	G	T	0.108	1.93E-28	4.67E-04	GPX6	MD Inferior Longitudinal Right	1.22E-08	5.696687
113	rs34676049	6	28453618	intergenic	G	T	0.108	1.93E-28	4.67E-04	GPX6	L1 Inferior Fronto Occipital fasciculus Left	1.87E-08	5.624051
113	rs34676049	6	28453618	intergenic	G	T	0.108	1.93E-28	4.67E-04	GPX6	MD Frontal Aslant Tract Right	1.34E-08	5.680266
113	rs34676049	6	28453618	intergenic	G	T	0.108	1.93E-28	4.67E-04	GPX6	L1 Fronto Insular tract4 Right	2.47E-13	7.320299
113	rs34676049	6	28453618	intergenic	G	T	0.108	1.93E-28	4.67E-04	GPX6	ICVF Inferior Fronto Occipital fasciculus Right	1.17E-10	-6.443583
113	rs34676049	6	28453618	intergenic	G	T	0.108	1.93E-28	4.67E-04	GPX6	MD Inferior Fronto Occipital fasciculus Right	1.21E-09	6.078994
113	rs34676049	6	28453618	intergenic	G	T	0.108	1.93E-28	4.67E-04	GPX6	ICVF Corpus callosum	2.61E-10	-6.320328
113	rs34676049	6	28453618	intergenic	G	T	0.108	1.93E-28	4.67E-04	GPX6	L3 Superior Londgitudinal Fasciculus III Right	1.06E-08	5.721071
113	rs34676049	6	28453618	intergenic	G	T	0.108	1.93E-28	4.67E-04	GPX6	MD Corpus callosum	2.09E-08	5.604680
113	rs34676049	6	28453618	intergenic	G	T	0.108	1.93E-28	4.67E-04	GPX6	MD Superior Londgitudinal Fasciculus III Left	2.08E-08	5.604830
113	rs34676049	6	28453618	intergenic	G	T	0.108	1.93E-28	4.67E-04	GPX6	ICVF Inferior Fronto Occipital fasciculus Left	6.73E-09	-5.797605
113	rs34676049	6	28453618	intergenic	G	T	0.108	1.93E-28	4.67E-04	GPX6	L1 Superior Londgitudinal Fasciculus II Left	3.44E-13	7.276020
113	rs34676049	6	28453618	intergenic	G	T	0.108	1.93E-28	4.67E-04	GPX6	L1 Fronto Insular tract3 Right	1.07E-11	6.796639
113	rs34676049	6	28453618	intergenic	G	T	0.108	1.93E-28	4.67E-04	GPX6	ICVF Frontal Aslant Tract Right	6.57E-09	-5.801609
113	rs34676049	6	28453618	intergenic	G	T	0.108	1.93E-28	4.67E-04	GPX6	L2 Corpus callosum	1.67E-09	6.026969
113	rs34676049	6	28453618	intergenic	G	T	0.108	1.93E-28	4.67E-04	GPX6	L2 Superior Londgitudinal Fasciculus III Right	1.16E-08	5.706085
113	rs34676049	6	28453618	intergenic	G	T	0.108	1.93E-28	4.67E-04	GPX6	L3 Inferior Fronto Occipital fasciculus Right	8.08E-09	5.766854
113	rs34676049	6	28453618	intergenic	G	T	0.108	1.93E-28	4.67E-04	GPX6	ICVF Frontal Aslant Tract Left	4.05E-08	-5.488788
113	rs34676049	6	28453618	intergenic	G	T	0.108	1.93E-28	4.67E-04	GPX6	ICVF Superior Londgitudinal Fasciculus III Right	6.62E-09	-5.800200
113	rs34676049	6	28453618	intergenic	G	T	0.108	1.93E-28	4.67E-04	GPX6	MD Superior Londgitudinal Fasciculus II Left	2.50E-09	5.961392
113	rs34676049	6	28453618	intergenic	G	T	0.108	1.93E-28	4.67E-04	GPX6	L3 Corpus callosum	2.01E-08	5.565992
113	rs34676049	6	28453618	intergenic	G	T	0.108	1.93E-28	4.67E-04	GPX6	ICVF Inferior Longitudinal Right	1.16E-09	-6.085480
113	rs34676049	6	28453618	intergenic	G	T	0.108	1.93E-28	4.67E-04	GPX6	L2 Superior Londgitudinal Fasciculus I Left	6.62E-09	5.800228
113	rs34676049	6	28453618	intergenic	G	T	0.108	1.93E-28	4.67E-04	GPX6	L1 Inferior Longitudinal Right	3.33E-08	5.523263
113	rs34676049	6	28453618	intergenic	G	T	0.108	1.93E-28	4.67E-04	GPX6	MD Arcuate Posterior Segment Left	4.20E-08	5.482204
113	rs34676049	6	28453618	intergenic	G	T	0.108	1.93E-28	4.67E-04	GPX6	OD Fronto Insular tract4 Right	3.73E-15	-7.863522
113	rs34676049	6	28453618	intergenic	G	T	0.108	1.93E-28	4.67E-04	GPX6	MO Fronto Insular tract4 Right	4.03E-13	7.254686
113	rs34676049	6	28453618	intergenic	G	T	0.108	1.93E-28	4.67E-04	GPX6	OD Fronto Insular tract3 Right	1.64E-09	-6.029859
113	rs34676049	6	28453618	intergenic	G	T	0.108	1.93E-28	4.67E-04	GPX6	MD Arcuate Long Segment Left	2.67E-08	5.561818
113	rs34676049	6	28453618	intergenic	G	T	0.108	1.93E-28	4.67E-04	GPX6	ICVF Inferior Longitudinal Left	2.44E-08	-5.577399
113	rs34676049	6	28453618	intergenic	G	T	0.108	1.93E-28	4.67E-04	GPX6	L3 Inferior Longitudinal Right	4.56E-08	5.467830
113	rs34676049	6	28453618	intergenic	G	T	0.108	1.93E-28	4.67E-04	GPX6	MD Superior Londgitudinal Fasciculus III Right	5.72E-09	5.824658
113	rs34676049	6	28453618	intergenic	G	T	0.108	1.93E-28	4.67E-04	GPX6	OD Superior Londgitudinal Fasciculus II Left	7.25E-10	-6.160626
113	rs34676049	6	28453618	intergenic	G	T	0.108	1.93E-28	4.67E-04	GPX6	MD Inferior Fronto Occipital fasciculus Left	1.52E-09	6.041849
113	rs34676049	6	28453618	intergenic	G	T	0.108	1.93E-28	4.67E-04	GPX6	L3 Arcuate Anterior Segment Right	2.20E-08	5.595221
113	rs34676049	6	28453618	intergenic	G	T	0.108	1.93E-28	4.67E-04	GPX6	L2 Arcuate Posterior Segment Left	1.48E-09	6.046767
113	rs3131856	6	29607101	intergenic	C	T	0.121	4.75E-33	7.66E-04	SUMO2P1	ICVF Fronto Insular tract4 Right	1.35E-08	-5.679114
113	rs3131856	6	29607101	intergenic	C	T	0.121	4.75E-33	7.66E-04	SUMO2P1	L3 Frontal Aslant Tract Right	1.93E-08	5.618324
113	rs3131856	6	29607101	intergenic	C	T	0.121	4.75E-33	7.66E-04	SUMO2P1	MD Superior Londgitudinal Fasciculus II Right	1.51E-08	5.659956
113	rs3131856	6	29607101	intergenic	C	T	0.121	4.75E-33	7.66E-04	SUMO2P1	L1 Inferior Longitudinal Left	1.12E-08	5.710885

Genomic Locus	Lead SNP	chr	Position	Functional category	Non-effect allele	Effect allele	MAF	mvgwasP (discovery -British-)	mvgwasP (replication -non British-)	Nearest gene	Central endophenotypes	univariate P value	univariate Z
113	rs3131856	6	29607101	intergenic	C	T	0.121	4.75E-33	7.66E-04	SUMO2P1	ICVF Arcuate Anterior Segment Right	3.66E-09	-5.899024
113	rs3131856	6	29607101	intergenic	C	T	0.121	4.75E-33	7.66E-04	SUMO2P1	ICVF Fronto Insular tract3 Right	1.25E-08	-5.692288
113	rs3131856	6	29607101	intergenic	C	T	0.121	4.75E-33	7.66E-04	SUMO2P1	MD Arcuate Anterior Segment Right	1.27E-08	5.690148
113	rs3131856	6	29607101	intergenic	C	T	0.121	4.75E-33	7.66E-04	SUMO2P1	MD Inferior Longitudinal Right	9.78E-09	5.734440
113	rs3131856	6	29607101	intergenic	C	T	0.121	4.75E-33	7.66E-04	SUMO2P1	L1 Inferior Fronto Occipital fasciculus Left	9.96E-09	5.731369
113	rs3131856	6	29607101	intergenic	C	T	0.121	4.75E-33	7.66E-04	SUMO2P1	MD Frontal Aslant Tract Right	8.89E-10	6.128223
113	rs3131856	6	29607101	intergenic	C	T	0.121	4.75E-33	7.66E-04	SUMO2P1	L1 Fronto Insular tract4 Right	2.09E-13	7.342959
113	rs3131856	6	29607101	intergenic	C	T	0.121	4.75E-33	7.66E-04	SUMO2P1	ICVF Fronto Insular tract2 Right	2.26E-08	-5.590801
113	rs3131856	6	29607101	intergenic	C	T	0.121	4.75E-33	7.66E-04	SUMO2P1	ICVF Inferior Fronto Occipital fasciculus Right	1.19E-10	-6.440825
113	rs3131856	6	29607101	intergenic	C	T	0.121	4.75E-33	7.66E-04	SUMO2P1	MD Inferior Fronto Occipital fasciculus Right	1.10E-09	6.093867
113	rs3131856	6	29607101	intergenic	C	T	0.121	4.75E-33	7.66E-04	SUMO2P1	ICVF Corpus callosum	1.59E-10	-6.396698
113	rs3131856	6	29607101	intergenic	C	T	0.121	4.75E-33	7.66E-04	SUMO2P1	L3 Superior Londgitudinal Fasciculus III Right	4.26E-09	5.873738
113	rs3131856	6	29607101	intergenic	C	T	0.121	4.75E-33	7.66E-04	SUMO2P1	MD Corpus callosum	3.01E-09	5.930985
113	rs3131856	6	29607101	intergenic	C	T	0.121	4.75E-33	7.66E-04	SUMO2P1	MD Superior Londgitudinal Fasciculus III Left	1.26E-09	6.072826
113	rs3131856	6	29607101	intergenic	C	T	0.121	4.75E-33	7.66E-04	SUMO2P1	ICVF Inferior Fronto Occipital fasciculus Left	9.24E-10	-6.122008
113	rs3131856	6	29607101	intergenic	C	T	0.121	4.75E-33	7.66E-04	SUMO2P1	L1 Superior Londgitudinal Fasciculus II Left	5.25E-13	7.218646
113	rs3131856	6	29607101	intergenic	C	T	0.121	4.75E-33	7.66E-04	SUMO2P1	L1 Fronto Insular tract3 Right	1.70E-10	6.385829
113	rs3131856	6	29607101	intergenic	C	T	0.121	4.75E-33	7.66E-04	SUMO2P1	ICVF Frontal Aslant Tract Right	1.08E-09	-6.097056
113	rs3131856	6	29607101	intergenic	C	T	0.121	4.75E-33	7.66E-04	SUMO2P1	L2 Uncinate Right	2.39E-08	5.581312
113	rs3131856	6	29607101	intergenic	C	T	0.121	4.75E-33	7.66E-04	SUMO2P1	L2 Corpus callosum	1.90E-10	6.369065
113	rs3131856	6	29607101	intergenic	C	T	0.121	4.75E-33	7.66E-04	SUMO2P1	L2 Superior Londgitudinal Fasciculus III Right	2.57E-09	5.956911
113	rs3131856	6	29607101	intergenic	C	T	0.121	4.75E-33	7.66E-04	SUMO2P1	L3 Superior Londgitudinal Fasciculus III Left	2.76E-08	5.556049
113	rs3131856	6	29607101	intergenic	C	T	0.121	4.75E-33	7.66E-04	SUMO2P1	L3 Inferior Fronto Occipital fasciculus Right	3.27E-09	5.917425
113	rs3131856	6	29607101	intergenic	C	T	0.121	4.75E-33	7.66E-04	SUMO2P1	L2 Superior Londgitudinal Fasciculus III Left	1.30E-08	5.685667
113	rs3131856	6	29607101	intergenic	C	T	0.121	4.75E-33	7.66E-04	SUMO2P1	L3 Inferior Fronto Occipital fasciculus Left	2.65E-08	5.562922
113	rs3131856	6	29607101	intergenic	C	T	0.121	4.75E-33	7.66E-04	SUMO2P1	ICVF Frontal Aslant Tract Left	6.04E-09	-5.815518
113	rs3131856	6	29607101	intergenic	C	T	0.121	4.75E-33	7.66E-04	SUMO2P1	MD Frontal Aslant Tract Left	7.53E-09	5.778638
113	rs3131856	6	29607101	intergenic	C	T	0.121	4.75E-33	7.66E-04	SUMO2P1	ICVF Superior Londgitudinal Fasciculus III Right	1.91E-09	-6.005011
113	rs3131856	6	29607101	intergenic	C	T	0.121	4.75E-33	7.66E-04	SUMO2P1	MD Arcuate Anterior Segment Left	3.85E-10	6.260021
113	rs3131856	6	29607101	intergenic	C	T	0.121	4.75E-33	7.66E-04	SUMO2P1	MD Superior Londgitudinal Fasciculus II Left	7.62E-09	5.776615
113	rs3131856	6	29607101	intergenic	C	T	0.121	4.75E-33	7.66E-04	SUMO2P1	L1 Frontal Aslant Tract Left	2.27E-10	6.341587
113	rs3131856	6	29607101	intergenic	C	T	0.121	4.75E-33	7.66E-04	SUMO2P1	L2 Inferior Fronto Occipital fasciculus Left	1.93E-08	5.617859
113	rs3131856	6	29607101	intergenic	C	T	0.121	4.75E-33	7.66E-04	SUMO2P1	L3 Corpus callosum	7.74E-09	5.774076
113	rs3131856	6	29607101	intergenic	C	T	0.121	4.75E-33	7.66E-04	SUMO2P1	ICVF Inferior Longitudinal Right	2.45E-09	-5.964970
113	rs3131856	6	29607101	intergenic	C	T	0.121	4.75E-33	7.66E-04	SUMO2P1	L2 Superior Londgitudinal Fasciculus I Right	4.03E-08	5.489443
113	rs3131856	6	29607101	intergenic	C	T	0.121	4.75E-33	7.66E-04	SUMO2P1	L2 Superior Londgitudinal Fasciculus I Left	7.78E-09	5.773072
113	rs3131856	6	29607101	intergenic	C	T	0.121	4.75E-33	7.66E-04	SUMO2P1	L1 Inferior Longitudinal Right	3.66E-08	5.506381
113	rs3131856	6	29607101	intergenic	C	T	0.121	4.75E-33	7.66E-04	SUMO2P1	MD Arcuate Posterior Segment Left	6.51E-09	5.803170
113	rs3131856	6	29607101	intergenic	C	T	0.121	4.75E-33	7.66E-04	SUMO2P1	OD Fronto Insular tract4 Right	2.36E-13	-7.326691
113	rs3131856	6	29607101	intergenic	C	T	0.121	4.75E-33	7.66E-04	SUMO2P1	L3 Arcuate Anterior Segment Left	2.24E-08	5.592437
113	rs3131856	6	29607101	intergenic	C	T	0.121	4.75E-33	7.66E-04	SUMO2P1	MO Fronto Insular tract4 Right	1.36E-12	7.087693
113	rs3131856	6	29607101	intergenic	C	T	0.121	4.75E-33	7.66E-04	SUMO2P1	L1 Frontal Aslant Tract Right	2.41E-10	6.332573
113	rs3131856	6	29607101	intergenic	C	T	0.121	4.75E-33	7.66E-04	SUMO2P1	MD Arcuate Long Segment Left	3.25E-09	5.918553
113	rs3131856	6	29607101	intergenic	C	T	0.121	4.75E-33	7.66E-04	SUMO2P1	ICVF Inferior Longitudinal Left	2.02E-08	-5.609984
113	rs3131856	6	29607101	intergenic	C	T	0.121	4.75E-33	7.66E-04	SUMO2P1	ICVF Superior Londgitudinal Fasciculus III Left	4.44E-08	-5.472580
113	rs3131856	6	29607101	intergenic	C	T	0.121	4.75E-33	7.66E-04	SUMO2P1	L3 Inferior Longitudinal Right	2.75E-08	5.556880
113	rs3131856	6	29607101	intergenic	C	T	0.121	4.75E-33	7.66E-04	SUMO2P1	MD Superior Londgitudinal Fasciculus III Right	1.37E-09	6.058673
113	rs3131856	6	29607101	intergenic	C	T	0.121	4.75E-33	7.66E-04	SUMO2P1	OD Superior Londgitudinal Fasciculus II Left	3.88E-11	-6.608602
113	rs3131856	6	29607101	intergenic	C	T	0.121	4.75E-33	7.66E-04	SUMO2P1	MD Inferior Fronto Occipital fasciculus Left	4.18E-10	6.247118
113	rs3131856	6	29607101	intergenic	C	T	0.121	4.75E-33	7.66E-04	SUMO2P1	L3 Arcuate Anterior Segment Right	4.67E-09	5.858363
113	rs3131856	6	29607101	intergenic	C	T	0.121	4.75E-33	7.66E-04	SUMO2P1	L2 Arcuate Posterior Segment Left	1.75E-10	6.381562
114	rs9380899	6	39794806	intronic	G	C	0.271	8.76E-12	5.17E-01	DAAM2	ISOVF Superior Londgitudinal Fasciculus II Right	3.30E-09	-5.915786
114	rs9380899	6	39794806	intronic	G	C	0.271	8.76E-12	5.17E-01	DAAM2	ISOVF Inferior Longitudinal Right	2.06E-10	-6.356746
114	rs9380899	6	39794806	intronic	G	C	0.271	8.76E-12	5.17E-01	DAAM2	L1 Fronto Insular tract1 Left	1.88E-08	-5.622600
114	rs9380899	6	39794806	intronic	G	C	0.271	8.76E-12	5.17E-01	DAAM2	MD Fronto Insular tract1 Left	1.33E-09	-6.063797
114	rs9380899	6	39794806	intronic	G	C	0.271	8.76E-12	5.17E-01	DAAM2	ISOVF Inferior Fronto Occipital fasciculus Right	8.79E-09	-5.752652
114	rs9380899	6	39794806	intronic	G	C	0.271	8.76E-12	5.17E-01	DAAM2	ISOVF Inferior Longitudinal Left	8.48E-10	-6.135636
114	rs9380899	6	39794806	intronic	G	C	0.271	8.76E-12	5.17E-01	DAAM2	ISOVF Superior Londgitudinal Fasciculus II Left	5.77E-11	-6.549600
114	rs9380899	6	39794806	intronic	G	C	0.271	8.76E-12	5.17E-01	DAAM2	ISOVF Superior Londgitudinal Fasciculus I Left	1.40E-08	-5.673401
114	rs9380899	6	39794806	intronic	G	C	0.271	8.76E-12	5.17E-01	DAAM2	ISOVF Superior Londgitudinal Fasciculus I Right	3.28E-09	-5.917070
114	rs9380899	6	39794806	intronic	G	C	0.271	8.76E-12	5.17E-01	DAAM2	ICVF Fronto Insular tract1 Left	2.32E-08	5.585966
114	rs9380899	6	39794806	intronic	G	C	0.271	8.76E-12	5.17E-01	DAAM2	L2 Fronto Insular tract1 Left	4.99E-10	-6.219405
114	rs9380899	6	39794806	intronic	G	C	0.271	8.76E-12	5.17E-01	DAAM2	ISOVF Corpus callosum	4.90E-09	-5.850381
114	rs9380899	6	39794806	intronic	G	C	0.271	8.76E-12	5.17E-01	DAAM2	MD Uncinate Left	2.94E-08	-5.545184
117	rs3799711	6	126075313	intronic	C	T	0.480	2.29E-27	3.15E-01	HEY2	MO Frontal Aslant Tract Right	4.12E-08	5.485424
118	rs1120786	6	126808637	intergenic	G	T	0.450	2.50E-22	4.85E-01	MIR588	MO Superior Londgitudinal Fasciculus III Left	9.03E-09	-5.748096
118	rs1120786	6	126808637	intergenic	G	T	0.450	2.50E-22	4.85E-01	MIR588	MO Frontal Aslant Tract Left	2.38E-10	-6.334651
119	rs12192990	6	151021978	intronic	G	C	0.412	5.37E-34	3.98E-01	PLEKHG1	ISOVF Superior Londgitudinal Fasciculus II Left	9.91E-10	-6.110826
122	rs798487	7	2802943	intronic	A	G	0.298	4.19E-17	1.46E-01	AMZ1:GNA12	MO Corpus callosum	8.32E-10	6.138724
122	rs798487	7	2802943	intronic	A	G	0.298	4.19E-17	1.46E-01	AMZ1:GNA12	ISOVF Superior Londgitudinal Fasciculus III Left	1.18E-13	7.419111
122	rs798487	7	2802943	intronic	A	G	0.298	4.19E-17	1.46E-01	AMZ1:GNA12	ISOVF Arcuate Anterior Segment Left	1.94E-09	6.002895
122	rs798487	7	2802943	intronic	A	G	0.298	4.19E-17	1.46E-01	AMZ1:GNA12	L1 Frontal Superior Longitudinal Left	8.69E-10	6.131798
122	rs798487	7	2802943	intronic	A	G	0.298	4.19E-17	1.46E-01	AMZ1:GNA12	MO Arcuate Long Segment Left	5.39E-10	-6.207380
122	rs798487	7	2802943	intronic	A	G	0.298	4.19E-17	1.46E-01	AMZ1:GNA12	ISOVF Arcuate Anterior Segment Right	8.09E-10	6.143071
122	rs798487	7	2802943	intronic	A	G	0.298	4.19E-17	1.46E-01	AMZ1:GNA12	ISOVF Superior Londgitudinal Fasciculus III Right	2.16E-10	6.349821
122	rs798487	7	2802943	intronic	A	G	0.298	4.19E-17	1.46E-01	AMZ1:GNA12	ISOVF Arcuate Posterior Segment Right	3.31E-10	6.283404
123	rs67248060	7	18899163	intronic	T	C	0.366	1.33E-22	4.78E-01	HDAC9	MD Inferior Longitudinal Left	4.49E-11	6.586911
123	rs67248060	7	18899163	intronic	T	C	0.366	1.33E-22	4.78E-01	HDAC9	L1 Inferior Longitudinal Left	2.94E-09	5.934912
123	rs67248060	7	18899163	intronic	T	C	0.366	1.33E-22	4.78E-01	HDAC9	L2 Inferior Longitudinal Left	4.56E-10	6.233689
123	rs67248060	7	18899163	intronic	T	C	0.366	1.33E-22	4.78E-01	HDAC9	MD Inferior Longitudinal Right	3.21E-10	6.288206
123	rs67248060	7	18899163	intronic	T	C	0.366	1.33E-22	4.78E-01	HDAC9	ISOVF Superior Londgitudinal Fasciculus III Left	4.41E-09	5.868137
123	rs67248060	7	18899163	intronic	T	C	0.366	1.33E-22	4.78E-01	HDAC9	MD Superior Londgitudinal Fasciculus III Left	7.78E-09	5.773181
123	rs67248060	7	18899163	intronic	T	C	0.366	1.33E-22	4.78E-01	HDAC9	L3 Arcuate Long Segment Left	1.62E-08	5.648053
123	rs67248060	7	18899163	intronic	T	C	0.366	1.33E-22	4.78E-01	HDAC9	L1 Frontal Aslant Tract Left	3.04E-08	5.539132
123	rs67248060	7	18899163	intronic	T	C	0.366	1.33E-22	4.78E-01	HDAC9	L3 Inferior Longitudinal Left	7.83E-09	5.772115
123	rs67248060	7	18899163	intronic	T	C	0.366	1.33E-22	4.78E-01	HDAC9	L3 Arcuate Long Segment Right	2.47E-09	5.963298
123	rs67248060	7	18899163	intronic	T	C	0.366	1.33E-22	4.78E-01	HDAC9	MD Arcuate Long Segment Right	2.53E-09	5.959328
123	rs67248060	7	18899163	intronic	T	C	0.366	1.33E-22	4.78E-01	HDAC9	L2 Inferior Longitudinal Right	5.53E-11	6.556022
123	rs67248060	7	18899163	intronic	T	C	0.366	1.33E-22	4.78E-01	HDAC9	L1 Superior Londgitudinal Fasciculus III Left	1.91E-08	5.620210
123	rs67248060	7	18899163	intronic	T	C	0.366	1.33E-22	4.78E-01	HDAC9	MD Arcuate Long Segment Left	2.21E-08	5.594746
123	rs67248060	7	18899163	intronic	T	C	0.366	1.33E-22	4.78E-01	HDAC9	L3 Inferior Longitudinal Right	3.01E-09	5.931266
126	rs17686617	7	29346518	intronic	T	C	0.313	1.36E-09	1.94E-01	CHN2	OD Fronto Insular tract1 Right	7.41E-11	-6.512116
126	rs17686617	7	29346518	intronic	T	C	0.313	1.36E-09	1.94E-01	CHN2	FA Fronto Insular tract1 Right	3.46E-14	7.579913
128	rs74504435	7	54949256	intergenic	G	A	0.094	5.65E-41	1.26E-01	SNORA73	L3 Superior Londgitudinal Fasciculus II Left	3.80E-08	-5.500030
128	rs74504435	7	54949256	intergenic	G	A	0.094	5.65E-41	1.26E-01	SNORA73	L1 Arcuate Anterior Segment Right	1.36E-09	-6.059934
128	rs74504435	7	54949256	intergenic	G	A	0.094	5.65E-41	1.26E-01	SNORA73	MD Superior Londgitudinal Fasciculus II Right	9.13E-09	-5.746166
128	rs74504435	7	54949256	intergenic	G	A	0.094	5.65E-41	1.26E-01	SNORA73	ICVF Superior Londgitudinal Fasciculus II Right	1.71E-18	8.774712
128	rs74504435	7	54949256	intergenic	G	A	0.094	5.65E-41	1.26E-01	SNORA73	ICVF Arcuate Anterior Segment Right	4.46E-21	9.421088

Genomic Locus	Lead SNP	chr	Position	Functional category	Non-effect allele	Effect allele	MAF	mvgwasP (discovery -British-)	mvgwasP (replication -non British-)	Nearest gene	Central endophenotypes	univariate P value	univariate Z
128	rs74504435	7	54949256	intergenic	G	A	0.094	5.65E-41	1.26E-01	SNORA73	MD Arcuate Anterior Segment Right	9.19E-09	-5.744974
128	rs74504435	7	54949256	intergenic	G	A	0.094	5.65E-41	1.26E-01	SNORA73	L1 Inferior Fronto Occipital fasciculus Left	4.84E-09	-5.852606
128	rs74504435	7	54949256	intergenic	G	A	0.094	5.65E-41	1.26E-01	SNORA73	ICVF Arcuate Long Segment Left	4.60E-23	9.889944
128	rs74504435	7	54949256	intergenic	G	A	0.094	5.65E-41	1.26E-01	SNORA73	L3 Superior Londgitudinal Fasciculus I Left	1.37E-10	-6.418751
128	rs74504435	7	54949256	intergenic	G	A	0.094	5.65E-41	1.26E-01	SNORA73	ICVF Fronto Insular tract5 Right	3.68E-09	5.897804
128	rs74504435	7	54949256	intergenic	G	A	0.094	5.65E-41	1.26E-01	SNORA73	ICVF Inferior Fronto Occipital fasciculus Right	2.85E-11	6.653920
128	rs74504435	7	54949256	intergenic	G	A	0.094	5.65E-41	1.26E-01	SNORA73	L1 Arcuate Anterior Segment Left	3.56E-09	-5.903230
128	rs74504435	7	54949256	intergenic	G	A	0.094	5.65E-41	1.26E-01	SNORA73	ICVF Corpus callosum	2.30E-20	9.247327
128	rs74504435	7	54949256	intergenic	G	A	0.094	5.65E-41	1.26E-01	SNORA73	ICVF Arcuate Posterior Segment Right	3.15E-21	9.457741
128	rs74504435	7	54949256	intergenic	G	A	0.094	5.65E-41	1.26E-01	SNORA73	MD Corpus callosum	2.11E-08	-5.603133
128	rs74504435	7	54949256	intergenic	G	A	0.094	5.65E-41	1.26E-01	SNORA73	OD Superior Londgitudinal Fasciculus III Left	9.10E-09	5.746649
128	rs74504435	7	54949256	intergenic	G	A	0.094	5.65E-41	1.26E-01	SNORA73	L1 Arcuate Long Segment Right	8.17E-09	-5.764897
128	rs74504435	7	54949256	intergenic	G	A	0.094	5.65E-41	1.26E-01	SNORA73	L3 Arcuate Posterior Segment Right	1.85E-09	-6.010487
128	rs74504435	7	54949256	intergenic	G	A	0.094	5.65E-41	1.26E-01	SNORA73	ICVF Fronto Insular tract3 Left	8.69E-16	8.044037
128	rs74504435	7	54949256	intergenic	G	A	0.094	5.65E-41	1.26E-01	SNORA73	MD Superior Londgitudinal Fasciculus III Left	1.94E-08	-5.616898
128	rs74504435	7	54949256	intergenic	G	A	0.094	5.65E-41	1.26E-01	SNORA73	ICVF Inferior Fronto Occipital fasciculus Left	3.21E-09	5.920425
128	rs74504435	7	54949256	intergenic	G	A	0.094	5.65E-41	1.26E-01	SNORA73	ICVF Frontal Aslant Tract Right	1.46E-14	7.690597
128	rs74504435	7	54949256	intergenic	G	A	0.094	5.65E-41	1.26E-01	SNORA73	L1 Inferior Fronto Occipital fasciculus Right	3.93E-10	-6.256966
128	rs74504435	7	54949256	intergenic	G	A	0.094	5.65E-41	1.26E-01	SNORA73	ICVF Frontal Superior Longitudinal Left	9.51E-13	7.137372
128	rs74504435	7	54949256	intergenic	G	A	0.094	5.65E-41	1.26E-01	SNORA73	L1 Arcuate Posterior Segment Left	2.91E-11	-6.651234
128	rs74504435	7	54949256	intergenic	G	A	0.094	5.65E-41	1.26E-01	SNORA73	MD Arcuate Posterior Segment Right	1.53E-12	-7.071857
128	rs74504435	7	54949256	intergenic	G	A	0.094	5.65E-41	1.26E-01	SNORA73	ICVF Superior Londgitudinal Fasciculus II Left	7.31E-17	8.341923
128	rs74504435	7	54949256	intergenic	G	A	0.094	5.65E-41	1.26E-01	SNORA73	L3 Arcuate Long Segment Left	3.26E-11	-6.634489
128	rs74504435	7	54949256	intergenic	G	A	0.094	5.65E-41	1.26E-01	SNORA73	L1 Arcuate Long Segment Left	1.41E-08	-5.672214
128	rs74504435	7	54949256	intergenic	G	A	0.094	5.65E-41	1.26E-01	SNORA73	ICVF Frontal Aslant Tract Left	9.18E-14	7.452236
128	rs74504435	7	54949256	intergenic	G	A	0.094	5.65E-41	1.26E-01	SNORA73	ICVF Superior Londgitudinal Fasciculus III Right	3.23E-15	7.881730
128	rs74504435	7	54949256	intergenic	G	A	0.094	5.65E-41	1.26E-01	SNORA73	ICVF Frontal Superior Longitudinal Right	5.68E-16	8.096022
128	rs74504435	7	54949256	intergenic	G	A	0.094	5.65E-41	1.26E-01	SNORA73	OD Inferior Fronto Occipital fasciculus Left	4.68E-09	5.858164
128	rs74504435	7	54949256	intergenic	G	A	0.094	5.65E-41	1.26E-01	SNORA73	MD Arcuate Anterior Segment Left	1.98E-08	-5.613436
128	rs74504435	7	54949256	intergenic	G	A	0.094	5.65E-41	1.26E-01	SNORA73	L3 Arcuate Posterior Segment Left	4.54E-08	-5.468626
128	rs74504435	7	54949256	intergenic	G	A	0.094	5.65E-41	1.26E-01	SNORA73	MD Superior Londgitudinal Fasciculus II Left	2.62E-08	-5.565105
128	rs74504435	7	54949256	intergenic	G	A	0.094	5.65E-41	1.26E-01	SNORA73	ICVF Arcuate Posterior Segment Left	1.32E-21	9.547923
128	rs74504435	7	54949256	intergenic	G	A	0.094	5.65E-41	1.26E-01	SNORA73	ICVF Fronto Insular tract5 Left	7.29E-09	5.784136
128	rs74504435	7	54949256	intergenic	G	A	0.094	5.65E-41	1.26E-01	SNORA73	ICVF Arcuate Long Segment Right	1.51E-21	9.534019
128	rs74504435	7	54949256	intergenic	G	A	0.094	5.65E-41	1.26E-01	SNORA73	OD Superior Londgitudinal Fasciculus III Right	9.70E-09	5.735882
128	rs74504435	7	54949256	intergenic	G	A	0.094	5.65E-41	1.26E-01	SNORA73	ICVF Inferior Longitudinal Right	6.78E-14	7.492059
128	rs74504435	7	54949256	intergenic	G	A	0.094	5.65E-41	1.26E-01	SNORA73	L3 Arcuate Long Segment Right	4.39E-12	-6.924090
128	rs74504435	7	54949256	intergenic	G	A	0.094	5.65E-41	1.26E-01	SNORA73	L1 Inferior Longitudinal Right	1.43E-08	-5.669635
128	rs74504435	7	54949256	intergenic	G	A	0.094	5.65E-41	1.26E-01	SNORA73	MD Arcuate Posterior Segment Left	2.60E-12	-6.997674
128	rs74504435	7	54949256	intergenic	G	A	0.094	5.65E-41	1.26E-01	SNORA73	ICVF Arcuate Anterior Segment Left	1.30E-22	9.785637
128	rs74504435	7	54949256	intergenic	G	A	0.094	5.65E-41	1.26E-01	SNORA73	ICVF Superior Londgitudinal Fasciculus I Right	2.48E-19	8.989747
128	rs74504435	7	54949256	intergenic	G	A	0.094	5.65E-41	1.26E-01	SNORA73	OD Inferior Longitudinal Right	3.43E-08	5.517864
128	rs74504435	7	54949256	intergenic	G	A	0.094	5.65E-41	1.26E-01	SNORA73	MD Superior Londgitudinal Fasciculus I Right	3.64E-08	-5.507713
128	rs74504435	7	54949256	intergenic	G	A	0.094	5.65E-41	1.26E-01	SNORA73	MD Arcuate Long Segment Right	5.24E-13	-7.218870
128	rs74504435	7	54949256	intergenic	G	A	0.094	5.65E-41	1.26E-01	SNORA73	OD Inferior Fronto Occipital fasciculus Right	4.55E-09	5.862860
128	rs74504435	7	54949256	intergenic	G	A	0.094	5.65E-41	1.26E-01	SNORA73	ICVF Superior Londgitudinal Fasciculus I Left	3.54E-19	8.950493
128	rs74504435	7	54949256	intergenic	G	A	0.094	5.65E-41	1.26E-01	SNORA73	L1 Arcuate Posterior Segment Right	6.63E-11	-6.528706
128	rs74504435	7	54949256	intergenic	G	A	0.094	5.65E-41	1.26E-01	SNORA73	L1 Superior Londgitudinal Fasciculus III Left	4.09E-11	-6.600720
128	rs74504435	7	54949256	intergenic	G	A	0.094	5.65E-41	1.26E-01	SNORA73	L3 Superior Londgitudinal Fasciculus II Right	6.96E-09	-5.791797
128	rs74504435	7	54949256	intergenic	G	A	0.094	5.65E-41	1.26E-01	SNORA73	L1 Corpus callosum	1.01E-08	-5.728680
128	rs74504435	7	54949256	intergenic	G	A	0.094	5.65E-41	1.26E-01	SNORA73	MD Arcuate Long Segment Left	2.59E-12	-6.998517
128	rs74504435	7	54949256	intergenic	G	A	0.094	5.65E-41	1.26E-01	SNORA73	ICVF Uncinate Right	1.50E-10	6.404902
128	rs74504435	7	54949256	intergenic	G	A	0.094	5.65E-41	1.26E-01	SNORA73	ICVF Fronto Insular tract4 Left	5.70E-09	5.825317
128	rs74504435	7	54949256	intergenic	G	A	0.094	5.65E-41	1.26E-01	SNORA73	L3 Superior Londgitudinal Fasciculus I Right	1.05E-10	-6.459763
128	rs74504435	7	54949256	intergenic	G	A	0.094	5.65E-41	1.26E-01	SNORA73	ICVF Uncinate Left	2.48E-08	5.574950
128	rs74504435	7	54949256	intergenic	G	A	0.094	5.65E-41	1.26E-01	SNORA73	ICVF Inferior Longitudinal Left	6.00E-12	6.879745
128	rs74504435	7	54949256	intergenic	G	A	0.094	5.65E-41	1.26E-01	SNORA73	ICVF Superior Londgitudinal Fasciculus III Left	6.91E-19	8.876381
128	rs74504435	7	54949256	intergenic	G	A	0.094	5.65E-41	1.26E-01	SNORA73	L2 Arcuate Posterior Segment Right	6.12E-09	-5.813545
128	rs74504435	7	54949256	intergenic	G	A	0.094	5.65E-41	1.26E-01	SNORA73	L3 Arcuate Anterior Segment Right	2.57E-09	-5.957055
128	rs74504435	7	54949256	intergenic	G	A	0.094	5.65E-41	1.26E-01	SNORA73	L2 Arcuate Posterior Segment Left	6.68E-10	-6.173398
128	rs74504435	7	54949256	intergenic	G	A	0.094	5.65E-41	1.26E-01	SNORA73	ICVF Frontal Inferior longitudinal Right	9.06E-11	6.481797
128	rs74504435	7	54949256	intergenic	G	A	0.094	5.65E-41	1.26E-01	SNORA73	MD Superior Londgitudinal Fasciculus I Left	2.17E-09	-5.984436
128	rs10244020	7	55108994	intronic	C	T	0.472	1.02E-10	1.83E-01	EGFR	ICVF Arcuate Anterior Segment Right	3.13E-10	-6.292061
128	rs10244020	7	55108994	intronic	C	T	0.472	1.02E-10	1.83E-01	EGFR	ICVF Arcuate Long Segment Left	2.10E-10	-6.354154
128	rs10244020	7	55108994	intronic	C	T	0.472	1.02E-10	1.83E-01	EGFR	ICVF Corpus callosum	3.66E-09	-5.898645
128	rs10244020	7	55108994	intronic	C	T	0.472	1.02E-10	1.83E-01	EGFR	ICVF Arcuate Posterior Segment Right	9.84E-09	-5.733533
128	rs10244020	7	55108994	intronic	C	T	0.472	1.02E-10	1.83E-01	EGFR	ICVF Fronto Insular tract3 Left	1.36E-09	-6.060690
128	rs10244020	7	55108994	intronic	C	T	0.472	1.02E-10	1.83E-01	EGFR	ICVF Frontal Superior Longitudinal Right	1.16E-08	-5.706071
128	rs10244020	7	55108994	intronic	C	T	0.472	1.02E-10	1.83E-01	EGFR	ICVF Arcuate Posterior Segment Left	2.76E-09	-5.945157
128	rs10244020	7	55108994	intronic	C	T	0.472	1.02E-10	1.83E-01	EGFR	ICVF Arcuate Long Segment Right	3.25E-09	-5.918395
128	rs10244020	7	55108994	intronic	C	T	0.472	1.02E-10	1.83E-01	EGFR	ICVF Arcuate Anterior Segment Left	6.14E-11	-6.540215
128	rs10244020	7	55108994	intronic	C	T	0.472	1.02E-10	1.83E-01	EGFR	ICVF Superior Londgitudinal Fasciculus I Right	8.41E-09	-5.760040
128	rs10244020	7	55108994	intronic	C	T	0.472	1.02E-10	1.83E-01	EGFR	ICVF Superior Londgitudinal Fasciculus I Left	1.26E-09	-6.071950
128	rs10244020	7	55108994	intronic	C	T	0.472	1.02E-10	1.83E-01	EGFR	L1 Superior Londgitudinal Fasciculus III Left	2.33E-08	5.585584
128	rs10244020	7	55108994	intronic	C	T	0.472	1.02E-10	1.83E-01	EGFR	ICVF Uncinate Right	8.73E-10	-6.131089
128	rs10244020	7	55108994	intronic	C	T	0.472	1.02E-10	1.83E-01	EGFR	ICVF Uncinate Left	4.85E-08	-5.456876
128	rs10244020	7	55108994	intronic	C	T	0.472	1.02E-10	1.83E-01	EGFR	ICVF Inferior Longitudinal Left	1.45E-08	-5.667219
128	rs10244020	7	55108994	intronic	C	T	0.472	1.02E-10	1.83E-01	EGFR	ICVF Superior Londgitudinal Fasciculus III Left	2.06E-09	-5.993196
129	rs10252734	7	81418596	intergenic	G	T	0.400	5.23E-12	2.30E-01	HGF	MO Uncinate Left	8.14E-09	5.765552

Genomic Locus	Lead SNP	chr	Position	Functional category	Non-effect allele	Effect allele	MAF	mvgwasP (discovery -British-)	mvgwasP (replication -non British-)	Nearest gene	Central endophenotypes	univariate P value	univariate Z
131	rs6967285	7	96200086	NaN	C	T	0.308	6.42E-37	3.87E-02	SHFM1	L1 Frontal Inferior longitudinal Left	5.16E-09	5.841953
131	rs6967285	7	96200086	NaN	C	T	0.308	6.42E-37	3.87E-02	SHFM1	MO Frontal Inferior longitudinal Left	9.64E-16	8.031332
137	rs6973339	7	134388544	intergenic	T	G	0.358	2.90E-10	3.26E-01	AC009276.4	L3 Fronto Insular tract2 Right	2.95E-09	-5.934413
137	rs6973339	7	134388544	intergenic	T	G	0.358	2.90E-10	3.26E-01	AC009276.4	L1 Fronto Insular tract1 Left	2.83E-09	-5.941052
137	rs6973339	7	134388544	intergenic	T	G	0.358	2.90E-10	3.26E-01	AC009276.4	MD Fronto Insular tract1 Left	6.62E-11	-6.528975
137	rs6973339	7	134388544	intergenic	T	G	0.358	2.90E-10	3.26E-01	AC009276.4	L2 Fronto Insular tract1 Left	6.43E-10	-6.179634
137	rs6973339	7	134388544	intergenic	T	G	0.358	2.90E-10	3.26E-01	AC009276.4	L3 Fronto Insular tract1 Left	3.31E-11	-6.632168
137	rs6973339	7	134388544	intergenic	T	G	0.358	2.90E-10	3.26E-01	AC009276.4	ISOVF Superior Londgitudinal Fasciculus III Right	1.60E-10	-6.395215
137	rs6973339	7	134388544	intergenic	T	G	0.358	2.90E-10	3.26E-01	AC009276.4	MD Fronto Insular tract2 Right	9.34E-10	-6.120214
139	rs4725995	7	150819169	intronic	T	C	0.305	3.86E-19	3.41E-01	AGAP3	OD Superior Londgitudinal Fasciculus II Right	3.48E-09	5.907303
139	rs4725995	7	150819169	intronic	T	C	0.305	3.86E-19	3.41E-01	AGAP3	FA Arcuate Anterior Segment Right	1.25E-11	-6.773807
139	rs4725995	7	150819169	intronic	T	C	0.305	3.86E-19	3.41E-01	AGAP3	OD Corpus callosum	1.52E-08	5.659817
139	rs4725995	7	150819169	intronic	T	C	0.305	3.86E-19	3.41E-01	AGAP3	FA Arcuate Long Segment Left	8.33E-12	-6.832737
139	rs4725995	7	150819169	intronic	T	C	0.305	3.86E-19	3.41E-01	AGAP3	OD Arcuate Long Segment Left	2.58E-13	7.314647
139	rs4725995	7	150819169	intronic	T	C	0.305	3.86E-19	3.41E-01	AGAP3	FA Arcuate Long Segment Right	3.73E-08	-5.502952
139	rs4725995	7	150819169	intronic	T	C	0.305	3.86E-19	3.41E-01	AGAP3	OD Superior Londgitudinal Fasciculus III Right	1.38E-12	7.086284
139	rs4725995	7	150819169	intronic	T	C	0.305	3.86E-19	3.41E-01	AGAP3	OD Arcuate Long Segment Right	1.32E-09	6.064667
139	rs4725995	7	150819169	intronic	T	C	0.305	3.86E-19	3.41E-01	AGAP3	OD Arcuate Anterior Segment Right	1.31E-12	7.093535
139	rs4725995	7	150819169	intronic	T	C	0.305	3.86E-19	3.41E-01	AGAP3	OD Superior Londgitudinal Fasciculus II Left	3.00E-08	5.541545
140	rs4128399	7	151498679	intronic	C	T	0.160	8.29E-19	2.19E-03	PRKAG2	MD Inferior Longitudinal Left	2.04E-08	5.608267
140	rs4128399	7	151498679	intronic	C	T	0.160	8.29E-19	2.19E-03	PRKAG2	ISOVF Superior Londgitudinal Fasciculus II Right	9.86E-09	5.733136
140	rs4128399	7	151498679	intronic	C	T	0.160	8.29E-19	2.19E-03	PRKAG2	L1 Frontal Superior Longitudinal Right	1.18E-12	7.108039
140	rs4128399	7	151498679	intronic	C	T	0.160	8.29E-19	2.19E-03	PRKAG2	ISOVF Frontal Superior Longitudinal Left	1.93E-08	5.618468
140	rs4128399	7	151498679	intronic	C	T	0.160	8.29E-19	2.19E-03	PRKAG2	L2 Inferior Longitudinal Left	9.54E-09	5.738766
140	rs4128399	7	151498679	intronic	C	T	0.160	8.29E-19	2.19E-03	PRKAG2	ISOVF Arcuate Posterior Segment Left	2.35E-10	6.336557
140	rs4128399	7	151498679	intronic	C	T	0.160	8.29E-19	2.19E-03	PRKAG2	MD Corpus callosum	3.67E-08	5.506024
140	rs4128399	7	151498679	intronic	C	T	0.160	8.29E-19	2.19E-03	PRKAG2	L1 Frontal Superior Longitudinal Left	3.38E-09	5.912036
140	rs4128399	7	151498679	intronic	C	T	0.160	8.29E-19	2.19E-03	PRKAG2	L1 Superior Londgitudinal Fasciculus II Left	1.00E-10	6.466457
140	rs4128399	7	151498679	intronic	C	T	0.160	8.29E-19	2.19E-03	PRKAG2	L2 Uncinate Right	1.24E-08	5.693566
140	rs4128399	7	151498679	intronic	C	T	0.160	8.29E-19	2.19E-03	PRKAG2	ISOVF Superior Londgitudinal Fasciculus II Left	5.65E-09	5.826932
140	rs4128399	7	151498679	intronic	C	T	0.160	8.29E-19	2.19E-03	PRKAG2	L1 Superior Londgitudinal Fasciculus II Right	3.67E-09	5.898425
140	rs4128399	7	151498679	intronic	C	T	0.160	8.29E-19	2.19E-03	PRKAG2	MD Superior Londgitudinal Fasciculus II Left	2.31E-08	5.587143
140	rs4128399	7	151498679	intronic	C	T	0.160	8.29E-19	2.19E-03	PRKAG2	L2 Uncinate Left	4.41E-08	5.473645
140	rs4128399	7	151498679	intronic	C	T	0.160	8.29E-19	2.19E-03	PRKAG2	L3 Uncinate Left	3.23E-08	5.528486
140	rs4128399	7	151498679	intronic	C	T	0.160	8.29E-19	2.19E-03	PRKAG2	L1 Superior Londgitudinal Fasciculus I Right	7.74E-13	7.165696
140	rs4128399	7	151498679	intronic	C	T	0.160	8.29E-19	2.19E-03	PRKAG2	ISOVF Corpus callosum	9.95E-09	5.731514
140	rs4128399	7	151498679	intronic	C	T	0.160	8.29E-19	2.19E-03	PRKAG2	L3 Uncinate Right	1.33E-09	6.063460
140	rs4128399	7	151498679	intronic	C	T	0.160	8.29E-19	2.19E-03	PRKAG2	L2 Inferior Longitudinal Right	2.71E-08	5.558971
140	rs4128399	7	151498679	intronic	C	T	0.160	8.29E-19	2.19E-03	PRKAG2	L2 Arcuate Anterior Segment Left	1.40E-08	5.673169
140	rs4128399	7	151498679	intronic	C	T	0.160	8.29E-19	2.19E-03	PRKAG2	L1 Corpus callosum	4.68E-12	6.914902
140	rs4128399	7	151498679	intronic	C	T	0.160	8.29E-19	2.19E-03	PRKAG2	MD Uncinate Left	4.22E-08	5.481263
140	rs4128399	7	151498679	intronic	C	T	0.160	8.29E-19	2.19E-03	PRKAG2	L1 Superior Londgitudinal Fasciculus I Left	7.29E-14	7.482568
141	rs4075359	8	9487813	intronic	C	T	0.376	1.73E-13	7.90E-02	TNKS	L2 Fronto Insular tract1 Right	5.10E-09	-5.843722
141	rs4075359	8	9487813	intronic	C	T	0.376	1.73E-13	7.90E-02	TNKS	MO Fronto Insular tract1 Right	8.56E-09	5.757000
142	rs71548883	8	23101514	intronic	CT	C	0.384	8.31E-21	3.02E-01	CHMP7	OD Superior Londgitudinal Fasciculus II Left	1.81E-10	6.376720
143	rs403185	8	26476721	intronic	G	A	0.408	1.84E-17	5.67E-02	DPYSL2	MO Fronto Insular tract3 Right	1.85E-10	6.373438
146	rs2978101	8	101679224	intergenic	G	T	0.461	7.07E-20	2.26E-02	SNX31	ISOVF Inferior Fronto Occipital fasciculus Left	8.40E-10	6.137168
146	rs2978101	8	101679224	intergenic	G	T	0.461	7.07E-20	2.26E-02	SNX31	ICVF Superior Londgitudinal Fasciculus II Right	6.81E-13	7.183274
146	rs2978101	8	101679224	intergenic	G	T	0.461	7.07E-20	2.26E-02	SNX31	ICVF Arcuate Anterior Segment Right	5.13E-12	6.902002
146	rs2978101	8	101679224	intergenic	G	T	0.461	7.07E-20	2.26E-02	SNX31	L2 Inferior Longitudinal Left	3.45E-08	-5.516780
146	rs2978101	8	101679224	intergenic	G	T	0.461	7.07E-20	2.26E-02	SNX31	MD Inferior Longitudinal Right	3.60E-08	-5.509247
146	rs2978101	8	101679224	intergenic	G	T	0.461	7.07E-20	2.26E-02	SNX31	ICVF Arcuate Long Segment Left	1.57E-11	6.741319
146	rs2978101	8	101679224	intergenic	G	T	0.461	7.07E-20	2.26E-02	SNX31	ISOVF Inferior Longitudinal Right	2.35E-11	6.682158
146	rs2978101	8	101679224	intergenic	G	T	0.461	7.07E-20	2.26E-02	SNX31	ICVF Inferior Fronto Occipital fasciculus Right	1.65E-15	7.965027
146	rs2978101	8	101679224	intergenic	G	T	0.461	7.07E-20	2.26E-02	SNX31	ICVF Corpus callosum	1.39E-13	7.397416
146	rs2978101	8	101679224	intergenic	G	T	0.461	7.07E-20	2.26E-02	SNX31	ICVF Arcuate Posterior Segment Right	3.98E-15	7.855561
146	rs2978101	8	101679224	intergenic	G	T	0.461	7.07E-20	2.26E-02	SNX31	ISOVF Inferior Fronto Occipital fasciculus Right	4.89E-14	7.534830
146	rs2978101	8	101679224	intergenic	G	T	0.461	7.07E-20	2.26E-02	SNX31	ICVF Inferior Fronto Occipital fasciculus Left	3.88E-14	7.564957
146	rs2978101	8	101679224	intergenic	G	T	0.461	7.07E-20	2.26E-02	SNX31	ICVF Frontal Aslant Tract Right	3.41E-09	5.910363
146	rs2978101	8	101679224	intergenic	G	T	0.461	7.07E-20	2.26E-02	SNX31	ICVF Frontal Inferior longitudinal Left	1.04E-08	5.724078
146	rs2978101	8	101679224	intergenic	G	T	0.461	7.07E-20	2.26E-02	SNX31	ICVF Superior Londgitudinal Fasciculus II Left	2.53E-12	7.001664
146	rs2978101	8	101679224	intergenic	G	T	0.461	7.07E-20	2.26E-02	SNX31	ISOVF Superior Londgitudinal Fasciculus I Right	1.09E-09	6.095389
146	rs2978101	8	101679224	intergenic	G	T	0.461	7.07E-20	2.26E-02	SNX31	ICVF Frontal Aslant Tract Left	1.24E-08	5.693650
146	rs2978101	8	101679224	intergenic	G	T	0.461	7.07E-20	2.26E-02	SNX31	ICVF Superior Londgitudinal Fasciculus III Right	2.04E-11	6.702926
146	rs2978101	8	101679224	intergenic	G	T	0.461	7.07E-20	2.26E-02	SNX31	ICVF Frontal Superior Longitudinal Right	4.41E-08	5.473718
146	rs2978101	8	101679224	intergenic	G	T	0.461	7.07E-20	2.26E-02	SNX31	ICVF Arcuate Posterior Segment Left	8.50E-14	7.462383
146	rs2978101	8	101679224	intergenic	G	T	0.461	7.07E-20	2.26E-02	SNX31	ICVF Arcuate Long Segment Right	3.95E-16	8.140216
146	rs2978101	8	101679224	intergenic	G	T	0.461	7.07E-20	2.26E-02	SNX31	ICVF Inferior Longitudinal Right	6.86E-20	9.129819
146	rs2978101	8	101679224	intergenic	G	T	0.461	7.07E-20	2.26E-02	SNX31	ICVF Arcuate Anterior Segment Left	5.84E-09	5.821140
146	rs2978101	8	101679224	intergenic	G	T	0.461	7.07E-20	2.26E-02	SNX31	ISOVF Corpus callosum	2.27E-14	7.634487
146	rs2978101	8	101679224	intergenic	G	T	0.461	7.07E-20	2.26E-02	SNX31	ICVF Superior Londgitudinal Fasciculus I Right	2.04E-13	7.346278
146	rs2978101	8	101679224	intergenic	G	T	0.461	7.07E-20	2.26E-02	SNX31	L3 Uncinate Right	6.41E-09	-5.805656
146	rs2978101	8	101679224	intergenic	G	T	0.461	7.07E-20	2.26E-02	SNX31	ICVF Superior Londgitudinal Fasciculus I Left	1.29E-14	7.706855
146	rs2978101	8	101679224	intergenic	G	T	0.461	7.07E-20	2.26E-02	SNX31	ISOVF Arcuate Anterior Segment Right	6.45E-09	5.804698
146	rs2978101	8	101679224	intergenic	G	T	0.461	7.07E-20	2.26E-02	SNX31	L2 Arcuate Long Segment Right	1.25E-09	-6.073634
146	rs2978101	8	101679224	intergenic	G	T	0.461	7.07E-20	2.26E-02	SNX31	ISOVF Superior Londgitudinal Fasciculus III Right	1.41E-08	5.671565
146	rs2978101	8	101679224	intergenic	G	T	0.461	7.07E-20	2.26E-02	SNX31	ICVF Uncinate Right	2.67E-14	7.613238
146	rs2978101	8	101679224	intergenic	G	T	0.461	7.07E-20	2.26E-02	SNX31	ICVF Uncinate Left	1.37E-12	7.086858
146	rs2978101	8	101679224	intergenic	G	T	0.461	7.07E-20	2.26E-02	SNX31	ICVF Inferior Longitudinal Left	5.13E-18	8.650554
146	rs2978101	8	101679224	intergenic	G	T	0.461	7.07E-20	2.26E-02	SNX31	ICVF Superior Londgitudinal Fasciculus III Left	1.07E-09	6.098848
146	rs2978101	8	101679224	intergenic	G	T	0.461	7.07E-20	2.26E-02	SNX31	L3 Inferior Longitudinal Right	8.56E-09	-5.757023
146	rs2978101	8	101679224	intergenic	G	T	0.461	7.07E-20	2.26E-02	SNX31	ICVF Frontal Inferior longitudinal Right	7.03E-09	5.790112
150	rs10283100	8	120596023	exonic	G	A	0.060	3.68E-16	2.47E-03	ENPP2	ISOVF Inferior Fronto Occipital fasciculus Left	3.63E-09	-5.900415
150	rs10283100	8	120596023	exonic	G	A	0.060	3.68E-16	2.47E-03	ENPP2	ISOVF Superior Londgitudinal Fasciculus II Right	6.43E-10	-6.179451
150	rs10283100	8	120596023	exonic	G	A	0.060	3.68E-16	2.47E-03	ENPP2	L3 Fronto Insular tract2 Right	1.19E-09	-6.081242
150	rs10283100	8	120596023	exonic	G	A	0.060	3.68E-16	2.47E-03	ENPP2	ISOVF Inferior Longitudinal Right	1.47E-09	-6.047472
150	rs10283100	8	120596023	exonic	G	A	0.060	3.68E-16	2.47E-03	ENPP2	ISOVF Superior Londgitudinal Fasciculus III Left	3.05E-12	-6.975427
150	rs10283100	8	120596023	exonic	G	A	0.060	3.68E-16	2.47E-03	ENPP2	ISOVF Arcuate Anterior Segment Left	2.61E-10	-6.320240
150	rs10283100	8	120596023	exonic	G	A	0.060	3.68E-16	2.47E-03	ENPP2	ISOVF Inferior Fronto Occipital fasciculus Right	1.15E-10	-6.445976
150	rs10283100	8	120596023	exonic	G	A	0.060	3.68E-16	2.47E-03	ENPP2	FA Fronto Insular tract1 Right	1.26E-08	5.691051
150	rs10283100	8	120596023	exonic	G	A	0.060	3.68E-16	2.47E-03	ENPP2	ISOVF Arcuate Long Segment Left	2.50E-11	-6.673502
150	rs10283100	8	120596023	exonic	G	A	0.060	3.68E-16	2.47E-03	ENPP2	ISOVF Superior Londgitudinal Fasciculus II Left	6.47E-11	-6.532426
150	rs10283100	8	120596023	exonic	G	A	0.060	3.68E-16	2.47E-03	ENPP2	ISOVF Superior Londgitudinal Fasciculus I Left	1.87E-08	-5.623256
150	rs10283100	8	120596023	exonic	G	A	0.060	3.68E-16	2.47E-03	ENPP2	ISOVF Superior Londgitudinal Fasciculus I Right	2.83E-09	-5.941041
150	rs10283100	8	120596023	exonic	G	A	0.060	3.68E-16	2.47E-03	ENPP2	L2 Fronto Insular tract1 Right	1.74E-09	-6.020413
150	rs10283100	8	120596023	exonic	G	A	0.060	3.68E-16	2.47E-03	ENPP2	ISOVF Corpus callosum	2.58E-09	-5.956311
150	rs10283100	8	120596023	exonic	G	A	0.060	3.68E-16	2.47E-03	ENPP2	ISOVF Arcuate Anterior Segment Right	1.88E-09	-6.008025
150	rs10283100	8	120596023	exonic	G	A	0.060	3.68E-16	2.47E-03	ENPP2	ISOVF Superior Londgitudinal Fasciculus III Right	1.84E-10	-6.374096
150	rs10283100	8	120596023	exonic	G	A	0.060	3.68E-16	2.47E-03	ENPP2	MD Fronto Insular tract2 Right	2.65E-08	-5.562866
150	rs10283100	8	120596023	exonic	G	A	0.060	3.68E-16	2.47E-03	ENPP2	ISOVF Arcuate Long Segment Right	1.39E-08	-5.674411
150	rs10283100	8	120596023	exonic	G	A	0.060	3.68E-16	2.47E-03	ENPP2	ISOVF Arcuate Posterior Segment Right	1.47E-10	-6.408176
151	rs55705857	8	130645692	ncRNA intronic	G	A	0.058	1.60E-24	8.28E-01	CCDC26	L3 Superior Londgitudinal Fasciculus II Left	1.13E-10	-6.449065
151	rs55705857	8	130645692	ncRNA intronic	G	A	0.058	1.60E-24	8.28E-01	CCDC26	MD Inferior Longitudinal Left	2.31E-11	-6.684639
151	rs55705857	8	130645692	ncRNA intronic	G	A	0.058	1.60E-24	8.28E-01	CCDC26	ICVF Fronto Insular tract4 Right	5.70E-14	7.514760

Genomic Locus	Lead SNP	chr	Position	Functional category	Non-effect allele	Effect allele	MAF	mvgwasP (discovery -British-)	mvgwasP (replication -non British-)	Nearest gene	Central endophenotypes	univariate P value	univariate Z
151	rs555705857	8	130645692	ncRNA intronic	G	A	0.058	1.60E-24	8.28E-01	CCDC26	FA Inferior Fronto Occipital fasciculus Right	8.73E-09	5.753741
151	rs555705857	8	130645692	ncRNA intronic	G	A	0.058	1.60E-24	8.28E-01	CCDC26	FA Superior Londgitudinal Fasciculus III Right	1.54E-12	7.071268
151	rs555705857	8	130645692	ncRNA intronic	G	A	0.058	1.60E-24	8.28E-01	CCDC26	ISOVF Inferior Fronto Occipital fasciculus Left	1.19E-10	6.440385
151	rs555705857	8	130645692	ncRNA intronic	G	A	0.058	1.60E-24	8.28E-01	CCDC26	ICVF Superior Londgitudinal Fasciculus II Right	2.62E-17	8.462566
151	rs555705857	8	130645692	ncRNA intronic	G	A	0.058	1.60E-24	8.28E-01	CCDC26	FA Inferior Longitudinal Left	4.46E-10	6.237167
151	rs555705857	8	130645692	ncRNA intronic	G	A	0.058	1.60E-24	8.28E-01	CCDC26	FA Inferior Fronto Occipital fasciculus Left	2.04E-13	7.346312
151	rs555705857	8	130645692	ncRNA intronic	G	A	0.058	1.60E-24	8.28E-01	CCDC26	ICVF Arcuate Anterior Segment Right	8.43E-25	10.282754
151	rs555705857	8	130645692	ncRNA intronic	G	A	0.058	1.60E-24	8.28E-01	CCDC26	MD Arcuate Anterior Segment Right	2.58E-10	-6.322328
151	rs555705857	8	130645692	ncRNA intronic	G	A	0.058	1.60E-24	8.28E-01	CCDC26	MD Inferior Longitudinal Right	6.99E-14	-7.488133
151	rs555705857	8	130645692	ncRNA intronic	G	A	0.058	1.60E-24	8.28E-01	CCDC26	ICVF Arcuate Long Segment Left	4.74E-25	10.338034
151	rs555705857	8	130645692	ncRNA intronic	G	A	0.058	1.60E-24	8.28E-01	CCDC26	L_3 Superior Londgitudinal Fasciculus I Left	1.95E-10	-6.365447
151	rs555705857	8	130645692	ncRNA intronic	G	A	0.058	1.60E-24	8.28E-01	CCDC26	ICVF Fronto Insular tract2 Right	1.56E-08	5.654623
151	rs555705857	8	130645692	ncRNA intronic	G	A	0.058	1.60E-24	8.28E-01	CCDC26	ICVF Fronto Insular tract5 Right	1.86E-08	5.624266
151	rs555705857	8	130645692	ncRNA intronic	G	A	0.058	1.60E-24	8.28E-01	CCDC26	FA Arcuate Anterior Segment Right	3.00E-10	6.298794
151	rs555705857	8	130645692	ncRNA intronic	G	A	0.058	1.60E-24	8.28E-01	CCDC26	FA Superior Londgitudinal Fasciculus I Left	8.94E-11	6.483948
151	rs555705857	8	130645692	ncRNA intronic	G	A	0.058	1.60E-24	8.28E-01	CCDC26	ICVF Inferior Fronto Occipital fasciculus Right	1.20E-28	11.103688
151	rs555705857	8	130645692	ncRNA intronic	G	A	0.058	1.60E-24	8.28E-01	CCDC26	FA Arcuate Long Segment Left	2.20E-11	6.691777
151	rs555705857	8	130645692	ncRNA intronic	G	A	0.058	1.60E-24	8.28E-01	CCDC26	MD Inferior Fronto Occipital fasciculus Right	5.61E-16	-8.097537
151	rs555705857	8	130645692	ncRNA intronic	G	A	0.058	1.60E-24	8.28E-01	CCDC26	ICVF Corpus callosum	1.81E-22	9.752142
151	rs555705857	8	130645692	ncRNA intronic	G	A	0.058	1.60E-24	8.28E-01	CCDC26	L_3 Superior Londgitudinal Fasciculus III Right	2.91E-11	-6.651113
151	rs555705857	8	130645692	ncRNA intronic	G	A	0.058	1.60E-24	8.28E-01	CCDC26	ICVF Arcuate Posterior Segment Right	6.60E-19	8.881521
151	rs555705857	8	130645692	ncRNA intronic	G	A	0.058	1.60E-24	8.28E-01	CCDC26	ISOVF Inferior Fronto Occipital fasciculus Right	2.59E-08	5.567106
151	rs555705857	8	130645692	ncRNA intronic	G	A	0.058	1.60E-24	8.28E-01	CCDC26	FA Frontal Inferior longitudinal Right	2.59E-09	5.955830
151	rs555705857	8	130645692	ncRNA intronic	G	A	0.058	1.60E-24	8.28E-01	CCDC26	ISOVF Inferior Londgitudinal Left	4.01E-08	5.490478
151	rs555705857	8	130645692	ncRNA intronic	G	A	0.058	1.60E-24	8.28E-01	CCDC26	L_2 Inferior Fronto Occipital fasciculus Right	5.49E-09	-5.831499
151	rs555705857	8	130645692	ncRNA intronic	G	A	0.058	1.60E-24	8.28E-01	CCDC26	L_3 Arcuate Posterior Segment Right	1.32E-09	-6.064775
151	rs555705857	8	130645692	ncRNA intronic	G	A	0.058	1.60E-24	8.28E-01	CCDC26	ICVF Fronto Insular tract3 Left	7.33E-11	6.513645
151	rs555705857	8	130645692	ncRNA intronic	G	A	0.058	1.60E-24	8.28E-01	CCDC26	MD Superior Londgitudinal Fasciculus III Left	4.72E-09	-5.856874
151	rs555705857	8	130645692	ncRNA intronic	G	A	0.058	1.60E-24	8.28E-01	CCDC26	ICVF Inferior Fronto Occipital fasciculus Left	6.76E-26	10.523144
151	rs555705857	8	130645692	ncRNA intronic	G	A	0.058	1.60E-24	8.28E-01	CCDC26	ICVF Frontal Aslant Tract Right	2.46E-17	8.469847
151	rs555705857	8	130645692	ncRNA intronic	G	A	0.058	1.60E-24	8.28E-01	CCDC26	L_1 Inferior Fronto Occipital fasciculus Right	1.83E-12	-7.046957
151	rs555705857	8	130645692	ncRNA intronic	G	A	0.058	1.60E-24	8.28E-01	CCDC26	MD Arcuate Posterior Segment Right	4.03E-10	-6.252764
151	rs555705857	8	130645692	ncRNA intronic	G	A	0.058	1.60E-24	8.28E-01	CCDC26	L_3 Superior Londgitudinal Fasciculus III Left	1.88E-10	-6.370729
151	rs555705857	8	130645692	ncRNA intronic	G	A	0.058	1.60E-24	8.28E-01	CCDC26	ICVF Frontal Inferior longitudinal Left	2.70E-11	6.662089
151	rs555705857	8	130645692	ncRNA intronic	G	A	0.058	1.60E-24	8.28E-01	CCDC26	ICVF Superior Londgitudinal Fasciculus II Left	5.85E-19	8.894826
151	rs555705857	8	130645692	ncRNA intronic	G	A	0.058	1.60E-24	8.28E-01	CCDC26	L_3 Inferior Fronto Occipital fasciculus Right	3.10E-16	-8.169504
151	rs555705857	8	130645692	ncRNA intronic	G	A	0.058	1.60E-24	8.28E-01	CCDC26	L_3 Inferior Fronto Occipital fasciculus Left	4.49E-14	-7.545919
151	rs555705857	8	130645692	ncRNA intronic	G	A	0.058	1.60E-24	8.28E-01	CCDC26	L_3 Arcuate Long Segment Left	2.04E-15	-7.939185
151	rs555705857	8	130645692	ncRNA intronic	G	A	0.058	1.60E-24	8.28E-01	CCDC26	ICVF Frontal Aslant Tract Left	8.66E-18	8.590551
151	rs555705857	8	130645692	ncRNA intronic	G	A	0.058	1.60E-24	8.28E-01	CCDC26	ICVF Superior Londgitudinal Fasciculus III Right	6.39E-21	9.383404
151	rs555705857	8	130645692	ncRNA intronic	G	A	0.058	1.60E-24	8.28E-01	CCDC26	ICVF Frontal Superior Longitudinal Right	5.64E-10	6.200257
151	rs555705857	8	130645692	ncRNA intronic	G	A	0.058	1.60E-24	8.28E-01	CCDC26	MD Superior Londgitudinal Fasciculus II Left	1.03E-08	-5.725007
151	rs555705857	8	130645692	ncRNA intronic	G	A	0.058	1.60E-24	8.28E-01	CCDC26	L_2 Inferior Fronto Occipital fasciculus Left	2.79E-11	-6.657268
151	rs555705857	8	130645692	ncRNA intronic	G	A	0.058	1.60E-24	8.28E-01	CCDC26	ICVF Arcuate Posterior Segment Left	1.13E-16	8.290203
151	rs555705857	8	130645692	ncRNA intronic	G	A	0.058	1.60E-24	8.28E-01	CCDC26	FA Arcuate Long Segment Right	4.90E-12	6.908508
151	rs555705857	8	130645692	ncRNA intronic	G	A	0.058	1.60E-24	8.28E-01	CCDC26	ICVF Fronto Insular tract5 Left	4.43E-11	6.588838
151	rs555705857	8	130645692	ncRNA intronic	G	A	0.058	1.60E-24	8.28E-01	CCDC26	ICVF Arcuate Long Segment Right	4.21E-25	10.349527
151	rs555705857	8	130645692	ncRNA intronic	G	A	0.058	1.60E-24	8.28E-01	CCDC26	L_3 Inferior Longitudinal Left	8.86E-14	-7.456818
151	rs555705857	8	130645692	ncRNA intronic	G	A	0.058	1.60E-24	8.28E-01	CCDC26	L_3 Corpus callosum	9.19E-09	-5.745014
151	rs555705857	8	130645692	ncRNA intronic	G	A	0.058	1.60E-24	8.28E-01	CCDC26	ICVF Inferior Longitudinal Right	2.01E-26	10.636774
151	rs555705857	8	130645692	ncRNA intronic	G	A	0.058	1.60E-24	8.28E-01	CCDC26	L_3 Arcuate Long Segment Right	3.36E-17	-8.433295
151	rs555705857	8	130645692	ncRNA intronic	G	A	0.058	1.60E-24	8.28E-01	CCDC26	FA Corpus callosum	5.78E-10	6.196290
151	rs555705857	8	130645692	ncRNA intronic	G	A	0.058	1.60E-24	8.28E-01	CCDC26	L_1 Inferior Longitudinal Right	3.81E-11	-6.611428
151	rs555705857	8	130645692	ncRNA intronic	G	A	0.058	1.60E-24	8.28E-01	CCDC26	MD Arcuate Posterior Segment Left	1.10E-08	-5.714354
151	rs555705857	8	130645692	ncRNA intronic	G	A	0.058	1.60E-24	8.28E-01	CCDC26	ICVF Arcuate Anterior Segment Left	4.76E-22	9.653247
151	rs555705857	8	130645692	ncRNA intronic	G	A	0.058	1.60E-24	8.28E-01	CCDC26	L_3 Arcuate Anterior Segment Left	1.32E-08	-5.682865
151	rs555705857	8	130645692	ncRNA intronic	G	A	0.058	1.60E-24	8.28E-01	CCDC26	ICVF Superior Londgitudinal Fasciculus I Right	2.64E-18	8.726104
151	rs555705857	8	130645692	ncRNA intronic	G	A	0.058	1.60E-24	8.28E-01	CCDC26	FA Inferior Longitudinal Right	1.20E-09	6.080603
151	rs555705857	8	130645692	ncRNA intronic	G	A	0.058	1.60E-24	8.28E-01	CCDC26	MD Arcuate Long Segment Right	1.36E-13	-7.400586
151	rs555705857	8	130645692	ncRNA intronic	G	A	0.058	1.60E-24	8.28E-01	CCDC26	ICVF Fronto Insular tract1 Right	1.92E-08	5.618860
151	rs555705857	8	130645692	ncRNA intronic	G	A	0.058	1.60E-24	8.28E-01	CCDC26	MO Inferior Longitudinal Right	1.79E-08	-5.630991
151	rs555705857	8	130645692	ncRNA intronic	G	A	0.058	1.60E-24	8.28E-01	CCDC26	ICVF Superior Londgitudinal Fasciculus I Left	5.00E-18	8.653414
151	rs555705857	8	130645692	ncRNA intronic	G	A	0.058	1.60E-24	8.28E-01	CCDC26	L_2 Arcuate Long Segment Right	2.33E-08	-5.585181
151	rs555705857	8	130645692	ncRNA intronic	G	A	0.058	1.60E-24	8.28E-01	CCDC26	L_2 Inferior Longitudinal Right	7.59E-09	-5.777286
151	rs555705857	8	130645692	ncRNA intronic	G	A	0.058	1.60E-24	8.28E-01	CCDC26	L_1 Superior Londgitudinal Fasciculus III Left	4.48E-08	-5.470777
151	rs555705857	8	130645692	ncRNA intronic	G	A	0.058	1.60E-24	8.28E-01	CCDC26	L_3 Superior Londgitudinal Fasciculus II Right	3.08E-09	-5.927317
151	rs555705857	8	130645692	ncRNA intronic	G	A	0.058	1.60E-24	8.28E-01	CCDC26	MD Arcuate Long Segment Left	3.98E-13	-7.256381
151	rs555705857	8	130645692	ncRNA intronic	G	A	0.058	1.60E-24	8.28E-01	CCDC26	ICVF Uncinate Right	4.19E-14	7.554971
151	rs555705857	8	130645692	ncRNA intronic	G	A	0.058	1.60E-24	8.28E-01	CCDC26	L_3 Superior Londgitudinal Fasciculus I Right	4.87E-09	-5.851553
151	rs555705857	8	130645692	ncRNA intronic	G	A	0.058	1.60E-24	8.28E-01	CCDC26	ICVF Uncinate Left	9.97E-14	7.441269
151	rs555705857	8	130645692	ncRNA intronic	G	A	0.058	1.60E-24	8.28E-01	CCDC26	ICVF Inferior Longitudinal Left	2.76E-25	10.389729
151	rs555705857	8	130645692	ncRNA intronic	G	A	0.058	1.60E-24	8.28E-01	CCDC26	ICVF Superior Londgitudinal Fasciculus III Left	4.81E-22	9.652244
151	rs555705857	8	130645692	ncRNA intronic	G	A	0.058	1.60E-24	8.28E-01	CCDC26	L_3 Inferior Longitudinal Right	6.00E-16	-8.089251
151	rs555705857	8	130645692	ncRNA intronic	G	A	0.058	1.60E-24	8.28E-01	CCDC26	MD Superior Londgitudinal Fasciculus III Right	6.68E-09	-5.798894
151	rs555705857	8	130645692	ncRNA intronic	G	A	0.058	1.60E-24	8.28E-01	CCDC26	L_3 Frontal Inferior longitudinal Right	1.18E-08	-5.703253
151	rs555705857	8	130645692	ncRNA intronic	G	A	0.058	1.60E-24	8.28E-01	CCDC26	MD Inferior Fronto Occipital fasciculus Left	5.51E-12	-6.891693
151	rs555705857	8	130645692	ncRNA intronic	G	A	0.058	1.60E-24	8.28E-01	CCDC26	L_3 Arcuate Anterior Segment Right	2.05E-13	-7.345529
151	rs555705857	8	130645692	ncRNA intronic	G	A	0.058	1.60E-24	8.28E-01	CCDC26	ICVF Frontal Inferior longitudinal Right	1.32E-16	8.271785
152	rs10102728	8	142205964	downstream	A	G	0.409	3.98E-16	4.91E-02	$DENND3_3$	FA Fronto Insular tract3 Right	3.87E-08	-5.496876
152	rs10102728	8	142205964	downstream	A	G	0.409	3.98E-16	4.91E-02	$DENND3_3$	OD Fronto Insular tract3 Right	9.18E-14	7.452224
153	rs6992333	8	144993377	exonic	G	A	0.430	3.58E-11	1.96E-01	PLEC	ICVF Corpus callosum	3.45E-08	-5.517017
154	rs679038	9	22029080	ncRNA intronic	A	G	0.421	1.68E-08	1.62E-01	RP11-145E5.5:CDKN2B-AS1	ICVF Superior Londgitudinal Fasciculus II Right	3.03E-08	5.539814
154	rs679038	9	22029080	ncRNA intronic	A	G	0.421	1.68E-08	1.62E-01	RP11-145E5.5:CDKN2B-AS1	ICVF Inferior Fronto Occipital fasciculus Right	7.19E-09	5.786518
154	rs679038	9	22029080	ncRNA intronic	A	G	0.421	1.68E-08	1.62E-01	RP11-145E5.5:CDKN2B-AS1	ICVF Corpus callosum	2.63E-13	7.312065
154	rs679038	9	22029080	ncRNA intronic	A	G	0.421	1.68E-08	1.62E-01	RP11-145E5.5:CDKN2B-AS1	ICVF Inferior Fronto Occipital fasciculus Left	1.15E-08	5.707463
154	rs679038	9	22029080	ncRNA intronic	A	G	0.421	1.68E-08	1.62E-01	RP11-145E5.5:CDKN2B-AS1	ICVF Frontal Aslant Tract Right	2.02E-08	5.610549
154	rs679038	9	22029080	ncRNA intronic	A	G	0.421	1.68E-08	1.62E-01	RP11-145E5.5:CDKN2B-AS1	ICVF Superior Londgitudinal Fasciculus II Left	1.42E-08	5.671400
154	rs679038	9	22029080	ncRNA intronic	A	G	0.421	1.68E-08	1.62E-01	RP11-145E5.5:CDKN2B-AS1	ICVF Superior Londgitudinal Fasciculus III Right	3.36E-09	5.912738
154	rs679038	9	22029080	ncRNA intronic	A	G	0.421	1.68E-08	1.62E-01	RP11-145E5.5:CDKN2B-AS1	ICVF Inferior Longitudinal Right	2.16E-08	5.598799
154	rs679038	9	22029080	ncRNA intronic	A	G	0.421	1.68E-08	1.62E-01	RP11-145E5.5:CDKN2B-AS1	ICVF Arcuate Anterior Segment Left	1.94E-08	5.616961
154	rs679038	9	22029080	ncRNA intronic	A	G	0.421	1.68E-08	1.62E-01	RP11-145E5.5:CDKN2B-AS1	ICVF Superior Londgitudinal Fasciculus I Right	6.17E-09	5.812016
154	rs679038	9	22029080	ncRNA intronic	A	G	0.421	1.68E-08	1.62E-01	RP11-145E5.5:CDKN2B-AS1	ICVF Superior Londgitudinal Fasciculus I Left	1.48E-08	5.663440
154	rs679038	9	22029080	ncRNA intronic	A	G	0.421	1.68E-08	1.62E-01	RP11-145E5.5:CDKN2B-AS1	ICVF Inferior Longitudinal Left	9.56E-09	5.738433

Genomic Locus	Lead SNP	chr	Position	Functional category	Non-effect allele	Effect allele	MAF	mvgwasP (discovery -British-)	mvgwasP (replication -non British-)	Nearest gene	Central endophenotypes	univariate P value	univariate Z
154	rs679038	9	22029080	ncRNA intronic	A	G	0.421	1.68E-08	1.62E-01	RP11-145E5.5:CDKN2B-AS1	ICVF Superior Londgitudinal Fasciculus III Left	2.37E-08	5.582359
154	rs679038	9	22029080	ncRNA intronic	A	G	0.421	1.68E-08	1.62E-01	RP11-145E5.5:CDKN2B-AS1	ICVF Frontal Inferior longitudinal Right	1.70E-08	5.640148
158	rs4744186	9	95932546	intergenic	T	C	0.431	2.93E-11	5.89E-02	WNK2	MO Inferior Fronto Occipital fasciculus Right	4.07E-08	-5.487729
160	rs911934	9	101637477	intergenic	G	T	0.313	1.75E-23	6.15E-01	RP11-92C4.3	MO Superior Londgitudinal Fasciculus II Left	2.34E-09	5.972391
160	rs911934	9	101637477	intergenic	G	T	0.313	1.75E-23	6.15E-01	RP11-92C4.3	OD Superior Londgitudinal Fasciculus III Left	4.47E-09	-5.865634
160	rs911934	9	101637477	intergenic	G	T	0.313	1.75E-23	6.15E-01	RP11-92C4.3	FA Fronto Insular tract2 Right	2.13E-08	-5.600782
161	rs10980607	9	113638375	intronic	T	C	0.216	8.06E-12	5.46E-01	LPAR1	ISOVF Frontal Aslant Tract Left	2.22E-11	-6.690899
161	rs10980607	9	113638375	intronic	T	C	0.216	8.06E-12	5.46E-01	LPAR1	ISOVF Inferior Fronto Occipital fasciculus Left	2.29E-13	-7.330749
161	rs10980607	9	113638375	intronic	T	C	0.216	8.06E-12	5.46E-01	LPAR1	ISOVF Superior Londgitudinal Fasciculus II Right	2.19E-11	-6.692491
161	rs10980607	9	113638375	intronic	T	C	0.216	8.06E-12	5.46E-01	LPAR1	ISOVF Fronto Insular tract1 Left	2.54E-08	-5.570679
161	rs10980607	9	113638375	intronic	T	C	0.216	8.06E-12	5.46E-01	LPAR1	ISOVF Inferior Longitudinal Right	3.38E-13	-7.278310
161	rs10980607	9	113638375	intronic	T	C	0.216	8.06E-12	5.46E-01	LPAR1	ISOVF Superior Londgitudinal Fasciculus III Left	1.15E-14	-7.721283
161	rs10980607	9	113638375	intronic	T	C	0.216	8.06E-12	5.46E-01	LPAR1	L1 Fronto Insular tract1 Left	4.50E-08	-5.469908
161	rs10980607	9	113638375	intronic	T	C	0.216	8.06E-12	5.46E-01	LPAR1	ISOVF Arcuate Anterior Segment Left	4.20E-10	-6.246323
161	rs10980607	9	113638375	intronic	T	C	0.216	8.06E-12	5.46E-01	LPAR1	MD Fronto Insular tract1 Left	3.72E-09	-5.895977
161	rs10980607	9	113638375	intronic	T	C	0.216	8.06E-12	5.46E-01	LPAR1	ISOVF Arcuate Posterior Segment Left	1.08E-08	-5.718293
161	rs10980607	9	113638375	intronic	T	C	0.216	8.06E-12	5.46E-01	LPAR1	ISOVF Uncinate Left	6.12E-11	-6.540843
161	rs10980607	9	113638375	intronic	T	C	0.216	8.06E-12	5.46E-01	LPAR1	ISOVF Inferior Fronto Occipital fasciculus Right	5.58E-12	-6.889935
161	rs10980607	9	113638375	intronic	T	C	0.216	8.06E-12	5.46E-01	LPAR1	ISOVF Inferior Longitudinal Left	4.75E-08	-5.460336
161	rs10980607	9	113638375	intronic	T	C	0.216	8.06E-12	5.46E-01	LPAR1	ISOVF Frontal Aslant Tract Right	1.91E-12	-7.040552
161	rs10980607	9	113638375	intronic	T	C	0.216	8.06E-12	5.46E-01	LPAR1	ISOVF Arcuate Long Segment Left	1.42E-10	-6.414102
161	rs10980607	9	113638375	intronic	T	C	0.216	8.06E-12	5.46E-01	LPAR1	ISOVF Superior Londgitudinal Fasciculus II Left	3.91E-11	-6.607297
161	rs10980607	9	113638375	intronic	T	C	0.216	8.06E-12	5.46E-01	LPAR1	ISOVF Superior Londgitudinal Fasciculus I Left	1.77E-13	-7.365130
161	rs10980607	9	113638375	intronic	T	C	0.216	8.06E-12	5.46E-01	LPAR1	ISOVF Superior Londgitudinal Fasciculus I Right	8.72E-14	-7.458979
161	rs10980607	9	113638375	intronic	T	C	0.216	8.06E-12	5.46E-01	LPAR1	L3 Fronto Insular tract1 Left	9.30E-09	-5.743039
161	rs10980607	9	113638375	intronic	T	C	0.216	8.06E-12	5.46E-01	LPAR1	ISOVF Corpus callosum	5.37E-11	-6.560209
161	rs10980607	9	113638375	intronic	T	C	0.216	8.06E-12	5.46E-01	LPAR1	ISOVF Arcuate Anterior Segment Right	9.73E-12	-6.810417
161	rs10980607	9	113638375	intronic	T	C	0.216	8.06E-12	5.46E-01	LPAR1	ISOVF Superior Londgitudinal Fasciculus III Right	1.04E-15	-8.022191
161	rs10980607	9	113638375	intronic	T	C	0.216	8.06E-12	5.46E-01	LPAR1	ISOVF Arcuate Long Segment Right	2.71E-10	-6.314615
161	rs10980607	9	113638375	intronic	T	C	0.216	8.06E-12	5.46E-01	LPAR1	ISOVF Arcuate Posterior Segment Right	1.23E-10	-6.435874
161	rs10980607	9	113638375	intronic	T	C	0.216	8.06E-12	5.46E-01	LPAR1	ISOVF Fronto Insular tract2 Right	4.86E-10	-6.223543
161	rs72748148	9	113677241	intronic	A	G	0.214	1.93E-33	2.41E-02	LPAR1	ISOVF Frontal Aslant Tract Left	1.34E-16	-8.269834
161	rs72748148	9	113677241	intronic	A	G	0.214	1.93E-33	2.41E-02	LPAR1	L3 Fronto Insular tract5 Right	1.82E-08	-5.628285
161	rs72748148	9	113677241	intronic	A	G	0.214	1.93E-33	2.41E-02	LPAR1	ISOVF Inferior Fronto Occipital fasciculus Left	1.27E-18	-8.808006
161	rs72748148	9	113677241	intronic	A	G	0.214	1.93E-33	2.41E-02	LPAR1	ISOVF Superior Londgitudinal Fasciculus II Right	3.27E-17	-8.436584
161	rs72748148	9	113677241	intronic	A	G	0.214	1.93E-33	2.41E-02	LPAR1	L1 Inferior Longitudinal Left	2.12E-08	-5.602080
161	rs72748148	9	113677241	intronic	A	G	0.214	1.93E-33	2.41E-02	LPAR1	L3 Fronto Insular tract2 Right	3.15E-13	-7.287794
161	rs72748148	9	113677241	intronic	A	G	0.214	1.93E-33	2.41E-02	LPAR1	MO Corpus callosum	1.37E-09	-6.059327
161	rs72748148	9	113677241	intronic	A	G	0.214	1.93E-33	2.41E-02	LPAR1	ISOVF Frontal Inferior longitudinal Right	3.00E-11	-6.646326
161	rs72748148	9	113677241	intronic	A	G	0.214	1.93E-33	2.41E-02	LPAR1	ISOVF Fronto Insular tract1 Left	8.13E-11	-6.498133
161	rs72748148	9	113677241	intronic	A	G	0.214	1.93E-33	2.41E-02	LPAR1	ISOVF Inferior Longitudinal Right	1.11E-19	-9.077440
161	rs72748148	9	113677241	intronic	A	G	0.214	1.93E-33	2.41E-02	LPAR1	ISOVF Superior Londgitudinal Fasciculus III Left	3.72E-22	-9.678659
161	rs72748148	9	113677241	intronic	A	G	0.214	1.93E-33	2.41E-02	LPAR1	L2 Fronto Insular tract2 Right	1.13E-08	-5.710529
161	rs72748148	9	113677241	intronic	A	G	0.214	1.93E-33	2.41E-02	LPAR1	L1 Fronto Insular tract1 Left	3.39E-20	-9.205697
161	rs72748148	9	113677241	intronic	A	G	0.214	1.93E-33	2.41E-02	LPAR1	ISOVF Arcuate Anterior Segment Left	3.27E-12	-6.965734
161	rs72748148	9	113677241	intronic	A	G	0.214	1.93E-33	2.41E-02	LPAR1	OD Corpus callosum	3.02E-08	5.540275
161	rs72748148	9	113677241	intronic	A	G	0.214	1.93E-33	2.41E-02	LPAR1	MD Fronto Insular tract1 Left	2.68E-25	-10.392461
161	rs72748148	9	113677241	intronic	A	G	0.214	1.93E-33	2.41E-02	LPAR1	ISOVF Arcuate Posterior Segment Left	4.87E-17	-8.389845
161	rs72748148	9	113677241	intronic	A	G	0.214	1.93E-33	2.41E-02	LPAR1	ISOVF Fronto Insular tract3 Left	2.02E-09	-5.995977
161	rs72748148	9	113677241	intronic	A	G	0.214	1.93E-33	2.41E-02	LPAR1	MO Frontal Superior Longitudinal Left	3.02E-09	-5.930633
161	rs72748148	9	113677241	intronic	A	G	0.214	1.93E-33	2.41E-02	LPAR1	MD Uncinate Right	1.06E-10	-6.458466
161	rs72748148	9	113677241	intronic	A	G	0.214	1.93E-33	2.41E-02	LPAR1	ISOVF Uncinate Left	1.23E-19	-9.066093
161	rs72748148	9	113677241	intronic	A	G	0.214	1.93E-33	2.41E-02	LPAR1	L3 Fronto Insular tract1 Right	2.37E-09	-5.970439
161	rs72748148	9	113677241	intronic	A	G	0.214	1.93E-33	2.41E-02	LPAR1	ISOVF Frontal Superior Longitudinal Right	6.66E-10	-6.174029
161	rs72748148	9	113677241	intronic	A	G	0.214	1.93E-33	2.41E-02	LPAR1	ISOVF Inferior Fronto Occipital fasciculus Right	1.95E-16	-8.224850
161	rs72748148	9	113677241	intronic	A	G	0.214	1.93E-33	2.41E-02	LPAR1	ISOVF Inferior Longitudinal Left	5.03E-12	-6.904810
161	rs72748148	9	113677241	intronic	A	G	0.214	1.93E-33	2.41E-02	LPAR1	ISOVF Frontal Aslant Tract Right	9.01E-19	-8.846719
161	rs72748148	9	113677241	intronic	A	G	0.214	1.93E-33	2.41E-02	LPAR1	L1 Frontal Superior Longitudinal Left	2.30E-09	-5.975233
161	rs72748148	9	113677241	intronic	A	G	0.214	1.93E-33	2.41E-02	LPAR1	ISOVF Arcuate Long Segment Left	2.85E-12	-6.984703
161	rs72748148	9	113677241	intronic	A	G	0.214	1.93E-33	2.41E-02	LPAR1	L2 Uncinate Right	2.92E-08	-5.545925
161	rs72748148	9	113677241	intronic	A	G	0.214	1.93E-33	2.41E-02	LPAR1	ISOVF Superior Londgitudinal Fasciculus II Left	4.35E-20	-9.179147
161	rs72748148	9	113677241	intronic	A	G	0.214	1.93E-33	2.41E-02	LPAR1	L1 Uncinate Left	1.26E-13	-7.410279
161	rs72748148	9	113677241	intronic	A	G	0.214	1.93E-33	2.41E-02	LPAR1	ISOVF Superior Londgitudinal Fasciculus I Left	4.63E-22	-9.656220
161	rs72748148	9	113677241	intronic	A	G	0.214	1.93E-33	2.41E-02	LPAR1	ISOVF Superior Londgitudinal Fasciculus I Right	3.41E-18	-8.696898
161	rs72748148	9	113677241	intronic	A	G	0.214	1.93E-33	2.41E-02	LPAR1	ICVF Fronto Insular tract1 Left	5.92E-16	8.090975
161	rs72748148	9	113677241	intronic	A	G	0.214	1.93E-33	2.41E-02	LPAR1	L2 Fronto Insular tract1 Left	2.19E-23	-9.963924
161	rs72748148	9	113677241	intronic	A	G	0.214	1.93E-33	2.41E-02	LPAR1	L3 Fronto Insular tract1 Left	2.98E-24	-10.160383
161	rs72748148	9	113677241	intronic	A	G	0.214	1.93E-33	2.41E-02	LPAR1	L2 Uncinate Left	1.53E-13	-7.384727
161	rs72748148	9	113677241	intronic	A	G	0.214	1.93E-33	2.41E-02	LPAR1	L2 Fronto Insular tract1 Right	6.39E-09	-5.806178
161	rs72748148	9	113677241	intronic	A	G	0.214	1.93E-33	2.41E-02	LPAR1	L3 Uncinate Left	1.52E-14	-7.686016
161	rs72748148	9	113677241	intronic	A	G	0.214	1.93E-33	2.41E-02	LPAR1	L1 Inferior Longitudinal Right	1.09E-08	-5.716389
161	rs72748148	9	113677241	intronic	A	G	0.214	1.93E-33	2.41E-02	LPAR1	L1 Fronto Insular tract2 Right	8.30E-10	-6.139060
161	rs72748148	9	113677241	intronic	A	G	0.214	1.93E-33	2.41E-02	LPAR1	L1 Superior Londgitudinal Fasciculus I Right	1.98E-08	-5.613986
161	rs72748148	9	113677241	intronic	A	G	0.214	1.93E-33	2.41E-02	LPAR1	ISOVF Corpus callosum	2.81E-17	-8.454127
161	rs72748148	9	113677241	intronic	A	G	0.214	1.93E-33	2.41E-02	LPAR1	MD Fronto Insular tract1 Right	4.98E-09	-5.847792
161	rs72748148	9	113677241	intronic	A	G	0.214	1.93E-33	2.41E-02	LPAR1	L3 Uncinate Right	1.07E-12	-7.120623
161	rs72748148	9	113677241	intronic	A	G	0.214	1.93E-33	2.41E-02	LPAR1	ISOVF Arcuate Anterior Segment Right	3.88E-15	-7.858609
161	rs72748148	9	113677241	intronic	A	G	0.214	1.93E-33	2.41E-02	LPAR1	L2 Frontal Aslant Tract Right	2.59E-08	-5.566990

Genomic Locus	Lead SNP	chr	Position	Functional category	Non-effect allele	Effect allele	MAF	mvgwasP (discovery -British-)	mvgwasP (replication -non British-)	Nearest gene	Central endophenotypes	univariate P value	univariate Z
161	rs72748148	9	113677241	intronic	A	G	0.214	1.93E-33	2.41E-02	LPAR1	ISOVF Fronto Insular tract1 Right	3.21E-10	-6.288212
161	rs72748148	9	113677241	intronic	A	G	0.214	1.93E-33	2.41E-02	LPAR1	ISOVF Fronto Insular tract3 Right	1.95E-09	-6.001919
161	rs72748148	9	113677241	intronic	A	G	0.214	1.93E-33	2.41E-02	LPAR1	ISOVF Superior Londgitudinal Fasciculus III Right	1.12E-23	-10.030878
161	rs72748148	9	113677241	intronic	A	G	0.214	1.93E-33	2.41E-02	LPAR1	MD Fronto Insular tract2 Right	1.09E-12	-7.119105
161	rs72748148	9	113677241	intronic	A	G	0.214	1.93E-33	2.41E-02	LPAR1	L1 Corpus callosum	1.16E-08	-5.705412
161	rs72748148	9	113677241	intronic	A	G	0.214	1.93E-33	2.41E-02	LPAR1	ISOVF Fronto Insular tract4 Right	9.59E-12	-6.812479
161	rs72748148	9	113677241	intronic	A	G	0.214	1.93E-33	2.41E-02	LPAR1	ISOVF Arcuate Long Segment Right	2.13E-17	-8.486320
161	rs72748148	9	113677241	intronic	A	G	0.214	1.93E-33	2.41E-02	LPAR1	MD Uncinate Left	7.73E-17	-8.335274
161	rs72748148	9	113677241	intronic	A	G	0.214	1.93E-33	2.41E-02	LPAR1	ISOVF Arcuate Posterior Segment Right	4.16E-22	-9.667040
161	rs72748148	9	113677241	intronic	A	G	0.214	1.93E-33	2.41E-02	LPAR1	ISOVF Fronto Insular tract2 Right	2.65E-17	-8.460913
161	rs72748148	9	113677241	intronic	A	G	0.214	1.93E-33	2.41E-02	LPAR1	MD Superior Londgitudinal Fasciculus I Left	4.60E-09	-5.860890
161	rs72748148	9	113677241	intronic	A	G	0.214	1.93E-33	2.41E-02	LPAR1	L1 Superior Londgitudinal Fasciculus I Left	1.77E-09	-6.017969
162	g:118957629 AAAG A	9	118957629	intronic	A	AAAG	0.424	1.55E-08	3.09E-02	PAPPA	OD Fronto Insular tract1 Right	8.32E-09	5.761927
162	g:118957629 AAAG A	9	118957629	intronic	A	AAAG	0.424	1.55E-08	3.09E-02	PAPPA	OD Fronto Insular tract2 Right	1.28E-08	5.688354
162	g:118957629 AAAG A	9	118957629	intronic	A	AAAG	0.424	1.55E-08	3.09E-02	PAPPA	FA Fronto Insular tract2 Right	1.99E-09	-5.998593
163	rs7030607	9	119245183	intronic	A	G	0.354	7.46E-16	7.30E-02	ASTN2	MO Fronto Insular tract2 Right	4.40E-09	-5.868554
167	rs774455421	10	25041543	intergenic	G	GAGACAGTCAAGTC	0.352	2.01E-09	2.43E-01	ARHGAP21	L3 Fronto Insular tract2 Right	2.93E-09	5.935474
167	rs774455421	10	25041543	intergenic	G	GAGACAGTCAAGTC	0.352	2.01E-09	2.43E-01	ARHGAP21	ISOVF Superior Londgitudinal Fasciculus III Left	5.63E-09	5.827325
167	rs774455421	10	25041543	intergenic	G	GAGACAGTCAAGTC	0.352	2.01E-09	2.43E-01	ARHGAP21	L2 Fronto Insular tract2 Right	2.36E-09	5.971008
167	rs774455421	10	25041543	intergenic	G	GAGACAGTCAAGTC	0.352	2.01E-09	2.43E-01	ARHGAP21	MD Fronto Insular tract1 Left	1.37E-11	6.760876
167	rs774455421	10	25041543	intergenic	G	GAGACAGTCAAGTC	0.352	2.01E-09	2.43E-01	ARHGAP21	ISOVF Uncinate Left	2.04E-11	6.702994
167	rs774455421	10	25041543	intergenic	G	GAGACAGTCAAGTC	0.352	2.01E-09	2.43E-01	ARHGAP21	L2 Fronto Insular tract1 Left	5.63E-12	6.888594
167	rs774455421	10	25041543	intergenic	G	GAGACAGTCAAGTC	0.352	2.01E-09	2.43E-01	ARHGAP21	L3 Fronto Insular tract1 Left	6.00E-12	6.879661
167	rs774455421	10	25041543	intergenic	G	GAGACAGTCAAGTC	0.352	2.01E-09	2.43E-01	ARHGAP21	ISOVF Corpus callosum	4.83E-08	5.457413
167	rs774455421	10	25041543	intergenic	G	GAGACAGTCAAGTC	0.352	2.01E-09	2.43E-01	ARHGAP21	ISOVF Superior Londgitudinal Fasciculus III Right	2.30E-08	5.587923
167	rs774455421	10	25041543	intergenic	G	GAGACAGTCAAGTC	0.352	2.01E-09	2.43E-01	ARHGAP21	ISOVF Fronto Insular tract2 Right	2.98E-09	5.932812
169	rs17537178	10	48442894	intergenic	G	A	0.267	3.61E-10	2.84E-01	GDF10	MO Arcuate Anterior Segment Left	4.24E-08	-5.480610
170	rs12240534	10	50318141	intronic	T	C	0.349	3.28E-10	1.67E-01	VSTM4	L1 Frontal Aslant Tract Left	7.73E-09	-5.774205
172	rs1163084	10	105039048	intronic	C	T	0.456	2.15E-15	1.09E-01	INA	L1 Superior Londgitudinal Fasciculus II Left	7.97E-10	-6.145560
172	rs1163084	10	105039048	intronic	C	T	0.456	2.15E-15	1.09E-01	INA	L2 Superior Londgitudinal Fasciculus III Left	1.71E-08	-5.639309
172	rs1163084	10	105039048	intronic	C	T	0.456	2.15E-15	1.09E-01	INA	L1 Superior Londgitudinal Fasciculus II Right	7.34E-09	-5.783010
172	rs1163084	10	105039048	intronic	C	T	0.456	2.15E-15	1.09E-01	INA	MD Superior Londgitudinal Fasciculus II Left	4.71E-08	-5.461939
172	rs1163084	10	105039048	intronic	C	T	0.456	2.15E-15	1.09E-01	INA	L1 Frontal Inferior longitudinal Right	3.50E-09	-5.906118
172	rs1163084	10	105039048	intronic	C	T	0.456	2.15E-15	1.09E-01	INA	L2 Arcuate Long Segment Left	1.06E-08	-5.721264
173	rs11394128	10	105454037	intronic	TG	T	0.485	3.49E-09	3.10E-01	SH3PXD2A	L3 Frontal Aslant Tract Right	2.52E-09	5.960046
173	rs11394128	10	105454037	intronic	TG	T	0.485	3.49E-09	3.10E-01	SH3PXD2A	MD Superior Londgitudinal Fasciculus II Right	1.82E-08	5.628171
173	rs11394128	10	105454037	intronic	TG	T	0.485	3.49E-09	3.10E-01	SH3PXD2A	L2 Frontal Inferior longitudinal Right	2.48E-08	5.574953
173	rs11394128	10	105454037	intronic	TG	T	0.485	3.49E-09	3.10E-01	SH3PXD2A	MD Arcuate Anterior Segment Right	2.06E-11	6.702052
173	rs11394128	10	105454037	intronic	TG	T	0.485	3.49E-09	3.10E-01	SH3PXD2A	ISOVF Frontal Inferior longitudinal Right	1.27E-08	5.690023
173	rs11394128	10	105454037	intronic	TG	T	0.485	3.49E-09	3.10E-01	SH3PXD2A	MD Frontal Aslant Tract Right	3.58E-10	6.271456
173	rs11394128	10	105454037	intronic	TG	T	0.485	3.49E-09	3.10E-01	SH3PXD2A	L1 Fronto Insular tract4 Right	3.58E-10	6.271275
173	rs11394128	10	105454037	intronic	TG	T	0.485	3.49E-09	3.10E-01	SH3PXD2A	ICVF Fronto Insular tract5 Right	9.24E-09	-5.744131
173	rs11394128	10	105454037	intronic	TG	T	0.485	3.49E-09	3.10E-01	SH3PXD2A	MD Fronto Insular tract5 Right	4.31E-09	5.871715
173	rs11394128	10	105454037	intronic	TG	T	0.485	3.49E-09	3.10E-01	SH3PXD2A	L3 Frontal Aslant Tract Left	1.72E-10	6.384426
173	rs11394128	10	105454037	intronic	TG	T	0.485	3.49E-09	3.10E-01	SH3PXD2A	MD Inferior Fronto Occipital fasciculus Right	3.64E-08	5.507334
173	rs11394128	10	105454037	intronic	TG	T	0.485	3.49E-09	3.10E-01	SH3PXD2A	L3 Superior Londgitudinal Fasciculus III Right	1.78E-10	6.379106
173	rs11394128	10	105454037	intronic	TG	T	0.485	3.49E-09	3.10E-01	SH3PXD2A	MD Fronto Insular tract3 Right	4.45E-12	6.922156
173	rs11394128	10	105454037	intronic	TG	T	0.485	3.49E-09	3.10E-01	SH3PXD2A	MD Superior Londgitudinal Fasciculus III Left	2.90E-11	6.651702
173	rs11394128	10	105454037	intronic	TG	T	0.485	3.49E-09	3.10E-01	SH3PXD2A	L1 Fronto Insular tract3 Right	3.17E-13	7.287167
173	rs11394128	10	105454037	intronic	TG	T	0.485	3.49E-09	3.10E-01	SH3PXD2A	ISOVF Arcuate Long Segment Left	2.68E-08	5.560958
173	rs11394128	10	105454037	intronic	TG	T	0.485	3.49E-09	3.10E-01	SH3PXD2A	MD Arcuate Posterior Segment Right	4.35E-08	5.476052
173	rs11394128	10	105454037	intronic	TG	T	0.485	3.49E-09	3.10E-01	SH3PXD2A	MD Fronto Insular tract5 Left	9.18E-10	6.123049
173	rs11394128	10	105454037	intronic	TG	T	0.485	3.49E-09	3.10E-01	SH3PXD2A	L2 Superior Londgitudinal Fasciculus III Right	7.95E-13	7.161967
173	rs11394128	10	105454037	intronic	TG	T	0.485	3.49E-09	3.10E-01	SH3PXD2A	L3 Superior Londgitudinal Fasciculus III Left	1.07E-09	6.098268
173	rs11394128	10	105454037	intronic	TG	T	0.485	3.49E-09	3.10E-01	SH3PXD2A	L3 Inferior Fronto Occipital fasciculus Right	3.47E-08	5.519286
173	rs11394128	10	105454037	intronic	TG	T	0.485	3.49E-09	3.10E-01	SH3PXD2A	L2 Frontal Aslant Tract Left	3.90E-10	6.257858
173	rs11394128	10	105454037	intronic	TG	T	0.485	3.49E-09	3.10E-01	SH3PXD2A	L2 Superior Londgitudinal Fasciculus III Left	2.87E-12	6.983901
173	rs11394128	10	105454037	intronic	TG	T	0.485	3.49E-09	3.10E-01	SH3PXD2A	L2 Arcuate Anterior Segment Right	3.01E-10	6.298478
173	rs11394128	10	105454037	intronic	TG	T	0.485	3.49E-09	3.10E-01	SH3PXD2A	L3 Inferior Fronto Occipital fasciculus Left	5.11E-10	6.215735
173	rs11394128	10	105454037	intronic	TG	T	0.485	3.49E-09	3.10E-01	SH3PXD2A	MD Frontal Aslant Tract Left	2.49E-11	6.673952
173	rs11394128	10	105454037	intronic	TG	T	0.485	3.49E-09	3.10E-01	SH3PXD2A	L2 Fronto Insular tract3 Right	3.15E-09	5.923461
173	rs11394128	10	105454037	intronic	TG	T	0.485	3.49E-09	3.10E-01	SH3PXD2A	L2 Superior Londgitudinal Fasciculus II Right	2.15E-09	5.985867
173	rs11394128	10	105454037	intronic	TG	T	0.485	3.49E-09	3.10E-01	SH3PXD2A	L1 Superior Londgitudinal Fasciculus III Right	2.07E-11	6.700780
173	rs11394128	10	105454037	intronic	TG	T	0.485	3.49E-09	3.10E-01	SH3PXD2A	L1 Frontal Aslant Tract Left	1.09E-08	5.716483
173	rs11394128	10	105454037	intronic	TG	T	0.485	3.49E-09	3.10E-01	SH3PXD2A	L2 Inferior Fronto Occipital fasciculus Left	2.24E-09	5.979554
173	rs11394128	10	105454037	intronic	TG	T	0.485	3.49E-09	3.10E-01	SH3PXD2A	L3 Arcuate Long Segment Right	5.89E-09	5.819831
173	rs11394128	10	105454037	intronic	TG	T	0.485	3.49E-09	3.10E-01	SH3PXD2A	MD Frontal Inferior longitudinal Right	4.67E-12	6.915294
173	rs11394128	10	105454037	intronic	TG	T	0.485	3.49E-09	3.10E-01	SH3PXD2A	L1 Frontal Inferior longitudinal Right	4.02E-10	6.253362
173	rs11394128	10	105454037	intronic	TG	T	0.485	3.49E-09	3.10E-01	SH3PXD2A	MD Arcuate Long Segment Right	2.07E-09	5.992299
173	rs11394128	10	105454037	intronic	TG	T	0.485	3.49E-09	3.10E-01	SH3PXD2A	L2 Arcuate Long Segment Left	3.84E-09	5.890733
173	rs11394128	10	105454037	intronic	TG	T	0.485	3.49E-09	3.10E-01	SH3PXD2A	L2 Frontal Aslant Tract Right	7.84E-09	5.771908
173	rs11394128	10	105454037	intronic	TG	T	0.485	3.49E-09	3.10E-01	SH3PXD2A	L1 Frontal Aslant Tract Right	4.11E-08	5.485941
173	rs11394128	10	105454037	intronic	TG	T	0.485	3.49E-09	3.10E-01	SH3PXD2A	MD Arcuate Long Segment Left	5.56E-10	6.202544
173	rs11394128	10	105454037	intronic	TG	T	0.485	3.49E-09	3.10E-01	SH3PXD2A	MD Superior Londgitudinal Fasciculus III Right	1.26E-12	7.098201
173	rs11394128	10	105454037	intronic	TG	T	0.485	3.49E-09	3.10E-01	SH3PXD2A	L3 Frontal Inferior longitudinal Right	2.48E-09	5.962479
173	rs11394128	10	105454037	intronic	TG	T	0.485	3.49E-09	3.10E-01	SH3PXD2A	L1 Fronto Insular tract5 Right	7.13E-09	5.787877
173	rs11394128	10	105454037	intronic	TG	T	0.485	3.49E-09	3.10E-01	SH3PXD2A	MD Inferior Fronto Occipital fasciculus Left	6.19E-10	6.185414
173	rs11394128	10	105454037	intronic	TG	T	0.485	3.49E-09	3.10E-01	SH3PXD2A	L3 Arcuate Anterior Segment Right	9.00E-09	5.748548
173	rs11191829	10	105614452	intronic	T	G	0.353	3.25E-13	1.84E-01	SH3PXD2A	L3 Frontal Aslant Tract Right	4.51E-08	5.469700
173	rs11191829	10	105614452	intronic	T	G	0.353	3.25E-13	1.84E-01	SH3PXD2A	MD Frontal Aslant Tract Right	4.35E-08	5.475984
173	rs11191829	10	105614452	intronic	T	G	0.353	3.25E-13	1.84E-01	SH3PXD2A	L3 Frontal Aslant Tract Left	2.45E-10	6.330116
173	rs11191829	10	105614452	intronic	T	G	0.353	3.25E-13	1.84E-01	SH3PXD2A	L2 Fronto Insular tract5 Right	6.44E-09	5.804848
173	rs11191829	10	105614452	intronic	T	G	0.353	3.25E-13	1.84E-01	SH3PXD2A	MD Frontal Aslant Tract Left	1.19E-09	6.081922
173	rs11191829	10	105614452	intronic	T	G	0.353	3.25E-13	1.84E-01	SH3PXD2A	MD Frontal Inferior longitudinal Right	5.47E-09	5.832240
173	rs11191829	10	105614452	intronic	T	G	0.353	3.25E-13	1.84E-01	SH3PXD2A	FA Superior Londgitudinal Fasciculus II Left	3.84E-08	-5.497944
173	rs11191829	10	105614452	intronic	T	G	0.353	3.25E-13	1.84E-01	SH3PXD2A	L3 Frontal Inferior longitudinal Right	8.69E-09	5.754528
174	rs17089699	10	118692698	intronic	G	A	0.249	2.67E-66	9.69E-03	KIAA1598	OD Superior Londgitudinal Fasciculus II Right	2.38E-20	-9.243890
174	rs17089699	10	118692698	intronic	G	A	0.249	2.67E-66	9.69E-03	KIAA1598	MO Superior Londgitudinal Fasciculus II Left	2.65E-08	5.563143
174	rs17089699	10	118692698	intronic	G	A	0.249	2.67E-66	9.69E-03	KIAA1598	OD Superior Londgitudinal Fasciculus II Left	5.18E-28	-10.972486
175	rs10901817	10	126443404	intronic	T	A	0.427	1.26E-19	5.77E-01	RP11-12J10.3:METTL10	OD Superior Londgitudinal Fasciculus I Left	5.40E-09	-5.834318
175	rs10901817	10	126443404	intronic	T	A	0.427	1.26E-19	5.77E-01	RP11-12J10.3:METTL10	OD Superior Londgitudinal Fasciculus I Right	7.70E-09	-5.774954
177	rs1045502	11	252818	UTR3	A	G	0.086	1.81E-14	4.19E-01	PSMD13	MD Inferior Longitudinal Left	3.75E-08	5.502308
177	rs1045502	11	252818	UTR3	A	G	0.086	1.81E-14	4.19E-01	PSMD13	ICVF Inferior Fronto Occipital fasciculus Right	3.68E-12	-6.949093
177	rs1045502	11	252818	UTR3	A	G	0.086	1.81E-14	4.19E-01	PSMD13	MD Inferior Fronto Occipital fasciculus Right	5.46E-09	5.832408
177	rs1045502	11	252818	UTR3	A	G	0.086	1.81E-14	4.19E-01	PSMD13	ICVF Inferior Fronto Occipital fasciculus Left	3.35E-10	-6.281672
177	rs1045502	11	252818	UTR3	A	G	0.086	1.81E-14	4.19E-01	PSMD13	L3 Inferior Fronto Occipital fasciculus Right	1.59E-08	5.651218
177	rs1045502	11	252818	UTR3	A	G	0.086	1.81E-14	4.19E-01	PSMD13	ICVF Inferior Longitudinal Right	2.71E-08	-5.559071
177	rs1045502	11	252818	UTR3	A	G	0.086	1.81E-14	4.19E-01	PSMD13	MD Inferior Fronto Occipital fasciculus Left	4.37E-08	5.475337
179	rs2071020	11	10478228	intronic	T	C	0.452	4.99E-19	7.47E-01	AMPD3	L1 Arcuate Anterior Segment Right	1.15E-08	-5.706316
179	rs2071020	11	10478228	intronic	T	C	0.452	4.99E-19	7.47E-01	AMPD3	L1 Inferior Longitudinal Left	2.30E-09	-5.975033
179	rs2071020	11	10478228	intronic	T	C	0.452	4.99E-19	7.47E-01	AMPD3	OD Superior Londgitudinal Fasciculus II Right	2.40E-10	6.332986
179	rs2071020	11	10478228	intronic	T	C	0.452	4.99E-19	7.47E-01	AMPD3	L1 Inferior Fronto Occipital fasciculus Left	1.49E-11	-6.749355
179	rs2071020	11	10478228	intronic	T	C	0.452	4.99E-19	7.47E-01	AMPD3	OD Superior Londgitudinal Fasciculus III Left	8.57E-10	6.133904
179	rs2071020	11	10478228	intronic	T	C	0.452	4.99E-19	7.47E-01	AMPD3	L1 Arcuate Long Segment Right	5.61E-13	-7.209757
179	rs2071020	11	10478228	intronic	T	C	0.452	4.99E-19	7.47E-01	AMPD3	L1 Superior Londgitudinal Fasciculus II Left	4.60E-16	-8.121512
179	rs2071020	11	10478228	intronic	T	C	0.452	4.99E-19	7.47E-01	AMPD3	L1 Inferior Fronto Occipital fasciculus Right	1.69E-11	-6.730411
179	rs2071020	11	10478228	intronic	T	C	0.452	4.99E-19	7.47E-01	AMPD3	L1 Arcuate Posterior Segment Left	3.52E-09	-5.905094

Genomic Locus	Lead SNP	chr	Position	Functional category	Non-effect allele	Effect allele	MAF	mvgwasP (discovery -British-)	mvgwasP (replication -non British-)	Nearest gene	Central endophenotypes	univariate P value	univariate Z
179	rs2071020	11	10478228	intronic	T	C	0.452	4.99E-19	7.47E-01	AMPD3	L1 Arcuate Long Segment Left	3.68E-13	-7.266913
179	rs2071020	11	10478228	intronic	T	C	0.452	4.99E-19	7.47E-01	AMPD3	L1 Superior Londgitudinal Fasciculus II Right	1.94E-14	-7.654833
179	rs2071020	11	10478228	intronic	T	C	0.452	4.99E-19	7.47E-01	AMPD3	OD Inferior Fronto Occipital fasciculus Left	5.01E-10	6.218775
179	rs2071020	11	10478228	intronic	T	C	0.452	4.99E-19	7.47E-01	AMPD3	L1 Superior Londgitudinal Fasciculus III Right	1.31E-10	-6.425599
179	rs2071020	11	10478228	intronic	T	C	0.452	4.99E-19	7.47E-01	AMPD3	MD Superior Londgitudinal Fasciculus II Left	4.38E-08	-5.474896
179	rs2071020	11	10478228	intronic	T	C	0.452	4.99E-19	7.47E-01	AMPD3	L1 Frontal Aslant Tract Left	4.42E-09	-5.867518
179	rs2071020	11	10478228	intronic	T	C	0.452	4.99E-19	7.47E-01	AMPD3	OD Superior Londgitudinal Fasciculus III Right	1.07E-21	9.569702
179	rs2071020	11	10478228	intronic	T	C	0.452	4.99E-19	7.47E-01	AMPD3	L1 Inferior Longitudinal Right	8.10E-09	-5.766260
179	rs2071020	11	10478228	intronic	T	C	0.452	4.99E-19	7.47E-01	AMPD3	MD Arcuate Long Segment Right	1.81E-08	-5.629699
179	rs2071020	11	10478228	intronic	T	C	0.452	4.99E-19	7.47E-01	AMPD3	L1 Arcuate Posterior Segment Right	1.88E-09	-6.008128
179	rs2071020	11	10478228	intronic	T	C	0.452	4.99E-19	7.47E-01	AMPD3	L1 Superior Londgitudinal Fasciculus III Left	1.54E-08	-5.657168
179	rs2071020	11	10478228	intronic	T	C	0.452	4.99E-19	7.47E-01	AMPD3	L1 Frontal Aslant Tract Right	8.66E-10	-6.132242
179	rs2071020	11	10478228	intronic	T	C	0.452	4.99E-19	7.47E-01	AMPD3	L1 Corpus callosum	2.23E-13	-7.334509
179	rs2071020	11	10478228	intronic	T	C	0.452	4.99E-19	7.47E-01	AMPD3	OD Superior Londgitudinal Fasciculus II Left	8.97E-11	6.483333
182	rs2585753	11	19895756	intronic	G	C	0.226	1.52E-11	4.18E-03	NAV2	OD Superior Londgitudinal Fasciculus II Right	1.47E-08	5.665564
182	rs2585753	11	19895756	intronic	G	C	0.226	1.52E-11	4.18E-03	NAV2	OD Arcuate Long Segment Left	1.15E-09	6.087171
182	rs2585753	11	19895756	intronic	G	C	0.226	1.52E-11	4.18E-03	NAV2	L1 Arcuate Long Segment Left	2.80E-10	-6.309202
182	rs2585753	11	19895756	intronic	G	C	0.226	1.52E-11	4.18E-03	NAV2	L1 Superior Londgitudinal Fasciculus II Right	2.86E-09	-5.939723
182	rs2585753	11	19895756	intronic	G	C	0.226	1.52E-11	4.18E-03	NAV2	OD Fronto Insular tract4 Right	2.65E-08	5.563294
183	rs7935166	11	44636547	intronic	A	G	0.133	4.43E-41	3.00E-01	CD82	MD Inferior Longitudinal Left	3.00E-11	-6.646595
183	rs7935166	11	44636547	intronic	A	G	0.133	4.43E-41	3.00E-01	CD82	ICVF Fronto Insular tract4 Right	1.29E-18	8.806952
183	rs7935166	11	44636547	intronic	A	G	0.133	4.43E-41	3.00E-01	CD82	L3 Frontal Aslant Tract Right	8.73E-09	-5.753635
183	rs7935166	11	44636547	intronic	A	G	0.133	4.43E-41	3.00E-01	CD82	MD Superior Londgitudinal Fasciculus II Right	3.32E-09	-5.915153
183	rs7935166	11	44636547	intronic	A	G	0.133	4.43E-41	3.00E-01	CD82	OD Uncinate Left	1.66E-08	5.644237
183	rs7935166	11	44636547	intronic	A	G	0.133	4.43E-41	3.00E-01	CD82	ICVF Fronto Insular tract3 Right	5.55E-16	8.098833
183	rs7935166	11	44636547	intronic	A	G	0.133	4.43E-41	3.00E-01	CD82	MD Arcuate Anterior Segment Right	3.37E-09	-5.912384
183	rs7935166	11	44636547	intronic	A	G	0.133	4.43E-41	3.00E-01	CD82	L1 Frontal Superior Longitudinal Right	8.26E-09	-5.762968
183	rs7935166	11	44636547	intronic	A	G	0.133	4.43E-41	3.00E-01	CD82	L2 Inferior Longitudinal Left	3.91E-11	-6.607318
183	rs7935166	11	44636547	intronic	A	G	0.133	4.43E-41	3.00E-01	CD82	MD Inferior Longitudinal Right	1.00E-09	-6.108635
183	rs7935166	11	44636547	intronic	A	G	0.133	4.43E-41	3.00E-01	CD82	L1 Inferior Fronto Occipital fasciculus Left	2.56E-10	-6.323429
183	rs7935166	11	44636547	intronic	A	G	0.133	4.43E-41	3.00E-01	CD82	MD Frontal Aslant Tract Right	8.18E-12	-6.835427
183	rs7935166	11	44636547	intronic	A	G	0.133	4.43E-41	3.00E-01	CD82	L3 Superior Londgitudinal Fasciculus I Left	4.54E-09	-5.863207
183	rs7935166	11	44636547	intronic	A	G	0.133	4.43E-41	3.00E-01	CD82	L1 Fronto Insular tract4 Right	2.27E-10	-6.341546
183	rs7935166	11	44636547	intronic	A	G	0.133	4.43E-41	3.00E-01	CD82	ICVF Fronto Insular tract2 Right	5.67E-09	5.826119
183	rs7935166	11	44636547	intronic	A	G	0.133	4.43E-41	3.00E-01	CD82	ICVF Fronto Insular tract5 Right	8.18E-19	8.857488
183	rs7935166	11	44636547	intronic	A	G	0.133	4.43E-41	3.00E-01	CD82	MD Fronto Insular tract5 Right	3.72E-08	-5.503679
183	rs7935166	11	44636547	intronic	A	G	0.133	4.43E-41	3.00E-01	CD82	L3 Frontal Aslant Tract Left	5.65E-09	-5.826885
183	rs7935166	11	44636547	intronic	A	G	0.133	4.43E-41	3.00E-01	CD82	OD Corpus callosum	1.79E-08	5.630854
183	rs7935166	11	44636547	intronic	A	G	0.133	4.43E-41	3.00E-01	CD82	ICVF Inferior Fronto Occipital fasciculus Right	4.36E-08	5.475505
183	rs7935166	11	44636547	intronic	A	G	0.133	4.43E-41	3.00E-01	CD82	L1 Arcuate Anterior Segment Left	1.43E-09	-6.051881
183	rs7935166	11	44636547	intronic	A	G	0.133	4.43E-41	3.00E-01	CD82	MD Uncinate Right	2.24E-20	-9.250391
183	rs7935166	11	44636547	intronic	A	G	0.133	4.43E-41	3.00E-01	CD82	MD Inferior Fronto Occipital fasciculus Right	4.86E-09	-5.851793
183	rs7935166	11	44636547	intronic	A	G	0.133	4.43E-41	3.00E-01	CD82	L3 Superior Londgitudinal Fasciculus III Right	3.09E-08	-5.536238
183	rs7935166	11	44636547	intronic	A	G	0.133	4.43E-41	3.00E-01	CD82	ICVF Arcuate Posterior Segment Right	9.76E-09	5.734837
183	rs7935166	11	44636547	intronic	A	G	0.133	4.43E-41	3.00E-01	CD82	MD Corpus callosum	9.04E-12	-6.821042
183	rs7935166	11	44636547	intronic	A	G	0.133	4.43E-41	3.00E-01	CD82	MD Fronto Insular tract3 Right	1.22E-09	-6.077554
183	rs7935166	11	44636547	intronic	A	G	0.133	4.43E-41	3.00E-01	CD82	MD Superior Londgitudinal Fasciculus III Left	5.43E-10	-6.206237
183	rs7935166	11	44636547	intronic	A	G	0.133	4.43E-41	3.00E-01	CD82	L1 Frontal Superior Longitudinal Left	1.56E-08	-5.655115
183	rs7935166	11	44636547	intronic	A	G	0.133	4.43E-41	3.00E-01	CD82	ICVF Inferior Fronto Occipital fasciculus Left	2.19E-10	6.347123
183	rs7935166	11	44636547	intronic	A	G	0.133	4.43E-41	3.00E-01	CD82	L1 Superior Londgitudinal Fasciculus II Left	5.04E-10	-6.217701
183	rs7935166	11	44636547	intronic	A	G	0.133	4.43E-41	3.00E-01	CD82	L1 Fronto Insular tract3 Right	4.62E-12	-6.916677
183	rs7935166	11	44636547	intronic	A	G	0.133	4.43E-41	3.00E-01	CD82	ICVF Frontal Aslant Tract Right	3.16E-09	5.922854
183	rs7935166	11	44636547	intronic	A	G	0.133	4.43E-41	3.00E-01	CD82	L1 Arcuate Posterior Segment Left	5.21E-13	-7.219803
183	rs7935166	11	44636547	intronic	A	G	0.133	4.43E-41	3.00E-01	CD82	MD Fronto Insular tract2 Left	1.44E-11	-6.754264
183	rs7935166	11	44636547	intronic	A	G	0.133	4.43E-41	3.00E-01	CD82	MD Arcuate Posterior Segment Right	8.39E-09	-5.760334
183	rs7935166	11	44636547	intronic	A	G	0.133	4.43E-41	3.00E-01	CD82	L2 Uncinate Right	1.64E-14	-7.675854
183	rs7935166	11	44636547	intronic	A	G	0.133	4.43E-41	3.00E-01	CD82	L2 Corpus callosum	7.20E-10	-6.161658
183	rs7935166	11	44636547	intronic	A	G	0.133	4.43E-41	3.00E-01	CD82	L1 Uncinate Left	2.74E-21	-9.472294
183	rs7935166	11	44636547	intronic	A	G	0.133	4.43E-41	3.00E-01	CD82	L2 Superior Londgitudinal Fasciculus III Right	1.88E-11	-6.715219
183	rs7935166	11	44636547	intronic	A	G	0.133	4.43E-41	3.00E-01	CD82	L1 Uncinate Right	1.83E-21	-9.514327
183	rs7935166	11	44636547	intronic	A	G	0.133	4.43E-41	3.00E-01	CD82	L2 Frontal Aslant Tract Left	5.24E-12	-6.899039
183	rs7935166	11	44636547	intronic	A	G	0.133	4.43E-41	3.00E-01	CD82	L2 Superior Londgitudinal Fasciculus III Left	3.61E-08	-5.508933
183	rs7935166	11	44636547	intronic	A	G	0.133	4.43E-41	3.00E-01	CD82	L3 Inferior Fronto Occipital fasciculus Left	7.83E-12	-6.841568
183	rs7935166	11	44636547	intronic	A	G	0.133	4.43E-41	3.00E-01	CD82	L1 Arcuate Long Segment Left	1.80E-08	-5.630673
183	rs7935166	11	44636547	intronic	A	G	0.133	4.43E-41	3.00E-01	CD82	ICVF Frontal Aslant Tract Left	1.84E-08	5.626633
183	rs7935166	11	44636547	intronic	A	G	0.133	4.43E-41	3.00E-01	CD82	MD Frontal Aslant Tract Left	2.74E-13	-7.306380
183	rs7935166	11	44636547	intronic	A	G	0.133	4.43E-41	3.00E-01	CD82	L1 Superior Londgitudinal Fasciculus II Right	3.19E-10	-6.289041
183	rs7935166	11	44636547	intronic	A	G	0.133	4.43E-41	3.00E-01	CD82	MD Fronto Insular tract4 Right	1.60E-11	-6.738610
183	rs7935166	11	44636547	intronic	A	G	0.133	4.43E-41	3.00E-01	CD82	ICVF Frontal Superior Longitudinal Right	3.69E-09	5.897623
183	rs7935166	11	44636547	intronic	A	G	0.133	4.43E-41	3.00E-01	CD82	MD Arcuate Anterior Segment Left	4.63E-10	-6.231158
183	rs7935166	11	44636547	intronic	A	G	0.133	4.43E-41	3.00E-01	CD82	L1 Superior Londgitudinal Fasciculus III Right	2.47E-13	-7.320760
183	rs7935166	11	44636547	intronic	A	G	0.133	4.43E-41	3.00E-01	CD82	MD Superior Londgitudinal Fasciculus II Left	1.76E-08	-5.634188
183	rs7935166	11	44636547	intronic	A	G	0.133	4.43E-41	3.00E-01	CD82	L1 Frontal Aslant Tract Left	1.49E-12	-7.075807
183	rs7935166	11	44636547	intronic	A	G	0.133	4.43E-41	3.00E-01	CD82	L2 Inferior Fronto Occipital fasciculus Left	4.50E-10	-6.235694
183	rs7935166	11	44636547	intronic	A	G	0.133	4.43E-41	3.00E-01	CD82	ICVF Arcuate Posterior Segment Left	2.88E-08	5.548351
183	rs7935166	11	44636547	intronic	A	G	0.133	4.43E-41	3.00E-01	CD82	L2 Uncinate Left	1.33E-17	-8.541140
183	rs7935166	11	44636547	intronic	A	G	0.133	4.43E-41	3.00E-01	CD82	ICVF Fronto Insular tract5 Left	4.61E-15	7.837180
183	rs7935166	11	44636547	intronic	A	G	0.133	4.43E-41	3.00E-01	CD82	L3 Inferior Longitudinal Left	2.40E-09	-5.968362
183	rs7935166	11	44636547	intronic	A	G	0.133	4.43E-41	3.00E-01	CD82	L3 Uncinate Left	4.61E-16	-8.121341

Genomic Locus	Lead SNP	chr	Position	Functional category	Non-effect allele	Effect allele	MAF	mvgwasP (discovery -British-)	mvgwasP (replication -non British-)	Nearest gene	Central endophenotypes	univariate P value	univariate Z
183	rs7935166	11	44636547	intronic	A	G	0.133	4.43E-41	3.00E-01	CD82	ICVF Inferior Longitudinal Right	1.69E-09	6.025463
183	rs7935166	11	44636547	intronic	A	G	0.133	4.43E-41	3.00E-01	CD82	ICVF Fronto Insular tract2 Left	3.08E-11	6.642601
183	rs7935166	11	44636547	intronic	A	G	0.133	4.43E-41	3.00E-01	CD82	L2 Superior Londgitudinal Fasciculus I Left	2.18E-08	-5.597317
183	rs7935166	11	44636547	intronic	A	G	0.133	4.43E-41	3.00E-01	CD82	MD Arcuate Posterior Segment Left	8.22E-11	-6.496578
183	rs7935166	11	44636547	intronic	A	G	0.133	4.43E-41	3.00E-01	CD82	ICVF Arcuate Anterior Segment Left	6.55E-09	5.801954
183	rs7935166	11	44636547	intronic	A	G	0.133	4.43E-41	3.00E-01	CD82	L1 Superior Londgitudinal Fasciculus I Right	1.25E-12	-7.100267
183	rs7935166	11	44636547	intronic	A	G	0.133	4.43E-41	3.00E-01	CD82	MD Superior Londgitudinal Fasciculus I Right	3.05E-12	-6.975488
183	rs7935166	11	44636547	intronic	A	G	0.133	4.43E-41	3.00E-01	CD82	OD Uncinate Right	1.41E-11	6.756473
183	rs7935166	11	44636547	intronic	A	G	0.133	4.43E-41	3.00E-01	CD82	L3 Uncinate Right	9.80E-15	-7.741835
183	rs7935166	11	44636547	intronic	A	G	0.133	4.43E-41	3.00E-01	CD82	ICVF Fronto Insular tract1 Right	1.27E-08	5.690148
183	rs7935166	11	44636547	intronic	A	G	0.133	4.43E-41	3.00E-01	CD82	L2 Frontal Aslant Tract Right	6.15E-10	-6.186447
183	rs7935166	11	44636547	intronic	A	G	0.133	4.43E-41	3.00E-01	CD82	L2 Arcuate Long Segment Right	2.40E-08	-5.580369
183	rs7935166	11	44636547	intronic	A	G	0.133	4.43E-41	3.00E-01	CD82	L2 Fronto Insular tract4 Right	4.54E-09	-5.863335
183	rs7935166	11	44636547	intronic	A	G	0.133	4.43E-41	3.00E-01	CD82	L2 Inferior Longitudinal Right	3.28E-09	-5.916980
183	rs7935166	11	44636547	intronic	A	G	0.133	4.43E-41	3.00E-01	CD82	L1 Superior Londgitudinal Fasciculus III Left	2.11E-11	-6.698349
183	rs7935166	11	44636547	intronic	A	G	0.133	4.43E-41	3.00E-01	CD82	L1 Frontal Aslant Tract Right	1.58E-11	-6.740627
183	rs7935166	11	44636547	intronic	A	G	0.133	4.43E-41	3.00E-01	CD82	L1 Corpus callosum	6.35E-16	-8.082476
183	rs7935166	11	44636547	intronic	A	G	0.133	4.43E-41	3.00E-01	CD82	MD Arcuate Long Segment Left	4.19E-08	-5.482443
183	rs7935166	11	44636547	intronic	A	G	0.133	4.43E-41	3.00E-01	CD82	ICVF Uncinate Right	2.31E-19	8.997533
183	rs7935166	11	44636547	intronic	A	G	0.133	4.43E-41	3.00E-01	CD82	L3 Superior Londgitudinal Fasciculus I Right	4.77E-08	-5.459506
183	rs7935166	11	44636547	intronic	A	G	0.133	4.43E-41	3.00E-01	CD82	ICVF Uncinate Left	2.40E-20	9.242638
183	rs7935166	11	44636547	intronic	A	G	0.133	4.43E-41	3.00E-01	CD82	ICVF Inferior Longitudinal Left	1.54E-10	6.401334
183	rs7935166	11	44636547	intronic	A	G	0.133	4.43E-41	3.00E-01	CD82	MD Uncinate Left	1.06E-22	-9.806170
183	rs7935166	11	44636547	intronic	A	G	0.133	4.43E-41	3.00E-01	CD82	L2 Arcuate Posterior Segment Right	1.65E-08	-5.645565
183	rs7935166	11	44636547	intronic	A	G	0.133	4.43E-41	3.00E-01	CD82	MD Superior Londgitudinal Fasciculus III Right	5.68E-12	-6.887526
183	rs7935166	11	44636547	intronic	A	G	0.133	4.43E-41	3.00E-01	CD82	MD Inferior Fronto Occipital fasciculus Left	1.24E-13	-7.412484
183	rs7935166	11	44636547	intronic	A	G	0.133	4.43E-41	3.00E-01	CD82	L2 Arcuate Posterior Segment Left	2.59E-08	-5.566814
183	rs7935166	11	44636547	intronic	A	G	0.133	4.43E-41	3.00E-01	CD82	MD Superior Londgitudinal Fasciculus I Left	1.98E-12	-7.035870
183	rs7935166	11	44636547	intronic	A	G	0.133	4.43E-41	3.00E-01	CD82	L1 Superior Londgitudinal Fasciculus I Left	4.95E-11	-6.572323
185	rs57630229	11	82409631	ncRNA intronic	A	G	0.113	4.35E-08	3.58E-01	RP11-179A16.1	ICVF Superior Londgitudinal Fasciculus II Right	4.56E-09	-5.862409
185	rs57630229	11	82409631	ncRNA intronic	A	G	0.113	4.35E-08	3.58E-01	RP11-179A16.1	ICVF Arcuate Anterior Segment Right	8.88E-09	-5.750896
185	rs57630229	11	82409631	ncRNA intronic	A	G	0.113	4.35E-08	3.58E-01	RP11-179A16.1	ICVF Inferior Fronto Occipital fasciculus Right	3.89E-11	-6.608027
185	rs57630229	11	82409631	ncRNA intronic	A	G	0.113	4.35E-08	3.58E-01	RP11-179A16.1	ICVF Corpus callosum	5.59E-10	-6.201643
185	rs57630229	11	82409631	ncRNA intronic	A	G	0.113	4.35E-08	3.58E-01	RP11-179A16.1	ICVF Arcuate Posterior Segment Right	4.63E-08	-5.464835
185	rs57630229	11	82409631	ncRNA intronic	A	G	0.113	4.35E-08	3.58E-01	RP11-179A16.1	ICVF Inferior Fronto Occipital fasciculus Left	7.78E-09	-5.773175
185	rs57630229	11	82409631	ncRNA intronic	A	G	0.113	4.35E-08	3.58E-01	RP11-179A16.1	ICVF Superior Londgitudinal Fasciculus II Left	2.95E-09	-5.934521
185	rs57630229	11	82409631	ncRNA intronic	A	G	0.113	4.35E-08	3.58E-01	RP11-179A16.1	ICVF Arcuate Long Segment Right	1.29E-09	-6.068043
185	rs57630229	11	82409631	ncRNA intronic	A	G	0.113	4.35E-08	3.58E-01	RP11-179A16.1	ICVF Inferior Longitudinal Right	3.38E-11	-6.628824
185	rs57630229	11	82409631	ncRNA intronic	A	G	0.113	4.35E-08	3.58E-01	RP11-179A16.1	ICVF Arcuate Anterior Segment Left	1.16E-10	-6.443883
185	rs57630229	11	82409631	ncRNA intronic	A	G	0.113	4.35E-08	3.58E-01	RP11-179A16.1	ICVF Superior Londgitudinal Fasciculus I Right	3.80E-10	-6.261879
185	rs57630229	11	82409631	ncRNA intronic	A	G	0.113	4.35E-08	3.58E-01	RP11-179A16.1	ICVF Superior Londgitudinal Fasciculus I Left	1.73E-11	-6.727402
185	rs57630229	11	82409631	ncRNA intronic	A	G	0.113	4.35E-08	3.58E-01	RP11-179A16.1	ICVF Uncinate Right	8.05E-09	-5.767369
185	rs57630229	11	82409631	ncRNA intronic	A	G	0.113	4.35E-08	3.58E-01	RP11-179A16.1	ICVF Inferior Longitudinal Left	8.25E-13	-7.156860
185	rs57630229	11	82409631	ncRNA intronic	A	G	0.113	4.35E-08	3.58E-01	RP11-179A16.1	ICVF Superior Londgitudinal Fasciculus III Left	9.75E-09	-5.734947
187	rs11020080	11	92578985	intronic	A	G	0.387	9.29E-12	7.11E-02	FAT3	MO Frontal Aslant Tract Left	1.19E-10	6.440155
187	rs11020080	11	92578985	intronic	A	G	0.387	9.29E-12	7.11E-02	FAT3	MO Frontal Aslant Tract Right	3.32E-11	6.631689
191	rs636406	11	114031092	intronic	G	C	0.358	2.80E-09	6.12E-01	ZBTB16	ICVF Fronto Insular tract4 Right	5.40E-09	-5.834258
191	rs636406	11	114031092	intronic	G	C	0.358	2.80E-09	6.12E-01	ZBTB16	OD Corpus callosum	4.21E-10	-6.246028
193	rs10841784	12	21441577	intronic	C	T	0.283	9.57E-09	5.77E-01	SLCO1A2	MO Frontal Aslant Tract Left	3.11E-08	5.534957
195	rs7305286	12	28282047	intergenic	G	A	0.307	3.24E-17	4.99E-04	CCDC91	OD Inferior Fronto Occipital fasciculus Right	1.90E-08	-5.620547
199	rs10876870	12	56478002	intronic	C	A	0.425	4.56E-09	2.20E-01	ERBB3	ICVF Arcuate Posterior Segment Left	1.20E-08	-5.700107
202	rs4479056	12	79938856	ncRNA intronic	A	G	0.307	3.57E-34	3.65E-01	RP11-359M6.1	FA Frontal Superior Longitudinal Right	1.97E-09	6.000019
202	rs4479056	12	79938856	ncRNA intronic	A	G	0.307	3.57E-34	3.65E-01	RP11-359M6.1	MD Arcuate Anterior Segment Left	4.71E-08	-5.461994
202	rs4479056	12	79938856	ncRNA intronic	A	G	0.307	3.57E-34	3.65E-01	RP11-359M6.1	L2 Arcuate Anterior Segment Left	2.59E-08	-5.566930
202	rs4479056	12	79938856	ncRNA intronic	A	G	0.307	3.57E-34	3.65E-01	RP11-359M6.1	L3 Frontal Superior Longitudinal Right	1.09E-09	-6.095297
203	rs77436242	12	99640159	exonic	C	G	0.048	3.03E-10	5.36E-01	ANKS1B	OD Arcuate Long Segment Right	1.03E-08	-5.726373
204	rs12146713	12	106476805	intronic	C	T	0.096	7.00E-35	1.99E-01	NUAK1	MO Frontal Aslant Tract Left	2.42E-19	-8.992431
204	rs12146713	12	106476805	intronic	C	T	0.096	7.00E-35	1.99E-01	NUAK1	FA Frontal Aslant Tract Left	4.92E-13	-7.227460
204	rs12146713	12	106476805	intronic	C	T	0.096	7.00E-35	1.99E-01	NUAK1	OD Frontal Aslant Tract Right	1.66E-15	7.964608
204	rs12146713	12	106476805	intronic	C	T	0.096	7.00E-35	1.99E-01	NUAK1	OD Frontal Aslant Tract Left	5.44E-18	8.643663
204	rs12146713	12	106476805	intronic	C	T	0.096	7.00E-35	1.99E-01	NUAK1	MO Frontal Aslant Tract Right	2.09E-17	-8.488629
204	rs12146713	12	106476805	intronic	C	T	0.096	7.00E-35	1.99E-01	NUAK1	FA Frontal Aslant Tract Right	6.60E-13	-7.187463
204	rs12146713	12	106476805	intronic	C	T	0.096	7.00E-35	1.99E-01	NUAK1	FA Fronto Insular tract3 Right	1.01E-08	-5.729880
204	rs12146713	12	106476805	intronic	C	T	0.096	7.00E-35	1.99E-01	NUAK1	OD Fronto Insular tract2 Left	3.24E-09	5.919036
205	rs536700128	12	107063485	intronic	GA	G	0.243	1.13E-13	3.57E-01	RP11-144F15.1:RFX4	ICVF Inferior Longitudinal Right	1.44E-08	-5.668403
205	rs536700128	12	107063485	intronic	GA	G	0.243	1.13E-13	3.57E-01	RP11-144F15.1:RFX4	ICVF Inferior Longitudinal Left	6.48E-09	-5.803986
206	rs11114035	12	109102983	intronic	A	T	0.438	1.01E-08	8.17E-01	CORO1C	MO Superior Londgitudinal Fasciculus I Left	5.72E-11	-6.550892
207	rs7137828	12	111932800	intronic	T	C	0.484	2.99E-29	6.03E-01	ATXN2	ISOVF Arcuate Anterior Segment Left	1.00E-08	-5.729885
207	rs7137828	12	111932800	intronic	T	C	0.484	2.99E-29	6.03E-01	ATXN2	ISOVF Arcuate Anterior Segment Right	1.59E-08	-5.651534
207	rs10219716	12	112503474	ncRNA exonic	A	T	0.085	1.60E-09	3.98E-01	NAA25:RP1-267L14.3	OD Inferior Fronto Occipital fasciculus Left	2.86E-09	5.939208
208	rs9739560	12	118461574	intronic	A	T	0.418	3.29E-17	1.33E-01	RFC5	ISOVF Inferior Fronto Occipital fasciculus Left	5.08E-13	7.223065
208	rs9739560	12	118461574	intronic	A	T	0.418	3.29E-17	1.33E-01	RFC5	ICVF Superior Londgitudinal Fasciculus II Right	4.43E-17	8.400980
208	rs9739560	12	118461574	intronic	A	T	0.418	3.29E-17	1.33E-01	RFC5	ICVF Arcuate Anterior Segment Right	4.09E-18	8.676232
208	rs9739560	12	118461574	intronic	A	T	0.418	3.29E-17	1.33E-01	RFC5	ICVF Arcuate Long Segment Left	1.02E-14	7.736411
208	rs9739560	12	118461574	intronic	A	T	0.418	3.29E-17	1.33E-01	RFC5	ISOVF Inferior Longitudinal Right	6.62E-15	7.791568
208	rs9739560	12	118461574	intronic	A	T	0.418	3.29E-17	1.33E-01	RFC5	L3 Superior Londgitudinal Fasciculus I Left	4.48E-10	-6.236474
208	rs9739560	12	118461574	intronic	A	T	0.418	3.29E-17	1.33E-01	RFC5	FA Superior Londgitudinal Fasciculus I Left	1.09E-09	6.095569
208	rs9739560	12	118461574	intronic	A	T	0.418	3.29E-17	1.33E-01	RFC5	ICVF Inferior Fronto Occipital fasciculus Right	8.70E-18	8.589965
208	rs9739560	12	118461574	intronic	A	T	0.418	3.29E-17	1.33E-01	RFC5	ICVF Corpus callosum	2.07E-17	8.489798
208	rs9739560	12	118461574	intronic	A	T	0.418	3.29E-17	1.33E-01	RFC5	ICVF Arcuate Posterior Segment Right	4.28E-13	7.246513
208	rs9739560	12	118461574	intronic	A	T	0.418	3.29E-17	1.33E-01	RFC5	ISOVF Inferior Fronto Occipital fasciculus Right	2.54E-15	7.911853
208	rs9739560	12	118461574	intronic	A	T	0.418	3.29E-17	1.33E-01	RFC5	ISOVF Inferior Longitudinal Left	1.03E-12	7.126878
208	rs9739560	12	118461574	intronic	A	T	0.418	3.29E-17	1.33E-01	RFC5	ICVF Inferior Fronto Occipital fasciculus Left	7.01E-16	8.070367
208	rs9739560	12	118461574	intronic	A	T	0.418	3.29E-17	1.33E-01	RFC5	ICVF Frontal Aslant Tract Right	6.38E-11	6.534641
208	rs9739560	12	118461574	intronic	A	T	0.418	3.29E-17	1.33E-01	RFC5	ICVF Superior Londgitudinal Fasciculus II Left	1.31E-15	7.993908
208	rs9739560	12	118461574	intronic	A	T	0.418	3.29E-17	1.33E-01	RFC5	L3 Inferior Fronto Occipital fasciculus Right	1.80E-08	-5.630211
208	rs9739560	12	118461574	intronic	A	T	0.418	3.29E-17	1.33E-01	RFC5	ICVF Frontal Aslant Tract Left	3.46E-11	6.625414
208	rs9739560	12	118461574	intronic	A	T	0.418	3.29E-17	1.33E-01	RFC5	ICVF Superior Londgitudinal Fasciculus III Right	2.90E-13	7.299065
208	rs9739560	12	118461574	intronic	A	T	0.418	3.29E-17	1.33E-01	RFC5	ICVF Frontal Superior Longitudinal Right	8.57E-09	5.756766
208	rs9739560	12	118461574	intronic	A	T	0.418	3.29E-17	1.33E-01	RFC5	ICVF Arcuate Posterior Segment Left	1.85E-11	6.717327
208	rs9739560	12	118461574	intronic	A	T	0.418	3.29E-17	1.33E-01	RFC5	ICVF Arcuate Long Segment Right	8.09E-18	8.598315
208	rs9739560	12	118461574	intronic	A	T	0.418	3.29E-17	1.33E-01	RFC5	ICVF Inferior Longitudinal Right	1.34E-18	8.801924
208	rs9739560	12	118461574	intronic	A	T	0.418	3.29E-17	1.33E-01	RFC5	L3 Arcuate Long Segment Right	1.38E-08	-5.676084
208	rs9739560	12	118461574	intronic	A	T	0.418	3.29E-17	1.33E-01	RFC5	ICVF Arcuate Anterior Segment Left	1.05E-10	6.459120

Genomic Locus	Lead SNP	chr	Position	Functional category	Non-effect allele	Effect allele	MAF	mvgwasP (discovery -British-)	mvgwasP (replication -non British-)	Nearest gene	Central endophenotypes	univariate P value	univariate Z
208	rs9739560	12	118461574	intronic	A	T	0.418	3.29E-17	1.33E-01	RFC5	ICVF Superior Londgitudinal Fasciculus I Right	7.26E-21	9.369839
208	rs9739560	12	118461574	intronic	A	T	0.418	3.29E-17	1.33E-01	RFC5	ICVF Superior Londgitudinal Fasciculus I Left	1.43E-21	9.540087
208	rs9739560	12	118461574	intronic	A	T	0.418	3.29E-17	1.33E-01	RFC5	FA Superior Londgitudinal Fasciculus I Right	1.60E-08	5.649961
208	rs9739560	12	118461574	intronic	A	T	0.418	3.29E-17	1.33E-01	RFC5	L3 Superior Londgitudinal Fasciculus I Right	8.81E-10	-6.129682
208	rs9739560	12	118461574	intronic	A	T	0.418	3.29E-17	1.33E-01	RFC5	ICVF Inferior Longitudinal Left	3.41E-18	8.696955
208	rs9739560	12	118461574	intronic	A	T	0.418	3.29E-17	1.33E-01	RFC5	ICVF Superior Londgitudinal Fasciculus III Left	8.55E-12	6.828963
208	rs9739560	12	118461574	intronic	A	T	0.418	3.29E-17	1.33E-01	RFC5	ISOVF Arcuate Long Segment Right	1.34E-08	5.681119
208	rs9739560	12	118461574	intronic	A	T	0.418	3.29E-17	1.33E-01	RFC5	L3 Inferior Longitudinal Right	3.32E-08	-5.523523
208	rs9739560	12	118461574	intronic	A	T	0.418	3.29E-17	1.33E-01	RFC5	ICVF Frontal Inferior longitudinal Right	7.77E-09	5.773470
215	rs11838776	13	111040681	intronic	A	G	0.277	3.42E-10	2.91E-03	COL4A2	L1 Fronto Insular tract5 Right	9.24E-09	-5.744197
218	rs160459	14	59074136	intergenic	C	A	0.459	4.19E-31	5.26E-01	DACT1	OD Arcuate Posterior Segment Right	1.04E-10	6.460670
218	rs160459	14	59074136	intergenic	C	A	0.459	4.19E-31	5.26E-01	DACT1	MO Inferior Fronto Occipital fasciculus Right	5.96E-12	-6.880632
218	rs160459	14	59074136	intergenic	C	A	0.459	4.19E-31	5.26E-01	DACT1	OD Inferior Fronto Occipital fasciculus Left	4.44E-11	6.588698
218	rs160459	14	59074136	intergenic	C	A	0.459	4.19E-31	5.26E-01	DACT1	MO Inferior Fronto Occipital fasciculus Left	6.60E-13	-7.187519
218	rs160459	14	59074136	intergenic	C	A	0.459	4.19E-31	5.26E-01	DACT1	FA Arcuate Posterior Segment Left	3.30E-12	-6.964461
218	rs160459	14	59074136	intergenic	C	A	0.459	4.19E-31	5.26E-01	DACT1	OD Arcuate Posterior Segment Left	1.17E-13	7.419671
218	rs160459	14	59074136	intergenic	C	A	0.459	4.19E-31	5.26E-01	DACT1	FA Arcuate Posterior Segment Right	6.96E-10	-6.166933
222	rs7142211	14	91910995	intergenic	A	G	0.443	4.74E-08	4.17E-01	SMEK1	MO Corpus callosum	1.18E-08	5.703206
224	rs355522344	14	100283856	intronic	T	C	0.382	2.60E-23	3.21E-01	EML1	FA Fronto Insular tract1 Right	4.66E-08	5.463867
227	rs5812099	15	39633877	ncRNA intronic	AG	A	0.090	2.15E-171	2.63E-06	RP11-624L4.1	L2 Frontal Inferior longitudinal Right	5.68E-09	-5.825873
227	rs5812099	15	39633877	ncRNA intronic	AG	A	0.090	2.15E-171	2.63E-06	RP11-624L4.1	MO Arcuate Anterior Segment Right	1.25E-10	6.433193
227	rs5812099	15	39633877	ncRNA intronic	AG	A	0.090	2.15E-171	2.63E-06	RP11-624L4.1	L1 Arcuate Anterior Segment Left	6.52E-15	7.793374
227	rs5812099	15	39633877	ncRNA intronic	AG	A	0.090	2.15E-171	2.63E-06	RP11-624L4.1	L1 Superior Londgitudinal Fasciculus II Left	4.70E-09	-5.857297
227	rs5812099	15	39633877	ncRNA intronic	AG	A	0.090	2.15E-171	2.63E-06	RP11-624L4.1	FA Arcuate Anterior Segment Left	2.83E-28	11.026975
227	rs5812099	15	39633877	ncRNA intronic	AG	A	0.090	2.15E-171	2.63E-06	RP11-624L4.1	OD Arcuate Anterior Segment Left	1.67E-67	-17.359497
227	rs5812099	15	39633877	ncRNA intronic	AG	A	0.090	2.15E-171	2.63E-06	RP11-624L4.1	OD Arcuate Anterior Segment Right	4.89E-14	-7.534763
227	rs5812099	15	39633877	ncRNA intronic	AG	A	0.090	2.15E-171	2.63E-06	RP11-624L4.1	L2 Arcuate Anterior Segment Left	2.05E-27	-10.847632
227	rs5812099	15	39633877	ncRNA intronic	AG	A	0.090	2.15E-171	2.63E-06	RP11-624L4.1	MO Arcuate Anterior Segment Left	5.17E-53	15.325490
229	rs12438742	15	61947280	ncRNA intronic	G	C	0.429	1.36E-08	2.57E-01	RP11-507B12.1	MD Fronto Insular tract1 Left	1.48E-10	-6.407499
229	rs12438742	15	61947280	ncRNA intronic	G	C	0.429	1.36E-08	2.57E-01	RP11-507B12.1	ISOVF Superior Londgitudinal Fasciculus II Left	8.12E-09	-5.766015
229	rs12438742	15	61947280	ncRNA intronic	G	C	0.429	1.36E-08	2.57E-01	RP11-507B12.1	ICVF Fronto Insular tract1 Left	5.11E-09	5.843706
229	rs12438742	15	61947280	ncRNA intronic	G	C	0.429	1.36E-08	2.57E-01	RP11-507B12.1	L2 Fronto Insular tract1 Left	3.05E-11	-6.644206
229	rs12438742	15	61947280	ncRNA intronic	G	C	0.429	1.36E-08	2.57E-01	RP11-507B12.1	L3 Fronto Insular tract1 Left	3.29E-12	-6.964846
229	rs12438742	15	61947280	ncRNA intronic	G	C	0.429	1.36E-08	2.57E-01	RP11-507B12.1	L3 Uncinate Right	3.85E-08	-5.497742
233	rs2342118	15	85693016	intergenic	A	G	0.325	7.28E-30	1.84E-03	PDE8A	L1 Fronto Insular tract1 Left	8.81E-11	6.486072
233	rs2342118	15	85693016	intergenic	A	G	0.325	7.28E-30	1.84E-03	PDE8A	ISOVF Arcuate Anterior Segment Left	9.15E-10	-6.123517
233	rs2342118	15	85693016	intergenic	A	G	0.325	7.28E-30	1.84E-03	PDE8A	MD Fronto Insular tract1 Left	4.24E-11	6.595551
233	rs2342118	15	85693016	intergenic	A	G	0.325	7.28E-30	1.84E-03	PDE8A	ICVF Fronto Insular tract1 Left	5.34E-12	-6.896238
233	rs2342118	15	85693016	intergenic	A	G	0.325	7.28E-30	1.84E-03	PDE8A	L2 Fronto Insular tract1 Left	3.56E-10	6.272156
233	rs2342118	15	85693016	intergenic	A	G	0.325	7.28E-30	1.84E-03	PDE8A	L3 Fronto Insular tract1 Left	1.51E-08	5.660958
235	rs6224	15	91423543	intronic	T	G	0.475	9.79E-16	6.63E-01	FURIN	OD Superior Londgitudinal Fasciculus II Left	1.75E-09	6.019806
240	rs1948948	16	51442679	intergenic	T	C	0.438	3.49E-53	5.03E-04	RP11-437L7.1	MD Inferior Longitudinal Left	1.57E-12	-7.067952
240	rs1948948	16	51442679	intergenic	T	C	0.438	3.49E-53	5.03E-04	RP11-437L7.1	L3 Frontal Aslant Tract Right	1.28E-08	-5.688487
240	rs1948948	16	51442679	intergenic	T	C	0.438	3.49E-53	5.03E-04	RP11-437L7.1	ISOVF Frontal Aslant Tract Left	4.19E-31	-11.598536
240	rs1948948	16	51442679	intergenic	T	C	0.438	3.49E-53	5.03E-04	RP11-437L7.1	ISOVF Inferior Fronto Occipital fasciculus Left	1.89E-34	-12.240321
240	rs1948948	16	51442679	intergenic	T	C	0.438	3.49E-53	5.03E-04	RP11-437L7.1	ISOVF Superior Londgitudinal Fasciculus II Right	3.60E-19	-8.948692
240	rs1948948	16	51442679	intergenic	T	C	0.438	3.49E-53	5.03E-04	RP11-437L7.1	L1 Inferior Longitudinal Left	1.19E-13	-7.417851
240	rs1948948	16	51442679	intergenic	T	C	0.438	3.49E-53	5.03E-04	RP11-437L7.1	L3 Fronto Insular tract2 Right	6.92E-14	-7.489465
240	rs1948948	16	51442679	intergenic	T	C	0.438	3.49E-53	5.03E-04	RP11-437L7.1	L1 Frontal Superior Longitudinal Right	4.77E-13	-7.231695
240	rs1948948	16	51442679	intergenic	T	C	0.438	3.49E-53	5.03E-04	RP11-437L7.1	ISOVF Frontal Superior Longitudinal Left	3.75E-12	-6.946328
240	rs1948948	16	51442679	intergenic	T	C	0.438	3.49E-53	5.03E-04	RP11-437L7.1	L2 Inferior Longitudinal Left	2.18E-09	-5.983779
240	rs1948948	16	51442679	intergenic	T	C	0.438	3.49E-53	5.03E-04	RP11-437L7.1	ISOVF Frontal Inferior longitudinal Right	6.34E-14	-7.500895
240	rs1948948	16	51442679	intergenic	T	C	0.438	3.49E-53	5.03E-04	RP11-437L7.1	MD Inferior Longitudinal Right	2.40E-09	-5.967835
240	rs1948948	16	51442679	intergenic	T	C	0.438	3.49E-53	5.03E-04	RP11-437L7.1	L1 Inferior Fronto Occipital fasciculus Left	2.41E-08	-5.579727
240	rs1948948	16	51442679	intergenic	T	C	0.438	3.49E-53	5.03E-04	RP11-437L7.1	ISOVF Fronto Insular tract1 Left	8.52E-09	-5.757797
240	rs1948948	16	51442679	intergenic	T	C	0.438	3.49E-53	5.03E-04	RP11-437L7.1	MD Frontal Aslant Tract Right	7.32E-12	-6.851298
240	rs1948948	16	51442679	intergenic	T	C	0.438	3.49E-53	5.03E-04	RP11-437L7.1	ISOVF Fronto Insular tract5 Left	8.32E-09	-5.761852
240	rs1948948	16	51442679	intergenic	T	C	0.438	3.49E-53	5.03E-04	RP11-437L7.1	ISOVF Inferior Longitudinal Right	9.00E-33	-11.922783
240	rs1948948	16	51442679	intergenic	T	C	0.438	3.49E-53	5.03E-04	RP11-437L7.1	ISOVF Superior Londgitudinal Fasciculus III Left	3.03E-36	-12.571383
240	rs1948948	16	51442679	intergenic	T	C	0.438	3.49E-53	5.03E-04	RP11-437L7.1	L2 Fronto Insular tract2 Right	1.10E-09	-6.093798
240	rs1948948	16	51442679	intergenic	T	C	0.438	3.49E-53	5.03E-04	RP11-437L7.1	L1 Fronto Insular tract1 Left	4.81E-15	-7.831842
240	rs1948948	16	51442679	intergenic	T	C	0.438	3.49E-53	5.03E-04	RP11-437L7.1	ISOVF Arcuate Anterior Segment Left	1.18E-27	-10.897984
240	rs1948948	16	51442679	intergenic	T	C	0.438	3.49E-53	5.03E-04	RP11-437L7.1	FA Fronto Insular tract4 Right	1.88E-11	6.714804
240	rs1948948	16	51442679	intergenic	T	C	0.438	3.49E-53	5.03E-04	RP11-437L7.1	MD Fronto Insular tract1 Left	2.84E-20	-9.224957
240	rs1948948	16	51442679	intergenic	T	C	0.438	3.49E-53	5.03E-04	RP11-437L7.1	ISOVF Arcuate Posterior Segment Left	7.24E-27	-10.731527
240	rs1948948	16	51442679	intergenic	T	C	0.438	3.49E-53	5.03E-04	RP11-437L7.1	ISOVF Fronto Insular tract3 Left	4.10E-23	-9.901495
240	rs1948948	16	51442679	intergenic	T	C	0.438	3.49E-53	5.03E-04	RP11-437L7.1	L1 Arcuate Anterior Segment Left	2.78E-08	-5.554983
240	rs1948948	16	51442679	intergenic	T	C	0.438	3.49E-53	5.03E-04	RP11-437L7.1	MD Uncinate Right	4.20E-11	-6.596882
240	rs1948948	16	51442679	intergenic	T	C	0.438	3.49E-53	5.03E-04	RP11-437L7.1	ISOVF Uncinate Left	2.01E-31	-11.661393
240	rs1948948	16	51442679	intergenic	T	C	0.438	3.49E-53	5.03E-04	RP11-437L7.1	ISOVF Frontal Superior Longitudinal Right	3.98E-15	-7.855568
240	rs1948948	16	51442679	intergenic	T	C	0.438	3.49E-53	5.03E-04	RP11-437L7.1	ISOVF Inferior Fronto Occipital fasciculus Right	1.38E-32	-11.886983
240	rs1948948	16	51442679	intergenic	T	C	0.438	3.49E-53	5.03E-04	RP11-437L7.1	MD Corpus callosum	2.31E-09	-5.974549
240	rs1948948	16	51442679	intergenic	T	C	0.438	3.49E-53	5.03E-04	RP11-437L7.1	MD Fronto Insular tract3 Right	7.79E-10	-6.149131
240	rs1948948	16	51442679	intergenic	T	C	0.438	3.49E-53	5.03E-04	RP11-437L7.1	ISOVF Inferior Longitudinal Left	1.09E-34	-12.284741
240	rs1948948	16	51442679	intergenic	T	C	0.438	3.49E-53	5.03E-04	RP11-437L7.1	L3 Fronto Insular tract4 Right	2.21E-13	-7.335303
240	rs1948948	16	51442679	intergenic	T	C	0.438	3.49E-53	5.03E-04	RP11-437L7.1	ISOVF Frontal Aslant Tract Right	5.80E-31	-11.570776
240	rs1948948	16	51442679	intergenic	T	C	0.438	3.49E-53	5.03E-04	RP11-437L7.1	MD Superior Londgitudinal Fasciculus III Left	7.77E-09	-5.773475
240	rs1948948	16	51442679	intergenic	T	C	0.438	3.49E-53	5.03E-04	RP11-437L7.1	L1 Frontal Superior Longitudinal Left	2.48E-17	-8.468582
240	rs1948948	16	51442679	intergenic	T	C	0.438	3.49E-53	5.03E-04	RP11-437L7.1	ISOVF Arcuate Long Segment Left	1.07E-20	-9.328694
240	rs1948948	16	51442679	intergenic	T	C	0.438	3.49E-53	5.03E-04	RP11-437L7.1	L2 Uncinate Right	3.91E-09	-5.888014
240	rs1948948	16	51442679	intergenic	T	C	0.438	3.49E-53	5.03E-04	RP11-437L7.1	ISOVF Superior Londgitudinal Fasciculus II Left	1.84E-17	-8.503740
240	rs1948948	16	51442679	intergenic	T	C	0.438	3.49E-53	5.03E-04	RP11-437L7.1	L1 Uncinate Left	8.62E-13	-7.150984
240	rs1948948	16	51442679	intergenic	T	C	0.438	3.49E-53	5.03E-04	RP11-437L7.1	ISOVF Fronto Insular tract2 Left	2.54E-10	-6.324742
240	rs1948948	16	51442679	intergenic	T	C	0.438	3.49E-53	5.03E-04	RP11-437L7.1	L1 Uncinate Right	4.73E-08	-5.461263
240	rs1948948	16	51442679	intergenic	T	C	0.438	3.49E-53	5.03E-04	RP11-437L7.1	ISOVF Superior Londgitudinal Fasciculus I Left	1.24E-23	-10.020595
240	rs1948948	16	51442679	intergenic	T	C	0.438	3.49E-53	5.03E-04	RP11-437L7.1	L2 Frontal Aslant Tract Left	4.20E-13	-7.248983
240	rs1948948	16	51442679	intergenic	T	C	0.438	3.49E-53	5.03E-04	RP11-437L7.1	ISOVF Superior Londgitudinal Fasciculus I Right	3.50E-24	-10.144611
240	rs1948948	16	51442679	intergenic	T	C	0.438	3.49E-53	5.03E-04	RP11-437L7.1	ICVF Fronto Insular tract1 Left	2.08E-10	6.355411
240	rs1948948	16	51442679	intergenic	T	C	0.438	3.49E-53	5.03E-04	RP11-437L7.1	L2 Superior Londgitudinal Fasciculus III Left	6.63E-09	-5.800040
240	rs1948948	16	51442679	intergenic	T	C	0.438	3.49E-53	5.03E-04	RP11-437L7.1	MD Frontal Aslant Tract Left	1.81E-11	-6.720930

Genomic Locus	Lead SNP	chr	Position	Functional category	Non-effect allele	Effect allele	MAF	mvgwasP (discovery -British-)	mvgwasP (replication -non British-)	Nearest gene	Central endophenotypes	univariate P value	univariate Z
240	rs1948948	16	51442679	intergenic	T	C	0.438	3.49E-53	5.03E-04	RP11-437L7.1	L2 Fronto Insular tract1 Left	3.45E-20	-9.203854
240	rs1948948	16	51442679	intergenic	T	C	0.438	3.49E-53	5.03E-04	RP11-437L7.1	L1 Superior Londgitudinal Fasciculus II Right	2.66E-08	-5.562406
240	rs1948948	16	51442679	intergenic	T	C	0.438	3.49E-53	5.03E-04	RP11-437L7.1	MD Fronto Insular tract4 Right	4.47E-13	-7.240599
240	rs1948948	16	51442679	intergenic	T	C	0.438	3.49E-53	5.03E-04	RP11-437L7.1	MD Frontal Superior Longitudinal Left	2.20E-10	-6.346476
240	rs1948948	16	51442679	intergenic	T	C	0.438	3.49E-53	5.03E-04	RP11-437L7.1	L2 Fronto Insular tract3 Right	4.65E-10	-6.230620
240	rs1948948	16	51442679	intergenic	T	C	0.438	3.49E-53	5.03E-04	RP11-437L7.1	MD Arcuate Anterior Segment Left	2.52E-08	-5.571724
240	rs1948948	16	51442679	intergenic	T	C	0.438	3.49E-53	5.03E-04	RP11-437L7.1	ISOVF Uncinate Right	5.95E-13	-7.201692
240	rs1948948	16	51442679	intergenic	T	C	0.438	3.49E-53	5.03E-04	RP11-437L7.1	L1 Superior Londgitudinal Fasciculus III Right	1.52E-08	-5.658797
240	rs1948948	16	51442679	intergenic	T	C	0.438	3.49E-53	5.03E-04	RP11-437L7.1	L1 Frontal Aslant Tract Left	1.09E-08	-5.716690
240	rs1948948	16	51442679	intergenic	T	C	0.438	3.49E-53	5.03E-04	RP11-437L7.1	L3 Fronto Insular tract1 Left	4.67E-20	-9.171462
240	rs1948948	16	51442679	intergenic	T	C	0.438	3.49E-53	5.03E-04	RP11-437L7.1	L2 Uncinate Left	2.32E-15	-7.922768
240	rs1948948	16	51442679	intergenic	T	C	0.438	3.49E-53	5.03E-04	RP11-437L7.1	L2 Fronto Insular tract3 Left	2.19E-11	-6.692442
240	rs1948948	16	51442679	intergenic	T	C	0.438	3.49E-53	5.03E-04	RP11-437L7.1	L3 Inferior Longitudinal Left	1.51E-08	-5.660341
240	rs1948948	16	51442679	intergenic	T	C	0.438	3.49E-53	5.03E-04	RP11-437L7.1	MD Fronto Insular tract3 Left	1.82E-17	-8.504939
240	rs1948948	16	51442679	intergenic	T	C	0.438	3.49E-53	5.03E-04	RP11-437L7.1	L3 Uncinate Left	1.29E-13	-7.407371
240	rs1948948	16	51442679	intergenic	T	C	0.438	3.49E-53	5.03E-04	RP11-437L7.1	FA Fronto Insular tract3 Right	3.13E-09	5.924379
240	rs1948948	16	51442679	intergenic	T	C	0.438	3.49E-53	5.03E-04	RP11-437L7.1	L1 Inferior Longitudinal Right	3.28E-10	-6.284919
240	rs1948948	16	51442679	intergenic	T	C	0.438	3.49E-53	5.03E-04	RP11-437L7.1	L1 Fronto Insular tract2 Right	1.34E-13	-7.402395
240	rs1948948	16	51442679	intergenic	T	C	0.438	3.49E-53	5.03E-04	RP11-437L7.1	L1 Superior Londgitudinal Fasciculus I Right	4.04E-14	-7.559687
240	rs1948948	16	51442679	intergenic	T	C	0.438	3.49E-53	5.03E-04	RP11-437L7.1	ISOVF Corpus callosum	8.44E-29	-11.135353
240	rs1948948	16	51442679	intergenic	T	C	0.438	3.49E-53	5.03E-04	RP11-437L7.1	ISOVF Fronto Insular tract5 Right	4.21E-14	-7.554257
240	rs1948948	16	51442679	intergenic	T	C	0.438	3.49E-53	5.03E-04	RP11-437L7.1	MD Superior Londgitudinal Fasciculus I Right	3.19E-11	-6.637685
240	rs1948948	16	51442679	intergenic	T	C	0.438	3.49E-53	5.03E-04	RP11-437L7.1	MD Fronto Insular tract1 Right	5.92E-10	-6.192632
240	rs1948948	16	51442679	intergenic	T	C	0.438	3.49E-53	5.03E-04	RP11-437L7.1	L3 Uncinate Right	1.17E-11	-6.783972
240	rs1948948	16	51442679	intergenic	T	C	0.438	3.49E-53	5.03E-04	RP11-437L7.1	ISOVF Arcuate Anterior Segment Right	1.02E-26	-10.700133
240	rs1948948	16	51442679	intergenic	T	C	0.438	3.49E-53	5.03E-04	RP11-437L7.1	L2 Frontal Aslant Tract Right	1.17E-11	-6.783446
240	rs1948948	16	51442679	intergenic	T	C	0.438	3.49E-53	5.03E-04	RP11-437L7.1	ISOVF Fronto Insular tract1 Right	9.15E-18	-8.584225
240	rs1948948	16	51442679	intergenic	T	C	0.438	3.49E-53	5.03E-04	RP11-437L7.1	L2 Fronto Insular tract4 Right	1.64E-14	-7.676052
240	rs1948948	16	51442679	intergenic	T	C	0.438	3.49E-53	5.03E-04	RP11-437L7.1	L1 Fronto Insular tract3 Left	1.38E-08	-5.676036
240	rs1948948	16	51442679	intergenic	T	C	0.438	3.49E-53	5.03E-04	RP11-437L7.1	ISOVF Fronto Insular tract3 Right	8.58E-18	-8.591556
240	rs1948948	16	51442679	intergenic	T	C	0.438	3.49E-53	5.03E-04	RP11-437L7.1	L2 Arcuate Anterior Segment Left	6.97E-09	-5.791714
240	rs1948948	16	51442679	intergenic	T	C	0.438	3.49E-53	5.03E-04	RP11-437L7.1	L1 Superior Londgitudinal Fasciculus III Left	3.50E-09	-5.906023
240	rs1948948	16	51442679	intergenic	T	C	0.438	3.49E-53	5.03E-04	RP11-437L7.1	L1 Frontal Aslant Tract Right	5.33E-10	-6.209126
240	rs1948948	16	51442679	intergenic	T	C	0.438	3.49E-53	5.03E-04	RP11-437L7.1	ISOVF Superior Londgitudinal Fasciculus III Right	2.29E-35	-12.410405
240	rs1948948	16	51442679	intergenic	T	C	0.438	3.49E-53	5.03E-04	RP11-437L7.1	MD Fronto Insular tract2 Right	1.22E-15	-8.002872
240	rs1948948	16	51442679	intergenic	T	C	0.438	3.49E-53	5.03E-04	RP11-437L7.1	L1 Corpus callosum	1.36E-15	-7.989204
240	rs1948948	16	51442679	intergenic	T	C	0.438	3.49E-53	5.03E-04	RP11-437L7.1	L3 Fronto Insular tract3 Right	5.44E-11	-6.558371
240	rs1948948	16	51442679	intergenic	T	C	0.438	3.49E-53	5.03E-04	RP11-437L7.1	ISOVF Fronto Insular tract4 Right	8.86E-20	-9.102043
240	rs1948948	16	51442679	intergenic	T	C	0.438	3.49E-53	5.03E-04	RP11-437L7.1	ISOVF Arcuate Long Segment Right	7.21E-19	-8.871556
240	rs1948948	16	51442679	intergenic	T	C	0.438	3.49E-53	5.03E-04	RP11-437L7.1	MD Uncinate Left	8.28E-17	-8.327213
240	rs1948948	16	51442679	intergenic	T	C	0.438	3.49E-53	5.03E-04	RP11-437L7.1	ISOVF Arcuate Posterior Segment Right	9.54E-27	-10.705966
240	rs1948948	16	51442679	intergenic	T	C	0.438	3.49E-53	5.03E-04	RP11-437L7.1	L3 Fronto Insular tract3 Left	4.99E-11	-6.571171
240	rs1948948	16	51442679	intergenic	T	C	0.438	3.49E-53	5.03E-04	RP11-437L7.1	MD Frontal Superior Longitudinal Right	1.01E-10	-6.465592
240	rs1948948	16	51442679	intergenic	T	C	0.438	3.49E-53	5.03E-04	RP11-437L7.1	ISOVF Fronto Insular tract2 Right	1.22E-19	-9.067351
240	rs1948948	16	51442679	intergenic	T	C	0.438	3.49E-53	5.03E-04	RP11-437L7.1	MD Superior Londgitudinal Fasciculus I Left	3.70E-11	-6.615631
240	rs1948948	16	51442679	intergenic	T	C	0.438	3.49E-53	5.03E-04	RP11-437L7.1	L1 Superior Londgitudinal Fasciculus I Left	2.96E-16	-8.174842
240	16:51495932 CAA C	16	51495932	intergenic	C	CAA	0.362	1.21E-08	5.29E-02	RP11-437L7.1	ISOVF Inferior Longitudinal Right	3.34E-08	5.522509
240	16:51495932 CAA C	16	51495932	intergenic	C	CAA	0.362	1.21E-08	5.29E-02	RP11-437L7.1	ISOVF Superior Londgitudinal Fasciculus III Left	3.33E-08	5.523200
240	16:51495932 CAA C	16	51495932	intergenic	C	CAA	0.362	1.21E-08	5.29E-02	RP11-437L7.1	ISOVF Arcuate Anterior Segment Left	7.09E-09	5.788814
240	16:51495932 CAA C	16	51495932	intergenic	C	CAA	0.362	1.21E-08	5.29E-02	RP11-437L7.1	ISOVF Arcuate Posterior Segment Left	1.95E-08	5.616352
242	rs55845372	16	86606321	intergenic	C	T	0.188	1.25E-09	4.79E-03	FOXL1	MD Uncinate Left	3.18E-08	5.531323
243	rs4843552	16	87233516	intergenic	A	G	0.422	6.18E-105	1.00E-05	C16orf95	MD Inferior Longitudinal Left	1.21E-09	6.078831
243	rs4843552	16	87233516	intergenic	A	G	0.422	6.18E-105	1.00E-05	C16orf95	ISOVF Frontal Aslant Tract Left	1.62E-13	7.377121
243	rs4843552	16	87233516	intergenic	A	G	0.422	6.18E-105	1.00E-05	C16orf95	ISOVF Inferior Fronto Occipital fasciculus Left	9.21E-15	7.749760
243	rs4843552	16	87233516	intergenic	A	G	0.422	6.18E-105	1.00E-05	C16orf95	OD Uncinate Left	2.81E-08	-5.552777
243	rs4843552	16	87233516	intergenic	A	G	0.422	6.18E-105	1.00E-05	C16orf95	ISOVF Superior Londgitudinal Fasciculus II Right	4.90E-12	6.908374
243	rs4843552	16	87233516	intergenic	A	G	0.422	6.18E-105	1.00E-05	C16orf95	L1 Inferior Longitudinal Left	2.71E-13	7.308094
243	rs4843552	16	87233516	intergenic	A	G	0.422	6.18E-105	1.00E-05	C16orf95	MO Frontal Aslant Tract Left	1.29E-08	-5.687231
243	rs4843552	16	87233516	intergenic	A	G	0.422	6.18E-105	1.00E-05	C16orf95	MO Corpus callosum	8.75E-18	8.589240
243	rs4843552	16	87233516	intergenic	A	G	0.422	6.18E-105	1.00E-05	C16orf95	L2 Inferior Longitudinal Left	2.86E-09	5.939563
243	rs4843552	16	87233516	intergenic	A	G	0.422	6.18E-105	1.00E-05	C16orf95	ISOVF Frontal Inferior longitudinal Right	7.76E-13	7.165323
243	rs4843552	16	87233516	intergenic	A	G	0.422	6.18E-105	1.00E-05	C16orf95	ISOVF Inferior Longitudinal Right	6.23E-24	10.088202
243	rs4843552	16	87233516	intergenic	A	G	0.422	6.18E-105	1.00E-05	C16orf95	ISOVF Superior Londgitudinal Fasciculus III Left	2.78E-24	10.167005
243	rs4843552	16	87233516	intergenic	A	G	0.422	6.18E-105	1.00E-05	C16orf95	ISOVF Arcuate Anterior Segment Left	5.91E-14	7.509994
243	rs4843552	16	87233516	intergenic	A	G	0.422	6.18E-105	1.00E-05	C16orf95	OD Corpus callosum	7.16E-17	-8.344282
243	rs4843552	16	87233516	intergenic	A	G	0.422	6.18E-105	1.00E-05	C16orf95	ISOVF Arcuate Posterior Segment Left	1.10E-25	10.477164
243	rs4843552	16	87233516	intergenic	A	G	0.422	6.18E-105	1.00E-05	C16orf95	ISOVF Fronto Insular tract3 Left	7.82E-09	5.772310
243	rs4843552	16	87233516	intergenic	A	G	0.422	6.18E-105	1.00E-05	C16orf95	ISOVF Uncinate Left	2.87E-09	5.938600
243	rs4843552	16	87233516	intergenic	A	G	0.422	6.18E-105	1.00E-05	C16orf95	ISOVF Inferior Fronto Occipital fasciculus Right	2.46E-18	8.733873
243	rs4843552	16	87233516	intergenic	A	G	0.422	6.18E-105	1.00E-05	C16orf95	ISOVF Inferior Longitudinal Left	1.90E-25	10.425342
243	rs4843552	16	87233516	intergenic	A	G	0.422	6.18E-105	1.00E-05	C16orf95	ISOVF Frontal Aslant Tract Right	3.77E-12	6.945392
243	rs4843552	16	87233516	intergenic	A	G	0.422	6.18E-105	1.00E-05	C16orf95	OD Superior Londgitudinal Fasciculus I Left	5.92E-14	-7.509811
243	rs4843552	16	87233516	intergenic	A	G	0.422	6.18E-105	1.00E-05	C16orf95	L1 Inferior Fronto Occipital fasciculus Right	2.13E-10	6.351509
243	rs4843552	16	87233516	intergenic	A	G	0.422	6.18E-105	1.00E-05	C16orf95	MO Uncinate Left	7.01E-09	5.790744
243	rs4843552	16	87233516	intergenic	A	G	0.422	6.18E-105	1.00E-05	C16orf95	ISOVF Arcuate Long Segment Left	4.58E-21	9.418393
243	rs4843552	16	87233516	intergenic	A	G	0.422	6.18E-105	1.00E-05	C16orf95	ISOVF Superior Londgitudinal Fasciculus II Left	4.79E-14	7.537532
243	rs4843552	16	87233516	intergenic	A	G	0.422	6.18E-105	1.00E-05	C16orf95	L1 Uncinate Left	1.25E-12	7.099697
243	rs4843552	16	87233516	intergenic	A	G	0.422	6.18E-105	1.00E-05	C16orf95	ISOVF Superior Londgitudinal Fasciculus I Left	5.68E-12	6.887392
243	rs4843552	16	87233516	intergenic	A	G	0.422	6.18E-105	1.00E-05	C16orf95	ISOVF Superior Londgitudinal Fasciculus I Right	7.15E-11	6.517524
243	rs4843552	16	87233516	intergenic	A	G	0.422	6.18E-105	1.00E-05	C16orf95	L1 Fronto Insular tract1 Right	2.11E-09	5.989119
243	rs4843552	16	87233516	intergenic	A	G	0.422	6.18E-105	1.00E-05	C16orf95	OD Inferior Fronto Occipital fasciculus Left	4.92E-10	-6.221516
243	rs4843552	16	87233516	intergenic	A	G	0.422	6.18E-105	1.00E-05	C16orf95	MO Inferior Fronto Occipital fasciculus Left	7.81E-11	6.504158
243	rs4843552	16	87233516	intergenic	A	G	0.422	6.18E-105	1.00E-05	C16orf95	OD Superior Londgitudinal Fasciculus III Right	2.32E-09	-5.973849
243	rs4843552	16	87233516	intergenic	A	G	0.422	6.18E-105	1.00E-05	C16orf95	MD Fronto Insular tract3 Left	1.80E-09	6.015110
243	rs4843552	16	87233516	intergenic	A	G	0.422	6.18E-105	1.00E-05	C16orf95	L1 Inferior Longitudinal Right	3.13E-10	6.292103
243	rs4843552	16	87233516	intergenic	A	G	0.422	6.18E-105	1.00E-05	C16orf95	ISOVF Fronto Insular tract5 Right	1.07E-08	5.719076
243	rs4843552	16	87233516	intergenic	A	G	0.422	6.18E-105	1.00E-05	C16orf95	OD Inferior Fronto Occipital fasciculus Right	6.86E-10	-6.169381
243	rs4843552	16	87233516	intergenic	A	G	0.422	6.18E-105	1.00E-05	C16orf95	MO Superior Londgitudinal Fasciculus I Left	6.74E-11	6.526415

Genomic Locus	Lead SNP	chr	Position	Functional category	Non-effect allele	Effect allele	MAF	mvgwasP (discovery -British-)	mvgwasP (replication -non British-)	Nearest gene	Central endophenotypes	univariate P value	univariate Z
243	rs4843552	16	87233516	intergenic	A	G	0.422	6.18E-105	1.00E-05	C16orf95	ISOVF Arcuate Anterior Segment Right	2.05E-19	9.010571
243	rs4843552	16	87233516	intergenic	A	G	0.422	6.18E-105	1.00E-05	C16orf95	MO Fronto Insular tract1 Right	5.41E-11	6.559071
243	rs4843552	16	87233516	intergenic	A	G	0.422	6.18E-105	1.00E-05	C16orf95	ISOVF Fronto Insular tract3 Right	1.91E-10	6.368767
243	rs4843552	16	87233516	intergenic	A	G	0.422	6.18E-105	1.00E-05	C16orf95	ISOVF Superior Londgitudinal Fasciculus III Right	6.60E-25	10.306270
243	rs4843552	16	87233516	intergenic	A	G	0.422	6.18E-105	1.00E-05	C16orf95	ISOVF Arcuate Long Segment Right	3.35E-22	9.689214
243	rs4843552	16	87233516	intergenic	A	G	0.422	6.18E-105	1.00E-05	C16orf95	ISOVF Arcuate Posterior Segment Right	1.32E-31	11.697289
243	rs4843552	16	87233516	intergenic	A	G	0.422	6.18E-105	1.00E-05	C16orf95	MO Superior Londgitudinal Fasciculus I Right	1.89E-09	6.007268
243	rs4843552	16	87233516	intergenic	A	G	0.422	6.18E-105	1.00E-05	C16orf95	L1 Superior Londgitudinal Fasciculus I Left	2.04E-10	6.358565
244	rs111398992	16	89992613	intronic	T	G	0.131	1.17E-31	9.85E-04	TUBB3:TUBB3	ICVF Superior Londgitudinal Fasciculus II Left	2.19E-08	-5.596418
244	rs111398992	16	89992613	intronic	T	G	0.131	1.17E-31	9.85E-04	TUBB3:TUBB3	FA Arcuate Long Segment Right	9.41E-09	-5.741011
244	rs111398992	16	89992613	intronic	T	G	0.131	1.17E-31	9.85E-04	TUBB3:TUBB3	FA Arcuate Posterior Segment Right	2.81E-09	-5.942300
244	rs111398992	16	89992613	intronic	T	G	0.131	1.17E-31	9.85E-04	TUBB3:TUBB3	L2 Arcuate Long Segment Right	3.00E-08	5.541514
244	rs111398992	16	89992613	intronic	T	G	0.131	1.17E-31	9.85E-04	TUBB3:TUBB3	FA Superior Londgitudinal Fasciculus II Left	1.85E-10	-6.373403
244	rs111398992	16	89992613	intronic	T	G	0.131	1.17E-31	9.85E-04	TUBB3:TUBB3	L2 Superior Londgitudinal Fasciculus II Left	2.20E-08	5.595579
245	rs2131704	17	1970898	intronic	T	C	0.425	8.01E-19	6.48E-03	SMG6	ISOVF Frontal Aslant Tract Left	4.82E-09	5.853128
245	rs2131704	17	1970898	intronic	T	C	0.425	8.01E-19	6.48E-03	SMG6	L2 Frontal Inferior longitudinal Left	9.88E-11	6.468839
245	rs2131704	17	1970898	intronic	T	C	0.425	8.01E-19	6.48E-03	SMG6	ISOVF Superior Londgitudinal Fasciculus II Right	5.38E-11	6.560103
245	rs2131704	17	1970898	intronic	T	C	0.425	8.01E-19	6.48E-03	SMG6	ISOVF Superior Londgitudinal Fasciculus III Left	6.57E-10	6.176070
245	rs2131704	17	1970898	intronic	T	C	0.425	8.01E-19	6.48E-03	SMG6	ISOVF Superior Londgitudinal Fasciculus II Left	1.25E-12	7.100065
245	rs2131704	17	1970898	intronic	T	C	0.425	8.01E-19	6.48E-03	SMG6	ICVF Fronto Insular tract1 Left	1.52E-08	-5.659543
245	rs2131704	17	1970898	intronic	T	C	0.425	8.01E-19	6.48E-03	SMG6	L3 Fronto Insular tract1 Left	4.11E-09	5.879842
245	rs2131704	17	1970898	intronic	T	C	0.425	8.01E-19	6.48E-03	SMG6	ISOVF Arcuate Anterior Segment Right	4.76E-10	6.226859
245	rs2131704	17	1970898	intronic	T	C	0.425	8.01E-19	6.48E-03	SMG6	L2 Arcuate Anterior Segment Left	8.83E-09	5.751782
245	rs2131704	17	1970898	intronic	T	C	0.425	8.01E-19	6.48E-03	SMG6	ISOVF Superior Londgitudinal Fasciculus III Right	1.82E-10	6.375862
245	rs11078865	17	2109109	intronic	A	T	0.371	1.11E-12	1.74E-01	SMG6	ISOVF Superior Londgitudinal Fasciculus II Right	2.57E-08	5.568768
245	rs11078865	17	2109109	intronic	A	T	0.371	1.11E-12	1.74E-01	SMG6	ISOVF Frontal Inferior longitudinal Right	2.02E-09	5.996412
245	rs11078865	17	2109109	intronic	A	T	0.371	1.11E-12	1.74E-01	SMG6	ISOVF Superior Londgitudinal Fasciculus II Left	7.39E-09	5.781866
248	rs7210118	17	13047713	intergenic	T	C	0.414	1.54E-24	6.24E-02	RP11-488L1.1	MO Arcuate Anterior Segment Right	1.34E-08	5.681293
248	rs7210118	17	13047713	intergenic	T	C	0.414	1.54E-24	6.24E-02	RP11-488L1.1	OD Fronto Insular tract5 Right	4.02E-08	5.489937
248	rs7210118	17	13047713	intergenic	T	C	0.414	1.54E-24	6.24E-02	RP11-488L1.1	FA Fronto Insular tract5 Right	1.37E-08	-5.677719
250	rs4994353	17	28386280	intronic	A	T	0.443	9.63E-36	9.98E-02	EFCAB5	L2 Fronto Insular tract3 Right	1.86E-08	5.624326
250	rs4994353	17	28386280	intronic	A	T	0.443	9.63E-36	9.98E-02	EFCAB5	OD Fronto Insular tract4 Right	8.64E-09	5.755564
250	rs4994353	17	28386280	intronic	A	T	0.443	9.63E-36	9.98E-02	EFCAB5	MO Fronto Insular tract3 Right	4.12E-13	-7.251425
250	rs4994353	17	28386280	intronic	A	T	0.443	9.63E-36	9.98E-02	EFCAB5	MO Fronto Insular tract4 Right	1.14E-09	-6.088497
250	rs4994353	17	28386280	intronic	A	T	0.443	9.63E-36	9.98E-02	EFCAB5	L1 Fronto Insular tract3 Left	1.32E-09	6.064515
250	rs4994353	17	28386280	intronic	A	T	0.443	9.63E-36	9.98E-02	EFCAB5	OD Fronto Insular tract3 Right	5.92E-11	6.545823
252	rs9898671	17	42935321	intronic	A	G	0.161	1.30E-21	1.05E-01	EFTUD2	MD Inferior Longitudinal Left	7.41E-09	5.781324
252	rs9898671	17	42935321	intronic	A	G	0.161	1.30E-21	1.05E-01	EFTUD2	ICVF Fronto Insular tract4 Right	3.38E-16	-8.159079
252	rs9898671	17	42935321	intronic	A	G	0.161	1.30E-21	1.05E-01	EFTUD2	FA Inferior Fronto Occipital fasciculus Right	2.03E-12	-7.032563
252	rs9898671	17	42935321	intronic	A	G	0.161	1.30E-21	1.05E-01	EFTUD2	ISOVF Inferior Fronto Occipital fasciculus Left	6.66E-12	-6.864728
252	rs9898671	17	42935321	intronic	A	G	0.161	1.30E-21	1.05E-01	EFTUD2	ICVF Superior Londgitudinal Fasciculus II Right	8.44E-15	-7.760720
252	rs9898671	17	42935321	intronic	A	G	0.161	1.30E-21	1.05E-01	EFTUD2	FA Inferior Longitudinal Left	1.88E-10	-6.370832
252	rs9898671	17	42935321	intronic	A	G	0.161	1.30E-21	1.05E-01	EFTUD2	FA Inferior Fronto Occipital fasciculus Left	2.51E-11	-6.672679
252	rs9898671	17	42935321	intronic	A	G	0.161	1.30E-21	1.05E-01	EFTUD2	ICVF Arcuate Anterior Segment Right	5.19E-17	-8.382328
252	rs9898671	17	42935321	intronic	A	G	0.161	1.30E-21	1.05E-01	EFTUD2	ICVF Fronto Insular tract3 Right	1.02E-14	-7.736565
252	rs9898671	17	42935321	intronic	A	G	0.161	1.30E-21	1.05E-01	EFTUD2	L2 Inferior Longitudinal Left	5.72E-10	6.198027
252	rs9898671	17	42935321	intronic	A	G	0.161	1.30E-21	1.05E-01	EFTUD2	MD Inferior Longitudinal Right	1.77E-10	6.380083
252	rs9898671	17	42935321	intronic	A	G	0.161	1.30E-21	1.05E-01	EFTUD2	L1 Inferior Fronto Occipital fasciculus Left	2.61E-11	6.667175
252	rs9898671	17	42935321	intronic	A	G	0.161	1.30E-21	1.05E-01	EFTUD2	ICVF Arcuate Long Segment Left	1.20E-16	-8.283003
252	rs9898671	17	42935321	intronic	A	G	0.161	1.30E-21	1.05E-01	EFTUD2	ISOVF Inferior Longitudinal Right	1.45E-14	-7.691506
252	rs9898671	17	42935321	intronic	A	G	0.161	1.30E-21	1.05E-01	EFTUD2	ICVF Fronto Insular tract2 Right	4.98E-13	-7.225827
252	rs9898671	17	42935321	intronic	A	G	0.161	1.30E-21	1.05E-01	EFTUD2	ICVF Fronto Insular tract5 Right	1.57E-14	-7.681764
252	rs9898671	17	42935321	intronic	A	G	0.161	1.30E-21	1.05E-01	EFTUD2	FA Superior Londgitudinal Fasciculus I Left	3.18E-09	-5.921886
252	rs9898671	17	42935321	intronic	A	G	0.161	1.30E-21	1.05E-01	EFTUD2	ICVF Inferior Fronto Occipital fasciculus Right	1.65E-29	-11.279678
252	rs9898671	17	42935321	intronic	A	G	0.161	1.30E-21	1.05E-01	EFTUD2	MD Uncinate Right	3.57E-10	6.271670
252	rs9898671	17	42935321	intronic	A	G	0.161	1.30E-21	1.05E-01	EFTUD2	MD Inferior Fronto Occipital fasciculus Right	1.44E-16	8.261505
252	rs9898671	17	42935321	intronic	A	G	0.161	1.30E-21	1.05E-01	EFTUD2	ICVF Corpus callosum	8.45E-21	-9.353854
252	rs9898671	17	42935321	intronic	A	G	0.161	1.30E-21	1.05E-01	EFTUD2	ICVF Arcuate Posterior Segment Right	3.30E-14	-7.585894
252	rs9898671	17	42935321	intronic	A	G	0.161	1.30E-21	1.05E-01	EFTUD2	ISOVF Inferior Fronto Occipital fasciculus Right	6.95E-12	-6.858622
252	rs9898671	17	42935321	intronic	A	G	0.161	1.30E-21	1.05E-01	EFTUD2	MD Corpus callosum	6.07E-09	5.814762
252	rs9898671	17	42935321	intronic	A	G	0.161	1.30E-21	1.05E-01	EFTUD2	ISOVF Inferior Longitudinal Left	3.67E-13	-7.267374
252	rs9898671	17	42935321	intronic	A	G	0.161	1.30E-21	1.05E-01	EFTUD2	L2 Inferior Fronto Occipital fasciculus Right	2.64E-13	7.311419
252	rs9898671	17	42935321	intronic	A	G	0.161	1.30E-21	1.05E-01	EFTUD2	ICVF Fronto Insular tract3 Left	6.94E-12	-6.858874
252	rs9898671	17	42935321	intronic	A	G	0.161	1.30E-21	1.05E-01	EFTUD2	MD Superior Londgitudinal Fasciculus III Left	1.18E-09	6.083137
252	rs9898671	17	42935321	intronic	A	G	0.161	1.30E-21	1.05E-01	EFTUD2	ICVF Inferior Fronto Occipital fasciculus Left	1.27E-29	-11.302757
252	rs9898671	17	42935321	intronic	A	G	0.161	1.30E-21	1.05E-01	EFTUD2	ICVF Frontal Aslant Tract Right	1.08E-17	-8.564941
252	rs9898671	17	42935321	intronic	A	G	0.161	1.30E-21	1.05E-01	EFTUD2	L1 Inferior Fronto Occipital fasciculus Right	4.27E-09	5.873306
252	rs9898671	17	42935321	intronic	A	G	0.161	1.30E-21	1.05E-01	EFTUD2	ICVF Frontal Superior Longitudinal Left	2.55E-08	-5.569652
252	rs9898671	17	42935321	intronic	A	G	0.161	1.30E-21	1.05E-01	EFTUD2	L2 Uncinate Right	1.34E-08	5.681353
252	rs9898671	17	42935321	intronic	A	G	0.161	1.30E-21	1.05E-01	EFTUD2	L2 Corpus callosum	3.49E-09	5.906570
252	rs9898671	17	42935321	intronic	A	G	0.161	1.30E-21	1.05E-01	EFTUD2	L3 Superior Londgitudinal Fasciculus III Left	8.75E-09	5.753364
252	rs9898671	17	42935321	intronic	A	G	0.161	1.30E-21	1.05E-01	EFTUD2	ICVF Frontal Inferior longitudinal Left	3.46E-08	-5.516528
252	rs9898671	17	42935321	intronic	A	G	0.161	1.30E-21	1.05E-01	EFTUD2	ICVF Superior Londgitudinal Fasciculus II Left	1.23E-14	-7.712840
252	rs9898671	17	42935321	intronic	A	G	0.161	1.30E-21	1.05E-01	EFTUD2	L3 Inferior Fronto Occipital fasciculus Right	6.35E-18	8.626054
252	rs9898671	17	42935321	intronic	A	G	0.161	1.30E-21	1.05E-01	EFTUD2	L3 Inferior Fronto Occipital fasciculus Left	8.88E-17	8.318906
252	rs9898671	17	42935321	intronic	A	G	0.161	1.30E-21	1.05E-01	EFTUD2	ICVF Frontal Aslant Tract Left	2.98E-18	-8.712070
252	rs9898671	17	42935321	intronic	A	G	0.161	1.30E-21	1.05E-01	EFTUD2	MD Frontal Aslant Tract Left	2.93E-08	5.545475
252	rs9898671	17	42935321	intronic	A	G	0.161	1.30E-21	1.05E-01	EFTUD2	ICVF Superior Londgitudinal Fasciculus III Right	1.78E-18	-8.770265
252	rs9898671	17	42935321	intronic	A	G	0.161	1.30E-21	1.05E-01	EFTUD2	ICVF Frontal Superior Longitudinal Right	1.46E-09	-6.048875
252	rs9898671	17	42935321	intronic	A	G	0.161	1.30E-21	1.05E-01	EFTUD2	L1 Superior Londgitudinal Fasciculus III Right	4.70E-08	5.462389
252	rs9898671	17	42935321	intronic	A	G	0.161	1.30E-21	1.05E-01	EFTUD2	L2 Inferior Fronto Occipital fasciculus Left	1.02E-13	7.438096
252	rs9898671	17	42935321	intronic	A	G	0.161	1.30E-21	1.05E-01	EFTUD2	ICVF Arcuate Posterior Segment Left	8.79E-18	-8.588773
252	rs9898671	17	42935321	intronic	A	G	0.161	1.30E-21	1.05E-01	EFTUD2	L2 Uncinate Left	3.18E-09	5.922222
252	rs9898671	17	42935321	intronic	A	G	0.161	1.30E-21	1.05E-01	EFTUD2	ICVF Fronto Insular tract5 Left	2.20E-08	-5.595381
252	rs9898671	17	42935321	intronic	A	G	0.161	1.30E-21	1.05E-01	EFTUD2	ICVF Arcuate Long Segment Right	3.40E-17	-8.431910
252	rs9898671	17	42935321	intronic	A	G	0.161	1.30E-21	1.05E-01	EFTUD2	L3 Inferior Longitudinal Left	1.08E-09	6.097661
252	rs9898671	17	42935321	intronic	A	G	0.161	1.30E-21	1.05E-01	EFTUD2	L3 Corpus callosum	1.48E-08	5.663868
252	rs9898671	17	42935321	intronic	A	G	0.161	1.30E-21	1.05E-01	EFTUD2	L3 Uncinate Left	7.59E-10	6.153343
252	rs9898671	17	42935321	intronic	A	G	0.161	1.30E-21	1.05E-01	EFTUD2	ICVF Inferior Longitudinal Right	3.87E-26	-10.575571
252	rs9898671	17	42935321	intronic	A	G	0.161	1.30E-21	1.05E-01	EFTUD2	ICVF Fronto Insular tract2 Left	7.81E-09	-5.772611

Genomic Locus	Lead SNP	chr	Position	Functional category	Non-effect allele	Effect allele	MAF	mvgwasP (discovery -British-)	mvgwasP (replication -non British-)	Nearest gene	Central endophenotypes	univariate P value	univariate Z
252	rs9898671	17	42935321	intronic	A	G	0.161	1.30E-21	1.05E-01	EFTUD2	FA Corpus callosum	3.75E-09	-5.894754
252	rs9898671	17	42935321	intronic	A	G	0.161	1.30E-21	1.05E-01	EFTUD2	MD Arcuate Posterior Segment Left	1.33E-08	5.682804
252	rs9898671	17	42935321	intronic	A	G	0.161	1.30E-21	1.05E-01	EFTUD2	ICVF Arcuate Anterior Segment Left	1.23E-13	-7.413912
252	rs9898671	17	42935321	intronic	A	G	0.161	1.30E-21	1.05E-01	EFTUD2	ICVF Superior Londgitudinal Fasciculus I Right	1.10E-16	-8.293817
252	rs9898671	17	42935321	intronic	A	G	0.161	1.30E-21	1.05E-01	EFTUD2	FA Inferior Longitudinal Right	1.13E-13	-7.424624
252	rs9898671	17	42935321	intronic	A	G	0.161	1.30E-21	1.05E-01	EFTUD2	MD Arcuate Long Segment Right	1.82E-08	5.628614
252	rs9898671	17	42935321	intronic	A	G	0.161	1.30E-21	1.05E-01	EFTUD2	L3 Uncinate Right	2.50E-10	6.326886
252	rs9898671	17	42935321	intronic	A	G	0.161	1.30E-21	1.05E-01	EFTUD2	ICVF Fronto Insular tract1 Right	5.99E-11	-6.543898
252	rs9898671	17	42935321	intronic	A	G	0.161	1.30E-21	1.05E-01	EFTUD2	ICVF Superior Londgitudinal Fasciculus I Left	1.41E-17	-8.533936
252	rs9898671	17	42935321	intronic	A	G	0.161	1.30E-21	1.05E-01	EFTUD2	FA Superior Londgitudinal Fasciculus I Right	2.64E-08	-5.563913
252	rs9898671	17	42935321	intronic	A	G	0.161	1.30E-21	1.05E-01	EFTUD2	L2 Inferior Longitudinal Right	4.25E-11	6.594964
252	rs9898671	17	42935321	intronic	A	G	0.161	1.30E-21	1.05E-01	EFTUD2	L1 Superior Londgitudinal Fasciculus III Left	5.66E-09	5.826410
252	rs9898671	17	42935321	intronic	A	G	0.161	1.30E-21	1.05E-01	EFTUD2	MD Arcuate Long Segment Left	1.54E-09	6.040081
252	rs9898671	17	42935321	intronic	A	G	0.161	1.30E-21	1.05E-01	EFTUD2	ICVF Uncinate Right	4.59E-19	-8.921781
252	rs9898671	17	42935321	intronic	A	G	0.161	1.30E-21	1.05E-01	EFTUD2	ICVF Uncinate Left	1.66E-18	-8.778083
252	rs9898671	17	42935321	intronic	A	G	0.161	1.30E-21	1.05E-01	EFTUD2	ICVF Inferior Longitudinal Left	1.95E-24	-10.201391
252	rs9898671	17	42935321	intronic	A	G	0.161	1.30E-21	1.05E-01	EFTUD2	ICVF Superior Londgitudinal Fasciculus III Left	2.73E-17	-8.457517
252	rs9898671	17	42935321	intronic	A	G	0.161	1.30E-21	1.05E-01	EFTUD2	L3 Inferior Longitudinal Right	3.50E-13	7.273562
252	rs9898671	17	42935321	intronic	A	G	0.161	1.30E-21	1.05E-01	EFTUD2	MD Uncinate Left	1.26E-09	6.072453
252	rs9898671	17	42935321	intronic	A	G	0.161	1.30E-21	1.05E-01	EFTUD2	MD Superior Londgitudinal Fasciculus III Right	1.04E-08	5.723300
252	rs9898671	17	42935321	intronic	A	G	0.161	1.30E-21	1.05E-01	EFTUD2	MD Inferior Fronto Occipital fasciculus Left	5.12E-17	8.383865
252	rs9898671	17	42935321	intronic	A	G	0.161	1.30E-21	1.05E-01	EFTUD2	ICVF Frontal Inferior longitudinal Right	3.19E-13	-7.286234
252	rs12936234	17	43177951	intronic	C	T	0.350	8.59E-26	4.26E-01	NMT1	L3 Superior Londgitudinal Fasciculus II Left	4.93E-08	-5.453659
252	rs12936234	17	43177951	intronic	C	T	0.350	8.59E-26	4.26E-01	NMT1	MD Inferior Longitudinal Left	1.14E-10	-6.446471
252	rs12936234	17	43177951	intronic	C	T	0.350	8.59E-26	4.26E-01	NMT1	L3 Frontal Aslant Tract Right	4.27E-11	-6.594373
252	rs12936234	17	43177951	intronic	C	T	0.350	8.59E-26	4.26E-01	NMT1	L1 Arcuate Anterior Segment Right	8.22E-09	-5.763863
252	rs12936234	17	43177951	intronic	C	T	0.350	8.59E-26	4.26E-01	NMT1	FA Superior Londgitudinal Fasciculus III Right	1.58E-08	5.652183
252	rs12936234	17	43177951	intronic	C	T	0.350	8.59E-26	4.26E-01	NMT1	L2 Frontal Inferior longitudinal Right	5.05E-10	-6.217573
252	rs12936234	17	43177951	intronic	C	T	0.350	8.59E-26	4.26E-01	NMT1	L1 Inferior Longitudinal Left	4.65E-10	-6.230509
252	rs12936234	17	43177951	intronic	C	T	0.350	8.59E-26	4.26E-01	NMT1	ICVF Superior Londgitudinal Fasciculus II Right	2.15E-16	8.213282
252	rs12936234	17	43177951	intronic	C	T	0.350	8.59E-26	4.26E-01	NMT1	ICVF Arcuate Anterior Segment Right	3.50E-19	8.951795
252	rs12936234	17	43177951	intronic	C	T	0.350	8.59E-26	4.26E-01	NMT1	MD Arcuate Anterior Segment Right	1.83E-12	-7.046851
252	rs12936234	17	43177951	intronic	C	T	0.350	8.59E-26	4.26E-01	NMT1	MD Inferior Longitudinal Right	1.04E-10	-6.461462
252	rs12936234	17	43177951	intronic	C	T	0.350	8.59E-26	4.26E-01	NMT1	L1 Inferior Fronto Occipital fasciculus Left	1.17E-12	-7.108515
252	rs12936234	17	43177951	intronic	C	T	0.350	8.59E-26	4.26E-01	NMT1	ICVF Arcuate Long Segment Left	1.77E-16	8.236456
252	rs12936234	17	43177951	intronic	C	T	0.350	8.59E-26	4.26E-01	NMT1	MD Frontal Aslant Tract Right	3.44E-12	-6.958353
252	rs12936234	17	43177951	intronic	C	T	0.350	8.59E-26	4.26E-01	NMT1	L3 Superior Londgitudinal Fasciculus I Left	4.54E-12	-6.919325
252	rs12936234	17	43177951	intronic	C	T	0.350	8.59E-26	4.26E-01	NMT1	ICVF Fronto Insular tract2 Right	1.16E-08	5.705945
252	rs12936234	17	43177951	intronic	C	T	0.350	8.59E-26	4.26E-01	NMT1	FA Superior Londgitudinal Fasciculus I Left	4.11E-09	5.879756
252	rs12936234	17	43177951	intronic	C	T	0.350	8.59E-26	4.26E-01	NMT1	L3 Frontal Aslant Tract Left	1.07E-08	-5.719615
252	rs12936234	17	43177951	intronic	C	T	0.350	8.59E-26	4.26E-01	NMT1	ICVF Inferior Fronto Occipital fasciculus Right	1.40E-18	8.797159
252	rs12936234	17	43177951	intronic	C	T	0.350	8.59E-26	4.26E-01	NMT1	MD Inferior Fronto Occipital fasciculus Right	8.76E-14	-7.458318
252	rs12936234	17	43177951	intronic	C	T	0.350	8.59E-26	4.26E-01	NMT1	ICVF Corpus callosum	5.96E-19	8.892698
252	rs12936234	17	43177951	intronic	C	T	0.350	8.59E-26	4.26E-01	NMT1	L3 Superior Londgitudinal Fasciculus III Right	6.49E-12	-6.868485
252	rs12936234	17	43177951	intronic	C	T	0.350	8.59E-26	4.26E-01	NMT1	ICVF Arcuate Posterior Segment Right	6.51E-13	7.189411
252	rs12936234	17	43177951	intronic	C	T	0.350	8.59E-26	4.26E-01	NMT1	MD Corpus callosum	3.51E-11	-6.623479
252	rs12936234	17	43177951	intronic	C	T	0.350	8.59E-26	4.26E-01	NMT1	L2 Inferior Fronto Occipital fasciculus Right	4.00E-10	-6.254042
252	rs12936234	17	43177951	intronic	C	T	0.350	8.59E-26	4.26E-01	NMT1	MD Superior Londgitudinal Fasciculus III Left	5.72E-12	-6.886349
252	rs12936234	17	43177951	intronic	C	T	0.350	8.59E-26	4.26E-01	NMT1	ICVF Inferior Fronto Occipital fasciculus Left	4.64E-20	9.172001
252	rs12936234	17	43177951	intronic	C	T	0.350	8.59E-26	4.26E-01	NMT1	ICVF Frontal Aslant Tract Right	1.31E-18	8.804800
252	rs12936234	17	43177951	intronic	C	T	0.350	8.59E-26	4.26E-01	NMT1	L1 Inferior Fronto Occipital fasciculus Right	9.66E-10	-6.114912
252	rs12936234	17	43177951	intronic	C	T	0.350	8.59E-26	4.26E-01	NMT1	ICVF Frontal Superior Longitudinal Left	4.94E-08	5.453383
252	rs12936234	17	43177951	intronic	C	T	0.350	8.59E-26	4.26E-01	NMT1	MD Arcuate Posterior Segment Right	4.29E-08	-5.478418
252	rs12936234	17	43177951	intronic	C	T	0.350	8.59E-26	4.26E-01	NMT1	L2 Corpus callosum	6.41E-11	-6.533843
252	rs12936234	17	43177951	intronic	C	T	0.350	8.59E-26	4.26E-01	NMT1	L2 Superior Londgitudinal Fasciculus III Right	7.65E-14	-7.476193
252	rs12936234	17	43177951	intronic	C	T	0.350	8.59E-26	4.26E-01	NMT1	L3 Superior Londgitudinal Fasciculus III Left	2.67E-09	-5.950765
252	rs12936234	17	43177951	intronic	C	T	0.350	8.59E-26	4.26E-01	NMT1	ICVF Frontal Inferior longitudinal Left	2.77E-12	6.988805
252	rs12936234	17	43177951	intronic	C	T	0.350	8.59E-26	4.26E-01	NMT1	ICVF Superior Londgitudinal Fasciculus II Left	1.03E-15	8.022761
252	rs12936234	17	43177951	intronic	C	T	0.350	8.59E-26	4.26E-01	NMT1	L3 Inferior Fronto Occipital fasciculus Right	8.39E-13	-7.154669
252	rs12936234	17	43177951	intronic	C	T	0.350	8.59E-26	4.26E-01	NMT1	L2 Frontal Aslant Tract Left	1.16E-11	-6.784984
252	rs12936234	17	43177951	intronic	C	T	0.350	8.59E-26	4.26E-01	NMT1	L2 Superior Londgitudinal Fasciculus III Left	9.52E-11	-6.474453
252	rs12936234	17	43177951	intronic	C	T	0.350	8.59E-26	4.26E-01	NMT1	L2 Arcuate Anterior Segment Right	2.82E-10	-6.308267
252	rs12936234	17	43177951	intronic	C	T	0.350	8.59E-26	4.26E-01	NMT1	L3 Inferior Fronto Occipital fasciculus Left	2.21E-13	-7.335474
252	rs12936234	17	43177951	intronic	C	T	0.350	8.59E-26	4.26E-01	NMT1	L3 Arcuate Long Segment Left	2.35E-11	-6.682587
252	rs12936234	17	43177951	intronic	C	T	0.350	8.59E-26	4.26E-01	NMT1	ICVF Frontal Aslant Tract Left	1.84E-16	8.232224
252	rs12936234	17	43177951	intronic	C	T	0.350	8.59E-26	4.26E-01	NMT1	MD Frontal Aslant Tract Left	2.82E-10	-6.308636
252	rs12936234	17	43177951	intronic	C	T	0.350	8.59E-26	4.26E-01	NMT1	ICVF Superior Londgitudinal Fasciculus III Right	9.63E-20	9.093077
252	rs12936234	17	43177951	intronic	C	T	0.350	8.59E-26	4.26E-01	NMT1	ICVF Frontal Superior Longitudinal Right	8.32E-14	7.465089
252	rs12936234	17	43177951	intronic	C	T	0.350	8.59E-26	4.26E-01	NMT1	L1 Superior Londgitudinal Fasciculus III Right	4.89E-14	-7.534736
252	rs12936234	17	43177951	intronic	C	T	0.350	8.59E-26	4.26E-01	NMT1	MD Superior Londgitudinal Fasciculus II Left	2.07E-08	-5.605913
252	rs12936234	17	43177951	intronic	C	T	0.350	8.59E-26	4.26E-01	NMT1	FA Frontal Aslant Tract Right	3.48E-09	5.907332
252	rs12936234	17	43177951	intronic	C	T	0.350	8.59E-26	4.26E-01	NMT1	L2 Inferior Fronto Occipital fasciculus Left	1.91E-11	-6.712912
252	rs12936234	17	43177951	intronic	C	T	0.350	8.59E-26	4.26E-01	NMT1	ICVF Arcuate Posterior Segment Left	2.44E-12	7.006712
252	rs12936234	17	43177951	intronic	C	T	0.350	8.59E-26	4.26E-01	NMT1	FA Arcuate Long Segment Right	1.01E-08	5.728553
252	rs12936234	17	43177951	intronic	C	T	0.350	8.59E-26	4.26E-01	NMT1	ICVF Arcuate Long Segment Right	5.98E-16	8.089640
252	rs12936234	17	43177951	intronic	C	T	0.350	8.59E-26	4.26E-01	NMT1	L3 Inferior Longitudinal Left	3.01E-10	-6.298156
252	rs12936234	17	43177951	intronic	C	T	0.350	8.59E-26	4.26E-01	NMT1	L3 Corpus callosum	5.65E-10	-6.199831
252	rs12936234	17	43177951	intronic	C	T	0.350	8.59E-26	4.26E-01	NMT1	ICVF Inferior Longitudinal Right	1.90E-18	8.762899
252	rs12936234	17	43177951	intronic	C	T	0.350	8.59E-26	4.26E-01	NMT1	L3 Arcuate Long Segment Right	5.87E-09	-5.820370
252	rs12936234	17	43177951	intronic	C	T	0.350	8.59E-26	4.26E-01	NMT1	L2 Superior Londgitudinal Fasciculus I Left	7.61E-10	-6.152815
252	rs12936234	17	43177951	intronic	C	T	0.350	8.59E-26	4.26E-01	NMT1	MD Frontal Inferior longitudinal Right	2.14E-13	-7.339872
252	rs12936234	17	43177951	intronic	C	T	0.350	8.59E-26	4.26E-01	NMT1	L1 Inferior Longitudinal Right	1.14E-09	-6.088805
252	rs12936234	17	43177951	intronic	C	T	0.350	8.59E-26	4.26E-01	NMT1	MD Arcuate Posterior Segment Left	1.19E-08	-5.701523
252	rs12936234	17	43177951	intronic	C	T	0.350	8.59E-26	4.26E-01	NMT1	L1 Frontal Inferior longitudinal Right	2.17E-11	-6.693975
252	rs12936234	17	43177951	intronic	C	T	0.350	8.59E-26	4.26E-01	NMT1	ICVF Arcuate Anterior Segment Left	2.12E-13	7.340867
252	rs12936234	17	43177951	intronic	C	T	0.350	8.59E-26	4.26E-01	NMT1	ICVF Superior Londgitudinal Fasciculus I Right	1.12E-18	8.822734
252	rs12936234	17	43177951	intronic	C	T	0.350	8.59E-26	4.26E-01	NMT1	MD Superior Londgitudinal Fasciculus I Right	7.20E-09	-5.786273
252	rs12936234	17	43177951	intronic	C	T	0.350	8.59E-26	4.26E-01	NMT1	MD Arcuate Long Segment Right	1.80E-09	-6.015049
252	rs12936234	17	43177951	intronic	C	T	0.350	8.59E-26	4.26E-01	NMT1	ICVF Fronto Insular tract1 Right	1.01E-12	7.128941
252	rs12936234	17	43177951	intronic	C	T	0.350	8.59E-26	4.26E-01	NMT1	ICVF Superior Londgitudinal Fasciculus I Left	5.38E-19	8.904042
252	rs12936234	17	43177951	intronic	C	T	0.350	8.59E-26	4.26E-01	NMT1	L2 Frontal Aslant Tract Right	3.28E-13	-7.282560
252	rs12936234	17	43177951	intronic	C	T	0.350	8.59E-26	4.26E-01	NMT1	L2 Arcuate Long Segment Right	2.61E-10	-6.320038
252	rs12936234	17	43177951	intronic	C	T	0.350	8.59E-26	4.26E-01	NMT1	L1 Superior Londgitudinal Fasciculus III Left	4.44E-11	-6.588599

Genomic Locus	Lead SNP	chr	Position	Functional category	Non-effect allele	Effect allele	MAF	mvgwasP (discovery -British-)	mvgwasP (replication -non British-)	Nearest gene	Central endophenotypes	univariate P value	univariate Z
252	rs12936234	17	43177951	intronic	C	T	0.350	8.59E-26	4.26E-01	NMT1	L1 Corpus callosum	8.29E-10	-6.139214
252	rs12936234	17	43177951	intronic	C	T	0.350	8.59E-26	4.26E-01	NMT1	MD Arcuate Long Segment Left	2.19E-11	-6.692511
252	rs12936234	17	43177951	intronic	C	T	0.350	8.59E-26	4.26E-01	NMT1	L3 Superior Londgitudinal Fasciculus I Right	7.68E-10	-6.151304
252	rs12936234	17	43177951	intronic	C	T	0.350	8.59E-26	4.26E-01	NMT1	ICVF Uncinate Left	1.32E-10	6.424898
252	rs12936234	17	43177951	intronic	C	T	0.350	8.59E-26	4.26E-01	NMT1	ICVF Inferior Longitudinal Left	1.89E-19	9.019632
252	rs12936234	17	43177951	intronic	C	T	0.350	8.59E-26	4.26E-01	NMT1	ICVF Superior Londgitudinal Fasciculus III Left	7.04E-17	8.346312
252	rs12936234	17	43177951	intronic	C	T	0.350	8.59E-26	4.26E-01	NMT1	L3 Inferior Longitudinal Right	5.97E-11	-6.544370
252	rs12936234	17	43177951	intronic	C	T	0.350	8.59E-26	4.26E-01	NMT1	L2 Arcuate Posterior Segment Right	9.53E-12	-6.813432
252	rs12936234	17	43177951	intronic	C	T	0.350	8.59E-26	4.26E-01	NMT1	MD Superior Londgitudinal Fasciculus III Right	2.10E-14	-7.644257
252	rs12936234	17	43177951	intronic	C	T	0.350	8.59E-26	4.26E-01	NMT1	L3 Frontal Inferior longitudinal Right	2.44E-10	-6.330988
252	rs12936234	17	43177951	intronic	C	T	0.350	8.59E-26	4.26E-01	NMT1	MD Inferior Fronto Occipital fasciculus Left	2.58E-15	-7.909738
252	rs12936234	17	43177951	intronic	C	T	0.350	8.59E-26	4.26E-01	NMT1	L3 Arcuate Anterior Segment Right	5.57E-10	-6.202140
252	rs12936234	17	43177951	intronic	C	T	0.350	8.59E-26	4.26E-01	NMT1	L2 Arcuate Posterior Segment Left	9.41E-09	-5.741056
252	rs12936234	17	43177951	intronic	C	T	0.350	8.59E-26	4.26E-01	NMT1	ICVF Frontal Inferior longitudinal Right	4.68E-15	7.835126
252	rs12936234	17	43177951	intronic	C	T	0.350	8.59E-26	4.26E-01	NMT1	MD Superior Londgitudinal Fasciculus I Left	5.42E-11	-6.558962
252	rs113448888	17	44108482	UTR3	AGCCCTCT	A	0.224	2.09E-100	9.42E-05	KANSL1	ICVF Fronto Insular tract4 Right	4.77E-21	9.414109
252	rs113448888	17	44108482	UTR3	AGCCCTCT	A	0.224	2.09E-100	9.42E-05	KANSL1	L3 Frontal Aslant Tract Right	6.77E-14	-7.492325
252	rs113448888	17	44108482	UTR3	AGCCCTCT	A	0.224	2.09E-100	9.42E-05	KANSL1	L3 Fronto Insular tract5 Right	2.52E-10	-6.325852
252	rs113448888	17	44108482	UTR3	AGCCCTCT	A	0.224	2.09E-100	9.42E-05	KANSL1	L1 Arcuate Anterior Segment Right	4.21E-12	-6.929800
252	rs113448888	17	44108482	UTR3	AGCCCTCT	A	0.224	2.09E-100	9.42E-05	KANSL1	FA Superior Londgitudinal Fasciculus III Right	1.53E-12	7.071917
252	rs113448888	17	44108482	UTR3	AGCCCTCT	A	0.224	2.09E-100	9.42E-05	KANSL1	MD Superior Londgitudinal Fasciculus II Right	6.00E-10	-6.190473
252	rs113448888	17	44108482	UTR3	AGCCCTCT	A	0.224	2.09E-100	9.42E-05	KANSL1	L2 Frontal Inferior longitudinal Right	1.67E-16	-8.243386
252	rs113448888	17	44108482	UTR3	AGCCCTCT	A	0.224	2.09E-100	9.42E-05	KANSL1	ICVF Superior Londgitudinal Fasciculus II Right	6.59E-16	8.077825
252	rs113448888	17	44108482	UTR3	AGCCCTCT	A	0.224	2.09E-100	9.42E-05	KANSL1	FA Frontal Aslant Tract Left	2.51E-08	5.572442
252	rs113448888	17	44108482	UTR3	AGCCCTCT	A	0.224	2.09E-100	9.42E-05	KANSL1	ICVF Arcuate Anterior Segment Right	1.92E-20	9.266726
252	rs113448888	17	44108482	UTR3	AGCCCTCT	A	0.224	2.09E-100	9.42E-05	KANSL1	ICVF Fronto Insular tract3 Right	2.31E-15	7.923565
252	rs113448888	17	44108482	UTR3	AGCCCTCT	A	0.224	2.09E-100	9.42E-05	KANSL1	MD Arcuate Anterior Segment Right	9.24E-14	-7.451329
252	rs113448888	17	44108482	UTR3	AGCCCTCT	A	0.224	2.09E-100	9.42E-05	KANSL1	L2 Fronto Insular tract5 Left	3.94E-08	-5.493468
252	rs113448888	17	44108482	UTR3	AGCCCTCT	A	0.224	2.09E-100	9.42E-05	KANSL1	ICVF Arcuate Long Segment Left	2.87E-15	7.896446
252	rs113448888	17	44108482	UTR3	AGCCCTCT	A	0.224	2.09E-100	9.42E-05	KANSL1	MD Frontal Aslant Tract Right	6.58E-12	-6.866481
252	rs113448888	17	44108482	UTR3	AGCCCTCT	A	0.224	2.09E-100	9.42E-05	KANSL1	L1 Fronto Insular tract4 Right	5.20E-09	-5.840796
252	rs113448888	17	44108482	UTR3	AGCCCTCT	A	0.224	2.09E-100	9.42E-05	KANSL1	ICVF Fronto Insular tract2 Right	3.20E-12	6.968833
252	rs113448888	17	44108482	UTR3	AGCCCTCT	A	0.224	2.09E-100	9.42E-05	KANSL1	ICVF Fronto Insular tract5 Right	1.33E-14	7.702506
252	rs113448888	17	44108482	UTR3	AGCCCTCT	A	0.224	2.09E-100	9.42E-05	KANSL1	MD Fronto Insular tract5 Right	3.72E-16	-8.147222
252	rs113448888	17	44108482	UTR3	AGCCCTCT	A	0.224	2.09E-100	9.42E-05	KANSL1	L3 Frontal Aslant Tract Left	4.06E-10	-6.251584
252	rs113448888	17	44108482	UTR3	AGCCCTCT	A	0.224	2.09E-100	9.42E-05	KANSL1	ICVF Inferior Fronto Occipital fasciculus Right	7.86E-09	5.771488
252	rs113448888	17	44108482	UTR3	AGCCCTCT	A	0.224	2.09E-100	9.42E-05	KANSL1	L1 Arcuate Anterior Segment Left	4.71E-08	-5.461763
252	rs113448888	17	44108482	UTR3	AGCCCTCT	A	0.224	2.09E-100	9.42E-05	KANSL1	ICVF Corpus callosum	3.47E-18	8.694963
252	rs113448888	17	44108482	UTR3	AGCCCTCT	A	0.224	2.09E-100	9.42E-05	KANSL1	L3 Superior Londgitudinal Fasciculus III Right	1.01E-15	-8.025881
252	rs113448888	17	44108482	UTR3	AGCCCTCT	A	0.224	2.09E-100	9.42E-05	KANSL1	ICVF Arcuate Posterior Segment Right	2.97E-15	7.892362
252	rs113448888	17	44108482	UTR3	AGCCCTCT	A	0.224	2.09E-100	9.42E-05	KANSL1	FA Frontal Inferior longitudinal Right	1.29E-14	7.706437
252	rs113448888	17	44108482	UTR3	AGCCCTCT	A	0.224	2.09E-100	9.42E-05	KANSL1	MD Corpus callosum	4.72E-10	-6.228287
252	rs113448888	17	44108482	UTR3	AGCCCTCT	A	0.224	2.09E-100	9.42E-05	KANSL1	MD Fronto Insular tract3 Right	9.63E-12	-6.811997
252	rs113448888	17	44108482	UTR3	AGCCCTCT	A	0.224	2.09E-100	9.42E-05	KANSL1	OD Superior Londgitudinal Fasciculus III Left	4.36E-08	5.475424
252	rs113448888	17	44108482	UTR3	AGCCCTCT	A	0.224	2.09E-100	9.42E-05	KANSL1	L3 Fronto Insular tract4 Right	7.94E-11	-6.501814
252	rs113448888	17	44108482	UTR3	AGCCCTCT	A	0.224	2.09E-100	9.42E-05	KANSL1	ICVF Fronto Insular tract3 Left	6.81E-09	5.795490
252	rs113448888	17	44108482	UTR3	AGCCCTCT	A	0.224	2.09E-100	9.42E-05	KANSL1	MD Superior Londgitudinal Fasciculus III Left	7.03E-11	-6.520116
252	rs113448888	17	44108482	UTR3	AGCCCTCT	A	0.224	2.09E-100	9.42E-05	KANSL1	ICVF Inferior Fronto Occipital fasciculus Left	1.29E-13	7.406764
252	rs113448888	17	44108482	UTR3	AGCCCTCT	A	0.224	2.09E-100	9.42E-05	KANSL1	L1 Fronto Insular tract3 Right	4.30E-10	-6.242550
252	rs113448888	17	44108482	UTR3	AGCCCTCT	A	0.224	2.09E-100	9.42E-05	KANSL1	ICVF Frontal Aslant Tract Right	1.47E-23	10.003880
252	rs113448888	17	44108482	UTR3	AGCCCTCT	A	0.224	2.09E-100	9.42E-05	KANSL1	ICVF Frontal Superior Longitudinal Left	1.01E-13	7.439213
252	rs113448888	17	44108482	UTR3	AGCCCTCT	A	0.224	2.09E-100	9.42E-05	KANSL1	L3 Fronto Insular tract5 Left	5.39E-09	-5.834753
252	rs113448888	17	44108482	UTR3	AGCCCTCT	A	0.224	2.09E-100	9.42E-05	KANSL1	FA Fronto Insular tract5 Left	3.70E-08	5.504426
252	rs113448888	17	44108482	UTR3	AGCCCTCT	A	0.224	2.09E-100	9.42E-05	KANSL1	OD Arcuate Long Segment Left	6.27E-11	6.537106
252	rs113448888	17	44108482	UTR3	AGCCCTCT	A	0.224	2.09E-100	9.42E-05	KANSL1	L2 Corpus callosum	2.63E-10	-6.319340
252	rs113448888	17	44108482	UTR3	AGCCCTCT	A	0.224	2.09E-100	9.42E-05	KANSL1	L2 Superior Londgitudinal Fasciculus III Right	1.73E-14	-7.669107
252	rs113448888	17	44108482	UTR3	AGCCCTCT	A	0.224	2.09E-100	9.42E-05	KANSL1	L3 Superior Londgitudinal Fasciculus III Left	1.47E-11	-6.751075
252	rs113448888	17	44108482	UTR3	AGCCCTCT	A	0.224	2.09E-100	9.42E-05	KANSL1	ICVF Frontal Inferior longitudinal Left	1.36E-10	6.420523
252	rs113448888	17	44108482	UTR3	AGCCCTCT	A	0.224	2.09E-100	9.42E-05	KANSL1	ICVF Superior Londgitudinal Fasciculus II Left	8.57E-14	7.461195
252	rs113448888	17	44108482	UTR3	AGCCCTCT	A	0.224	2.09E-100	9.42E-05	KANSL1	L2 Frontal Aslant Tract Left	4.92E-09	-5.849972
252	rs113448888	17	44108482	UTR3	AGCCCTCT	A	0.224	2.09E-100	9.42E-05	KANSL1	L2 Fronto Insular tract5 Right	5.41E-16	-8.101933
252	rs113448888	17	44108482	UTR3	AGCCCTCT	A	0.224	2.09E-100	9.42E-05	KANSL1	FA Arcuate Anterior Segment Left	5.30E-10	6.209936
252	rs113448888	17	44108482	UTR3	AGCCCTCT	A	0.224	2.09E-100	9.42E-05	KANSL1	L2 Arcuate Anterior Segment Right	6.25E-09	-5.810029
252	rs113448888	17	44108482	UTR3	AGCCCTCT	A	0.224	2.09E-100	9.42E-05	KANSL1	L1 Arcuate Long Segment Left	6.66E-12	-6.864748
252	rs113448888	17	44108482	UTR3	AGCCCTCT	A	0.224	2.09E-100	9.42E-05	KANSL1	ICVF Frontal Aslant Tract Left	6.76E-20	9.131427
252	rs113448888	17	44108482	UTR3	AGCCCTCT	A	0.224	2.09E-100	9.42E-05	KANSL1	MD Frontal Aslant Tract Left	1.25E-09	-6.073605
252	rs113448888	17	44108482	UTR3	AGCCCTCT	A	0.224	2.09E-100	9.42E-05	KANSL1	MD Fronto Insular tract4 Right	9.29E-15	-7.748572
252	rs113448888	17	44108482	UTR3	AGCCCTCT	A	0.224	2.09E-100	9.42E-05	KANSL1	L2 Fronto Insular tract3 Right	6.38E-11	-6.534633
252	rs113448888	17	44108482	UTR3	AGCCCTCT	A	0.224	2.09E-100	9.42E-05	KANSL1	ICVF Superior Londgitudinal Fasciculus III Right	2.06E-24	10.196471
252	rs113448888	17	44108482	UTR3	AGCCCTCT	A	0.224	2.09E-100	9.42E-05	KANSL1	L2 Superior Londgitudinal Fasciculus II Right	1.60E-10	-6.395434
252	rs113448888	17	44108482	UTR3	AGCCCTCT	A	0.224	2.09E-100	9.42E-05	KANSL1	ICVF Frontal Superior Longitudinal Right	3.13E-16	8.168255
252	rs113448888	17	44108482	UTR3	AGCCCTCT	A	0.224	2.09E-100	9.42E-05	KANSL1	MD Arcuate Anterior Segment Left	2.36E-12	-7.011338
252	rs113448888	17	44108482	UTR3	AGCCCTCT	A	0.224	2.09E-100	9.42E-05	KANSL1	L3 Arcuate Posterior Segment Left	2.24E-08	-5.592107
252	rs113448888	17	44108482	UTR3	AGCCCTCT	A	0.224	2.09E-100	9.42E-05	KANSL1	L1 Superior Londgitudinal Fasciculus III Right	4.59E-12	-6.917627
252	rs113448888	17	44108482	UTR3	AGCCCTCT	A	0.224	2.09E-100	9.42E-05	KANSL1	FA Frontal Aslant Tract Right	2.63E-09	5.953340
252	rs113448888	17	44108482	UTR3	AGCCCTCT	A	0.224	2.09E-100	9.42E-05	KANSL1	ICVF Arcuate Posterior Segment Left	5.64E-18	8.639585
252	rs113448888	17	44108482	UTR3	AGCCCTCT	A	0.224	2.09E-100	9.42E-05	KANSL1	ICVF Fronto Insular tract5 Left	1.55E-16	8.252289
252	rs113448888	17	44108482	UTR3	AGCCCTCT	A	0.224	2.09E-100	9.42E-05	KANSL1	ICVF Arcuate Long Segment Right	5.31E-16	8.104108
252	rs113448888	17	44108482	UTR3	AGCCCTCT	A	0.224	2.09E-100	9.42E-05	KANSL1	L3 Corpus callosum	8.84E-10	-6.129007
252	rs113448888	17	44108482	UTR3	AGCCCTCT	A	0.224	2.09E-100	9.42E-05	KANSL1	FA Arcuate Posterior Segment Left	5.21E-09	5.840375
252	rs113448888	17	44108482	UTR3	AGCCCTCT	A	0.224	2.09E-100	9.42E-05	KANSL1	ICVF Fronto Insular tract2 Left	2.13E-10	6.351675
252	rs113448888	17	44108482	UTR3	AGCCCTCT	A	0.224	2.09E-100	9.42E-05	KANSL1	L2 Superior Londgitudinal Fasciculus I Right	1.49E-08	-5.662994
252	rs113448888	17	44108482	UTR3	AGCCCTCT	A	0.224	2.09E-100	9.42E-05	KANSL1	L2 Superior Londgitudinal Fasciculus I Left	2.26E-11	-6.688449
252	rs113448888	17	44108482	UTR3	AGCCCTCT	A	0.224	2.09E-100	9.42E-05	KANSL1	MD Frontal Inferior longitudinal Right	1.01E-15	-8.026225
252	rs113448888	17	44108482	UTR3	AGCCCTCT	A	0.224	2.09E-100	9.42E-05	KANSL1	ICVF Arcuate Anterior Segment Left	1.13E-20	9.323019
252	rs113448888	17	44108482	UTR3	AGCCCTCT	A	0.224	2.09E-100	9.42E-05	KANSL1	L3 Arcuate Anterior Segment Left	1.49E-12	-7.075450
252	rs113448888	17	44108482	UTR3	AGCCCTCT	A	0.224	2.09E-100	9.42E-05	KANSL1	ICVF Superior Londgitudinal Fasciculus I Right	1.06E-17	8.567202
252	rs113448888	17	44108482	UTR3	AGCCCTCT	A	0.224	2.09E-100	9.42E-05	KANSL1	MD Superior Londgitudinal Fasciculus I Right	4.61E-10	-6.231920
252	rs113448888	17	44108482	UTR3	AGCCCTCT	A	0.224	2.09E-100	9.42E-05	KANSL1	MD Arcuate Long Segment Right	6.25E-09	-5.809891
252	rs113448888	17	44108482	UTR3	AGCCCTCT	A	0.224	2.09E-100	9.42E-05	KANSL1	ICVF Fronto Insular tract1 Right	7.15E-11	6.517571

Genomic Locus	Lead SNP	chr	Position	Functional category	Non-effect allele	Effect allele	MAF	mvgwasP (discovery -British-)	mvgwasP (replication -non British-)	Nearest gene	Central endophenotypes	univariate P value	univariate Z
252	rs113448888	17	44108482	UTR3	AGCCCTCT	A	0.224	2.09E-100	9.42E-05	KANSL1	ICVF Superior Londgitudinal Fasciculus I Left	1.89E-16	8.228704
252	rs113448888	17	44108482	UTR3	AGCCCTCT	A	0.224	2.09E-100	9.42E-05	KANSL1	L2 Frontal Aslant Tract Right	9.00E-09	-5.748508
252	rs113448888	17	44108482	UTR3	AGCCCTCT	A	0.224	2.09E-100	9.42E-05	KANSL1	L2 Fronto Insular tract4 Right	7.75E-16	-8.058115
252	rs113448888	17	44108482	UTR3	AGCCCTCT	A	0.224	2.09E-100	9.42E-05	KANSL1	L2 Arcuate Anterior Segment Left	3.60E-09	-5.901651
252	rs113448888	17	44108482	UTR3	AGCCCTCT	A	0.224	2.09E-100	9.42E-05	KANSL1	L1 Superior Londgitudinal Fasciculus III Left	3.98E-12	-6.938008
252	rs113448888	17	44108482	UTR3	AGCCCTCT	A	0.224	2.09E-100	9.42E-05	KANSL1	L3 Superior Londgitudinal Fasciculus II Right	6.49E-09	-5.803720
252	rs113448888	17	44108482	UTR3	AGCCCTCT	A	0.224	2.09E-100	9.42E-05	KANSL1	L1 Frontal Aslant Tract Right	3.32E-08	-5.523667
252	rs113448888	17	44108482	UTR3	AGCCCTCT	A	0.224	2.09E-100	9.42E-05	KANSL1	MD Arcuate Long Segment Left	3.61E-09	-5.901251
252	rs113448888	17	44108482	UTR3	AGCCCTCT	A	0.224	2.09E-100	9.42E-05	KANSL1	L3 Superior Londgitudinal Fasciculus I Right	1.63E-09	-6.030634
252	rs113448888	17	44108482	UTR3	AGCCCTCT	A	0.224	2.09E-100	9.42E-05	KANSL1	ICVF Uncinate Left	9.39E-11	6.476456
252	rs113448888	17	44108482	UTR3	AGCCCTCT	A	0.224	2.09E-100	9.42E-05	KANSL1	ICVF Inferior Longitudinal Left	4.52E-08	5.469307
252	rs113448888	17	44108482	UTR3	AGCCCTCT	A	0.224	2.09E-100	9.42E-05	KANSL1	ICVF Superior Londgitudinal Fasciculus III Left	3.00E-20	9.218880
252	rs113448888	17	44108482	UTR3	AGCCCTCT	A	0.224	2.09E-100	9.42E-05	KANSL1	MD Superior Londgitudinal Fasciculus III Right	1.14E-15	-8.010875
252	rs113448888	17	44108482	UTR3	AGCCCTCT	A	0.224	2.09E-100	9.42E-05	KANSL1	L3 Frontal Inferior longitudinal Right	7.77E-16	-8.057838
252	rs113448888	17	44108482	UTR3	AGCCCTCT	A	0.224	2.09E-100	9.42E-05	KANSL1	L1 Fronto Insular tract5 Right	6.62E-13	-7.186988
252	rs113448888	17	44108482	UTR3	AGCCCTCT	A	0.224	2.09E-100	9.42E-05	KANSL1	L3 Arcuate Anterior Segment Right	3.45E-10	-6.277266
252	rs113448888	17	44108482	UTR3	AGCCCTCT	A	0.224	2.09E-100	9.42E-05	KANSL1	L2 Arcuate Posterior Segment Left	1.48E-09	-6.046922
252	rs113448888	17	44108482	UTR3	AGCCCTCT	A	0.224	2.09E-100	9.42E-05	KANSL1	ICVF Frontal Inferior longitudinal Right	3.48E-24	10.145278
255	rs36090413	17	62984671	intergenic	C	G	0.081	3.35E-10	1.56E-01	AMZ2P1	MO Corpus callosum	3.15E-08	5.533045
256	rs62086046	17	65982943	intergenic	T	C	0.204	8.58E-19	3.20E-02	BPTF	L3 Superior Londgitudinal Fasciculus II Left	1.85E-08	-5.625138
256	rs62086046	17	65982943	intergenic	T	C	0.204	8.58E-19	3.20E-02	BPTF	MD Inferior Longitudinal Left	9.40E-09	-5.741251
256	rs62086046	17	65982943	intergenic	T	C	0.204	8.58E-19	3.20E-02	BPTF	ICVF Fronto Insular tract4 Right	1.18E-10	6.442344
256	rs62086046	17	65982943	intergenic	T	C	0.204	8.58E-19	3.20E-02	BPTF	FA Superior Londgitudinal Fasciculus III Right	6.31E-13	7.193666
256	rs62086046	17	65982943	intergenic	T	C	0.204	8.58E-19	3.20E-02	BPTF	MD Superior Londgitudinal Fasciculus II Right	2.29E-08	-5.588580
256	rs62086046	17	65982943	intergenic	T	C	0.204	8.58E-19	3.20E-02	BPTF	ICVF Superior Londgitudinal Fasciculus II Right	2.34E-09	5.972586
256	rs62086046	17	65982943	intergenic	T	C	0.204	8.58E-19	3.20E-02	BPTF	ICVF Arcuate Anterior Segment Right	1.06E-11	6.798595
256	rs62086046	17	65982943	intergenic	T	C	0.204	8.58E-19	3.20E-02	BPTF	MD Arcuate Anterior Segment Right	2.03E-11	-6.703756
256	rs62086046	17	65982943	intergenic	T	C	0.204	8.58E-19	3.20E-02	BPTF	L2 Inferior Longitudinal Left	9.09E-09	-5.746980
256	rs62086046	17	65982943	intergenic	T	C	0.204	8.58E-19	3.20E-02	BPTF	ICVF Arcuate Long Segment Left	4.25E-10	6.244595
256	rs62086046	17	65982943	intergenic	T	C	0.204	8.58E-19	3.20E-02	BPTF	L3 Superior Londgitudinal Fasciculus I Left	3.19E-08	-5.530726
256	rs62086046	17	65982943	intergenic	T	C	0.204	8.58E-19	3.20E-02	BPTF	FA Arcuate Anterior Segment Right	1.95E-10	6.365264
256	rs62086046	17	65982943	intergenic	T	C	0.204	8.58E-19	3.20E-02	BPTF	FA Superior Londgitudinal Fasciculus I Left	2.01E-08	5.611010
256	rs62086046	17	65982943	intergenic	T	C	0.204	8.58E-19	3.20E-02	BPTF	ICVF Inferior Fronto Occipital fasciculus Right	2.99E-08	5.542209
256	rs62086046	17	65982943	intergenic	T	C	0.204	8.58E-19	3.20E-02	BPTF	ICVF Corpus callosum	2.90E-09	5.937271
256	rs62086046	17	65982943	intergenic	T	C	0.204	8.58E-19	3.20E-02	BPTF	L3 Superior Londgitudinal Fasciculus III Right	2.43E-14	-7.625566
256	rs62086046	17	65982943	intergenic	T	C	0.204	8.58E-19	3.20E-02	BPTF	ICVF Arcuate Posterior Segment Right	3.41E-11	6.627475
256	rs62086046	17	65982943	intergenic	T	C	0.204	8.58E-19	3.20E-02	BPTF	FA Frontal Inferior longitudinal Right	5.36E-09	5.835643
256	rs62086046	17	65982943	intergenic	T	C	0.204	8.58E-19	3.20E-02	BPTF	L3 Arcuate Posterior Segment Right	6.48E-10	-6.178168
256	rs62086046	17	65982943	intergenic	T	C	0.204	8.58E-19	3.20E-02	BPTF	ICVF Fronto Insular tract3 Left	2.70E-10	6.314979
256	rs62086046	17	65982943	intergenic	T	C	0.204	8.58E-19	3.20E-02	BPTF	FA Superior Londgitudinal Fasciculus III Left	8.29E-10	6.139187
256	rs62086046	17	65982943	intergenic	T	C	0.204	8.58E-19	3.20E-02	BPTF	MD Superior Londgitudinal Fasciculus III Left	4.85E-12	-6.909955
256	rs62086046	17	65982943	intergenic	T	C	0.204	8.58E-19	3.20E-02	BPTF	ICVF Inferior Fronto Occipital fasciculus Left	1.86E-09	6.009659
256	rs62086046	17	65982943	intergenic	T	C	0.204	8.58E-19	3.20E-02	BPTF	ICVF Frontal Aslant Tract Right	1.14E-08	5.708940
256	rs62086046	17	65982943	intergenic	T	C	0.204	8.58E-19	3.20E-02	BPTF	L1 Arcuate Posterior Segment Left	8.74E-09	-5.753613
256	rs62086046	17	65982943	intergenic	T	C	0.204	8.58E-19	3.20E-02	BPTF	MD Arcuate Posterior Segment Right	2.43E-10	-6.331325
256	rs62086046	17	65982943	intergenic	T	C	0.204	8.58E-19	3.20E-02	BPTF	L1 Uncinate Left	4.13E-09	-5.878865
256	rs62086046	17	65982943	intergenic	T	C	0.204	8.58E-19	3.20E-02	BPTF	L2 Superior Londgitudinal Fasciculus III Right	6.91E-13	-7.181209
256	rs62086046	17	65982943	intergenic	T	C	0.204	8.58E-19	3.20E-02	BPTF	L3 Superior Londgitudinal Fasciculus III Left	1.00E-11	-6.805963
256	rs62086046	17	65982943	intergenic	T	C	0.204	8.58E-19	3.20E-02	BPTF	L1 Uncinate Right	5.78E-10	-6.196222
256	rs62086046	17	65982943	intergenic	T	C	0.204	8.58E-19	3.20E-02	BPTF	ICVF Superior Londgitudinal Fasciculus II Left	4.58E-09	5.861682
256	rs62086046	17	65982943	intergenic	T	C	0.204	8.58E-19	3.20E-02	BPTF	L2 Frontal Aslant Tract Left	2.18E-08	-5.596940
256	rs62086046	17	65982943	intergenic	T	C	0.204	8.58E-19	3.20E-02	BPTF	L2 Superior Londgitudinal Fasciculus III Left	1.49E-10	-6.406449
256	rs62086046	17	65982943	intergenic	T	C	0.204	8.58E-19	3.20E-02	BPTF	L2 Arcuate Anterior Segment Right	5.11E-10	-6.215729
256	rs62086046	17	65982943	intergenic	T	C	0.204	8.58E-19	3.20E-02	BPTF	L3 Arcuate Long Segment Left	2.60E-12	-6.997996
256	rs62086046	17	65982943	intergenic	T	C	0.204	8.58E-19	3.20E-02	BPTF	ICVF Frontal Aslant Tract Left	8.70E-10	6.131659
256	rs62086046	17	65982943	intergenic	T	C	0.204	8.58E-19	3.20E-02	BPTF	MD Frontal Aslant Tract Left	1.24E-08	-5.693994
256	rs62086046	17	65982943	intergenic	T	C	0.204	8.58E-19	3.20E-02	BPTF	ICVF Superior Londgitudinal Fasciculus III Right	6.66E-14	7.494323
256	rs62086046	17	65982943	intergenic	T	C	0.204	8.58E-19	3.20E-02	BPTF	L3 Arcuate Posterior Segment Left	9.13E-12	-6.819616
256	rs62086046	17	65982943	intergenic	T	C	0.204	8.58E-19	3.20E-02	BPTF	L1 Superior Londgitudinal Fasciculus III Right	3.81E-10	-6.261736
256	rs62086046	17	65982943	intergenic	T	C	0.204	8.58E-19	3.20E-02	BPTF	MD Superior Londgitudinal Fasciculus II Left	1.40E-09	-6.055503
256	rs62086046	17	65982943	intergenic	T	C	0.204	8.58E-19	3.20E-02	BPTF	ICVF Arcuate Posterior Segment Left	1.39E-11	6.759462
256	rs62086046	17	65982943	intergenic	T	C	0.204	8.58E-19	3.20E-02	BPTF	ICVF Arcuate Long Segment Right	4.14E-12	6.932214
256	rs62086046	17	65982943	intergenic	T	C	0.204	8.58E-19	3.20E-02	BPTF	L3 Inferior Longitudinal Left	6.14E-09	-5.813009
256	rs62086046	17	65982943	intergenic	T	C	0.204	8.58E-19	3.20E-02	BPTF	L3 Uncinate Left	3.02E-09	-5.930460
256	rs62086046	17	65982943	intergenic	T	C	0.204	8.58E-19	3.20E-02	BPTF	ICVF Inferior Longitudinal Right	4.75E-08	5.460561
256	rs62086046	17	65982943	intergenic	T	C	0.204	8.58E-19	3.20E-02	BPTF	L3 Arcuate Long Segment Right	6.54E-12	-6.867298
256	rs62086046	17	65982943	intergenic	T	C	0.204	8.58E-19	3.20E-02	BPTF	L2 Superior Londgitudinal Fasciculus I Left	2.59E-10	-6.321685
256	rs62086046	17	65982943	intergenic	T	C	0.204	8.58E-19	3.20E-02	BPTF	MD Frontal Inferior longitudinal Right	1.50E-09	-6.044406
256	rs62086046	17	65982943	intergenic	T	C	0.204	8.58E-19	3.20E-02	BPTF	MD Arcuate Posterior Segment Left	3.49E-12	-6.956464
256	rs62086046	17	65982943	intergenic	T	C	0.204	8.58E-19	3.20E-02	BPTF	ICVF Superior Londgitudinal Fasciculus I Right	4.65E-08	5.464090
256	rs62086046	17	65982943	intergenic	T	C	0.204	8.58E-19	3.20E-02	BPTF	MD Arcuate Long Segment Right	7.99E-11	-6.500809
256	rs62086046	17	65982943	intergenic	T	C	0.204	8.58E-19	3.20E-02	BPTF	ICVF Superior Londgitudinal Fasciculus I Left	3.75E-08	5.502016
256	rs62086046	17	65982943	intergenic	T	C	0.204	8.58E-19	3.20E-02	BPTF	L2 Arcuate Anterior Segment Left	1.38E-09	-6.057307
256	rs62086046	17	65982943	intergenic	T	C	0.204	8.58E-19	3.20E-02	BPTF	L1 Superior Londgitudinal Fasciculus III Left	1.20E-08	-5.699958
256	rs62086046	17	65982943	intergenic	T	C	0.204	8.58E-19	3.20E-02	BPTF	L3 Superior Londgitudinal Fasciculus II Right	3.90E-08	-5.495300
256	rs62086046	17	65982943	intergenic	T	C	0.204	8.58E-19	3.20E-02	BPTF	MD Arcuate Long Segment Left	1.25E-10	-6.433398
256	rs62086046	17	65982943	intergenic	T	C	0.204	8.58E-19	3.20E-02	BPTF	ICVF Uncinate Right	1.73E-08	5.637310
256	rs62086046	17	65982943	intergenic	T	C	0.204	8.58E-19	3.20E-02	BPTF	ICVF Uncinate Left	1.33E-10	6.424104
256	rs62086046	17	65982943	intergenic	T	C	0.204	8.58E-19	3.20E-02	BPTF	ICVF Inferior Longitudinal Left	2.26E-08	5.590897
256	rs62086046	17	65982943	intergenic	T	C	0.204	8.58E-19	3.20E-02	BPTF	ICVF Superior Londgitudinal Fasciculus III Left	8.32E-11	6.494637
256	rs62086046	17	65982943	intergenic	T	C	0.204	8.58E-19	3.20E-02	BPTF	MD Uncinate Left	4.30E-09	-5.872214
256	rs62086046	17	65982943	intergenic	T	C	0.204	8.58E-19	3.20E-02	BPTF	MD Superior Londgitudinal Fasciculus III Right	1.46E-13	-7.390531
256	rs62086046	17	65982943	intergenic	T	C	0.204	8.58E-19	3.20E-02	BPTF	L3 Frontal Inferior longitudinal Right	4.22E-10	-6.245563

Genomic Locus	Lead SNP	chr	Position	Functional category	Non-effect allele	Effect allele	MAF	mvgwasP (discovery -British-)	mvgwasP (replication -non British-)	Nearest gene	Central endophenotypes	univariate P value	univariate Z
256	rs62086046	17	65982943	intergenic	T	C	0.204	8.58E-19	3.20E-02	BPTF	MD Inferior Fronto Occipital fasciculus Left	4.15E-08	-5.484500
256	rs62086046	17	65982943	intergenic	T	C	0.204	8.58E-19	3.20E-02	BPTF	L3 Arcuate Anterior Segment Right	2.83E-12	-6.985743
256	rs62086046	17	65982943	intergenic	T	C	0.204	8.58E-19	3.20E-02	BPTF	ICVF Frontal Inferior longitudinal Right	2.66E-10	6.317254
256	rs62086046	17	65982943	intergenic	T	C	0.204	8.58E-19	3.20E-02	BPTF	MD Superior Londgitudinal Fasciculus I Left	2.67E-08	-5.561961
259	rs77006879	17	73866798	intergenic	G	GT	0.184	1.36E-13	4.55E-02	TRIM47	ICVF Arcuate Anterior Segment Right	8.96E-11	6.483498
259	rs77006879	17	73866798	intergenic	G	GT	0.184	1.36E-13	4.55E-02	TRIM47	ICVF Arcuate Long Segment Left	2.48E-09	5.962580
259	rs77006879	17	73866798	intergenic	G	GT	0.184	1.36E-13	4.55E-02	TRIM47	L3 Superior Londgitudinal Fasciculus III Right	5.97E-09	-5.817535
259	rs77006879	17	73866798	intergenic	G	GT	0.184	1.36E-13	4.55E-02	TRIM47	ICVF Inferior Fronto Occipital fasciculus Left	2.41E-09	5.967464
259	rs77006879	17	73866798	intergenic	G	GT	0.184	1.36E-13	4.55E-02	TRIM47	ICVF Frontal Aslant Tract Right	3.76E-09	5.894606
259	rs77006879	17	73866798	intergenic	G	GT	0.184	1.36E-13	4.55E-02	TRIM47	L2 Superior Londgitudinal Fasciculus III Right	3.31E-08	-5.524297
259	rs77006879	17	73866798	intergenic	G	GT	0.184	1.36E-13	4.55E-02	TRIM47	ICVF Frontal Inferior longitudinal Left	1.49E-08	5.662640
259	rs77006879	17	73866798	intergenic	G	GT	0.184	1.36E-13	4.55E-02	TRIM47	ICVF Frontal Aslant Tract Left	1.07E-09	6.098347
259	rs77006879	17	73866798	intergenic	G	GT	0.184	1.36E-13	4.55E-02	TRIM47	ICVF Superior Londgitudinal Fasciculus III Right	1.58E-13	7.380429
259	rs77006879	17	73866798	intergenic	G	GT	0.184	1.36E-13	4.55E-02	TRIM47	ICVF Arcuate Posterior Segment Left	3.61E-08	5.508947
259	rs77006879	17	73866798	intergenic	G	GT	0.184	1.36E-13	4.55E-02	TRIM47	MD Frontal Inferior longitudinal Right	3.69E-08	-5.505205
259	rs77006879	17	73866798	intergenic	G	GT	0.184	1.36E-13	4.55E-02	TRIM47	ICVF Arcuate Anterior Segment Left	3.49E-10	6.275271
259	rs77006879	17	73866798	intergenic	G	GT	0.184	1.36E-13	4.55E-02	TRIM47	ICVF Fronto Insular tract1 Right	1.21E-08	5.698591
259	rs77006879	17	73866798	intergenic	G	GT	0.184	1.36E-13	4.55E-02	TRIM47	ICVF Uncinate Left	4.66E-08	5.463651
259	rs77006879	17	73866798	intergenic	G	GT	0.184	1.36E-13	4.55E-02	TRIM47	ICVF Superior Londgitudinal Fasciculus III Left	2.46E-12	7.005540
259	rs77006879	17	73866798	intergenic	G	GT	0.184	1.36E-13	4.55E-02	TRIM47	ICVF Frontal Inferior longitudinal Right	3.80E-12	6.944276
260	rs9966170	18	35029506	intronic	G	A	0.360	1.24E-28	5.40E-01	CELF4	ISOVF Inferior Fronto Occipital fasciculus Right	3.01E-09	-5.931266
264	rs62127993	19	3298646	ncRNA intronic	A	G	0.135	2.58E-10	3.58E-01	AC010649.1	L1 Arcuate Anterior Segment Right	6.42E-09	5.805445
264	rs62127993	19	3298646	ncRNA intronic	A	G	0.135	2.58E-10	3.58E-01	AC010649.1	OD Arcuate Anterior Segment Right	2.49E-09	-5.961935
265	rs7256295	19	4071814	intergenic	A	G	0.223	6.17E-09	9.02E-01	ZBTB7A	L2 Uncinate Left	2.39E-09	5.969056
265	rs7256295	19	4071814	intergenic	A	G	0.223	6.17E-09	9.02E-01	ZBTB7A	L3 Uncinate Left	4.90E-08	5.454833
265	rs7256295	19	4071814	intergenic	A	G	0.223	6.17E-09	9.02E-01	ZBTB7A	L3 Uncinate Right	1.49E-08	5.662840
267	rs10403210	19	13103638	intergenic	C	T	0.466	4.69E-08	4.17E-02	NFIX	MO Superior Londgitudinal Fasciculus I Left	4.92E-08	-5.454230
271	rs429358	19	45411941	exonic	C	T	0.156	1.20E-16	5.37E-02	APOE	MD Inferior Longitudinal Left	1.25E-10	-6.433351
271	rs429358	19	45411941	exonic	C	T	0.156	1.20E-16	5.37E-02	APOE	L1 Inferior Longitudinal Left	6.70E-09	-5.798157
271	rs429358	19	45411941	exonic	C	T	0.156	1.20E-16	5.37E-02	APOE	L2 Inferior Longitudinal Left	8.48E-10	-6.135756
271	rs429358	19	45411941	exonic	C	T	0.156	1.20E-16	5.37E-02	APOE	MD Inferior Longitudinal Right	1.15E-09	-6.087099
271	rs429358	19	45411941	exonic	C	T	0.156	1.20E-16	5.37E-02	APOE	ISOVF Inferior Longitudinal Right	4.27E-08	-5.479396
271	rs429358	19	45411941	exonic	C	T	0.156	1.20E-16	5.37E-02	APOE	ISOVF Inferior Longitudinal Left	1.04E-08	-5.723498
271	rs429358	19	45411941	exonic	C	T	0.156	1.20E-16	5.37E-02	APOE	MD Arcuate Posterior Segment Right	3.10E-08	-5.535967
271	rs429358	19	45411941	exonic	C	T	0.156	1.20E-16	5.37E-02	APOE	L3 Inferior Longitudinal Left	2.37E-09	-5.970211
271	rs429358	19	45411941	exonic	C	T	0.156	1.20E-16	5.37E-02	APOE	L2 Inferior Longitudinal Right	5.35E-10	-6.208383
271	rs429358	19	45411941	exonic	C	T	0.156	1.20E-16	5.37E-02	APOE	L1 Arcuate Posterior Segment Right	4.11E-08	-5.486218
271	rs429358	19	45411941	exonic	C	T	0.156	1.20E-16	5.37E-02	APOE	L3 Inferior Longitudinal Right	2.23E-09	-5.979769
277	rs202393	20	45195738	intronic	C	T	0.160	1.77E-12	4.82E-01	SLC13A3	L3 Superior Londgitudinal Fasciculus II Left	1.84E-09	-6.011205
277	rs202393	20	45195738	intronic	C	T	0.160	1.77E-12	4.82E-01	SLC13A3	ICVF Superior Londgitudinal Fasciculus II Right	1.55E-10	6.400141
277	rs202393	20	45195738	intronic	C	T	0.160	1.77E-12	4.82E-01	SLC13A3	ICVF Arcuate Anterior Segment Right	3.18E-10	6.289534
277	rs202393	20	45195738	intronic	C	T	0.160	1.77E-12	4.82E-01	SLC13A3	ICVF Arcuate Long Segment Left	3.34E-11	6.630756
277	rs202393	20	45195738	intronic	C	T	0.160	1.77E-12	4.82E-01	SLC13A3	L3 Superior Londgitudinal Fasciculus I Left	4.35E-08	-5.476129
277	rs202393	20	45195738	intronic	C	T	0.160	1.77E-12	4.82E-01	SLC13A3	FA Superior Londgitudinal Fasciculus I Left	1.43E-10	6.412748
277	rs202393	20	45195738	intronic	C	T	0.160	1.77E-12	4.82E-01	SLC13A3	FA Arcuate Long Segment Left	2.05E-08	5.607661
277	rs202393	20	45195738	intronic	C	T	0.160	1.77E-12	4.82E-01	SLC13A3	FA Superior Londgitudinal Fasciculus II Right	2.86E-08	5.549502
277	rs202393	20	45195738	intronic	C	T	0.160	1.77E-12	4.82E-01	SLC13A3	ICVF Superior Londgitudinal Fasciculus II Left	2.60E-11	6.667417
277	rs202393	20	45195738	intronic	C	T	0.160	1.77E-12	4.82E-01	SLC13A3	L3 Arcuate Long Segment Left	1.54E-09	-6.040641
277	rs202393	20	45195738	intronic	C	T	0.160	1.77E-12	4.82E-01	SLC13A3	L2 Superior Londgitudinal Fasciculus II Right	4.50E-08	-5.469984
277	rs202393	20	45195738	intronic	C	T	0.160	1.77E-12	4.82E-01	SLC13A3	MD Superior Londgitudinal Fasciculus II Left	2.06E-09	-5.993312
277	rs202393	20	45195738	intronic	C	T	0.160	1.77E-12	4.82E-01	SLC13A3	FA Arcuate Long Segment Right	2.18E-08	5.596899
277	rs202393	20	45195738	intronic	C	T	0.160	1.77E-12	4.82E-01	SLC13A3	ICVF Arcuate Long Segment Right	5.22E-09	5.839931
277	rs202393	20	45195738	intronic	C	T	0.160	1.77E-12	4.82E-01	SLC13A3	L3 Arcuate Long Segment Right	2.79E-08	-5.554389
277	rs202393	20	45195738	intronic	C	T	0.160	1.77E-12	4.82E-01	SLC13A3	ICVF Superior Londgitudinal Fasciculus I Right	2.94E-09	5.935183
277	rs202393	20	45195738	intronic	C	T	0.160	1.77E-12	4.82E-01	SLC13A3	L2 Arcuate Long Segment Left	4.46E-08	-5.471526
277	rs202393	20	45195738	intronic	C	T	0.160	1.77E-12	4.82E-01	SLC13A3	ICVF Superior Londgitudinal Fasciculus I Left	3.43E-10	6.277932
277	rs202393	20	45195738	intronic	C	T	0.160	1.77E-12	4.82E-01	SLC13A3	FA Superior Londgitudinal Fasciculus I Right	2.16E-10	6.349478
277	rs202393	20	45195738	intronic	C	T	0.160	1.77E-12	4.82E-01	SLC13A3	L3 Superior Londgitudinal Fasciculus II Right	1.09E-08	-5.715910
277	rs202393	20	45195738	intronic	C	T	0.160	1.77E-12	4.82E-01	SLC13A3	MD Arcuate Long Segment Left	1.92E-09	-6.004597
277	rs202393	20	45195738	intronic	C	T	0.160	1.77E-12	4.82E-01	SLC13A3	L3 Superior Londgitudinal Fasciculus I Right	1.51E-08	-5.660032
277	rs202393	20	45195738	intronic	C	T	0.160	1.77E-12	4.82E-01	SLC13A3	L2 Superior Londgitudinal Fasciculus II Left	2.07E-09	-5.992548
277	rs2694896	20	45237143	intronic	G	A	0.385	4.95E-08	3.64E-01	SLC13A3	ISOVF Frontal Aslant Tract Left	6.36E-09	5.807053
277	rs2694896	20	45237143	intronic	G	A	0.385	4.95E-08	3.64E-01	SLC13A3	ISOVF Inferior Fronto Occipital fasciculus Left	2.56E-08	5.569129
277	rs2694896	20	45237143	intronic	G	A	0.385	4.95E-08	3.64E-01	SLC13A3	ISOVF Superior Londgitudinal Fasciculus II Right	5.20E-13	7.219841
277	rs2694896	20	45237143	intronic	G	A	0.385	4.95E-08	3.64E-01	SLC13A3	ISOVF Superior Londgitudinal Fasciculus III Left	5.22E-15	7.821460
277	rs2694896	20	45237143	intronic	G	A	0.385	4.95E-08	3.64E-01	SLC13A3	ISOVF Arcuate Anterior Segment Left	5.74E-15	7.809432
277	rs2694896	20	45237143	intronic	G	A	0.385	4.95E-08	3.64E-01	SLC13A3	ISOVF Arcuate Posterior Segment Left	3.74E-14	7.569572
277	rs2694896	20	45237143	intronic	G	A	0.385	4.95E-08	3.64E-01	SLC13A3	ISOVF Inferior Longitudinal Left	6.05E-13	7.199361
277	rs2694896	20	45237143	intronic	G	A	0.385	4.95E-08	3.64E-01	SLC13A3	ISOVF Frontal Aslant Tract Right	4.62E-11	6.582644
277	rs2694896	20	45237143	intronic	G	A	0.385	4.95E-08	3.64E-01	SLC13A3	ISOVF Arcuate Long Segment Left	2.50E-10	6.326993
277	rs2694896	20	45237143	intronic	G	A	0.385	4.95E-08	3.64E-01	SLC13A3	ISOVF Superior Londgitudinal Fasciculus II Left	2.44E-16	8.198424
277	rs2694896	20	45237143	intronic	G	A	0.385	4.95E-08	3.64E-01	SLC13A3	ISOVF Arcuate Anterior Segment Right	8.85E-11	6.485454
277	rs2694896	20	45237143	intronic	G	A	0.385	4.95E-08	3.64E-01	SLC13A3	ISOVF Superior Londgitudinal Fasciculus III Right	6.40E-13	7.191623
277	rs2694896	20	45237143	intronic	G	A	0.385	4.95E-08	3.64E-01	SLC13A3	ISOVF Arcuate Posterior Segment Right	1.63E-08	5.647213
277	rs6011998	20	45269867	intronic	T	C	0.042	9.31E-10	3.66E-01	SLC13A3	ISOVF Superior Londgitudinal Fasciculus II Right	3.12E-08	5.534480
277	rs6011998	20	45269867	intronic	T	C	0.042	9.31E-10	3.66E-01	SLC13A3	ISOVF Superior Londgitudinal Fasciculus III Left	1.35E-08	5.680163
277	rs6011998	20	45269867	intronic	T	C	0.042	9.31E-10	3.66E-01	SLC13A3	ISOVF Arcuate Anterior Segment Left	4.07E-10	6.251509
277	rs6011998	20	45269867	intronic	T	C	0.042	9.31E-10	3.66E-01	SLC13A3	ISOVF Arcuate Posterior Segment Left	1.93E-15	7.945830
277	rs6011998	20	45269867	intronic	T	C	0.042	9.31E-10	3.66E-01	SLC13A3	ISOVF Inferior Longitudinal Left	3.16E-09	5.923089
277	rs6011998	20	45269867	intronic	T	C	0.042	9.31E-10	3.66E-01	SLC13A3	ISOVF Arcuate Long Segment Left	3.20E-08	5.529942
277	rs6011998	20	45269867	intronic	T	C	0.042	9.31E-10	3.66E-01	SLC13A3	ISOVF Superior Londgitudinal Fasciculus II Left	5.36E-10	6.208230
277	rs6011998	20	45269867	intronic	T	C	0.042	9.31E-10	3.66E-01	SLC13A3	ISOVF Superior Londgitudinal Fasciculus III Right	4.98E-09	5.847971
277	rs6011998	20	45269867	intronic	T	C	0.042	9.31E-10	3.66E-01	SLC13A3	ISOVF Arcuate Posterior Segment Right	8.61E-09	5.756125
279	rs72626592	20	55528415	intergenic	T	C	0.036	1.58E-09	3.84E-01	AL117380.2	MO Fronto Insular tract4 Right	3.91E-08	5.494954
280	rs6062264	20	61154871	intronic	T	C	0.279	2.12E-08	4.59E-01	C20orf166	L3 Superior Londgitudinal Fasciculus II Left	1.93E-09	-6.003847
280	rs6062264	20	61154871	intronic	T	C	0.279	2.12E-08	4.59E-01	C20orf166	FA Superior Londgitudinal Fasciculus III Right	2.14E-08	5.600387
280	rs6062264	20	61154871	intronic	T	C	0.279	2.12E-08	4.59E-01	C20orf166	ICVF Superior Londgitudinal Fasciculus II Right	4.39E-08	5.474291
280	rs6062264	20	61154871	intronic	T	C	0.279	2.12E-08	4.59E-01	C20orf166	FA Inferior Longitudinal Left	3.85E-08	5.497431
280	rs6062264	20	61154871	intronic	T	C	0.279	2.12E-08	4.59E-01	C20orf166	FA Arcuate Anterior Segment Right	1.27E-08	5.690684
280	rs6062264	20	61154871	intronic	T	C	0.279	2.12E-08	4.59E-01	C20orf166	FA Arcuate Long Segment Left	3.97E-10	6.255168
280	rs6062264	20	61154871	intronic	T	C	0.279	2.12E-08	4.59E-01	C20orf166	ICVF Corpus callosum	1.22E-08	5.697427
280	rs6062264	20	61154871	intronic	T	C	0.279	2.12E-08	4.59E-01	C20orf166	ICVF Frontal Superior Longitudinal Left	3.05E-10	6.296423

Genomic Locus	Lead SNP	chr	Position	Functional category	Non-effect allele	Effect allele	MAF	mvgwasP (discovery -British-)	mvgwasP (replication -non British-)	Nearest gene	Central endophenotypes	univariate P value	univariate Z
280	rs6062264	20	61154871	intronic	T	C	0.279	2.12E-08	4.59E-01	C20orf166	FA Superior Londgitudinal Fasciculus II Right	3.05E-08	5.538525
280	rs6062264	20	61154871	intronic	T	C	0.279	2.12E-08	4.59E-01	C20orf166	ICVF Superior Londgitudinal Fasciculus II Left	6.88E-11	6.523167
280	rs6062264	20	61154871	intronic	T	C	0.279	2.12E-08	4.59E-01	C20orf166	L3 Corpus callosum	1.59E-08	-5.652092
280	rs6062264	20	61154871	intronic	T	C	0.279	2.12E-08	4.59E-01	C20orf166	FA Corpus callosum	1.46E-10	6.409307
280	rs6062264	20	61154871	intronic	T	C	0.279	2.12E-08	4.59E-01	C20orf166	FA Superior Londgitudinal Fasciculus II Left	1.13E-11	6.788361
282	rs9608859	22	30667277	intergenic	C	T	0.437	2.31E-12	5.74E-01	OSM	ICVF Superior Londgitudinal Fasciculus II Right	1.31E-11	-6.767972
282	rs9608859	22	30667277	intergenic	C	T	0.437	2.31E-12	5.74E-01	OSM	FA Inferior Longitudinal Left	9.36E-09	-5.742006
282	rs9608859	22	30667277	intergenic	C	T	0.437	2.31E-12	5.74E-01	OSM	ICVF Arcuate Anterior Segment Right	9.40E-12	-6.815330
282	rs9608859	22	30667277	intergenic	C	T	0.437	2.31E-12	5.74E-01	OSM	ICVF Arcuate Long Segment Left	8.38E-12	-6.831812
282	rs9608859	22	30667277	intergenic	C	T	0.437	2.31E-12	5.74E-01	OSM	ICVF Inferior Fronto Occipital fasciculus Right	5.53E-15	-7.814322
282	rs9608859	22	30667277	intergenic	C	T	0.437	2.31E-12	5.74E-01	OSM	MD Inferior Fronto Occipital fasciculus Right	4.53E-08	5.468767
282	rs9608859	22	30667277	intergenic	C	T	0.437	2.31E-12	5.74E-01	OSM	ICVF Corpus callosum	8.28E-14	-7.465787
282	rs9608859	22	30667277	intergenic	C	T	0.437	2.31E-12	5.74E-01	OSM	ICVF Arcuate Posterior Segment Right	1.32E-09	-6.064682
282	rs9608859	22	30667277	intergenic	C	T	0.437	2.31E-12	5.74E-01	OSM	ICVF Inferior Fronto Occipital fasciculus Left	7.32E-15	-7.778804
282	rs9608859	22	30667277	intergenic	C	T	0.437	2.31E-12	5.74E-01	OSM	ICVF Frontal Aslant Tract Right	6.98E-12	-6.858133
282	rs9608859	22	30667277	intergenic	C	T	0.437	2.31E-12	5.74E-01	OSM	ICVF Superior Londgitudinal Fasciculus II Left	6.33E-10	-6.181892
282	rs9608859	22	30667277	intergenic	C	T	0.437	2.31E-12	5.74E-01	OSM	L3 Inferior Fronto Occipital fasciculus Right	1.85E-09	6.010664
282	rs9608859	22	30667277	intergenic	C	T	0.437	2.31E-12	5.74E-01	OSM	L3 Inferior Fronto Occipital fasciculus Left	3.18E-10	6.289503
282	rs9608859	22	30667277	intergenic	C	T	0.437	2.31E-12	5.74E-01	OSM	L3 Arcuate Long Segment Left	1.11E-08	5.713369
282	rs9608859	22	30667277	intergenic	C	T	0.437	2.31E-12	5.74E-01	OSM	ICVF Frontal Aslant Tract Left	1.24E-12	-7.101399
282	rs9608859	22	30667277	intergenic	C	T	0.437	2.31E-12	5.74E-01	OSM	ICVF Superior Londgitudinal Fasciculus III Right	2.96E-09	-5.933574
282	rs9608859	22	30667277	intergenic	C	T	0.437	2.31E-12	5.74E-01	OSM	ICVF Frontal Superior Longitudinal Right	3.56E-09	-5.903279
282	rs9608859	22	30667277	intergenic	C	T	0.437	2.31E-12	5.74E-01	OSM	FA Arcuate Long Segment Right	4.24E-08	-5.480486
282	rs9608859	22	30667277	intergenic	C	T	0.437	2.31E-12	5.74E-01	OSM	ICVF Arcuate Long Segment Right	3.95E-12	-6.938846
282	rs9608859	22	30667277	intergenic	C	T	0.437	2.31E-12	5.74E-01	OSM	ICVF Inferior Longitudinal Right	3.75E-13	-7.264328
282	rs9608859	22	30667277	intergenic	C	T	0.437	2.31E-12	5.74E-01	OSM	L3 Arcuate Long Segment Right	2.48E-08	5.574378
282	rs9608859	22	30667277	intergenic	C	T	0.437	2.31E-12	5.74E-01	OSM	ICVF Superior Londgitudinal Fasciculus I Right	2.85E-13	-7.301488
282	rs9608859	22	30667277	intergenic	C	T	0.437	2.31E-12	5.74E-01	OSM	ICVF Superior Londgitudinal Fasciculus I Left	1.67E-12	-7.059527
282	rs9608859	22	30667277	intergenic	C	T	0.437	2.31E-12	5.74E-01	OSM	ICVF Inferior Longitudinal Left	1.03E-13	-7.437239
282	rs9608859	22	30667277	intergenic	C	T	0.437	2.31E-12	5.74E-01	OSM	ICVF Superior Londgitudinal Fasciculus III Left	2.18E-10	-6.347764
282	rs9608859	22	30667277	intergenic	C	T	0.437	2.31E-12	5.74E-01	OSM	MD Inferior Fronto Occipital fasciculus Left	6.07E-09	5.814822
282	rs9608859	22	30667277	intergenic	C	T	0.437	2.31E-12	5.74E-01	OSM	ICVF Frontal Inferior longitudinal Right	3.70E-08	-5.504648
282	rs2267161	22	30953295	exonic	T	C	0.306	2.46E-12	2.57E-02	GAL3ST1	MD Inferior Longitudinal Left	7.22E-09	5.785687
282	rs2267161	22	30953295	exonic	T	C	0.306	2.46E-12	2.57E-02	GAL3ST1	ICVF Superior Londgitudinal Fasciculus II Right	1.11E-14	-7.726407
282	rs2267161	22	30953295	exonic	T	C	0.306	2.46E-12	2.57E-02	GAL3ST1	ICVF Arcuate Anterior Segment Right	2.57E-18	-8.729145
282	rs2267161	22	30953295	exonic	T	C	0.306	2.46E-12	2.57E-02	GAL3ST1	MD Inferior Longitudinal Right	3.70E-09	5.897037
282	rs2267161	22	30953295	exonic	T	C	0.306	2.46E-12	2.57E-02	GAL3ST1	L1 Inferior Fronto Occipital fasciculus Left	5.69E-11	6.551687
282	rs2267161	22	30953295	exonic	T	C	0.306	2.46E-12	2.57E-02	GAL3ST1	ICVF Arcuate Long Segment Left	2.48E-19	-8.989658
282	rs2267161	22	30953295	exonic	T	C	0.306	2.46E-12	2.57E-02	GAL3ST1	FA Arcuate Anterior Segment Right	2.66E-09	-5.951242
282	rs2267161	22	30953295	exonic	T	C	0.306	2.46E-12	2.57E-02	GAL3ST1	FA Superior Londgitudinal Fasciculus I Left	4.67E-10	-6.229846
282	rs2267161	22	30953295	exonic	T	C	0.306	2.46E-12	2.57E-02	GAL3ST1	ICVF Inferior Fronto Occipital fasciculus Right	2.04E-16	-8.219492
282	rs2267161	22	30953295	exonic	T	C	0.306	2.46E-12	2.57E-02	GAL3ST1	FA Arcuate Long Segment Left	1.52E-08	-5.659434
282	rs2267161	22	30953295	exonic	T	C	0.306	2.46E-12	2.57E-02	GAL3ST1	MD Inferior Fronto Occipital fasciculus Right	1.40E-10	6.416151
282	rs2267161	22	30953295	exonic	T	C	0.306	2.46E-12	2.57E-02	GAL3ST1	ICVF Corpus callosum	9.09E-18	-8.584882
282	rs2267161	22	30953295	exonic	T	C	0.306	2.46E-12	2.57E-02	GAL3ST1	ICVF Arcuate Posterior Segment Right	2.03E-13	-7.346629
282	rs2267161	22	30953295	exonic	T	C	0.306	2.46E-12	2.57E-02	GAL3ST1	FA Superior Londgitudinal Fasciculus III Left	2.15E-08	-5.599728
282	rs2267161	22	30953295	exonic	T	C	0.306	2.46E-12	2.57E-02	GAL3ST1	MD Superior Londgitudinal Fasciculus III Left	4.25E-08	5.479950
282	rs2267161	22	30953295	exonic	T	C	0.306	2.46E-12	2.57E-02	GAL3ST1	ICVF Inferior Fronto Occipital fasciculus Left	6.79E-15	-7.788240
282	rs2267161	22	30953295	exonic	T	C	0.306	2.46E-12	2.57E-02	GAL3ST1	ICVF Frontal Aslant Tract Right	2.18E-13	-7.337182
282	rs2267161	22	30953295	exonic	T	C	0.306	2.46E-12	2.57E-02	GAL3ST1	L1 Inferior Fronto Occipital fasciculus Right	7.73E-11	6.505677
282	rs2267161	22	30953295	exonic	T	C	0.306	2.46E-12	2.57E-02	GAL3ST1	L1 Arcuate Posterior Segment Left	4.27E-08	5.479177
282	rs2267161	22	30953295	exonic	T	C	0.306	2.46E-12	2.57E-02	GAL3ST1	L3 Superior Londgitudinal Fasciculus III Left	1.21E-08	5.697902
282	rs2267161	22	30953295	exonic	T	C	0.306	2.46E-12	2.57E-02	GAL3ST1	ICVF Superior Londgitudinal Fasciculus II Left	5.29E-15	-7.819823
282	rs2267161	22	30953295	exonic	T	C	0.306	2.46E-12	2.57E-02	GAL3ST1	L3 Inferior Fronto Occipital fasciculus Right	9.20E-09	5.744784
282	rs2267161	22	30953295	exonic	T	C	0.306	2.46E-12	2.57E-02	GAL3ST1	L3 Inferior Fronto Occipital fasciculus Left	7.38E-09	5.782038
282	rs2267161	22	30953295	exonic	T	C	0.306	2.46E-12	2.57E-02	GAL3ST1	L3 Arcuate Long Segment Left	3.55E-12	6.953980
282	rs2267161	22	30953295	exonic	T	C	0.306	2.46E-12	2.57E-02	GAL3ST1	ICVF Frontal Aslant Tract Left	1.08E-13	-7.431097
282	rs2267161	22	30953295	exonic	T	C	0.306	2.46E-12	2.57E-02	GAL3ST1	ICVF Superior Londgitudinal Fasciculus III Right	2.33E-14	-7.630974
282	rs2267161	22	30953295	exonic	T	C	0.306	2.46E-12	2.57E-02	GAL3ST1	ICVF Arcuate Posterior Segment Left	1.43E-13	-7.393747
282	rs2267161	22	30953295	exonic	T	C	0.306	2.46E-12	2.57E-02	GAL3ST1	ICVF Arcuate Long Segment Right	3.82E-16	-8.144250
282	rs2267161	22	30953295	exonic	T	C	0.306	2.46E-12	2.57E-02	GAL3ST1	ICVF Inferior Longitudinal Right	1.93E-16	-8.226645
282	rs2267161	22	30953295	exonic	T	C	0.306	2.46E-12	2.57E-02	GAL3ST1	L3 Arcuate Long Segment Right	7.28E-09	5.784271
282	rs2267161	22	30953295	exonic	T	C	0.306	2.46E-12	2.57E-02	GAL3ST1	FA Corpus callosum	4.41E-08	-5.473407
282	rs2267161	22	30953295	exonic	T	C	0.306	2.46E-12	2.57E-02	GAL3ST1	L1 Inferior Longitudinal Right	1.30E-08	5.685912
282	rs2267161	22	30953295	exonic	T	C	0.306	2.46E-12	2.57E-02	GAL3ST1	MD Arcuate Posterior Segment Left	1.20E-09	6.080398
282	rs2267161	22	30953295	exonic	T	C	0.306	2.46E-12	2.57E-02	GAL3ST1	ICVF Arcuate Anterior Segment Left	7.30E-14	-7.482401
282	rs2267161	22	30953295	exonic	T	C	0.306	2.46E-12	2.57E-02	GAL3ST1	ICVF Superior Londgitudinal Fasciculus I Right	1.02E-17	-8.572181
282	rs2267161	22	30953295	exonic	T	C	0.306	2.46E-12	2.57E-02	GAL3ST1	OD Inferior Fronto Occipital fasciculus Right	4.21E-08	-5.481617
282	rs2267161	22	30953295	exonic	T	C	0.306	2.46E-12	2.57E-02	GAL3ST1	ICVF Superior Londgitudinal Fasciculus I Left	6.75E-17	-8.351324
282	rs2267161	22	30953295	exonic	T	C	0.306	2.46E-12	2.57E-02	GAL3ST1	FA Superior Londgitudinal Fasciculus I Right	1.50E-08	-5.661112
282	rs2267161	22	30953295	exonic	T	C	0.306	2.46E-12	2.57E-02	GAL3ST1	MD Arcuate Long Segment Left	5.95E-12	6.880805
282	rs2267161	22	30953295	exonic	T	C	0.306	2.46E-12	2.57E-02	GAL3ST1	ICVF Uncinate Right	5.44E-10	-6.205921
282	rs2267161	22	30953295	exonic	T	C	0.306	2.46E-12	2.57E-02	GAL3ST1	L3 Superior Londgitudinal Fasciculus I Right	4.25E-08	5.479936
282	rs2267161	22	30953295	exonic	T	C	0.306	2.46E-12	2.57E-02	GAL3ST1	ICVF Inferior Longitudinal Left	2.46E-15	-7.915699
282	rs2267161	22	30953295	exonic	T	C	0.306	2.46E-12	2.57E-02	GAL3ST1	ICVF Superior Londgitudinal Fasciculus III Left	3.62E-16	-8.150557
282	rs2267161	22	30953295	exonic	T	C	0.306	2.46E-12	2.57E-02	GAL3ST1	L3 Inferior Longitudinal Right	3.17E-08	5.531535
282	rs2267161	22	30953295	exonic	T	C	0.306	2.46E-12	2.57E-02	GAL3ST1	MD Inferior Fronto Occipital fasciculus Left	1.75E-10	6.381978
282	rs2267161	22	30953295	exonic	T	C	0.306	2.46E-12	2.57E-02	GAL3ST1	L3 Arcuate Anterior Segment Right	1.89E-09	6.006789
282	rs2267161	22	30953295	exonic	T	C	0.306	2.46E-12	2.57E-02	GAL3ST1	ICVF Frontal Inferior longitudinal Right	1.01E-13	-7.439879
283	rs738443	22	38458681	ncRNA intronic	A	G	0.381	3.31E-18	4.80E-01	PICK1:RP5-1039K5.13	L3 Frontal Aslant Tract Right	2.17E-08	5.597846
283	rs738443	22	38458681	ncRNA intronic	A	G	0.381	3.31E-18	4.80E-01	PICK1:RP5-1039K5.13	FA Inferior Fronto Occipital fasciculus Right	3.98E-09	-5.884952
283	rs738443	22	38458681	ncRNA intronic	A	G	0.381	3.31E-18	4.80E-01	PICK1:RP5-1039K5.13	FA Superior Londgitudinal Fasciculus III Right	8.41E-09	-5.759977
283	rs738443	22	38458681	ncRNA intronic	A	G	0.381	3.31E-18	4.80E-01	PICK1:RP5-1039K5.13	FA Inferior Longitudinal Left	9.92E-09	-5.732161
283	rs738443	22	38458681	ncRNA intronic	A	G	0.381	3.31E-18	4.80E-01	PICK1:RP5-1039K5.13	FA Inferior Fronto Occipital fasciculus Left	9.12E-09	-5.746274
283	rs738443	22	38458681	ncRNA intronic	A	G	0.381	3.31E-18	4.80E-01	PICK1:RP5-1039K5.13	ICVF Arcuate Anterior Segment Right	9.19E-12	-6.818605
283	rs738443	22	38458681	ncRNA intronic	A	G	0.381	3.31E-18	4.80E-01	PICK1:RP5-1039K5.13	ICVF Arcuate Long Segment Left	5.77E-13	-7.205757
283	rs738443	22	38458681	ncRNA intronic	A	G	0.381	3.31E-18	4.80E-01	PICK1:RP5-1039K5.13	L3 Superior Londgitudinal Fasciculus I Left	2.93E-08	5.545628
283	rs738443	22	38458681	ncRNA intronic	A	G	0.381	3.31E-18	4.80E-01	PICK1:RP5-1039K5.13	ICVF Inferior Fronto Occipital fasciculus Right	5.58E-10	-6.201727
283	rs738443	22	38458681	ncRNA intronic	A	G	0.381	3.31E-18	4.80E-01	PICK1:RP5-1039K5.13	FA Arcuate Long Segment Left	1.87E-09	-6.008915
283	rs738443	22	38458681	ncRNA intronic	A	G	0.381	3.31E-18	4.80E-01	PICK1:RP5-1039K5.13	MD Inferior Fronto Occipital fasciculus Right	9.86E-09	5.733180
283	rs738443	22	38458681	ncRNA intronic	A	G	0.381	3.31E-18	4.80E-01	PICK1:RP5-1039K5.13	ICVF Corpus callosum	4.52E-12	-6.919862
283	rs738443	22	38458681	ncRNA intronic	A	G	0.381	3.31E-18	4.80E-01	PICK1:RP5-1039K5.13	L3 Superior Londgitudinal Fasciculus III Right	1.20E-08	5.699634
283	rs738443	22	38458681	ncRNA intronic	A	G	0.381	3.31E-18	4.80E-01	PICK1:RP5-1039K5.13	ICVF Arcuate Posterior Segment Right	4.48E-08	-5.470729
283	rs738443	22	38458681	ncRNA intronic	A	G	0.381	3.31E-18	4.80E-01	PICK1:RP5-1039K5.13	FA Frontal Inferior longitudinal Right	8.32E-10	-6.138665
283	rs738443	22	38458681	ncRNA intronic	A	G	0.381	3.31E-18	4.80E-01	PICK1:RP5-1039K5.13	FA Superior Londgitudinal Fasciculus III Left	3.44E-09	-5.908906

Genomic Locus	Lead SNP	chr	Position	Functional category	Non-effect allele	Effect allele	MAF	mvgwasP (discovery -British-)	mvgwasP (replication -non British-)	Nearest gene	Central endophenotypes	univariate P value	univariate Z
283	rs738443	22	38458681	ncRNA intronic	A	G	0.381	3.31E-18	4.80E-01	PICK1:RP5-1039K5.13	MD Superior Londgitudinal Fasciculus III Left	1.66E-08	5.643807
283	rs738443	22	38458681	ncRNA intronic	A	G	0.381	3.31E-18	4.80E-01	PICK1:RP5-1039K5.13	ICVF Inferior Fronto Occipital fasciculus Left	8.09E-10	-6.143095
283	rs738443	22	38458681	ncRNA intronic	A	G	0.381	3.31E-18	4.80E-01	PICK1:RP5-1039K5.13	ICVF Frontal Aslant Tract Right	3.51E-08	-5.514008
283	rs738443	22	38458681	ncRNA intronic	A	G	0.381	3.31E-18	4.80E-01	PICK1:RP5-1039K5.13	L3 Superior Londgitudinal Fasciculus III Left	5.07E-10	6.216850
283	rs738443	22	38458681	ncRNA intronic	A	G	0.381	3.31E-18	4.80E-01	PICK1:RP5-1039K5.13	L3 Inferior Fronto Occipital fasciculus Right	3.00E-12	6.977807
283	rs738443	22	38458681	ncRNA intronic	A	G	0.381	3.31E-18	4.80E-01	PICK1:RP5-1039K5.13	L3 Inferior Fronto Occipital fasciculus Left	8.96E-13	7.145681
283	rs738443	22	38458681	ncRNA intronic	A	G	0.381	3.31E-18	4.80E-01	PICK1:RP5-1039K5.13	L3 Arcuate Long Segment Left	1.02E-14	7.737274
283	rs738443	22	38458681	ncRNA intronic	A	G	0.381	3.31E-18	4.80E-01	PICK1:RP5-1039K5.13	ICVF Superior Londgitudinal Fasciculus III Right	7.81E-09	-5.772468
283	rs738443	22	38458681	ncRNA intronic	A	G	0.381	3.31E-18	4.80E-01	PICK1:RP5-1039K5.13	FA Frontal Aslant Tract Right	3.95E-08	-5.492995
283	rs738443	22	38458681	ncRNA intronic	A	G	0.381	3.31E-18	4.80E-01	PICK1:RP5-1039K5.13	ICVF Arcuate Posterior Segment Left	2.73E-08	-5.557851
283	rs738443	22	38458681	ncRNA intronic	A	G	0.381	3.31E-18	4.80E-01	PICK1:RP5-1039K5.13	ICVF Arcuate Long Segment Right	5.24E-11	-6.564042
283	rs738443	22	38458681	ncRNA intronic	A	G	0.381	3.31E-18	4.80E-01	PICK1:RP5-1039K5.13	L3 Inferior Longitudinal Left	1.87E-08	5.623294
283	rs738443	22	38458681	ncRNA intronic	A	G	0.381	3.31E-18	4.80E-01	PICK1:RP5-1039K5.13	L3 Corpus callosum	1.11E-08	5.712612
283	rs738443	22	38458681	ncRNA intronic	A	G	0.381	3.31E-18	4.80E-01	PICK1:RP5-1039K5.13	ICVF Inferior Longitudinal Right	8.87E-09	-5.751019
283	rs738443	22	38458681	ncRNA intronic	A	G	0.381	3.31E-18	4.80E-01	PICK1:RP5-1039K5.13	L3 Arcuate Long Segment Right	7.02E-10	6.165690
283	rs738443	22	38458681	ncRNA intronic	A	G	0.381	3.31E-18	4.80E-01	PICK1:RP5-1039K5.13	FA Corpus callosum	9.70E-11	-6.471490
283	rs738443	22	38458681	ncRNA intronic	A	G	0.381	3.31E-18	4.80E-01	PICK1:RP5-1039K5.13	ICVF Superior Londgitudinal Fasciculus I Right	4.24E-09	-5.874402
283	rs738443	22	38458681	ncRNA intronic	A	G	0.381	3.31E-18	4.80E-01	PICK1:RP5-1039K5.13	FA Inferior Longitudinal Right	4.47E-08	-5.471067
283	rs738443	22	38458681	ncRNA intronic	A	G	0.381	3.31E-18	4.80E-01	PICK1:RP5-1039K5.13	MD Arcuate Long Segment Right	2.41E-09	5.967378
283	rs738443	22	38458681	ncRNA intronic	A	G	0.381	3.31E-18	4.80E-01	PICK1:RP5-1039K5.13	ICVF Superior Londgitudinal Fasciculus I Left	2.70E-09	-5.949066
283	rs738443	22	38458681	ncRNA intronic	A	G	0.381	3.31E-18	4.80E-01	PICK1:RP5-1039K5.13	FA Superior Londgitudinal Fasciculus I Right	2.34E-11	-6.682975
283	rs738443	22	38458681	ncRNA intronic	A	G	0.381	3.31E-18	4.80E-01	PICK1:RP5-1039K5.13	L1 Arcuate Posterior Segment Right	3.97E-08	5.491966
283	rs738443	22	38458681	ncRNA intronic	A	G	0.381	3.31E-18	4.80E-01	PICK1:RP5-1039K5.13	MD Arcuate Long Segment Left	8.29E-12	6.833361
283	rs738443	22	38458681	ncRNA intronic	A	G	0.381	3.31E-18	4.80E-01	PICK1:RP5-1039K5.13	L3 Superior Londgitudinal Fasciculus I Right	4.42E-10	6.238563
283	rs738443	22	38458681	ncRNA intronic	A	G	0.381	3.31E-18	4.80E-01	PICK1:RP5-1039K5.13	ICVF Inferior Longitudinal Left	1.58E-08	-5.652328
283	rs738443	22	38458681	ncRNA intronic	A	G	0.381	3.31E-18	4.80E-01	PICK1:RP5-1039K5.13	ICVF Superior Londgitudinal Fasciculus III Left	3.98E-09	-5.885161
283	rs738443	22	38458681	ncRNA intronic	A	G	0.381	3.31E-18	4.80E-01	PICK1:RP5-1039K5.13	L3 Inferior Longitudinal Right	3.59E-10	6.271020
283	rs738443	22	38458681	ncRNA intronic	A	G	0.381	3.31E-18	4.80E-01	PICK1:RP5-1039K5.13	L3 Frontal Inferior longitudinal Right	2.43E-08	5.578298
283	rs738443	22	38458681	ncRNA intronic	A	G	0.381	3.31E-18	4.80E-01	PICK1:RP5-1039K5.13	MD Inferior Fronto Occipital fasciculus Left	6.63E-10	6.174699
283	rs738443	22	38458681	ncRNA intronic	A	G	0.381	3.31E-18	4.80E-01	PICK1:RP5-1039K5.13	L3 Arcuate Anterior Segment Right	1.75E-09	6.019113
285	rs61748567	22	50685332	exonic	A	G	0.017	1.39E-22	3.23E-01	HDAC10:MAPK12	OD Superior Londgitudinal Fasciculus II Right	1.17E-10	6.442761
285	rs61748567	22	50685332	exonic	A	G	0.017	1.39E-22	3.23E-01	HDAC10:MAPK12	OD Arcuate Posterior Segment Right	7.86E-09	5.771396
285	rs61748567	22	50685332	exonic	A	G	0.017	1.39E-22	3.23E-01	HDAC10:MAPK12	OD Superior Londgitudinal Fasciculus III Right	4.33E-11	6.592241
285	rs61748567	22	50685332	exonic	A	G	0.017	1.39E-22	3.23E-01	HDAC10:MAPK12	FA Superior Londgitudinal Fasciculus II Left	4.07E-09	-5.881400
285	rs61748567	22	50685332	exonic	A	G	0.017	1.39E-22	3.23E-01	HDAC10:MAPK12	OD Superior Londgitudinal Fasciculus II Left	1.93E-15	7.945961

Appendix E

Résumé en français

Abstract in French

Sujet : L'architecture génétique du connectome du langage dans le cerveau humain

Motivations et contextes

Le langage est une composante essentielle de la vie humaine en raison de son rôle central dans les interactions sociales, la transmission culturelle, et la structuration de nos pensées. De part son omniprésence, le langage peut sembler avoir un caractère simple, mais celui-ci n'est pas suffisamment compris en tant que phénomène et processus. Dans différents contextes et sous différentes formes, les chercheurs soulignent le caractère particulier du langage par rapport aux autres capacités humaines. En conséquence, de nombreuses hypothèses entourent ce sujet dont celle relative à son origine. Le langage possède une dimension inhérente d'apprentissage, mais aussi une aspect innée qui se manifeste par le babillage des nourrissons, par exemple. Il est intéressant de noter que ce phénomène ne s'observe pas pour d'autres pratiques culturelles et qu'il est spécifique au langage. Le langage existe donc dans un espace unique, à la conjonction entre l'inné et l'acquis, entre individu et société.

Le langage est un phénomène à la fois biologique et social, il peut être abordé avec une grande variété de méthodes qui incluent les méthodes et les modèles explicatifs des sciences dites dures, ainsi que les outils offerts par les sciences humaines et sociales. La première approche se concentre sur les bases cognitives du langage et les différents aspects de son origine biologique qui permettent à l'espèce humaine d'apprendre et d'utiliser le langage. Elle tisse des relations étroites entre les neurosciences cognitives, la biologie humaine et aussi les statistiques qui fournissent des instruments précis pour sa modélisation. La deuxième approche, quant à elle, se concentre sur les relations entre le langage et la société, l'histoire, la philologie et la littérature. La nature même du langage, sa complexité, et son statut hybride justifient une pluralité d'approches et de méthodes. La présente thèse s'inscrit dans la première approche présentée ci-dessus et son objectif principal est de contribuer à l'étude de la neurobiologie du langage.

.

L'étude des causes biologiques des troubles du langage a suscité un vif intérêt pour la cartographie des gènes sous-jacents à cette capacité cognitive. Jusqu'à récemment, les racines biologiques du langage étaient principalement investiguées via des études de lésions, où les patients présentaient des troubles spécifiques du langage tels que les troubles du développement du langage et la dyslexie. L'imagerie-génétique est un domaine scientifique émergent qui bénéficie des propriétés non-invasives des techniques d'imagerie comme l'imagerie par résonance magnétique, qui permettent de "voir" le cerveau en fonctionnement, et du génotypage à haut débit par puces à ADN ou séquençage, qui permet de mesurer la variabilité génétique individuelle. Ces techniques permettent l'acquisition systématique des caractéristiques anatomiques et fonctionnelles du cerveau d'un individu ainsi que de son génotype. La possibilité d'acquérir ces données dans la population générale permet de mener des études sur des questions ouvertes de neurosciences cliniques et fondamentales. Les outils de la science des données nous permettent d'étudier comment la génétique et l'environnement modulent la fonction ou l'anatomie du cerveau humain ainsi que le comportement humain qui en découle. Avec la disponibilité récente de cohortes à grande échelle, il est devenu possible d'étudier le langage dans la population générale. L'objectif principal de cette thèse est de mettre en exergue les gènes qui sous-tendent le langage humain, améliorant ainsi notre compréhension des fondements génétiques du langage humain. À cette fin, nous avons étudié les variants génétiques communs qui s'associent aux traits quantitatifs, dérivés d'IRM fonctionnel de repos, liés au langage chez l'humain. Nous avons mis en avant les variations inter-individuelles de la fonction et de la structure du cerveau qui reflètent des traits neurocognitifs spécifiques du langage et avons testé les associations potentielles entre cette variabilité inter-individuelle observée et le profil génotypique. Cette étude a tiré parti de deux cohortes à grande échelle bien connues et adaptées aux études d'imagerie génétique : "UK Biobank" et "Human Connectome Project". Ces deux cohortes comprennent un génotypage en génome entier et une grande variété d'endophénotypes allant de données psychométriques et démographiques, en passant par la neuro-imagerie.

Déroulement du manuscrit de thèse

Le langage humain est un trait complexe. On s'attend à ce que différents types de variants génétiques affectent sa variabilité. Cette thèse vise à étudier les associations entre variations génétiques inter-individuelles et variations des endophénotypes dérivés des IRM cérébraux et liés au langage, afin de proposer des gènes jouant un rôle dans le fondement du langage chez l'humain.

Ce manuscrit de thèse est organisé comme suit :

Chapitre 4 : *Heritability of human language*

Dans ce chapitre, nous proposons une étude approfondie de l'héritabilité du langage humain caractérisé par des phénotypes intermédiaires soigneusement choisis. Plus particulièrement, nous avons évalué l'héritabilité de phénotypes dérivés de la psychométrie et de l'imagerie en tirant profit de deux ressources à grande échelle actuellement disponibles : le Human Connectome Project (HCP) et la UK Biobank (UKB) et ce, en utilisant des approches à l'état de l'art. Ces

(endo)phénotypes comprennent la connectivité fonctionnelle (CF) à l'état de repos, la connectivité structurelle et l'activation neural relative au langage. Nous avons observé une hiérarchie des estimations de l'héritabilité du langage avec 19,4-71,7 % pour les scores cognitifs du langage, 11,4-48,7 % pour la CF au repos et 14,4-34,9 % pour les activations neuronal du langage. La connectivité fonctionnelle au repos présente de faibles niveaux d'héritabilité par rapport aux scores cognitifs et aux caractéristiques structurelles, tant dans la population générale que dans les études sur les jumeaux. Ces observations sont cohérentes avec les héritabilités obtenues sur la population générale par [Elliott et al., 2018] qui a rapporté de faibles niveaux d'héritabilité pour la CF à l'état de repos par rapport aux endophénotypes structurels et de diffusion. En ce qui concerne la variabilité inter-cohorte, nous avons observé, et ce en accord avec la littérature, des valeurs d'héritabilité plus élevées dans les études généalogiques par rapport aux études d'héritabilité basées sur le génotypage. Les origines possibles de ces divergences ont été étudiées selon un plan expérimental qui prend en compte les dissimilarités entre les deux cohortes.

Chapitre 5 : *Shared genetic variance between language-related performance, language-brain activations and language functional connectivity*

Nous nous sommes intéressés en particulier aux données d'IRM fonctionnelle à l'état de repos et à leur pertinence pour l'étude de fonctions cognitives telles que le langage. Ce type de données offre de multiples avantages. Contrairement aux données d'IRM fonctionnelle basé sur une tâche, il est exempt de paradigme et, de ce fait, est plus facile à mettre en œuvre dans de très grandes cohortes comme UK Biobank. Par ailleurs l'IRM fonctionnelle à l'état de repos suscite un vif intérêt par la communauté scientifique du fait que certaines populations ont des difficultés à s'engager dans des tâches spécifiques. Bien que les données d'IRMf au repos soient considérées comme héritable, peu de connaissance existent sur leur relation avec le processus cognitif lié au langage.

Dans ce chapitre, nous abordons la question de l'héritabilité partagée en explorant la variabilité génétique commune qui expliquerait à la fois la variabilité des données d'IRMf et celles des mesures plus directes du langage en tant que processus cognitif. Pour ce faire, nous avons estimé les corrélations phénotypiques et génétiques entre les capacités cognitives mesurées par les tests psychométriques, les activations neuronales et les données de repos dans le langage. À cette fin, nous avons tiré parti de la cohorte du Human Connectome Project qui comprend à la fois, des scores liés au langage, des données d'IRMf basées sur des tâches de langage ainsi que des données d'IRMf en état de repos. Les résultats montrent une étiologie partagée entre la connectivité fonctionnelle à l'état de repos et les activations neuronales. Les résultats sont donc en faveur de l'existence d'un lien entre les données de l'état de repos et les données basées sur les tâches, tant sur le plan phénotypique que génétique, en ce qui concerne l'organisation cérébrale du langage humain.

Chapitre 6 : *The genetic architecture of human language functional connectome*

Dans ce chapitre, nous avons contribué à la compréhension de l'architecture génétique de la connectivité fonctionnelle du langage en mettant en évidence certains gènes liés au processus du langage. Nous avons extrait des phénotypes intermédiaire du langage - 300 paramètres de

connectivité fonctionnelle - à partir de données d'IRM à l'état de repos dans la plus grande cohorte d'imagerie-génétique sur population générale existante à ce jour (UK Biobank). Afin de s'assurer que ces endophénotypes reflètent bien la fonction du langage dans le cerveau, nous avons adopté une approche basée sur des régions d'intérêt pour l'estimation de la CF. Ces régions du langage ont été identifiées et dérivées d'une méta-analyse complète des études d'IRM fonctionnelle basées sur des expériences sollicitant explicitement le langage. Cette approche rend les endophénotypes comparables entre les individus et convient donc à une étude d'association. Nous avons appliqué un filtre sur l'héritabilité des CFs pour n'en garder qu'un sous ensemble significativement héritable. Nous avons ensuite mis en oeuvre une étude pangénomique multivariée afin de tirer parti de la structure de corrélation entre les CFs et de découvrir des loci potentiellement pléiotropes. Suite à une annotation fonctionnelle fine de ces loci, nous avons mis en évidence des gènes potentiels liés au langage, notamment :

- Le gène *EPHA3* présent dans le locus 3p11.1 avec un rôle potentiel dans le réseau *fronto-temporal sémantique*,
- Le gène *THBS1*, modulé par le locus 15q14, associé à la connectivité fonctionnelle présente dans l'interaction *perception-moteur* requise pour le langage, et
- Le gène *PLCE1* présent dans le locus 10q23.33 avec un rôle potentiel dans le *réseau bilatérale fronto-temporal auditif-moteur*.

Ces gènes pourraient être considérés comme prioritaires pour étudier le langage dans un modèle génétique approprié. Un nombre croissant de travaux avance que les études sur le langage devraient prendre en compte les données d'IRM fonctionnelle de repos en population générale afin de se concentrer sur l'organisation neurobiologique du langage dans sa globalité et sur la façon dont elle soutient le langage naturel, c'est-à-dire tel qu'il est utilisé dans la vie de tous les jours [Hasson et al., 2018]. D'un point de vue clinique, de tels conditions d'investigation sont hautement souhaitables car il est nécessaire de cartographier les zones du langage chez les patients incapables d'effectuer des tâches linguistiques [Branco et al., 2016, Klingbeil et al., 2019, Park et al., 2020, Ramage et al., 2020]. En cherchant à valider nos résultats obtenus sur les endophénotypes CF par l'étude d'autres endophénotypes dérivés de l'IRM de diffusion qui informent sur la connectivté anatomique, nous avons essayé de donner un point de vue du connectome fonctionnel et structurel de l'organisation du langage dans le cerveau. Enfin, de récentes approches d'imagerie génétique telles que les études pangénomique multivariées, nous ont permis d'augmenter la puissance statistique et de contourner les problématique lié aux très faibles tailles d'effet. Nous pensons que ces approches sont prometteuses et qu'elles seront largement diffusées dans le domaine de l'imagerie génétique et au-delà. Avec l'approche présentée, nous avons essayé de contribuer à ces tendances innovantes et d'ouvrir la voie à d'autres approches alternatives utilisant l'IRMf de repos pour étudier le langage naturel et ses fondements génétiques.

Chapitre 7 : *The genetic architecture of anatomical connectivity in human language*

Dans ce chapitre, nous avons adopté un plan expérimental similaire à celui présenté dans le chapitre 6 pour étudier l'architecture génétique de la connectivité anatomique à l'échelle de toute la connectivité structurelle actuellement connue dans le langage. Nous avons extrait les endophénotypes de connectivité anatomique (CA) du langage à partir d'acquisitions pondérées en diffusion disponibles dans la cohorte UK Biobank. Nous avons adopté une approche basée sur régions d'intérêt pour l'estimation de la CA avec des tracts de matière blanche du langage bien connus. Après avoir filtré ces endophénotypes en considérant leur héritabilité, nous avons mis en oeuvre une étude pangénomique multivariée afin de tirer parti de la structure de corrélation entre la connectivité structurelle et de découvrir des loci pléiotropes potentiels. Nous avons ainsi mis en évidence des gènes potentiels liés au traitement du langage. Ces gènes pourraient être prioritisés pour étudier le langage dans un modèle génétique approprié. Les résultats suggèrent de nouveaux gènes candidats qui sont liés à des voies biologiques déjà présumées être importantes dans le développement du cerveau humain et le langage. Dans l'ensemble, ces résultats proposent une nouvelle vision de l'architecture génétique du langage chez l'homme.

Discussion, limitations

Une approche intégrative. Nous avons suivi une approche intégrative dans notre étude de l'architecture génétique du langage. Tout d'abord, en validant nos résultats sur les endophénotypes CF de l'IRM fonctionnelle de repos avec les endophénotypes dérivés de l'IRM de diffusion, nous avons essayé de fournir un point de vue à la fois fonctionnel et structurel du connectome de l'organisation du langage dans le cerveau. Deuxièmement, nous avons utilisé des approches récentes d'association imagerie-génétique telles que les études pangénomique multivariées, qui nous ont permis d'augmenter la puissance statistique et de contourner les petites tailles d'effet produites par des variants génétiques sur ces endophénotypes initiaux. Nous pensons que ces approches sont prometteuses et qu'elles seront largement diffusées dans le domaine de l'imagerie-génétique et au-delà. Avec l'approche présentée, nous avons essayé de contribuer à ces tendances innovantes et d'ouvrir la voie à d'autres approches alternatives d'IRMf au repos pour étudier le langage naturel et ses fondements génétiques.

Une étude en population générale. Nous avons mené notre étude sur une cohorte de la population générale en sélectionnant des (endo)phénotypes du langage à l'état de l'art. Nous pensons qu'elle offre un cadre alternatif intéressant aux études basées sur les troubles du langage. Les cohortes de la population générale fournissent une multitude de mesures qui permettent de développer des (endo)phénotypes d'intérêt, y compris pour les processus cognitifs complexes. Cette approche offre une alternative prometteuse au paradigme cas-témoins.

Conclusion

Le langage est un élément central de la vie humaine. Comprendre comment nous sommes capables d'acquérir et d'utiliser ce trait hautement complexe a nécessité le développement de nombreuses descriptions du langage à plusieurs niveaux. D'une part, nous avons exploité des scores

de traitement du langage bien caractérisés et des phénotypes intermédiaires. D'autre part, nous avons appliqué des méthodes d'association pour identifier les gènes liés aux différences comportementales et comprendre leur impact sur le développement et le fonctionnement du cerveau en examinant la fonction cellulaire des protéines que codent ces gènes et les voies biologiques dans lesquelles ils sont impliqués. Une compréhension plus complète du langage humain nécessitera d'intégrer les résultats des différentes stratégies entreprises et des différents niveaux de description.

Dans cette thèse, nous avons abordé la question de la base génétique du langage humain en utilisant des méthodes à l'état de l'art : en mettant en évidence la variabilité inter-individuelle du cerveau et en évaluant le rôle des variants génétiques communs pris dans l'ensemble du génome sans *a priori* sur des gènes candidats potentiels. Nous avons relié ces recherches aux connaissances actuelles sur les performances cognitives liées au langage et aux mécanismes moléculaires connus dans le cerveau et le développement. Les résultats de cette thèse fournissent de nouveaux points d'entrée pour de futurs travaux visant à combler le fossé entre la contribution génétique et le processus du langage humain.

* * *
* *
*

Bibliography

The gene ontology resource: enriching a gold mine. *Nucleic Acids Research*, 49(D1):D325–D334, 2021.

Alexandre Abraham, Fabian Pedregosa, Michael Eickenberg, Philippe Gervais, Andreas Mueller, Jean Kossaifi, Alexandre Gramfort, Bertrand Thirion, and Gaël Varoquaux. Machine learning for neuroimaging with scikit-learn. *Frontiers in neuroinformatics*, 8:14, 2014.

Fidel Alfaro-Almagro, Mark Jenkinson, Neal K Bangerter, Jesper LR Andersson, Ludovica Griffanti, Gwenaëlle Douaud, Stamatios N Sotiropoulos, Saad Jbabdi, Moises Hernandez-Fernandez, Emmanuel Vallee, et al. Image processing and quality control for the first 10,000 brain imaging datasets from uk biobank. *Neuroimage*, 166:400–424, 2018.

David B Allison, Bonnie Thiel, Pamela St Jean, Robert C Elston, Ming C Infante, and Nicholas J Schork. Multiple phenotype modeling in gene-mapping studies of quantitative traits: power advantages. *The American Journal of Human Genetics*, 63(4):1190–1201, 1998.

Laura Almasy and John Blangero. Multipoint quantitative-trait linkage analysis in general pedigrees. *The American Journal of Human Genetics*, 62(5):1198–1211, 1998.

Jesper LR Andersson and Stamatios N Sotiropoulos. Non-parametric representation and prediction of single-and multi-shell diffusion-weighted mri data using gaussian processes. *Neuroimage*, 122:166–176, 2015.

Heidi Anthoni, Marco Zucchelli, Hans Matsson, Bertram Müller-Myhsok, Ingegerd Fransson, Johannes Schumacher, Satu Massinen, Päivi Onkamo, Andreas Warnke, Heide Griesemann, et al. A locus on 2p12 containing the co-regulated mrpl19 and c2orf3 genes is associated to dyslexia. *Human molecular genetics*, 16(6):667–677, 2007.

John Ashburner and Karl J Friston. Voxel-based morphometry—the methods. *Neuroimage*, 11 (6):805–821, 2000.

Michael Ashburner, Catherine A Ball, Judith A Blake, David Botstein, Heather Butler, J Michael Cherry, Allan P Davis, Kara Dolinski, Selina S Dwight, Janan T Eppig, et al. Gene ontology: tool for the unification of biology. *Nature genetics*, 25(1):25–29, 2000.

Deanna M Barch, Gregory C Burgess, Michael P Harms, Steven E Petersen, Bradley L Schlaggar, Maurizio Corbetta, Matthew F Glasser, Sandra Curtiss, Sachin Dixit, Cindy Feldt, et al. Function in the human connectome: task-fmri and individual differences in behavior. *Neuroimage*, 80:169–189, 2013.

Christopher W Bartlett, Judy F Flax, Mark W Logue, Veronica J Vieland, Anne S Bassett, Paula Tallal, and Linda M Brzustowicz. A major susceptibility locus for specific language impairment is located on 13q21. *The American Journal of Human Genetics*, 71(1):45–55, 2002.

Christopher W Bartlett, Judy F Flax, Mark W Logue, Brett J Smith, Veronica J Vieland, Paula Tallal, and Linda M Brzustowicz. Examination of potential overlap in autism and language loci on chromosomes 2, 7, and 13 in two independent samples ascertained for specific language impairment. *Human heredity*, 57(1):10–20, 2004.

T Mark Beasley, Stephen Erickson, and David B Allison. Rank-based inverse normal transformations are increasingly used, but are they merited? *Behavior genetics*, 39(5):580–595, 2009.

Christian F Beckmann and Stephen M Smith. Probabilistic independent component analysis for functional magnetic resonance imaging. *IEEE transactions on medical imaging*, 23(2): 137–152, 2004.

Emma Belton, Claire H Salmond, Kate E Watkins, Faraneh Vargha-Khadem, and David G Gadian. Bilateral brain abnormalities associated with dominantly inherited verbal and orofacial dyspraxia. *Human brain mapping*, 18(3):194–200, 2003.

Michel Belyk and Steven Brown. The origins of the vocal brain in humans. *Neuroscience & Biobehavioral Reviews*, 77:177–193, 2017.

Sarah E Bergen, Charles O Gardner, and Kenneth S Kendler. Age-related changes in heritability of behavioral phenotypes over adolescence and young adulthood: a meta-analysis. *Twin Research and Human Genetics*, 10(3):423–433, 2007.

Jeffrey R Binder, Rutvik H Desai, William W Graves, and Lisa L Conant. Where is the semantic system? a critical review and meta-analysis of 120 functional neuroimaging studies. *Cerebral cortex*, 19(12):2767–2796, 2009.

Jeffrey R Binder, William L Gross, Jane B Allendorfer, Leonardo Bonilha, Jessica Chapin, Jonathan C Edwards, Thomas J Grabowski, John T Langfitt, David W Loring, Mark J Lowe, et al. Mapping anterior temporal lobe language areas with fmri: a multicenter normative study. *Neuroimage*, 54(2):1465–1475, 2011.

Bharat Biswal, F Zerrin Yetkin, Victor M Haughton, and James S Hyde. Functional connectivity in the motor cortex of resting human brain using echo-planar mri. *Magnetic resonance in medicine*, 34(4):537–541, 1995.

Bharat B Biswal, Maarten Mennes, Xi-Nian Zuo, Suril Gohel, Clare Kelly, Steve M Smith, Christian F Beckmann, Jonathan S Adelstein, Randy L Buckner, Stan Colcombe, et al. Toward discovery science of human brain function. *Proceedings of the National Academy of Sciences*, 107(10):4734–4739, 2010.

Gunnar Blom. *Statistical estimates and transformed beta-variables*. PhD thesis, Almqvist & Wiksell, 1958.

James R Booth, Douglas D Burman, Joel R Meyer, Darren R Gitelman, Todd B Parrish, and M Marsel Mesulam. Modality independence of word comprehension. *Human brain mapping*, 16(4):251–261, 2002.

Thomas J Bouchard. The wilson effect: the increase in heritability of iq with age. *Twin Research and Human Genetics*, 16(5):923–930, 2013.

Alan P Boyle, Eurie L Hong, Manoj Hariharan, Yong Cheng, Marc A Schaub, Maya Kasowski, Konrad J Karczewski, Julie Park, Benjamin C Hitz, Shuai Weng, et al. Annotation of functional variation in personal genomes using regulomedb. *Genome research*, 22(9):1790–1797, 2012.

Paulo Branco, Daniela Seixas, Sabine Deprez, Silvia Kovacs, Ronald Peeters, São L Castro, and Stefan Sunaert. Resting-state functional magnetic resonance imaging for language preoperative planning. *Frontiers in human neuroscience*, 10:11, 2016.

Korbinian Brodmann. Beiträge zur histologischen lokalisation der grosshirnrinde: Vi. die cortexgliederung des menschen. *Journal für Psychologie und Neurologie*, 10:231–246, 1909.

Toai Bui and J Nguyen. Neuroanatomy, cerebral hemisphere. 2019.

Brendan K Bulik-Sullivan, Po-Ru Loh, Hilary K Finucane, Stephan Ripke, Jian Yang, Nick Patterson, Mark J Daly, Alkes L Price, and Benjamin M Neale. Ld score regression distinguishes confounding from polygenicity in genome-wide association studies. *Nature genetics*, 47(3): 291–295, 2015.

Clare Bycroft, Colin Freeman, Desislava Petkova, Gavin Band, Lloyd T Elliott, Kevin Sharp, Allan Motyer, Damjan Vukcevic, Olivier Delaneau, Jared O'Connell, et al. The uk biobank resource with deep phenotyping and genomic data. *Nature*, 562(7726):203–209, 2018.

Mario Cáceres, Joel Lachuer, Matthew A Zapala, John C Redmond, Lili Kudo, Daniel H Geschwind, David J Lockhart, Todd M Preuss, and Carrolee Barlow. Elevated gene expression levels distinguish human from non-human primate brains. *Proceedings of the National Academy of Sciences*, 100(22):13030–13035, 2003.

Mario Cáceres, Carolyn Suwyn, Marcelia Maddox, James W Thomas, and Todd M Preuss. Increased cortical expression of two synaptogenic thrombospondins in human brain evolution. *Cerebral Cortex*, 17(10):2312–2321, 2007.

Vince D Calhoun, Tulay Adali, Godfrey D Pearlson, and James J Pekar. A method for making group inferences from functional mri data using independent component analysis. *Human brain mapping*, 14(3):140–151, 2001.

Amaia Carrion-Castillo, Antonietta Pepe, Xiang-Zhen Kong, Simon E Fisher, Bernard Mazoyer, Nathalie Tzourio-Mazoyer, Fabrice Crivello, and Clyde Francks. Genetic effects on planum temporale asymmetry and their limited relevance to neurodevelopmental disorders, intelligence or educational attainment. *cortex*, 124:137–153, 2020.

Jillian P Casey, Tiago Magalhaes, Judith M Conroy, Regina Regan, Naisha Shah, Richard Anney, Denis C Shields, Brett S Abrahams, Joana Almeida, Elena Bacchelli, et al. A novel approach of homozygous haplotype sharing identifies candidate genes in autism spectrum disorder. *Human genetics*, 131(4):565–579, 2012.

Marco Catani and Valentina Bambini. A model for social communication and language evolution and development (scaled). *Current opinion in neurobiology*, 28:165–171, 2014.

Marco Catani and Michel Thiebaut De Schotten. A diffusion tensor imaging tractography atlas for virtual in vivo dissections. *cortex*, 44(8):1105–1132, 2008.

Marco Catani and Stephanie J Forkel. Diffusion imaging methods in language sciences. *The Oxford Handbook of Neurolinguistics*, page 212, 2019.

Marco Catani, Derek K Jones, and Dominic H Ffytche. Perisylvian language networks of the human brain. *Annals of Neurology: Official Journal of the American Neurological Association and the Child Neurology Society*, 57(1):8–16, 2005.

Marco Catani, Flavio Dell'Acqua, Francesco Vergani, Farah Malik, Harry Hodge, Prasun Roy, Romain Valabregue, and Michel Thiebaut De Schotten. Short frontal lobe connections of the human brain. *cortex*, 48(2):273–291, 2012.

Christopher C Chang, Carson C Chow, Laurent CAM Tellier, Shashaank Vattikuti, Shaun M Purcell, and James J Lee. Second-generation plink: rising to the challenge of larger and richer datasets. *Gigascience*, 4(1):s13742–015, 2015.

Sreenivas Chavali, Fredrik Barrenas, Kartiek Kanduri, and Mikael Benson. Network properties of human disease genes with pleiotropic effects. *BMC systems biology*, 4(1):1–11, 2010.

Kulpreet Cheema, Amberley V Ostevik, Lindsey Westover, William E Hodgetts, and Jacqueline Cummine. Resting-state networks and reading in adults with and without reading impairments. *Journal of Neurolinguistics*, 60:101016, 2021.

Karen S Christopherson, Erik M Ullian, Caleb CA Stokes, Christine E Mullowney, Johannes W Hell, Azin Agah, Jack Lawler, Deane F Mosher, Paul Bornstein, and Ben A Barres. Thrombospondins are astrocyte-secreted proteins that promote cns synaptogenesis. *Cell*, 120(3): 421–433, 2005.

Maria-Daniela Cirnaru, Sicheng Song, Kizito-Tshitoko Tshilenge, Chuhyon Corwin, Justyna Mleczko, Carlos Galicia Aguirre, Houda Benlhabib, Jaroslav Bendl, John Fullard, Pasha Apontes, et al. Transcriptional and epigenetic characterization of early striosomes identifies foxf2 and olig2 as factors required for development of striatal compartmentation and neuronal phenotypic differentiation. *bioRxiv*, 2020.

Michael W Cole, Danielle S Bassett, Jonathan D Power, Todd S Braver, and Steven E Petersen. Intrinsic and task-evoked network architectures of the human brain. *Neuron*, 83(1):238–251, 2014.

1000 Genomes Project Consortium et al. A global reference for human genetic variation. *Nature*, 526(7571):68, 2015.

GTEx Consortium et al. Genetic effects on gene expression across human tissues. *Nature*, 550 (7675):204–213, 2017.

Sli Consortium et al. Highly significant linkage to the sli1 locus in an expanded sample of individuals affected by specific language impairment. *The American Journal of Human Genetics*, 74(6):1225–1238, 2004.

R Todd Constable, Kenneth R Pugh, Ella Berroya, W Einar Mencl, Michael Westerveld, Weijia Ni, and Donald Shankweiler. Sentence complexity and input modality effects in sentence comprehension: an fmri study. *NeuroImage*, 22(1):11–21, 2004.

Natalie Cope, John D Eicher, Haiying Meng, Christopher J Gibson, Karl Hager, Cheryl Lacadie, Robert K Fulbright, R Todd Constable, Grier P Page, and Jeffrey R Gruen. Variants in the dyx2 locus are associated with altered brain activation in reading-related brain regions in subjects with reading disability. *Neuroimage*, 63(1):148–156, 2012.

Jillian M Couto, Lissette Gomez, Karen Wigg, Tasha Cate-Carter, Jennifer Archibald, Barbara Anderson, Rosemary Tannock, Elizabeth N Kerr, Maureen W Lovett, Tom Humphries, et al. The kiaa0319-like (kiaa0319l) gene on chromosome 1p34 as a candidate for reading disabilities. *Journal of neurogenetics*, 22(4):295–313, 2008.

Simon R Cox, Stuart J Ritchie, Chloe Fawns-Ritchie, Elliot M Tucker-Drob, and Ian J Deary. Structural brain imaging correlates of general intelligence in uk biobank. *Intelligence*, 76: 101376, 2019.

Alexandra M Cross, Reshma Ramdajal, Lien Peters, Matthew RJ Vandermeer, Elizabeth P Hayden, Jan C Frijters, Karen A Steinbach, Maureen W Lovett, Lisa MD Archibald, and Marc F Joanisse. Resting-state functional connectivity and reading subskills in children. *NeuroImage*, 243:118529, 2021.

Darina Czamara, Jennifer Bruder, Jessica Becker, Jürgen Bartling, Per Hoffmann, Kerstin Urte Ludwig, Bertram Müller-Myhsok, and Gerd Schulte-Körne. Association of a rare variant with mismatch negativity in a region between kiaa0319 and dcdc2 in dyslexia. *Behavior genetics*, 41(1):110–119, 2011.

Alessandro Daducci, Erick J Canales-Rodríguez, Hui Zhang, Tim B Dyrby, Daniel C Alexander, and Jean-Philippe Thiran. Accelerated microstructure imaging via convex optimization (amico) from diffusion mri data. *NeuroImage*, 105:32–44, 2015.

Philip S Dale, Ginette Dionne, Thalia C Eley, and Robert Plomin. Lexical and grammatical development: A behavioural genetic perspective. *Journal of child language*, 27(3):619–642, 2000.

Fahimeh Darki, Myriam Peyrard-Janvid, Hans Matsson, Juha Kere, and Torkel Klingberg. Three dyslexia susceptibility genes, dyx1c1, dcdc2, and kiaa0319, affect temporo-parietal white matter structure. *Biological psychiatry*, 72(8):671–676, 2012.

Fahimeh Darki, Myriam Peyrard-Janvid, Hans Matsson, Juha Kere, and Torkel Klingberg. Dcdc2 polymorphism is associated with left temporoparietal gray and white matter structures during development. *Journal of Neuroscience*, 34(43):14455–14462, 2014.

Gail Davies, Riccardo E Marioni, David C Liewald, W David Hill, Saskia P Hagenaars, Sarah E Harris, Stuart J Ritchie, Michelle Luciano, Chloe Fawns-Ritchie, Donald Lyall, et al. Genome-wide association study of cognitive functions and educational attainment in uk biobank (n= 112 151). *Molecular psychiatry*, 21(6):758–767, 2016.

CGF De Kovel, FA Hol, JGAM Heister, JJHT Willemen, LA Sandkuijl, B Franke, and GW Padberg. Genomewide scan identifies susceptibility locus for dyslexia on xq27 in an extended dutch family. *Journal of medical genetics*, 41(9):652–657, 2004.

Christiaan A de Leeuw, Joris M Mooij, Tom Heskes, and Danielle Posthuma. Magma: generalized gene-set analysis of gwas data. *PLoS Comput Biol*, 11(4):e1004219, 2015.

Karen E Deffenbacher, Judith B Kenyon, Denise M Hoover, Richard K Olson, Bruce F Pennington, John C DeFries, and Shelley D Smith. Refinement of the 6p21. 3 quantitative trait locus influencing dyslexia: linkage and association analyses. *Human Genetics*, 115(2):128–138, 2004.

Emily L Dennis, Neda Jahanshad, Jeffrey D Rudie, Jesse A Brown, Kori Johnson, Katie L McMahon, Greig I de Zubicaray, Grant Montgomery, Nicholas G Martin, Margaret J Wright, et al. Altered structural brain connectivity in healthy carriers of the autism risk gene, cntnap2. *Brain connectivity*, 1(6):447–459, 2011.

Rahul S Desikan, Florent Ségonne, Bruce Fischl, Brian T Quinn, Bradford C Dickerson, Deborah Blacker, Randy L Buckner, Anders M Dale, R Paul Maguire, Bradley T Hyman, et al. An automated labeling system for subdividing the human cerebral cortex on mri scans into gyral based regions of interest. *Neuroimage*, 31(3):968–980, 2006.

Nina F Dronkers. The pursuit of brain–language relationships. *Brain and Language*, 71(1): 59–61, 2000.

Hugues Duffau, Peggy Gatignol, Dominique Denvil, Manuel Lopes, and Laurent Capelle. The articulatory loop: study of the subcortical connectivity by electrostimulation. *Neuroreport*, 14(15):2005–2008, 2003.

John D Eicher, Natalie R Powers, Laura L Miller, Natacha Akshoomoff, David G Amaral, Cinnamon S Bloss, Ondrej Libiger, Nicholas J Schork, Burcu F Darst, BJ Casey, et al. Genome-wide association study of shared components of reading disability and language impairment. *Genes, Brain and Behavior*, 12(8):792–801, 2013.

John D Eicher, Angela M Montgomery, Natacha Akshoomoff, David G Amaral, Cinnamon S Bloss, Ondrej Libiger, Nicholas J Schork, Burcu F Darst, BJ Casey, Linda Chang, et al. Dyslexia and language impairment associated genetic markers influence cortical thickness and white matter in typically developing children. *Brain imaging and behavior*, 10(1):272–282, 2016.

Jennifer Stine Elam, Matthew F Glasser, Michael P Harms, Stamatios N Sotiropoulos, Jesper LR Andersson, Gregory C Burgess, Sandra W Curtiss, Robert Oostenveld, Linda J Larson-Prior, Jan-Mathijs Schoffelen, et al. The human connectome project: A retrospective. *NeuroImage*, page 118543, 2021.

Lloyd T Elliott, Kevin Sharp, Fidel Alfaro-Almagro, Sinan Shi, Karla L Miller, Gwenaëlle Douaud, Jonathan Marchini, and Stephen M Smith. Genome-wide association studies of brain imaging phenotypes in uk biobank. *Nature*, 562(7726):210–216, 2018.

Maxwell L Elliott, Annchen R Knodt, Megan Cooke, M Justin Kim, Tracy R Melzer, Ross Keenan, David Ireland, Sandhya Ramrakha, Richie Poulton, Avshalom Caspi, et al. General functional connectivity: Shared features of resting-state and task fmri drive reliable and heritable individual differences in functional brain networks. *NeuroImage*, 189:516–532, 2019.

Jason Ernst and Manolis Kellis. Chromhmm: automating chromatin-state discovery and characterization. *Nature methods*, 9(3):215–216, 2012.

Alan C Evans, Brain Development Cooperative Group, et al. The nih mri study of normal brain development. *Neuroimage*, 30(1):184–202, 2006.

Luciano Fadiga, Laila Craighero, Giovanni Buccino, and Giacomo Rizzolatti. Speech listening specifically modulates the excitability of tongue muscles: a tms study. *European journal of Neuroscience*, 15(2):399–402, 2002.

Manuel AR Ferreira and Shaun M Purcell. A multivariate test of association. *Bioinformatics*, 25(1):132–133, 2009.

LL Field, K Shumansky, J Ryan, D Truong, E Swiergala, and BJ Kaplan. Dense-map genome scan for dyslexia supports loci at 4q13, 16p12, 17q22; suggests novel locus at 7q36. *Genes, Brain and Behavior*, 12(1):56–69, 2013.

Deborah Finkel and Matt McGue. Age differences in the nature and origin of individual differences in memory: A behavior genetic analysis. *The International Journal of Aging and Human Development*, 47(3):217–239, 1998.

Bruce Fischl and Anders M. Dale. Measuring the thickness of the human cerebral cortex from magnetic resonance images. *Proceedings of the National Academy of Sciences of the United States of America*, 97(20):11050–11055, 2000.

Simon E Fisher and Sonja C Vernes. Genetics and the language sciences. *Annu. Rev. Linguist.*, 1(1):289–310, 2015.

Simon E Fisher, Faraneh Vargha-Khadem, Kate E Watkins, Anthony P Monaco, and Marcus E Pembrey. Localisation of a gene implicated in a severe speech and language disorder. *Nature genetics*, 18(2):168–170, 1998.

Simon E Fisher, Clyde Francks, Angela J Marlow, I Laurence MacPhie, Dianne F Newbury, Lon R Cardon, Yumiko Ishikawa-Brush, Alex J Richardson, Joel B Talcott, Javier Gayán, et al. Independent genome-wide scans identify a chromosome 18 quantitative-trait locus influencing dyslexia. *Nature genetics*, 30(1):86–91, 2002.

Adeen Flinker, Anna Korzeniewska, Avgusta Y Shestyuk, Piotr J Franaszczuk, Nina F Dronkers, Robert T Knight, and Nathan E Crone. Redefining the role of broca's area in speech. *Proceedings of the National Academy of Sciences*, 112(9):2871–2875, 2015.

Stephanie J Forkel, Michel Thiebaut de Schotten, Jamie M Kawadler, Flavio Dell'Acqua, Adrian Danek, and Marco Catani. The anatomy of fronto-occipital connections from early blunt dissections to contemporary tractography. *Cortex*, 56:73–84, 2014.

Michael D Fox and Marcus E Raichle. Spontaneous fluctuations in brain activity observed with functional magnetic resonance imaging. *Nature reviews neuroscience*, 8(9):700–711, 2007.

Julius Fridriksson, Dana Moser, Jack Ryalls, Leonardo Bonilha, Chris Rorden, and Gordon Baylis. Modulation of frontal lobe speech areas associated with the production and perception of speech movements. 2009.

Angela D Friederici. The brain basis of language processing: from structure to function. *Physiological reviews*, 91(4):1357–1392, 2011.

Angela D Friederici. *Language in our brain: The origins of a uniquely human capacity*. MIT Press, 2017.

Karl J Friston. Functional and effective connectivity in neuroimaging: a synthesis. *Human brain mapping*, 2(1-2):56–78, 1994.

Karl J Friston. Modalities, modes, and models in functional neuroimaging. *Science*, 326(5951): 399–403, 2009.

Karl J Friston, Andrew P Holmes, Keith J Worsley, J-P Poline, Chris D Frith, and Richard SJ Frackowiak. Statistical parametric maps in functional imaging: a general linear approach. *Human brain mapping*, 2(4):189–210, 1994.

Joaquin M Fuster. *Cortex and mind: Unifying cognition*. Oxford university press, 2002.

Bruno Galantucci, Carol A Fowler, and Michael T Turvey. The motor theory of speech perception reviewed. *Psychonomic bulletin & review*, 13(3):361–377, 2006.

Tessel E Galesloot, Kristel Van Steen, Lambertus ALM Kiemeney, Luc L Janss, and Sita H Vermeulen. A comparison of multivariate genome-wide association methods. *PloS one*, 9(4): e95923, 2014.

J Ganger, S Pinker, S Chawla, and A Baker. Heritability of early milestones of vocabulary and grammar: A twin study. *Unpublished manuscript*, 2002.

Katrin Gerstmann and Geraldine Zimmer. The role of the eph/ephrin family during cortical development and cerebral malformations. *Medical Research Archives*, 6(3), 2018.

Alessandro Gialluisi, Dianne F Newbury, Erik G Wilcutt, Richard K Olson, John C DeFries, William M Brandler, Bruce F Pennington, Shelley D Smith, Thomas S Scerri, Nuala H Simpson, et al. Genome-wide screening for dna variants associated with reading and language traits. *Genes, Brain and Behavior*, 13(7):686–701, 2014.

Alessandro Gialluisi, Tulio Guadalupe, Clyde Francks, and Simon E Fisher. Neuroimaging genetic analyses of novel candidate genes associated with reading and language. *Brain and language*, 172:9–15, 2017.

Richard A Gibbs, John W Belmont, Paul Hardenbol, Thomas D Willis, FL Yu, HM Yang, Lan-Yang Ch'ang, Wei Huang, Bin Liu, Yan Shen, et al. The international hapmap project. 2003.

Daniel A Gibson and Le Ma. Developmental regulation of axon branching in the vertebrate nervous system. *Development*, 138(2):183–195, 2011.

David C Glahn, Paul M Thompson, and John Blangero. Neuroimaging endophenotypes: strategies for finding genes influencing brain structure and function. *Human brain mapping*, 28(6):488–501, 2007.

Matthew F Glasser, Stamatios N Sotiropoulos, J Anthony Wilson, Timothy S Coalson, Bruce Fischl, Jesper L Andersson, Junqian Xu, Saad Jbabdi, Matthew Webster, Jonathan R Polimeni, et al. The minimal preprocessing pipelines for the human connectome project. *Neuroimage*, 80:105–124, 2013.

Gary H Glover. Overview of functional magnetic resonance imaging. *Neurosurgery Clinics*, 22 (2):133–139, 2011.

Irving I Gottesman and Todd D Gould. The endophenotype concept in psychiatry: etymology and strategic intentions. *American journal of psychiatry*, 160(4):636–645, 2003.

Michael D Greicius, Ben Krasnow, Allan L Reiss, and Vinod Menon. Functional connectivity in the resting brain: a network analysis of the default mode hypothesis. *Proceedings of the National Academy of Sciences*, 100(1):253–258, 2003.

Ludovica Griffanti, Gholamreza Salimi-Khorshidi, Christian F Beckmann, Edward J Auerbach, Gwenaëlle Douaud, Claire E Sexton, Enikő Zsoldos, Klaus P Ebmeier, Nicola Filippini, Clare E Mackay, et al. Ica-based artefact removal and accelerated fmri acquisition for improved resting state network imaging. *Neuroimage*, 95:232–247, 2014.

Yongtao Guan and Matthew Stephens. Practical issues in imputation-based association mapping. *PLoS genetics*, 4(12):e1000279, 2008.

Jennifer M Gurd, Katrin Amunts, Peter H Weiss, Oliver Zafiris, Karl Zilles, John C Marshall, and Gereon R Fink. Posterior parietal cortex is implicated in continuous switching between verbal fluency tasks: an fmri study with clinical implications. *Brain*, 125(5):1024–1038, 2002.

Peter Hagoort. *Human Language: From Genes and Brains to Behavior*. The MIT Press, 2019.

Michelle Hampson, Fuyuze Tokoglu, Zhongdong Sun, Robin J Schafer, Pawel Skudlarski, John C Gore, and R Todd Constable. Connectivity–behavior analysis reveals that functional connectivity between left ba39 and broca's area varies with reading ability. *Neuroimage*, 31(2): 513–519, 2006.

Yixing Han, Jianke Ren, Eunice Lee, Xiaoping Xu, Weishi Yu, and Kathrin Muegge. Lsh/hells regulates self-renewal/proliferation of neural stem/progenitor cells. *Scientific reports*, 7(1): 1–14, 2017.

Katariina Hannula-Jouppi, Nina Kaminen-Ahola, Mikko Taipale, Ranja Eklund, Jaana Nopola-Hemmi, Helena Kääriäinen, and Juha Kere. The axon guidance receptor gene robo1 is a candidate gene for developmental dyslexia. *PLoS genetics*, 1(4):e50, 2005.

Nicole Harlaar, Emma L Meaburn, Marianna E Hayiou-Thomas, Oliver SP Davis, Sophia Docherty, Ken B Hanscombe, Claire MA Haworth, Thomas S Price, Maciej Trzaskowski, Philip S Dale, et al. Genome-wide association study of receptive language ability of 12-year-olds. 2014.

Uri Hasson, Giovanna Egidi, Marco Marelli, and Roel M Willems. Grounding the neurobiology of language in first principles: The necessity of non-language-centric explanations for language comprehension. *Cognition*, 180:135–157, 2018.

Isabelle Hesling, Loic Labache, Marc Joliot, and Nathalie Tzourio-Mazoyer. Large-scale plurimodal networks common to listening to, producing and reading word lists: an fmri study combining task-induced activation and intrinsic connectivity in 144 right-handers. *Brain Structure and Function*, 224(9):3075–3094, 2019.

Gregory Hickok and David Poeppel. Dorsal and ventral streams: a framework for understanding aspects of the functional anatomy of language. *Cognition*, 92(1-2):67–99, 2004.

Gregory Hickok and David Poeppel. The cortical organization of speech processing. *Nature reviews neuroscience*, 8(5):393–402, 2007.

William G Hill, Michael E Goddard, and Peter M Visscher. Data and theory point to mainly additive genetic variance for complex traits. *PLoS genetics*, 4(2):e1000008, 2008.

Edith Hofer, Gennady V Roshchupkin, Hieab HH Adams, Maria J Knol, Honghuang Lin, Shuo Li, Habil Zare, Shahzad Ahmad, Nicola J Armstrong, Claudia L Satizabal, et al. Genetic determinants of cortical structure (thickness, surface area and volumes) among disease free adults in the charge consortium. *BioRxiv*, page 409649, 2018.

Sam Horng, Gabriel Kreiman, Charlene Ellsworth, Damon Page, Marissa Blank, Kathleen Millen, and Mriganka Sur. Differential gene expression in the developing lateral geniculate nucleus and medial geniculate nucleus reveals novel roles for zic4 and foxp2 in visual and auditory pathway development. *Journal of Neuroscience*, 29(43):13672–13683, 2009.

Ging-Yuek R Hsiung, Bonnie J Kaplan, Tracey L Petryshen, Shao Lu, and L Leigh Field. A dyslexia susceptibility locus (dyx7) linked to dopamine d4 receptor (drd4) region on chromosome 11p15. 5. *American Journal of Medical Genetics Part B: Neuropsychiatric Genetics*, 125 (1):112–119, 2004.

Rebecca L Jackson, Paul Hoffman, Gorana Pobric, and Matthew A Lambon Ralph. The semantic network at work and rest: differential connectivity of anterior temporal lobe subregions. *Journal of Neuroscience*, 36(5):1490–1501, 2016.

Kaja K Jasińska, Peter J Molfese, Sergey A Kornilov, W Einar Mencl, Stephen J Frost, Maria Lee, Kenneth R Pugh, Elena L Grigorenko, and Nicole Landi. The bdnf val66met polymorphism influences reading ability and patterns of neural activation in children. *PloS one*, 11(8): e0157449, 2016.

Mark Jenkinson, Peter Bannister, Michael Brady, and Stephen Smith. Improved optimization for the robust and accurate linear registration and motion correction of brain images. *Neuroimage*, 17(2):825–841, 2002.

Heidi Johansen-Berg and Timothy EJ Behrens. *Diffusion MRI: from quantitative measurement to in vivo neuroanatomy*. Academic Press, 2013.

Matthew B Johnson, Yuka Imamura Kawasawa, Christopher E Mason, Željka Krsnik, Giovanni Coppola, Darko Bogdanović, Daniel H Geschwind, Shrikant M Mane, Matthew W State, and Nenad Šestan. Functional and evolutionary insights into human brain development through global transcriptome analysis. *Neuron*, 62(4):494–509, 2009.

Marc Joliot, Gaël Jobard, Mikaël Naveau, Nicolas Delcroix, Laurent Petit, Laure Zago, Fabrice Crivello, Emmanuel Mellet, Bernard Mazoyer, and Nathalie Tzourio-Mazoyer. Aicha: An

atlas of intrinsic connectivity of homotopic areas. *Journal of neuroscience methods*, 254: 46–59, 2015.

O Parker Jones, NL Voets, JE Adcock, R Stacey, and S Jbabdi. Resting connectivity predicts task activation in pre-surgical populations. *NeuroImage: Clinical*, 13:378–385, 2017.

Hanna Julienne, Pierre Lechat, Vincent Guillemot, Carla Lasry, Chunzi Yao, Robinson Araud, Vincent Laville, Bjarni Vilhjalmsson, Hervé Ménager, and Hugues Aschard. Jass: Command line and web interface for the joint analysis of gwas results. *NAR genomics and bioinformatics*, 2(1):lqaa003, 2020.

Nina Kaminen, Katariina Hannula-Jouppi, Marjo Kestilä, Päivi Lahermo, Kurt Muller, M Kaaranen, B Myllyluoma, Arja Voutilainen, H Lyytinen, Jaana Nopola-Hemmi, et al. A genome scan for developmental dyslexia confirms linkage to chromosome 2p11 and suggests a new locus on 7q32. *Journal of medical genetics*, 40(5):340–345, 2003.

DE Kaplan, J Gayan, J Ahn, T-W Won, D Pauls, RK Olson, JC DeFries, F Wood, BF Pennington, GP Page, et al. Evidence for linkage and association with reading disability, on 6p21. 3-22. *The American Journal of Human Genetics*, 70(5):1287–1298, 2002.

Clare Kelly, Lucina Q Uddin, Zarrar Shehzad, Daniel S Margulies, F Xavier Castellanos, Michael P Milham, and Michael Petrides. Broca's region: linking human brain functional connectivity data and non-human primate tracing anatomy studies. *European Journal of Neuroscience*, 32(3):383–398, 2010.

Martin Kircher, Daniela M Witten, Preti Jain, Brian J O'Roak, Gregory M Cooper, and Jay Shendure. A general framework for estimating the relative pathogenicity of human genetic variants. *Nature genetics*, 46(3):310–315, 2014.

Lambertus Klei, Diana Luca, Bernie Devlin, and Kathryn Roeder. Pleiotropy and principal components of heritability combine to increase power for association analysis. *Genetic Epidemiology: The Official Publication of the International Genetic Epidemiology Society*, 32(1): 9–19, 2008.

Julian Klingbeil, Max Wawrzyniak, Anika Stockert, and Dorothee Saur. Resting-state functional connectivity: An emerging method for the study of language networks in post-stroke aphasia. *Brain and Cognition*, 131:22–33, 2019.

Chiung-Yuan Ko, Yu-Yi Chu, Shuh Narumiya, Jhih-Ying Chi, Tomoyuki Furuyashiki, Tomohiro Aoki, Shao-Ming Wang, Wen-Chang Chang, and Ju-Ming Wang. The ccaat/enhancer-binding protein delta/mir135a/thrombospondin 1 axis mediates pge2-induced angiogenesis in alzheimer's disease. *Neurobiology of aging*, 36(3):1356–1368, 2015.

Michihiko Koeda, Atsushi Watanabe, Kumiko Tsuda, Miwako Matsumoto, Yumiko Ikeda, Woochan Kim, Amane Tateno, Banyar Than Naing, Hiroyuki Karibe, Takashi Shimada, et al. Interaction effect between handedness and cntnap2 polymorphism (rs7794745 genotype) on

voice-specific frontotemporal activity in healthy individuals: an fmri study. *Frontiers in behavioral neuroscience*, 9:87, 2015.

Maki S Koyama, Clare Kelly, Zarrar Shehzad, Deepak Penesetti, F Xavier Castellanos, and Michael P Milham. Reading networks at rest. *Cerebral cortex*, 20(11):2549–2559, 2010.

Maki S Koyama, Adriana Di Martino, Xi-Nian Zuo, Clare Kelly, Maarten Mennes, Devika R Jutagir, F Xavier Castellanos, and Michael P Milham. Resting-state functional connectivity indexes reading competence in children and adults. *Journal of Neuroscience*, 31(23):8617–8624, 2011.

Veena Kumar, Paula L Croxson, and Kristina Simonyan. Structural organization of the laryngeal motor cortical network and its implication for evolution of speech production. *Journal of Neuroscience*, 36(15):4170–4181, 2016.

Loic Labache, M Joliot, Jérôme Saracco, Gaël Jobard, I Hesling, Laure Zago, Emmanuel Mellet, Laurent Petit, Fabrice Crivello, B Mazoyer, et al. A sentence supramodal areas atlas (sensaas) based on multiple task-induced activation mapping and graph analysis of intrinsic connectivity in 144 healthy right-handers. *Brain Structure and Function*, 224(2):859–882, 2019.

Satu Lamminmäki, Satu Massinen, Jaana Nopola-Hemmi, Juha Kere, and Riitta Hari. Human robo1 regulates interaural interaction in auditory pathways. *Journal of Neuroscience*, 32(3):966–971, 2012.

Nicole Landi and Meaghan V Perdue. Neuroimaging genetics studies of specific reading disability and developmental language disorder: A review. *Language and linguistics compass*, 13(9):e12349, 2019.

Nicole Landi, Stephen J Frost, W Einar Mencl, Jonathan L Preston, Leslie K Jacobsen, Maria Lee, Carolyn Yrigollen, Kenneth R Pugh, and Elena L Grigorenko. The comt val/met polymorphism is associated with reading-related skills and consistent patterns of functional neural activation. *Developmental science*, 16(1):13–23, 2013.

Ellen F Lau, Colin Phillips, and David Poeppel. A cortical network for semantics:(de) constructing the n400. *Nature reviews neuroscience*, 9(12):920–933, 2008.

Isobel D Lawrenson, Sabine H Wimmer-Kleikamp, Peter Lock, Simone M Schoenwaelder, Michelle Down, Andrew W Boyd, Paul F Alewood, and Martin Lackmann. Ephrin-a5 induces rounding, blebbing and de-adhesion of epha3-expressing 293t and melanoma cells by crkii and rho-mediated signalling. *Journal of cell science*, 115(5):1059–1072, 2002.

Yann Le Guen, Marie Amalric, Philippe Pinel, Christophe Pallier, and Vincent Frouin. Shared genetic aetiology between cognitive performance and brain activations in language and math tasks. *Scientific reports*, 8(1):1–11, 2018.

Yann Le Guen, Slim Karkar, Antoine Grigis, Cathy Philippe, Jean-François Mangin, and Vincent Frouin. Heritability of surface area and cortical thickness: a comparison between the human

connectome project and the uk biobank dataset. In *2019 IEEE 16th International Symposium on Biomedical Imaging (ISBI 2019)*, pages 1887–1890. IEEE, 2019.

Yann Le Guen, François Leroy, Cathy Philippe, IMAGEN Consortium, Jean-François Mangin, Ghislaine Dehaene-Lambertz, and Vincent Frouin. Enhancer Locus in ch14q23.1 Modulates Brain Asymmetric Temporal Regions Involved in Language Processing. *Cerebral Cortex*, 05 2020.

Olivier Ledoit and Michael Wolf. A well-conditioned estimator for large-dimensional covariance matrices. *Journal of multivariate analysis*, 88(2):365–411, 2004.

Megan H Lee, Christopher D Smyser, and Joshua S Shimony. Resting-state fmri: a review of methods and clinical applications. *American Journal of neuroradiology*, 34(10):1866–1872, 2013.

Sang Hong Lee, Jian Yang, Michael E Goddard, Peter M Visscher, and Naomi R Wray. Estimation of pleiotropy between complex diseases using single-nucleotide polymorphism-derived genomic relationships and restricted maximum likelihood. *Bioinformatics*, 28(19):2540–2542, 2012.

Jean-Michel Lemée, David Hassanein Berro, Florian Bernard, Eva Chinier, Louis-Marie Leiber, Philippe Menei, and Aram Ter Minassian. Resting-state functional magnetic resonance imaging versus task-based activity for language mapping and correlation with perioperative cortical mapping. *Brain and behavior*, 9(10):e01362, 2019.

Jason P Lerch, André JW van der Kouwe, Armin Raznahan, Tomáš Paus, Heidi Johansen-Berg, Karla L Miller, Stephen M Smith, Bruce Fischl, and Stamatios N Sotiropoulos. Studying neuroanatomy using mri. *Nature neuroscience*, 20(3):314–326, 2017.

Zhi-Pei Liang and Paul C Lauterbur. *Principles of magnetic resonance imaging*. SPIE Optical Engineering Press Belllingham, WA, 2000.

Alvin M Liberman and Ignatius G Mattingly. The motor theory of speech perception revised. *Cognition*, 21(1):1–36, 1985.

Frédérique Liégeois, Torsten Baldeweg, Alan Connelly, David G Gadian, Mortimer Mishkin, and Faraneh Vargha-Khadem. Language fmri abnormalities associated with foxp2 gene mutation. *Nature neuroscience*, 6(11):1230–1237, 2003.

Jake Lin, Rubina Tabassum, Samuli Ripatti, and Matti Pirinen. Metaphat: Detecting and decomposing multivariate associations from univariate genome-wide association statistics. *Frontiers in genetics*, 11:431, 2020.

Nikos K Logothetis. What we can do and what we cannot do with fmri. *Nature*, 453(7197): 869–878, 2008.

Junfeng Lu, Han Zhang, NU Farrukh Hameed, Jie Zhang, Shiwen Yuan, Tianming Qiu, Dinggang Shen, and Jinsong Wu. An automated method for identifying an independent component analysis-based language-related resting-state network in brain tumor subjects for surgical planning. *Scientific reports*, 7(1):1–16, 2017.

Lina Lu, Hui Guo, Yu Peng, Guanglei Xun, Yanling Liu, Zhimin Xiong, Di Tian, Yalan Liu, Wei Li, Xiaojuan Xu, et al. Common and rare variants of the thbs1 gene associated with the risk for autism. *Psychiatric genetics*, 24(6):235–240, 2014.

Zhenjie Lu and Jonathan Kipnis. Thrombospondin 1—a key astrocyte-derived neurogenic factor. *The FASEB Journal*, 24(6):1925–1934, 2010.

Michelle Luciano, David M Evans, Narelle K Hansell, Sarah E Medland, Grant W Montgomery, Nicholas G Martin, Margaret J Wright, and Timothy C Bates. A genome-wide association study for reading and language abilities in two population cohorts. *Genes, Brain and Behavior*, 12(6):645–652, 2013.

Rizzi Luigi. *Compléxité des structures linguistiques, simplicité des mécanismes du langage*. Fayard, 2021.

Reedik Mägi and Andrew P Morris. Gwama: software for genome-wide association meta-analysis. *BMC bioinformatics*, 11(1):1–6, 2010.

Teri A Manolio, Francis S Collins, Nancy J Cox, David B Goldstein, Lucia A Hindorff, David J Hunter, Mark I McCarthy, Erin M Ramos, Lon R Cardon, Aravinda Chakravarti, et al. Finding the missing heritability of complex diseases. *Nature*, 461(7265):747–753, 2009.

Jonathan Marchini, Lon R Cardon, Michael S Phillips, and Peter Donnelly. The effects of human population structure on large genetic association studies. *Nature genetics*, 36(5): 512–517, 2004.

Jonathan Marchini, Bryan Howie, Simon Myers, Gil McVean, and Peter Donnelly. A new multipoint method for genome-wide association studies by imputation of genotypes. *Nature genetics*, 39(7):906–913, 2007.

Cecilia Marino, Paola Scifo, Pasquale A Della Rosa, Sara Mascheretti, Andrea Facoetti, Maria L Lorusso, Roberto Giorda, Monica Consonni, Andrea Falini, Massimo Molteni, et al. The dcdc2/intron 2 deletion and white matter disorganization: focus on developmental dyslexia. *Cortex*, 57:227–243, 2014.

Guillaume Marrelec, Alexandre Krainik, Hugues Duffau, Mélanie Pélégrini-Issac, Stéphane Lehéricy, Julien Doyon, and Habib Benali. Partial correlation for functional brain interactivity investigation in functional mri. *Neuroimage*, 32(1):228–237, 2006.

Shashwath A Meda, Joel Gelernter, Jeffrey R Gruen, Vince D Calhoun, Haiying Meng, Natalie A Cope, and Godfrey D Pearlson. Polymorphism of dcdc2 reveals differences in cortical morphology of healthy individuals—a preliminary voxel based morphometry study. *Brain imaging and behavior*, 2(1):21–26, 2008.

Arthur Mensch, Gaël Varoquaux, and Bertrand Thirion. Compressed online dictionary learning for fast resting-state fmri decomposition. In *2016 IEEE 13th International Symposium on Biomedical Imaging (ISBI)*, pages 1282–1285. IEEE, 2016.

M-Marsel Mesulam. Large-scale neurocognitive networks and distributed processing for attention, language, and memory. *Annals of Neurology: Official Journal of the American Neurological Association and the Child Neurology Society*, 28(5):597–613, 1990.

M-Marsel Mesulam, Cynthia K Thompson, Sandra Weintraub, and Emily J Rogalski. The wernicke conundrum and the anatomy of language comprehension in primary progressive aphasia. *Brain*, 138(8):2423–2437, 2015.

Jeremy A Miller, Song-Lin Ding, Susan M Sunkin, Kimberly A Smith, Lydia Ng, Aaron Szafer, Amanda Ebbert, Zackery L Riley, Joshua J Royall, Kaylynn Aiona, et al. Transcriptional landscape of the prenatal human brain. *Nature*, 508(7495):199–206, 2014.

Karla L Miller, Fidel Alfaro-Almagro, Neal K Bangerter, David L Thomas, Essa Yacoub, Junqian Xu, Andreas J Bartsch, Saad Jbabdi, Stamatios N Sotiropoulos, Jesper LR Andersson, et al. Multimodal population brain imaging in the uk biobank prospective epidemiological study. *Nature neuroscience*, 19(11):1523–1536, 2016.

Grigorios Nasios, Efthymios Dardiotis, and Lambros Messinis. From broca and wernicke to the neuromodulation era: insights of brain language networks for neurorehabilitation. *Behavioural neurology*, 2019, 2019.

Dianne F Newbury, Laura Winchester, Laura Addis, Silvia Paracchini, Lyn-Louise Buckingham, Ann Clark, Wendy Cohen, Hilary Cowie, Katharina Dworzynski, Andrea Everitt, et al. Cmip and atp2c2 modulate phonological short-term memory in language impairment. *The American Journal of Human Genetics*, 85(2):264–272, 2009.

Guiyan Ni, Gerhard Moser, Stephan Ripke, Benjamin M Neale, Aiden Corvin, James TR Walters, Kai-How Farh, Peter A Holmans, Phil Lee, Brendan Bulik-Sullivan, et al. Estimation of genetic correlation via linkage disequilibrium score regression and genomic restricted maximum likelihood. *The American Journal of Human Genetics*, 102(6):1185–1194, 2018.

Nobuyuki Nishitani and Riitta Hari. Temporal dynamics of cortical representation for action. *Proceedings of the National Academy of Sciences*, 97(2):913–918, 2000.

Uta Noppeney and Cathy J Price. Retrieval of abstract semantics. *Neuroimage*, 22(1):164–170, 2004.

Ron Nudel, Nuala H Simpson, Gillian Baird, Anne O'Hare, Gina Conti-Ramsden, Patrick F Bolton, Elizabeth R Hennessy, SLI Consortium, SM Ring, G Davey Smith, et al. Genome-wide association analyses of child genotype effects and parent-of-origin effects in specific language impairment. *Genes, Brain and Behavior*, 13(4):418–429, 2014.

Dale R Nyholt. Seca: Snp effect concordance analysis using genome-wide association summary results. *Bioinformatics*, 30(14):2086–2088, 2014.

Lauren J O'Donnell and Carl-Fredrik Westin. An introduction to diffusion tensor image analysis. *Neurosurgery Clinics*, 22(2):185–196, 2011.

Paul F O'Reilly, Clive J Hoggart, Yotsawat Pomyen, Federico CF Calboli, Paul Elliott, Marjo-Riitta Jarvelin, and Lachlan JM Coin. Multiphen: joint model of multiple phenotypes can increase discovery in gwas. *PloS one*, 7(5):e34861, 2012.

Christophe Pallier, Anne-Dominique Devauchelle, and Stanislas Dehaene. Cortical representation of the constituent structure of sentences. *Proceedings of the National Academy of Sciences*, 108(6):2522–2527, 2011.

Anand S Pandit, Gareth Ball, A David Edwards, and Serena J Counsell. Diffusion magnetic resonance imaging in preterm brain injury. *Neuroradiology*, 55(2):65–95, 2013.

Hae Jeong Park, Su Kang Kim, Jong Woo Kim, Won Sub Kang, and Joo-Ho Chung. Association of thrombospondin 1 gene with schizophrenia in korean population. *Molecular biology reports*, 39(6):6875–6880, 2012.

Ki Yun Park, John J Lee, Donna Dierker, Laura M Marple, Carl D Hacker, Jarod L Roland, Daniel S Marcus, Mikhail Milchenko, Michelle M Miller-Thomas, Tammie L Benzinger, et al. Mapping language function with task-based vs. resting-state functional mri. *PloS one*, 15(7): e0236423, 2020.

Elena B Pasquale. Eph-ephrin bidirectional signaling in physiology and disease. *Cell*, 133(1): 38–52, 2008.

Meaghan V Perdue, Sara Mascheretti, Sergey A Kornilov, Kaja K Jasińska, Kayleigh Ryherd, W Einar Mencl, Stephen J Frost, Elena L Grigorenko, Kenneth R Pugh, and Nicole Landi. Common variation within the setbp1 gene is associated with reading-related skills and patterns of functional neural activation. *Neuropsychologia*, 130:44–51, 2019.

Robin L Peterson and Bruce F Pennington. Developmental dyslexia. *Annual review of clinical psychology*, 11:283–307, 2015.

Tracey L Petryshen, Bonnie J Kaplan, Ming Fu Liu, Norma Schmill de French, Rose Tobias, Martha L Hughes, and L Leigh Field. Evidence for a susceptibility locus on chromosome 6q influencing phonological coding dyslexia. *American journal of Medical genetics*, 105(6): 507–517, 2001.

KC Sreedharan Pillai. Some new test criteria in multivariate analysis. *The Annals of Mathematical Statistics*, pages 117–121, 1955.

Philippe Pinel, Fabien Fauchereau, Antonio Moreno, Alexis Barbot, Mark Lathrop, Diana Zelenika, Denis Le Bihan, Jean-Baptiste Poline, Thomas Bourgeron, and Stanislas Dehaene.

Genetic variants of foxp2 and kiaa0319/ttrap/them2 locus are associated with altered brain activation in distinct language-related regions. *Journal of Neuroscience*, 32(3):817–825, 2012.

Nicholas A Popp, Dianke Yu, Bridgett Green, Emily Y Chew, Baitang Ning, Chi-Chao Chan, and Jingsheng Tuo. Functional single nucleotide polymorphism in il- 17 a 3' untranslated region is targeted by mi r-4480 in vitro and may be associated with age-related macular degeneration. *Environmental and molecular mutagenesis*, 57(1):58–64, 2016.

Heather F Porter and Paul F O'Reilly. Multivariate simulation framework reveals performance of multi-trait gwas methods. *Scientific reports*, 7(1):1–12, 2017.

Jonathan D Power, Alexander L Cohen, Steven M Nelson, Gagan S Wig, Kelly Anne Barnes, Jessica A Church, Alecia C Vogel, Timothy O Laumann, Fran M Miezin, Bradley L Schlaggar, et al. Functional network organization of the human brain. *Neuron*, 72(4):665–678, 2011.

Leslie Pray. Discovery of dna structure and function: Watson and crick. *Nature Education*, 1 (1), 2008.

Shaun Purcell. Variance components models for gene–environment interaction in twin analysis. *Twin Research and Human Genetics*, 5(6):554–571, 2002.

Shaun Purcell, Benjamin Neale, Kathe Todd-Brown, Lori Thomas, Manuel AR Ferreira, David Bender, Julian Maller, Pamela Sklar, Paul IW De Bakker, Mark J Daly, et al. Plink: a tool set for whole-genome association and population-based linkage analyses. *The American journal of human genetics*, 81(3):559–575, 2007.

Ting Qi, Yang Wu, Jian Zeng, Futao Zhang, Angli Xue, Longda Jiang, Zhihong Zhu, Kathryn Kemper, Loic Yengo, Zhili Zheng, et al. Identifying gene targets for brain-related traits using transcriptomic and methylomic data from blood. *Nature communications*, 9(1):1–12, 2018.

Marcus E Raichle, Ann Mary MacLeod, Abraham Z Snyder, William J Powers, Debra A Gusnard, and Gordon L Shulman. A default mode of brain function. *Proceedings of the National Academy of Sciences*, 98(2):676–682, 2001.

Amy E Ramage, Semra Aytur, and Kirrie J Ballard. Resting-state functional magnetic resonance imaging connectivity between semantic and phonological regions of interest may inform language targets in aphasia. *Journal of Speech, Language, and Hearing Research*, 63(9): 3051–3067, 2020.

Vasily Ramensky, Peer Bork, and Shamil Sunyaev. Human non-synonymous snps: server and survey. *Nucleic acids research*, 30(17):3894–3900, 2002.

J Steven Reznick, Robin Corley, JoAnn Robinson, and Adam P Matheny Jr. A longitudinal twin study of intelligence in the second year. *Monographs of the society for research in child development*, pages i–160, 1997.

Sally-Ann Rhea, Josh B Bricker, Sally J Wadsworth, and Robin P Corley. The colorado adoption project. *Twin Research and Human Genetics*, 16(1):358–365, 2013.

Stuart J Ritchie, David Alexander Dickie, Simon R Cox, Maria del C Valdes Hernandez, Janie Corley, Natalie A Royle, Alison Pattie, Benjamin S Aribisala, Paul Redmond, Susana Muñoz Maniega, et al. Brain volumetric changes and cognitive ageing during the eighth decade of life. *Human brain mapping*, 36(12):4910–4925, 2015.

D Roeske, KU Ludwig, N Neuhoff, J Becker, J Bartling, J Bruder, FF Brockschmidt, A Warnke, H Remschmidt, P Hoffmann, et al. First genome-wide association scan on neurophysiological endophenotypes points to trans-regulation effects on slc2a3 in dyslexic children. *Molecular psychiatry*, 16(1):97–107, 2011.

K Rojkova, E Volle, M Urbanski, F Humbert, F Dell'Acqua, and M Thiebaut De Schotten. Atlasing the frontal lobe connections and their variability due to age and education: a spherical deconvolution tractography study. *Brain Structure and Function*, 221(3):1751–1766, 2016.

Jerker Rönnberg, Mary Rudner, and Martin Ingvar. Neural correlates of working memory for sign language. *Cognitive Brain Research*, 20(2):165–182, 2004.

Alexander Rudov, Marco Bruno Luigi Rocchi, Augusto Accorsi, Giorgio Spada, Antonio Domenico Procopio, Fabiola Olivieri, Maria Rita Rippo, and Maria Cristina Albertini. Putative mirnas for the diagnosis of dyslexia, dyspraxia, and specific language impairment. *Epigenetics*, 8(10):1023–1029, 2013.

Gholamreza Salimi-Khorshidi, Gwenaëlle Douaud, Christian F Beckmann, Matthew F Glasser, Ludovica Griffanti, and Stephen M Smith. Automatic denoising of functional mri data: combining independent component analysis and hierarchical fusion of classifiers. *Neuroimage*, 90: 449–468, 2014.

Jeanne E Savage, Philip R Jansen, Sven Stringer, Kyoko Watanabe, Julien Bryois, Christiaan A De Leeuw, Mats Nagel, Swapnil Awasthi, Peter B Barr, Jonathan RI Coleman, et al. Genome-wide association meta-analysis in 269,867 individuals identifies new genetic and functional links to intelligence. *Nature genetics*, 50(7):912–919, 2018.

Thomas S Scerri, Fahimeh Darki, Dianne F Newbury, Andrew JO Whitehouse, Myriam Peyrard-Janvid, Hans Matsson, Qi W Ang, Craig E Pennell, Susan Ring, John Stein, et al. The dyslexia candidate locus on 2p12 is associated with general cognitive ability and white matter structure. *PloS one*, 7(11):e50321, 2012.

Benjamin J Schmiedel, Divya Singh, Ariel Madrigal, Alan G Valdovino-Gonzalez, Brandie M White, Jose Zapardiel-Gonzalo, Brendan Ha, Gokmen Altay, Jason A Greenbaum, Graham McVicker, et al. Impact of genetic polymorphisms on human immune cell gene expression. *Cell*, 175(6):1701–1715, 2018.

Jean-Luc Schwartz, Marc Sato, and Luciano Fadiga. The common language of speech perception and action: a neurocognitive perspective. *Revue française de linguistique appliquée*, 13(2): 9–22, 2008.

Jean-Luc Schwartz, Anahita Basirat, Lucie Ménard, and Marc Sato. The perception-for-action-control theory (pact): A perceptuo-motor theory of speech perception. *Journal of Neurolinguistics*, 25(5):336–354, 2012.

Zhiqiang Sha, Dick Schijven, Amaia Carrion-Castillo, Marc Joliot, Bernard Mazoyer, Simon E Fisher, Fabrice Crivello, and Clyde Francks. The genetic architecture of structural left-right asymmetry of the human brain. *Nature Human Behaviour*, pages 1–14, 2021.

Stephen T Sherry, M-H Ward, M Kholodov, J Baker, Lon Phan, Elizabeth M Smigielski, and Karl Sirotkin. dbsnp: the ncbi database of genetic variation. *Nucleic acids research*, 29(1): 308–311, 2001.

Chet C Sherwood, Francys Subiaul, and Tadeusz W Zawidzki. A natural history of the human mind: tracing evolutionary changes in brain and cognition. *Journal of anatomy*, 212(4): 426–454, 2008.

Michael A Skeide, Holger Kirsten, Indra Kraft, Gesa Schaadt, Bent Müller, Nicole Neef, Jens Brauer, Arndt Wilcke, Frank Emmrich, Johannes Boltze, et al. Genetic dyslexia risk variant is related to neural connectivity patterns underlying phonological awareness in children. *Neuroimage*, 118:414–421, 2015.

Michael A Skeide, Indra Kraft, Bent Müller, Gesa Schaadt, Nicole E Neef, Jens Brauer, Arndt Wilcke, Holger Kirsten, Johannes Boltze, and Angela D Friederici. Nrsn1 associated grey matter volume of the visual word form area reveals dyslexia before school. *Brain*, 139(10): 2792–2803, 2016.

Stephen M Smith, Mark Jenkinson, Heidi Johansen-Berg, Daniel Rueckert, Thomas E Nichols, Clare E Mackay, Kate E Watkins, Olga Ciccarelli, M Zaheer Cader, Paul M Matthews, et al. Tract-based spatial statistics: voxelwise analysis of multi-subject diffusion data. *Neuroimage*, 31(4):1487–1505, 2006.

Stephen M Smith, Peter T Fox, Karla L Miller, David C Glahn, P Mickle Fox, Clare E Mackay, Nicola Filippini, Kate E Watkins, Roberto Toro, Angela R Laird, et al. Correspondence of the brain's functional architecture during activation and rest. *Proceedings of the national academy of sciences*, 106(31):13040–13045, 2009.

Stephen M Smith, Karla L Miller, Gholamreza Salimi-Khorshidi, Matthew Webster, Christian F Beckmann, Thomas E Nichols, Joseph D Ramsey, and Mark W Woolrich. Network modelling methods for fmri. *Neuroimage*, 54(2):875–891, 2011.

Beate St Pourcain, Rolieke AM Cents, Andrew JO Whitehouse, Claire MA Haworth, Oliver SP Davis, Paul F O'Reilly, Susan Roulstone, Yvonne Wren, Qi W Ang, Fleur P Velders, et al. Common variation near robo2 is associated with expressive vocabulary in infancy. *Nature communications*, 5(1):1–9, 2014.

Matthew Stephens. A unified framework for association analysis with multiple related phenotypes. *PloS one*, 8(7):e65245, 2013.

W Dale Stevens, Dwight J Kravitz, Cynthia S Peng, Michael Henry Tessler, and Alex Martin. Privileged functional connectivity between the visual word form area and the language system. *Journal of Neuroscience*, 37(21):5288–5297, 2017.

Karin Stromswold. The heritability of language: A review and metaanalysis of twin, adoption, and linkage studies. *Language*, pages 647–723, 2001.

Aravind Subramanian, Pablo Tamayo, Vamsi K Mootha, Sayan Mukherjee, Benjamin L Ebert, Michael A Gillette, Amanda Paulovich, Scott L Pomeroy, Todd R Golub, Eric S Lander, et al. Gene set enrichment analysis: a knowledge-based approach for interpreting genome-wide expression profiles. *Proceedings of the National Academy of Sciences*, 102(43):15545–15550, 2005.

Cathie Sudlow, John Gallacher, Naomi Allen, Valerie Beral, Paul Burton, John Danesh, Paul Downey, Paul Elliott, Jane Green, Martin Landray, et al. Uk biobank: an open access resource for identifying the causes of a wide range of complex diseases of middle and old age. *Plos med*, 12(3):e1001779, 2015.

D Szklarczyk et al. The string database in 2017: quality-controlled protein–protein association networks, made broadly accessible nucleic acids res., 45. *D362–D368*, 2017.

Mikko Taipale, Nina Kaminen, Jaana Nopola-Hemmi, Tuomas Haltia, Birgitta Myllyluoma, Heikki Lyytinen, Kurt Muller, Minna Kaaranen, Perttu J Lindsberg, Katariina Hannula-Jouppi, et al. A candidate gene for developmental dyslexia encodes a nuclear tetratricopeptide repeat domain protein dynamically regulated in brain. *Proceedings of the National Academy of Sciences*, 100(20):11553–11558, 2003.

Geoffrey CY Tan, Thomas F Doke, John Ashburner, Nicholas W Wood, and Richard SJ Frackowiak. Normal variation in fronto-occipital circuitry and cerebellar structure with an autism-associated polymorphism of cntnap2. *Neuroimage*, 53(3):1030–1042, 2010.

I Tavor, O Parker Jones, RB Mars, SM Smith, TE Behrens, and S Jbabdi. Task-free mri predicts individual differences in brain activity during task performance. *Science*, 352(6282):216–220, 2016.

Peter E Thijssen, Yuya Ito, Giacomo Grillo, Jun Wang, Guillaume Velasco, Hirohisa Nitta, Motoko Unoki, Minako Yoshihara, Mikita Suyama, Yu Sun, et al. Mutations in cdca7 and hells cause immunodeficiency–centromeric instability–facial anomalies syndrome. *Nature communications*, 6(1):1–8, 2015.

Bertrand Thirion, Gaël Varoquaux, Elvis Dohmatob, and Jean-Baptiste Poline. Which fmri clustering gives good brain parcellations? *Frontiers in neuroscience*, 8:167, 2014.

Moriah E Thomason and Paul M Thompson. Diffusion imaging, white matter, and psychopathology. *Annual review of clinical psychology*, 7:63–85, 2011.

Paul M Thompson, Kiralee M Hayashi, Rebecca A Dutton, Ming-Chang Chiang, Alex D Leow, Elizabeth R Sowell, Greig De Zubicaray, James T Becker, Oscar L Lopez, Howard J Aizenstein, et al. Tracking alzheimer's disease. *Annals of the New York Academy of Sciences*, 1097:183, 2007.

Paul M Thompson, Tian Ge, David C Glahn, Neda Jahanshad, and Thomas E Nichols. Genetics of the connectome. *Neuroimage*, 80:475–488, 2013.

Yanmei Tie, Laura Rigolo, Isaiah H Norton, Raymond Y Huang, Wentao Wu, Daniel Orringer, Srinivasan Mukundan Jr, and Alexandra J Golby. Defining language networks from resting-state fmri for surgical planning—a feasibility study. *Human brain mapping*, 35(3):1018–1030, 2014.

Pascale Tremblay and Anthony Steven Dick. Broca and wernicke are dead, or moving past the classic model of language neurobiology. *Brain and language*, 162:60–71, 2016.

Patrick Turley, Raymond K Walters, Omeed Maghzian, Aysu Okbay, James J Lee, Mark Alan Fontana, Tuan Anh Nguyen-Viet, Robbee Wedow, Meghan Zacher, Nicholas A Furlotte, et al. Multi-trait analysis of genome-wide association summary statistics using mtag. *Nature genetics*, 50(2):229–237, 2018.

Travis H Turner, Julius Fridriksson, Julie Baker, David Eoute Jr, Leonardo Bonilha, and Christopher Rorden. Obligatory broca's area modulation associated with passive speech perception. *Neuroreport*, 20(5):492, 2009.

Nathalie Tzourio-Mazoyer, Brigitte Landeau, Dimitri Papathanassiou, Fabrice Crivello, Olivier Etard, Nicolas Delcroix, Bernard Mazoyer, and Marc Joliot. Automated anatomical labeling of activations in spm using a macroscopic anatomical parcellation of the mni mri single-subject brain. *Neuroimage*, 15(1):273–289, 2002.

Julia Uddén, Tineke M Snijders, Simon E Fisher, and Peter Hagoort. A common variant of the cntnap2 gene is associated with structural variation in the left superior occipital gyrus. *Brain and language*, 172:16–21, 2017.

Sven J van der Lee, Gennady V Roshchupkin, Hieab HH Adams, Helena Schmidt, Edith Hofer, Yasaman Saba, Reinhold Schmidt, Albert Hofman, Najaf Amin, Cornelia M van Duijn, et al. Gray matter heritability in family-based and population-based studies using voxel-based morphometry. *Human brain mapping*, 38(5):2408–2423, 2017.

Dennis van der Meer, Oleksandr Frei, Tobias Kaufmann, Alexey A Shadrin, Anna Devor, Olav B Smeland, Wesley K Thompson, Chun Chieh Fan, Dominic Holland, Lars T Westlye, et al. Understanding the genetic determinants of the brain with mostest. *Nature communications*, 11(1):1–9, 2020.

Sophie Van der Sluis, Danielle Posthuma, and Conor V Dolan. Tates: efficient multivariate genotype-phenotype analysis for genome-wide association studies. *PLoS genetics*, 9(1): e1003235, 2013.

David C Van Essen, Kamil Ugurbil, Edward Auerbach, Deanna Barch, Timothy EJ Behrens, Richard Bucholz, Acer Chang, Liyong Chen, Maurizio Corbetta, Sandra W Curtiss, et al. The human connectome project: a data acquisition perspective. *Neuroimage*, 62(4):2222–2231, 2012.

David C Van Essen, Stephen M Smith, Deanna M Barch, Timothy EJ Behrens, Essa Yacoub, Kamil Ugurbil, Wu-Minn HCP Consortium, et al. The wu-minn human connectome project: an overview. *Neuroimage*, 80:62–79, 2013.

Faraneh Vargha-Khadem, Kate E Watkins, CJ Price, John Ashburner, Katie J Alcock, Alan Connelly, Richard SJ Frackowiak, Karl J Friston, ME Pembrey, Mortimer Mishkin, et al. Neural basis of an inherited speech and language disorder. *Proceedings of the National Academy of Sciences*, 95(21):12695–12700, 1998.

Francesco Vergani, Luis Lacerda, Juan Martino, Johannes Attems, Christopher Morris, Patrick Mitchell, Michel Thiebaut de Schotten, and Flavio Dell'Acqua. White matter connections of the supplementary motor area in humans. *Journal of Neurology, Neurosurgery & Psychiatry*, 85(12):1377–1385, 2014.

Sonja C Vernes, Dianne F Newbury, Brett S Abrahams, Laura Winchester, Jérôme Nicod, Matthias Groszer, Maricela Alarcón, Peter L Oliver, Kay E Davies, Daniel H Geschwind, et al. A functional genetic link between distinct developmental language disorders. *New England Journal of Medicine*, 359(22):2337–2345, 2008.

Mathieu Vigneau, Virginie Beaucousin, Pierre-Yves Herve, Hugues Duffau, Fabrice Crivello, Olivier Houde, Bernard Mazoyer, and Nathalie Tzourio-Mazoyer. Meta-analyzing left hemisphere language areas: phonology, semantics, and sentence processing. *Neuroimage*, 30(4): 1414–1432, 2006.

Mathieu Vigneau, Virginie Beaucousin, Pierre-Yves Hervé, Gael Jobard, Laurent Petit, Fabrice Crivello, Emmanuel Mellet, Laure Zago, Bernard Mazoyer, and Nathalie Tzourio-Mazoyer. What is right-hemisphere contribution to phonological, lexico-semantic, and sentence processing?: Insights from a meta-analysis. *Neuroimage*, 54(1):577–593, 2011.

Peter M Visscher, William G Hill, and Naomi R Wray. Heritability in the genomics era—concepts and misconceptions. *Nature reviews genetics*, 9(4):255–266, 2008.

Urmo Võsa, Annique Claringbould, Harm-Jan Westra, Marc Jan Bonder, Patrick Deelen, Biao Zeng, Holger Kirsten, Ashis Saha, Roman Kreuzhuber, Silva Kasela, et al. Unraveling the polygenic architecture of complex traits using blood eqtl metaanalysis. *BioRxiv*, page 447367, 2018.

Louise V Wain, Nick Shrine, Suzanne Miller, Victoria E Jackson, Ioanna Ntalla, María Soler Artigas, Charlotte K Billington, Abdul Kader Kheirallah, Richard Allen, James P Cook, et al. Novel insights into the genetics of smoking behaviour, lung function, and chronic obstructive pulmonary disease (uk bileve): a genetic association study in uk biobank. *The Lancet Respiratory Medicine*, 3(10):769–781, 2015.

Daifeng Wang, Shuang Liu, Jonathan Warrell, Hyejung Won, Xu Shi, Fabio CP Navarro, Declan Clarke, Mengting Gu, Prashant Emani, Yucheng T Yang, et al. Comprehensive functional genomic resource and integrative model for the human brain. *Science*, 362(6420), 2018.

Kai Wang, Mingyao Li, and Hakon Hakonarson. Annovar: functional annotation of genetic variants from high-throughput sequencing data. *Nucleic acids research*, 38(16):e164–e164, 2010.

Kyoko Watanabe, Erdogan Taskesen, Arjen Van Bochoven, and Danielle Posthuma. Functional mapping and annotation of genetic associations with fuma. *Nature communications*, 8(1):1–11, 2017.

Kate E Watkins, Faraneh Vargha-Khadem, John Ashburner, Richard E Passingham, Alan Connelly, Karl J Friston, Richard SJ Frackowiak, Mortimer Mishkin, and David G Gadian. Mri analysis of an inherited speech and language disorder: structural brain abnormalities. *Brain*, 125(3):465–478, 2002.

DH Whalen. The motor theory of speech perception. In *Oxford Research Encyclopedia of Linguistics*. 2019.

Heather C Whalley, Garret O'Connell, Jessika E Sussmann, Anna Peel, Andrew C Stanfield, Marianna E Hayiou-Thomas, Eve C Johnstone, Stephen M Lawrie, Andrew M McIntosh, and Jeremy Hall. Genetic variation in cntnap2 alters brain function during linguistic processing in healthy individuals. *American Journal of Medical Genetics Part B: Neuropsychiatric Genetics*, 156(8):941–948, 2011.

Arndt Wilcke, Carolin Ligges, Jana Burkhardt, Michael Alexander, Christiane Wolf, Elfi Quente, Peter Ahnert, Per Hoffmann, Albert Becker, Bertram Müller-Myhsok, et al. Imaging genetics of foxp2 in dyslexia. *European Journal of Human Genetics*, 20(2):224–229, 2012.

Cristen J Willer, Yun Li, and Gonçalo R Abecasis. Metal: fast and efficient meta-analysis of genomewide association scans. *Bioinformatics*, 26(17):2190–2191, 2010.

Stephen M Wilson, Ayşe Pinar Saygin, Martin I Sereno, and Marco Iacoboni. Listening to speech activates motor areas involved in speech production. *Nature neuroscience*, 7(7):701–702, 2004.

Wojciech Wiszniewski, Jill V Hunter, Neil A Hanchard, Jason R Willer, Chad Shaw, Qi Tian, Anna Illner, Xueqing Wang, Sau W Cheung, Ankita Patel, et al. Tm4sf20 ancestral deletion and susceptibility to a pediatric disorder of early language delay and cerebral white matter hyperintensities. *The American Journal of Human Genetics*, 93(2):197–210, 2013.

Chong Wu. Multi-trait genome-wide analyses of the brain imaging phenotypes in uk biobank. *Genetics*, 215(4):947–958, 2020.

Hua-Dong Xiang, Hubert M Fonteijn, David G Norris, and Peter Hagoort. Topographical functional connectivity pattern in the perisylvian language networks. *Cerebral cortex*, 20(3): 549–560, 2010.

Jian Yang, Beben Benyamin, Brian P McEvoy, Scott Gordon, Anjali K Henders, Dale R Nyholt, Pamela A Madden, Andrew C Heath, Nicholas G Martin, Grant W Montgomery, et al. Common snps explain a large proportion of the heritability for human height. *Nature genetics*, 42 (7):565–569, 2010.

Jian Yang, S Hong Lee, Michael E Goddard, and Peter M Visscher. Gcta: a tool for genome-wide complex trait analysis. *The American Journal of Human Genetics*, 88(1):76–82, 2011.

Jian Yang, Andrew Bakshi, Zhihong Zhu, Gibran Hemani, Anna AE Vinkhuyzen, Sang Hong Lee, Matthew R Robinson, John RB Perry, Ilja M Nolte, Jana V van Vliet-Ostaptchouk, et al. Genetic variance estimation with imputed variants finds negligible missing heritability for human height and body mass index. *Nature genetics*, 47(10):1114–1120, 2015.

Hui Zhang, Torben Schneider, Claudia A Wheeler-Kingshott, and Daniel C Alexander. Noddi: practical in vivo neurite orientation dispersion and density imaging of the human brain. *Neuroimage*, 61(4):1000–1016, 2012.

Rui Zhang, Nan-Nan Zhong, Xiao-Gang Liu, Han Yan, Chuan Qiu, Yan Han, Wei Wang, Wei-Kun Hou, Yue Liu, Cheng-Ge Gao, et al. Is the efnb2 locus associated with schizophrenia? single nucleotide polymorphisms and haplotypes analysis. *Psychiatry research*, 180(1):5–9, 2010.

Daria V Zhernakova, Patrick Deelen, Martijn Vermaat, Maarten Van Iterson, Michiel Van Galen, Wibowo Arindrarto, Peter Van't Hof, Hailiang Mei, Freerk Van Dijk, Harm-Jan Westra, et al. Identification of context-dependent expression quantitative trait loci in whole blood. *Nature genetics*, 49(1):139–145, 2017.

Wensheng Zhu and Heping Zhang. Why do we test multiple traits in genetic association studies? *Journal of the Korean Statistical Society*, 38(1):1–10, 2009.

Or Zuk, Eliana Hechter, Shamil R Sunyaev, and Eric S Lander. The mystery of missing heritability: Genetic interactions create phantom heritability. *Proceedings of the National Academy of Sciences*, 109(4):1193–1198, 2012.

* * *
* *
*

université PARIS-SACLAY

ÉCOLE DOCTORALE
Physique et ingénierie : Electrons, Photons, Sciences du vivant (EOBE)

Titre : L'architecture génétique du connectome du langage dans le cerveau humain

Mots clés : imagerie-génétique, IRM fonctionnelle de repos, IRM de diffusion, Langage, GWAS multivariée, UK Biobank.

Résumé : Le langage est une composante essentielle de la vie humaine en raison de son rôle central dans les interactions sociales, la transmission culturelle, et la structuration de nos pensées. Grâce à l'étude des troubles du développement du langage parlé et écrit, tel que la dyslexie, un nombre croissant de gènes ont été identifiés et étiquetés comme étant impliqués dans leurs étiologies. Des études d'association cas-témoins sont mises en œuvre, mais souffrent d'un manque de puissance statistique et peinent à produire des résultats significatifs. Parallèlement à cela, des études de neuro-imagerie ont contribué de manière significative à la compréhension des aspects structurels et fonctionnels du langage dans le cerveau. La disponibilité récente des cohortes de grande taille comportant à la fois de la neuro-imagerie et de la génétique tels que "UK Biobank" et le "Human Connectome Project" a rendu possible l'étude du langage dans les populations générales via des phénotypes intermédiaires (endophénotypes). En effet, ceux-là donnent accès à des mesures biologiquement pertinentes de la variabilité individuelle des supports structurels et fonctionnels du langage et sont par conséquent adaptés à la recherche d'associations génétiques. Dans cette thèse, nous souhaitons d'une part, mettre en évidence la variation interindividuelle de la structure et/ou de la fonction cérébrale qui reflète des traits neurocognitifs spécifiques ; d'autre part, tirer profit de cette variabilité pour mettre en évidence la base génétique de leur architecture cérébrale. Pour ce faire, nous avons étudié la neurobiologie du langage à l'aide de la connectivité fonctionnelle (CF) des régions corticales périsylviennes mesurée à l'état de repos, ainsi qu'à partir de la connectivité anatomique (CA) mesuré sur des faisceaux de matière blanche déterminé par l'IRM de diffusion et connus comme étant liés au langage. Tout d'abord, nous présentons une étude approfondie de l'héritabilité du langage en exploitant des endophénotypes du connectome du langage humain extraits des deux cohortes susmentionnées. Les résultats obtenus sont conformes aux estimations de l'héritabilité rapportées dans la littérature et confirment que l'organisation cérébrale liée au langage est en partie sous-tendue par la génétique. Deuxièmement, pour les endophénotypes de CF avec une héritabilité significative, nous avons réalisé une étude d'association multivariée pangénomique sur 32.186 participants de la cohorte UK Biobank. Vingt loci sont significativement associés aux CF du langage, dont trois sont répliqués dans un échantillon indépendant (ethnicité non britannique de UKB, N=4.754). L'annotation fonctionnelle approfondie pointe notamment vers le gène EPHA3 avec un rôle dans le réseau sémantique fronto-pariéto-temporal, et le gène THBS1 avec un rôle dans l'interaction perception-moteur, requise dans le langage. Enfin, de la même manière, pour les endophénotypes de CA avec une héritabilité significative, nous avons effectué une étude d'association multivariée pangénomique sur 31.775 participants de la cohorte UK Biobank. 278 loci sont significativement associés aux CA du langage, dont ceux précédemment associés à des endophénotypes de CF. En conclusion, ce travail a permis d'étudier les bases génétiques du langage humain en utilisant des approches génomiques à l'état de l'art et ce, en développant des endophénotypes originaux associés au langage. Les gènes suggérés par l'analyse fournissent des pistes d'investigation dans des modèles animaux ou cellulaires du langage. Aussi, alors que de plus en plus de cohortes sont construites en population générale, ce travail renforce notre conviction que ce type de cohortes "multi-phénotypées" permet d'augmenter la puissance statistique et de pallier les faibles tailles d'effet en neuro-imagerie afin d'étudier des questions ouvertes en neuroscience. De nombreux autres domaines des neurosciences pourraient probablement bénéficier de ce type de méthodologie.

université PARIS-SACLAY

ÉCOLE DOCTORALE
Physique et ingénierie : Electrons, Photons, Sciences du vivant (EOBE)

Title : The genetic architecture of the human language connectome

Keywords : Imaging-genetics, Resting-state functional MRI, diffusion MRI, Language, multivariate GWAS, UK Biobank.

Abstract : Language is an essential component of human life because of its central role in social interaction, cultural transmission, and for structuring our thoughts. Through developmental disorders of spoken and written language studies such as dyslexia, a growing number of genes have been identified and labelled as implicated in language etiology. Case-control studies suffering from a lack of statistical power, struggle to uncover significant variants. In parallel, neuroimaging studies have significantly contributed to the understanding of structural and functional aspects of language in the human brain. The recent availability of large-scale cohorts comprising both neuroimaging and genetics data such as the UK Biobank and the Human Connectome Project, have made it possible to study language in the general population via image-derived phenotypes (IDP). Indeed, these IDPs give access to biologically relevant measurements of individual variability and are consequently suitable for the search of genetic associations. In this thesis, we aim to first, highlight the inter-individual variation in brain structure and/or function of language ; second, take advantage of this variability to study the genetic basis of the brain's infrastructure for language. For this, we used task-free functional connectivity (FC), extracted from perisylvian cortical regions as well as from anatomical connectivity (AC) measured using well-known language related white matter bundles determined from diffusion MRI. First, we present an in-depth study of language heritability using human language connectome as endophenotypes extracted from the two aforementioned large-scale cohorts. The results found are consistent with the heritability estimates reported in the literature and support that the language-related brain organization is partly underpinned by genetic. Secondly, using the significantly heritable FC endophenotypes, we performed a multivariate genome-wide association study on 32,186 participants from UK Biobank. Twenty genomic loci were found significantly associated with language FCs, out of which three were replicated in an independent sample (the UK Biobank non-British sample, N=4.754). The functional annotation highlighted noticeably the EPHA3 gene associated with FCs of the fronto-parieto-temporal semantic network, and the THBS1 gene with a potential role in the perceptual-motor interaction required for language processing. Finally, using the significantly heritable AC endophenotypes, we performed a multivariate genome-wide association study on 31.775 participants from UK Biobank. 278 genomic loci were found significantly associated with language ACs including those previously associated with FC endophenotypes. As a conclusion, this work contributed to uncovering the neurobiology of human language using state-of-the-art genomic approaches and by developing novel language endophenotypes. The genes pinpointed in this work open new leads for investigations of neurobiology of language using animal and cellular models. Furthermore, as more and more cohorts are being built in the general population, this work strengthens our belief that multi-modal data collection in large-scale cohorts allow us to increase statistical power and to circumvent the small effect sizes in neuroimaging in order to investigate open neuroscience questions. Many other neuroscience fields could probably benefit from this type of methodology.